MINERALOGY
in the System of Earth Sciences

Scientific Works

EMIL CONSTANTINESCU

MINERALOGY
in the System of Earth Sciences

EMIL CONSTANTINESCU

MINERALOGY
in the System of Earth Sciences

Scientific Works

MINERALOGY IN THE SYSTEM OF THE EARTH SCIENCES

Cover: Elena Drăgulelei Dumitru

CONTENTS

Foreword

I. New mineral occurences

II.   Rock forming minerals

III. Mineralogy of ore deposits

IV. Mineral textures

V. Mineralogy and petrogenesis

VI. Mineralogy of secondary processes

VII. Mineralogy and petrochemistry

VIII. Syntheses

Introduction by the Mineralogical Society of Great Britain & Ireland

The Mineralogical Society is pleased to endorse the publication of ,,Mineralogy in the System of Earth Sciences", a book including many of the published works by Professor Emil Constantinescu, and presented now in this volume, in his honour. This work, in eight sections, testifies to the immense breadth of interest of Constantinescu, with subjects varying from new mineral occurrences to alpine mineralogy.

The Society awarded Honorary Membership to Professor Constantinescu "in recognition of his strong association with the Mineralogical Society Of Great Britain and Ireland".This in an honour limited to twenty mineralogists, at any time, resident outside of the UK.

Professor Constantinescu is one of the number of eminent ore mineralogists based in Romania. The universities in that country, at specially that in Bucharest continue to produce some of the first ore in mineralogists in the world. Since his time as a lecturer at the University of Bucharest, after which he became Rector of that institution, Professor Constantinescu has maintained his interest in mineralogy. This commitment to education is undoubtedly a very important part of his programme of regeneration for Romania.

The Mineralogical Society welcomes scientist from Romania to its meetings, and invites them to continue to submit their papers to the Society publications. The link between Romania and the Society is important to mineralogists in the UK, and we hope that it will continue for many years.

B.E. Leake
President of the Mineralogical Society of Great Britain and Ireland

September 1999

Foreword

Romania plays - and always played - an important role in the Earth Sciences. This is a consequence of its richness in mineral resources and of its interesting and varied geology, but equally of its old traditions in mining as well as in the scientific investigation of mineral deposits and geologic objects in general.

In the teaching of and in the research in mineralogy with all its branches the Romanian Universities were and are important institutions going back in time long before World War I. A great number of minerals was first discovered from localities in Romania. This holds for instance for the famous gold and telluride minerals from Transylvania. They were and are investigated all over the world, and the results contributed greatly to progress of science. In this context we should recollect that the chemical element tellurium was discovered in material from Transylvania at the end of the 18th century. But the international interest in such minerals from Romania is by far not only a historical phenomenon: it clearly continues in our days. A typical example for this is the complex lead-antimony-gold sulfide-telluride mineral nagyágite. It got its present name by Haidinger 1845, but it was known already more than half a century earlier. Although samples with centimeter sized plates of nagyágite are to be found in many of the better mineral collections, a generally accepted chemical formula could not be established up to the present. And only very recently combined single crystal X-ray work on natural and synthetic material allowed the determination of the main features of its atomic arrangement; but many details await further work.

Of equal importance as the minerals and ore deposits are the rocks on the territory of Romania. For instance, every petrographer in the world knows the alkaline rocks of Ditrău. But they are, of course, not the only ones that are famous also abroad. Let us think also only of the "banatites" and their contact phenomena, including skarn deposits.

Bucharest University is a research and teaching institution of mineralogy and petrology for more than a century. Quite a number of its staff members were and are highly renowned not only for in their home country, but also abroad: Of the deceased ones Ludovic Mrazec and Dan Giuşcă are probably first of all to be mentioned in this context. Today one of the outstanding personalities in mineralogy at the Bucharest University is Prof. Dr. Dr. h. c. mult. Emil Constantinescu. This Foreword is not the place to pay tribute to all his activities, of whatever great importance they are, but rather to say a few words on the mineralogist Emil Constantinescu.

He started studies in Earth Sciences at Bucharest University in 1961, received in 1966 the Diploma in Geology, and in 1979 he became Doctor in Geological Studies. Since 1991 he is the Professor for Mineralogy-Crystallography. An excellent training under the guidance mainly of Prof. Dan Giuşcă combined with broad interests and high working capacity caused that Prof. Emil Constantinescu became soon on eof the leading figures in Romanian Earth Sciences.

The topics of his publications cover a wide field. He worked on several of the key problems of Romanian mineralogy and petrography, for instance on problems of the alkali massif of Ditrău, and on "banatites", including their contacts and connected mineralizations. Other papers deal with ore mineralogy, Alpine-type veins in the Carpathians, micrographic feldspar-quartz intergrowths, pyrophyllite and its petrologic implications, various mineral occurrences in Romania and their peculiarities, and fractal features in mineralogy. He published not only in Romania but also in renowned journals abroad. Not to be forgotten are his textbooks - important teaching aids for Romanian students.

A longer stay at Duke University, North Carolina, shorter visits to many institutions in Earth Sciences all over the world and participation in a great number of international congresses made him widely known and - together with his scientific achievements - led to a remarkable number of honors here in Romania as well as abroad.

The volume is structured in eight chapters grouping the papers of Prof. Emil Constantinescu according to several main directions of his scientific research activity. Thus, the volume is opened by a chapter dealing with the new or unusual mineral occurrences of vesuvianite, pyrrophillite, adularia and vivianite from various localities across Romania. Following, is the chapter on rock forming minerals which contains important papers concerning the mineralogy of the alkaline massif of Ditrău and of the banatites. The chapter on the mineralogy of ore deposits groups several works contributing to a better knowledge of the economic geology of certain mineralizations such as porphyry copper deposits, bismuth minerals and manganese ore deposits. The chapter dedicated to the study of mineral intergrowths contain original contributions to the knowledge of myrmekites and fractal-like textures.

The other chapters - mineralogy and petrogenesis (with papers on skarn occurrences, the alkaline massif from Ditrău), mineralogy of secondary processes (with contributions to the study of hydrothermal alterations), mineralogy and geochemistry - reflects the wide spectrum of topics approached by Prof. Emil Constantinescu in his research.

The volume ends with several syntheses such as gold mineralogy in Romania, foidic rocks in Romanian Carpathians and Upper Cretaceous - Paleogene magmatic series in the Carpathian - Balkan region.

With only few words about the mineralogist Emil Constantinescu, we will let his works speak for their author.

Prof. J. Zemann, Vienna, July 28th, 1999

I. NEW MINERAL OCCURRENCES

Crandallite in the phosphate association from Cioclovina cave, (Sureanu Mts., Romania)

EMIL CONSTANTINESCU
ŞTEFAN MARINCEA
CONSTANTIN CRĂCIUN

Crandallite, ideally $CaAl_3(PO_4)_2(OH)_5 \cdot H_2O$, is a quite widespread mineral in the guano-bearing cave deposits throughout the world. Over 20 occurences of crandallite in such deposits have been reported worldwide (Palache et al., 1951; Nriagu and Moore. 1984), but the mineral was never mentioned in the similar deposits from Romania. In this paper, we describe the first occurrence of crandallite in Romania. The mineral was identified in Cioclovina cave from Sureanu Mountains, South Carpathians.

1. Geological setting

Located at about 16 km east-southeast of Haţeg, the major city in the area, Cioclovina cave from is worldwide famous as the type locality of ardealite $[Ca_2H(PO_4)(SO_4) \cdot 4H_2O]$, which was first described in the bat guano deposit inside by Schadler (1932). During the first half of the XXth century, the cave was extensively mined for guano: about 32000 tons of this precious fertilizer were extracted according to Bleahu (1976).

The mineral association from Cioclovina cave is typical for a "dry" system of phosphate-bearing cave deposits. An extended analysis of the associated minerals, including the carbonate phases, is reserved for further studies. The list of these minerals, restricted to the species occurring in the crandallite-bearing zones, includes ardealite, brushite, taranakite, gypsum, hydroxylapatite, kaolinite and illite.

Crandallite was identified in samples located at 130 – 180 m westward from the natural entrance in the cave (Fig. 1). A secondary man-made entrance assures an easier access.

2. Physical properties

The mineral occurs as crusts of dull appearance or as earthy masses of yellowish-white crystals, intimately associated with brushite
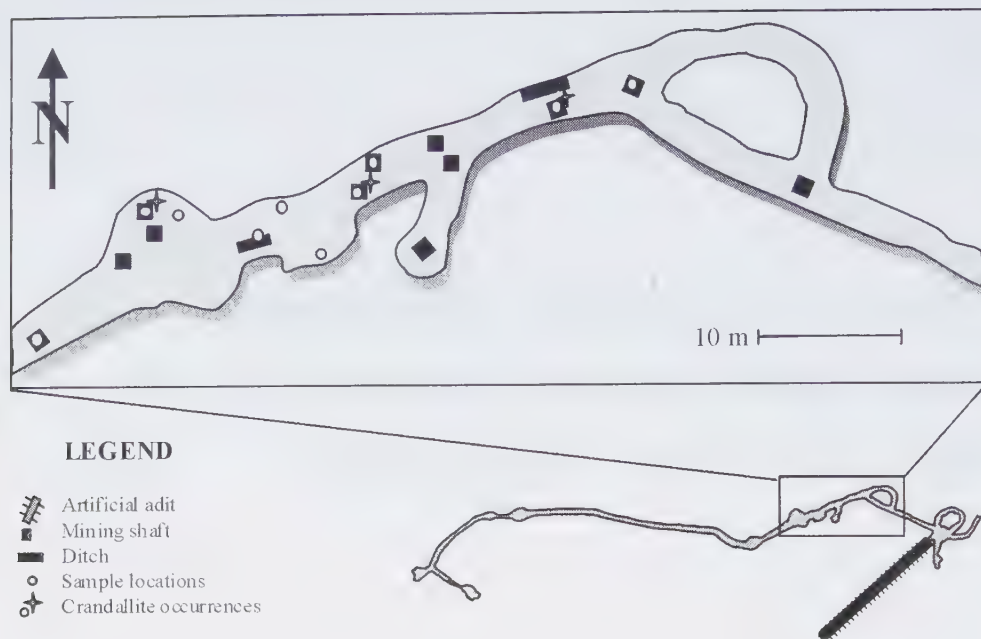
Fig. 1. Sketch of Cioclovina cave with the location of the crandallite occurences.

and ardealite, which are distinctly white in color. Because of the intimate intergrown, the mineral is difficult to separate from the admixed phases, which implies that the present work is largely based on analyses of impure material.

Crystals of crandallite are too small to permit a good optical characterization. The indices of refraction which may be estimated by immersion in calibrated oils, using sodium light (λ = 589 nm) are ε = 1.620(5) and ω = 1.610(5). They are slightly smaller than those given by Palache et al. (1951) for crandallite from Fairfield, Utah [ε = 1.627(4) and ω = 1.620(2)].

3. X-ray Powder Diffraction data

The X-ray powder-diffraction analysis of a carefully hand-picked separate was performed with a DRON 3 apparatus, operated at 35 kV and 20 mA, using Ni-filtered Cu Kα radiation (l = 1.5406 Å). The data were collected over the 2θ range 5-100°, using a step size of 1° 2θ

and a 2 s counting time at each step. Synthetic spinel (a = 8.0835 Å) was used as an internal standard.

The main reflections which are unambiguously ascribable to crandallite [d in Å (I), (hkl)] occur at 4.850 Å (100), (012); 2.938 Å (100), (113); 2.434 Å (55), (024); 2.171 Å (65), (107); 2.146 Å (45), (116); 2.002 Å (90), (214); 1.899 Å (80), (033); 1.797 Å (22), (009); 1.368 Å (40), (232) and (137); and 1.339 Å (18), (039). The unit-cell parameters determined by three cycles of least-squares refinement of the data given above are a = 7.027(14) Å and c = 16.210(29) Å. They are larger than those given for this mineral in PDF 33-257 [a = 7.0062(4) Å and c = 16.192(1) Å], which accounts for (slight) chemical differences between the samples.

4. Chemical data

There was insufficient material totally exempted from impurities for an efficient determination of the mineral chemistry by

wet-chemical methods. In spite of this inconvenient, an analysis of a material containing mainly crandallite with minor brushite and very few ardealite was obtained. The primary analysis (in wt.%) yields: $CaO = 17.32$, $SO_3 = 1.80$, $Fe_2O_3 = 0.06$, $Al_2O_3 = 30.91$, $P_2O_5 = 35.94$, $H_2O = 16.40$ (as deduced on the basis of the thermogravimetric curve, from what 6.28 wt.% is clearly bounded in the acid phosphate). Subtracting 7.73 wt.% of stoichiometric ardealite, in order to eliminate SO_3, it is possible to derive a chemical composition corresponding to a "purer" crandallite. The chemistry of the remainder (in wt.%) is: $CaO = 14.80$, $Fe_2O_3 = 0.06$, $Al_2O_3 = 30.91$, $P_2O_5 = 34.35$, $H_2O = 14.58$. It leads, after the recalculation of the number of ions on the basis of 2 P atoms, to the formula:

$$Ca_{1.091}(Al_{2.505}Fe^{3+}_{0.003})(PO_4)_2(OH)_{3.706} \cdot 0.974H_2O.$$

This formula is Al- and (OH)-depleted, which suggests that small quantities of brushite are still admixed with crandallite.

5. Thermal analyses

A parallel record of thermogravimetric (TGA), differential thermogravimetric (DTG)
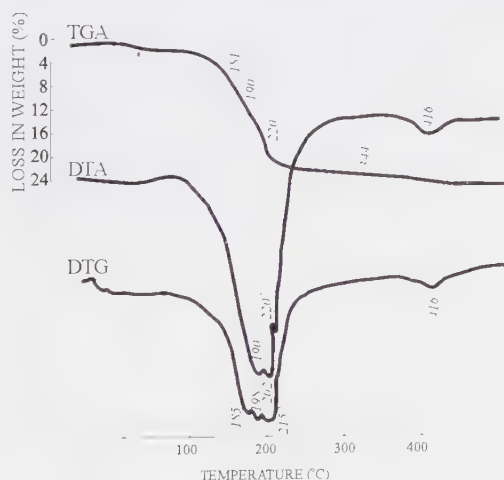
Fig. 2. Thermal analysis of crandallite samples.

and differential thermal analysis (DTA) curves of a separate containing crandallite, brushite and traces of ardealite was made using a MOM Q-1500 D derivatograph, applying a heating rate of 5°C/min, in static air. The thermal curves are given in Figure 2. The major differential thermal effects between 20°C and 500°C are basically attributable to a series of dehydrations involving the structurally bound H_2O then the (OH) groups. The triplet of endothermic peaks recorded on the DTA curve at 190, 202 and 220°C (185, 198 and 215°C on the DTG curve), marks a major loss of structurally bound H_2O. According to Todor (1981 - private communication) the endothermic effects in Figure 2 may be assigned to the three admixed phases in the analyzed material, namely to crandallite, brushite and finally to ardealite. The endothermic effect marked at 416°C on the DTA curve (410°C on the DTG curve) is essentially related to the dehydration of $CaHPO_4$ (monetite), which breaks down into amorphous $Ca_2P_2O_7$ and H_2O (Murray and Dietrich, 1956). The loss in weight recorded on the TGA curve during this process was used to calculate the content of water related to the acid phosphate (see above). A last endothermic effect, not reproduced here because its irrelevance, was recorded on the DTA curve at about 975°C and is probably due to the breakdown of $CaSO_4$ resulted by the thermal decomposition of ardealite.

6. Infrared absorbtion study

A detail of the infrared absorption spectrum recorded for the same separate in the fundamental OH-stretching region is given in Figure 3. The spectrum was recorded with a SPECORD M-80 infrared spectrometer, using a standard pressed-disk technique, after embedding a small amount of mechanically ground phosphate (2.5 wt.%) in dry KBr and compacting under 2500 N/cm^2 pressure.

The section of the infrared spectrum in Figure 3, shows in the principal OH-stretching
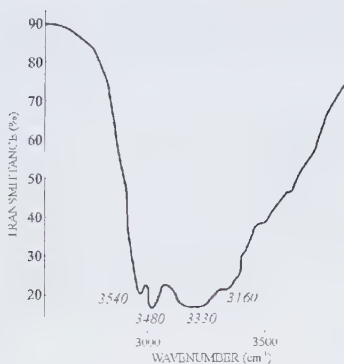
Fig. 3. Fragment of the infrared spectra of crandallite showing the principal OH-stretching region.

region, two prominent absorption bands centered at ~3540 cm^{-1} and ~3480 cm^{-1} respectively, a broad band centered at ~3330 cm^{-1} and a poorly resolved band (a shoulder of this former) at ~3160 cm^{-1}.

Inspection of the structure proposed for ardealite by Sakae et al. (1978) and for brushite by Jones and Smith (1962) indicates two distinct $(HPO_4)^{2-}$ positions in their structures and owing to that, four OH-stretching bands are expected to occur in each of these minerals. The high-wavenumber bands in each structure are characteristic for weak hydrogen bonds in hydroxyl groups, whereas the broad bands centered at lower wavenumbers correspond to stronger hydrogen bonds, similar to those that may be encountered in the water molecule. It is the same for crandallite, which nominally contains both H_2O and (OH) groups and whose infrared spectrum must contain three bands in the OH-stretching region (Ross, 1974). In an infrared spectrum of a mixture of the three minerals, it is to expect that the bands overlap and a sole and poorly resolved absorption band (probably the one centered at ~3330 cm^{-1}) may characterize the antisymmetric stretching of the H_2O molecules.

The band at ~3160 cm^{-1} is then of particular interest, because it has an enough low frequency for an OH band. As shown by

Nakamoto et al. (1955), the frequency of an OH-stretching band is a function of the strength of the hydrogen bond, lower wavenumbers being characteristic of stronger hydrogen bonds. It results that this band may tentatively be ascribed to a very strong hydrogen bond, i.e., to the OH-P(Al) stretching in crandallite. A similar absorption band was encountered at 3140 cm^{-1} in the spectrum of pure crandallite and at 3100 cm^{-1} in the spectrum of wavellite (Ross, 1974). It is of note that in brushite one of the low-wavenumber bands in the OH-stretching region also occur at ~3150 cm^{-1} (Ross, 1974). The presence of this band in our spectrum, together with a doublet of bands at ~870 and 825 cm^{-1}, that probably materialize out-of-plane OH bendings, may however account for the presence of crandallite or of another aluminum phosphate at Cioclovina.

7. Discussion and conclusions

In spite of the difficulties in obtaining pure material, the data obtained during this preliminary study provide further information on the mineralogical properties of crandallite from this first occurrence in Romania. It is generally accepted that crandallite in such deposits is formed by interaction between phosphatic solutions, derived from the breakdown of guano, and clay minerals. The presence in vicinity of illite and kaolinite flakes and their diminished presence in the "terra rossa" near the guano deposit are strong indicators that this kind of genesis may be accepted. The presence of crandallite at Cioclovina indicates a basic pH since this mineral precipitates and is stable in slightly alkaline environment (Haseman et al., 1950).

References

Bleahu M. (1976), Peşteri din România. Ed. Ştiintifică şi Enciclopedică, Bucharest.

Haseman   J.F., Brown E.H., Whitt C.D. (1950), Some reaction of phosphate with

clay and hydrous oxides of iron and aluminum. *Soil Sci.*, **70**, 257-271.

Jones D.W., Smith J.A. (1962) Structure of brushite, $CaHPO_4 \cdot 2H_2O$. *J. Chem. Soc.*, 1414-1420.

Murray J.W., Dietrich R.V. (1956), Brushite and taranakite from Pig Hole Cave, Giles County, Virginia. *Am. Mineral.*, **41**, 270-280.

Nakamoto K., Margoshes M., Rundle R.E. (1955) Stretching frequencies as a function of distances in hydrogen bonds. *Journ. American Chem. Soc.*, **77**, 6480-6486.

Nriagu J.O., Moore P.B. (1984) Phosphate minerals: Their properties and general modes of occurrence. In Phosphate minerals. Chap. 1, 1-136, Springer Verlag, Berlin, Germany

Palache C., Berman H., Frondel C. (1951), The system of mineralogy II. John Wiley & Sons, New York, N.Y.

Ross S.D. (1974) Phosphates and other oxyanions of group V. In The infrared spectra of minerals. Mineralogical Society Monograph 4, V.C. Farmer Ed., London, 383-422.

Sakae T., Nagata H., Sudo T. (1978) The crystal structure of synthetic calcium phosphate-sulfate hydrate, $Ca_2HPO_4SO_4 \cdot 4H_2O$ and its relation to brushite and gypsum. *Am. Mineral.*, 63, 520-527.

Schadler T. (1932) Ardealit, ein neues Mineral $CaHPO_4 \cdot CaSO_4 + 4H_2O$. *Central-bl. Miner. Abt.* **A**, 40-41.

Vesuvianite in skarns at Sasca Montană

EMIL CONSTANTINESCU

Due to its interesting crystallography, to the complications of its internal structure, to the peculiar variations of its chemistry and optical constants, vesuvianite was the object of numerous mineralogical studies, most of the known occurences being used by various authors for complex investigation of its properties.

In Romania, vesuvianite was studied by Doll (1874), Weibull (1896), Koch (1925), Cădere (1927) in samples from Oravița, by Murgoci (1900) in samples from the Parâng massif and more recently it was described by Superceanu (1958) at Ciclova, Cioflică (1960) at Măgureaua Vaței and Rafalet (1963) at Pietroasa – Budureasa.

The presence of vesuvianite at Sasca Montană has not yet been reported in the geological literature, even though the neighbou-ring localities – Oravița, Dognecea, Ocna de Fier – have been quoted along with Vesuvius, Piémont, Wiliui, as reference areas for this mineral (Klockman's Mineralogie, 1967). The ore deposits at Sasca Montană have been known as a classical area for the study of contact metamorphic minerals.

Vesuvianite occurs in skarns formed at the contact between the Laramian magmatites and the Mesozoic carbonate rocks from the Reşița – Moldova Nouă syncline; the mineral was identified in the surroundings of the Sasca Montană village, between Dealul Orașului and Valea Morii. Two types of vesuvianite-bearing skarns have been distinguished: vesuvianite skarns, consisting mostly of vesuvianite (80%) and calcite, and vesuvianite-garnetiferous skarns, with vesuvianite (making up 20 to 40 % of the rock) accompanied by garnet and other contact metamorphic minerals. The vesuvianitites have been identified within an exposure located 250 m NE of the church in Dealul Orașului. Vesuvianite occurs as single crystals 0.8 cm long and 0.3 cm wide, or as intergrowths of 2 to 4 individuals, without attaining larger crystal agglomeration known as "vesuvianfels". The remainder of the rock consists of large greyish-bluish, polysintetically twinned calcite crystals. In some areas, partial silicification of the rock is caused by calcite replacement by quartz.

The garnet-vesuvianite skarns crop out on the southern slope of Dealul lui Ciucar. They are

compact, brown-greyish and spoted because of the distribution of the two dominant minerals. The typical assemblage is grossularite-vesuvianite, accompanied by subordinate amounts of salite, wollastonite, tremolite, zoisite, epidote, calcite; vein minerals are quartz, laumontite and stilbite. Skarns resembling this type also occur in the neighbourhood of the villages Stânăpari - Cărbunari, at about 10 km south of Sasca Montană; microscopic examination of samples from drilling exploration enabled the separation of a garnet-vesuvianite skarn area with considerable development.

This paper presents the main crystallographic, chemical/structural and microscopic properties of vesuvianite crystals from the exposures in Dealul Orașului. For comparison, microscopic observations and quantitative measurements of the refractive indices, specific weight and hardness of vesuvianite from garnet-vesuvianite skarns from Dealul lui Ciucar and Stînăpari Plateau were carried out.

Crystallographic data

The crystals analyzed represent a combination of tetragonal prism faces of the species I and II, with faces of tetragonal dipyramid, species I.

In all cases, they show prismatic habit, elongated parallel to C axis; the short prismatic specimens, often mentioned as habit variations in other occurences, are missing here. The prismatic character is accentuated by the dominance of the {110} over the {100} form.

The following forms have been identified: {100}, {110}, {111}, {101}, {001}, {011} and {210}, {120}, {201}, {311}, {331}. Examination of 70 individuals shows that all crystals display the forms {100}, {110}, {010} or {111}, but in most cases, forms {101}, {001}, {210}, {120}, {201}, {311}, {331} and {001} occur more often.
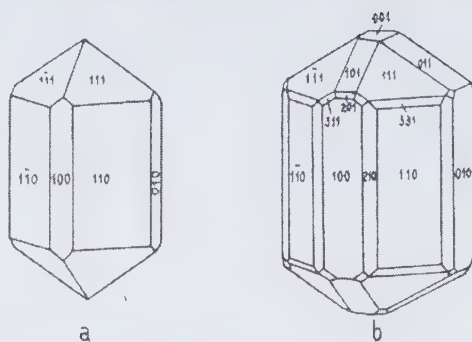
Fig. 1. Prismatic vesuvianite crystals. a) Vesuvianite from Pegueres (after Lacroix); b) Vesuvianite from Piedmont (after Goldschmidt).

According to the literature, the combination of the faces of the analyzed crystals is intermediate between the two types of the prismatic habit: the first model was descibed by Lacroix (1893) in Pegueres – Pyrénées (Fig. 1a) whereas the second model was described by Zepharovich (1864) in Piémont and Nauman fide Goldschmidt (1918) at the Vesuvius (Fig.. 1b).

Crystals showing combinations of faces between the quoted models are well known, but in most cases the crystal preserves its holoedric symmetry, while in our case not all the symmetric, holoedric faces occur. Forms {210}, {120}, {311}, {201}, {331} are accidental, transitory to the equilibrated forms of the first model. The measurements of crystal lographic angles are given in Table 1.

The studied vesuvianite specimens typically display complications of the external crystal geometry. Only 6 or 7 from 70 crystals show a holoedric external symmetry. In most cases, they either display geometric complications such as vicinal faces, growth strikings, corrosion figures, or various types of intergrowths.

Their various aspects have probably different genetic explanations, starting with the fixation of certain impurities in the lattice, or even twinning, at certain angles, of two crystals formed in two distinct crystallisation centres,

Table 1. Crystallographic angles of vesuvianite

Faces	Medium values measured	Calculated values
(110):(111)	52°51'	52°26'6"
(101):(100)	61°40'	61°50'10"
(101):(001)	28°10'	28°9'50"
(201):(100)	43°30'	40°2'30"

and ultimately to internal lattice disorder. In both isolated and intergrown crystals (Fig. 1, Plate III; Fig. 4, Plate III, respectively) each individual shows irregularities indicating a pronounced "structural sensitivity" ("Strukturenpfindlich" according to Smekal) in respect to various types of lattice flaws (after Dekeyser, Amelincks, 1957).

In the analysed crystals, the dominant type of intergrowth is the association of two crystals under an apparently constant accute angle (about 30°) (Figs. 2, 3, 4, Plate III), resembling the "cross of Saint Andrew" penetration twins. Detailed macroscopic and microscopic examination indicates that the angle between the C axes differ in vertical plane and that the crystals are twisted. This resembles certain quartz prisms which combine twisted or spiral groups, which are the consequence of growth deficiencies, due to initial deviations from perfect parallelism of the unit cells. Considering lattice differences, it is possible to explain the various growth strikings (Figs. 1, 7, Plate III) as well as distinct irregularities of the crystal faces.

Structural - chemical data

The chemical composition of vesuvianite from Sasca Montană (Dealul Orașului) is shown in table 2. Compared to the theoretical composition or to similar chemical analyses from literature, they indicate a vesuvianite with medium composition, having 5.25% Fe contents (4.87% as Fe_2O_3), that is higher than normal values, without attaining the concen-

trations of iron varieties (duparcite): 7.8% Fe_2O_3, 3.96 FeO (Nicolet, 1932; Phan, 1967).

The enrichment in Fe_2O_3 is not correlated (like in case of other the Fe-rich vesuvianites) with the depletion of Al_2O_3 contents, which shows high values. The Al_2O_3/Fe_2O_3 ratio of the analysed vesuvianite is 17.29/4.87%, as opposed to 12.66/4.36% of vesuvianite from Akhmat – Urals (Miashnikov, 1940), 13.36/4.15% (FeO 2.15%) of vesuvianite from Iron Mountains – New Mexico (Deer et al., 1965) and 15.62/2.81% (FeO 2.96%) of vesuvianite from Turnback Lake – Canada (Meen, 1968). Compared to the Fe_2O_3/FeO ratios from the forementioned Akhmat, Iron Mountains and Turnback Lake vesuvianites, it is clear that the oxidation of iron has also occured in vesuvianite from Sasca (Fe_2O_3 4.87% - FeO 0.36%).

The considerable Fe contents of vesuvianite from Sasca Montană (Dealul Orașului) determines the physical properties like hardness, specific weight and refringence, which are higher compared to the low iron vesuvianites already known (Gadeke, 1939). The Fe_2O_3/FeO ratio probably controls the yellowish green color and the high transparency of crystals, resembling the color and transparency of vesuvianites with similar degree of iron oxidation (Deer et al., 1965).

The great chemical variation of vesuvianite explains the difficulty to establish a widely applicable formula. After compiling the modern chemical analyses (Deer et al., 1962; Barth, 1963), Howie (1967) suggested a formula which is most suitable for the analytical results: $X_{10-u}Y_{6+u}$ $Si_9(O,OH,F)_{38}$, where u ± 1, with X = Ca Mn, Na, K; Y = Mg, Fe, Ti, Al, Cu, and where the structural positions of Mg and Ca are exchangeable.

The structural formula of the analysed vesuvianite (Table 2), calculated in the basis of 76 (O,OH) is given below: $(Ca_{9.36}Mn_{0.07}Na_{0.05}K_{0.08})_{9.56}(Mg_{1.07}Fe_{0.075}Fe_{0.88}$ $Ti_{0.142}Al_{4.496})_{6.66}(Si_{8.58}Al_{0.42})_9(O,OH)_{38}$. It shows the position of Mn, Na ad K as isomorphous with Ca,

Table 2. Chemical analyses of vesuvianite from Sasca Montană (Dealul Orașului)

	Contents (%)	Number of ions in the basis of 76 (O, OH)	
SiO_2	35.55	Si	17.168
TiO_2	0.78	Al	0.832 / 18.00
Al_2O_3	17.29	Al	8.993
Fe_2O_3	4.87	Fe^{3+}	1.760
FeO	0.36	Ti	0.284 / 13.33
MnO	0.31	Mg	2.146
MgO	3.00	Fe^{2+}	0.151
CaO	36.22	Mn	0.141
Na_2O	0.13	Na	0.113 / 19.13
K_2O	0.28	Ca	18.716
H_2O^+	1.00	K	0.162
H_2O^-	0.35	OH	3.248
Total	100.14		

[1] Analyst: I. Merches – Prospecting Enterprise and Laboratories C.G.S.

the position of Mg as isomorphous exclusively with Fe and Al isomorphous with Fe and Si.

Similar to major elements, the contents of minor elements represent medium values. The Cu, Be and Ce, which if in large amounts determine the varieties cypryne (Kurbatov, 1922), Be-vesuvianite (Hurlbut,1955) and Ce-vesuvianite show low amounts or are absent. The values for Ni (920 ppm) and Co (300 ppm) are remarcable compared to the known data. We noticed the presence of Be which occurs in the lattice of vesuvianite as result of substitution of the group $(SiO_4)^{-4}$ (Ri=2,90Å) with the group $(BeO_4)^{-6}$ (Ri=2,90Å) and the presence of B, which significantly modifies some optical properties (Table 6). B can occur either as an endocryptical isomorph with group $(SiO_4)^{-4}$ (Rankama, Sahama, 1952), or as a mobile form within the $(BO_3)^{-3}$ complex which is replacing the $(OH)_3$ group (Serdicenco et al., 1968).

The Cu content, which within the quoted formula appears as isomorphous with Mg, Fe and Ti, is probably related to some mechanical impurities.

Table 3. Minor constituents in vesuvianite and in grey calcite from Sasca Montană (Dealul Orașului)

Element	Wavelength (Å)	Vesuvianite (ppm)	Grey calcite (ppm)
Cu	3271	15	10
Pb	2833	traces	3
Zn	3350	150	-
Mn	2950	900	500
Ni	3050	920	traces
Co	3409	300	-
Cr	3014	40	-
Sn	2840	15	-
As	2350	30	traces
B	2500	650	45
Be	2650	40	-
Ag	3382	-	0.3
Mo	3171	traces	traces

The chemical characterization was completed with the X-ray analysis of vesuvianite. (Debye Scherer method on powdered sample). The results are given in Table 4.

Table 4. X-ray powder diffraction data for vesuvianite

Nr.	d (Å)	I/I_0
1	2.9734	9
2	2.7757	6
3	2.6143	4
4	2.5636	2
5	1.9179	1
6	1.6322	1
7	1.5789	4
8	1.5649	1
9	0.8812	1
10	0.8680	5

Several chemical-structural features of the Sasca Montană vesuvianite have been studied by means of IR absorption spectra which indicated the presence of OH group - bands at 3440, 3632 cm^{-1} and the state of hydration of the partly altered crystals. The thermodifferential analysis is given in Plate IV.

Table 5. Physical properties of vesuvianite from Sasca Montană

Determined properties	Sample provenance	
	Vesuvianite –Dealul Oraşului	Garnet-vesuvianite skarn Dealul lui Ciucar
Specific weight	3.4	3.3
Hardness	1054 kg/mm^2 (6.75 on Mohs's scale)	887kg/mm^2 (6.50 on Mohs's scale)
Refringence	Note: it changes in various zones of the crystal A:n = 1.710; B:n = 1.730; C:n = 1.735;	np = 1.720; ng = 1.725

Table 6. Microscopic features of vesuvianite from Sasca Montană

Optical properties	Vesuvianite - Dealul Oraşului		Vesuvianite – Dealul lui Ciucar
outline	euhedral		anhedral
color	colorless		light yellow
pleochroism	not pleochroic		neither yellow, nor colorless
cleavage	no cleavage		imperfect after (100) and (110)
extinction	c·ng = 0		c/ng = 0
zoning	intense zoning		not zoned
	central zone, middle and terminal zone		
Ng Np	0.000	0.010	0.005
Optical properties	2Vă = 60° to 64° uniaxial negative		uniaxial negative

The physical constants of the Sasca Montană vesuvianite, in direct relation with the chemistry of the analyzed samples, have been determined for the two types considered and are shown in Table 5.

Microscopic data

The determinations were carried out on vesuvianitite samples from Dealul Oraşului and on garnet-vesuvianite skarns from Dealul lui Ciucar. The microscopic data from Table 6 indicate that vesuvianite from the two occurences differ largely in their optic properties and complete the observations concerning the difference in aspect and in the parageneses evidenced through microscopic examination. The examination in thin sections of vesuvianite from Dealul Oraşului allowed a detailed analysis, on crystal scale, of the aspects revealed by chemical-structural and crystallographic analyses. These data concern crystal zoning and the pattern of inclusions within the crystal.

Zoning

The zoning of vesuvianite may be noticed both on macroscopic scale, as linear variation of the color intensity and evidenced microscopically by differences in relief and bireffringence. It is worth noting that:
- zoning is a general feature, appearing in all analyzed crystals;
- in all cases the zones show a euhedral outline;

Photo 1

Fig. 2. Relations between chemistry and optical features (N and S) on Trogger diagram. II - Vesuvianite from Dealul lui Ciucar; A, B, C - zones of the types A, B, C of vesuvianite from Dealul Oraşului.

which represent the transition to A-type zones (Photo 1).

The chemical data given for vesuvianite concern the mineral as a whole. However, one must take into account that the analyzed crystals are characterized by a significant inhomogeneity, as suggested by the strong variation and zoning of the physical properties.

- their sequence and relative development are constant, regardless of the crystal size;
- all zones show simultaneous extinction, indicating the same optical orientation.

Three types of zones with distinct properties have been separated:

A. zones with abnormal interference colors deep brown-Berlin light blue, refringence = 1,710, biaxial positive;

B. zones with yellow birefringence colors, value 0.010, refringence = 1.730, uniaxial negative;

C. zones with vivid yellow birefringence colors, value 0.10, refringence = 1.735, uniaxial negative.

The A-type zones form the central, largest part of the crystal (about 1/2 of the section) and the very narrow marginal part. The C-type zones form the middle sector, well developed and bordered by two thin bands of B-type zones

Using the relation between the optical properties and the participation of certain chemical elements, established by a comparative study of a great numer of various samples (Trogger, 1952; Oftedhal, 1965), we tried to estimate the chemical character of different zones within the same crystal; consequently, according to Trogger diagram (fig. 2) a small content of Fe(Ti) corresponds to A-type zones, a high content to C-type zones and a , medium to high content to B-type zones. The content of OH(B) is higher in A-type zones, compared to B- and C-type zones.

The variation of Fe(Ti) contents with zonality is shown in a Fe+Ti vs. distance diagram (Fig. 3). The pattern is typical to the recurrent zoning and documents the transitional character of B-type zones, with contents close to those corresponding to C-type zones. The
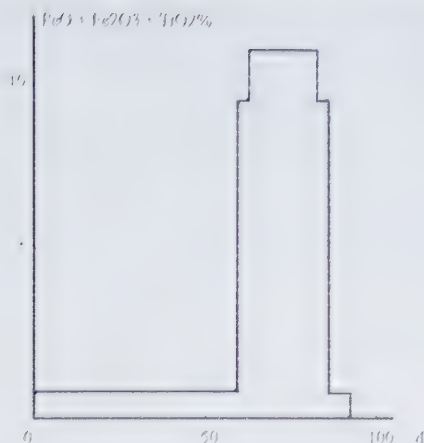
Fig. 3. The variation of $FeO \cdot Fe_2O_3 \cdot TiO_2$ as a function of distance (Note: the measurement of distances was made in microscopic conventional divisions, in sections parallel to the (100) prism faces and after sections normal to C axis (Photo 1).

strong rightward assymmetry reveals the small development of the last zone compared to the central one. The steep jump visible at the passage from zone A to zone B suggests that a strong change in the chemistry of the fluids has occurred, which might imply the existence of an iron-rich front coeval with the development of zones B and C.

These considerations concerning the chemistry variations within the crystal zones are confirmed quantitatively by means of microprobe analysis. Such studies have been carried out lately upon crystals of zoned garnet (Howie, 1967) and zircon (Veniale, Pigorini, 1968).

Considering the crystallography of the analyzed mineral, the euhedral character of zones enables the reconstruction of another aspect of the crystal history: the variation of the growth velocity for different faces. This variation, clearly expressed in certain cases (Photos 5, 6, 7) can eventually lead to the dissapearence of the faces existing in intermediate stages of crystal development. We note the scarce

development of forms {201}, {311}, {331}. Microscopic observations clearly show the crystal tendency toward equilibrated forms and the sensitivity of weakly developed faces to the variations in the growth velocity on different directions. We also notice that the perturbation of the relative growth velocity upon different directions is usually superimposed onto zone C, being synchronous with a rise in iron content.

Inclusions

In nearly all vesuvianite crystals we note the presence, usually within the central zone, of inclusions of isotropic, mostly euhedral garnet.

We synthesized the investigations of the following facts:
- garnet only appears in the skarns studied as inclusions in vesuvianite;
- the marginal zones of the inclusions indicate a more or less advanced replacement of garnet by vesuvianite. The initial outlines of the inclusion are clearly distinguished with crossed polars, due to the difference in the birefringence of the replacing vesuvianite as compared to the host-crystal;
- the limits of the inclusion will be different compared to the association of faces typical for garnet and vesuvianite;
- all the marginal parts of the birefringent inclusions show simultaneous extinction, displaying a common optical orientation not only between themselves, but also with the host crystal;
- the birefringence color of the marginal zone of the inclusions is always light yellow, identical with the birefringence color of the B-type zones of crystals having a medium Fe content.

The marginal zones of the inclusions show euhedral outlines toward the host-crystal and irregular borders toward the central part of

the inclusion. These were formed as a consequence of the peripheral transformations of the instable garnet grains in the conditions of a higher potential of OH and B in vesuvianite.

This process was facilitated by the chemical similarities of vesuvianite and certain phases of the grandite series (McConnel, 1939) which show no difference in what concerns the presence of volatiles (B, F) and of OH groups. It was also facilitated by the structural resemblances between these two minerals, where certain parts of the structures are common (according to Warren and Modell, 1931) and the dimension of C unit-cell parameter of vesuvianite equals in length the a unit-cell parameter of grossularite.

Crystallogenetic considerations

The following conclusions resulted from this study:

The formation of vesuvianite crystals from Dealul Oraşului probably took place within an isotropic environment, represented by a homogeneous limestone, which enabled the development of their euhedral zoning.

The constant character of the succession and the relative dimensions of A-, B- and C- type zones in crystals of different dimensions indicates that they developed during a single generation.

During their development, the most stable vesuvianite includes garnet crystals and partly alters them to vesuvianite.

The presence of large amounts of garnet inclusions, mainly in the first stage of vesuvianite formation, was probably the cause of disorders of its internal lattice, which determined the abundance of crystal dislocations. There was a discontinuous, rhythmic variation in chemistry during crystallisation, due to changing contents of Fe, Ti, B, OH,

which resulted in zones with well developed optical properties.

Zoning in vesuvianite is recurrent; the Fe content variation is well expressed, as a single strong maximum, which might indicate the existence of an iron-rich front in the evolution of the fluids, which lasted till the formation of the B- and C-type zones.

During crystal formation, the growth velocity has varied in different directions, determining various development of faces and, in extreme cases, their dissappearence. The sensitivity of weakly developed faces toward these variations and the tendency toward equilibrated forms during the final phases has determined – in the studied crystals – the predominance of combinations of prism faces, species I and II, and of species I faces of bypiramid.

The disturbance in the development velocity along different directions is generally superimposed onto C-type zone, being synchronous with sudden changes in iron contents.

Acknowledgements

References

Barth, T. F. W. (1963) vesuvianite from Kristiansand; other occurences in Norway; the general formula of vesuvianite. *Norsk. Geol. Tidsskr.*, **43**, 457-472.

Beus A. A. (1957). "On beryllium idocrase" *Trans. min. muz. Akad. nauk SSSR,* vol **8**, 25.

Buckley H. E. (1958) "Crystal Growth" J. Wiley & Sons, New York.

Chumakov A. A., Morozov Al., Ginzburg I. V. (1948) Idocrazi v zapadnovo Kieva. *Dokl. Akad. Nauk SSSR,* **61**, 1099.

Cioflică G. (1960) Contribuţii la cunoaşterea

fenomenelor de contact de la Măgureaua Vaței (M. Drocea). *Studii și cercet. Acad.*, **5**, 3.

Connel Mc. D. (1939) Note on the chemical similarity of idocrase and certain garnets. *Amer. Min.*, **24**, 62.

Deckeyser W., Amelinkcs S. (1955) Les dislocations et la croissance des cristaux. Paris, Masson Cie.

Deer W. A., Howie R. A., Zussman J. (1965) Rock forming minerals, Longmans, London, pp. 113.

Duparc L., Gysin M. (1927) Sur la genévite, un nouveau minéral. *Bull. Soc. Franc. Min.*, vol **50**, 41.

Gädeke R. (1939) Die gesetzmässigen Zusammenhänge und Anomalien in der Vesuvian gruppe und einigen anderen Kalksilikaten. *Chemie der Erde*, **11**, 592.

Goldschmidt V. (1918) Atlas der Krystallformen, vol. 4, Universitat-buchhandlung, Heidelberg.

Howie R. A. (1967) Curent trends in mineralogy. *Earth. Sc. Rev.*, **3**, 31-46

Hurlbut C. S. Jr. (1955) Beryllian idocrase from Franklin, New-Jersey. *Amer. Min.*, **40**, 118.

Lacroix A. (1893). Mineralogie de la France. Paris, vol. I.

Marka G. (1869) Einige Notizen uber das Banater-Gebirge. *Jahrbuch der K. K.*, **19**, 299-318, Wien.

Nicolet S. E. (1932). Un minéral nouveau, la duparcite. *Schweiz. Min. Petr. Mitt.*, **12**, 543.

Oftedahl I. W. (1964) Vesuvianite as a host mineral for boron. *Norsk. geol. Tidsskr.*, **44**, 377-383.

Pabst A. (1936) Vesuvianite from Georgetown, California. *Amer. Min.*, **21**, 1.

Ramdohr P., Strunz H. (1967) Klockmann's Lehrbuch der Mineralogie, I. Enke Verlag, Stuttgart.

Rădulescu D., Dimitrescu R. (1966) Mineralogia topografică a României. Ed. Acad. RSR, București.

Rock Al. (1925) Uber der Vesuvian uns Scheelit von Ciclova (jud. Caraș). *Föld. Kozl.*, **55**.

Serdicenco D. N. et al. (1968) Vezuvianî iz skarnirovannîh porod Srednei Azii i ih himiceskaia konstituția. *Dokl. Akad. Nauk. SSSR* **180**, 2, 452-455.

Superceanu C. (1958) Skarne vezuvianice și granatice cu conținut de beriliu și bor în zăcămîntul de contact de la Ciclova - Banatul de SV. *Rev. Minelor*, **9**, 12, 552-562.

Talic R. (1957). Vezuvian u skarnu potoj Cuke. *Zborn Rud. geol. fak.*, Univ. Beogradu, V **5**, 45-53.

Trofer B. W. E. (1952) Tabellen zur optischen bestimmung der gesteinbildenden Minerale, Stuttgart.

Warren B. E., Modell D. I. (1931). The structure of vesuvianite. *Z. Krist.*, **78**, 422-424.

Weibull M. (1896). Studien über Vezuvian. *Z. Krist.*, **25**, 1-37.
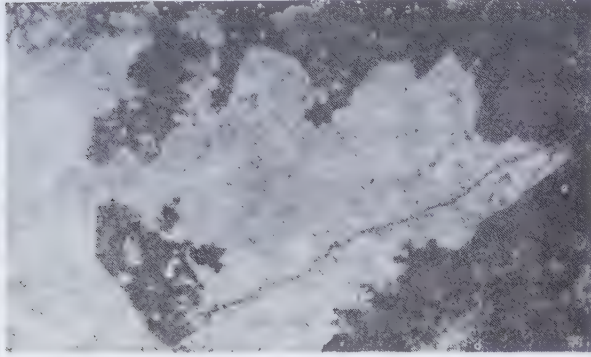
Photo 2
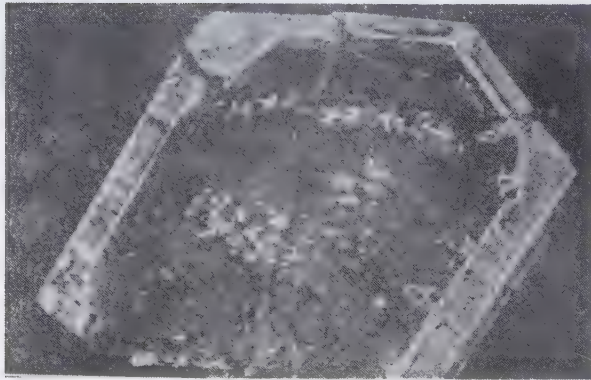
Photo 3
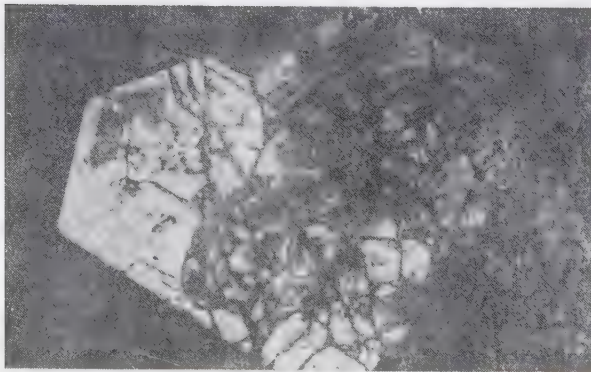
Photo 4

Photo 2. Garnet-vesuvianite skarn from Dealul lui Ciucar; anhedral vesuvianite in the center, garnet completely extinguished and calcite at right; N +, 10x.

Photo 3. Vesuvianite crystal from Dealul Oraşului: vertical dislocation, marked by growth strikings in the outer morphology of the crystal (section oriented along C axis).

Photo 4. Intergrowth between two crystals at a certain angle.
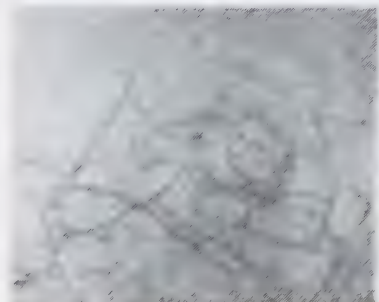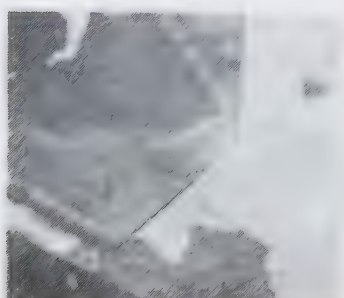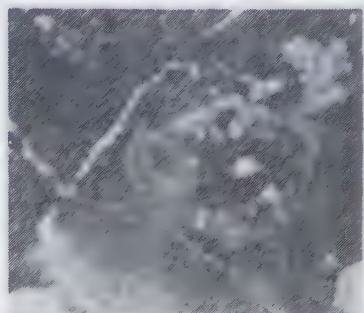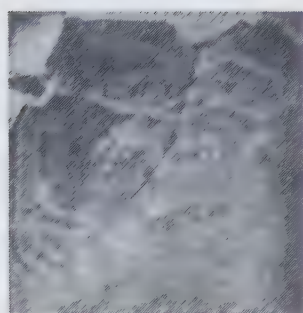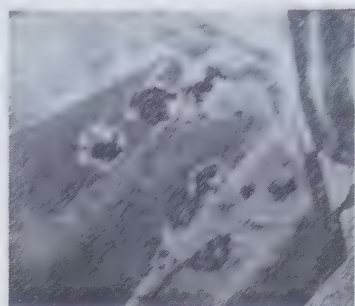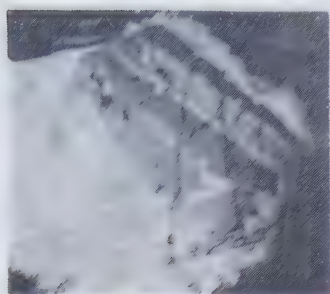
Photo 5. Vesuvianite crystal in calcite from Dealul Orașului. Note the garnet inclusions; N +, 10x

Photo 6. Detail from the crystal shown in Photo 5; N +, 25x

Photo 7. Association of two vesuvianite crystals in calcite; N +, 10x

Photos 8 and 10. Detail of section from Photo 7, showing a garnet inclusion marginally altered to one fringent vesuvianite.
    Photo 8. Euhedral inclusion of vesuvianite distinguishable by the difference in the birefringence color; N +, 25x
    Photo 10. Irregular limits of the central, garnet part and the marginal, vesuvianite part of the inclusion due to the difference in relief; N +, 25x

Photo 9. Vesuvianite in polysynthetically twinned calcite (Dealul Orașului). Note the difference between the euhedral outline of zones showing different stages of crystal development. This aspect can also be recognized in Photos 2 and 3.
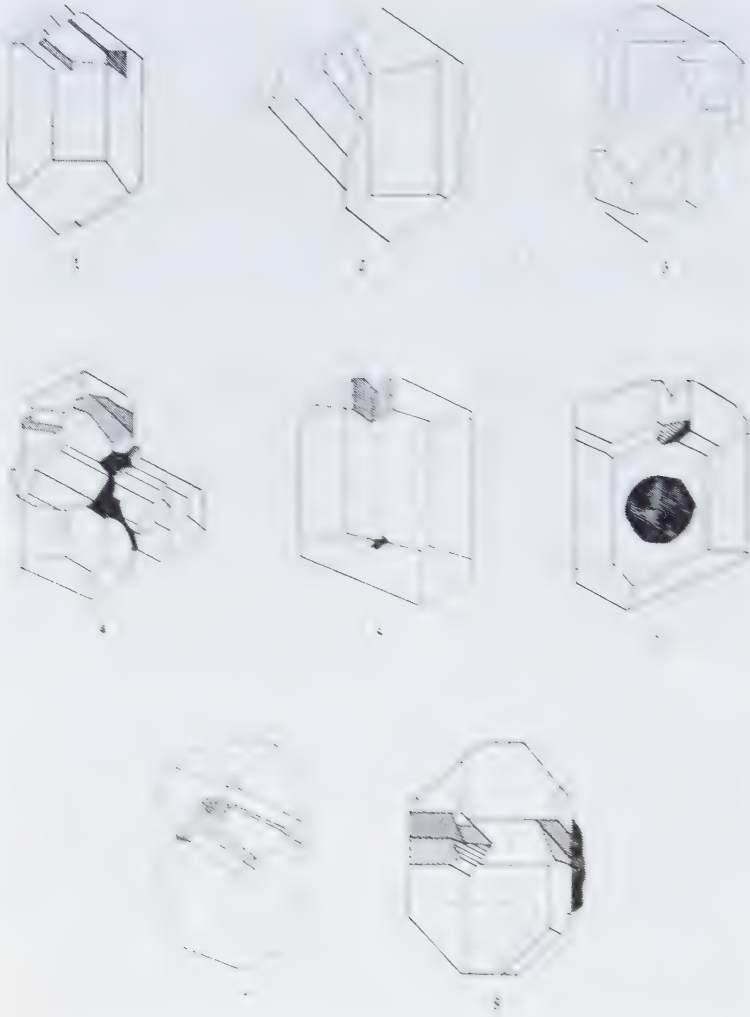
Pyrophyllite from anchimetamorphic schists in Parâng Mountains, South Carpathians, Romania. Petrogenetic significance

GHEORGHE C. POPESCU
EMIL CONSTANTINESCU

The pyrophyllite occurrences studied in this paper outcrop on the northern border of the Parâng Mountains in the Izvorul (1) and Jieț (2) zones, and are located within the anchimetamorphic schists of the Schela Formation (Fig. 1).

The Schela Formation (SF) designates a complex of anchimetamorphic rocks formed of metaconglomerates, coaly metasandstones, pyrophyllite-chloritoid schists and anthracite lenses. The term was introduced by Dupark and Mrazec (1893) to define a complex of sedimentary rocks in the zone of the Schela Gorj locality. Later, Manolescu (1932), Streckeisen (1934) and Paliuc (1937) have pointed out its regional spreading towards the contact of the Getic Nappe with the Danubian Autochthon, and assigned it a Liassic (Manolescu, 1932) or Carboniferous age (Dupark, Mrazec, 1893; Semaka, 1968).

The anchimetamorphic character of SF was underlined by Mutihac and Popescu (1981; 1982).

Within the South Carpathians, pyrophyllite was described for the first time by Paliuc (1972) at Schela Gorj. Ianovici et al. (1981) carried out detailed research on the composition and structure of pyrophyllite from this occurrence.

Occurrence and mode of presentation

Pyrophyllite occurs in two characteristic environments: (a) as a component of anchimetamorphic schists together with quartz, chloritoid, paragonite/muscovite, anthracite, and (b) in Alpine veins associated with quartz, paragonite/muscovite, chlorite. In the first case, pyrophyllite is the most frequent component of the rock (~ 70%) and appears as lamellae parallel to
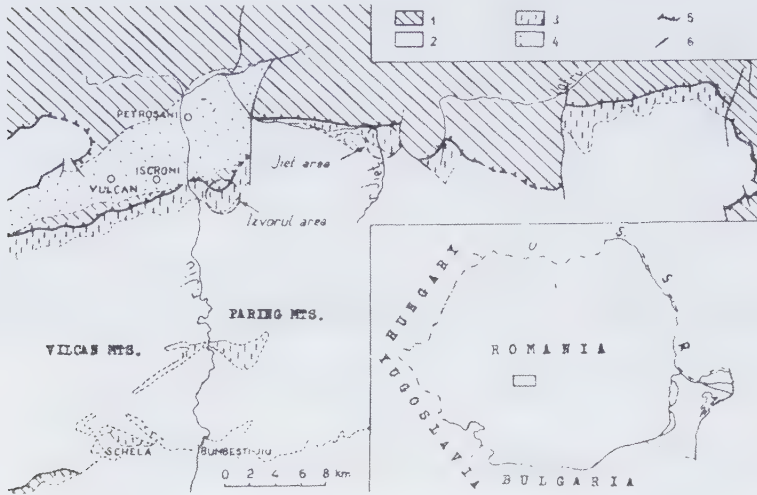
Fig. 1. Simplified geological map of the Central Southern Carpathians showing main sample localities (in circles); 1. Getic nappe; 2. Danubian units; 3. Schela Formation; 4. Petroşani basin; 5. Thrust; 6. Fault.
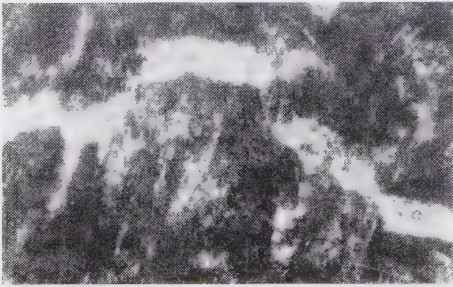
Fig. 2. Pyrophyllite veins in pyrophyllite schists, N+, 120 X.
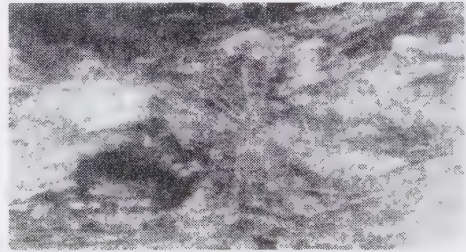
Fig. 4. Micaceous schists with radial chloritoid, N II, 120 X
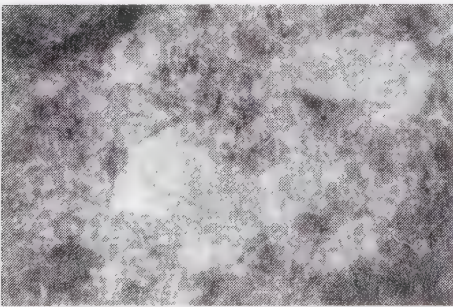
Fig. 3. Relic quartz in pyrophyllite vein, N II, 120 X.

the schistosity plane, disseminated among quartz granules and as grain agglomerations randomly distributed in the rock mass. In the second case, it appears as nests, lenses and veinlets (Fig. 2-4).

The color of pyrophyllite varies from pearly white in Alpine veins, greenish-white in pyrophyllitic schists, to blackish-bluish-gray in pyrophyllite and anthracite schists.

In thin sections pyrophyllite appears as scales and elongated leaflets with anhedral shape, generally having submillimetric

Fig. 5. Electron microscope microphotograph of pyrophyllite.

dimensions. It is colorless or slightly green-ish. Colors of birefringence vary from gray to greenish-yellow. $\alpha^{\wedge}c$ extinction=8-10°. The $2V\alpha$ angle determined in basal sections varies between 54-58°. The habit of pyro-phyllite crystals was studied using electron microscope JEOL, JSM-15 (Fig. 5).

X-ray data

Interplanar distances and intensities are shown in Table 1 and Fig. 6. They are generally sim-ilar to those of other natural pyrophyllites from anchimetamorphic schists. Thus, values corresponding to the (006) reflection, i.e., 3.045 Å for secondary pyrophyllite from Alpine veins and 3. 039-3. 055 A for pyro-phyllite from schists, fall close to the values of 3. 066 Å determined for the pyrophyllite from anchimetamorphic schists of Glarus Alps (Frey, 1978), to 3. 035 A determined for the pyrophyllite from anchimetamorphic schists of Schela Gorj - South Carpathians (Ianovici et al., 1981). These values are lower than those obtained for synthetic pyrophyllites, i.e., 3.068 Å (Rosenberg, 1974).

An important role in characterizing some phyllosilicates was given to the crystallinity index, considered to be a sensible index for their genesis (Dunoyer de Segonzac, 1969 - for illite; White, 1962 - for muscovite). For the

analysed pyrophyllite the crystallinity index was calculated taking into account the ratio between the height of the peak corresponding to the (002) peak and its thickness at half-height, measured in mm, according to the method proposed by Ianovici et al. (1981).

This index values is 122 for pyrophyllite from veins and 47 for pyrophyllite from schists (average of five analyses). Both val-ues indicate a high degree of crystallinity, comparable to that of pyrophyllites with sim-ilar genesis from the Schela Gorj occurrence

Table 1. X-ray diffraction data of pyrophyllite (Phillips diffractometer, CuKα radiation, Ni-filter, 35Kv, 15mA)

Alpine veins sample 149			Anchimetamorphic schists; sample 126	
d. A	I	hkl	d. A	I
9.0544	49.5	002	9.0175	80.6
4.5344	7.2	004	4.5668	40.52
3.0455	100	006	3.0455	100
-	-	200	2.5265	4.83
2.4012	2.34	132	2.4086	7.25
2.2905	10.92	008	2.2916	2.77
1.8391	21.5	0.0.10	1.8391	5.31
1.5289	23.48		1.5395	12.56
1.3799	6.26		1.4817	2.77
1.3644	8.40		1.3824	1.51
			1.3710	1.33

(65 and 35, respectively) and by far superior to hydrothermal pyrophyllites from Romania (Tălagiu, Cavnic), with an index of 8 (Ianovici et al., 1981). At the same time, there is a strong difference of crystallinity between secondary pyrophyllite and pyro-phyllite from schists.

Diffractograms of pyrophyllitic schists point out the participation of chloritoid in their com-position (reflections at 4.41 Å and 2.94 - 2.96 Å), of ferriferous chlorite (reflections at 14.1 - 7.07 - 4.66 - 3.55 Å) and of quartz (Fig. 6). Some diffractograms made on samples collect-
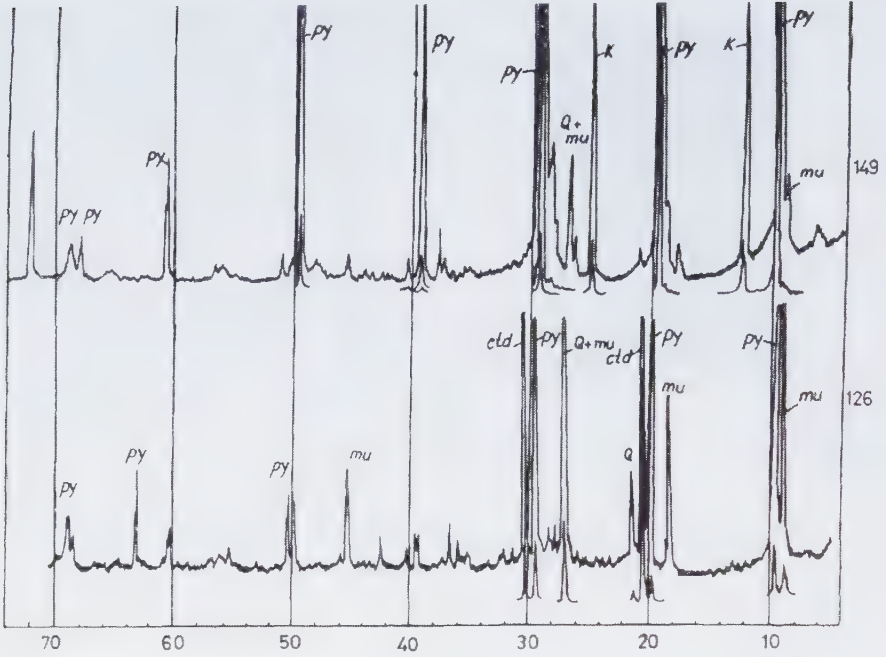
Fig. 6. X-ray diffractograms of pyrophyllite (sample 149) and pyrophyllite-bearing rocks (sample 126).
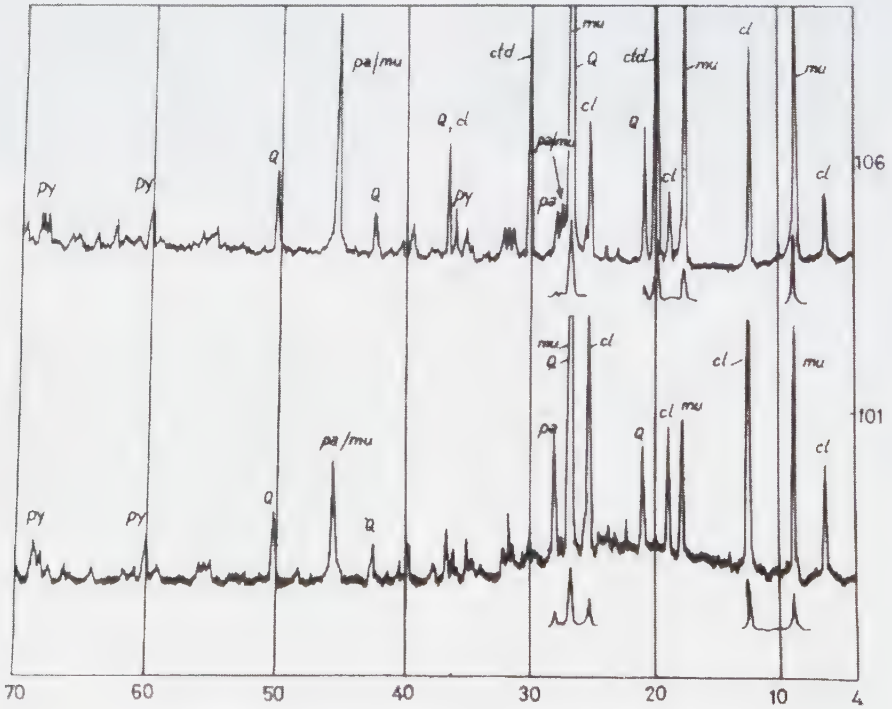
Fig. 7. X-ray diffractograms of paragonite/muscovite-bearing rocks.

ed from anchimetamorphic schists (samples 101, 106) point out the presence of pyrophyllite in lower amounts and the predominance of some micaceous minerals: muscovite, paragonite/muscovite and paragonite (Fig. 7).

The identification of paragonite/muscovite was made according to the reflection at 9.62-9.99 Å (strong) and 3.25 and 1.96 Å (weaker), which show the presence of a phengitic mixture paragonite/muscovite in a ratio of 6/4. A doubling of the reflection at 3.32 Å for paragonite/muscovite with the reflection at 3.18-3.19 Å specific for muscovite can be noticed. Paragonite/muscovite is relatively abundant in micaceous schists, but low amounts were identified in pyrophyllic schists as well. It represents in fact a mixture between muscovite and paragonite formed under conditions intermediary between diagenesis and metamor-

phism, through the transformation of Na-bearing illites (Frey, 1969).

Paragonite was identified due to the presence of the basal reflection 3.19 Å which in some samples, matches with the reflection 3.24 Å of paragonite/muscovite. This seem to be characteristic for schists having a transitory state between diagenesis and metamorphism.

IR spectroscopy

IR-spectra of pyrophyllite (spectrophotometer Zeiss UR 20, KBr) point out a series of absorption bands of high intensity ascribable to Si-O bonds: 485, 1070 and 1125 cm^{-1} or to Si-O-Al bonds: 540 cm^{-1} (Fig. 8A). The diagram also clearly shows a triplet characteristics for pyrophyllite, formed of three absorp-
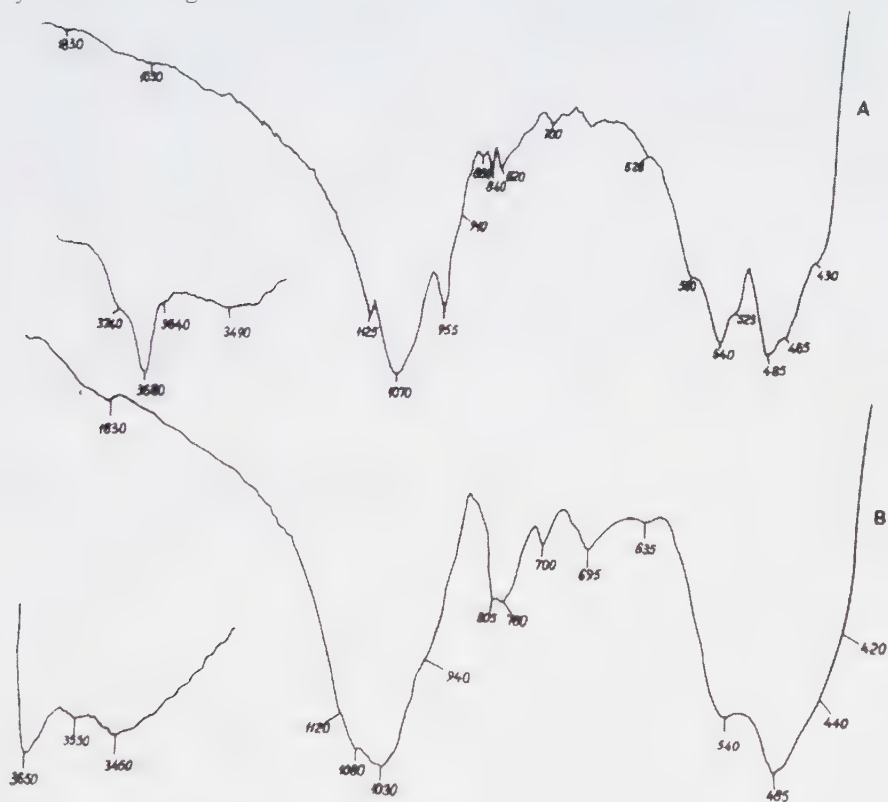
Fig. 8. IR-spectra of pyrophyllite-bearing rocks (A) and paragonite/muscovite-bearing rocks (B)

tion bands, 820, 840 and 860 cm⁻¹. The dioctahedral character of the network is confirmed by the absorption bands from 955 cm⁻¹ (Al-O-H) and 3680 cm⁻¹ (Al-OH). The presence of the inflexion from 3740 cm⁻¹ indicates a deviation from the ideal structure, as this band is determined by symmetrical vibrations of OH-groups and is practically inactive in IR for networks with perfect symmetry (Farmer, Russel, 1964).

As concerns minerals associated to pyrophyllite on the spectrum represented in Fig. 8B, the absorption bands from 485 cm⁻¹ (Si-O), 540 cm⁻¹ (Si-O-Al)VI, 1030 cm⁻¹ (Si-O) and 1120 cm⁻¹ (Si-O) reflect the presence of a micaceous mineral. The rather high value of the absorption band from 3650 cm⁻¹ suggests an isomorphous substitution of Al by Mg in octahedral levels, therefore the presence of a phengitic term. The low intensity absorption band from 3550 cm⁻¹ certifies the presence of chlorite. The doublet formed by the absorption bands from 780 cm⁻¹ and 805 cm⁻¹, as well as the band from 1080 cm⁻¹ indicate the presence of quartz.

Thermal analysis

Thermal-differential and thermal-gravimetric analyses allow a clear distinction between pyrophyllite and other minerals possible to be confused with (talc, sericite). This type of analyses allow also an evaluation of the pyrophyllite crystallinity (Kisch, 1975). DTA curves (Fig. 9) show a strong endothermal at 760° C due to the loss of OH-groups and a weak exothermal peak at 1200° C due to the transformation into mullite. A weak endothermal peak is also noticed at 573° C, representing the polymorphous transformation $\alpha \rightarrow \beta$ of quartz. The exothermal inflexion from 200-250° C is due to the presence of anthracite. The TG curve indicates only a well marked

Table 2. Chemical analyses of pyrophyllite

Oxides	Samples			
	149	126	91	101
SiO_2	64.19	59.85	65.58	61.48
TiO_2	0.01	1.10	0.46	1.20
Al_2O_3	28.77	25.19	22.09	16.77
Fe_2O_3	0.40	5.40	3.90	6.80
MnO	-	0.21	0.08	0.12
MgO	0.14	1.02	0.50	2.75
CaO	0.16	0.63	0.42	0.56
Na_2O	0.14	0.72	1.02	2.40
K_2O	0.20	1.64	0.10	3.32
H_2O	5.73	.	.	
Total	99.74	95.76	94.15	95.40

149-from Alpine veins; 126 and 91-from pyrophyllite schists;
101- from micaceous schists
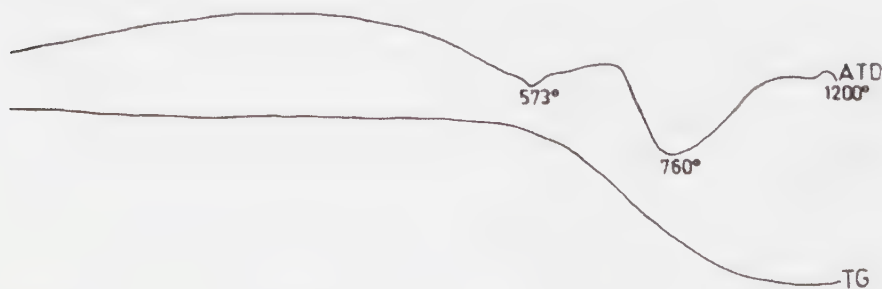
Fig. 9. DTA-curves of pyrophyllite.

slope at 760° C due to weight loss caused by elimination of OH-groups.

Chemical composition

The chemical composition of pyrophyllite and of pyrophyllitic schists from the Izvorul and Jieț zones is given in Table 2. The weight percents of the main oxides are similar to those of pyrophyllite from Schela Gorj (Paliuc, 1972) and to other pyrophyllites from anchimetamorphic zones, with some unimportant differences concerning the content in Al_2O_3, SiO_2 and Na_2O.

Mineralogenetic and petrogenetic considerations

All observation data in the studied area have pointed out the presence of pyrophyllite within the following characteristic associations:
1. Pyrophyllite-chloritoid-quartz-anthracite, within pyrophyllitic schists;
2. Muscovite-paragonite/muscovite-quartz-chlorite-chloritoid-pyrophyllite-paragonite-anthracite, within micaceous schists;
3. Chloritoid-quartz-pyrophyllite-anthracite, within schists with chloritoid;
4. Quartz-anthracite-muscovite-pyrophyllite, within quartzitic schists;
5. Quartz-pyrophyllite-chloritoid-chlorite-kaolinite, in Alpine veins.

Recent research on "anchimetamorphic zones" or "anchizone" (Kübler, 1967) has established its position between the zone of late diagenesis and the epizone of regional metamorphism (incorporating the green-schist facies).

In order to recognize the anchimetamorphic zone, the following criteria were proposed: the crystallinity degree of illite (Kübler, 1967; Dunoyer et al., 1966), the appearance of pyrophyllite at the expense of kaolinite in Al-rich rocks (Kübler, 1968), the carbonization degree of ranks of coal and coaly matter, marked by

the presence of anthracite (Karweil, 1956; Teichmüller, 1967; Kisch, 1975), the association paragonite-phengite-mixed layer phengite/paragonite (Kisch, 1974). Some of these criteria can be corroborated in a satisfactory way in different geological zones.

Within the South Carpathians, the Schela Formation was considered to stand either for a complex of sedimentary rocks (Dupark, Mrazec, 1893; Manolescu, 1932), or for a complex of epimetamorphic rocks - an upper horizon of the Tulișa Series (Pavelescu, 1966). The associations of minerals characteristic for this formation (1-4), characterized by the presence of pyrophyllite as well as of the anthracite and the paragonite/muscovite, demonstrate its anchimetamorphic character.

Pyrophyllite formation takes place according to the following reactions:

1 kaolinite + 2 quartz $\rightarrow$ 1 pyrophyllite + 1 H_2O
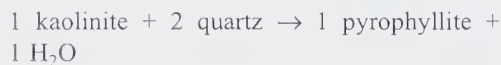
The hydrothermal synthesis of pyrophyllite from kaolinite and quartz was achieved at a temperature of 400° C (Althaus, 1966). The temperature of the reaction in which pyrophyllite forms from kaolinite + quartz is also hardly dependent on the P_{H_2O} (Winkler, 1967). According to Thompson (1970), the equilibrium temperature of this reaction is approximately 330-340° C at P_{H_2O}, 2 Kbar.

The pyrophyllite rocks are characterized by the dominance of alumosilicates and show quartz and kaolinite relics indicating the existence of an initial material with a clayey (kaolinitic)-sandy character with lenses and coaly disseminations. The temperature was determined on the basis of measurements of homogeneity temperature of fluid inclusions within quartz of Alpine veins. The results of 50 determinations are shown in the Fig. 10, indicating a frequency maximum between 160-180° C.

As concerns pressure, the burying depth of SF can be evaluated by stratigraphic criteria to be between 3 and 4 km. A forming depth larger than 3 km is indicated according to Teichmüller and Teichmüller (1967) by the presence of anthracite. The anthracite stage of the coal from SF was established in the studied zones by reflectivity determinations (R%=9.80-14.45 for 487, 552, 591 and 658 nm, using silica standard) and by X-ray diffraction (d_{002}=3.40-3.5 Å).

Taking into account the geological and petrographic characteristics, the Schela Formation of the South Carpathians can be paralleled with the anchimetamorphic formations from the Glarus Alps zone. While appreciating the formation conditions of pyrophyllite in the Glarus Alps zone, Frey (1978) takes into consideration a temperature of ~ 200° C and a total pressure of 1-2 Kbar. The low formation temperature is explained by the high water activity in metamorphic reactions (a = 0.1-0.2), justified by the very high content of methane which is present in the solutions.

Unlike the Glarus Alps zone, within the Schela Formation from the South Carpathians, carbonatic minerals are absent and anthracite is present in rather high amount. The absence of any initial carbonatic rocks allows us to appreciate that metamorphic solutions were devoid of CO_2. On the other hand, the elastic character of anthracite grains from pyrophyllite schists and the nucleation on these grainss of silicate minerals (quartz, pyrophyllite, chloritoid) demonstrate the non-participation of the carbonatic phase in the blastesis reactions and therefore the absence of methane in solutions.

In these conditions we believe that the formations of pyrophyllite from kaolinite and quartz took place in an open system under osmotic conditions. Figure 11 presents the equilibrium curves: kaolinite + quartz → pyrophyllite + H_2O according to experimental data (1) and calculated according to thermodynamic data (2) and (3). The slope of curves 2 and 3 was

calculated by equation:

$$dP/dT = \Delta s \text{ reaction}/\Delta Vs \quad (\text{Şeclăman, 1981})$$

The ΔG, Δs and ΔVs values were calculated starting from thermodynamic constants of the implied phases (Robie et al., 1978) obtaining thus: ΔG reaction = 13.986 joules/mols; Δs = 142.15 Joules/mole; ΔVs = 17.06 cm3/mol.
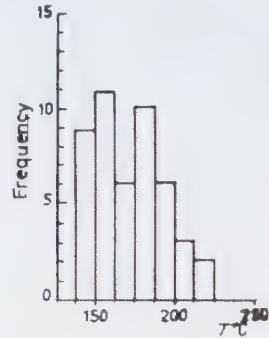
Fig. 10. Temperature histogram of fluid inclusions in quartz from Alpine veins.
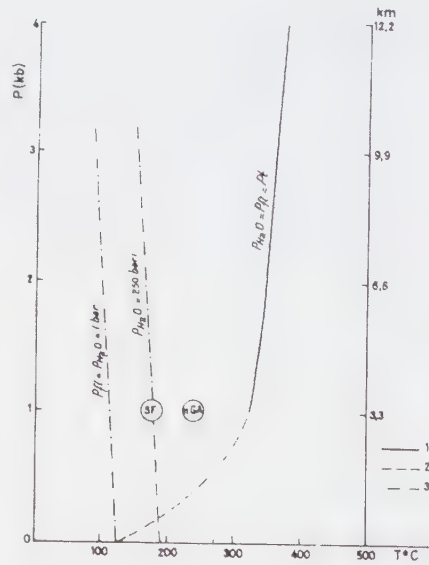
Fig. 11. Estimated P-T conditions of the Schela Formation (SF) in comparison with the Northern Glarus Alps (nGA). 1. experimental curve (Thompson, 1970); 2 - curve estimated by thermodynamic data; 3 - calculated curve.

The regime determined for Alpine veins was: temperature 160-180° C, pressure ~1 Kbar = 3.3 km, and P_{H_2O} ~250 bar. The difference between the values of pressure regime within the Alpine veins (250 bar) and those of the adjacent zones (1 kbar) was determined by stress which acted as a over-pressure.

Acknowledgements

References:

Althaus E. (1966) Der Stabilitätsbereich des Pyrophyllits unter dem Einflub von Sauren. I. *Mitteinlung. Beitr. Mineral. Petrol* . **13**. 1.

Dunoyer de Segonzac G. (1969) Les minéraux argilleux dans la diagenése. Passage an métamorphisme. Mém. 29, *Serv. Carte Géol. Als. Lorr*. **320**.

Dunoyer de Segonzac G., Ferrero J., Kubler B. (1966) Sur la cristallinité de l'illite dans la diagenése et l'anchimétamorphisme. *Sedimentology*, **10**, 137-143.

Dupark J., Mrazec L. (1893) Sur un schist ŕ chloritoid des Carpathes. *C. R. Acad. Sci.* Paris.

Frey M. (1969) A mixed layer paragonitę/phengite of low-grade metamorphic origin. *Contr. Mineral. Petrol*, **24**, 63-65.

Frey M. (1978) Progressive low-grade metamorphism of Black Shale formation, Central Swiss Alps, with special reference to pyrophyllite and margarite-bearing assemblages. *J. of Petrol.*, **19**, 1, 95-133.

Ianovici V., Neacşu G., Neacşu V. (1981) Pyrophyllite occurrences and their genetic relation with the kaolin minerals in Romania. *Rev. Roum. Géol.Géophys. Géogr.*, s. Géol., 25, **1-17**.

Karweil J. (1956) Die Metamorphose der Kohlen von Standpunkt der physikalischen Chemie. *Deutsche Geol. Gesell. Zeitschr.*, **107 (1955)**, 132-139.

Kisch H. I. (1974) Anthracite and meta-anthracite coal ranks associated with "anchimetamorphism" and "very low-stage" metamorphism. *Koninke Nedul. Akadem.* Wetenschappen, Amsterdam Proceed., Ser. B, **77(2)**, 81-118.

Kisch H. I. (1975) Coal rank and "very low-stage" metamorphic mineral facies in associated sedimentary rocks. An introduction. Colloque Intern. Pétrographie matiére organique des sédiments. Paris, Sept., 1973. Ed. HNRS, 117-121.

Kübler B. (1967) La cristallinité de l'illite et les zones tout à fait supérieures de métamorphisme. Coll. étages tectoniques, Neuchâttel, 105-121.

Kübler B. (1968) Evolution quantitative du métamorphisme par la cristallinité de l'illite. *Bull. Centr. Rech. Pan, SNPA,* **2**, 385-397.

Manolescu G. (1932) Das Alter der Schela Formation. Bull. Soc. Roum. Géol., I.

Mutihac V., Popescu Gh. C. (1981) Anchimétamorphisme et position de la formation de Schela dans la structogénése des Carpathes Méridionales. Carpatho-Balkan Geol. Assoc., 12th Congress, Sept. 8-13. Bucharest, Romania, Abstracts, 293-294.

Mutihac V., Popescu Gh. C. (1982) Sur le caractére anchimétamorphique de la formation de Schela des Carpathes Méridionales centrales. *Rév. Roum. Géol., Géoph. Géogr., s. Géologie*, **26**, 47-56.

Paliuc G. (1937) Etude géologique et pétrographique de massif du Parŕng et des Munţii Cîmpii (Carpathes Méridionales, Roumanie). *An. Inst. Géol.*, **18**

Paliuc G. (1972) Pirofilitul din formaţiunea de Schela. *D. S. Inst. Geol.*, **58**, 45-65.

Pavelescu L. (1966) Cercetări geologice şi petrografice în bazinul văii Jiului transilvănean şi al văii Jieţului. *St. cerc. geol. geof. geogr., Ser. geol.*, **11**, 151-169.

Robie R. A., Hemingway B. S., Fisher J. R. (1978) Thermodynamic properties of minerals and related substances at 1 bar (105 Pascals) pressure and at higher temperatures. *U. S. Geol. Survey Bull.*, **1452**, 426.

Rosenberg P. E. (1974) Pyrophyllite solid solutions in the system Al_2O_3-SiO_2-H_2O. *Am. Mineral.*, **59**, **254-260**.

Semaka Al. (1968) Despre vârsta formațiunii de Schela. Asoc. Geol. Carpato-Balc. Congr. V., II, 2, Bucuresti.

Șeclăman M. (1981) Introducere în termodinamica sistemelor și proceselor minerale. Ed. Acad. R. S. România, București, 147 p.

Streickeisen A. (1934) Observațiuni geologice în Carpații Meridionali între Valea Oltului și Valea Jiului. *D. S. Inst. Geol. Rom.*, **17**.

Teichmüller M., Teichmüller R. (1967) Diagenesis of coal (coalification). Diagenesis in sediments. Ed. G. Larsen, G. V. Chilinger, Elsevier, 391-415.

Thompson A. B. (1970) A note on the kaolinite-pyrophyllite equilibrium. *Am. J. Sci.*, **268**, 454-458.

White J. L. (1962) X-ray diffraction studies on weathering of muscovite. *Soil. Sci.*, **93**, 16-21.

Winkler H. G. F. (1967) Die Genese der metamorphen Gesteine. 2 Auflage, Berlin, Springer-Verlag, 237.

The crystallographic, optic and chemical-structural features of adularia from the Alpine veins of Romania: a contribution to the "adularia problem"

EMIL CONSTANTINESCU
GAVRIL SABĂU

The term "adularia" was introduced by Pini (1873) after he examined the crystals collected from St. Gothard (Swiss Alps). Pini considered "adularia" to be a type of monoclinic K-feldspar having a specific habitus and a genesis associated to the alpine dykes. Later crystallographic measurements (Hintze 1897, Goldschimdt 1916. Niggli 1923. Ramdohr 1948) pointed out the monoclinic symmetry of adularia. The microscopic studies (Alling 1923, Barth 1928, Kohler 1948) demonstrated the existence of triclinic adularia twinned after albite-periclin and akline-B laws (specific twins for triclinic symmetry).

Other optical data obtained by Chaison (1950), Ansilewski (1958) and Nowakovski (1959) show a large variation of the optical indicatrix position as well as of the 2V angle within different adularia crystals. The X-ray studies (Laves 1950,1952; Smidt 1972) and the infrared absorption studies (Hafner, Laves

1957) revealed that optical triclinic adularia have constants that correspond to a triclinic lattice.

Consequently, the adularia was considered (Banbauer, Laves 1960) an intermediary metastable stage between sanidine (disordered Al/Si distribution) and microcline (ordered Al/Si distribution).

In Romania, the adularia was first optically determined for the first time by Giuşcă (1968) who described it as a K-feldspar of neoformation, resulted by hydrotermal alteration of Neogene volcanites of Gutâi Mountains. Later, Giuşcă identified adularia within different ore deposits from Eastern Carpathians, Banat, Dobrogea and Apuseni Mountains. Due to its constant association with gold, Cu-W or Cu-Mo mineralization, the adularia was considered by Giuşcă as a metallogenetic indicator

The adularia occurrences from Parâng Mts. which represent the first alpine dykes discovered in Romanian Carpathians. They offer a great number of well developed crystals suitable for different and complex mineralogical examination. The obtained data for different adularia crystals show the modification of optical and structural features within individual crystals due to the variation of genetic conditions.

Occurrence and paragenesis

The herein examined adularia was identified within several dykes from Parâng Mts. The most representative adularia crystals were collected from a quarry localized on the left slope of the Gruniu valley (Maleia) at 9.3 km East from Petroşani.

The host rocks consist of chlorite, epidote and actinolite bearing schist, belonging to Drăgşani Group. Here, the migmatization is considered to be related to the sinkinematic Parâng granite (Ungureanu, 1974).The Alpine dykes are developed along N-S oriented discordant fractures. The dykes length is about 1-3 m and the width is 2-50 cm.

The paragenesis of the dykes consist of: a) quartz (big sized crystals up to 20 cm); they are colorless, white, smoky or greenish, having well developed prism or ditrigonal pyramid faces; b) chlorite (ripidolite) in compact green aggregates; c) actinolite as fine needles within quartz and adularia crystals; d) epidote in developed yellow-brownish crystals (2-4 mm); e) sphene; g) apatite.

Morphology of adularia crystals

There were 97 adularia crystals analysed. The short prismatic crystals are 1-4 cm in size. The (110), (1-10), (001) and (201) faces are well developed. Some crystals show a predominant development of (20-1) face on the expense of the (001) face (Fig. 1).

Within the sections perpendicular on C axis a color variation with a zoning feature may be noticed: the central part is dark or dark gray, while the external parts turn to milky-white bands.

The (110) face shows two cleavage directions: one of very good quality parallel to (001) and another one of good quality parallel to (010).

There were frequently noticed twins after to (001) plane (Manebach type) and (021) planes (Baveno types). Complex twins are also present (Baveno + Manebach).

Beside the monoclinic type twins, some adularia crystals show striation on (20-1) faces suggesting pericline (001) or akline-B (100) twins, which are typical for triclinic symmetry.

Chemical composition

Compared with other chemical analyses found in mineralogical literature (Table 1), our analyses show a lower content of Na. We can also notice the lower content of Ca and the higher content of Ba when comparing to the analyses 3 and 4 (Dauphiné – France and Taiwan, respectively). According to Veibel and Meyer (1957), who examined the Ba content of adularia from Cavradischlucht-Alps (analysis no. 5), it is possible that the higher Ca content of some of our own analyses does not reflect errors in the determination of Ba but the concentration tendency of this element within adularia.

The structural formula of Maleia adularia calculated in the basis of 32(O) basis is : $K_{3.092}Na_{0.245}Ba_{0.100}Ca_{0.022}Si_{11.901}Al_{4.427}O_{32}$. The participation of feldspar end-members (expressed in mole%) is : FK 89% Ab 7% Cs 3% An 1%. The lower content of Na and Ca indicates that the optical and structural heterogeneity is exclusively due to the structural variations.
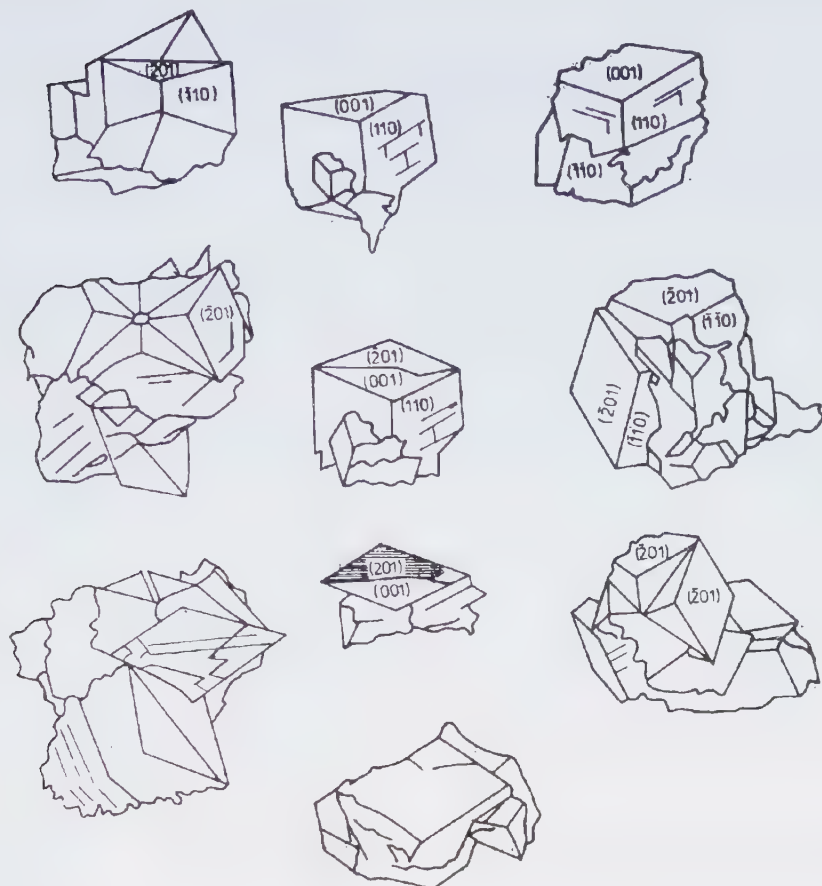
Fig. 1. Morphology of the adularia crystals from Gruniu – Parâng Mts., Southern Carpathians.

Table 1. Chemical analyses of adularia

Oxides %	1	2	3	4	5
SiO_2	64.20	64.00	64.87	64.45	62.3
Al_2O_3	19.26	19.25	18.51	18.97	19.6
Fe_2O_3	0.11	-	0.23	0.07	-
FeO	0.09	-	-	0.25	-
MgO	0.05	-	-	0.03	-
CaO	0.12	0.15	0.23	0.53	0.01
BaO	1.42	0.41	0.92	-	2.6
Na_2O	0.70	1.86	1.99	0.95	1.05
K_2O	13.04	14.01	13.08	14.98	14.2
H_2O^+	0.63	0.50	-	0.11	0.08
H_2O	0.07	0.50	0.07	0.06	-

Structural features

X-ray data. The X-ray diffraction analysis was done by diffractometer method. The $d\alpha/n$ and I/100 values (Table 2) are similar to the data obtained for other adularia crystals from different Alpine dykes.

The detailed morphology of the different peaks in the region 2θ: 22-25° C suggests the inhomogeneity of the analysed crystal. All the reflections in this area (Fig. 2) are ascribable to the (130) planes in both monoclinic and triclinic K-feldspar. However, the monoclinic symmetry prevails. The calculated triclinicity gives $\Delta = 0.8$.

Table 2. The d/n and I/I_0 values of the adularia from Maleia

Adularia (Maleia)		Adularia (Tirol; Gruner, 1936)	
d/n	I	d/n	I
3.930	10	3.940	1
3.766	15	3.770	4
3.450	10	3.480	2
3.290	20	3.313	10
3.229	100	3.227	8
2.985	35	2.995	4
2.889	10	2.901	2
2.760	10	2.763	2
2.550	25	2.560	6
2.319	10	2.319	1
2.154	10	2.165	4
2.119	10	2.119	2
2.049	10	2.050	1
1.887	45	1.881	1
1.795	35	1.792	8
1.615	10	1.622	2
1.449	15	1.447	2
1.406	10	1.402	2
1.382	10	1.381	2
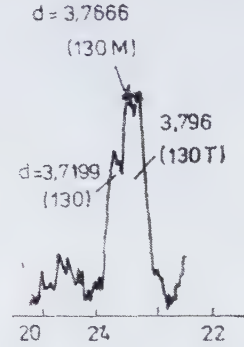
Fig. 2. Detail of 2θ: 22-25° diffractograme of the adularia from Gruniu.

Infrared absorption spectroscopy. The IR absorption spectrum (Fig. 3) shows bands corresponding to bond-stretching: Si-O (1142-1100 cm⁻¹); Si(Al)-O(1044-1010 cm⁻¹); Si-Al-Si (742-782 cm⁻¹) and the bond deformation: Si-O-Si (539 cm⁻¹).

The values of these bands fit the values known for adularia from different occurrences compiled by Gadsen (1975) and they are typical for different transition stages between triclinic and monoclinic terms.

Fig. 3. Infrared absorption spectrum of the adularia form Gruniu.

Within microcline, the minimum transition value of 645 cm⁻¹ moves to 650 cm⁻¹ as a measure of increased triclinicity (Δ). Within the sanidine, the minimum value appears at 639 cm⁻¹ and as a measure of ordering it moves to 650 cm⁻¹. The position of the absorp-

tion bands within the domains 18.3-18.7 μm and 15.4-15.8 μm that was illustrated within a Hafner - Laves diagram, shows an intermediate ordering stage.

Microscopic features

A number of 27 thin sections were analysed. Some of them were oriented parallel to the (110), (001), (201) faces or perpendicular to the Z axis.

The universal stage measurements showed optical inhomogeneity within different zones of the same crystals by variation of the 2V angle (67-83°) and cΛγ extinction angle (12-17°).

Uniaxial zones were identified, too. Zoned structures given by thin lamellae parallel to the (110) prism faces that surround a more developed inner zone (Fig. 4) were also observed. In this case, the central zone shows values closer to the monoclinic symmetry whereas the external zones have typical values for intermediate microcline. The linking zone of lamellae where the prism faces make acute angles, is more representative values for an ordered configuration than the zone where the same faces make an obtuse angle. Typical values for monoclinic symmetry and albite-pericline type twin were also noticed in the vicinity of certain cracks and inclusions.

Conclusions

According to its morphology, chemistry, structures and optical properties, the adularia from Maleia-Parâng presents the typical features for "Alpine dykes" type adularia. Although it is well known in different occurrences from the Alpino-Carpathian chain, it was not known until now within the Romanian Carpathians. By its statute, even as a metastable phase, the adularia from each occurrence show typical features that could contribute to the knowledge some of its mineralogenetic aspects.
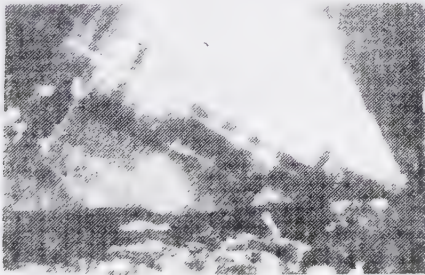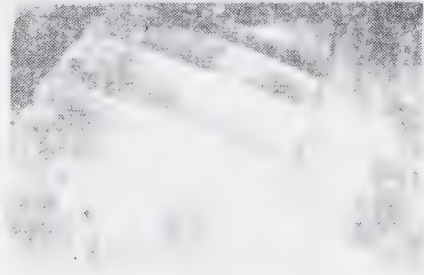
a　　　　　b
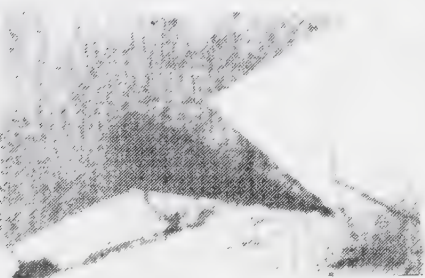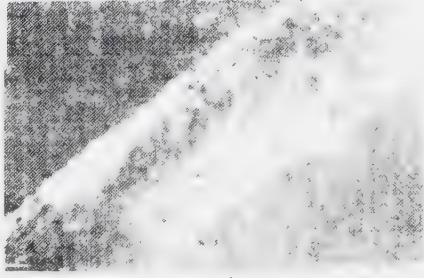
c　　　　　d

Fig. 4. Microscopic images of adularia from Gruniu.

One of the question raised was: are the triclinic zones formed during the final crystallization stages or do they represent a result of a subsequent transformation (a triclinization of a monoclinic feldspar)? The occurrence and the parageneses exclude the possibility of crystallization at temperatures higher than 400° C (geothermometrical determination on fluid inclusions from associated quartz give temperatures up to 180° C). So, there are no appropriate conditions for the formation of a stable monoclinic phase. The speed of crystallization process which control the formation of a partial disordered structure rather than an ordered one is responsible here for the appearance of a monoclinic metastable stage within the stability field of triclinic K-feldspar. This possibility is perfectly in agreement to the monoclinic symmetry of the isolated crystals and to the observed twinning symmetry of Manebach and Baveno types.

The striation on the (201) face do not represent the twin planes of albite type (specific for triclinic symmetry as considered by Nowakowsky, 1959) but limits of certain zones with different degrees of Si-Al ordering, oriented parallel to (100) face, as suggested by Bambauer and Laves (1960).

The microscopic observations on adularia from Maleia-Parâng pointed out the tendency of symmetry changing in time from monoclinic to triclinic. The domains with higher ordering – showed by the 2Vα and cΛγ angles and the pericline + albite twins – are disposed within the marginal zones, parallel to the (110) faces, around the inclusions and cracks.

These elements allow to associate the kinetics of transformations to specific properties of the crystalline lattice from the vicinity of certain surfaces. According to these observations, we may consider two possibilities:

1) In the vicinity of the monoclinic crystal surface there is an exceeding amount of free energy (due to the superficial tension), which rises the motrical force of the polimorphous inversion. This mechanism is also responsible for the higher ordering degree within the zones where the (110) prism faces make acute angles;

2) On the internal or external crystal surfaces (closer to inclusions and cracks), there existed an adsorbed water based fluid which catalyzed the transformation of the metastable monoclinic phase to an ordered triclinic phase.

References

Alling H.L. (1923) The mineralogy of the feldspar. *J. Geol.* **21**, p. 281-305.

Ansilewski J. (1958) On microcline and triclinic adularia from Bialkie Góry gneisses (Polish Sudeten). *Bull. Acad. Pol. Sci., Serie Sci. Chim., Geol. et Geogr.* **VI**, 10, p. 275-282.

Bambauer H.U., Laves F. (1960) Phasenzustände des Adulars und ihre genetische Deutung, *Fortschr. Min.* **38** (Vortragsreferat).

Bambauer H.U., Laves F. (1966) Zum Adularproblem. *Sweiz Min. Petr. Mitt.*

Barth T. F. W. (1928) Ein neuer Zwilling bei triklinem Feldspat, Aklin B, *Z. Krist.* **68**, p. 473-475.

Chaisson U. (1950) The optics of triclinic adularia. *J. geol.* **58**, p. 537-547, 5.

Deer W. A., Howie R.A., Zussman J. (1967), Rock forming minerals. Loggmans, London.

Gadsden J.A. (1975) Infrared spectra of minerals and related inorganic compounds, Butlerworth Co. London.

Giuşcă D. (1960) Adularizarea vulcanitelor din regiunea Baia Mare. *St. cerc. geol., geofiz., geogr., ser. Geol.*, **3**, V. Bucuresti.

Goldschmidt V. (1916) Atlas der Krystallformen, Heidelberg.

Hafner St., Laves F. (1957) Ordnung / Unordnung und Ultrarotabsorption II. Variation der Lage und Intensität einger

Absorbtionen von feldspäten. Zur Struktur von Orthoklas und Adular. *Z. Krist.* **103**, p. 204-225.

Köhler A. (1948) Zur optic des Adulars *N. Jb. Min. Abh.* **5-8**, p. 49-55;

Hintze C. (1897) Handbuch der Mineralogie, Bd. II, Leipzig.

Laves F. (1952) Phase relations of the alkali feldspar; I. Introductory remarks; II The stable and pseudostable phase relations in the alkalifeldspar system. *J. geol.* **60**, p. 436-450, p. 549-574.

Laves F. (1960) Al/Si - Verteilungen, Phasentransformationen und Namen der Alkalifeldspäte. *Z. Krist.* **113**, Von-laue-Festschrift II.

Niggli P. (1923) Lehrbuch der Mineralogie, Berlin.

Nowakowski A. (1959) On the adularized dyke rock in the vicinity of Klimontów (holy. Cross Mts.) *Bull. Akad. Pol. Sci. serie Sci. Chim. Geol, Geogr.* **VII**, 10, p. 751-757.

Ramdohr P. (1948) Klockmanns Lehrbuch der Mineralogie, Stuttgart.

Tuttle O.F. (1952) Optical studies on alkali feldspar. *Am. J. Sci.* Bowen Volume, p. 553-567.

Weibel M. (1957) Zum Chemismus der alpinen Adulare (II). *Schweiz. Min. Petr. Mitt.* **37**, 2, p. 545-553.

Weibel M., Meyer F. (1957) Zum Chemismus der alpinen Adulare (I). *Schweiz. Min. Petr. Mitt.* **37**, 1, p. 153-158.

First occurence of coloradoite in Romania

GHEORGHE C. POPESCU
EMIL CONSTANTINESCU

Coloradoite was first discovered on the occasion of the revision of the material collected by prof. Petrulian, at present deposited in the collection of the Department of Mineralogy Bucharest University. This paper deals with the microscopic description of this mineral.

Coloradoite samples comes from Stănija, one of the best-known telluride occurences in the mostly auro-argentiferous metallogenetic sub-province of the Apuseni Mountains, Romania (fig. 1).

Fig. 1. The Stănija gold deposit within the metallogenetic province of the Apuseni Mountains (Romania).

At Stănija, coloradoite occurs as a substitution "rim" of the krenerite and sylvanite grains, or disposed on the krennerite cleavage and fissures (Plate I). Its colour is light grey, with a brownish hue in comparison with krennerite. The polishing hardness is smaller than that of the krennerite and sylvanite.

The reflectivity of coloradoite has been determined in the visible spectrum with interference filters 487, 552, 591 and 658 mμ, using a silicium standard.

The dispersion curve, drawn up on the basis of the reflectivity measurements, displays an obvious similarity with that of the coloradoite of Kalgoorlie (Australia) (Fig. 2a). However, the curve generally indicates low reflectivity values for the coloradoite of Stănija in comparison with the coloradoite of Kalgoorlie. The outline of the curve is not only similar, but also conformable to that considered by Bezsmertnaya et al. (1973) as a standard for coloradoite (Fig. 2b).

Coloradoite is isotropic and does not show internal reflexes.

Coloradoite of Stănija was also studied using the electronic microprobe type Jeol Y/ A - 5A. The analysis has been carried out by comparison with the gold and silver tellurides. In these conditions, the distinct distribution of Au and

Ag, on one hand, and of Hg, on the other hand, has confirmed the optical determinations coloradoite existence at Stănija, as well as its association with the krennerite and sylvanite (Plate II).

The spatial relationships between coloradoite and krennerite— sylvanite indicate its subsequent formation in comparison with the gold and silver tellurides. Coloradoite seems to end the series of tellurides formed during the hydrothermal process at Stănija.
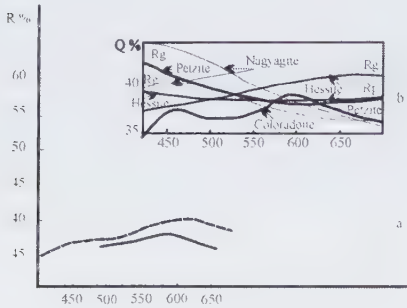
Fig. 2. Reflectivity dispersion curves: a) for the coloradoite of Stănija (solid line) versus the coloradoite of Kalgoorlie (dashed line); b) for the "standard" coloradoite versus petzite, nagyagite and hessite (after Bezsmertnaya et al., 1973).

References

Bezsmertnaya S. M., Civileva N. T., Agroshkin S. L., Bocek Y. L., Lebedeva M. S., Loghinova A. L. (1973). *Determination of ore minerals in polished section by their reflectances and hardness.* (in Russian). Nedra, Moskva, p. **244**.

Picot P., Johan Z. (1982), *Atlas of ore minerals*, B.R.G.M. - Elsevier, p. **458**.

Plate I. Occurrence and structural relationships between coloradoite, krennerite and sylvanite.
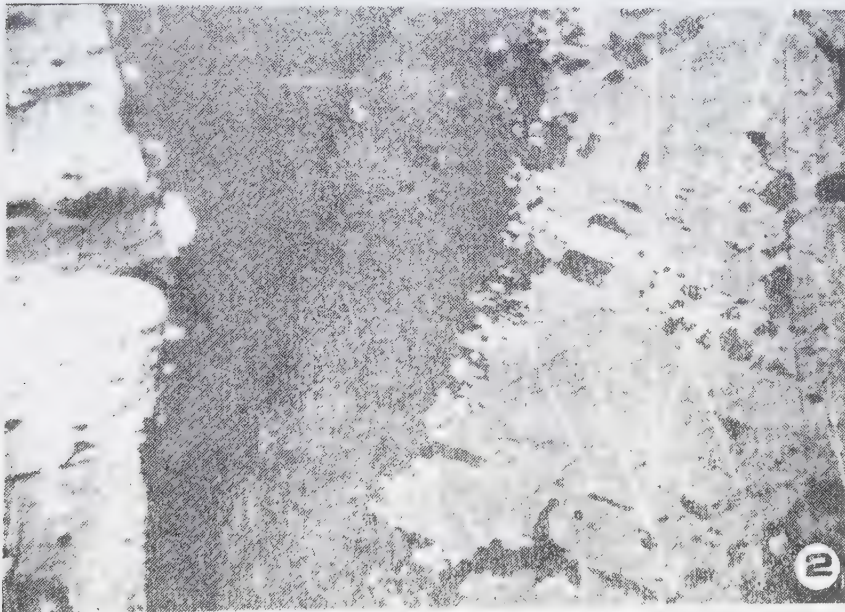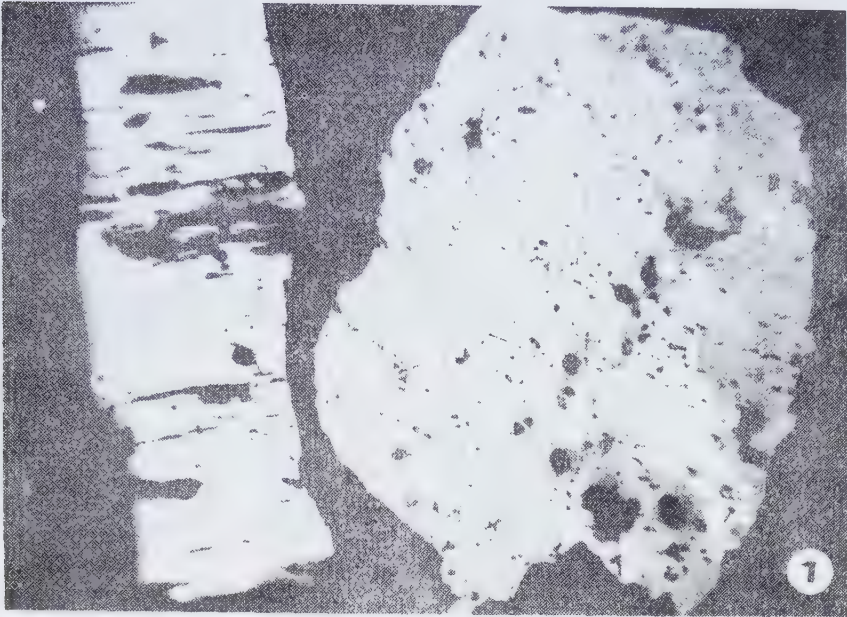
1. Coloradoite replaces krennerite centripetally on fissures and partially along cleavage. To the left, a krennerite crystal with visible cleavage, x 120;
2. Details in the micro photograph 1 with N+. Coloradoite isotropy and sylvanite distribution (anisotropic and twinned) at the krennerite-coloradoite limit. x 250.

Plate II. Electron photographs at the coloradoite-krennerite-sylvanite limit. x 600
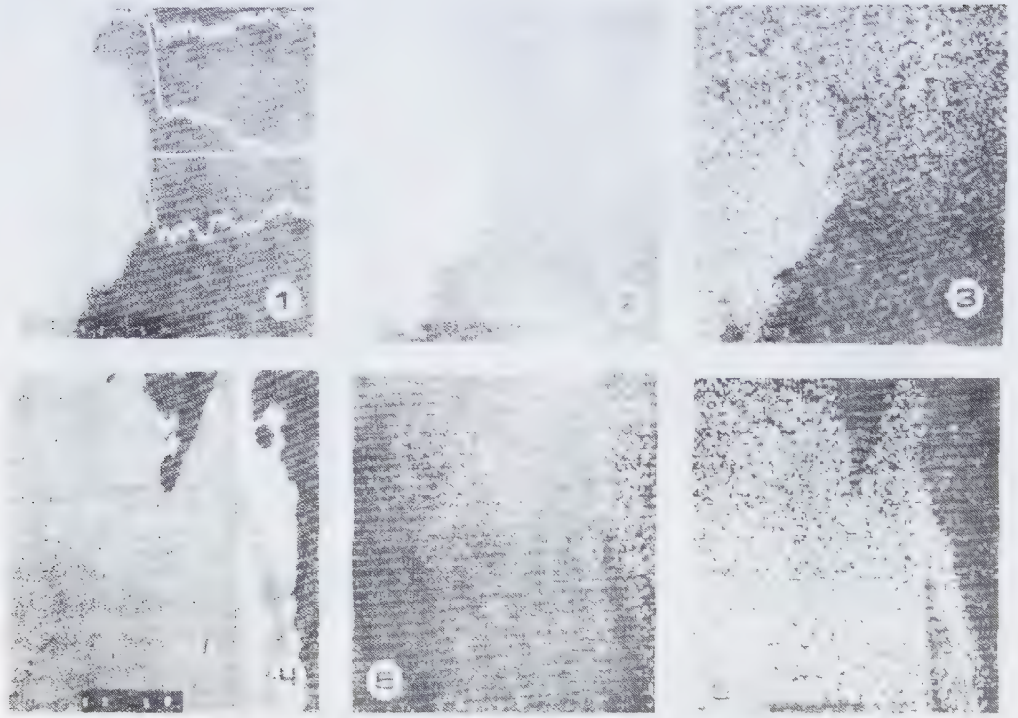
1. X-ray analysis for Te, Au and Ag along a profile superposed to the composition image;
2. Idem for Hg;
3. X-ray image of the Hg distribution at the coloradoite-krennerite+sylvanite limit;
4. Composition image of the krennerite replacement by coloradoite;
5. X-ray image of the Hg distribution presented in the electron photograph 4;
6. X-ray image of the Ag distribution presented in the electron photograph 4.

Clintonite in the skarn occurrence of Oravița (Romania). Particularities of the chemical composition and of the crystal structure

EMIL CONSTANTINESCU
GHEORGHE C. POPESCU

The skarn occurrences in Banat, developed at the contact of Laramian magmatites, represent classic areas for the study of contact metamorphism (von Cotta, 1864; Marka, 1869). For a long time, the contact rocks have been considered as calcic skarns; garnets, vesuvianite and Ca-pyroxenes have been the main minerals drawing the attention of the mineralogical research.

Recently, a series of minerals characteristic to magnesian skarns and to their related hydrothermal alterations, have been pointed out: flogopite, palygorskite, antigorite - Ocna de Fier (Kissling, 1967); humite, forsterite, flogopite, chrysotile, antigorite, sepiolite, sheridanite, saponite - Sasca Montană (Constantinescu, 1971, 1977, 1980); humite, forsterite, sepiolite - Moldova Nouă (Gheorghiță, 1975; Gheorghițescu, 1977).

Occurrence. Clintonite was identified in an outcrop located at the confluence of Oravița valley with Crișenilor brook (Fig. 1), in skarns developed along the contact between a body of Laramian diorites (andesine 64.55%; ortho-clase 2.9%, quartz 4.19%, pyroxene 3.9%, hornblende 3.1%, biotite 6%) and Jurassic limestones.

Skarns consist of compact masses of green-yellowish garnets (70 mole % grossularite, 14 mole % andradite, 11.2 mole % almandine; 6.3 mole % pyrope) and vesuvianite, with centimetric porphyroblasts of dark-brown garnet (84 mole % grossularite, 5 mole % andradite, 1 mole % almandine; 8 mole % pyrope).

Clintonite occurs in tabular crystals of intense marine green color, 0.5-1 cm in diameter, aggregated in nests where it associates with brown porphyroblastic garnet and vesuvianite (Fig. 2). By alteration, clintonite loses color and becomes white and transparent, resembling muscovite.

Physical and chemical properties. Under the microscope, clintonite is colorless or weakly pleochroic: pale yellow - green yellowish; the cleavage is perfect after (001), $c^\wedge np = 5^\circ$; $2Vnp = 31^\circ$, $np = 1.65$.
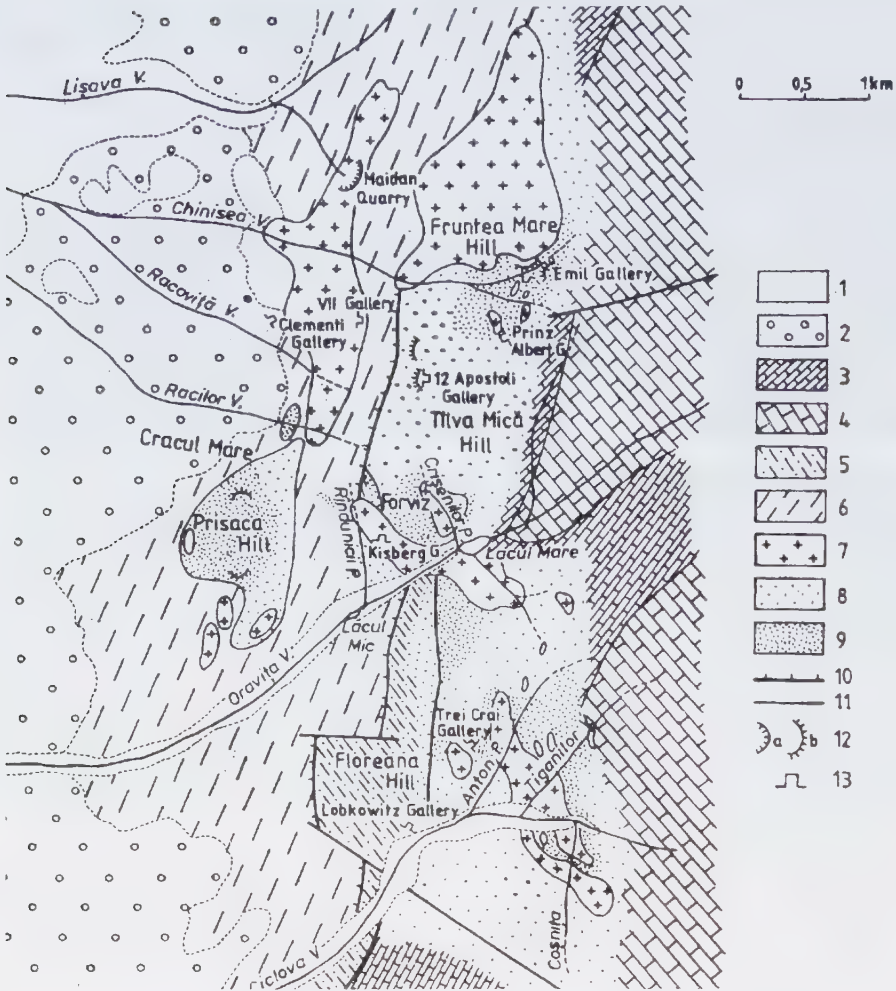
Fig. 1. Geological sketch of Oravița-Ciclova zone. 1, Pleistocene (gravel, sand, clays); 2, (conglomerates, sandstones); 3, Cretaceous (marls, calcareous clays, chert-bearing limestones, reef limestones); 4, Jurassic (chert-bearing limestones, sublithographic limestones); Permian (lithic sandstones, clay shales); 6, Precambrian (muscovite-biotite paragneisses, muscovite schists with albite porphyroblasts, amphibolites, muscovite-bearing quartzites; 7, Laramian magmatites (granodiorites, diorites, monzodiorites); 8, hornfels; 9, skarns; 10, Oravita tectonic line; 11, faults; 12 a, quarry; b, mining dump 13, mining adit.

The chemical analysis and the number of ions calculated in the basis 24 (O,OH) (Table 1), indicate values that are largely similar with those determined for clintonites at Zlataust (Urals) and Monzoni (Italy) and for xantophyllites from Adamello (Italy) and Cerstmore (California). The chemical-structural formula derived for clintonite from Oravița is $Ca_{1.760}$ $(Mg, Fe_{4.027}A_{11.320})[Si_{2.515}Al_{5.485}O_{20}]$ $(OH)_4$. If margarite can be regarded as a derivative of muscovite by a K $\rightarrow$ Ca, then the brittle micas of the clintonite-xantophylite type can be considered a calcic analogue of flogopite. From the formula we note the low content of Si, reflecting a $^{IV}Al/Si$ ratio bigger than 2/1 and counterweighing the K $\rightarrow$ Ca and the $Mg \rightarrow$ ^{VI}Al (3.7/1.3) substitutions.
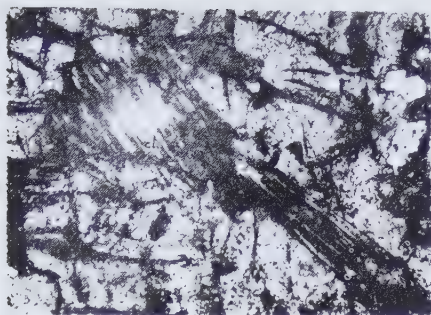
Fig. 2. Clintonite in vesuvianite, NII, 150X.

Table 1. Chemical analysis of clintonite from Oravița valley

Table 2. The 2θ, d, and I values measured for clintonite from Oravița

No.	2θ	d	I	No.	2θ	d	I
1	6.02	14.7	40	16	41.18	2.19	7
2	9.25	9.56	20	17	42.98	2.10	23
3	18.48	4.80	13	18	44.48	2.03	3
4	24.00	3.70	1	19	47.18	1.92	100
5	25.10	3.54	12	20	54.26	1.69	7
6	27.80	3.20	29	21	54.45	1.68	4
7	29.45	3.03	7	22	54.40	1.60	15
8	31.79	2.81	13	23	62.00	1.49	12
9	32.60	2.74	5	24	62.64	1.48	35
10	34.45	2.60	15	25	68.12	1.37	30
11	35.10	2.55	29	26	71.80	1.31	16
12	36.85	2.43	7	27	71.96	1.31	15
13	37.32	2.40	4	28	75.40	1.26	4
14	38.10	2.36	6	29	79.42	1.20	34
15	39.66	2.27	3	30	70.65	1.20	36

Oxides	wt. %	Number of ions in the basis of 24 (O,OH)		
SiO_2	18.40	Si	2.515	
Al_2O_3	42.19	Al	5.485	8.00
Fe_2O_3	2.59	Al	1.320	
FeO	0.46	Fe^{3+}	0.263	
MnO	0.05	Fe^{2+}	0.049	
MgO	18.21	Mg	3.715	
CaO	12.02	Ca	1.760	5.35
TiO_2	-			
H_2O^+	6.23			

The interplanar distances "d" and the relative intensities I/100 (Table 2) calculated from the diffractogram (Fig. 3) are similar to those published by Forman et al. (1967, fide Farmer and Velde, 1973) and Harada, Kodama (1965, fide op. cit.). '

The thermal-differential analysis shows an endothermic effect at 1020° C indicating the loss of OH.

Remarkable diagnostic elements and structural details result from the infrared absorbtion spectra that allow the distinction between different species of brittle micas. The IR spectrum of clintonite from Oravița (Fig. 4) shows in the domain 600-1100 cm^{-1}, three well defined absorption bands at 652, 797 and 943 cm^{-1}, as well as a weak inflexion at 903 cm^{-1}. In the interval 3000-3800 cm^{-1}, there are two inflexions at 3415 and 3620 cm^{-1}.

After Farmer and Velde (1973), in margarite and ephesite, the tetrahedral layers containing Si and Al in equal proportions, are ordered. Therefore, the absorption bands in the spectra are sharp and show no vibration of the Al-O-Al bond. The tetrahedral layers are disordered and show a strong absorption band corresponding to Al-O-Al bond in the region of 800 cm^{-1}. The frequencies corresponding to the elongating vibrations of the OH group (3000-3800 cm^{-1}) are affected by the ionic substitutions in the tetrahedral and octahedral layers, which allows an estimation of the chemical composition of the tetrahedral layers of clintonite.

The discussion on the chemical-structural features requires a series of details concerning the nomenclature of the brittle, tri-octahedral micas. For their designation, with the exception of clintonite, a series of other names have been in use, such as: xantophylite, seyberite, valuévite, brandisite, disterite, holmesite and chrysophane. Forman and Kodama (1967, fide Farmer and Velde, 1973) analysed these minerals by X-ray diffraction, but did not notice essential structural differences among this group.

Deer et al. (1965) proposed that only two phases be retained among the tri-octahedral
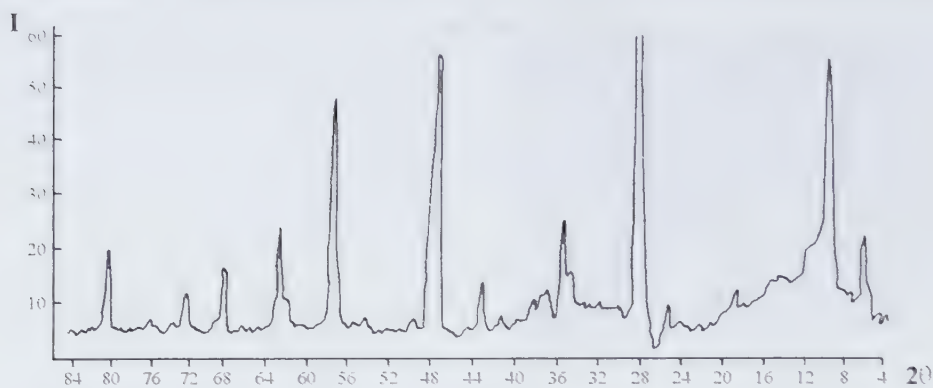
Fig. 3. The diffractogram of clintonite from Oravița. Philips diffractometer, CuKa radiation, Ni filter.
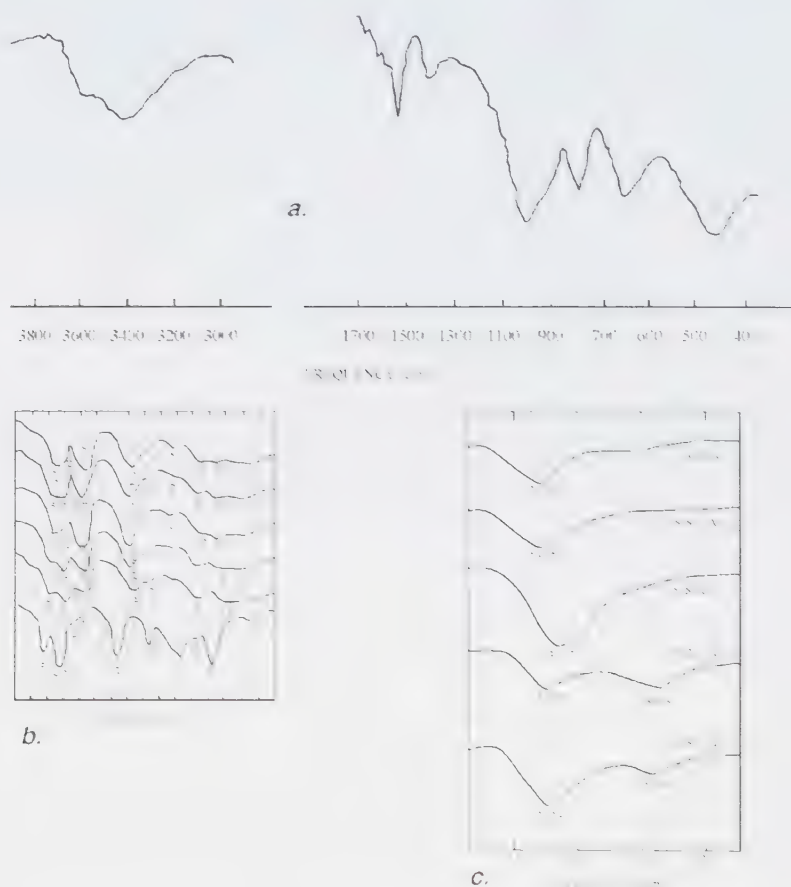
Fig. 4. (a) Infrared absorption spectra of clintonite from Oravița; (b) Infrared spectra of synthetic clintonites (C) and natural clintonites with various tetrahedral compositions; (c) Hydroxyl stretching absorption of clintonites (N natural, S synthetic); tetrahedral compositions are indicated (b and c, after Farmer and Velde, 1973).

micas: clintonite and xantophylite, which are optically distinguishable by the position of the plane of optical axes (P.O.A.) in relation with the face (010). The authors made also a critical analysis of the published data, concluding that phases described as valuévite are xantophyllites, whereas those described as brandisite and seyberite, represent in fact clintonites.

The data we obtained on clintonite and the comparison of the structural constants with those published in various sources do not reflect decisive differences able to validate all these phases as distinct species.

Microscopical investigations carried out with the universal stage on sections cut parallel to (001) showed that P.O.A. is prependicular on (010), thus confirming the diagnosis given for clintonite.

Genetic siginificance. The occurrence of clintonite at Oravița reflects a hypothermal transitory stage of evolution of the inner contact aureole, developed towards the end of the main skarn formation process. At a regional scale the formation of clintonite follows shortly the depostion of vesuvianite and can be paralleled with the occurrence of scapolite and tourmaline, signifying a stage abbundant in volatiles and mineralizers (B, F, OH) and with an increased mobility of Mg and Al.

References

Constantinescu E. (1971) Observații asupra skarnelor și mineralizațiilor cuprifere laramice de la Sasca Montană. *Analele Universității București*, **XX**, 65-74.

Constantinescu E. (1977) Studiul mineralogic al alterațiilor hidrotermale ale banatitelor de la Sasca Montană. *Analele Universității București*, **XXVI**, 59-75.

Constantinescu E. (1980) Mineralogeneza skarnelor de la Sasca Montană. 158 p., Edit. Academiei, București.

Deer W.A., Howie R.A. Zussman J. (1965) Rock forming minerals. Longmans, London.

Farmer V.C., Velde B (1973) Effects of structural order and disorder on the infrared spectra of brittle micas. *Mineralogical Magazine*, **39**, 282–288.

Gheorghiță I. (1975) Studiul mineralogic și petrografic al regiunii Moldova Nouă (zona Suvorov - Valea Mare). *Studii Tehnice și Economice*, **I/11**, 188 p.

Gheorghițescu D. (1972) Considerații privind mineralogia skarnelor cu mineralizații cuprifere de la Vărad. *St. cerc. geol. geof. geogr., s. geol.*, **17/1**, 49-66.

Kissling Al. (1967) Studii mineralogice și petrografice în zona de exoskarn de la Ocna de Fier (Banat). Edit Acad. Rom., 129 p., București.

Marka G. (1869) Einige Notizen über das Banater-Gebirge. *Jahrb. d.k.k. geol. R.A.*, **XIX**, 318-349.

von Cotta, B. (1865) Erzlagerstätten in Banat und Serbien. 105 p., W. Braumüller, Wien.

Relatively unoxidized vivianite in limnic coal from Căpeni, Baraolt Basin, Romania

ŞTEFAN MARINCEA
EMIL CONSTANTINESCU
JEAN LADRIERE-INAN

Vivianite in limnic coal from Căpeni, Baraolt Basin, Romania, is partially oxidized, despite the strongly reducing environment. The main reflections of its X-ray powder pattern may be indexed on a monoclinic cell with a 10.037(10), b 13.464(9), c 4.723(5) Å and β 102.55(4)° (space group $I2/m$) or a 10.113(14) , b 13.464(9) , c 4.723(5) Å and β 104.38(3)° (space group $C2/m$). The thermal analyses, taken in air, show effects attributable to the oxidation of Fe^{2+} to Fe^{3+} ions, *i.e.* the splitting of the first endothermic effect at about 190° C, the presence of a supplementary exothermic peak at 270°C on the DTA curve and a gradual dehydration on the TGA curve. The Mössbauer spectrum consists, however, of four quadrupole doublets associated with two sites occupied by ferrous iron and two occupied by ferric iron. Approximately 13 % of Fe (2) and 15% of Fe (1) are oxidized to Fe^{3+}. The infrared absorption spectrum shows a splitting of the fundamental H-O-H stretching at 3000 - 3500 cm $^{-1}$, as well as the absence of an (OH) band at about 3370 cm $^{-1}$, confirming a slight oxidation of the sample analyzed. Chemical analyses show that only 18 to 22 % of iron are oxidized to Fe^{3+} and that less than 7.2 % of the octahedra are occupied by cations other than iron. On the basis of the geological setting and on the trace-element chemistry, diagenetic formation in anoxic low-sulfide sediments is indicated. Partial oxidation is due to exposure to air following collection.

Introduction

Vivianite is quite widespread in sedimentary fields in Romania. It is mentioned in pellitic and psammitic rocks by Cădere (1928) and Rădulescu & Dimitrescu (1966), but has not been reported in coal. Nevertheless, occurrences in coal are mentioned by Palache *et al.* (1951) in Germany (Meklenburg) and France (Commentry, Cransac). In this paper, we describe a first occurrence of vivianite in Romanian coal. An extensive analytical investigation was deemed necessary in view of peculiarities due to the strongly reducing environment in coal deposits.

Geological setting

At Căpeni (Baraolt Basin, Bârsei Depression, East Carpathians), vivianite has been found in lignite hosted by a sedimentary sequence of Pliocene age. Lignite in this deposit is a soft dull coal containing 30 to 50% by weight humodetrinite (Borcoş *et al.* 1984). It occurs as beds included in a marly-sandy horizon that belongs to the post-tectonic cover of the Bârsei Depression. This horizon consists in an alternation of marls, tuffaceous marls and sands, with lignite intercalations. The palyno-logical content indicates a Pliocene age, whereas the microfauna and the sedimentary environment suggest a limnic origin for the whole sequence.

An X-ray diffraction study of the mineral con-tent of the Căpeni coal led to the identification, in addition to vivianite, of kaolinite, illite, gyp-sum, pyrite, marcasite, quartz, K-feldspar and calcite. Furthermore, some minor minerals, such as interlayered illite-smectite, siderite and iron sulfates with different degrees of hydration (*i.e.* szomolnokite, melanterite, jarosite) also occur.

Vivianite forms earthy nodular aggregates enclosed by marl that contains abundant coaly organic matter. These marly sequences invari-ably occur nearby the limit between the coal beds and the surrounding pelites, and are com-monly interbedded with pure coal.

The nodules of vivianite range from a few mm to more than 4 cm in diameter. They have a round shape, a spheroidal to discoidal devel-opment, and a rough surface. The constituent crystals, up to 0.1 mm in size, are very closely packed and randomly oriented.

Physical properties

A microscopic study shows that the blue-indi-go color of the earthy concretions, which indi-cates a certain degree of oxidation, has a strong pseudochromatic nature. The flat, pris-matic crystals studied in immersion are translucent to transparent and are pleochroic in light blue (α) to light green shades (β and γ). Polysynthetic twins on (010), usually recorded in oxidized vivianite (Dormann *et al.* 1982), were not observed.

The mean indices of refraction, determined in immersion using oblique illumination and sodium light (λ = 589 nm) vary between 1.63(1) and 1.65(2). The average indices of refraction, calculated from the composition in Table 1 (sample 2) and measured densities, according to the Gladstone-Dale law (Mandarino 1976), are n = 1.649(5) and n = 1.652(2), respectively, in reasonable agree-ment with the measured values.

A change in the macroscopic color, from indi-go blue to brown, occurs after heating at 100° C, and indicates a rapid superficial oxidation followed by a partial dehydration.

The density of a vivianite aggregate, measured at 22° C, by means of a pyknometer, using toluene as displacement fluid, is 2.70(1) g/cm^3. It agrees well with the value of 2.69(2) g/cm^3 established for isolated crystals by sink-float in bromoform-toluene solutions. Both values are slightly lower than that calculated on the basis of the molecular weight deduced from the chemical data in Table 1 (sample 2) and using the cell parameters in Table 2, *i.e.* 2.718 g/cm^3.

The differences are, however, minor and may be due to the different degrees of oxidation of the samples analyzed.

Thermal analyses

The thermal curves for a sample of vivianite from Căpeni are given in Figure 1. They were drawn using a MOM 1500 D derivatograph with Pt-Pt Rh thermocouple, at a mean heating rate of 10° C per min, in air. The vivianite used for analysis, as well as for other measure-ments, was gently pulverized by mechanical

Table 1. Chemical composition of vivianite from Căpeni

OXIDE	SAMPLE 1*	SAMPLE 2*	SAMPLE 3**	SAMPLE 4**	SAMPLE 5**
Fe_2O_3	8.50	10.27	9.307 [3]	9.401 [3]	9.158 [3]
FeO	34.47	32.34	33.169	33.505	32.643
MnO	-	0.92	0.922	1.284	0.923
CaO	-	0.14	0.379	0.216	0.267
MgO	-	0.60	0.505	0.938	0.756
P_2O_5	28.22	26.91	27.966	29.393	27.831
H_2O	28.70	28.38	27.752 [2]	25.263 [2]	28.422 [2]
Total	99.89	99.56 [1]	100.00	100.00	100.00
		Number of ions on the basis of 2 P atoms			
Fe^{3+}	0.536	0.678	0.592	0.568	0.585
Fe^{2+}	2.413	2.381	2.344	2.252	2.317
Mn	-	0.069	0.066	0.087	0.066
Ca	-	0.013	0.034	0.018	0.025
Mg	-	0.078	0.064	0.112	0.096
P	2.000	2.000	2.000	2.000	2.000
$(OH)^-$	0.434	1.116	0.792	0.642	0.763
H_2O	7.566	6.884	7.208	7.358	7.237

* wet-chemical analyses. Results reported in weight %.
** microprobe analyses. Mean of 4, 5, 5 point analyses.
(1) includes 14.73 % H2O+ and 13.65 % H2O-.
(2) deduced by difference.
(3) assumed on the basis of wet-chemical tests.

Table 2. Cell parameters of selected samples of vivianite

a. Refined in space group C 2 m					
LOCATION	REFERENCE	a (Å)	b (Å)	c (Å)	β
(?)	Yamaguti (1936)*	9.997	13.370	4.696	104.27°
Monserrat (Bolivia)	Barth (1937)	10.039	13.388	4.687	104.30°
Ashio (Japan)	Mori & Ito (1950)	10.08	13.43	4.70	104.50°
Huanuni (Bolivia)	Fejdi et al. (1980)	10.086	13.441	4.703	104.27°
Kamysh-Burun (Russia)	Dormann et al. (1982)	10.117	13.394	4.684	104.70°
Căpeni (Romania)	this work	10.113	13.464	4.723	104.38°
b. Refined in space group I 2/m					
LOCATION	REFERENCE	a (Å)	b (Å)	c (Å)	β
(?)	Yamaguti (1936)**	9.962	13.40	4.70	102.62°
Monserrat (Bolivia)	Barth (1937)**	9.975	13.388	4.687	102.78°
Ashio (Japan)	Mori & Ito (1950)**	9.99	13.43	4.70	102.57°
Lake Biwa (Japan)	Nakano (1992)	10.05	13.51	4.70	102.41°
- (SYNTHETIC)	PDF 30-0662	10.034	13.449	4.707	102.65°
Căpeni (Romania)	this work	10.037	13.464	4.723	102.55°

* as given by Barth (1937).
** as calculated by Donnay et al. (1963).

grinding under acetone then dried in flowing nitrogen, in order to reduce oxidation.

The thermal behavior of vivianite, and particularly its differential thermal responses, has been studied extensively. As mentioned by Rodgers & Henderson (1986) and Rodgers (1989), all previous studies showed that the major differential thermal effects between 20°C and 1000°C are basically attributable to a series of dehydrations and structural reorganization. Our interpretation of the thermal curves in Figure 1 confirms this inference.

The doublet of endothermic peaks recorded on the differential thermal analysis (DTA) curve at 183°C and 205°C, respectively (178°C and 200°C on the differential thermogravimetric, DTG curve) marks a major loss of structurally bound H_2O. The splitting of this major endotherm is obviously due to an overlapped exothermic effect, which clearly marks the beginning of oxidation of Fe^{2+} to Fe^{3+} (Dormann et al. 1982).

The weight loss calculated for this step on the basis of the thermogravimetric (TGA) curve is of about 15.5wt.%, similar to the loss reported by Dormann et al. (1982) for a slightly oxidized sample of vivianite from Anloua (Cameroon). The total loss in weight recorded by this curve, 24% in conditions of a weak increase in weight induced by the oxidation [+4.7% according to Dormann et al. (1982)], suggests that the calculated loss of H_2O approximates 5.2 molecules. This agrees with earlier determinations of Manly (1950) and Kleber et al. (1965), who estimated that this first endotherm corresponds to the depletion of five molecules of structurally bound H_2O.

The exothermic peak recorded on the DTA curve at 270°C corresponds to another phase of oxidation of Fe^{2+} to Fe^{3+}. Such an effect was not reported by Tien & Waugh (1969) or by Dormann et al. (1982), but was found by Rao (1965) at 250°C and by Vochten et al. (1979) at 260°C, and assigned to a phase transformation (Vochten et al. 1979).

The endothermic effect marked at 360°C on the DTA curve (355°C on the DTG curve) is essentially related to the loss of another two molecules of H_2O, though that loss in H_2O may be rather regarded as a dehydroxylation of a transitional phase than as a true dehydration (Dormann et al. 1982). The cumulative loss in weight recorded on the TGA curve is about 21.5 wt.%, which represents about 90% of the total H_2O lost.

An important feature of the thermal record (Fig. 1) is the absence of another endothermic effect, found by Manly (1950), Rao (1965), Kleber et al. (1965) or Tien et al. (1969) on the DTA curves of many samples, between 380 and 470°C. A similar behavior was, however, reported by Bocchi et al. (1971) for the vivianite from Anloua (Cameroon) and can be easily regarded as a progressive loss of the last molecule of H_2O, bound as hydroxyl groups in some ferric hydroxy-metaphosphates. The end of the decrease in weight marked on the TGA curve
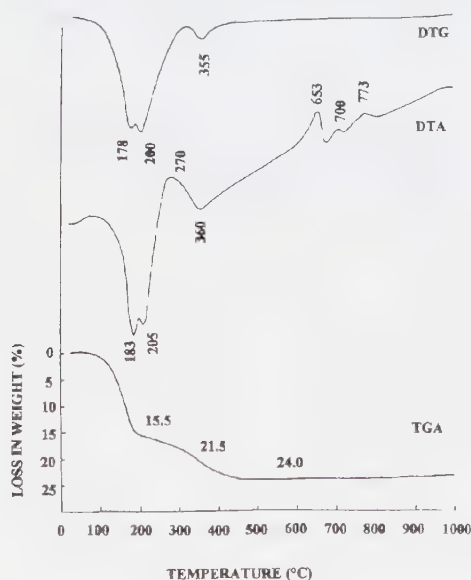

Fig. 1. Thermal curves recorded for a vivianite from Căpeni: differential thermogravimetric (top), differential thermal analysis (middle) and thermogravimetric (bottom).

corresponds to a temperature of about 470°C, the same as that reported by Tien et al. (1969) for the end of the dehydration of a vivianite from Kansas. The total weight-loss recorded on the TGA curve is 24 wt.%. After the theoretical correction of (+) 4.7 wt. % due to the oxidation of Fe^{2+} to Fe^{3+}, this loss closely approximates the total H_2O content determined by using the Penfield method (28.38 wt.%).

The exothermic effect recorded at 653°C on the DTA curve marks a major structural transformation that brings about the formation of α-$FePO_4$, $Fe(PO_3)_3$ and, occasionally, of γ-Fe_2O_3 (maghemite) (Rodgers & Henderson 1986, Rodgers 1989). Subsequently, a gradual structural reorganization, a polymorphic transformation according to Tien & Waugh (1969), gives two others small exotherms at 700 and 773°C, respectively (Fig. 1).

The fusion (or decomposition) which usually occurs between 1000 and 1200°C (Rodgers & Henderson 1986) is announced by the beginning, on the DTA and DTG curves, of an endothermic effect in the range 980°C and 970°C, respectively. This effect is visible with difficulty in Figure 1 because of drift in the apparatus, but it was clearly recorded at a lower heating rate, 5°C/min.

An X-ray powder-diffraction study of the breakdown products resulted after heating at 1000°C and cooling in air indicates the presence, as a major phase, of the ferric orthophosphate (α-$FePO_4$: PDF 29-0715). The main reflections recorded for this compound [*d* in Å (*I*)]occur at 3.461 (100), 4.382 (25), 2.362 (15), 2.180 (15), 1.871 (15) and 1.623 (10). Some supplementary reflections are attributable to admixed hydrous ortho- and metaphosphates.

Although the differences in thermal behavior between unoxidized and oxidized vivianite or between vivianite and metavivianite are too slight to be used for discrimination (Rodgers & Henderson 1986), vivianite from Căpeni

behaves as a typical unoxidized or moderately oxidized vivianite. This conclusion is supported by the recording in its thermal curves of all the effects which are generally attributable to the $Fe^{2+} \rightarrow Fe^{3+}$ transition in such compounds, *i.e.*, the splitting of the first endotherm, a supplementary exothermic peak at 270°C on the DTA curve, and a gradual dehydration on the TGA curve.

Mössbauer spectroscopy

Mössbauer spectroscopy has been used by many authors in order to estimate the degree of natural or artificial oxidation of vivianite. Thus, the studies of Vochten et al. (1979), De Grave *et al.* (1980), McCammon & Burns (1980), Dormann & Poullen (1980), Dormann *et al.* (1982) showed that the Mössbauer spectra of oxidized vivianite can be described by means of four quadrupole doublets. They differ from the spectra of unoxidized vivianite, which show only two quadrupole doublets (Gonser & Grant 1967; Mattievich & Danon 1977).

This different behavior has a structural explanation. Crystal-structure refinements reported by Mori & Ito (1950) and by Fejdi *et al.* (1980) show that, in vivianite, the octahedrally coordinated iron occupies two different structural sites, namely Fe(1) and Fe(2). Iron in the Fe(1) sites is found to be six-fold-coordinated to four H_2O ligands in a rhombic plane and by two trans oxygen atoms belonging to the $(PO_4)^{3-}$ groups. The Fe(2) sites are coordinated by two H_2O ligands in *cis* position and by four atoms of oxygen belonging to the $(PO_4)^{3-}$ groups. As a result the Mössbauer spectra of unoxidized vivianite could be decomposed into two sets of asymmetric quadrupole-split doublets associated with the two ferrous-iron-bearing sites (Gonser & Grant 1967; Mattievich & Danon 1977). The number of quadrupole splits is obviously double in oxidized vivianite because analogous ferric-iron-bearing sites occur.
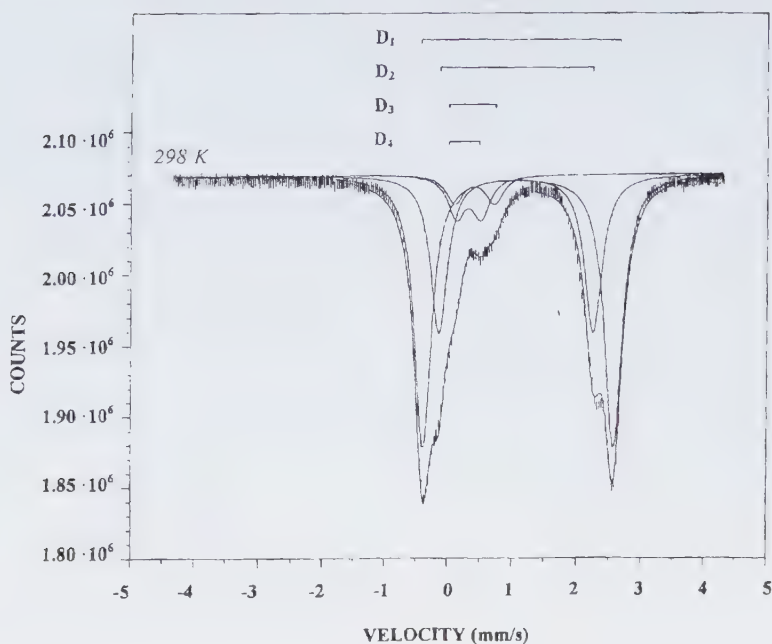
Fig. 2. Room-temperature ^{57}Fe Mössbauer spectrum of vivianite from Căpeni. Quadrupole doublets are indicated on top.

The ^{57}Fe Mössbauer spectroscopy was consequently considered as appropriate for the study of the degree of oxidation of our mineral. A Mössbauer spectrum was obtained on a time-mode spectrometer, using a constant acceleration drive. A ^{57}Co source in a Rh matrix was used, with initial activity of 5 mCi.

The spectrum was recorded at 298 K. The hyperfine parameters were determined by fitting a sum of Lorentzian lines to the experimental Mössbauer spectrum, using a least-squares iterative program.

The spectrum (Fig. 2) can be described satisfactorily by four quadrupole doublets, referred as D1, D2, D3 and D4 by Vochten *et al.* (1979); these mark the two ferrous-iron and two ferric-iron sites. The spectrum shows excellent agreement with the ones given by Vochten et al. (1979), Dormann and Poullen (1980), Dormann *et al.* (1982) and Nembrini

et al. (1983) for partially oxidized vivianite. The hyperfine parameters, isomer shift I.S. (δ) and quadrupole splitting Q.S. (Δ) obtained, the relative distributions of iron in ferrous-iron and ferric-iron sites (α), and the assignment of the four doublets to the various iron species, are presented in Table 3. The assignment of the Fe^{2+} doublets is based on the values of the isomer shift and of the quadrupole splitting found in pure vivianite by Mattievich and Danon (1977); these are also given in Table 3.

The two Fe^{3-} doublets were ascribed to the (1) and (2) sites in order to maintain a Fe(2): Fe (1) ratio that approximates 2:1, as expected. Taking into account the results, we can estimate that 13% of Fe (2) and about 15% of Fe (1) are Fe^{3+}. This finding agrees very well with the structural premises (iron coordinated to four H_2O ligands is more easily oxidizable) and with chemical data given below.

Table 3. Mössbauer hyperfine parameters, relative iron distributions (a) and sites assignment fitted to the spectrum in figure 2 *

SAMPLE	QUADRUPOLE DOUBLET	I.S. (mm/s)	Q.S. (mm/s)	α (%)	SITE	Fe^{2+}/Fe^{3+}	$Fe(2)/Fe(1)$
VIVIANITE	D_1	1.17(3)	2.38(5)	31.6	$Fe^{2+}(1)$		
FROM	D_2	1.20(3)	2.95(5)	54.6	$Fe^{2+}(2)$		
CAPENI	D_3	0.53(3)	0.61(5)	5.7	$Fe^{3+}(1)$	6.25	1.68
	D_4	0.44(3)	0.32(5)	8.1	$Fe^{3+}(2)$		
SYNTHETIC	D_1	1.15(3)	2.51(5)	33.3	$Fe^{2+}(1)$		
VIVIANITE	D_2	1.20(3)	2.97(5)	66.7	$Fe^{2+}(2)$	∞	2.00

* as compared with similar data given by Mattievich and Danon (1977) for synthetic vivianite.

Infrared absorption study

An infrared absorption spectrum of a vivianite sample from Căpeni was recorded in the frequency range between 250 and 4000 cm⁻¹, using a SPECORD M-80 spectrometer. The spectrum was obtained using a standard pressed-disk technique, after embedding a small amount of mechanically ground vivianite (2.5 wt.%) in dry KBr and compacting under 2500 N cm² pressure. The spectrum is given in Figure 3, together with a similar spectrum recorded for a sample of slightly oxidized vivianite from Anloua (Cameroon).

The main absorption bands are attributable to the vibrational modes of the hydrogen-bounded systems (hydroxyl groups, water of crystallization and adsorbed water) and of the $(PO_4)^{3-}$ groups. Their assignment is substantially facilitated by the previous results of Brunel and Vierne (1970), Vochten et al. (1979) and Piriou and Poullen (1987). The assignment of the main bands recorded in the two samples analyzed is consequently attempted in Table 4. An estimation of the degree of oxidation has been attempted on the basis of the infrared absorp-

tion data. The relevant structural effect of the substitution of the H_2O ligands by hydroxyl groups, which follow the Fe^{2+} to Fe^{3+} transition, is thought to be the distortion of the octahedra of the structure (Piriou and Poullen 1987). The resultant effect on the infrared spectrum is the decrease in intensity of the absorption bands around 3450 and 3160 cm⁻¹ (Piriou and Poullen 1987). These bands, which express the v_3 antisymmetric stretching of the H_2O molecules, are very strong in the infrared spectrum of our material (Fig. 3). This fact, as well as the evident splitting of the 3000-3500 cm⁻¹ band, indicates the presence at Căpeni of vivianite sensu stricto. On the other hand, the lack of the band at about 3260 cm⁻¹, which express the v_1' symmetric stretching of H_2O in unoxidized vivianite (Piriou and Poullen 1987), indicates a certain degree of oxidation. In both analyzed samples, this 3260 cm⁻¹ absorption band is absent and not covered by another one at about 3370 cm⁻¹, found in metavivianite and assigned to $(OH)^-$ groups (Piriou and Poullen 1987). This behavior is quite normal since the 3370 cm⁻¹ band is weak or absent in the spectra of vivianite sensu stricto. We conclude that the vivianite from Căpeni is only slightly oxidized
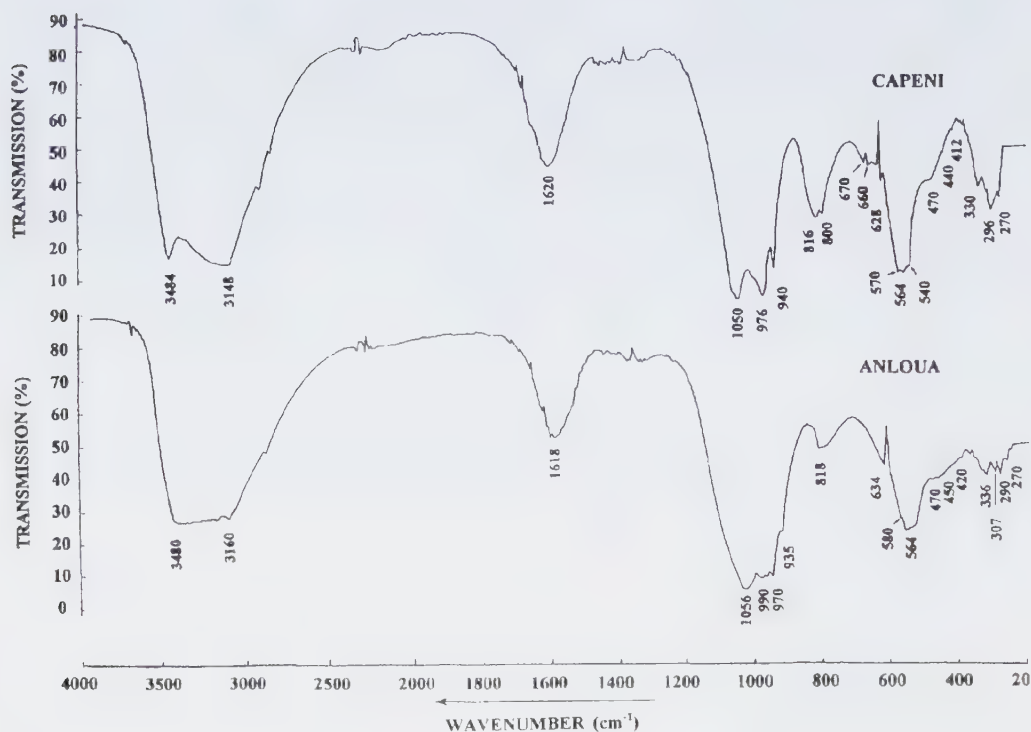
Fig. 3. Infrared spectra of vivianites from Căpeni (top) and Anloua (bottom).

and does not contain any admixed metavivianite. As can be seen in Table 4, the main absorption bands due to the $(PO_4)^{3-}$ groups lie in the 900 to 1000 cm^{-1} and 500 to 600 cm^{-1} regions. Both stretchings in the first spectral range and bendings in the second were practically recorded at the same frequencies by Tien and Waugh (1969), Brunel and Vierne (1970) and Vochten et al. (1979). It seems, therefore, that the position of the absorption bands due to this functional molecular group is not dependent on interatomic environment (e.g., on Fe^{2+} to Fe^{3+} transitions).

More relevant in this respect seem to be the low-frequency bands between 250 and 600 cm^{-1}, and particularly those below 400 cm^{-1}, which in the majority of cases can be assigned

to the internal vibrations of octahedra, which express metal-oxygen stretching and bending modes (Brunel and Vierne 1970; Vochten et al. 1979).

As the different extents of the iron oxidation in the samples induce differences in the bond strengths, the vibrational frequencies are expected to vary as a function of degree of oxidation. A comparison of our data with those of Vochten et al. (1979) for unoxidized vivianite from Anloua, Cameroon (which absorbs at 268 cm^{-1}, 304 cm^{-1}, 368 cm^{-1}, etc.) and for oxidized vivianite from Retie, Belgium (which absorbs at 272 cm^{-1}, 292 cm^{-1}, 330 cm^{-1}, etc.) indicates that the Căpeni vivianite is only slightly oxidized.

Table 4. Positions and assumptions concerning the infrared absorption bands recorder for vivianite from Căpeni and Anloua

Structural group	Vibrational mode	Căpeni	Anloua
H_2O	v_3' antisymmetric stretching	3484 cm^{-1}	3480 cm^{-1}
H_2O	v_3 antisymmetric stretching	3148 cm^{-1}	3160 cm^{-1}
H_2O	H-OH bending	1620 cm^{-1}	1618 cm^{-1}
$(PO_4)^{3-}$	v_3 antisymmetric stretching	1050 cm^{-1}	1056 cm^{-1}
$(PO_4)^{3-}$	v_1' symmetric stretching	976 cm^{-1}	970 cm^{-1}
$(PO_4)^{3-}$	v_1 symmetric stretching	940 cm^{-1}	935 cm^{-1}
H_2O	π [1]	816 cm^{-1}	818 cm^{-1}
H_2O	π [1]	800 cm^{-1}	-
-	metal-oxygen vibration [2]	670 cm^{-1}	-
-	metal-oxygen vibration [2]	660 cm^{-1}	-
H_2O (?)	(OH) libration (?)	628 cm^{-1}	634 cm^{-1}
-	metal-oxygen vibration [2]	570 cm^{-1}	580 cm^{-1}
$(PO_4)^{3-}$	v_4' antisymmetric bending	564 cm^{-1}	564 cm^{-1}
-	metal-oxygen vibration [2]	540 cm^{-1}	-
$(PO_4)^{3-}$	v_4 antisymmetric bending [3]	470 cm^{-1}	470 cm^{-1}
-	metal-oxygen vibration [3]	440 cm^{-1}	450 cm^{-1}
$(PO_4)^{3-}$	v_2 symmetric bending [3]	412 cm^{-1}	420 cm^{-1}
-	metal-oxygen vibration [3]	330 cm^{-1}	336 cm^{-1}
-	metal-oxygen vibration [3]	296 cm^{-1}	290 cm^{-1}
-	metal-oxygen vibration [3]	270 cm^{-1}	270 cm^{-1}

(1) assigned by Brunel and Vierne (1970) to the H2O ligands in the FeO4(H2O)2 and FeO2(H2O)4 groups.
(2) assumed by Brunel and Vierne (1970).
(3) as supposed by us.

X-ray powder-difraction data

The X-ray powder-diffraction analysis of a vivianite sample from Căpeni was performed with an automated Siemens D-5000 Krystalloflex diffractometer, using graphite-monochromatized CuKa radiation (λ = 1.54056 Å), at 40 kV and 30 mA. The pattern was collected in a 2θ range 10-45°, using a step size of 0.04° 2θ and a 2-second counting time at each step. Synthetic silicon, with an *a* of 5.4309 Å (PDF 27-1402) was used as internal standard. The data obtained are given in Table 5, together with those given by Sameshima *et al.* (1985) and in PDF 30-662 for synthetic Fe$_3$(PO$_4$)$_2$ ·8H$_2$O. The pattern shows that the vivianite from Căpeni does not contain admixed metavivianite. No

reflections are assignable to this mineral, and particularly the prominent ones close to 8.6 and 2.8 Å respectively, mentioned by Sameshima *et al.* (1985). Some additional reflections were found, however, at 7.019, 3.998, 3.485 and 2.821 Å. Excepting the first and the third, these are barely visible above background. These reflections are coincident with or close to the lines of bobierrite at 6.96, 4.00, 3.48 and 2.81 Å, mentioned by Fazier *et al.* (1963). Taking into account the possibility that some other lines of bobierrite are obscured by vivianite reflections, and the detection of a bobierrite-like phase by Sameshima *et al.* (1985) in many vivianite admixtures, it appears that bobierrite also is present at Căpeni.

Table 5. X-ray powder-difraction data for vivianite from Căpeni* and for synthetic $Fe_3(PO_4)_2.8H_2O$

Crt. no.	Căpeni $d_{obs}(Å)$	$d_{calc}(Å)$	I/I_0	Syntetic $d_{obs}(Å)^{(1)}$	$d_{obs}(Å)^{(2)}$	I/I_0	(hkl)
1	7.9712	7.9218	14	7.89	7.93	13	(110)
2	6.7481	6.7322	100	6.71	6.73	100	(020)
3	4.9014	4.8984	20	4.90	4.90	12	(200)
4	4.3587	4.3615	3	4.40	4.341	2	(011)
5	4.0689	4.0804	10	4.10	4.081	12	(130)
6	3.8509	3.8605	11	3.88	3.849	7	(101)
7	3.6484	3.6516	3	3.65	-	-	(-211)
8	3.2198	3.2158	17	3.22	3.210	16	(031)
9	2.9876	2.9887	20	2.99	2.985	10	(-301)
10	2.9760	2.9683	21	-	2.960	8	(211)
11	2.7140	2.7316	15	2.73	2.728	9	(-321)
12	2.7140	2.7106	15	-	2.706	9	(-141)
13	2.6379	2.6406	7	2.65	2.637	6	(330)
14	2.5989	2.5966	3	-	2.593	4	(-150)
15	2.5328	2.5371	10	2.54	2.530	8	(141)
16	2.4267	2.4275	10	2.44	2.421	6	(301)
17	2.3216	2.3253	5	2.33	2.321	7	(051)
18	2.2360	2.2349	8	2.25	2.233	5	(-341)
19	2.1820	2.1807	7	2.20	2.173	2	(022)

$CuK_\alpha 1 = 1.54056$ Å

(1) data from Sameshima *et al.* (1985)
(2) data from PDF 30-0662

A monoclinic cell of vivianite, with *a* 10.037(10), *b* 13.464(9), *c* 4.723(5) Å, b 102.55(4)° (space group *I2/m*) was found to correctly describe the average diffraction-symmetry of all the reflections given in Table 5. The cell parameters were determined by five cycles of least-squares refinement of the data in the table, using the computer program of Appleman and Evans (1973), as revised for microcomputer use by Benoit (1986). All the reflections in Table 5 could be also indexed in space group *C2/m*, found for vivianite by Mori and Ito (1950) or by Fejdi *et al.* (1980). A monoclinic cell with *a* 10.113(14) , *b* 13.464(9), *c* 4.723(5) Å, b = 104.38(3)° could also be used to describe the structure.

In both cases, the cell parameters obtained are in good agreement with those quoted for a number of natural specimens (Table 2). The derived unit-cell volume *V*, 623.001 Å·, gives, for Z = 2 and considering as average composition that of sample 2 in Table 1, a calculated density of 2.718 g/cm·. This value is in excellent agreement with those quoted by Donnay et al. (1963) for vivianite from some other occurrences (2.70 < D_x < 2.72 g/cm·). Our value must reflect, therefore, a certain degree of oxidation of the sample, which normally induces a decrease in weight due to the replacement of (OH) for H_2O.

Chemical data

Material for wet-chemical analysis was selected by hand-picking and magnetic separation. A partial and a complete analysis on two different separates (samples 1 and 2 in Table 1)

were carried out in order to test the variability of the oxidation state of iron. The concentration of P was determined by gravimetry (Maxwell 1968), and that of Mn, Ca, and Mg by atomic absorption spectrometry. The FeO content was determined titrimetrically following a modified Pratt method (Maxwell 1968), whereby Fe^{2+} is titrated in a boric-phosphoric hydrofluoric acid medium against $K_2Cr_2O_7$, using barium diphenylamine sulfonate as an indicator. The total iron content was determined by the volumetric method of Hume and Kolthoff (1957) from which the Fe_2O_3 content was obtained in a straightforward manner. As expected, a difference between the two samples occurs, but both analyses confirm the slight oxidation previously inferred: 18.2 and respectively 22.2 % of the iron, respectively, is oxidized to Fe3+. This normally induces the substitution of some H_2O ligands by $(OH)^-$ groups and the occurrence of these groups into formulae. As a consequence, the formula approximates closely to $Fe^{2+}_{3-x} Fe^{3+}_x (PO_4)_2 (OH)_x \cdot (8 - x) H_2O$, where $x <,= 1.2$ (Gamidov and Mamedov 1960, Dormann and Poullen 1980). Their proposed formula does not consider the presence of some other octahedrally coordinated cations such as Mn^{2+}, Ca or Mg, and also supposes the stoichiometric proportion of P. Although the partial composition in Table 1 fits close to 100% sum of wt.% oxides, showing that the isomorphous substitutions of Fe^{2+} by Mn^{2+}, Ca and Mg are minor, the other composition in the table indicate their presence.

Columns 3-5 represent results of electron-microprobe analyses on three separate grains, taken as an average of 4-5 random spot-analyses per grain. They were performed using a Cameca SX 50 microprobe. Operating conditions were 15 kV accelerating potential and 20 nA sample current on brass. Because the difficulties in performing electron-microprobe analyses on hydrated minerals such as vivianite (Autefage and Fontan 1985), the counting time was reduced at 10 s and a slightly defocused beam was used. The standards used were fluorapatite (P, Ca), hematite (Fe),

rhodonite (Mn) and synthetic forsterite (Mg). The oxidation state of iron was assumed on the basis of wet-chemical tests. Consequently, a Fe_2O_3:FeO ratio of 1:3.6, calculated as mean of the two wet-chemical determinations in Table 1, was applied to results of the microprobe analyses.

Taking into account the structural and compositional data reported before, the compositions in Table 1 were calculated on the basis of 4 P atoms (or 8 atoms of oxygen in the anhydrous and unhydroxylated compound). The general formula proposed by Gamidov and Mamedov (1960) was accepted as a basis for the calculations, and the proportions of $(OH)^-$ and H_2O were deduced following their scheme: $(OH)^-$ in order to maintain the charge balance and H_2O by difference. Mn was assumed to be in divalent state of oxidation.

The structural formulae show that: (1) The sum of Fe^{2+}, Mn^{2+}, Mg, Ca and Fe^{3+} invariably exceeds the stoichiometric number of 3 *apfu*. The slight excess over the stoichiometric proportion allowed in vivianite indicates the oxidation of Fe^{2+} to Fe^{3+} and shows that only relatively small amounts of $(OH)^-$ may proxy for $(PO_4)^{3-}$. (2) Manganese, generally recognized as the main isomorphous substituent of iron in vivianite (Palache et al. 1951, Ritz et al. 1974, Nakano 1992), is not abundant at Căpeni: 2.1 to 2.9% of the iron positions are occupied by manganese. Even considering the presence of other substituents such as Ca or Mg, the analyzed sample of vivianite is remarkably pure: fewer than 7.2% of the octahedral positions are occupied by other cations than iron. (3) As expected, the number of hydroxyl groups per formula unit does not exceed the limit of 1.2, beyond which the monoclinic structure of vivianite collapses to the triclinic symmetry of metavivianite (Dormann and Poullen 1980; Dormann *et al.* 1982).

As can be seen in Table 1, differences between the results of a complete wet-chemical analysis and the mean of the electron-microprobe

analyses 3-5 are minor. Consequently, the second composition listed in the table was considered as an average one and used for the calculation of the molecular weight. The accepted average composition corresponds to the higher degree of oxidation of the investigated samples. It leads to the formula: $(Fe^{2-}_{2.381}Mn^{2-}_{0.069}Ca_{0.013}Mg_{0.678})Fe^{3-}_{0.678}$ $(PO_4)_2(OH)_{1.116} \cdot 6.884 \ H_2O$, used for the calculation of molecular weight of 509.984 mass units, which gives the reported D_x.

Gladstone-Dale constants (Mandarino, 1981) were used to calculate a compatibility index of 0.016, indicating superior agreement among the average optical, physical and chemical data.

A study of trace-element concentrations in the vivianite from Căpeni confirms the purity of the sample. It was carried out by means of inductively coupled plasma-emission spectrometry, using a JOBIN-YVON 138 ULTRA-CE spectrometer. Only the siderophile elements such as Co (34.2 ppm), Ni (17.7 ppm), Zn (43.7 ppm) are well represented. They suggest, as well as the contents of Sc (5.5 ppm), Nb (3.4 ppm), Ti (10 ppm) and Th (2 ppm), some diadochic replacements of iron. An unusual enrichment in Ba (27.7 ppm) and the presence of Sr (2.4 ppm) are reported for a calcium content of 0.15 %.

The rare-earths elements (REE) are deficient in the Căpeni vivianite: the sample contains 8.94 ppm Y, 3.77 ppm La and 3.40 ppm Yb, which indicates a strong deficiency with respect to "normal" concentrations in sedimentary materials, approximately 230 ppm according to Herrmann (1978).

The chondrite-normalized concentrations of REE, with chondrite values from Herrmann (1978) illustrate a slight fractionation, since $(La/Yb)_N = 0.49$. Note that the heavy REE predominate over the light ones, as expected in lacustrine deposits.

Discussion

Generally, vivianite forms either from hydrothermal solutions or by direct precipitation from groundwater. It is obvious that at Căpeni hydrothermal activity need not be considered. A sedimentary-diagenetic mode of formation seems likely.

Rosenqvist (1970), Nembrini et al. (1983), Manning et al. (1991) and Nakano (1992), among others, speculated that aggregates of vivianite can grow by diffusion in pore water in reducing environments, such as the bottom sediments in limnic areas. Moreover, the factors necessary for the formation of vivianite, i.e., the presence of ferric oxy-hydroxides (Manning et al. 1991) and of organic (wood) remains (Nriagu and Dell 1974) and, implicitly of the electric field due to organic decomposition (Zelibor et al. 1988), all occurred in the sedimentary basin at Căpeni. Deposition and diagenesis occurred under fairly oxidizing conditions, since sulfides such as pyrite or marcasite are low in abundance in the vivianite-bearing sequences. However, as Manning *et al.* (1991) pointed out, in some other limnic areas the bottom sediments are sulfide-bearing. Therefore, if sulfur had been available, iron sulfides would have been able to form. Their scarcity, as well as that of the derivative sulfates (e.g., szomolnokite, melanterite, jarosite), may indicate an absence of sulfur in water during deposition. Consequently, at Căpeni, iron coming from a vent system precipitated as ferric oxy-hydroxides and then reduced to vivianite, in an environment that was sufficiently oxidizing to form $(PO_4)^{3-}$. This is entirely consistent with the affirmation of Berner (1981) which concluded that vivianite generally occurs in anoxic low-sulfide sediments.

Some supplementary conclusions may be drawn on the basis of the trace-element geochemistry of the vivianite. The enrichment in Ba and the presence of Sr, despite the low Ca

content, are not uncommon, since Ba becomes strongly concentrated into some lacustrine sediments such as shale, particularly in black shale. This behavior, which suggests a connection of Ba with organic matter (Puchelt 1974) explains its abundance in the samples of vivianite analyzed. On the other hand, it seems that the concentration of the REE is independent of Ca concentration. The deficiency in REE may be explained by the low pH, which favors dissolution of carbonates and mobilization of lanthanides. The low pH, which explains the low abundance of REE in shales and sandstones from coal-bearing deposits (Balashov *et al.* 1964) is common during crystallization of vivianite. The marked relative enrichment in heavy REE is anomalous only in appearance. According to Balashov et al. (1964), an increased acidity, i.e., a higher content of HCO_2^- in natural waters, causes a higher solubility of the heavier lanthanides, relative to the lighter ones. A preferential inflow of the heavy REE to the sedimentary basin is then to be presumed. This "excess" would precipitate with the iron and must be incorporated into the vivianite after the reduction of the initial ferric oxy-hydroxides.

All the physical and chemical data presented above show that the analyzed vivianite is partly oxidized. This oxidation probably occurred on exposure of the samples to air after their collection. One can infer that most of the museum and laboratory specimens which were analyzed by various authors were submitted to different degrees of oxidation upon removal from their initial environment.

Acknowledgments

References

Appleman D.E., Evans H.T. (1973) Indexing and least-squares refinement of powder diffraction data. *U.S. Geol. Surv., Comput. Contrib.* **20** (NTIS Doc. PB-216).

Autefage E.F., Fontan F. (1985) Comportement de minéraux hydratés au cours de leur analyse à la microsonde électronique. *Bull. Minéral.* **108**, 293-304.

Balashov Yu.A., Ronov A.B., Migdisov A.A. Turanskaya N.V. (1964) The effect of climate and facies environment on the fractionation of the rare elements during sedimentation *Geokhimiya* **8**, 951-969 (in Russ.).

Barth F.W. (1937) Crystallographic studies in the vivianite group. *Am. Mineral.* **22**, 325-341.

Benoit P.H. (1986) Adaptation to microcomputer of the Appleman-Evans program for indexing and least-squares refinement of powder-diffraction data for unit-cell dimensions. *Am. Mineral.* **72**, 1018-1019.

Berner R.A. (1981) A new geochemical classification of sedimentary environments. *J. Sed. Petrol.* **51**, 359-365.

Bocchi G., Bondi M., Foresti E., Nannetti M.C. (1971) Carracteristiche chimiche, termiche, ottiche e roentgenografiche della vivianite di Anloua (Cameroun). *Miner. Petrogr. Acta* **17**, 109-133.

Borcoş M., Kräutner H.G., Udubaşa G., Săndulescu M., Năstaseanu S. and Biţoianu C. (1984) Map of the mineral resources.Explanatory note. In Geological Atlas of Romania (1:1 000 000). Institute of Geology and Geophysics, Bucharest, Romania.

Brunel R., Vierne R. (1970) Spectres de réflexion infrarouge de minéraux monocristallins ou en poudre (II). *Bull. Soc. fr. Minéral. Cristallogr.* **93**, 328-340.

Cădere D.M. (1928) Fapte pentru a servi la descrierea mineralogică a României. *Mem. Sect. St. Acad. Rom.*, **ser.III, 6**, Bucureşti.

De Grave E., Vochten R., Dessein H., Chambaere D. (1980) Analysis of some oxidized vivianites. *J. Phys.*, **C 1**, Suppl. 41, 407-408.

Donnay J.D.H., Donnay G., Cox E.G., Kennard O., King Vernon M. (1963) Crystal Data. Determinative Tables (2nd ed.). Williams and Heintz, Washington, D.C.

Dormann J.L., Gasperin M., Poullen J.F. (1982) Etude structurale de la séquence d'oxydation de la vivianite, $Fe_3 (PO_4)_2 \cdot 8H_2O$. *Bull. Minéral.* **105**, 147-160.

Dormann J.L. and Poullen J.F. (1980) Etude par spectroscopie Mössbauer de vivianites oxydées naturelles. *Bull. Minéral.* **103**, 633-639.

Fazier A.W., Lehr J.R., Smith J.P. (1963) The magnesium phosphates hannayite, schertelite and bobierrite. *Am. Mineral.* **48**, 635-641.

Fejdi P., Poullen J.F., Gasperin M. (1980) Afinement de la structure de la vivianite $Fe_3^{2+} (PO_4)_2 \cdot 8H_2O$. *Bull. Minéral.* **103**, 135-138.

Gamidov R.S., Mamedov K.S. (1960) On the structure of vivianite and its derivates. Azerbaidzhan Khim. Zh. 4, 121-125 (in Russ.).

GonserU., Grant R.W. (1967) Determination of spin directions and electric field gradient axes in vivianite by polarized recoil-free g-rays. *Phys Stat.Solid.* **21**, 331-342.

Hermman A.G. (1978) Yttrium and lan-

thanides. In Handbook of Geochemistry II-5 (K.H. Wedepohl ed.). Springer Verlag, Berlin, Germany (39, 57-71, B-M, O).

Hume D.N., Kolthoff I.M. (1957) The use of cacotheline as an oxidation-reduction indicator before the volumetric determination of iron. *Anal. Chim. Acta* **16**, 415-418.

Kleber W., Wilde W., Frenzel M. (1965) The thermal decomposition and oxidation of bivalent iron in vivianite. *Chem. Erde* **24**, 77-93.

Mandarino J.A. (1976) The Gladstone-Dale relationship. I. Derivation of new constants. *Can. Mineral.* **14**, 498-502.

Mandarino J.A. (1981) The Gladstone-Dale relationship. IV. The compatibility concept and its application. *Can. Mineral.* **19**, 441-450.

Manly R.L., Jr. (1950) The differential thermal analysis of certain phosphates. *Am. Mineral.* **35**, 108-115.

Manning P.G., Murphy T.P., Prepas E.E. (1991) Intensive formation of vivianite in the bottom sediments of mesotropic Narrow Lake, Alberta. *Can. Mineral.* **29**, 77-85.

Mattievich E., Danon J. (1977) Hydrothermal synthesis and Mössbauer studies of ferrous phosphates of the homologous series $Fe_3^{2+} (PO_4)_2 (H_2O)_n$. J. Inorg. *Nucl.Chem.***39**, 569-580.

Maxwell J.A. (1968) Rock and mineral analysis. In Chemical Analysis. A Series of Monographs on Analytical Chemistry and Its Applications.(P.J. Elving, I.M. Kolthoff Eds.) Vol. 27, Interscience Publishers, London, U.K.

Mc Cammon C.A, Burns R.G. (1980) The oxidation mechanism of vivianite as studied by Mössbauer spectroscopy. *Am. Mineral.* **65**, 361-366.

Mori H., Ito T. (1950) The crystal structure of vivianite and simplesite. *Acta Crystallogr.* **3**, 1-6.

Nakano S. (1992) Manganoan vivianite in the bottom sediments of Lake Biwa, Japan. *Mineral. J.* (Japan) **16**, 96-107.

Nembrini G.P., Capobianco J.A., Viel M.,

Williams A.F. (1983) A Mössbauer and chemical study of the formation of vivianite in sediments from Lago Maggiore (Italy). *Geochim. Cosmochim. Acta* **47**, 1459-1464.

Nriagu J.O., Dell C.I. (1974) Diagenetic formation of iron phosphates in recent lake sediments. *Am. Mineral.* **59**, 934-946.

Palache C., Berman H., Frondel C. (1951) The system of mineralogy II. John Wiley and Sons, New York, N.Y.

Piriou B., Poullen J.F. (1987) Etude infrarouge des modes vibrationnels de l'eau dans la vivianite. *Bull. Minéral.* **110**, 697-710.

Puchelt H. (1974) Barium. In Handbook of Geochemistry II-4 (K.H. Wedepohl ed.). Springer Verlag, Berlin, Germany (56, B-O).

Rădulescu D., Dinitrescu R. (1966) Mineralogia topografica a României. Academic Ed., Bucharest, Romania.

Rao A.B. (1965) Note on the DTA study of some rare Brazilian phosphate minerals. *Mineral. Mag.* **35**, 427-428.

Ritz C., Essene E.J., Peacor D.R. (1974) Metavivianite, $Fe_3 (PO_4)_2 \cdot 8H_2O$, a new mineral. *Am. Mineral.* **59**, 896-899.

Rodgers K.A. (1989) The thermochemical behaviour of vivianite and vivianite / metavivianite admixtures from Borne (Netherlands) and Mangualde (Portugal). *Geol. Minjbouw* **68**, 257-262.

Rodgers K.A., Henderson G.S. (1986) The thermochemistry of some iron phosphate minerals: vivianite, metavivianite, baricite, ludlamite and vivianite / metavivianite admixtures. *Thermochim. Acta* **104**, 1-12.

Rosenqvist I.T. (1970) Formation of vivianite in Holocene clay sediments. *Lithos* **3**, 327-334.

Sameshima T., Henderson G.S., Black P.M. Rodgers K.A. (1985) X-ray diffraction studies of vivianite, metavivianite and baricite. *Mineral. Mag.* **49**, 81-85.

Tien P., Waugh T.C. (1969) Thermal and X-ray studies on earthy vivianite in Graneros Shale (Upper Cretaceous), Kansas. *Am. Mineral.* **54**, 1355-1362.

Tien P., Waugh T.C., Dilts R.L. (1969) Vivianite in Graneros Shale (Upper Cretaceous), Central Kansas. *Kansas Geol. Surv. Bull.* **194**, 21-24.

Vochten R., De Grave E., Stoops G. (1979) Petrographic, chemical and Mössbauer study of some oxidized vivianite nodules from Retie (Province of Antwerp, Belgium). *Neues Jahrb. Mineral., Abh.* **137**, 208-222.

Yamaguti T. (1936) Diffraction of cathode rays by vivianite. *Proc. Phys.-Mat. Soc. Japan (3)*, **18**, 372-379.

Zelibor J.L., Senftle F.E., Reinhardt J.L. (1988) A proposed mechanism for the formation of spherical vivianite crystal aggregates in sediments. *Sediment. Geol.* **59**, 125-142.

II. ROCK FORMING MINERALS

The garnets in the skarn at Sasca Montană

EMIL CONSTANTINESCU

The garnets from Sasca Montană (Banat, Romania) are mainly represented by a mixture of grossularite and andradite, but in contrast with other garnets from the Banat province, they contain a relatively high proportion of pyralspite. Some garnet crystals have euhedral zoning with a striking optical anizotropy. The paper suggests that anizotropic zones are a consequence of the variation in the proportion of aluminum and iron.

The garnets in the skarns associated to the Laramian magmatites of Banat, due to their participation , as well as through their chemical and structural characteristics, have attracted long ago the attention of the researches, outlining a classical area for the study of these minerals.

The research undertaken on the garnets of Sasca Montană skarns has been focused on their complex characterization in terms of chemical composition structure and physical properties, but also on the some aspects related to their optical and composition anomalies.

The garnets represent the essential component of the thermal and metasomatic contact area, both with regard to their participation in most of the primary associations, characteristic to the different skarn types: apobanititic (+ diopside + vesuvianite); periskarns (+ K-feldspar + aegirine-augite); apocalcareous (+ wollastonite); apodolomite (+ tremolite + humites + anthophyllite), as well as of the secondary associations (epidote + calcite).

The garnets form compact monomineralic masses or appear as crystalloblasts in wollastonitites, shaped as nests and stripes, or making up accumulations of euhedral crystals in a matrix of largely recrystallized calcite or in geodes.

The euhedral crystals have rhomboidal dodecahedron and trapezohedron faces, or combinations of faces of dodecahedron and trapezohedron. The following forms were identified: {110}, {111}, {100}, {211} and {311}.

The color varies within a wide range: from black, dark brown, brown, to yellowish-brown, yellow, yellowish-green, grass-green, dark-green and withe. Despite of some attempts to correlate the color with the presence of different terms from the grandite series, or with the influence of some chemical substitutions – justified by correlations of elements in particular cases – it is difficult to give an explanation for such a wide color variation of the garnets from Sasca Montană. The spe-

Table 1. Chemical analyses of the garnets from Sasca Montană skarns

Sample/Oxides%	328	330	331	332
SiO_2	35.86	39.40	36.46	36.70
TiO_2	0.15	0.60	0.14	0.41
Al_2O_3	4.60	21.14	3.31	18.39
Fe_2O_3	25.31	3.91	26.22	11.20
FeO	0.49	0.89	0.57	1.62
MnO	0.17	0.15	0.35	0.18
MgO	2.30	0.61	0.86	1.90
CaO	29.33	32.40	31.85	29.50
H_2O^+	0.10	0.07	0.04	0.06
$H_2O_2^-$	0.66	0.59	0.30	0.38
Total	99.98	99.76	100.10	100.42

Number of ions in the basis of 24(0)

Si	5.916	6	5.515	6.00	6.015	-	5.626	6.00
Al	0.084		0.485		-		0.374	
Al	0.807		3.773		0.641		2.841	
Fe³⁺	0.130	3.95	0.209	4.04	3.253	3.91	1.197	4.08
Ti	0.018		0.058		0.017		0.047	
Mg	0.017		0.227		0.078		0.537	
Fe²⁺	0.067	5.96	0.203	6.05	0.048	6.07	0.023	5.97
Mn	0.023		0.217		0.213		0.217	
Ca	5.148		5.136		5.360		5.211	

Proportion of end members (in mole %)

andradite	79.9	5.1	85.8	29.8
grossularite	5.1	84.1	8.3	57.5
almandine	1.1	3.4	0.8	0.4
pyrope	13.5	3.8	1.4	8.9
spessartine	0.4	3.6	3.7	3.4

Physical constants

n	1.83	1.75	1.87	1.77
G	3.78	3.61	3.89	3.69
a(Å)	11.95 Å +/-0.005	11.87 Å +/-0.008	12.36 Å +/-0.008	11.92 Å +/-0.005
D	1.188 kg/mm² (7.25 Mohs)	1.038 kg/mm² (6.37 Mohs)	1.089 kg/mm² (7.25 Mohs)	1.093 kg/mm² (6.9 Mohs)

328 - yellowish - green grandite, Sasca Română; 330 - light brown grandite, Stanapari; 331 - dark green grandite, Cărbunari; 332 - dark reddish - brown grandite, Dealul Orașului.

cific weight determinations pointed out values between 3.61 and 3.89 (Table 1), but there was no indication of a major variation among the analyzed samples.

The micro-hardness tests (Table 1) show values between 1033 kg/sq.mm and 1189 kg/sq.mm higher for the high-andradite terms.
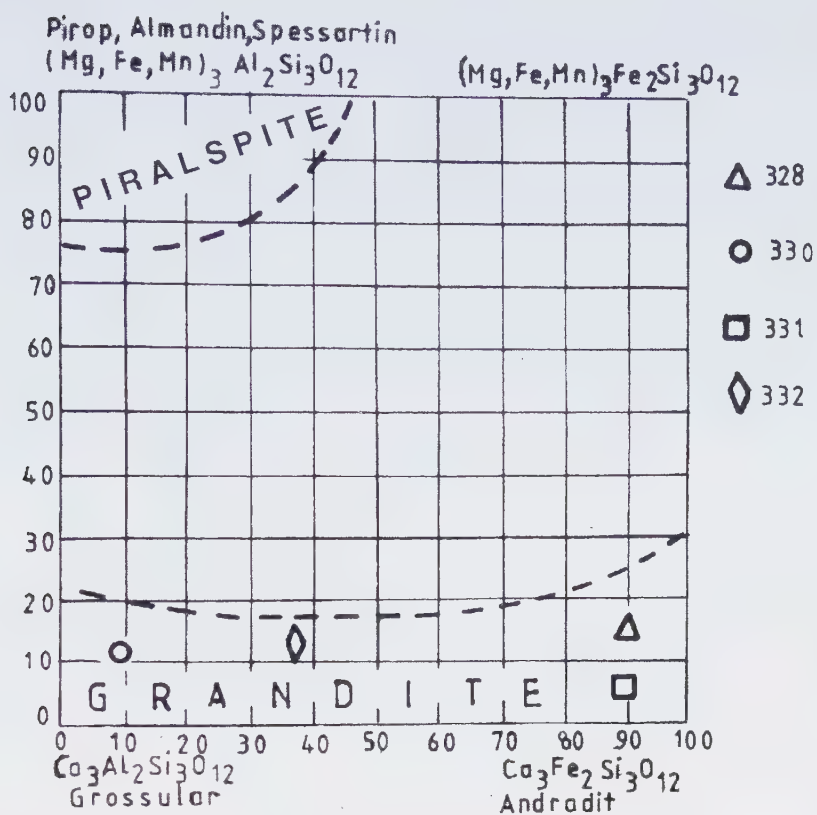
Fig. 1. Projection of values representing end members (in mole%) obtained for garnets of Sasca Montană, on the Boecke diagram: 328 - Sasca Română; 330 - Stânăpari; 331 - Cărbunari; 332 - Dealul Orașului.

The values of refraction indexes tested with M.U.F., according to the Nikitin method on nine samples (Table 1, Fig. 2), vary between 1.74 and 1.87.

Crystal-chemistry of the garnets

Garnets represent a group of minerals the formula: $X_3Y_2(ZO_4)$, where: $X=Ca^{2+}$, Fe^{2+}; $Y = Fe^{3+}$, Al^{3+}, Cr^{3+}; $Z= Si^{4+}$ (Al^{3+}), where the coordination number may be 8, for the cations: Ca^{2+}, Mg^{2+}, Mn^{2+}, or 6 for the cations: Fe^{3+}, Al^{3+}, Cr^{3+} and Si^{4+}, (Al^{3+}).

In a synthesis of a large number of chemical analyses, Boeke (1914) noticed that there are two series – the pyralspites $(Mg, Fe, Mn)_3Al_2(SiO_4)$ and ugrandites – $Ca_3(Al,Fe,Cr)_2(SiO_4)_3$,

separated by a wide miscibility gap (Fig. 2). The garnets from the skarns are generally represented by grandites, while those from crystalline schists are represented by pyralspites, due to the control exerted by the pressure in the environment where the rock is formed. In order to define the chemical composition of the Sasca Montană garnets, four chemical analyses were carried out, that made it possible to calculate the structural formula, relating them to the basis of 24(O) (Table 1). The composition in end members of the garnets recalculated in molecular ratios, is also given in Table 1.

The analyzed garnets (samples 328, 330, 331, 332) as well as the garnets whose chemical composition was deducted from X-ray powder

diffraction and from IR spectroscopy (samples 329, 333, 334, 339) have an outstanding compositional variety, covering the range from 85.8 mole% andradite, to 84.1 mole% of grossularite. This differentiates them from the almost exclusively andraditic garnets of Ocna de Fier (Kisling, 1967), Dognecea (Vlad, 1975), Moldova Nouă (Gheorghiță, 1975) or Oravița where the occurrence of the grossularite is a characteristic (Moencke 1962); Cioflică et al. 1975). The projection of the chemical composition of the Sasca Montană garnets onto the Boecke diagram, (Fig. 1), emphasizes an important participation of pyralspites.
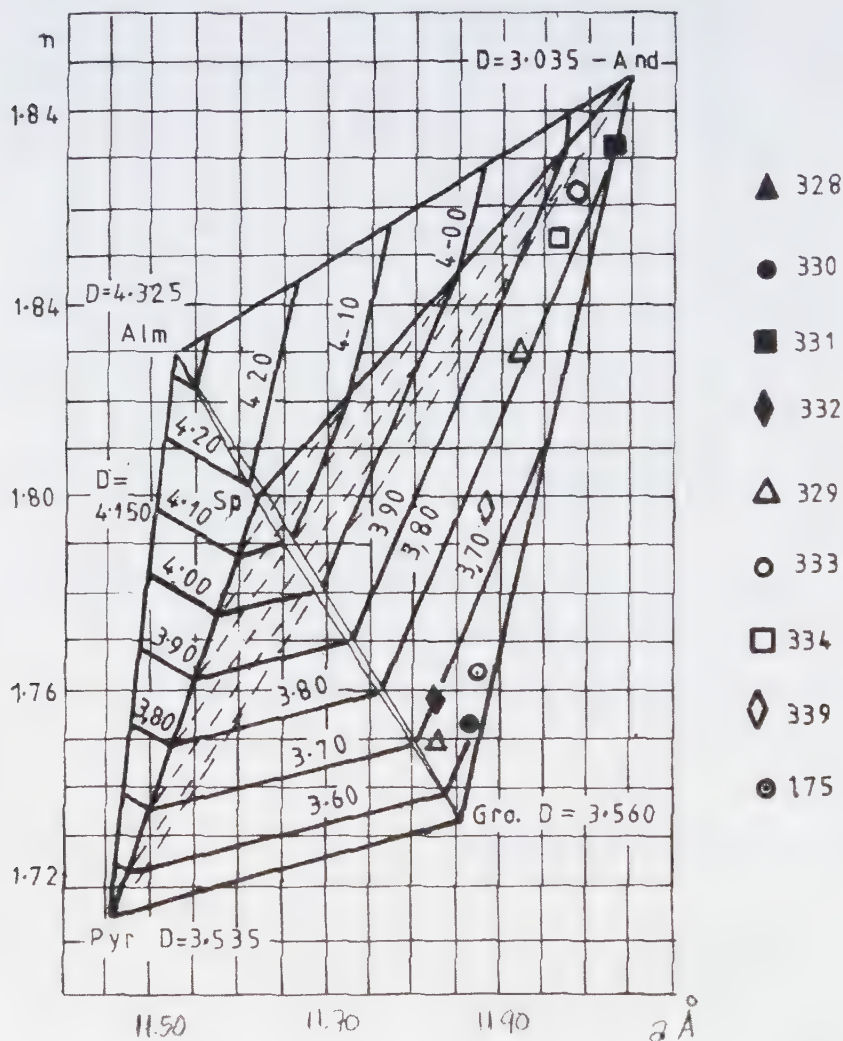

Fig. 2. Projection of the "a" unit-cell parameter, of the "n" refraction index and of the "G" specific weight of the Sasca Montană garnets in the Winchell diagram: 328 - Sasca Română; 330 - Stânăpari; 331 - Cărbunari; 332 - Dealul Orașului; 329 - Ogașul lui Ilie; 333 - Valea Gheorghe; 334 - Sasca Română; 339 - Dealul Gheorghe; 175 - Cioaca Înaltă.

X-ray diffraction study

The unit-cell parameter is considered an essential element to the garnets diagnosis. The variation diagrams and the regression curves for garnets identification (Ford, Fleischer and Skinner diagrams) are based upon the linear variation of the "a" reticular parameter and upon several physical properties (refraction index, specific weight), along with the change in the chemical composition. This variation is valid for the miscibility between two end-members: the emergence of several component terms that change linearity may bring about consistent errors.

In order to solve out this problem, Winchell (1958) drew up tetrahedral diagrams where the refraction index and the unit-cell parameter, taken as independent variables are considered the ordinate and the abscissa respectively, while the chemical composition and the specific weight are considered as functions of these two variables.

The composition of the analyzed garnets may thus be determined following fields, delimited by three or four extreme terms. On the diagram in Fig. 2 there are the values of the "a" parameter; calculated from the reflexes measured on diffractograms [4] and the values of the specific weight and refraction indexes obtained on nine garnets. In comparison with the end member participation, one can notice that the presence in samples 328, 330, 331 and 332 of pyralspites (mainly pyrope) entails a drop in the values of the 'a" unit-cell parameter, below the values set when only the grossularite-andradite ratio is considered.

Infrared absorption analysis

Structural details and determinative indications may be obtained on garnets by means of the infra-red analysis. The interpretation of the absorption spectra of garnets was the topic of the works published by Moencke (1966), Tarte (1960), Dimanche and Tarte (1965). The main results may be summarized as follows:

- The IR spectra have patterns very specific to this group of minerals, clearly different from that of other types of silicates.

- The aspect of the diagrams is largely similar, irrespective of the nature of the bivalent or trivalent cations, with the exception of the titanium varieties of the melanite-skorlomite-ivarite series, where the aspect of the spectrum is modified because the Ti partially replaces Si in tetrahedral coordination, creating characteristic absorption bands.

- The possibility to separate the pyralspites from ugrandites is given by the fact that in case of pyralspites, there are two bands within the range 280-350 cm^{-1}, that are not found in ugrandites. The bands are ascribed to the metal-oxygen vibrations of the bivalent cations (Fe^{2+}, Mn^{2+}, Mg^{2+}), in octahedral coordination. Within the ugrandites series, the bivalent cation is represented by the Ca, while the Ca-O ionic bands do not yield a proper intensity to the absorption bands in this field.

- Characteristic details for different types of garnets of the two series may be noticed in the area of the spectrum with frequencies below 500 cm^{-1}. As a consequence of the fact that the absorption bands of this area are linked to the metal-oxygen vibrations, their position is mainly determined by the nature of the cations.

- In the case of isomorphous substitutions, a migration of the bands was noticed, pendant to the cations replacements. One can establish a connection between the variation of the band frequencies and the variation of the parameter "a". This variation is valid for bands frequencies that exceed 500 cm^{-1}.

The interpretation of the aspect of the absorption bands on the spectra of the Sasca Montană garnets and the comparison of the frequency

values with the literature data, emphasize that we may deal with grandites of intermediate composition. At the same time one could notice a variation of the values of the diagnostic bands which can be related, as a whole, to the variation of the "a" unit-cell parameter.

Optical and compositional characteristics

Optical anomalies. Most of the Sasca Montană garnets are isotropic. Yet, anisotropic garnets could sometimes be detected. In general, they are largely developed, with a euhedral outline, and divided into zones that can be seen on the microscope, through variations of the color intensity. They develop in free spaces or in veins and are late in comparison with the isotropic garnets.

The anisotropic garnets have two types of optical anomalies: (1) sectorial anomalies – in the crystals appear divided into sectors, generally with a triangular form, pointing to the centre of the grain. The limits between the sectors are either clear or diffuse. Generally, opposite sectors have the same optical orientation; (2) lamellar anomalies - the crystals have a system of lamellae of variable widths alternately isotropic and anisotropic, and parallel with the border of the granules. The lamellae are distinguishable by the in color of birefringence (variable from 0.001 to 0.005) and the color seen with one polar (from colorless to yellowish). The angle of optical axes varies within the anisotropic areas from 20 to 70 degrees.

The problem of the anisotropy of garnets was brought up by many works; the phenomenon was mainly related to grandites, to the variation of the iron content, degree of order and disorder in the network and crystallization kinetics.

Our electron microprobe study on birefringent garnets from Dealul Gheorghe, Sasca Montană, showed that the alternation of isotropic and anisotropic lamellae corresponds to a regular modification of iron and aluminum content, hereby suggesting a rhythmic variation of the Fe/Al potential within the metasomatic process. Verkaeren (1971) presumes, with regard to the isotropic garnets of Sardaigne that the Fe/Al division into zones might have been caused by the circulation on the rock fractures during the last stage of skarn formation of a residual fluid richer in iron that caused the alternation of garnets.

The microscopic examination of the anisotropic garnets from Sasca Montată pointed out a massive diopside replacement, yet this presence has no impact on the linearity of the limits between the isotropic and anisotropic zones. This finding suggests the existence of deforming twin crystals. If this hypothesis is true, it could represent an argument for a genetic mechanism similar to the one mentioned by Verkaeren.

Characteristics of the composition. A remarkable feature of the analyzed garnets is related to the relatively high content of pyralspites (15.0; 12.7; 10.8; 5.9% mole%, Table 1), as compared to most grandite analyses published the literature. It is worth mentioning that one of the highest content of pyralspites regarding the grandites of the primary skarns can be identified in an analysis of the andradite from Ocna de Fier, Zombory (1934), *fide* Deer et al. (1965) – with 89.3% and 9.7% sp. 1% alm. A high content of pyralspites was also identified in the garnets of Dognecea skarns (Vlad, 1974), as well as in the Oravița garnets (Cioflică et al.).

If the subsequent studies will confirm this tendency, it could be seen as a noticeable peculiarity of the mineralogy of to the Banat skarns. Even in this context, the Sasca Montană garnets are individualized by a scarce presence, within the above mentioned percentages (13.5%, 8.9%) of the pyrope molecules in the calcic garnets of the primary skarns. The limits and particularities of the miscibility between the grandites and pyralspites is high-

ly interesting due to the differences, in terms of the ionic ray, between the Ca^{-2} cations, on one hand, and the Mg, Fe^{-2}, Al, on the other hand enough to cause changes of structure.

The diagram of the mutual solubilities among the end-members of the garnets group (Boecke), has represented lately the object of many debates and reviewing attempts, starting from different syntheses and laboratory tests performed over a longer period of time. Nemec (1967) analysed the miscibility between pyralspites and grandites as a function of several experimental data and of the petrographic context of the analyzed garnets. He considered that only the grossularite-spessartine occurrence is stable inside the facies of the pyroxene hornfels, due to the fact the spessartine is the only garnet from the pyralspite group that may be synthesized at low atmospheric pressures and temperatures. The synthesis of almandine and pyrope was performed at high temperatures and pressures according to the test data obtain by Coes (1955), Boyd and England (1959). Nemec sustains that the grossularite-almandine miscibility is possible solely within the conditions of the granulite facies.

Sobolev (1964), who studied different stages of miscibility between the grossularite and pyrope in the eclogites of Jakutsk, considers that only the high pressure of 20-30Kb may have generated the formation of mixed crystals between these members, despite the difference of ionic ray of both Mg and Ca.

However, Dimanche (1969) described in the region of Ginevro (Elba) a ferroan grossularite with 16% almandine, in skarns whose protogene character is well proved. In order to explain this composition he resorted to Gilbert's experimental data (1966) who obtain grossularite- and almandine-rich garnets, by dehydrating amphiboles, under a low oxygen fugacity and under a fluid phase pressure rated at about 500 bars. Dimanche considers that in the case of environments responsive to a con-

venient temperature, the oxygen fugacity, and less the total pressure, determine the composition of some garnets.

The relatively high content of pyrope in some garnets from Sasca Montană also suggests that there may exist a notable Mg-Ca substitution considered until now as difficult to achieve under the low pressure specific to the skarns.

Acknowledgements

References

Cioflică Gr., Vlad Ş., Vasiliu C. (1967) Granaţii din skarnele de la Băiţa Bihorului, *St. cerc. geol. geofiz. geog., ser. geol.* **12**, 1.

Deer, Howie, Zussman (1963) Rock forming minerals, Logmans, London.

Dimanche F., (1969) Sur les particularites d'un grenat issu des skarns a magnetite du Ginevro (île d'Elbe, Italie), *Bul. Soc. Fr. Min. Crist.* **92**, 468-471.

Gentile A.L., Roy R., (1960) Isomorphism and crystalline solubility in the garnet family, *Amer. Min.*, **45**.

Gheorghiţă I. (1975) Studiul mineralogic şi petrografic al regiunii Moldova Nouă, *St. teh. şi ec.*, **11**, 1-188.

Gheorghitescu D., (1975) Studiul mineralogic şi geochimic al formatiunilor de contact termic şi metasomatic de la Oraviţa (Coşovita), *D. S. Ins. Geol.*, **LXI**.

Gilbert M.C. (1966) Ssynthesis and stability relations of the relations of the homblende ferropargasite, *Amer. Journ. Sci*, **264**, 698-742.

Huckenholz H.G. (1969) Synthesis and stability of Ti-andradite, *Amer. Journ. Sci.*, **267**;

Huckenholz H.G., Yoder H.S. jr. (1971) Andradite stability in the $CaSiO_3$-Fe_2O_3 join up to 30 kb. *Neu Jahrb. f. Min.*, **114**;

Kalinin D.V. (1966) O sviazi anizotropii grana-
tov s sostavom i himiceskoi ovstanoscki ih
sinteza Dokl., *Ak. Nauk SSSR*, **172**;

Kissling Al., (1967) Studii mineralogice şi
petrografice îin zona de exoskarn de la
Ocna de Fier (Banat), Ed. Acad.,
Bucureşti.

Lee D.E. (1958) An andradite - spessartite gar-
net from Jajsberg Sweden, *Amer. Min.*, **43**.

Moenche H., (1962) - Mineral Spektren.
Akademie Verlag, Berlin.

Nemec D., (1967) The miscibility of the pyral-
spite and grandite molecules in garnets,
Min. mag., **36**; 389-403.

Skinner B.J. (1956) Physical properties of end
membres of the garnet group. *Am. Min.*, **41**;

Tarte P., (1960) Infra - Red - Spectrum of
Garnets: *Nature,* **186**, 234.

Tarte (1960) Recherches sur le spectre
infrarouge des silicates: *Silicates ind* **4**, 3-7.

Verkaeren J., (1971) Les grenats birefringents
des skarnes a magnetite de san Leone (sar-
daigne S-W): *Bull., Soc. fr. Min. Cris.*, **94**;
492-499.

Vlad Ş., (1974) Mineralogeneza skarnelor de
la Dognecea. Ed. Acad. Bucureşti.

Winchel H., (1958) The composition and
physical properties of garnet, *Am. Min.* **43**,
p. 595-596.

Nepheline from the alkaline massif of Ditrău

EMIL CONSTANTINESCU
NICOLAE ANASTASIU

Nepheline is found in foidic syenites, monzonites and essexites. The characteristic assemblages are: nepheline+microcline+albite; nepheline+microcline+biotite; nepheline+microcline+albite +biotite+hornblende; nepheline+microcline+albite+oligoclase+biotite; nepheline+microcline +albite+oligoclase+biotite+hornblende+pyroxene. Nepheline has euhedral, subhedral and anhedral forms and, often, presents "myrmekitic" intergrowths with kalsilite. The relationship between euhedral nepheline and microcline or albite, shows that this mineral was separated from the "primary magma" at the begining of its crystallisation, before the feldspars. The Ne, Ks, Q parameters (calculated from the chemical and X-ray analyses), projected on $NaAlSiO_4$ – $KAlSiO_4$ – SiO_2 diagram, indicate temperature of cristalisation around $550\text{-}600^0$ C. Certain chemical, structural and morphological features distinguish to nepheline from the centre of massif. The minerals formed by alteration of nepheline – cancrinite, sodalite, analcime, liebnerite – reflects "subsolidus transformation" in the presence of water.

The Ditrău massif belongs to the Tulgheş formation of the Eastern Carpathians. It consists of a great variety of alkaline rocks, bearing typical minerals such as: microcline, albite, oligoclase, nepheline, cancrinite, sodalite, biotite, amphiboles (hastingsite, arfvedsonite, hornblende, Mg-riebeckite, ossanite), titanaugite, diopsidic augite, aegirine etc. The main petrographic types consist of nepheline-bearing syenites, nepheline-bearing monzonites, essexites, alkali-feldspar syenites, foidic monzonites, diorites and ultramafites (Anastasiu, Constantinescu, 1976). The nepheline has a maximum frequency within the nepheline-bearing syenites from the central area (Valea Mare, Priczke creek), the marginal eastern area (Călugăr and Putna valleys) and southern area (upper course of Cianod valley, Cetății and Chiuruț valleys). The nepheline is also well represented within the nepheline-bearing monzonites and essexites from the northern area (Fig. 1).

Typical for Ditrău massif is considered to be the variety of nepheline—bearing mineral assemblages: nepheline + microcline + albite; nepheline + microcline + biotite; nepheline + microcline + albite + biotite + hornblende; nepheline + microcline + albite + oligoclase + biotite; nepheline + microcline + albite +
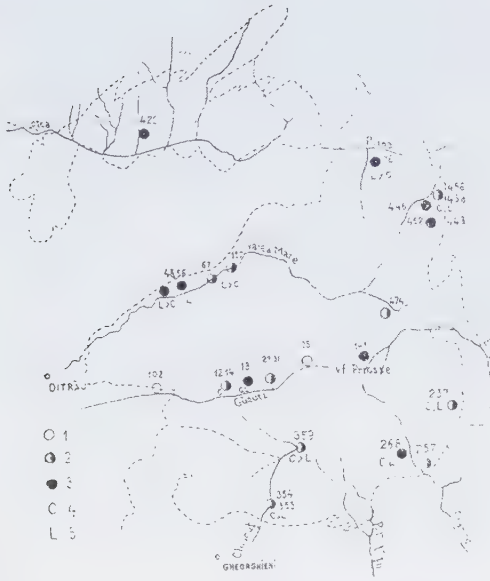
Fig. 1. Sketch of the Ditrău alkaline massif with the distribution of nepheline analyzed samples: 1, fresh nepheline; 2, partially altered nepheline; 3, totally altered nepheline; 4, cancrinite; 5, lieb-nerite.

oligoclase + biotite + hornblende + pyroxene. Beside all these mineral assemblages, there can be found accessory minerals such as zircon, apatite, sphene, epidote, orthite, ilmenite, garnet, and bastnäsite. The nepheline participation is 15-50% within the nepheline-bearing syenites, 10-35% within the nepheline-bearing monzonites and 1.5-35% within the essexites (Table 1).

Macroscopic and microscopic features

The detailed observations on the morphology and size of nepheline crystals, as well as on the paragenetical type, degree of transformation and occurrences are shown in Table 1. The data presented lead to the following general observations:

a) the crystal size within the above mentioned parageneses fall into a normal granular facies (1-2 mm) or into a pegmatoid facies, where the nepheline crystals frequently exceed 1 cm (Valea Mare, Putna creek and Chiruţul Mare);

b) the macroscopically and microscopically observed habits of nepheline crystals, show different forms:

-euhedral tetragonal or hexagonal crystals were frequently noticed within the medium grained and pegmatoidal nepheline-bearing syenites (especially on the upper course of Güdutz creek and within the waste deposits of the mining dumps from Valea Mare);

-subhedral crystals, where the crystallographic forms are intersected by mafic crystals (especially hornblende) or by secondary phases;

-anhedral crystals with interstitial patterns observed within the essexites and transformed nepheline-bearing rocks. Here, nepheline shows a relic aspect, without crystallographic faces.

Within most of the analyzed parageneses, the intergrowths between nepheline and other minerals are not so evident. As an exception, there are the samples from Güdutz creek, which have "myrmekite" type intergrowths between nepheline and K-feldspar. These intergrowths are localized at the limit between the two minerals, probably as a result of the later development of cancrinite.

Other mineral inclusions in nepheline are accidental. They appear mainly within nepheline-bearing monzonites and essexites, where nepheline includes hornblende, biotite and apatite.

The degree of nepheline transformation within the rocks from Ditrău massif differs from one type of rock to another, being more advanced within the coarse grained and pegmatoid facies from the marginal zone of the massif. The secondary products consist of cancrinite, liebnerite (paragonite), sodalite, analcime and natrolite. They appear as marginal accumulations, crack-fillings, reaction rims or pseudomorph after nepheline. In the last case, the forms of the replaced nepheline are perfectly preserved. The relations between the secondary phases that replace nepheline yield the following succession of minerals: cancrinite, liebnerite, and sodalite.

Table 1

Petrography (sample-occurrence)	Paragenese	Frequency	Size (mm)		Outline	Typical transformations
			Max.	Min.		
1.Nepheline-bearing syenites -67 Valea Mare Ditrău	Nepheline + Pl +Bi + Sodalite + Sf +Il +Hp	20%	>2	0.5	anhedral	(Li+C+S)
354 Chiuruțul Mare	Nepheline +Fk +Ab +Bi	25%	0.4-0.5		anhedral, subhedral pseudotetrag.	fresh
355 Chiuruțul Mare	Nepheline +Fk +Ab +Bi +H	20%	0.6-1	0.4	anhedral	Totally transformed (C>Li)
359 Chiuruțul Mare	Nepheline +Fk +Ab +Bi	30%	1-2		subhedral tetragonal prism	Partially transformed (C>Li)
268 Cianod	Nepheline +Fk +Bi	15%	1	0.5	anhedral	(C+Li)
488 Călugăr	Nepheline +Fk +Ab	30%	2-3	1	subhedral	(Li>C)
452 Călugăr	Nepheline +Fk +Ab +Bi	50%	2		anhedral	Totally transformed (Li>C)
453 Călugăr	Nepheline +Fk +Ab	25%	3		anhedral	Totally transformed (Li)
76 Putna	Nepheline +Fk +Ab + calcite	40%	0.6	0.8	anhedral	Totally transformed
44 Valea Mare	Nepheline +Fk +Ab +Bi	15%	5-6		anhedral	Totally transformed
14 Güdutz	Nepheline +Fk +Ab	20%	3-4		anhedral	Totally transformed (C+S)
2. Nepheline-bearing monzonites 12 Güdutz creek	Nepheline +Fk +Ab +Bi	15-20%	1		anhedral	Partially transformed (C)
29 Güdutz	Nepheline +Fk +Ab +Bi	10%	2		anhedral	Partially transformed (C)
31 Güdutz	Nepheline +Fk +Ab + Mo - Bi	20%	1		subhedral, pseudotetragonal prism	Fresh, intergrowth with kalsilite (photo 5,6)
446 Călugăr	Nepheline +Fk +Ab + Mo + Bi	25%	2	0.52	subhedral	Totally transformed
141 Pricske	Nepheline +Fk +Ab = Bi + Mo	35%			subhedral	Totally transformed (Li+C)
3. Essexites 19 Jolotca river	Nepheline +Ho + Bi + Fk + Plg	35%			anhedral (interstitial)	Totally transformed (Li+C)
48 Valea Mare	Nepheline +Plg + Bi + Fk + Ab	30%	2	0.5	subhedral	Totally transformed
56 Valea Mare	Nepheline + Plg + Fk + Ho + Bi		0.4-0.5		subhedral	Partially transformed (Li+C)
237 Balaș Lorincz	Nepheline + Fk + Plg + Ab + Bi	12%	15	0.5	subhedral anhedral	(Li+C)
Călugăr	Nepheline + Fk + Plg + Ho + Bi	20%	2	0.5	anhedral (interstitial)	Partially transformed (C+Li)

C=cancrinite; Li=liebnerite; S=sodalite

Within fresh syenites, nepheline coexists with cancrinite and sometimes with sodalite which fills the interstitial spaces. Within the rocks where nepheline is partially altered, the only mineral developed on the expense of nepheline is cancrinite. Within the rocks where the nepheline is completely altered, the transformation processes are represented by the appearance of liebnerite and cancrinite in different proportions. Within the pegmatoid facies aggregates of secondary minerals can be macroscopically distinguished. They have a greenish colour and a weak satin-like luster. The secondary minerals have carved out zones with sharp contours, such zones may be noticed on the exogenely altered surfaces of the exposed rocks.

Within the syenitic rocks, the aggregates of liebnerite formed on the expense of nepheline are close related to pink K-feldspar. No relation could be found between the determined refraction indexes (ε=1.530-1.535; ω=1.536-1.540), birefringence (0.003-0.004) and the variation of chemical composition.

Chemical and structural features

The theoretical composition of nepheline is considered to be $NaAlSiO_4$. Buerger (1974) proposed the formula $KNa_3Al_4Si_4O_{16}$ corresponding to the K content recorded by analyses. Later, different analyses showed SiO_2 in excess, as initially considered by Hann,

Buerger (1955). Eitel (1962) suggested that nepheline chemistry should be considered within the ternary system $NaAlSiO_4$-$KalSiO_4$-SiO_2 (nepheline-kalsilite-quartz).

After Donnay, nepheline represents a solid solution of kalsilite where the nepheline phase admits different amounts of K. Nepheline can therefore be described as sub-potasic, medium-potasic and per-potassic corresponding to $0<x<0.25$, $0.25<x<2.0$ and $2.0<x<4.73$ domains where x represents the number of K ions, calculated in the basis of 32(O).

The chemistry of nepheline from Ditrău syenites was determined by six chemical analyses (Table 2). The chemical composition of nepheline from the alkaline massifs of Sînîr, URSS (Panina, 1972) and Bratholmen, Norway (Tilley, Gittins, 1961). The main analyzed oxides of nepheline from Ditrău show values similar to that of Synyr and Bratholmen. They within are also comparable with the average values of for 18 nepheline analyses (published by Table 2, Sample 9 (Ciuhrovski, fide Deer et al., 1967).

The K values calculated in the analyses 1-4 (Table 2) belong to the potassic domain, showing trend to the per one. The values of Ne and Ks for the same analyses correspond to the $Ne_{73}Ks_{27}$-$Ne_{75}Ks_{21}Q$, i.e., to the Marozevicz-Buerger convergence domain (Tilley, 1954), considered to be typical for the nepheline-bearing syenites.

Table 2. Chemical analyses of nepheline.

Oxides	1	2	3	4	5	6	7	8	9
SiO_2	43.04	42.64	43 96	45.25	52.71	43.20	43.60	43.61	43.97
TiO_2	0.04	-	-	-	-	-	-	-	-
Al_2O_3	33.56	32.99	33.01	29.41	27.64	31.00	33.60	33.05	32.89
Fe_2O_3	0.47	0.41	0.87	-	-	-	0.29	0.85	-
MgO	0.05	-	-	-	1.70	0.48	0.34	0.05	-
CaO	0.56	0.30	-	1.69	0.06	1.10	0.72	0.53	0.43
Na_2O	16.61	16.17	15.84	14.36	11.22	-	14.48	16.09	15.73
K_2O	5.75	6.22	5.39	6.84	4.85	22.23	5.38	4.92	5.45
H_2O	0.34	1.10	0.67	2.11	0.94	1.99	0.28	0.70	-
Total	100.18	99.77	99.74	99.66	99.21	100.00	10.15	99.82	99.47

Samples 1-6 = nepheline from Ditrău Massif.

The results of three X-ray diffraction analyses on nepheline from the Ditrău syenites (Jolotca valley and Valea Mare) are given in the Table 3.

The d/n and I/100 values are close to those of the nepheline standard sample (Miheev, 1957). The X-ray diffraction patterns allowed the identification of kalsilite and analcime. These two minerals are intimately associated with nepheline; therefore very often they are difficult to be distinguished under the microscope.

Smith and Sahama (1954) showed that the 2θ values corresponding to 2022 and 2130 reflections have a systematical variation related to the K/(K+Na+Ca) ratio. Thus, the nepheline content within the solid solution can be calculated starting from certain linear equations.

The plot of the 2θ values measured for 2022 and 2130 reflections from samples 67 and 19 (Fig. 2), yielded 70-80 Ne.

Conclusions

The study of nepheline-bearing parageneses reveals the nepheline affinity for felsic minerals (microcline, albite). This could explain the nepheline distribution within the central-eastern and southern areas of the Ditrău massif. Mafic minerals (biotite, hornblende, and pyroxene) are less freguent in nepheline parageneses.

We mention the typical presence of the nepheline-albite paragenesis within the dyke facies (Putna and Aurora creek).

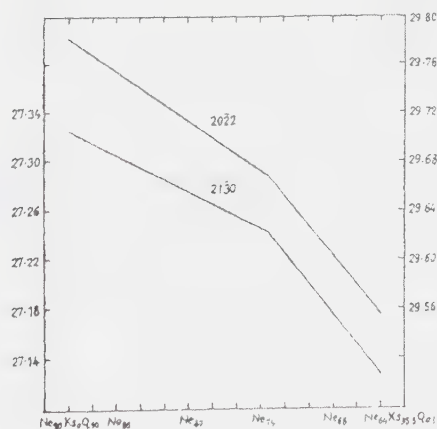The idiomorphism of the nepheline crystals (compared to the microcline and albite) and

Table 3. The d/n and I/100 values for Ditrău nepheline.

Nepheline sample 67 Valea Mare		Nepheline, sample 19, Jolotca valley		Nepheline Miheev, 1975	
d	I/100	d	I/100	d	I/100
4.20	10	4.29	19	7	4.315
3.83	15	3.83	84	9	4.157
3.70	22	2.875	100	9	3.258
3.25	100	2.577	31	10	2.001
3.035	14	2.489	11	8	2.873
2.903	20	2.386	31	8	2.563
2.755	4	2.108	59	5	2.489
2.625	5	2.343	30	4	2.393
2.563	10	1.983	8	10	2.338
2.472	5	1.886	10	8	2.297
2.326	4	1.821	4	2	2.175
2.156	48	1.721	5	4	2.117
2.127	22	1.714	5	8	2.078
1.987	5	1.689	10	6	1.921
1.927	3	1.634	13	4	1.880
1.853	6	1.614	25	5	1.785
1.835	5	1.598	11	4	1.687
1.790	5	1.469	10	4	1.630
1.738	3	1.347	5	6	1.611
1.690	7	1.314	10	4	1.595
1.632				10	1.553
1.618				6	1.465
1.596				7	1.410
1.514				1	1.406
1.456				8	1.380
				5	1.367
				2	1.338
				5	1.275
				3	1.250
				3	1.219
				8	1.198
				8	1.182
				6	1.136
				5	1.126

Fig. 2. 2θ values (CuKα) corresponding to 2130 and 2022 reflections of the Ditrău nepheline plotted the Hamilton & Mackenzie diagram (1960).

the absence of inclusions are the main arguments for the nepheline separation from magma before feldspars, during the initial stages of crystallization.

The Ne, Ks, Q values calculated from chemical analyses and X-ray diffraction data, and plotted to the diagram with isotherms of the system $NaAlSiO_4$-$KalSiO_4$-SiO_2 give a crystallization temperature of 550-600° C. However, some chemical, structural and morphological features suggest different genetic conditions for the nepheline in the central area of Ditrău massif and in the southern area, respectively.

The minerals formed by nepheline alteration (cancrinite, sodalite, analcime, and liebnerite) show the complexity of "subsolvus" transformation due to the presence of water in the system.

The spatial distribution of the nepheline alteration processes is partially related to the position of rocks within the massif and to their degree of crystallinity. The nepheline from the marginal zone and that of pegmatoid facies is more altered than the nepheline from other occurrences.

References

Anastasiu N., Constantinescu E. (1977) Observații mineralogice în rocile sienitice din masivul alcalin de la Ditrău, vol. Comunicări Geologie. Tipografia Univ. București, 77-84.

Anastasiu N., Constantinescu E., (1978) Feldspații potasici din masivul alcalin de la Ditrău. *D.S. Inst. geol. Geofîz.*, **LXIV**, 13-26;

Deer W. A., Howie R.A., Zussman J. (1967) Rock forming minerals, Logmans, London.

Donnay G., Schainer J., DonnayI.D. (1959) Nepheline solid solution, *Min. Mag.* **18**, 369.

Felner A. (1867) Chemische Unterschung der Gestein von Ditro, *Verch, K.K. Geol. R.A.,* **17**, 285-287;

Hamilton D.T., Mackenzie W.S. (1960) Nepheline solid solution in the system $NaAlSiO_4$ - $KalSiO_4$-SiO_2. *Journ Petr,.* **1**, 56.

Ianovici V. (1933) Etude sur le massif syenitique de Ditrău, region Jolotca, district Ciuc. *Rev. Muz., Geol. Miner. Univ. Cluj,* **4**, 2, 1-53.

Ianovici V., Ionescu J. (1972) Contribuții la mineralogia masivului alcalin de la Ditrău. I Amfibolii. *St. cerc. geol. geofîz. geogr., s. geol..* **XIV**, 2, 353.

Koch A. (1877) Mineralogische - petrografische notizen aus Siebenburgen Uber den Eleoliith und Sodalith von Ditro, *Tcherm. Min. Petr. Mitt.,* **1**, 332-336;

Miheev V.I. (1957) Rentgonometriceskii opredelitel mineralov. Gosthelizdat, Moskva.

Panina L.O. (1972) Mineralogogeneticeskaia karakteristica nekotorih scelocinih masivov prebikalia Nauka, Moskva.

Smith J.V., Sahama T.G. (1954) Determination of the composition of natural nephelines by a X-ray method. *Min. Mag.* **30**, 439.

Streckeisen A. (1952-1954) Das Nephelinsyenit Massif von Ditro. *Schw. Miner. Per. Mitt.* **54**, 1, Berna.

Tihonenkova R.P., Naciaeva I.A., Osokir E.D. (1971) Petrologhia kalievih scelocin h porod. Rauka. Moskva.

Tilley C.E. (1954) Nephelin - alkali feldspar paragenesis. *Amer. Journ Sci.*, **252**, 65;

Tilley C.E., Gittins J., (1961), Igneous nepheline-bearing rocks of the Haliburton Bancroft Province of Ontario. *Journ Petr,.* **2**, 38.
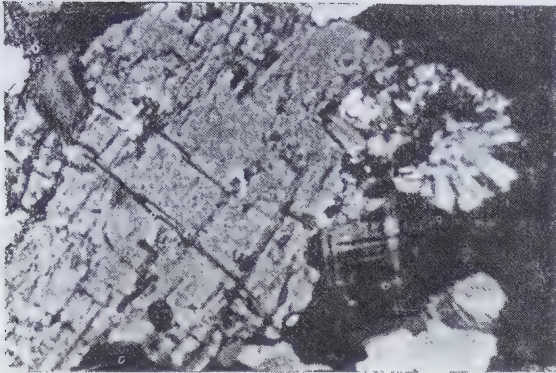
Plate 1

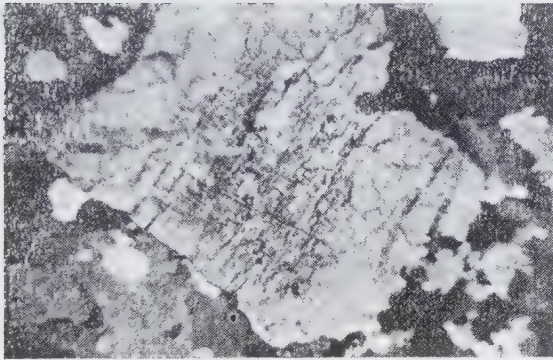**Photo 1**. Subhedral nepheline within spheroidal cancrinite. Chiruţul Mare creek, N+, x 40.

Photo 2. Subhedral fresh nepheline within the nepheline-bearing monzonites. Güdutz creek, N+ , x 40.
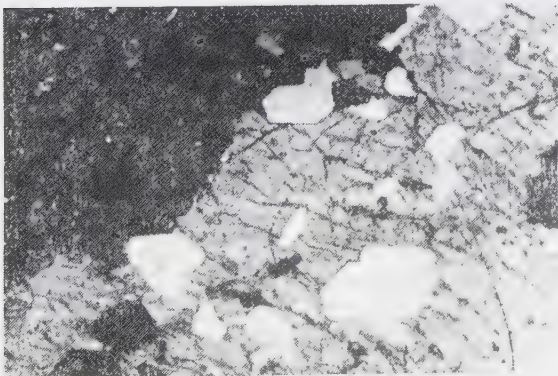

Photo 3. Apatite inclusions within the nepheline from essexites. Jolotca creek, N+, x 40.
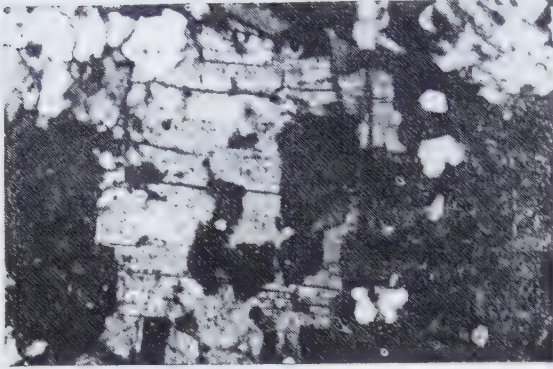
Plate 2

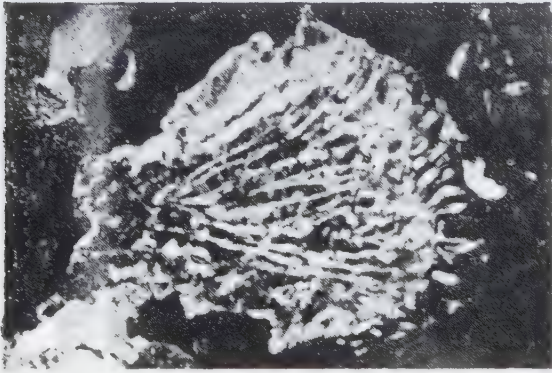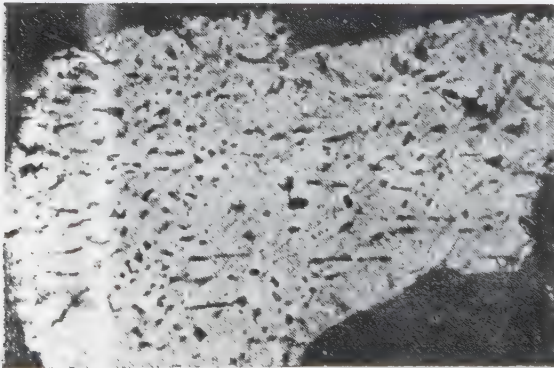**Photo 4.** Euhedral nepheline within the nepheline-bearing syenites. Valea Mare N+, x 40.

Photo 5-6. Kalsilite-nepheline "myrmekite" type intergrowth within nepheline-bearing monzonites. Güdutz creek. N+, x 40.

K-feldspars from the alkaline massif of Ditrău

NICOLAE ANASTASIU
EMIL CONSTANTINESCU

The K-feldspars of the Ditrău alkaline massif appear with a high frequency (35–50%) and always display anhedral crystal-grains, masses, pseudomorphs, veinlets intimately intergrown with albite or oligoclase of substitution and exsolution perthites and microperthites. The range of the optical properties of the K-feldspars ($2V\alpha = 70$–$80°$; b: $\gamma = 6$–$18°$, $N\beta = 1.518$–1.525) leads to the spatial and asymmetric zonality as against the shape and petrographical composition of the massif. The investigation carried out by X-ray diffraction and IR analysis confirmed the types of maximum and intermediate microcline with 0.9 and 0.5 triclinicity. These properties are due to the high instability of the K-felspars and were acquired subsequently to their crystallization and selective remobilization processes during conditions of slow cooling.

The Ditrău alkaline massif, unique in Romania by its size and petrographical variety, outcrops in the Central East Carpathians, as an internal component of Mesozoic-Crystalline Zone, in the Tulgheș Series.

Since Herbich's (1859) notification a lot of impressive research work has been carried out. Very profound and original contributions have been brought by Koch (1877–1880), Mauritz (1910–1925), Ianovici (1932–1968), Streckeisen (1931–1974), Codarcea et al. (1957) etc. As a result, Ditrău alkaline massif became well-known in the petrographical literature, being also mentioned in Sorensen's (1974) monography "The Alkaline Rocks".

The research carried-out so far involved chemical and mineralogical observations, as well as petrographical and structural details. The most important of these have been integrated in several genetic models: Ianovici (1933), Codarcea et al. (1957) and Streckeisen (1954, 1974). Recently, refined methodology – especially geophysical – has been taken into account – e.g. frequency analysis used for establishing effect-cumulative sources (the case of the total geomagnetic field anomaly – Botezatu et al., 1975).

The progress of the mineralogical and petrographical technologies during the last years and, by these, the detailed knowledge of the

mineral structural and optical properties and related petrogenetic significance – suggest the large field that is continously opening for new geological research on new aspects and genetic models. On the other hand, the accepted nomenclature of plutonic rocks (Streckeisen, 1968, 1974) recommends the use of the most suitable terms in Romanian literature in order to define parageneses that characterize the massif and, consequently, to integrate them in an unanimous accepted classification.

2. Geological setting of the Ditrău alkaline massif in the East Carpathians crystalline zone

The Ditrău alkaline massif is characterized by a large petrographical, mineralogical and chemical variety as well as by complicated structural and textural features. It outcops within crystalline schist—of Baikalian age, belonging to Mesozoic-Crystalline Zone of the East Carpatians (Gheorgheni - Tulgheş sector) and it is covered, between Valea Mare of Ditrău and Jolotca brook, by a sedimentary cover of Pliocene and Quaternary deposits.

The crystalline schists belonging to Tulgheş series are low-degree metamorphic (green schist facies), sometimes with a retromorph character (Popescu, 1970) and are petrographically represented by quartz-feldspar schists, quartz-biotite schists, quartzites with biotite (in Jolotca brook basin, Sărmaş level (Tg$_1$)-Mureşan, 1971; Popa, (1975), quartz-sericite schists, graphitic schists (westward of Cianod brook, Fagul Înalt level (Tg$_1$), Mureşan (1971; Popa, 1975). Between Belcina and Putna brooks, the middle complex of Tulgheş Series (Tg$_2$) consists of graphitic schists, sericite-graphite schists and sericite-chlorite schists (Mureşan, 1971; Popa, 1975).

The contact with the crystalline schists of Tulgheş Series is sharp and marked by mineralogical associations and structures diagnostic for thermal metamorphism: biotite, andalusite, cordierite (usually replaced by pinnite), corundum, spinel and rarely chloritoid and alkaline amphibole (Streckeisen, 1974) in phyllites with spotted and nodular structures or recrystallized quartzite.

The contact aureole of the massif has variable widths, from tens of meters to 2–3 km and is well developed in northwestward part, as well as between Chiuruţ, Cetăţii and Cianod brooks. Within the aureole, near the massif there are centrimetrical to metrical injections of syenites and quartz and felspar- bearing rocks displaying peculiar "lit-par-lit" textures (easy observable along Chiuruţ, Cianod, Holoşag and Teascului brooks).

3. Petrography and structure – general features

The Ditrău massif comprises a large variety of rocks composed of minerals specific for alkaline intrusions: microcline, albite, oligoclase, nepheline, cancrinite, sodalite, biotite, amphibole (Anastasiu, Constantinescu, 1976) hastingsite, arfvedsonite, hornblende, magnezioriebekite, ossanite, muscovite, Ti- and Fe-diopside, rarely quartz, accessory minerals (apatite, sphene, ilmenite, zircon, rutile, orthite, monazite, epidote etc.)

The structural features the rocks are controlled by their crystallinity degree and transitions between macro-, meso- and microcrystalline facies. The rocks textures, almost irrespective to type, display massive and orientated their arrangements (named "gneissic" by Codarcea et al., 1957 or "fluid" by Streckeisen, 1974).

The petrographic types, separated by integration (Anastasiu, Constantinescu, 1975) and data plotted in QAPF diagram (Committee for Plutonic Rocks Classification, IUGS, 1974) indicated foidic rocks, foides- and quartz/feldspar-bearing rocks, diorites and ultramafites (Figs. 1 and 2).
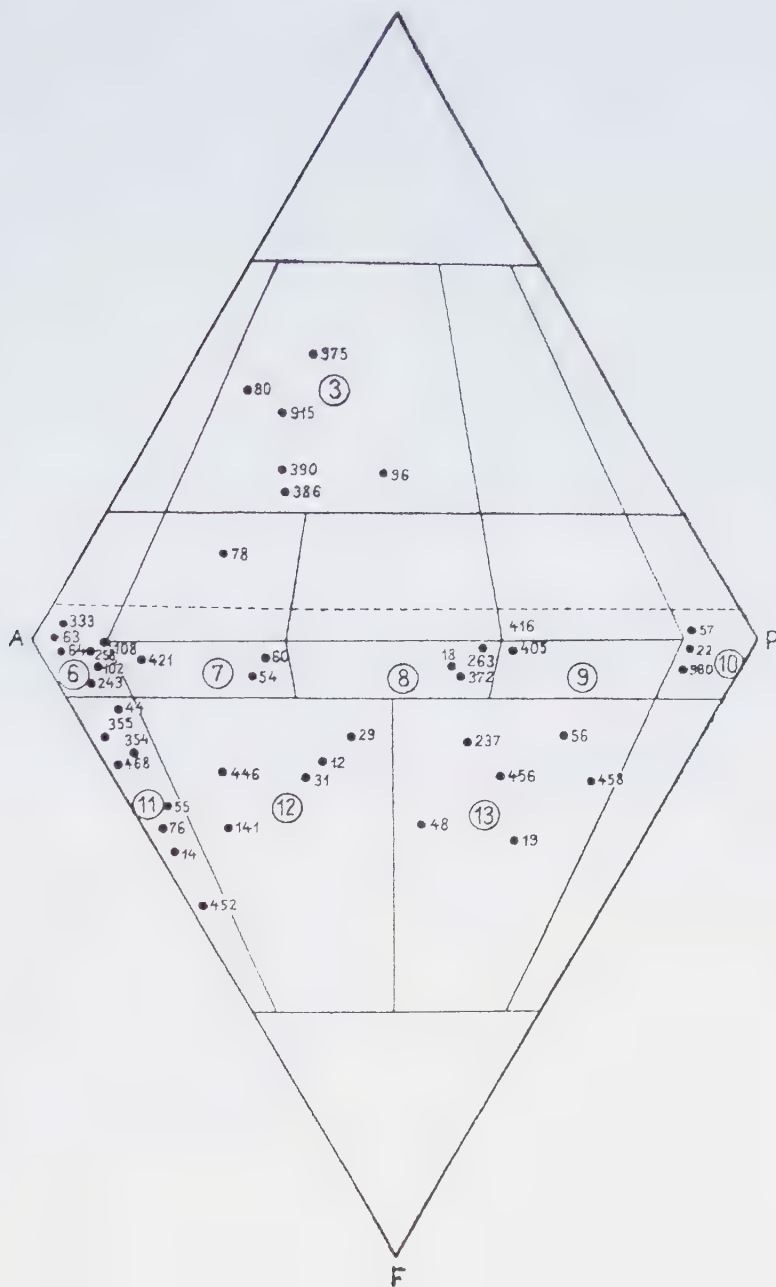
Fig. 1. The modal analysis (in QAPF diagram): 3, granites; 6, alkali-feldspar syenites with foides; 7, foidic syenites; 8, foidic monzonites; 9, monzonites with foides; 10, foidic diorites; 11, foidic syenites (nephelinic); 12, foidic monzosyenites; 13, essexites.
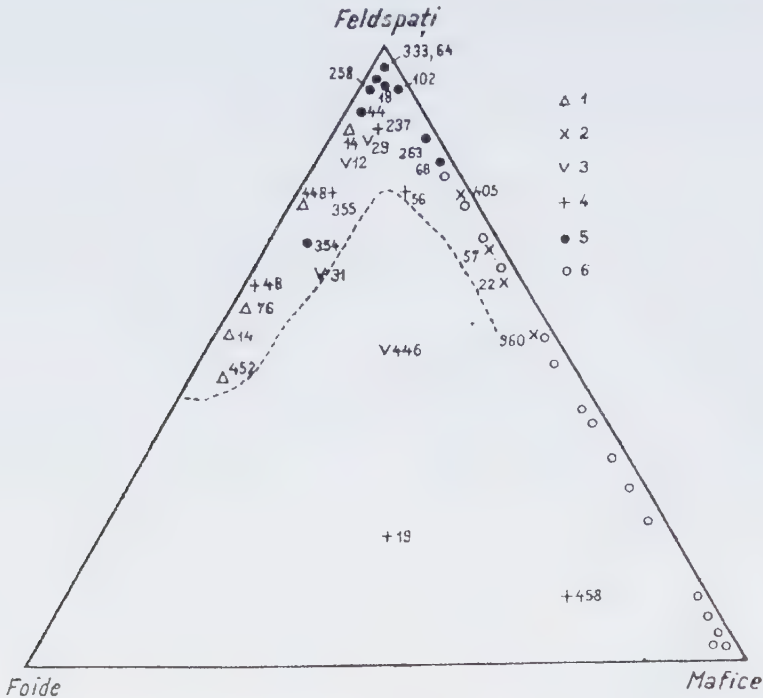
Fig. 2. Ternary diagram (end-members: feldspars, nepheline and femic minerals):1, foidic syenites; 2, foidic monzonites; 3, essexites; 4, syenitoides; 5, monzonites with foides; 6, diorites and hornblendites.

a) The foidic rocks - foidic syenites, foidic monzonites and essexites - represent the main part of the massif, being well-exposed in the central area (along Valea Mare brook, Belcina brook; Cianod brook; right tributaries of Putna brook) and displaying different structural facies and associations. Sometimes, the transition from a petrographic type to another is achieved gradually and could be revealed by the proportion of femic minerals or by sharp limits.

The foidic syenites are rocks prevalently leucocratic, white or pink, having a lower color-index (M < 10 - 15%).

The composition comprises the following minerals: K-feldspars, albite-oligoclase, nepheline (± cancrinite, ± sodalite), biotite, rarely hornblende, zircon, ilmenite, sphene, and apatite. The pink color is the effect of weathering – the ferrous pigment being retained by feldspars. These types preferentially outcrop along Putna brook basin, upper Belcina brook and in the southern area of the massif. Structurally, the pegmatoidic and mesocrystalline facies prevails. The microcrystalline facies – of nephelinic microsyenitic type – appear as irregular zones, nests or veins within pegmatoidic or normal foidic syenites bodies.

The foidic monzonites are lateral counterparts of foidic syenites and may farm intercalations within the essexite complex, mainly developed on Güdutz brook and Putna brook (right tributaries). Their composition is represented by K-feldspars, albite, oligoclase, nepheline, biotite, hornblende, sphene, apatite, epidote, and calcite with a mesocrystalline structure. The essexites outcropp along middle Jolotca brook , on Ditrău-Tulgheș road (29–26 km), in

open-pits on Güdutz brook and upper Putna brook, as a mineralogically and structurally heterogeneous complex. The composition is represented by plagioclase, oligoclase-andezine, K-feldspar, nepheline, amphibole and biotite, sphene, apatite, epidote. The structures are mesocrystalline or pegmatoidic, the texture being orientated due to femic minerals associated in "parallel bedding". None of these display linear elements, the minerals being associated in groups lacking any orientation. The syenitoide veins within the essexitic complex diversify the petrographical associations and suggest – by convergence with anatexic phenomena – similar structures with those related to migmatites ("agmatites, diadizite, nebulites-like aspects", Codarcea et al., 1957).

b) The foidic rocks include here syenitoides and monzonites, in which foides appear accidentally (< 10%). These types outcrop peripherally within foidic complexes as elongated, ring-like areas or as veins displaying variable thickness (0.50 2–3 m) intruded in adjacent rock bodies. The syenites and alkali-feldspar syenites are exposed along upper Turcului brook, lower Holoşag brook, cross Jolotca brook and reappear (under sedimentary cover) between Valea Mare and Güdutz brooks. Petrographically are leucocrate rocks, white or pink-colored, consisting of K-feldspars, albite or oligoclase, biotite, muscovite, nepheline and accessory minerals: zircon, apatite, ilmenite, rutile, sphene. Along Jolotca brook the marginal facies displays transitions to adjacent complexes, being enriched in quartz (eastward) and in femic minerals (westward). In the central-western areas the enrichment in nepheline and femic minerals makes the transition to essexites. The structures are usually meso- and microcrystalline with massive textures grading into orientated, ones when an increased content of femic minerals is present.

The monzonites and monzodiorites are found as transitional series between the above-mentioned complexes, in lens- (Güdutz and Cianod brooks) or concordant-shaped bodies

(Jolotca brook), the texture being massive or orientated. The compositions are mainly represented by K-feldspars, oligoclase - andezine ± albite, biotite ± amphibole; sphene, apatite, ilmenite, and epidote. The structures are hypidiomorph-mesocrystalline.

c) The quartz-feldspar-bearing rocks and the granitoides outcrop discontinuously along marginal zones. Very extended areas could be found along upper Jolotca brook, Czengeler - Lükone road and middle Cianod brook. The granitoides are mostly leucocrates, pink-colored and consist of K-feldspar, quartz, plagioclase, biotite, zircon, sphene, and apatite. The rock structure is allotriomorph-mesocrystalline microcrystalline; massive textures are ubiquitous.

d) The diorites and ultramafites form a complex along lower Jolotca brook , between Cibi Iacob brook and Teascului brook.

The parageneses that characterize the petrographic complexes from Ditrău alkaline massif have a leucocrate character (given by abundance of feldspars). At the scale, of the entire massif some systematic variations between feldspar types and, also, foidic/femic minerals are observed.

An increasing trend of the foidic content could be emphasized toward the core of the massif delineating a rounded zone (of syenite-nephelinic composition). The central zone is discontinuously surrounded by ring- like areas enriched in feldspars and poor in foides. The mineralogical zoning is marked by textural aspects and less by structural ones.

From this point of view, oriented textures from the massif marginal zones grade into massive ones towards to its central parts. The structural variation, from mezo- to large- crystallized (pegmatoide) facies or to those fine – crystallized lead to a inhomogeneous character that can not be correlated directional or transversal in the massif.

4. K-feldspars

This paper focuses on different characteristics of K-feldspars and try to reveal some conditions that – by controlling their genesis and spatial distribution – directly influenced the paragenetic, textural and structural relationships within the Ditrău alkaline massif.

The investigation involved a microscopic study on 200 thin sections (collected from the main rock types) revealing crystalline morphology, intergrowth and inclusions aspects, variations in feldspar optical properties and X-ray diffraction analysis and infrared absorption spectroscopy.

Frequency, sizes, morphology. The K-feldspars from the Ditrău alkaline massif very frequent minerals. The participation is around 40 - 50% excepting essexites (having contents under 35% - Table 1).

By analyzing the diagram of participation limits of the K-feldspars in different rock types, the following aspects could be emphasized (Fig. 3):

- a great variation in syenites, monzonites and granitoides; foidic syenites and monzonites display relatively constant contents;
- in all cases the maximal contents corre are sponding to leucocrate separations, in many

Table 1. Properties of K- feldspars from Ditrău massif alkaline rocks

	Nepheline syenites	Foidic monzonites	Essexites	Syenites	Monzonites	Granitoides
	Valea Mare, Putna brook, Chiurut brook, Gudutz brook	Putna Brook, Gudutz brook	Valea Mare, Putna brook, Jolotca brook, Gudutz brook, Balas Lorintz brook	Jolotca brook, Valea Mare, Gudutz brook, Cianod brook, Chiurut brook	Jolotca brook, Gudutz brook, Cianod brook	Jolotca brook, Czengeler, Cianod brook
Rock content %	50 - 60	40 50	10 - 35	25 - 70	30 60	30 – 60
Crystals morphology	Anhedral, elongated prismatic, isometric, irregular masses, filiform	Anhedral, granular, irregular masses	Anhedral, interstitial, granular	Anhedral Enhedral (total pseudomorphosis on plagioclase) filiform	Anhedral, interstitial, irregular masses	Anhedral, granular, connate
Nβ (γ α) Or maximal values	1.525 / 1.519 Or 94	1.523 Or 85	1.525 , 1.527 Or 75	1.523 1.525 1.518 Or 92	1.524 Or 84	1.522 Or 96
2 Vα extreme values (maximal frequency)	80 - 88° (84°)	70 - 85° (84°)	72 - 88°	70 - 86° (80°)	70 - 84°	76 - 86°(84°)
B : γ	14 - 18°	8 - 18°	10 - 18°	10 - 18°	10 - 16°	14 - 18°
Triclinicity (Δ) M M and M.I.	M.M.	M.I. M.M.	M.I M.M	M.I ˉM.M	M.I M.M	M.M
Macles	"grill"	"grill"	"grill"	"grill"	"grill"	"grill"
Concrescence	Microperthites, "vein" perthites, replacement perthites	Microperthites, "vein" perthites, replacement perthites, epitaxial character	"vein" perthites, replacement perthites	replacement perthites	Microperthites, "vein" perthites, replacement perthites	Microperthites, "string" perthites, "braid" perthite quantitative subordinated
Inclusions, alterations, deformations	Usually clear, kaolinized, fissures with calcite or albite	clear -	clear, weak deformations	clear very weak deformations (optical anomalies)	clear very weak deformations (optical anomalies)	clear and incipiently kaolinized weak deformations (Optical anomalies)

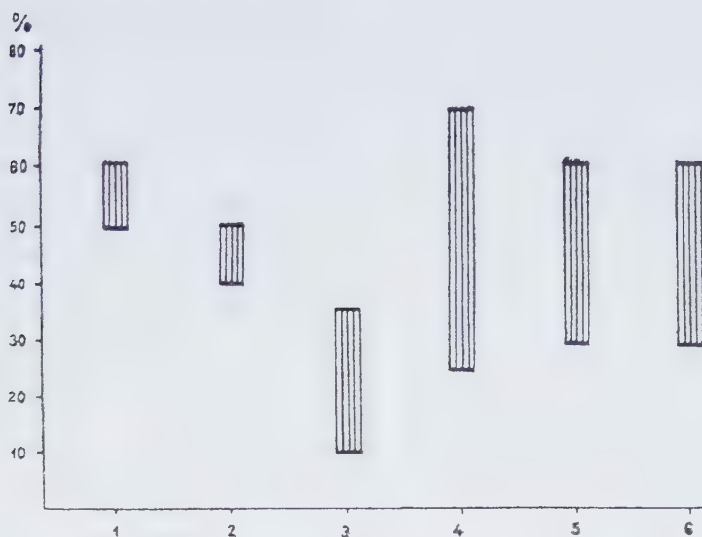M.M. – maximum microcline; M.I. intermediary microcline

Fig. 3. The average participation of the K-feldspars in the Ditrău alkaline massif: 1, foidic syenites; 2, foidic monzonites; 3, essexites; 4, syenitoides; 5, monzonites with foides ; 6, granitoides.

Table 2. K-feldspars sizes of the main rock types and associated structural facies (mm)

Rock type	Rock structure		
	Pegmatoide	Normal - granular	Microcrystalline
Alkali-feldspar syenites			
- massive	5 - 15	0.8 – 1.2	0.05 – 0.8
- vein	10 – 25	1. 2.0	
Monzonites		0.4 – 2.5	0.05 – 0.4
Foidic syenites	10 - 30	0.3 2.0	0.08 – 0.8
Essexites	15 – 25	0.4 1.5	
Granites	5 - 10	0.2 1.5	0.04 – 0.8

cases having a pegmatoid character. Crystal sizes are usually the same relative to the other paragenetic minerals and determine the pegmatoid structures – normal granular and microcrystalline – within each petrographical complex (Table 2).

From Table 2 it becomes clear that, excepting foidic syenites which frequently display pegmatitic structures along Valea Mare (observed on the samples from the old exploration wastes), the large crystallized structures of the other rock types define locally-developed facies in irregular or lens bodies.

The morphological features of the K-feldspar crystals vary according to the structural types of analyzed rocks and are not related to their parageneses. The observed morphologies are:

- Elongated prismatic crystals, without crystallographic faces; in spite of their prismatic development and the macroscopic idiomorphic faces, under microscope K-feldspars are

never developed with crystallographic faces. The crystals display irregular terminations. The limits with nepheline are sharp whereas the contacts with the plagioclases are fringed. The large crystals, from granitoides, foidic syenites and vein syenites frequently reveal fissures. These forms are found in pegmatoid rocks, especially in alkali-feldspar syenites and foidic syenites;

- Interstitial grains (meso- and microcrystalline), isometric, always uniform developed and in sub-millimetric sizes;
- Substitution structures – of different morphologies – affecting plagioclases; sometimes, within partial pseudomorphs K-feldspars are developed epitaxially, in the continuity of the plagioclases twins and cleavages. Within the pseudomorphos the habit is prismatic, and hypidiomorphic. The incipient substitutions, regularly developed and parallel with cleavages define antiperthites (in all rocks types);
- Grains relatively rounded – included in other K-feldspars and probably representing primary generations – appear in some alkali granites and foidic syenites;
- Filiform depositions, along some fissures or cleavages in plagioclases, appear in syenites, granites and foidic syenites.

The crystal morphologies suggest later crystallization of K-feldspar (generally confined), and on the other hand, its high mobility and affinity for plagioclases, which constitute a good support for K-feldspar to develop by replacement.

Intergrowths and inclusions. A general characteristic of K-feldspars from all the rock types is the lack of homogeneity and the appearance as various concrescence types with Na-feldspar.

The microscopic intergrowths are to microperthites and macroperthites categories, within which the Na-phase displays sizes > 0.05 mm and < 0.05 mm, respectively. Morphologically, the perthites from massif rocks belong to "string", "film", "vein"-perthite types

(Andersen, 1928; Smith, 1974) or to "replacement" and "braid" - perthite types (Alling, 1938 fide Smith, 1974).

In very fine intergrowths ("string" and "film" - perthites) the albite veinlets display sizes between 0.01 and 0.1 mm and appear developed in relative equal ratios with K-phase (Pl.2, Fig.1). As a rule, they appear on crystals borders but also as groups in different crystals parts. The albite lamellae are preferentially developed parallel to the (010) face. In replacement perthites the albitic phase appear as irregular relicts, with no crystallographic faces but having the same optical orientation. The albite - K-feldspar contact, in this case, does not follow specific crystallographic directions. The albitic phase frequently shows polysynthetic twins. Along Güdutz brook mixed intergrowths of "vein-replacement" type have been observed within alkali-feldspar syenites (K-phase that includes albite relict – "replacement" type intergrowth – is perthitic, that is, fine intergrowth "vein type"). In foidic syenites "braid" type perthite is very frequent – simultaneous intergrowths along two directions (110) and (110); in this case, the albitic phase is very fine and not showing polysynthetic twins.

No correlations could be found between perthite types and rock types. A possible explanation may be given by the absence of any rock-dependent facturs that controlled the formation of the perthites. Usually, "string" and "vein" type perthites are considered as separating products, and "replacement" types as being related to replacements. Their simultaneous presence in Ditrău rocks are arguments for the complexity of petrogenetic processes.

The feldspar twins are ubiquitous in the massif rocks, of them the "tartan"-twin of microcline is the most wide spread. "Tartan"-twin is closely associated with Carlsbad-twins in alkali – feldspar syenites and in microcrystalline facies of these or of foidic syenites. In

vein rocks – within which more frequent deformations have been remarked – "tartan" twin of microcline display also these effects.

The degree of nonhomogeneity of the K-feldspar has been emphasized by the high frequency of perthites and by the presence of plagioclase relicts within them. Excepting these inhomogeneous evidences, within K-feldspars albite idiomorphic inclusions in alkali-feldspar syenites and globular inclusions of quartz in granitoides could be observed. The rocks having an increased color index (essexites, diorites, ultramafites) the biotite and amphibole sometimes appear included within the K-feldspar. The accessory minerals (zircon, apatite, sphene, illmenite) are rarely found in relationship with K-feldspar.

Optical features of feldspars. The optic study of K-feldspars has been performed on 116 crystals from foidic syenites, foidic monzonites, syenitoides, essexites, monzonites (± foides) and granitoides. Sample locations and results are given in the Table 1. The K-feldspars optic and crystallographic properties depend on their structural state and on the Na content, respectively (Goldsmith, Laves, 1954; Mackenzie, 1954; Smith, 1961); accordingly, for their complete characterization, 2V and, extinction angles and refraction indexes have been determined. 2V-angle and extinction angle (β:γ) determinations (by using Fedorov method) pointed out the following features:
- 2Vα values of K-feldspars from all the massif rocks are between 70 - 88⁰ (Fig. 4);
- 2Vα values average limits for different rock types (Fig. 5) are distinct from a rock type to another.

More restricted limits have 2Vα values of K-feldspars from foidic syenites (80 - 88⁰) and granitoides (75 - 86⁰) and within larger limits (70 - 84⁰; 86⁰) are the values that characterize the feldspars from foidic monzonites, syenitoides and monzonites.
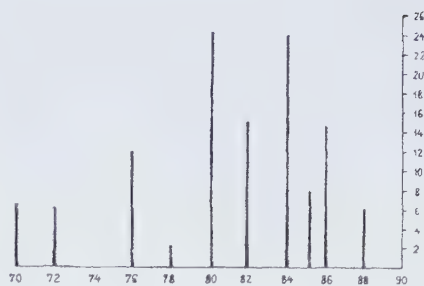

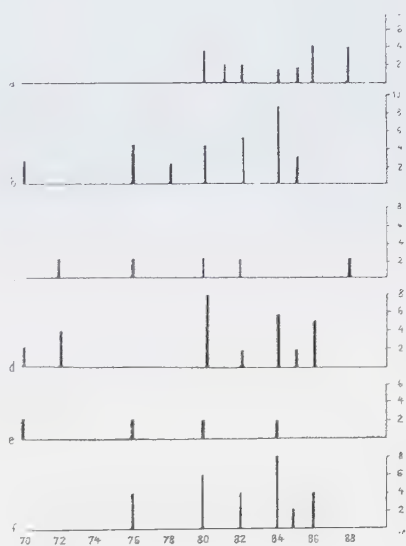**Fig. 4.** Limits of variation of 2Vα angle for K- feldspars from Ditrău alkaline rocks.

Fig. 5. Fields of 2Vα angle for K-feldspars from different rock types in Ditrău alkaline massif a, foidic syenites; b, foidic monzonites; c, essexites; d, syenitoides; e, monzonites with foides; f, granitoides.

For the main rocks of the massif the maximal frequency of a 2V-angle value is the same. Thus, within syenitoides the most frequent values belong to K-feldspars with 2Vα = 80⁰, in foidic monzonites and granitoides crystals with 2Vα = 84⁰. and in foidic syenites those

with $2V\alpha = 86^0$. The differences are small and cannot be a criterion for correlating each petrographic type. The lack of a strong variation of optic axes angle may be correlated with the same morphological characters that have been noticed for analyzed petrographical types.

The spatial distribution of measured $2V\alpha$ angle values (Fig. 6) – disregarding the associated petrographic type – suggests a trend of increased values ($2V\alpha = 84\text{--}86^0$) toward the north - eastern, southern marginal and central-western zones and decreased values ($2V\alpha = 76\text{--}80^0$) along a line that intersect the Jolotca

brook (between confluence with Simo brook and Teascului brook) and middle courses of Güdutz and Cianod brooks. The image suggests that no correlation between the massif central morphologic zone and a central zone that can be outlined on the basis of the discussed values.

The β:γ extinction angle values are between $6\text{--}18^0$ and correspond to intermediary microcline and maximal microcline state (Fig. 7).

Optically, the deviation from monoclinic symmetry could be predicted by the angle between

Fig. 6. Sketch showing 2Va value distribution for the K-feldspars in the Ditrău alkaline massif. 1, foidic syenites; 2, foidic monzonites; 3, essexites; 4, syenitoides; 5, monzonites with foides; 6, granitoides.

the "b" crystallographic axis and "γ" direction. Its value of it is 0^0 for feldspars with monoclinic symmetry (orthoclase) and could reach the maximal value of 18^0 for those with triclinic symmetry (maximal microcline). The intermediary states are possible and defined as intermediate microcline.
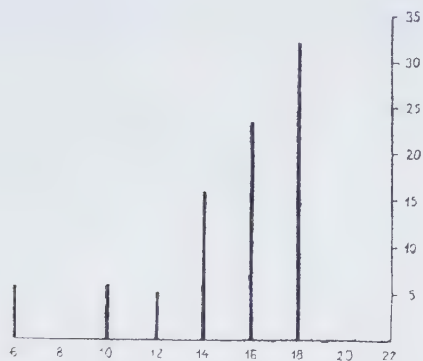
The values of $14-18^0$ have maximal frequency, showing a specific structural state for K-feldspar (i.e., maximal microcline with high degree of triclinicity). By simultaneous plotting $2V\alpha$ and $b:\gamma$ values in Laves-Vishwanathan diagram (Fig. 8) we may infer that K-feldspars from Ditrău alkaline rocks is represented by orthoclase microcline and sanidinic microcline with medium and high triclinicity.

Fig. 7. Limits of variation of b:γ extinction angles for the K-feldspars from Ditrău alkaline rocks.

For determining the Na content in the K-feldspar several measurements of refraction index have been carried-out in immersion, using standard liquids and Abbe refractometer (on 10 samples). The results obtained (Table 1) show a higher sodic character of the feldspars in essexites comparatively to the feldspars in other types of rocks. The feldspars from the granitoides and foidic syenites have the highest K content (>Or 90); Na values (<Or 65) are typical to alkali-feldspar syenites and monzonites.
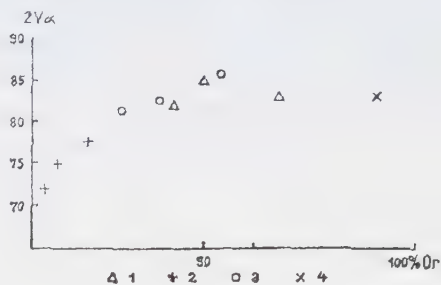

Fig. 9. The relationship between $2V\alpha$ and % Or for the K-feldspars from different rock types in the Ditrău alkaline massif. 1, foidic syenites; 2, essexites; 3, syenites; 4, granitoides.

Fig. 8. Plotting of 2V and b:γ values in Laves - Vishwanathan diagram for characterization of K-feldspars structural state. 1, foidic syenites; 2, essexites; 3, syenitoides; 4, monzonites with foides; 5, granitoides.

By correlating the N values with the 2V angles, a trend of increasing 2V value – simultaneously with decreasing Na content (Fig. 9) – could be remarked. The analyzed optical data suggest that K-feldspars from Ditrău alkaline massif are mainly represented by microcline, with a structural state characterized by a maximum to medium triclinicity degree, i.e., a high order degree in Al– Si relationship.

X-ray diffraction and I.R. absorption spec-troscopy analysis. The unit-cell size of the alkali feldspars depends on the degree order of Si and Al arrangement, and on the K/Na ratio. In the case of perthite the some dimensi ons depend on the degree of coherence between the K and Na zones. The outlining of these chemical-structural elements by X-ray diffrac-tion and I.R. spectrography represented the basis of some structural and petrological inter-pretations (Mackenzie, 1954; Mackenzie, Smith, 1955; Goldsmith, Laves, 1954), who outlined an image of feldspars genesis.

X-ray diffraction. 13 feldspar samples taken from the main massif rock types have been analyzed.

The comparison between calculated parame-ters (2θ, d, i) for 2θ = 10–55° domain and K-feldspars standard values – Borg and Smith (1969) shows the presence of microcline and perthitic intergrowth with albite. The details about the K-feldspars structural state have been obtained on the basis of the shape and positions of the (130) and (131) peaks.

The peak corresponding to (130) appears split-ted, which pleads for the presence of micro-cline, the amplitude marking the deviation from monoclinic symmetry (Mackenzie, 1954). The (130), (130 + 200) peak-shape and the distances between them, as well as the 2θ values (23-24⁰), show the presence of maxi-mum and intermediary microcline.

The calculation of triclinicity with Goldsmith and Laves (1954) method using (131), peaks showed values ranging mainly in 0.7-0.9 inter-val, corresponding to maximum microcline, and subordinately in 0.5-0.7 interval, corre-sponding to intermediary microcline.

The ratio between K and Na phases in alkaline feldspars has been determined on the basis of the d-values (201), (060), (204), (131), (1-31) peaks vs. to standard values for different per-centage of Or mole% in the low temperature

series microcline-albite (Orvill, 1967), and by means of the Wright diagram (1968) obtained on the basis of 2θ values, corresponding to (060) and (204) peaks (Fig. 10). The values obtained correspond to both end portions of the low-temperature albite-microcline series portions.

IR absorbtion spectroscopy in. 7 samples of K-feldspars have been measured between 300 and 1100 cm⁻¹ (Fig.11).
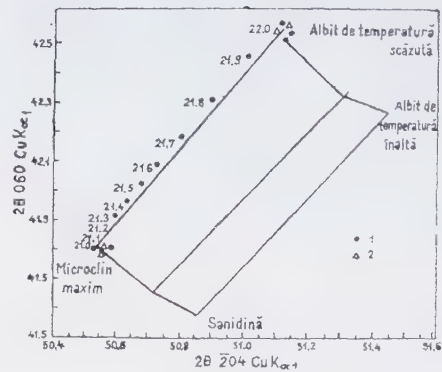

Fig. 10. 2θ 060/ 2θ 204 diagram for determination of K-feldspars structural type (Wright, 1968). 1, standard samples; 2, Ditrău feldspars.
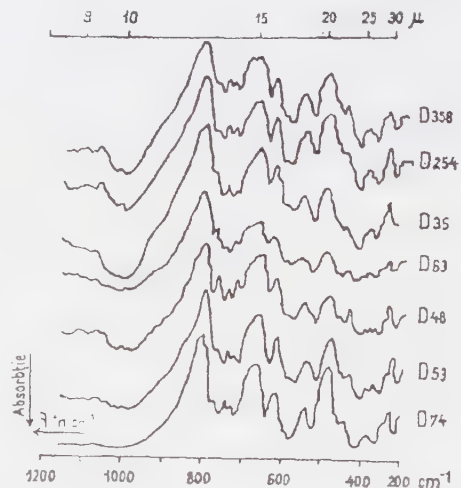

Fig. 11. The IR absorption spectra of the K- feldspars from Ditrău feldspars.

The shape and frequency of the main absorption bands obtained have been compared with the standard spectrum for the K-feldspars (Lyon, 1962; Van der Marel, 1969). The assignment of the characteristic bands has been after Iishi et al., 1971, fide Smith, 1974. Microcline is denoted by 1953 cm^{-1} and 1012 cm^{-1} diagnostic bands and by the more splited character of the bands when compared to sanidine and orthoclase.

The structural details of the K-feldspars are distinguished by slow changes of absorption bands position in 15.5 - 15.8 µm and 18.3-18.7 µm domains. The bands values of 15.5 - 15.8 µm and 18.3-18.7 µm plotted in Hafner-Laves diagram, completed by Smith, 1974, locates the Ditrău K-feldspar within microcline field, confirming that in spite of the some systematic instrumental errors, the main variations of absorption bands of K-feldspars are the result the order-disorder degree of Si - Al positions within the crystalline network. (Fig. 12).

Petrogenetic considerations. Because of their high frequency in igneous rocks, and especially, of the relationship between their nature (chemical, optical and structural) and genetic

conditions, the K-feldspars, constitute important petrogenetic minerals. In the case of Ditrău alkaline massif, because of their important participation, in almost all petrographic varieties, and of their peculiar characteristics, the K-feldspars are significant for the conditions in which the crystallization processes took place.

The study of the crystal morphology revealed the high degree of xenomorphism of K-feldspars due to late crystallization. The K-feldspars partial or total pseudomorphos after plagioclases are due to their high mobility and, probably, to their formation after the crystallization of plagioclase feldspars through selective remobilization processes in slow cooling conditions.

The study of intergrowths (perthites, antiperthites, twins) reveals a"high degree of mixing" between the K- and Na-phases. The forms described are the result of processes that evolved in subsolidus conditions and conducted, by selective replacements to perthites. During a subsequent stage characterized by a lower temperature (600–660°C) the exsolution perthites (string and vein-types) occurred. An argument for this is the presence of film- and vein-perthites within the K-feldspars that replace plagioclase determinining the "replacement"- type.

The development of "tartan"- type twins in the case of microcline formed on plagioclase, seems to be controlled by the presence of polysynthetic, albite type, ones, as both feldspars form epitaxial intergrowths having a common face - (010).

The optical properties of the feldspars and the X-ray and IR analyses, point to the unitary "structural" character of the K-feldspar from all types of rocks. A peculiar shape is represented by maximal microcline with high triclinicity specific to lower temperatures. Generally, the same structural state characterizes the K-feldspars from different rocks, and suggests the

Fig. 12. The IR absorption bands values of the Ditrău K-feldspars projected on the Hafner - Laves diagram.

possibility that the parageneses passed through similar petrogenetic conditions The spatial distribution of 2V angles outline a new zoning – conditioned by the massif cooling regime – asymmetrical in relation to the shape of the massif and to its petrographic constitution.

The asymmetry of this zone compared to geological limits outlined by erosion suggests a westward extensio, of the massif under Lăzarea crystalline structures or under the sediment cover and pyroclastic deposits from Gheorgheni Basin. This interpretation could be correlated with variations in cooling conditions, irrespective to the massif shape resulted from actual limits.

References

Alling H.L. (1938) Perthite types. *Journ. Geol.* **46**, Chicago.

Anastasiu N., Constantinescu E. (1976). Observații mineralogice în rocile sienitice din masivul Ditrău. Comunicări Geologie. Tipografia Universității București.

Borg I. Y., Smith D. K.(1969) Calculated powder pattern. Part II Six potassium feldspars and barium feldspar. *Amer. Min.* **54**, p. 163-181, Washington.

Codarcea Al., Codarcea-Dessila M., Ianovici V. (1957) Structura geologică a masivului de roci alcaline de la Ditrău. *Bul. Şt. Acad. R.P.R.* **II**, p. 3-4, București.

Goldsmith I.J.R., Laves F. (1954) Potassium Feldspar Structurally Intermediate between Microcline and Sanidine. *Geoch. Cosm. Acta,* **6**, p.100-118, London.

Ianovici V. (1933) Etude sur le masif syenitique de Ditrău, region Jolotca, district Ciuc. *Rev. Muz. Geol.-Miner. Univ. Cluj* **4**, 2, p. 1-53, Cluj.

Ionescu J. (1963) Studiul valorificării sienitelor alcalin nefelinice de la Ditrău ca înlocuitor al feldspatului în industria ceramică. *Stud.cerc. geol. geof. geogr.*, seria geol., **8**, 4, București.

Laves F., Hafner S. (1956). Infrared spectra of feldspars. *Zeitsch. Krist.* **108**, p. 56-63.

Laves F., Vishwanathan R. (1967). Relation between the Axial Angle and Triclinicity of K-Feldspars and Their Significance for Definition of "Stable" and "Unstable" States of Alkali Feldspars. *Schw. Miner. Petr. Mitt.*, **47**, 1, p.147-162, Berna.

Lyon R.J.P. (1962) Minerals in infrared. Stanford Research Institute.

Mackenzie W.S. (1954) The orthoclase - Microcline Inversion. *Min. Mag.* **30**, p. 354-366, London.

Mackenzie W.S., Smith J.V. (1955) The Alkali feldspars I-Ortoclase Microperthites. *Amer. Miner.* **40**, p. 707-732, Washington.

Mauritz B., Vendl M. (1923) Beitrage zur Kenntnis der Abyssichen Gesteine des Syenitstocks von Ditro. *Math. naturwtss. Ber. Ungarn.* **34** (1926-1927), p. 108-158 Budapesta.

Mureşan M.. (1968) The tectonic structure of the Southern Part of the Crystalline Mesozoic Zone in the Eastern Carpathians. *Rev. Roum. Geol. Geoph. Geogr., Ser.Geol.* **12**, 1, p. 55-59, București.

Orville P.M. (1967) Unit-cell parameters of microcline-low albite and the sanidine-high albite solid solution series. *Amer. Miner.* **52**, p. 58-86, Washington.

Popa Gh. (1975) Litostratigrafia Seriei de Tulgheş între Valea Putna şi Valea Belcina, Carpaţii Orientali, *D.S. Inst. Geol.* **LXI/5**, p. 151-177, București.

Popescu Gh.C. (1974) Studiul formaţiunilor cristaline cu sulfuri metalice din zona Bălan, Munţii Hăghimaş, Ciuc. M.M.P.G. O.D.P.T. Studii de sinteză, București.

Sorensen H. (1974) The Alkaline Rocks. John Willey. London.

Smith J.V. (1961) Experimental and Geological Evidence for the Stability of Alkali Feldspars. Cursill. Confer. 8, Madrid.

Smith J.V. (1974) Feldspars I - II, Springer-Verlag, Berlin.

Streckeisen A. (1952 -1954) Das Nephelinsyenit Massif von Ditrău. *Schw. Miner. Petr. Mitt.* **54**,1, Berne.

Streckeisen A. (1974) On the Origin and Age of the Nepheline Syenite massif of Ditrău. *Schw. Miner. Petr.Mitt*, **54**, 1, Berne.

Wright T. (1968) X-ray and Optical Study of Alkali Feldspar. *Amer. Miner.* **53**, Washington.
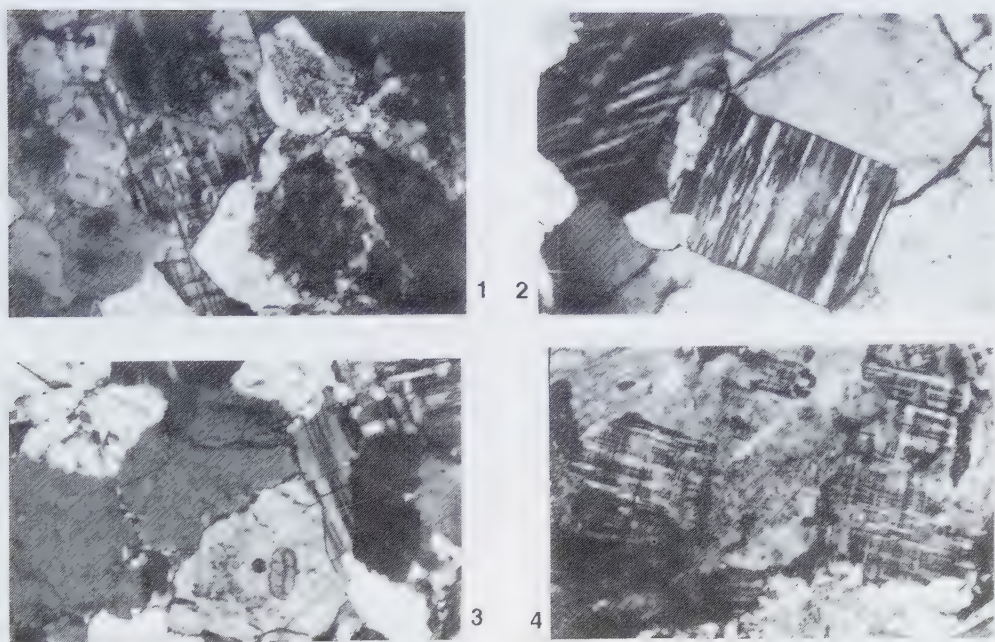
Plate I

Fig. 1. "Tartan"-twinned interstitial microcline; foidic monzonite, Jolotca brook; N+; X20.
Fig. 2. Euhedral grain of microcline; granitoide, Czengeler-Lückone; N+; X20.
Fig. 3. Interstial microcline; foidic syenites, Valea Mare; N+; X20.
Fig. 4. Microcline patches (partial pseudomorphs after plagioclase) foidic monzonites. Jolotca brook; N+; X20.
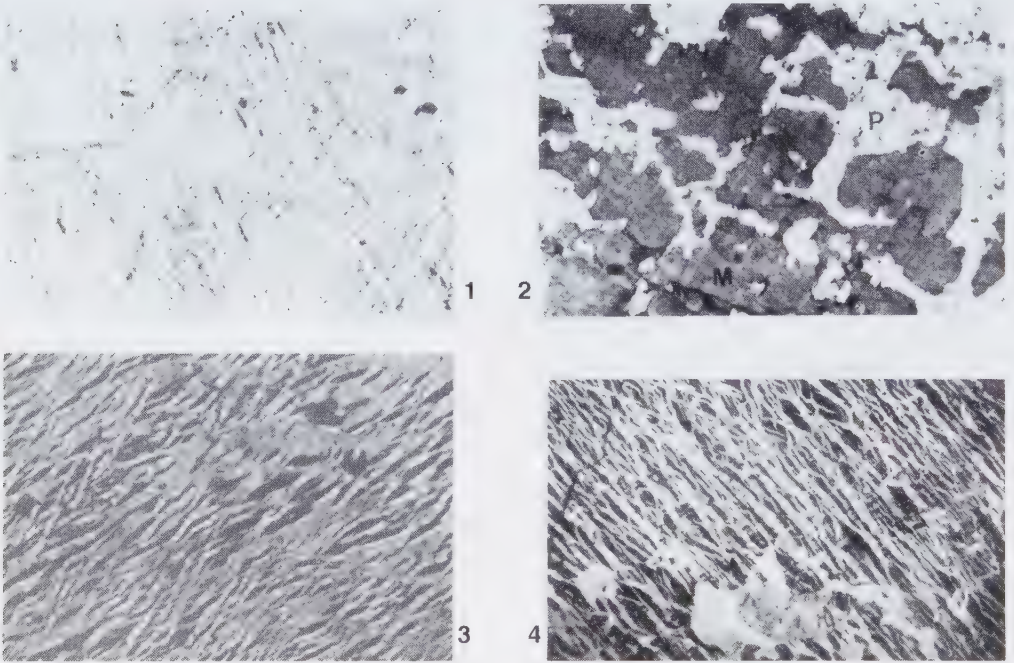
Plate II

Fig. 1. Exsolution perthites ("vein"-type) in microcline; alkali-feldspar syenites, Chiuruț brook; N+, X80.

Fig. 2. "Replacement"-type perthites; foidic monzonites, Güdutz brook; N+; X40.

Fig. 3. "Braid"-perthites in foidic monzonites, Güdutz brook; N+; X80.

Fig. 4. Microcline-perthite in essexites, Jolotca Brook; N+;X20.

Plate III
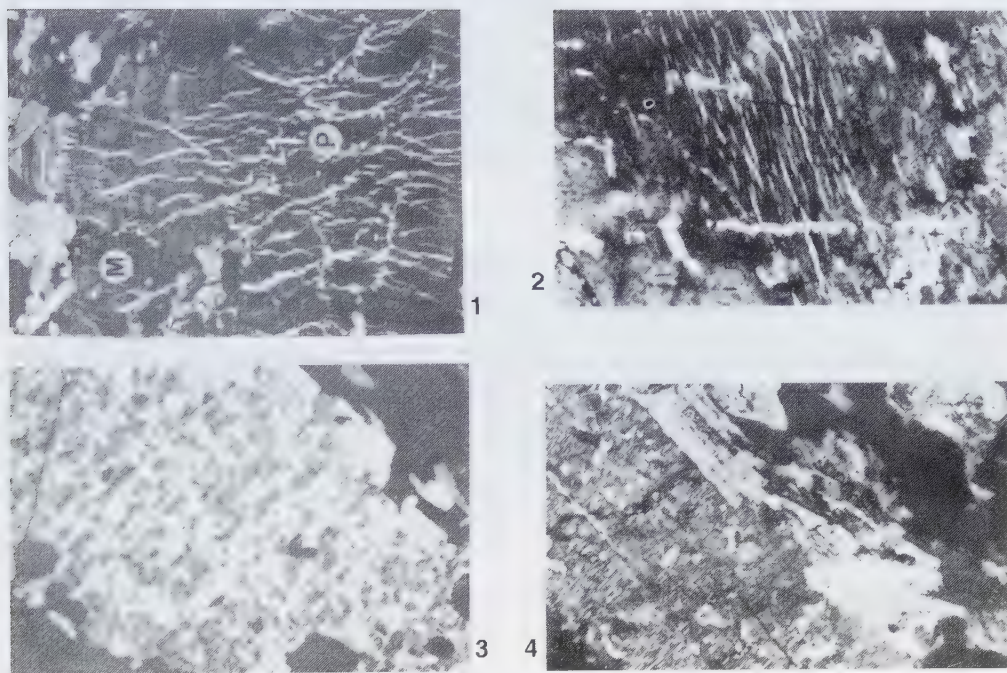
Fig. 1. "Braid"-perthites in microcline, foidic syenites, Güdutz brook; N+;X40.
Fig. 2. "Film" perthites in granitoides, Jolotca brook; N+; X20.
Fig. 3. Microcline patches developed on plagioclase (nearly total pseudomorhs), foidic monzonites, Jolotca brook; N+; X80.
Fig. 4. Microcline-perthite with plagioclase inclusions, syenitoides, Jolotca brook; N+; X80.

Plate IV
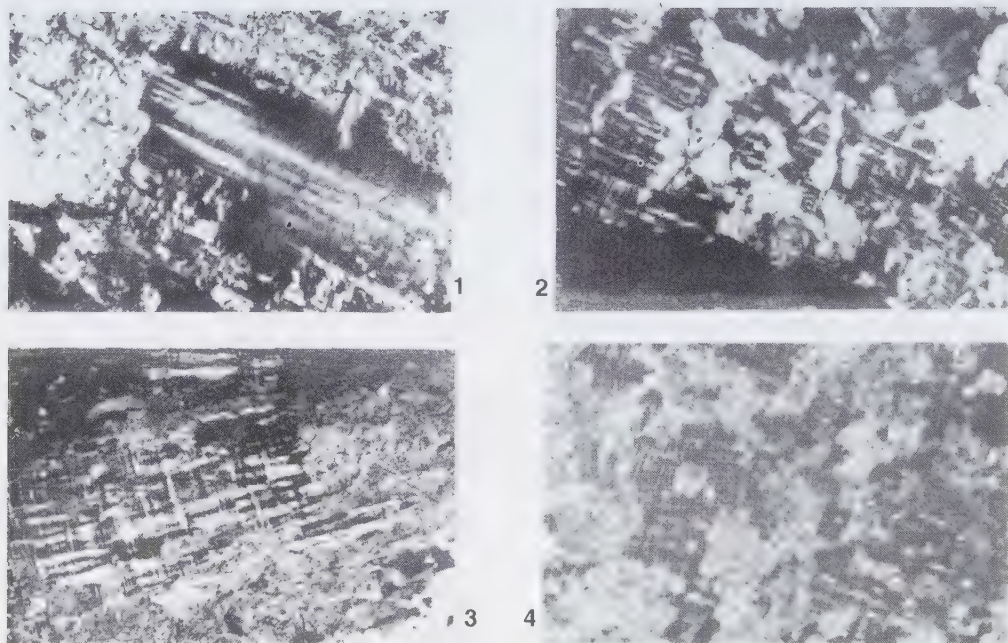
Fig. 1. Pseudomorph microcline after plagioclase, syenitoides, Valea Mare; N+; X20.
Fig. 2. "Tartan"-twinned microcline with inclusions of plagioclase, syenitoides, Valea Mare; N+; X20.
Fig. 3. "Tartan"-twinned microcline (plagioclase patches), alkali-feldspar syenites,
Valea Mare; N+; X20.
Fig. 4. Patches of microcline in sericitized plagioclase, foidic monzonites, Jolotca brook; N+; X20.
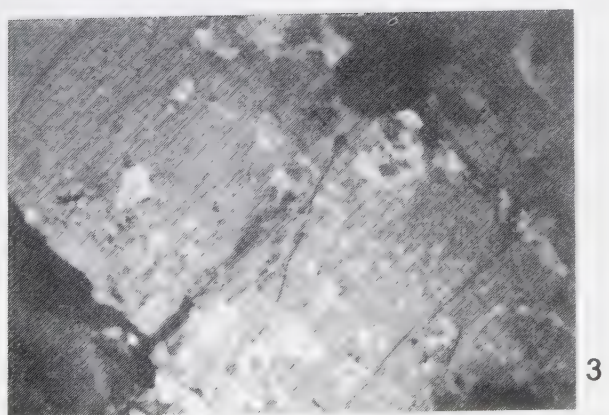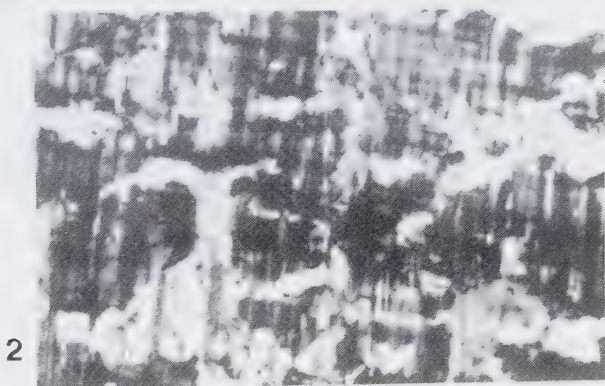
Plate V

Fig. 1. "Tartan"-twinned microcline, foidic syenites, Chiuruț brook; N+; X20.
Fig. 2. Epitaxial intergrowths of microcline and plagioclase, syenitoides, Valea Mare; N+; X20.
Fig. 3. Plagioclase relics in perthitic microcline, granitoides, Jolotca brook; N+; X20.

Plagioclase feldspars from the alkaline massif of Ditrău

NICOLAE ANASTASIU
EMIL CONSTANTINESCU

The plagioclases from the alkaline massif of Ditrău are albite and oligoclase-andesine. Grain size and crystal morphology, intergrowths (twins, antiperthites, myrmekites), optical (2V) and structural (XR), (IR) parameters were established as well as high order of plagioclases and low temperatures of crystallization. A petrologic genesis model was assumed. The plagioclases represent late crystallization minerals from alkaline natural melt; oligoclase-andesine was separated earlier than microcline but albite was formed both during plagioclase decalcification and during exsolution of alkaline feldspars.

In continuity of mineralogical observations about alkaline massif on Ditrău, begun in 1975, this study deals with the study of feldspars – minerals with the largest spread and with a sensible petrogenetic signification, within the massif. After ample studies (Ianovici, 1933, 1938; Codarcea, Ianovici, Codarcea, 1954, Streckeisen, 1954, 1960, 1974), which outlined a general image about the petrogenesis of the massif, our recent researching revealed several particularities, which enhance the mineralogical and petrographical diversity of Ditrău occurrence. The massif represents as complex unit, with two structural compartments:

a) Jolotca - Putna, north of Jolotca Valley;
b) Valea Mare - Gudutz - Belcina, south of Valea Mare – Ditrău, differentiated by the nature of petrographic members, by their extension and succession.

In the northern compartment, Jolotca - Putna, the petrographic members, younger from West to East, are represented by: a) ultramafites and mafites; b) diorites; c) monzodiorites and monzonites; d) syenitoides; e) granitoides. The foidic rocks, such as nepheline-bearing syenites, are subordinated and occur as marginal apophyses with circular contour. In the south compartment, Valea Mare-Gŭdutz-Belcina, the miscellaneous foidic rocks – foidic syenites, foidic monzonites, essexites – occupy the central part and marginally includes mafites and ultramafites. The foidic members are discontinuously bordered by monzonites, syenitoides and granitoides (Fig.1). The study of plagioclase feldspars – present in all petrographic types of the massif, excepting ultramafites – deals with their frequency and morphology, the intergrowth types, optical and chemical-structural elements and several aspects related to petroge-

Fig. 1. The distribution of An% content in plagioclase, within the alkaline massif of Ditrău.

netic evolution of the massif. Being a continuation of the research on K-feldspar (Anastasiu, Constantinescu, 1978) this study is based on a similar number of samples and follows the spatial spreading of plagioclase.

I. Frequency, size, morphological features

The plagioclase feldspars, belonging to major types of rocks in the alkaline massif of Ditrău, may be separated from chemical point of view, in sodic (albite) and sodic-calcic (oligoclase and andesine) forms; more calcic forms were quoted sporadically, without forming important masses (Codarcea et. al., 1954). Considering the cumulative participation of albite and mixed crystals – oligoclase and andesine – their frequency reflects variations related to the petrographic types and their spreading (Table 1 and Fig. 2).

In the compartment Jolotca-Putna, the plagioclase is the only salic fraction in mafites and

diorites, but its participation is restricted to (10-15 % and 35-50 %, respectively). In syenites and monzonites, the plagioclase is more frequent (35-55% and 40-60%, respectively) and is associated with K-feldspar. In granitoides (20-40%)and is associated with K-feldspar and quartz.

In the compartment Valea Mare-Güdutz-Belcina, the plagioclase content ranges in larger limits related to the participation of foides (nepheline, cancrinite, sodalite). The small contents (20-35%) are peculiar for the rocks with higher color index while the great ones (50-70%), from syenitoides and foidic syenitoid, are related to their leucocratic facies. Here, too, the mafite separations expose the lowes participation of plagioclase. In the massif, the crystal size (Table 1) equals that of other minerals in the paragenesis, but may form pegmatoid, normal granular and microcrystalline structures. The variation limits of anorthite (An%) content for feldspar from all types of rocks and the frequency histograms
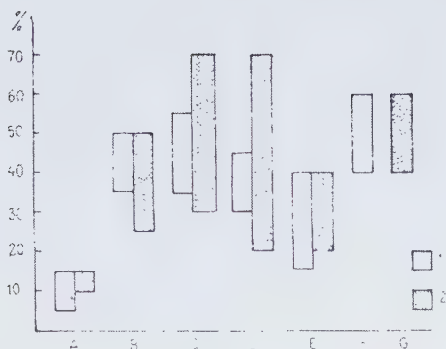
Fig. 2. The participation of plagioclase feldspars in the alkaline massif of Ditrău: 1-Jolotca-Putna compartment, 2-Valea Mare-Güdutz-Belcina compartment; A, mafites; B, diorites; C, syenitoides; D, foidic syenites; E, granitoides; F, monzonites; G, essexites.

(Fig. 3) reveal the following aspects:
- the maximum frequency of plagioclase in mafite at the border between oligoclase and andesine (An $_{20-45}$);
- in syenitoides and foidic syenitoides from both compartments, albite (An$_{0-10}$) coexists with oligoclase; in diorites from the southern compartment, it is associated with andesine (An$_{30-35}$);
- the frequency curve of anorthite content in the plagioclases from granitoides suggests the equal participation of albite and acid oligoclase, as an expression of the alkaline and normal facies of these rocks;
- monzonites and essexites tend to be depleted in albite.

In the studied paragenesis, albite and oligoclase often separate as two distinct phases, within characteristic morphology and properties.

Albite appears frequently in alkali-feldspar syenites, in foidic syenites and granitoides, and sometimes, tends to concentrate exclusively in monomineralic rocks with vein character – "albitites" ("Güdutz" open - pit, Valea Mare – Ditrău) In the CFF open - pit Putna basin, it occurs associated with nepheline,

forming mariupolite-type rocks (Sorensen, 1974). Albite shows the following habits:
- prismatic crystals, elongated, anhedral or subhedral, disposed in divergent aggregates;
- short prismatic crystals, usually anhedral, with pinacoid lateral faces (010) well developed, in granular aggregates, as inclusions in K-feldspar, or as recrystallization product on fissures (Pl. I, Fig.1);
- continuous or discontinuous coronas with variable width on the margins of oligoclase crystals (Pl. I, Fig. 2) in syenitoides and granitoides.
In all cases, the albite appears fresh and without inclusions.

Oligoclase occurs as subhedral prismatic crystals, or as interstitial agglomerations in diorites. Anhedral grains appear frequent as relics in the K-feldspar.

In syenites foidic monzonites, granitoides, and sericitized rocks, a slight caolinite pigment covers the plagioclase. The sericite develops as aggregates and sheets in the center of crystals (in some diorites, monzonites, and essexites). Generally, one could notice a more intense alteration with increasing content of Ca, and of crystal size.

In rocks with high color index, oligoclase includes idiomorphic crystals of sphene, epidote, hornblende and, biotite (Pl. II, Fig. 3, 4), In syenites, foidic syenites and granitoides it appears partially substituted by microcline.

II. Intergrowth and the optic of crystals

The intergrowths of plagioclases comprise twinning, antiperthites and myrmekites. The complex and various relationship of albite with the K-feldspars were previously analyzed (Anastasiu, Constantinescu, 1978). The twins have a polysynthetic character and are peculiar for all sodic phases, or sodic-calcic ones. The most frequent ones are the twinning after albite law (normal hemitropy), with associa-

Table 1

A. Structural compartment Jolotca – Putna Valley.

Petrographic type. Sample number - location	Paragenesis	Frequency %	Sizes (mn., max. in mm.)	Outline, habit	Anorthite content (%)	2 V (°)	Intergrowths, twins, transformations
1	2	3	4	5	6	7	8
1. Marites							
Coasta Băii	plg + amp + sph + ap + Ti-mg	5–15	20 0.4	Anhedral	25–53	(+)85 88	Poikilitic structures
Teascului Creek	plg + amp+ bi + sph + ap + Ti-mg	10–15	30 0.3	Anhedral	25–35	(+) 85 88	Albite-pericline twins,
Güdüz Creek	plg + amp+ px + sph + ap + Ti-mg	10	10 - 0.25	Anhedral	30 40	(+) 82–88	Fresh, rarely kaolinized
2. Diorites							
416 – Simo Creek	plg + amp + bi + px + ap + sph	40	5 0.2	Anhedral in "oceli"	20 35	(+)85–88	Poikilitic structures
300 Teascului Creek	plg + amp + px + sph + ap	35	10 0.3	Anhedral	25–35	(+) 85 88	Albite, Albite + Carlsbad twins
960 - 969, 340, 341 - Jolotca Valley	plg + amp + bi + sph + ap	50	10–0.2	Anhedral, subhedral	20 30	(−)86–90	Fresh, rarely with sericite, epidote, sausurite
3. Monzodiorites, monzonites							
372-405-408 – Jolotca Valley	plg + mi +amp + bi + ep + sph	40–60	5–0.2	Euhedral, subhedral, tabular, prismatic	10–25	(+)84–86	Albite coronas, rarely antipertithic fresh rarely with sericite and kaolinite
4. Syenitoides							
383-421-465-Jolotca Valley	plg + mi	35 55	4 -0.2	Euhedral, subhedral, prismatic	5–10 10–15	(+) 78–82 (+) 84 90	Albite coronas around oligoclase
5. Granitoides							
80-96–Czengeler Lukone	plg + mi	15–40	2 -0.2	Anhedral, subhedral	8–15	(+) 84–90	
386-390 Jolotca Valley	plg + mi +-q + bi + zr + ca	25–35	1 -0.4	Anhedral, short prismatic	8–18	(+)84–90	Albite twins, Carlsbad
975 Holo"ag Creek	plg + mi +q + bi + amp	20 25	15 -0.3	Euhedral, subhedral	15–20	(+) 88	Fresh, rarely with kaolinite, sericite
915-Turcului Creek	plg + mi +q + bi + ms + zr	15–20	15 0.3	Euhedral	10–15	(+)84–90	
6. Foidic syenites (apophyses) - Teasculu Creek, Fagului Creek	plg + ne + mi + bi + ca	30–45	2 0.2	Anhedral	0–8	(+)76–84 (-)88	Albite coronas, intergrowth with K- feldspar, partially kaolinized

Table 1 (continued)

B. Valea Mare – Guduţz. – Belcina structural compartment.

Petrographic type Sample number - location	Paragenesis	l-gneexx %	S % (min., max. m mm.)	Orans. habit	Anorthite content (%)	2V (°)	Intergrowths, twins, transformations
1. Foidic syenites 14, 35 - Güdütz Creek	plg + ne + mi + bi + ca	25-40	5-0.1	Euhedral	2-8	(+)78-84	Antiperthitic intergrowth
44, 476 Valea Mare	plg + ne + mi + bi + amp + px + so + ca + zr + ap	20-80	10-0.2	Euhedral, subhedral, prismatic	0-8 10-15	(+)76-82 (+)84-90	Albite, Albite-Carlsbad twins fresh, rarely kaolinized
448, 452 Călugăr Creek	plg + ne + mi + bi + ca	20-60	1-0.15		8-10		
2. Foidic monzonites 29, 31 Güdütz Creek	plg + mi + ne + bi + amp + px + zr + il + ap	40	2-0.2	Anhedral	10-20	(+)86-88	Albite, Albite Carlsbad twins
3. Essexites 19, 56 – Güdütz Creek, Valea Mare	plg + mi + ne + bi + amp	40-60	2-0.5	Subhedral	15-30	(-)86-90	Fresh, rarely with sericite
4. Mafites Tulgheş Ditrău road (km 26)	plg + amp + px + bi + sph + ap + ep + il	10-15	5-0.5	Anhedral, subhedral	20-35	(-)88-84	Poikilitic structures, Albite twins, fresh
Diorites Valea Crucea Tulgheş Ditrău road (km 18)	plg + amp + px + bi + sph + ap + Ti-mg	25-50	10-0.2	Anhedral, subhedral	20-30	(+)88-84	Antiperthitic exsolutions
18, 263 Güdütz Creek, Cetăţi	plg + mi + bi + amp + ap + sph	35-50		Subhedral, tabular, prismatic	0-8 15-25	(+)76-82 (-)86-90	Deformations, albite coronas, thin twins; fresh, partially kaolinized
6. Syenitoides 102,108 Güdütz	plg + mi + bi + ms + zr + ap	35-80	2-0.2	Euhedral	0-8	(+)76-82 (-)86-88	Fresh albite coronas
1014 Ciumod	plg + mi + bi + amp + zr + ap + xc	30-35	3-0.2	Subhedral, anhedral	10-20		thin twins, deformations partially kaolinized
7. Granitoides 101, 266, 1330- Güdütz Creek, Ciumod Creek, Aurora	plg + mi + q + bi + ms + zr + ap	20-40	1.5-0.1	Anhedral, subhedral	0-8 10-18	(+)76-82 (+)84-90	Fresh Partially kaolinized and sericitized

Abbreviations: px – pyroxenes, amp – amphiboles, bi - biotite, mi – microcline, q – quartz, ca – cancrinite, so – sodalite, ne – nepheline., il – ilmenite, ap – apatite, Ti-mg – Ti-magnetite, sph – sphene, xc – xenotime, ms – muscovite, zr – zircon, ep – epidote.

tion after plane (010) (pl. I, Fig. 1). The complex hemithropy twin, Albite-Carlsbad [(010) x (001)] (Pl. I, Fig. 3, 4) represents a subordinate type. The intergrowth after law Albite-A-A or Manebach appears sporadically. Thus, we may conclude that the high frequency of Albite and then, Albite-Carlsbad twins represent a rule for foidic and feldspar-rich rocks (syenites, monzonites) with sodic character, which resulted by slow crystallization at low temperature. The observation is sustained by the projection of twinning plane poles and of

twinning axes, that fit with the low-temperature curves in standard diagrams. The crystals forming the twins are wider in alkali-feldspar syenites, and thinner and elongated in syenitoides, granitoides, and, even, diorites; in essexites, they appear, simultaneously, thin and bulky.

Where the plagioclase presents deformation traces the twins are bent and torn up in steps or with variable width (e. q. in essexites occurring on the Ditrău-Tulgheş road, in foidic
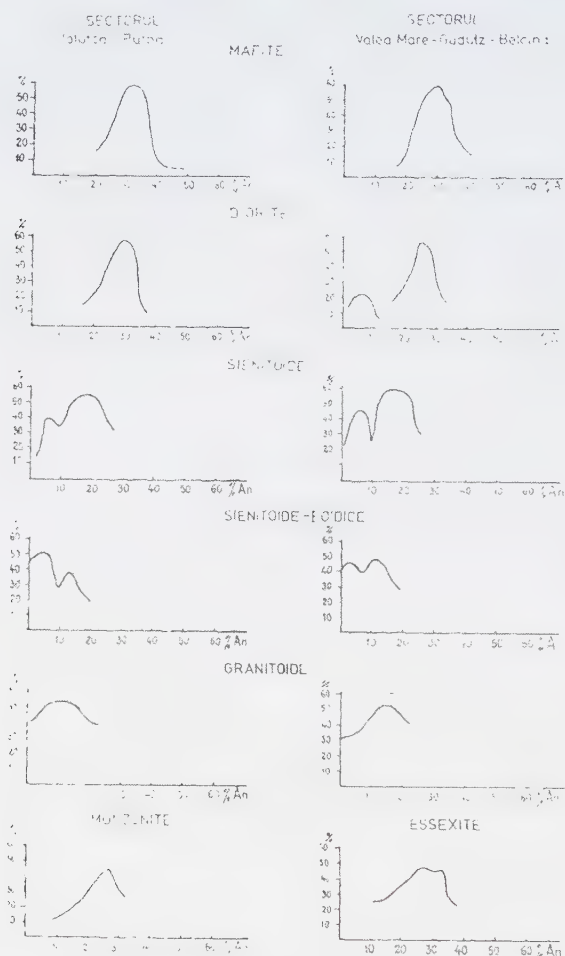
Fig. 3. Frequency and limits of variation for anorthite content (% An) of plagioclase from the main petrographic members of structural compartments Jolotca - Putna and Valea Mare - Güdutz - Belcina.

monzonite on Güdutz Creek or in granitoides on Holoşag Valley, the twins are bent and torn up in steps or with various breadths.

Though rare, the antiperthites occur in diorites, monzonites and all foidic rocks In nepheline syenites on Güdütz Creek and Putna Creek, the K-feldspar tend to develop as kaolinized veinlets in the mass of plagioclase or as short, idiomorphic crystals, parallel with the cleavage. The myrmekites outcrop exclusively in granitoides, on Holoşag Creek, Turcului Creek and in the upper course of Jolotca Valley. By universal stage study, there were determined the values of the 2V angle for plagioclases from diorites, syenitoides, foidic monzonites and syenites, granitoides and essexites (Table 1). The data correlate with the anorthite content of plagioclase and suggest, by their projection on Slemmons curves (1965) (Fig.4), crystallization at low-temperatures.

clase in almost all analyzed samples as well as its association with albite.

Compared with the data presented by Borg, Smith (1969) and Smith (1974) the "d" parameter for albite and its relative intensities, point out that our values correspond to low-temperature albite domain.

Seven analyses were made by IR absorption spectroscopy, in the range 200 cm^{-1} – 1,100 cm^{-1}. The spectra contain the diagnostic absorption bands for plagioclase feldspar (noted with asterisk on the figure), which vary with the anorthite content in the domains 15.3 - 16.2 and 18.2 - 18.9 μm.

The projection on Hafner, Laves and Thompson, Wodsworth diagrams reveals values corresponding to oligoclase and albite,indicating a low-temperature plagioclase (Fig. 5).
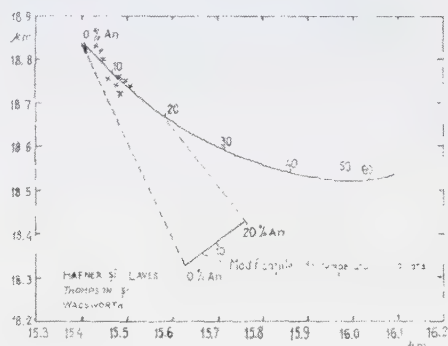

Fig. 4. 2V angles projection of plagioclase on Slemmons (1965) diagram: 1, diorites; 2, syenitoides; 3, monzonites; 4, foidic syenites; 5, granitoides; 6, essexites.

Fig. 5 Projection of IR absorption bands in the ranges 18.2-18.9 mm and 15.3 - 16.2mm on Hafner and Laves (1957) and Thompson and Wodsworth (1957) - diagram for the plagioclase feldspars from the alkaline massif of Ditrău.

III. X-ray diffraction and IR absorption spectroscopy data

The X-ray diffraction analyses were made on plagioclase feldspar from various types of rocks and occurrences, in the domain 2θ: 10-55°. The comparison of 2θ and dα/n parameters with the standard values (Miheev, 1957; ASTM) suggests the presence of oligo-

IV. Petrogenetic considerations

The plagioclase feldspars,and the K-feldspar, are ubiquitous minerals in the alkaline massif of Ditrău. Both minerals express the formation conditions and some petrogenetic aspects.

Table 2. The values 2q, dα/n and hkl obtained by X-rays diffraction, for the feldspars from the massif of Ditrău.

Sample 35

2θ	dα/n	hkl
13.65	6.485	0.20
22.05	4.031	-201
23.10	3.851	1-11
23.52	3.783	111
24.32	3.659	-130
25.55	3.487	-1-12
27.90	3.198	002
30.18	2.9615	1-31
30.50	2.931	0-22
31.25	2.8625	131
33.27	2.6925	-2-22
34.20	2.622	-3-12
34.95	2.567	-2-41
35.80	2.5255	1-121
38.55	2.3155	-331
40.48	2.2285	1-32
40.75	2.214	-223
42.60	2.1225	060
43.60	2.076	-2-41
45.20	2.006	-152

Sample 53

2θ	dα/n	hkl
13.63	6.475	0.20
13.88	6.38	001
24.48	3.670	-1-31
25.66	3.475	-221
26.40	3.376	-112
28.72	3.187	002
30.20	2.9595	-2-22
30.48	2.9335	0-22
30.78	2.905	041
31.25	2.8625	131
35.02	2.5825	-2-41
35.57	2.524	-241
36.70	2.449	-241
37.02	2.1285	-3-31
37.80	2.405	240
38.80	2.320	-113
41.79	2.1614	003
43.52	2.0795	2-41
45.74	1.9836	-422
47.10	1.9294	-0-22
48.18	1.8888	222

Sample 74

2θ	dα/n	hkl
13.65	6.485	020
13.89	6.373	020
22.08	4.02	-201
23.10	3.85	1-11
23.58	3.77	111
24.30	3.66	-1-31
25.50	3.483	-2-21
26.48	3.336	-221
27.92	3.195	040
28.32	3.151	-220
30.18	2.9615	1-31
30.35	2.9315	0.22
31.24	2.8635	1-31
32.11	2.7875	0-41
33.99	2.6375	-132
34.99	2.5745	-2-41
36.99	2.4305	-1-51
28.80	2.310	-3-31
41.30	2.186	042
41.80	2.161	060
42.50	2.127	060
43.60	2.076	311
45.35	1.999	222
47.15	1.9274	2-22
48.15	1.8898	-3-51
50.00	1.824	0-62
50.55	1.8056	043
51.42	1.7866	-204

Sample 80

2θ	dα/n	hkl
13.65	6.485	001
13.92	6.36	020
22.10	4.022	-201
23.60	3.77	111
24.30	3.663	1-31
25.60	3.48	-1-12
26.48	3.336	220
27.92	3.495	002
30.20	2.9595	1-31
30.55	2.9365	0-40
30.83	2.9005	0-41
32.20	2.780	0-41
34.00	2.637	-312
35.05	2.5605	-2-41
36.80	2.4425	-2-41
36.95	2.2433	-1-51
37.45	2.4015	-150
38.65	2.3295	-1-13
39.68	2.2715	-113
41.35	2.1835	-242
41.90	2.456	-223
42.59	2.423	060
43.61	2.0755	202
45.78	1.9848	-422
47.15	1.9275	400
48.20	1.888	-3-52
50.00	1.824	-0-62
50.15	1.812	400

Table 2 (continued)

Standard oligoclase A.S.T.M. II-1159		Low temperature albite, Standard Borg, Smith, 1967		
dα/n	dα/n	2θ	dα/n	hkl
6.4	1.74	13.88	6.376	0 20
4.5	1.70	15.88	5.581	-1 11
4.07	1.66	22.06	4.027	-2 01
3.67	1.562	23.06	3.854	1-11
3.47	1.524	23.54	3.777	1 11
3.18	1.490	24.32	3.668	-1-31
2.90	1.451	26.74	3.332	-2 21
2.80	1.416	27.96	3.194	0 02
2.67	1.403	30.12	2.965	1-31
2.59	1.381	30.50	2.931	0-22
2.52	1.364	31.24	2.962	1-31
2.43	1.325	32.14	2.782	0 41
2.37	1.315	33.98	2.637	-1 32
2.29	1.278	35.00	2.562	-2-41
2.16	1.262	36.86	2.431	-1-51
2.10	1.251	38.80	2.319	-3-31
2.07	1.233	41.26	2.187	0 42
2.01	1.220	42.50	2.125	0 60
1.95	1.190	45.30	2.004	-1 52
1.90	1.172	47.12	1.9270	2-22
1.87	1.155	48.14	1.8894	-3-51
1.83	1.133	50.08	1.8196	4 00
1.81	1.109	50.60	1.8027	1 13
1.77	1.060			
	1.037			
	1.025			
	1.014			
	1.986			

The study of crystal morphology and of the mineral relationships suggests that the plagioclase feldspars (as well as the K-feldspars – Anastasiu, Constantinescu, 1978) represent late crystallization minerals.

In the feldspar paragenesis, the terms "oligoclase – andesine" appeared before "microcline" and "albite". The albite may represent a recrystallization product formed by decalcification of plagioclase (in albite coronas) or by exsolution of K-feldspar (in the case of idiomorphic crystals included in K-feldspar or of those localized on fissures).

The albite neoformations from alkali-feldspar syenites and and from the mariupolite-type, reflect a petrographic disequilibrium, with the release of sodic phase and its remobilization by diffusion at microscopic scale in certain marginal areas of the massif.

The optic investigations of plagioclase, beside the results of X-ray diffraction and infrared spectroscopy, reveal the presence of crystals with high structural order. This fact, correlated with the projection of 2 V - %An values on low temperature curves (Slemmons, 1961) suggest similar inset and cooling conditions for all petrographic members which form the structural compartments of the alkaline massif of Ditrău.

References

Anastasiu N., Constantinescu E. (1974) Observații mineralogice în rocile sienitice din masivul Ditrău, *Com. Geol.,* Geologie, Univ. București.

Anastasiu N., Constantinescu E. (1978) Feldspații alcalini din masivul alcalin de la Ditrău. *D.S. Inst. Geol. Geof.,* **LXIV** (1976-1977), 13-36.

Borg I.Y., Smith D.K. (1968),Calculated powder patterns. Part II Five plagioclases, *Amer. Miner,* **53**, Washington.

Codarcea Al, Codarcea D. M., Ianovici V. (1957) Structura geologică a masivului de roci alcaline de la Ditrău, *Bul. Șt. Acad. R.P.R.,* **II**, 3-4, București.

Ianovici V. (1933/1934) Etude sur le massif syenitique de Ditrău, region Jolotca, district Ciuc, (Transilvania), *Rev. Muz. Mineral.,* **4**, 2, Univ. Cluj.

Laves F., Hafner S. (1956). Infrared spectra of feldspars, *Zeitsch Krist.,* **108**.

Lyon R.J.P., (1962), Minerals in infrared, Stanford Research. Institute.

Miheev V. (1957), Renigenometriceskii opredelitel mineralov, Gosgheolitehknizdat, Moscova.

Sorensen H. (1974). The alkaline Rocks, John Willey, London.

Streckeisen A., Hunziker J.C. (1974), On the origin and age of nephelin syenit massif of Ditrău (Transilvania, Romania), *Schw. Min. Petr. Mitt.,* **54**, 1.

Thompson C.S., Wodsworth M.E. (1957), Determination of the composition of plagioclase feldspars by means of infrared spectroscopy, *Am. Miner.,* **42**.

* * A.S.T.M. index to X-ray powder data file A.S.T.M., sp. *Tehn. Publ.,* **48**, L, II, New York.

Plate I.
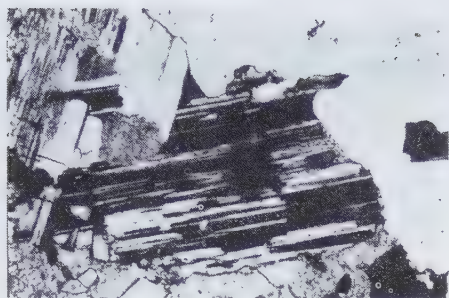
Fig. 1. Synthetically twinned albite in foidic monzonites; Balas Lorinz Creek, N +, x 40.
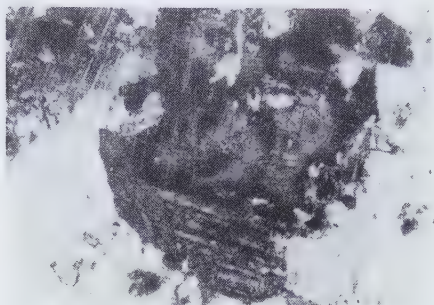
Fig. 2. Plagioclase anhedral crystal with albite corona, in monzodiorite, Jolotca Creek, N +, x 20.
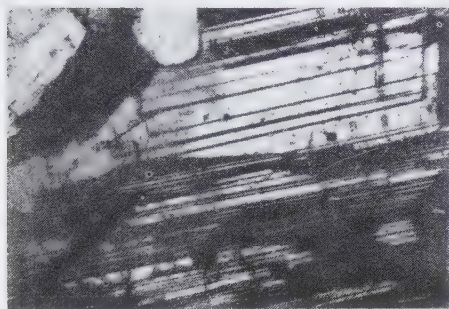
Fig. 3. Albite - Carlsbad twinning in plagioclase; syenite, Jolotca Creek, N +, x 40.
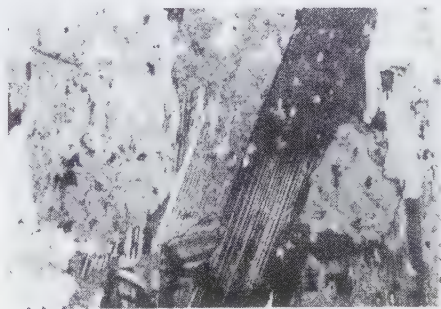
Fig. 4. Albite - Carlsbad twinning in oligoclase.

Plate II.
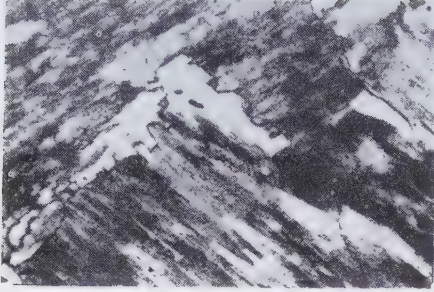
Fig. 1. Albite corona around albite; foidic syenite, Valea Mare – Ditrău, N+, x 40.
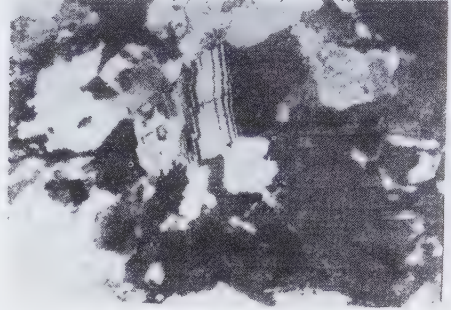
Fig. 2. Deformed plagioclases and albite neoformation in alkali-feldspar syenite; vein in Valea Mare – Ditrău, N +, x 20, x 40.
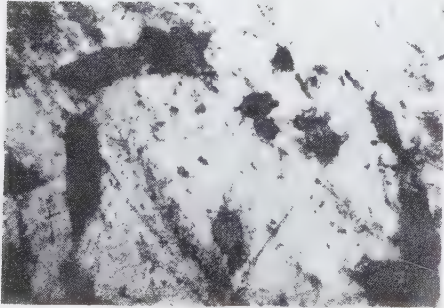
Fig. 3. Inclusions of idiomorphic sphene in plagioclase; diorite, Teascului Creek, N+, x 40.
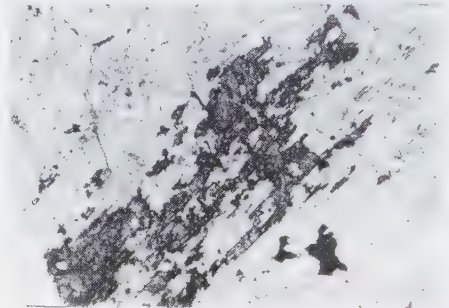
Fig. 4. Inclusions of epidote in the plagioclase; diorite, Teascului Creek, N +, x 40.

Plagioclase feldspars in the banatites from Maidan-Oravița, Romania

EMIL CONSTANTINESCU
GABRIEL BINDEA

By means of the universal stage, there were investigated the plagioclase feldspars in a series of banatitic bodies outcropping in the perimeter between Oravița and Maidan. Their mineralogical composition pointed out the presence of the following varieties: quartz monzodiorites diorites (M between 17% and 31%), quartz diorites, granodiorites, monzodiorites, granites and tonalites. Plotting points of these rocks form a field situated along the QPA angle bisectrix of the Streckeisen diagram. The anorthite content in plagioclase creates an obvious distinction between two lines of magmatic evolution. For the two feldspar populations, two frequency maxima are determined: 18% An and 42% An. According to the structural position of these subvolcanic bodies, plagioclase feldspars point out types characterized by a certain degree of structural disorder. In this context, it is noticed that about 50% of the two axis poles or of cleavage poles are plotted in the standard diagrams (Tröger, Wenk Parker Wenk) between the high and low tem perature curve according to a continuous order. The following correlations between the rock type and the plagioclase twins are remarked: in quartz granodiorites and monzodiorites, the only twins observed in the plagioclases are complex twins of Manebach Aklin A type; in plagioclases from diorites, complex twins of albite Ala B type are present, as well as parallel twins of Karlsbad type and normal twins such as Baveno and albite. In plagioclases from quartz diorites occur all the mentioned twins in about identical proportions. In other words the frequency of Karlsbad A, albite, Baveno, Albite Ala B twins increases with the rock basicity. Manebach twin is observed especial ly in more acid varieties. Zoned plagioclases, are characterized by the constant presence of about 3-4 recurrent zones of high basicity, distributed at certain intervals, in the context of a gradual acidity increase towards margins. They sugges crystals motion during the formation, according to some continuous circuits into a magmatic quasi-stratified chamber.

Tourmaline from Cioaca Înaltă zone (SW Banat)

EMIL CONSTANTINESCU

The Cioaca Înaltă zone, limited to the north by the Nera river and to the south by Ungurelu valley, is located east of Sasca Montană locality. The geological background includes Laramian magmatic bodies (banatites) represented mainly by porphyritic quartz-monzodiorites. They form a NS elongated body, emplaced into the Barremian-Aptian limestones of the Reșița-Moldova Nouă syncline.

Tourmaline was identified in isolated outcrops which cover a rectangle shaped area (150/30 m), usually covered in vegetation, located east of, and parallel to the banatite body. A progressive transition from partly altered banatities to rocks consisting almost exclusively of quartz and tourmaline is obvious. In an initial phase, the feldspars are transformed into a sericite and zoisite mass, while in an intermediate phase the rocks show a cavernous aspect, the voids probably corresponding to completely leached feldspars. Other minerals present are magnetite, hematite and brookite.

Macroscopic features

Tourmaline has a black color and appears as isolated, short or long prismatic crystals, with dimensions varying from 3-4 mm to 1.5 cm; radial aggregates also occur. They show combi-nations of prism faces (1011, 1101, 1110). Often they accumulate as bands or compact masses with 3-4 cm^2 or more.

Chemical and physical features

Tourmaline is a mineral with complex chemistry and numerous hypotheses have been advanced in order to establish its structure and formula. Most authors think it is a group with large chemical variability, between 5: dravite - $H_4NaMg_3Al_6B_3Si_6O_3$; schörlite -$H_8NaFe_3Al_6B_3Si_6O_{31}$; elbaite - $H_4NaLi_3Al_6B_3Si_6O_{31}$; tsilaisite - $H_4NaMn_3Al_6B_3Si_6O_{31}$ and uvite - $H_4CaMg_4Al_5B_3Si_6O_{31}$, with continuous solid solutions between dravite-schörlite (and uvite), schörlite-elbaite and with a miscibility gap between dravite and elbaite.

The chemical composition of tourmaline from Cioaca Înaltă (Table 1) corresponds to the isomorph series dravite-schörlite with low contents of uvitic components. The number of ions calculated in the basis of 31 (O,OH) (Table 1) reported to similar values calculated for 25 (shorlitic) tourmaline analyses by Deer et al. (1965) reveal high contents of Al^{3+} compared to the medium values of the dravite-schörlite series and a remarcable participation of Fe^{3+}.

Table 1.

Chemical analyses of tourmaline		Number of ions in the basis of 31 (O,OH)	
SiO_2	35.11	Si	5.869
TiO_2	0.46	B	2.814
B_2O_3	9.79	Al	6.000
Al_2O_3	36.63	Al	1.215
Fe_2O_3	3.83	Fe^{3+}	0.482
FeO	7.27	Mg	0.713
MnO	0.12	Ti	0.060
CaO	0.73	Fe^{2+}	1.025
Na_2O	1.06	Mn	0.010
MgO	2.87	Na	0.341
K_2O	0.13	Ca	0.120
H_2O^+	2.33	K	0.020
H_2O^-	0.20	OH	2.613
		$Fe^{2+} + Fe^{3+} + Mn$	1.517
Total	100.54		

The measured physical properties are shown in Table 2. The values of w, e and G on Winchell's diagram (1964) (Fig.1) correspond to a domaine situated between 60 and 80 mole%. schörlite. The informations obtained through X-ray diffraction, infrared spectroscopy and thermodifferential analysis show the chemical-structural particularities of the analysed samples.

Values *d* and *I* (Table 2, Fig. 2A) are generally similar to the values given by Miheev (1957) for the schörlite variety; on the diagramm of Deer et al. (1965), the values of *c* and *a* (Table 3) correspond to the domaine with 60-80 mole% schörlite.

The thermo-differential curve (Fig. 2B) shows an strong endothermal effect at 1020° C, due to Boron elimination of boron. For different types of tourmaline, the temperature of this peak varies from 1000 to 1100° C (Kauffman and Dilling, 1950). Elimination of the (OH)‑ group takes place in various ways for distinct tourmaline varieties (Kurylenko, 1950). It takes place at temperatures between 145 and 770° C. For the analysed tourmaline, this effect is weakly marked, appearing as a large band in the range of 100-300° C.

The infrared absorption spectrum of tourmaline is little discussed. The absorption band is difficult to ascribe in the absence of chemical analyses of synthetic minerals with compositions corresponding to the end-members of the isomorphous series. A large number of authors prefer to use the aspects regarding the color and pleochroism, using the absorption spectra in both visible and ultraviolet light (Faye et al., 1968; Marfounine et al., 1970). The infrared spectrum from Fig. 2C is similar with that obtained by Moenke (1962) for the schörlite from Ancone both as general appearence, and disposition of the bands characteristic for chains of Si-O-cations in the 400-1800 cm^{-1} domain. We note the inflections typical for the presence of the (OH)‑ groups of the 3400-3600 cm^{-1} interval and of the planar lattice BO_3 in the domain situated at 1600-1800 cm^{-1}.

Fig. 1. The values of refraction indexes, birefringence and specific weight measured for tourmaline from Cioaca Înaltă, ploted on the dravite-schörlite diagram (Winchell, 1964): 1, large zoned crystals; a, dark green central zone; b, light yellow marginal zone; 2, colorless needle shaped crystals.

Table 2. Values of 2α, d and I calculated from the diffractogram of tourmaline from Cioaca Înaltă

N°	2θ	d_α/n(Å)	I/100	hkil	N°	2θ	d_α/n(Å)	I/100	hkil
1	13.83	6.41	16	10$\bar{1}$1	14	51.12	1.7868	3	54$\bar{9}$0
2	17.73	5.004	10	20$\bar{2}$1	15	55.02	1.669	15	60$\bar{6}$3
3	19.28	4.604	31	30$\bar{3}$0	16	56.00	1.642	4	4373
4	20.90	4.250	60	21$\bar{3}$1	17	57.92	1.5922	22	5.5.10.0
5	22.35	3.978	100	22$\bar{4}$0	18	60.30	1.5349	8	9090
6	25.50	3.494	26	10$\bar{1}$2	19	64.00	1.4548	4	
7	34.78	2.5785	26	50$\bar{5}$1	20	65.18	1.4312	7	
8	37.75	2.383	3	0003	21	65.82	1.419	6	
9	38.30	2.350	2	10$\bar{1}$3	22	69.18	1.358	6	
10	42.48	2.127	18		23	70.89	1.3294	5	
11	44.30	2.0445	12	22$\bar{4}$3	24	72.05	1.3108	15	
12	47.35	1.9198	3	7071	25	74.32	1.2764	7	
13	50.20	1.8174	15	50$\bar{5}$3	26	77.98	1.2282	18	

Optical properties

Tourmaline occurs as isolated crystals, with euhedral and subhedral outlines, short prismatic to acicular. It forms fibrous and spherulitic aggregates of the "tourmaline sun" type, or as compact aggregates showing wavy extinction. Cleavage is imperfect after (1011).

Fig. 2. A, Diffractogram: rad. CuKa; Ni filters: Vg=1°/min; Vp=240mm/n; Phillips diffractometer. B, TDA curve: sample mass: 410 mg; platinum; MOM derivatograph; C, infrared absorption specta: KBr pill; 0.15 mg; Zeiss UR20 spectrometer.

The color of different crystals varies from intense green to greenish yellow and colorless. Crystals with more intense shades are strongly pleochroic: ω - colorless, yellowish green, pale bluish; ε - dark olive green. The interference colors vary from 0.024 to 0.034; the birefringence colors show little homogeneity and are often masked by the own color of the mineral.

A great number of large crystals are zoned. Zones parallel to the prism faces show a euhedral outline and are evidenced by variations of color and birefringence. They usually show a large central zone of dark green color and narrow, light yellow border zones (Pl I, Figs. 1, 2). Zoning can be oscilatory, seen as an alternation of very thin bands. In this case there is a tendency to pass from ditrigonal to trigonal habit. It is the case of fractured crystals which look like yellow veins, showing the same color as the marginal zones and cementing the fissures which cross the dark green colored central zone.

The refraction indices of the zoned tourmalines show slight variations between the central and the marginal zones, and remarcable variations between the values obtained for the strongly colored and for the colorless tourmaline (Fig. 1). The projection of indexes w and e (Fig. 3) shows that the interval of the virtual values corresponding to the total ions (Fe^2 + Fe^3 + Mn) in the basis of 31 (O, OH) is equal to 1.517, as calculated from the global chemical analysis (Table

Table 3. Physical properties of tourmaline from Cioaca Înaltă

$\omega = 1.662$	$a = 15.95 \pm 0.01$	$G = 3.20 \pm 0.02$
$\varepsilon = 1.634$	$c = 7.20 \pm 0.01$	D (VHN) = 1.176 kg/mm (7.25 Mohs)
$\Delta = 0.030$		

(Table 1), and suggesting modification of the Fe contents.

Discussion

The relations between the minerals reveal that tourmaline is a secondary mineral in the investigated area. In altered magmatites, biotite and feldspars of the primary mineralogical association have been replaced by a first generation of tourmaline, represented by large crystals with dark green color, highly pleochroic or colorless, often with radial habit. They occur along the contacts between the quartz grains or invading them (Figs. 2, 3).

The tourmalinisation in the Cioaca Înaltă zone involves a supply of boron. In the general frame of the postmagmatic phenomena from Sasca Montană, this indicates a substantial input of mineralizing agents (B, F, Cl), as indicated by the presence of scapolite, apatite, B- vesuvianite, etc.

The variation of optical properties (color, birefringence, refraction indices) is more obvious between the two generations of tourmaline than between different zones of large crystals of the first generation. This suggests the variation in time of the amount of various elements from tourmaline composition.

Even if the cause of the color variation is not yet solved, most authors suggest that the black color is due to the simultaneous presence of both Fe^{2+} and Fe^{3+} (Sobolev, 1949; Slivco, 1955, fide Deer et al., 1965), with Fe^{2+} ions dominant (Marfounine et al., 1970). The green color is related to the change of Fe^{2+} to Fe^{3+} (Faye et al., 1968). The increasingly lighter color to colorless may be due to an enhanced Mg content. The
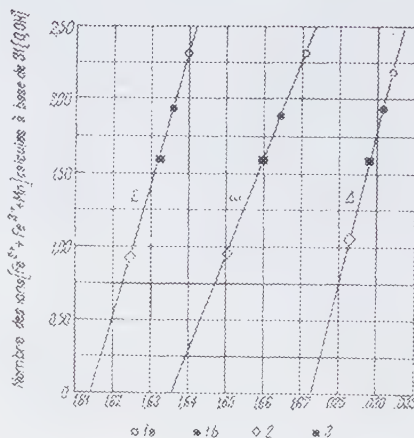
Fig. 3. Values of refractive indixes and birefringence ploted on the correlation diagram: optic properties-number of ions (Fe^{2+} + Fe^{3+} + Mn) in base 31 (O,OH) (Deer et al., 1965). 1, large zoned crystals; a, central, dark green zone; b, light yellow, marginal zone; 2, colorless needle shaped crystals; 3, virtual values corresponding to total Fe^{2+}, Fe^{3+}, Mn ions, calculated in the basis of 31 (O,OH) for the chemical analyses from Table 1.

variations of the refractive indexes and of the birefringence are correlated to a change in Fe/Mg ratio (Ward, 1931; Deer et al., 1965).

The analysed tourmalines are initially enriched in Fe and become subsequently enriched in Mg; this indicates a temperature drop with time (according to Staatz et al., 1955, at lowest temperatures, the schörlitic types are replaced by elbaitic types), as well as Mg enrichment, probably due to the dolomite limestones adjacent to the altered magmatites.

Oxigene fugacity is important in modifying Mg, Fe^{2+} and Fe^{3+} ratios. According to Mueller

(1961), MgO/MgO + FeO and Fe_2O_3/FeO ratios increase with increase in oxygen fugacity. The presence of iron oxides associated with tourmaline and the replacement of magnetite by hematite indicates a highly oxidizing environment. The persistence of oxidizing conditions untill a late alkaline stage suggests a low partial pressure of S in the postmagmatic solutions, which explains the absence of sulphides in the association.

The tourmaline-quartz association and several particular forms of the "tourmaline suns" are regarded as typical for the tourmaline-quartz facies of the greisenisation process (Nacovnic, fide Kourek, 1954). Consequently, in the Cioaca Înaltă zone a high temperature hydrothermal process took place, in conditions similar to those affecting the sericitised porphyries from Cananea, Llalagua, Mount Potosi (Schwartz, 1959).

In what concerns the regularity of the postmagmatic alteration process, the tourmaline-quartz association is considered a metallogenetic indicator for the porphyry or "pipe breccia" type copper ores in acid-intermediate rocks, as well as for some gold-quartz ores in granodioritic rocks (Boyle, 1970).

Generally speaking, the turmalinisation has affected only the southern, peripheral zone of the Sasca Montană ores and shows as a particular feature the association with iron or titanium oxides (magnetite, hematite and rutile, brookite, respectively).

References

Boyle R.W. (1970) Regularities in wall-rock alteration phenomena associated with epigenetic deposits. *Int. Un. Geol. Sci., A*, **2**: Problems of hydrothermal ore deposition, Schweizerbart, Stuttgart, 231-260.

Deer W., Howie R., Zussman J. (1965) Rock forming minerals, vol. I, Longmans, London, p. 311.

Faye G., Manning P., Nickel E. (1968) The polarized optical absorption spectra of tourmaline, cordierite, chloritoid and vivianite: ferrous-ferric electronic interaction as a source of pleochroism. *Amer. Min.,* **53**, 7,8.

Kauffman A. J. Jr., Dilling E. D. (1950) D.T.A. curves of certain minerals. *Econ. Geol.* **45**, 222.

Kourek H. H. (1954) Izmemennyie okloroundnye porody i poikovoe znacenie. Gosgueoltekhizdat, Moskva.

Kurylenco C. (1950) Analyse thermique de quelques tourmalines. *Bull. Soc. franc. Min. Crist.*, **73**, 49.

Marfounine et al. (1970) Opticeskie i mossbauerovskie spektry jeleza v tourmalinah. *Izd. AN. Ser. geol.,* **2**.

Miheev V. I. (1957) Rentghenometriceskii opredelitel mineralov. Gosgheoltekhizdat, Moskva.

Moenke H. (1962) Mineral Spektren. Akademie Verlag, Berlin.

Mueller R. (1961) Oxidation in high-temperature petrogenesis. *Amer. Jour. Sci.* **259**.

Schwartz G. M. (1959) Hydrothermal alteration. *Ec. Geol.,* **54**, 161-183.

Staatz M., Murata K., Glass J. (1955) Variation of composition and physical properties of tourmaline with its position in the pegmatite. *Amer. Min.,* **40**, 789.

Ward G. W. (1931) Chemical and optical study of the black tourmalines. *Amer. Min.,* **23**, 607.

Winchell A. N. (1964). Elements of optical Mineralogy. John Wiley, New York, p. 465.
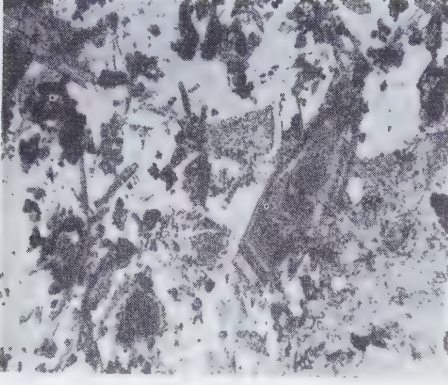
Plate I

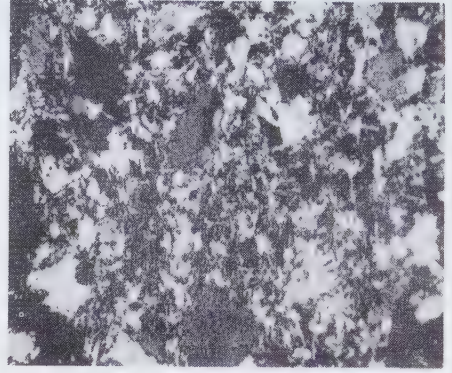**Fig. 1.** Zoned tourmaline crystals. NII (20 x).

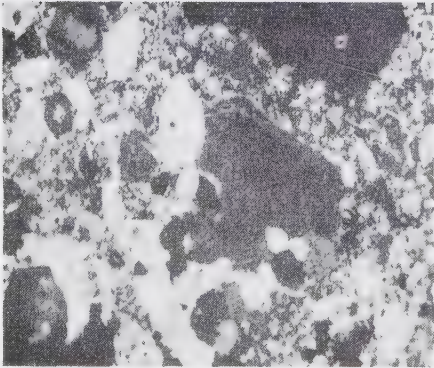**Fig. 2.** Needle shaped tourmaline crystals surrounded by and penetrating quartz. N + (40x).

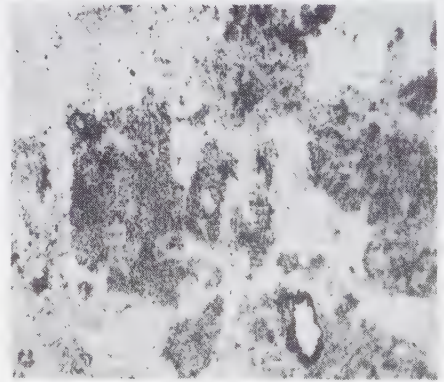**Fig. 3.** Zoned tourmaline corroded by quartz.

Fig. 4. Feldspars replaced by tourmaline and sericite (damourite). N + (20x).

On the mineralogy of syenites from the alkaline massif of Ditrău

NICOLAE ANASTASIU
EMIL CONSTANTINESCU

The study approaches three aspects connected with the mineralogy of alkali-feldspar and nepheline syenites from the alkaline body of Ditrău: a) the nature of the feldspars and their genesis; b) the morphology of nepheline and its alteration products; c) the sodalite-biotite assemblage. Within the rocks under study, K-feldspar is a maximum microcline with high triclinicity and high Si:Al order, formed at low temperatures. Optical investigations of plagioclase point out albite (An_{4-10}) and oligoclase (An_{15-20}) of low temperature modification and high Si:Al order. Nepheline appears with tetragonal and hexagonal symmetry either fresh, or altered. The orientation products are cancrinite, paragonite and sodalite. The sodalite-biotite assemblage has a post-magmatic character and was found as veins.

The alkaline massif of Ditrău, unique in our country by size and petrographical variety, lies in the central part of the East Carpathians, on the inner border of Mesozoic Crystalline Zone, within in Tulgheş Group.

Since its discovery by Herbich, in 1859, the massif constituted the object of study for many geologists, who contributed to its mineralogical, petrographical, chemical, structural and economic potential knowledge (Koch, 1877; Mauritz, 1913, Ianovici, 1929-1938, Streckeisen, 1931-1954, 1954, Codarcea et al., 1957).

The massif of Ditrău consists of a large variety of rocks (hornblendites, alkali-feldspar, syenites, monzodiorites, essexites, nepheline syenites, granites and alkali granites), their composition comprising, in various contents, minerals characteristic for alkaline bodies:

- *salic minerals*: orthoclase, microcline, albite, oligoclase, andesine, nepheline, cancrinite, sodalite, rarely quartz;
- *femic minerals*: amphibole (hornblende, Na-hornblende), biotite, Ti-augite, diopsidic augite, seldom olivine;
- *accessory minerals*: apatite, sphene, ilmenite, orthite, epidote, etc.

General structural features of the rocks are due to their degree of crystallinity and to the frequent transitions between the coarse, medium and micro-crystalline facies. Almost regardless of the petrographic type, the rocks show both massive and oriented fabric.

The alkali-feldspar syenites and nepheline syenites occur on large areas in the massif. A trend for an increasing content of fóides toward the center of the massif and for the development of a circular zone, with nepheline syenite composition is obvious. The central zone is discontinuous, surrounded by ring zones with rocks poor in in fóides or devoid of them. A textural zoning and to lesser extent, a structural one enhance the mineralogical zoning. Thus, the trend is from the oriented texture in the marginal zones,to massif ones in the central areas.
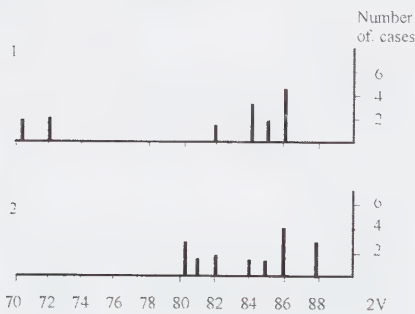
Fig. 1. Range of 2Vα angle for alkali-feldspar in syenites: 1-alkali-feldspar syenites; 2-nepheline syenites.

Mineralogical observations on alkali-feldspar and nepheline syenites concern:

1. morphological, optical and structural characters of alkali and plagioclase feldspar;

2. nepheline morphology and its secondary alteration products ;

3. sodalite-biotite association and its petrographic significance.
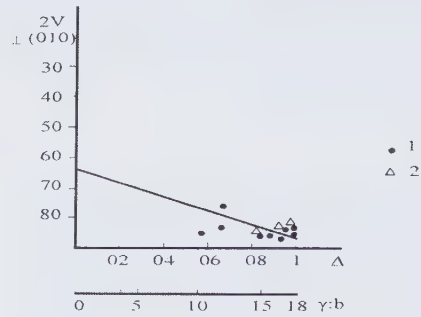
Fig. 2. Stability domains of K-feldspar on the Laves-Vishwanatan diagram: 1-alkali-feldspar syenite; 2-nepheline syenite.

1. Observations on feldspars

K-feldspars. The content of K-feldspar in syenites ranges from 25% to 70%. The morphologic aspects are diverse:
    - prismatic crystals without crystallographic faces;
        - interstial grains;
        - sheet and coronas on plagioclase;
        - filiform depositions.
Besides, it is noteworthy the simultaneous presence of perthites, as "string", "vein" (Andersen, 1928) and "replacement" types (Alling, 1932).
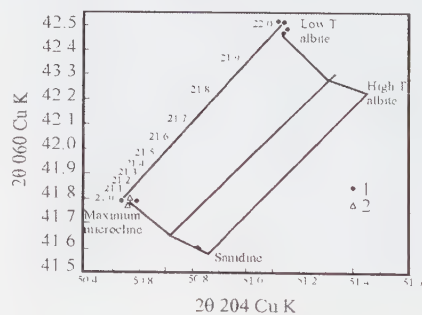
Fig. 3. The projection of 2θ (060) and 2θ (204) values obtained by X-rays diffraction, for the feldspars from syenite of Ditrău, on the diagram of Wright (1968). 1-alkali-feldspar syenite; 2-nepheline syenite.

As the optical and crystallographic properties of the alkali-feldspar depend on its structural state, and on the Na content (Goldsmith, Laves 1954; Smith, 1961), the 2V extinction angle and refractive index of the crystals were measured.
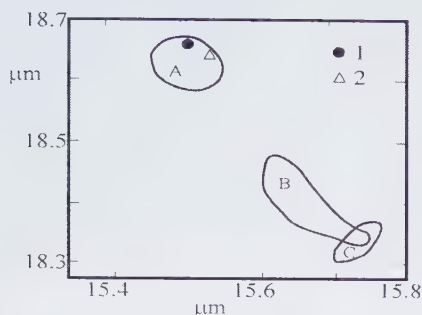

Fig. 4. A-microcline field; B-orthoclase field; C-sanidine field; 1-alkali-feldspar syenite; 2-nepheline syenite.

The values of 2V angle range between 70° and 86° for the feldspars in the alkali-feldspar syenites, and between 80° and 88° for the feldspars in the nepheline syenites (Fig. 1). The angle γ:b, measured in the same crystals is between 10° and 18° and characterizes the alkali-feldspars with medium and high triclinicity. The projection of both 2V and γ:b values on the Laves - Vishvanatan diagram allowed the characterization of alkali-feldspars from alkali-feldspar syenites and nepheline syenites as intermediary and maximum microcline, especially orthoclase-microcline type (Fig. 2).

Testing the structural state and the ordering degree Al : Si was carried out by X-ray diffraction and infrared absorption spectroscopy methods.

The projection of the 2 θ (060) and 2θ (204) values obtained by X-ray diffraction on the diagram of Wright (1968) confirms the presence of maximum microcline type crystals, with high order degree and high triclinicity (Fig.3).

On the Hafner Laves (1957) diagram, the wavelength of infrared adsorption bands in the domains 18.3 - 18.7 µm and 15.4 - 15.8 µm of the alkali-feldspar from syenites, plot in the field of microcline with high order degree (Fig.4).

As the same structural state characterizes the K-feldspar of both rock types – alkali-feldspar syenites and nepheline syenites – the parageneses belonging to the massif of Ditrău could have evolved in similar petrogenetic conditions, especially in identical cooling conditions, which might have allowed the achievement of the above mentioned parameters.

Plagioclase feldspars. The plagioclase content of alkali-feldspar syenites differs from that of nepheline syenites, ranging between 30 and 60% in the former, and between 6 and 15% in the later. The amount of plagioclase feldspar was estimated by counting both albite and various types of oligoclase-andesine. The crystals show various morphologies. The albite forms elongated prismatic crystals, without crystallographic faces and disposed in divergent aggregates or euhedral, short prismatic crystals, forming granular aggregates or inclusions in K-feldspar. Plagioclase feldspars appear either subhedral, or as corroded relics within the mass of K-feldspars.
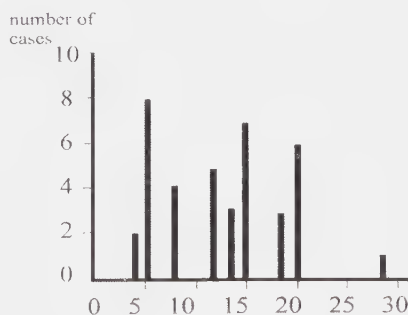

Fig. 5. Anorthite content of plagioclase from syenites.
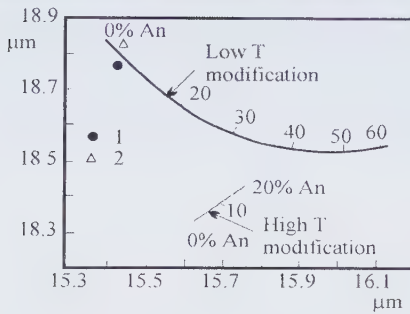
Fig. 6. The wavelength projection of IR absorption bands in the ranges 18.2 - 18.9 μm and 15.3 - 16.2 μm, on Hafner and Laves (1957) and Thompson and Wadsworth (1957) diagram for plagioclase feldspar from syenites; 1. alkali-feldspar syenites; 2. nepheline syenites.

In syenitic rocks, the anorthite content of feldspars, measured through optical studies, range between An_4 and An_{28} (Fig. 5). The two maxim in the figure correspond to albite and oligoclase. The simultaneous presence of Na-Ca feldspar (An_{12-20}) and of albite rises the question of conditions and time of their crystallization. In many cases, the mutual relationship of these minerals and their relationship with the K-feldspar suggest the secondary nature of albite.

The X-ray diffraction and infrared absorption spectroscopy indicated, in all cases, the presence of low temperature modifications with high order degree (Fig. 6).

The study of feldspars from alkali-feldspar and nepheline syenite gives significant information about their crystallization conditions . The morphology of crystals and their relationship reveal that:
   - both plagioclases and alkali-feldspars represent late crystallization minerals; the plagioclase feldspars have formed earlier in the crystallization process, followed by alkali-feldspars;
   - the partial or total pseudomorphs of K-feldspar after plagioclase have formed due to the high mobility of the former and are probably subsequent to their crystallization,

by selective remobilization during slow cooling conditions;
   - among the feldspar parageneses, the albite exposes a particular position, as in most cases seems to be a recrystallization product resulted either by decalcification of plagioclase, or by exsolution from the alkali-feldspar.

The perthites are the result of subsolidus processes, which have led initially to the formation of replacement perthite, as selective replacements favored by ionic diffusion. Exsolution perthites of string and vein type have formed during a later, lower temperature stage (600° - 660° C).

2. Nepheline morphology and its alteration products

In the nepheline syenites from the central part of the massif, the nepheline occurs frequently as idiomorph crystals, with short prismatic, square or hexagonal outline. The hexagonal symmetry is typical for low temperature forms (Hamilton, 1961). The nepheline crystals are either fresh, or replaced by late, post-magmatic associations (cancrinite, paragonite and sodalite). The nepheline syenites parageneses typically show "myrmekitic" intergrowths of nepheline and cancrinite as well as paragonite pseudomorphs formed in subsolidus domain, in the presence of H_2O (the instability of nepheline in the temperature range 400 - 500° C was experimentally proved by Boetcher, 1969).

3. Sodalite-biotite association

The sodalite-biotite association is typical for the nepheline syenites from the central-southern zone and reflects the diversity of post-magmatic processes affecting the Ditrău massif. Its presence – almost exclusively as veinlet – suggests an obvious tectonic control and deposition from solutions with complex composition (Cl, OH, Fe, etc.).

References

Codarcea Al., Codarcea M., Ianovici V. (1957) Structura geologică a masivului de roci alcaline de la Ditrău. *Buletin Şt. Acad RPR*, **3-4**, II, Bucureşti.

Sorensen H. (1974) The alkaline rocks. J. Willey & Sons, London.

Smith J., (1974) - Feldspars, vol. I - II, Springer - Verlag, Berlin.

Streckeisen A., (1952-1954) Das Nephelinsyenit - Massif von Ditro. *Schw. Min. Petr. Mitt.*, **32,** 34.

Streckeisen A., (1974) On the origin and age of the nepheline syenite massif of Ditro. *Schw. Min. Petr. Mitt.*, **54/1**.

Mineralogy and petrography of the Laramian igneous rocks between Nera Valley and Radimniuța Valley

EMIL CONSTANTINESCU

The studied zone lies in the south-west of Banat, limited northward by Cerna Valley, southward by Radimniuța Valley, westward by Calvaria and Tâlva Cerbului and eastward by Dealul Orașului and Bolborosu Valley.

Laramian igneous rocks crop out along 8 km, as longitudinal bodies forming two lineaments striking N–S: a main, western lineament and an eastern, less developed lineament, parallel with the Oravița Fault and with the Sasca, Crucea Otmanului and Nera fractures. The eruptive bodies of the western lineament are clustered in three sectors: northern (Sasca Română), central (Sasca Montană -dealul Gheorghe) and southern (Stânăpari– Cărbunari) (Marka, 1869; Constantinof, 1972).

In the eastern lineament, the Cioaca Înaltă body is the most remarkable; though known in the past (Cotta, 1864; Marka, 1869), the limits of this body were less clear, being concealed by the Quaternary sediments. The body was partly sampled by us in the isolated outcrop from the errosional plateau. The elongated shape of this body and its N-S trend have been precised by the exploration work carried out by IPEG Banatul.

The shape in depth is difficult to predict in the northern and the central sector, where the elliptic outline of the outcrop area enables to see the relationships with the pre-Laramian sediments. Instead, it was clearly revealed by the drillings in the southern sector. In the Stânăpari - Cărbunari sector, the Laramian intrusions, partly conformably emplaced into the Lower Cretaceous sediments, are exposed as a 200 m thick, sheet-shaped body, with N-S strike and 45-50°W dipping.

Mineralogical data

Laramian igeous rocks (banatites) consist dominantly of feldspars, mafic minerals (biotite, pyroxene, amphibole), usually making up 30% of the bulk rock composition.

Table 1. Frequency of twin types and the anorthite contents of the plagioclase from the main types of Laramian rocks

Rock type	Frequency of twin types (M%) Medium anorthite (An) contents	Normal twins	Parallel twins				Complex twins			Plan of association	
		Albite	Ala B	Ala A	Peri-cline	Carls bad	Albite-Carls bad	Albite Ala B	Mane bach Ala B	010	001
Granodiorite	M%	7.4	22.2	—	3.9		31.4	18.4	16.7	70	30
	An	24.5	30.2		27.0		26.3	28.5	31.3		
Quartz-diorite	M%	41.1	—	11.7	5.8		23.4			80	20
	An	35.5		342	34.3		37.0				
Monzodiorite	M%	—	12.4	9.4	6.2	3.1	29.3	18.1	20.7	58	42
	An		38.3	34.2	40.1	32.5	36.2	30.4	35.1		
Total frequency of twin types and hemitropies		17.3	12.2	7.5	5.7	1.1	30.1	12.8	133		
		17.3	26.5				56.2				

Accessory minerals are sphene, apatite, magnetite, seldom zircon, rutile.

The main component of the Laramian igneous rocks, the plagioclase, forms well individualised crystals within the rock mass. In porphyritic rocks, it appears as euhedral and subhedral crystals. The plagioclase shows prismatic, slightly tabular, seldom isometric habit. It shows remarcable freshness, move often in equigranular rocks and seldom in porphyritic rocks.

The anorthite contents of the plagioclase – tested by universal stage on 80 crystals – ranges between 25% and 48% An. The distribution of An contents clearly indicates the prevalence of andesine.

The plagioclase is particularly zoned, with normal or recurrent zonation. In some grains, recurrences are superimposed onto a generally normal background. Subordinately, crystals with anhedral zoning from hornblende or biotite-bearing granodiorites and diorites show a reverse recurrence. This may be considered a metasomatic zonation, resulted from the substitution of plagioclase with albite (Plate I, Fig. 1), as suggested by the jagged albite rims on feldspars. Various inclusions within some plagioclase grains show a honeycomb-type zonal distribution. Partially altered feldspar grains show a selective sericitization of the core, the zonation being highlighted by a kaolinitic dust.

The statistical distribution of the twinning types, joint planes and the variation of anorthite contents of the twinns both in the main rock types and in the whole mass of the igneous rocks are shown in Table 1.

The projection of poles of the twin axes onto the Ng - Na (Kaaden) stereogram suggests low and intermediate values for the formation temperature which is likely to indicate crystallization in plutonic and subvolcanic condition.

The K-feldspar is most commonly represented by orthoclase, with euhedral, subhedral or anhedral outline, often forming narrow zones within the granodiorite, bordering the plagioclase outlines. Sometimes it corrodes inwardly the anhedral plagioclase crystals (Plate I, Fig. 1).

In quartz-diorites, monzonites and monzodiorites, the K-feldspar appears as sheets, replacing the plagioclase or the mafic minerals (pyroxene, hornblende) (Plate I, Fig. 2).

In microgranites it forms graphic intergrowths with quartz (Plate I, Fig. 4); in some porphyritic rocks (granodiorites), orthoclase is present only in the groundmass. In alkaline rocks it often shows microperthitic or cryptoerthitic character (Plate I, Fig. 3). In such cases, the irregular aspect of albite veinlets and K-feldspar deformations indicate possible metasomatic perthites. The 2V angle, measured with the universal stage, ranges between

62° and 72°, indicating a monoclinic K-feldspar.

Quartz is granular, chiefly anhedral, seldom subhedral. It is quantitatively subordinated to feldspars and often forms irregular sheets including plagioclase, hornblende and biotite. It often corrodes orthoclase, formimg graphic intergrowths, feather-shaped and seldom myrmekitic structures.

In most rocks, amphiboles are represented by green pleochroic hornblende (γ - pale green; β - pale green; α - yellowish). The range of extinction angles measured with the universal stage is: $\gamma^\wedge c = 17°\text{-}23°$; $2V = 64\text{-}66°$. Amphiboles are twinned on (001) plane and show zoned structure. They often appear as clusters of hollowed crystals, facilitating the resorption and invasion by biotite lamellae. In other cases they show reaction rims of magnetite and pyroxene and inclusions of zircon and apatite. Seldom, a sodic variety (hastingsite) appears as prismatic or elongated crystals with the following scheme of pleochroism: γ – dark green; β – yellowish-brown; α – yellowish-green; $\gamma^\wedge c = 20°$, $2V = +28°$. Hornblende alters into a variety of fibrous actinolite, forming nests or bunches.

Usually, pyroxenes occur in basic rocks (diorites) and only seldom in granodiorites. They are represented by augite, as idiomorph crystals, elongated along c axis; they are slightly pleochroic, with purple colors. The optic constants – $\gamma^\wedge c = 46°$, $\Delta = 0.024$, $2V_\gamma = 68°$ – suggest an iron enrichment. In diorites, the pyroxenes are often replaced by brown hornblende. In other cases, they alter to hematite or limonite, opaque on rims and with small nests of limonite inward, finally being completely replaced by iron oxides.

In alkaline rocks (monzodiorites, syenites and alkali granites), they gradually change to augite-aegirine.

The values of extinction angles and 2V α, plotted on the Larsen-Trogger diagram (1968) correspond to several terms of the isomorphic series augite-aegirine, with 15-60% mol. aegirine. In thin sections they show gradual replacement of augite by aegirine or augite-aegirine.

Aegirine appears, rarely as independent, crystals elongated along c axis ($\gamma^\wedge c = 1\text{-}8°$; $\Delta = 0.05$).

The biotite occurs alone or associated with hornblende. It shows a marked pleochroism: α – brown; γ – yellow, and often forms phenocrysts spotted by feldspars or fine sheets with irregular outline within the interstices of feldspars (γ – green; β – brown; α – yellow). Frequently biotite replaces hornblende or form rims around magnetite grains, changing itself in pennine. The biotite includes plagioclase, magnetite, sphene, apatite, rutile (sagenite) and zircon, which generate a pleochroic aureole.

Accessory minerals are represented by sphene, apatite, zircon, rutile, magnetite, pyrite, with local enrichment in sphene and apatite, with remarcable dimensions. Sphene is often associated with magnetite, sometimes with a leucoxene appearance.

Petrographical data

The quantitative determination of mineral components allowed the separation of various types of rocks, mainly belonging, after diagram QAP - IUGS (Fig. 1) – Subcomission on the Systematics of Igneous Rocks Reccomendations (1973) – to quartz-diorites, granodiorites and quartz-monzonites.

Worth to be noted is the structural variation of igneous rocks, with a gradual transition from structures specific to the plutonic facies (diorites, quartz-diorites, granodiorites) to porphyry facies. This transition is well expressed, especially in hypabyssal rocks which prevail

in the region, by changes in phenocryst size and in the groundmass components. The transition allowed the separation, amongst the prevailing granodiorite porphyries, of porphyritic diorites and microdiorites, respectively. The characteristic presence, often exclusive, of one of the mafic minerals (biotite, hornblende, pyroxene) imposes varieties like: biotite-bearing granodiorites, hornblende–bearing quartz-diorites, pyroxene-bearing quartz-diorites. Besides, color index leads to mela- and leuco- varieties of the analized granodiorites, quartz-diorites and quartz-monzonites (Streckeisen, 1967).
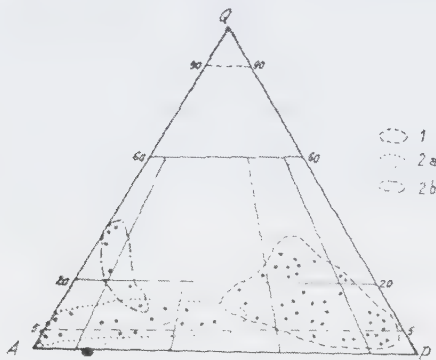
Fig. 1. QAP diagram (after reccomendations of the I.U.G.S. subcommission, 1973). 1. Rocks of the banatite bodies; quartz-diorites, granodiorites; 2. alkaline rocks from the periskarn areas: a., syenites, egirine-bearing alkali syenites, b., egirine-bearing alkali granites, graphic granites.

Based on these results, the participation of the main types of rocks separated are presented in Table 2. The systematic examination of the samples from the entire area indicates that the igneous rocks exposed between Nera Valley and Radimniuța Valley are represented mainly by hornblende quartz-diorites, hornblende and biotite granodiorites, pyroxene and hornblende quartz-monzodiorites.

The less widespread alkaline rocks (syenites, alkali syenites, alkali granites) are exposed on the eastern and western apophyses of the Sasca Montană body, in the extreme east part

of the Gheorghe body, and in the upper part of the Stânăpari body. They are usually disposed parallel to the contact between the eruptive bodies and the adjacent carbonate rocks, and show a remarkable, gradual transition from granodiorites and quartz-diorites to alkaline rocks, mostly due to the plagioclase replacement with K-feldspar.

A remarcable feature of the igneous rocks is given by the enclaves, which can be either "homeogeneous" or "enalogeneous" (Didier, 1973). More widespread are the microgranular xenoliths with a quartz-dioritic composition and a macroscopically darker color, as compared to the leucocratic granodioritic background. Usually xenoliths show small sizes and elliptical outline (large axis 2-12 cm) and typically occur in the peripheral zones of the bodies, seemingly parallel with them. Besides, schlieren or mafic rocks with quasi-circular outline appear, consisting mostly of hornblende and/or biotite, often twisted.

Enallogeneous xenoliths are represented by fragments of carbonate sediments, with various sizes and irregular outlines. At larger scale, the terminal branches of the Laramian apophyses can sometimes include limestone blocks (roof pendants) (Stânăpari Plateau).

Microtectonic data

Fractures typically occur within the Laramian igneous rocks as effects or late results of Laramian tectonics. The identification of the main fracture system is based on measurements of four outcrops from the Dealul lui Ciucar - Dealul Orașului zone. The measurements were projected in the diagram of Fig. 2. They evidence 4 maxima corresponding to 4 fracture systems: 1) N-S/50W; 2) 40-50°E/E; 3) E-W/80-90°; 4) E-W/N. Three of these fracture systems are dominant, while the fourth is subordinate.

The longitudinal fractures of the first system are parallel with the lineation of the Laramian

Table 2. Modal composition of the Laramian magmatites

Petro graphic type	Number of thin sections	Mineral constituents in %							
		Orto clase	Plagio clase	Quartz	Horn blende	Biotite	Augite	Aegirine-augite	Access ories
Diorite	5	3.1-4.3	44.1-47.3	3.9-4.8	412-43.2	—	1.0-6.5	----	1.2-2
Quartz-diorite	7	5.4-6.2	42.3-44.8	9.6-11.2	37.1-39.2	0.5-1.4	0.5-5.5	0.1-1	0.5-1.1
Quartz-monzo diorite	4	24.2-26.7	42.4-43.5	17.6-18.1	10.1-15.6	0.1-0.7	0.5-9.7	—	0.5-2.4
Granodi orite	14	5.4-6.2	13.2-14.6	52.4-54.3	19.7-20.3	12.4-13.2	0-4.5	—	0.4-2.2
Monzo nite	3	39.6-41.8	39.4-41.4	2.3-3.4	11.1-13.2	3.2-3.7	10.1-18.2	—	0.1-0.3
Quartz-monzo nite	3	45.2-57.3	44.7-58.2	5.6-9.3	8.7-12.3	1.2-1.7	7.9-9.3	—	0.2-1.3
Syenite	3	41.2-45.2	16-21.7	1.02-1.5	16.2-1.2	6.5-7	—	8.9-18.4	0.8-3.6
Alkali syenite	4	56.9-59.5	0-3.5	----	1.5-2.5	----	—	19.2-24.4	0.6-2.5
Alkali granite	3	53.8-60.4	0-5.9	20.2-35.2	0-3.4	—	--	4.9-24.8	0.5-2.5
Micro granites	3	70.1 4-72.1 1	—	27.18-28.72	—	.	---	—	0.4-1.8
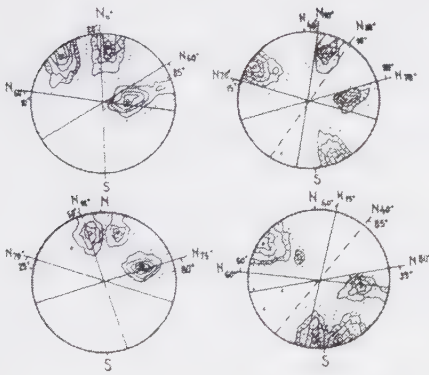
Fig. 2. Tectonograms of fissures measured in the magmatites in Dealul lui Ciucăr.

igneous body, pursuing local variations of this lineation. Aplitic or quartz veins form the infill of these fractures. Decimetric skarn bands may occur, showing the same orientation.

The fractures of the second system, less marked than those previously described, have a higher frequency and opposite dip, normal to the eruptive body, representing probably Q fractures (Cloos, 1936).

The fractures of the last two systems have an approximate E-W orientation, dipping south (system 3) or north (system 4). They split up the Laramian body into regular banks 0.40-1 m thick, intersecting the other systems and displace the quartz veinlets of the system "1". In mining works they often appear as friction fault planes and linear striations. Younger fractures are conformable with these strikes. The last two systems have probably an exokinetic character, while the first two have an endokinetic character.

Petrochemical data

The geochemical features of the Laramian igneous rocks result from 8 chemical analyses of the main petrographic types, most of them

widespread in the investigated bodies (Fig. 2). The silica contents, ranging between 57.90 - 69.32 % show an acid character. The Na_2O and K_2O range from 2.95 to 5.26 % and from 1.93 to 3.48 % respectively. These values largely correspond to the entire Banat region and, on a larger scale, to the whole Laramian province of Romania.

The small number of chemical analyses has left open the problem of the petrochemical character of the banatites in the studied area (between Nera Valley and Radimniuţa Valley). The use of a great number of diagrams in the processing of the results is justified by the special involvement of the local chemical trend compared to the chemical character of the Laramian province and yielded a suggestive comparison of the most useful parameters. The values of the Niggli parameters are shown in Table 5. The magma types (Niggli) is grandioritic, quartz-dioritic, opdalitic, trending toward alkaline magma (essexitic diorites).

The diagrams based on Niggli parameters suggest the following remarks:
- the diagram al-fm (Fig. 3a) reveals an isofalsemisalic character, with a local trend to salic character;
- in diagram mg-k (Fig. 3b) all the projected analyses concentrate in a zone limited by the diagonals 0.5 mq - 0.5 k and 0.9 mq-0.9 k, typical for the Laramian igneous rocks (Giuşcă et al., 1967). The field of maximum frequency is limited by the diagonals 0.7 mq - 0.7 k and 0.8 mq - 0.8 k, typical for rocks with alkaline or subalkaline affinities;
- the al-alk diagram (Fig. 3c) show a main clustering around the line alk = 1, as border between the field of intermediate and alkaline rocks, trending toward the alkaline. The c values (Fig. 3c) plot within the normal to upper limit of the field C (Burri, 1959);
- in diagram c/fm:mg (Fig. 3d), most analyses fall in the more calcic field, with Fe showing a slight tendency to dominate over Mg, a tendency more accentuated in rocks with lower

Ca contents;
- in diagram Q-L-M (Fig. 4), the studied magmatites are located in the field of calc-alkaline rocks, in a central position within the space of the banatites from Banat, outlined after Giuşcă (1966), they show a tendency for clustering toward the PF line;
- the variation diagram based on Niggli values (Fig. 5) shows a normal differentiation suite. The isofalic magma is quartz-dioritic, following the trend of subalkaline differentiation.

The normal evolution trends of the banatites are also indicated by the Nockolds-Allen diagram (Fig. 6) and by the shape of the curves showing the variation of the main cations with the Nockolds-Allen index. Considering the values of the felsic and differentiation indices (Table 6), it is noteworthy that the analysed rocks show an overall calc-alkaline chemistry, with an alkaline differentiation tendency.

The values of the trace elements from the magmatites (Table 4) are in the limits of the medium values typical for intermediate rocks (Turekian, Wedepohl, 1961; Vinogradov, 1962), confirming the tendencies of the major elements.

Petrogenetic considerations

The petrogenesis of the Laramian magmatites from SW Banat, which show an obvious tectonic control, is controlled by a system of deep, crustal faults.

The remarcable development of the banatite bodies, as well as the associated metallogenesis in the area between Nera and Radimniuţa valleys is correlated with the existence of a network of faults trending N-S and E-W. The meridian faults (Oraviţa, Sasca, Crucea Otmanului, Nera) have determined the distribution along longitudinal lineaments of the elongated, sheet–shaped bodies, while the apophyses extend parallel to the transverse fractures.

Table 3. Chemical analyses of the Laramian magmatites

Sample nr. Oxides %	121	272	83	307	274	436	139	210
SiO_2	69.32	66.56	60.21	61.12	63.08	60.02	57.90	63.50
Al_2O_3	14.83	14.74	17.05	17.00	17.59	15.11	19.00	13.70
Fe_2O_3	1.96	3.05	3.57	5.40	3.02	4.78	5.40	5.00
FeO	1.52	2.31	1.27	0.25	1.63	3.34	0.20	0.18
MnO	0	0.08	0.18	0.10	0.05	0.12	0.14	0.10
MgO	1.12	2.03	2.67	2.82	2.65	2.42	2.80	2.26
CaO	2.31	2.53	5.09	5.53	5.13	5.63	6.02	7.35
Na_2O	4.15	5.26	3.78	2.95	3.62	3.64	4.25	3.22
K_2O	3.48	2.87	2.10	2.04	1.93	3.18	2.16	3.37
TiO_2	0.08	0.16	0.66	0.60	0.16	0.11	0.10	0.12
P_2O_5	0.05	0.09	0.28	0.08	0.07	0.16	0.18	0.14
CO_2	0.59	0	1.23	0.10	0	0	0.18	0.10
S	0.37	0	0.63	0.12	0	0	0.18	0
H2O⁻	0.19	0.13	0.23	0.14	0.26	0.33 ˙	0.08	0.10
Total	100.76	100.05	99.98	98.75	99.98	100.14	99.89	99.94

Table 4. Trace elements of the Laramian magmatites

Sample nr. Trace elements (ppm)	121	272	83	307	274	436	139	210
V	80	70	70	85	64	58	60	60
Ni	16	18	20	20	17	16	15	20
Co	20	22	24	21	16	14	12	18
Cr	28	30	15	17	14	26	26	10
Ba	650	600	720	580	620	610	780	800
Sr	340	380	400	420	460	420	580	500
Li	28	26	20	24	10	12	16	25
Ga	16	18	14	16	18	22	15	5
Ge	5	7	11	9	14	12	7	5

The westward dip of the flat bodies, partly conformable with the Mesozoic sediments of the Reşiţa-Moldova Nouă syncline, indicates a tendency of rooting toward the main tectonic line-- Oraviţa Fault –which marks the overthrust of the Getic Nappe on the sediments of the Reşiţa-Moldova Nouă zone.

The analysis of a sequence of cross sections based on geological data from outcrops, mining works and drillings shows that in the study area, as opposed to the Oraviţa-Ciclova zone, the main eruptive bodies develop along the Sasca Fault, which continues south of the Danube with the Ridanj Krepoljin Fault.

The gradational transition from equigranular to porphyry structures and the optic properties of the plagioclase feldspars indicate that the rocks have been emplaced in subvolcanic conditions. The hypabyssal facies of the magmatites from the study area compared to the chiefly porphyritic facies at Moldova Nouă (Gheorghiţă, 1975; Gheorghiţescu, 1972) and to the abyssal facies at Oraviţa-Ciclova (Constantinof, 1972) probably represent the effect of differential erosion which might be due to the existence of tectonic compartments lowered in steps along transverse faults, rather than to a progressive southward sinking (Răileanu et al., 1967).

Table 5. Niggli values

Sample nr.	Si	al	Fm	c	alk	k	mg	ti
121	31.04	39.96	20.19	11.31	28.54	0.36	0.38	0.28
272	259.62	33.87	28.54	10.57	27.02	0.26	0.41	0.47
83	212.19	35.40	27.76	19.21	17.63	0.27	0.50	1.75
307	213.31	34.95	28.86	20.67	14.51	0.31	0.49	1.57
274	223.53	36.72	27.02	19.47	16.79	0.26	0.52	0.43
436	195.83	29.05	33.16	19.67	18.12	0.37	0.35	0.27
139	182.91	35.36	26.91	20.37	17.36	0.25	0.49	0.24
210	222.22	28.25	25.77	27.55	18.44	0.41	0.46	0.32

Sample nr.	P	W	cf m	Q	L	M			qz
121	0.10	0.54	0.56	51.45	42.04	6.51	0.162	10.798	102.89
272	0.15	0.53	0.37	45.03	43.36	11.61	0.113	4.164	51.56
83	0.42	0.69	0.69	44.31	43.25	12.44	0.335	3.732	41.69
307	0.12	0.93	0.69	46.47	40.71	12.83	0.413	4.520	55.25
274	0.10	0.62	0.72	46.82	41.89	11.29	0.363	5.020	56.37
436	0.22	0.56	0.59	40.43	41.17	18.40	0.232	2.117	23.34
139	0.24	0.93	0.76	39.81	47.02	13.16	0.341	1.929	13.47
210	0.21	0.94	1.07	44.34	37.89	17.77	0.210	3.222	48.47

Table 6. Values of felsic and differentiation index

Sample Nr.	F.I.	D.I.	Sample Nr.	F.I.	D.I.
121	9.158	11.363	274	20.623	6.166
272	13.080	9.721	436	13.868	6.508
83	19.940	5.877	139	18.906	4.823
307	20.951	5.564	210	16.108	6.076

F.I., felsic index (Kuno); D.I., differentiation index (Larsen, 1938, modified by Nockolds & Allen)

The origin of the banatitic magmas was considered within the Alpine tectono-structural framework (East-Mediterranean belt - Petraschek, 1956; global - Janković, 1974). Both hypotheses ascribe an important part of subduction processes in banatite magma genesis, regardless of the orientation of the subduction plane (Rădulescu, Săndulescu, 1973; Savu, Herz, 1974; Janković, 1974), They are regarded them as early, initial magmatites, emplaced in the rifting phase (Dewey, Bird, 1971), indicating an upper mantle source for magmas, with some crustal contamination. This is confirmed by the values of Sr/Sr ratio (0.708-0.714), established by analyses on Laramian rocks from eastern Serbia, Jugoslavia (Janković, Petcović, 1974).Complex processes of magmatic differentiation, taking place after magma formation, and partly the reaction with wall-rocks during the ascent of magma toward the surface, are controlled by local geotectonic conditions. The mineralogical and petrochemical data presented for the magmatites from the Nera Valley - Radimniuța Valley area indicate a single magmatic phase. The inhomogeneity of *in situ* differentiation has caused the formation of granodioritic, quartz-dioritic and quartz-monzodioritic zones, usually showing progressive transitions, without sharp contacts. The microdiorite xenoliths might represent products of a former stage of magmatism in the Laramian province, corresponding to the first stage of the Paleocene-Early Eocene magmatism (Cioflica, Vlad, 1973).
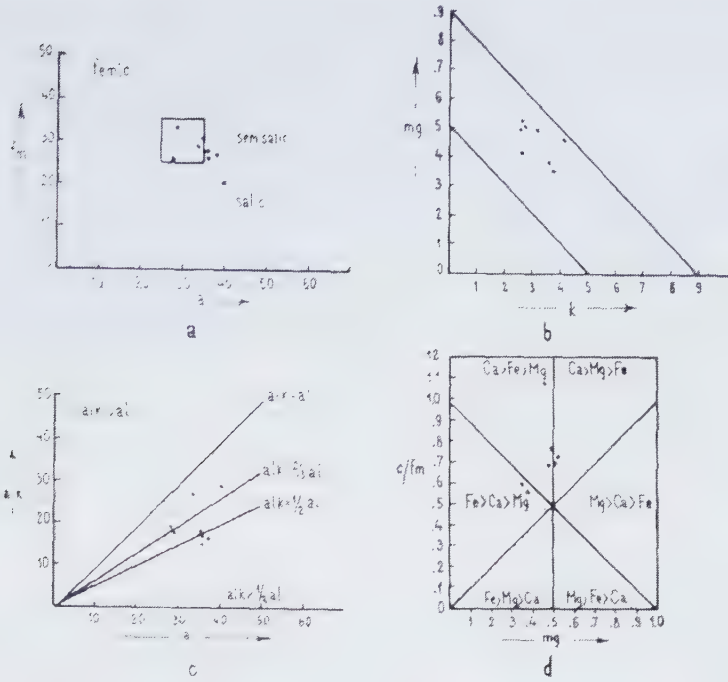
Fig. 3. Petrochemical diagrams: a. al - fm; b. k-mg; c. al-alk; d. mg - c/fm.

Fig. 4. Q.L.M. Diagram (Kp . Cal . Ne).

According to Giuşcă et al. (1967), the initial granodioritic magma of the banatitic province shows two trends: basic and alkaline. The absence of gabbros from the study area, as well as of lamprophyres, known in other, neighbouring sectors (Moldova Nouă, Oraviţa), correlated with the presence of remarcable amounts of quartz-monzodiorites supports the idea of a dominant alkaline differentiation trend, reflected by the petrochemical values discussed.

- The alkaline rocks (aegirine-bearing alkali syenites, K-syenites, aegirine-bearing alkali granites, graphic granites) which occur in the position of periskarns, as narrow bands at the contact of the magmatites with the carbonate rocks, represent the result of metasomatic replacements.

- various replacement stages, mapped in the field and identified in thin sections, concern the replacement of plagioclase with K-feldspar, the dissapearence of biotite and hornblende, the transformation of augite in augite-aegirine and aegirine, the development of replacement perthites. The graphic structures are the consequence of selective replacement of the perthitic feldspar by quartz, in the weak zones of the later, represented by deformation bands (Şeclăman, Constantinescu, 1972).
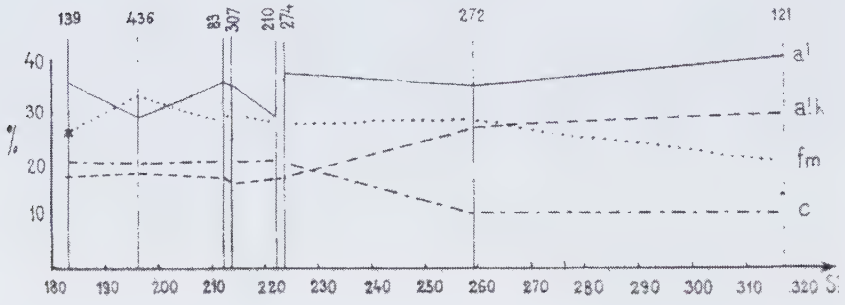
Fig. 5. The Niggli diagram.
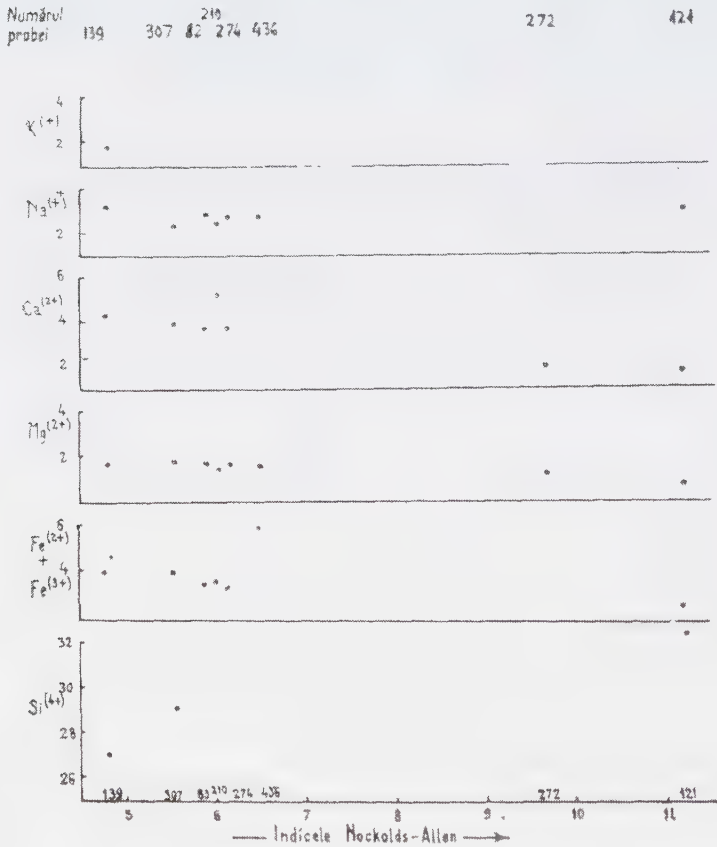
Fig. 6. The Nockolds - Allen diagram.

- The paragenesis and relationships of the minerals from the alkaline rocks relatively resemble those from the vicinity of carbonate xenoliths from certain granodioritic and dioritic massifs (Muir, 1953; Tilley, 1952).

- The still unclear mechanism of formation involves a transfer of silica, K, Na and Fe in a first phase. The reaction between magma and the carbonate rocks may have produced the silica depletion and the geochemical culmination of some basic elements (K_2O, Na_2O, FeO) (Reynolds, 1952).

- The particularities of the petrogenesis of alkaline rocks from Nera Valley - Radimniuța Valley, partly developed in subsolidus phase, are given by the discontinuous character and by the role of mineral deformation due to periodic reactivation of the microcrack system.

- An overview of the petrogenetic and metallogenetic processes accompanying the intrusion of the Laramian magmatites and affecting both the adjacent sedimentary complex and the intruded rocks, involves the consideration of mineral associations from the apobanatitic skarns and from the autometamorphic zones.

- The mineral neoformations resulted by the replacement of primary minerals or by direct deposition from solutions are represented by diopside, grandite, vesuvianite, antophyllite in the case of apobanatitic skarns (Constantinescu, 1971) and by tourmaline-quartz, fluorite-quartz, sericite-quartz and chloritic , and zeolitic clay associations (Constantinescu, 1976, 1977).

- The mentioned associations reveal a large thermal range (from the tourmaline-quartz to zeolitic association), the remarcable 'role of mineralizers (tourmaline, fluorite in the autometamorphosed magmatites; B-vesuvianite, scapolite in skarns) and the polyascendent evolution of postmagmatic fluids.

References

Burri C. (1959) Petrochemische Berechnungsmethoden auf aequivalenter grundlage, Basel u., Stuttgart.

Cloos E. (1936) Der Sierra Nevada pluton in Californien. *Neues Jahrb. Min. M.,* **76**.

Cioflica G. (1976) Die Entwicklung des laramischen magmatismus in Rumänien, *Acta Geol. Ac. Sci. H.,* **11**, 1-3.

Cioflica G., Vlad S. (1973) The correlation of laramian metallogenetic events belonging to the Carpatho-Balkan area, *Rev. roum. Géol., Géophys., Géogr, ser. Géol.,* **17**, 2.

Constantinescu E. (1971) Observații asupra skarnelor și mineralizației cuprifere laramice de la Sasca Montană. *Analele Univ. Buc.,* **XX**, 65-74.

Constantinescu E. (1976) Tourmaline de la zone de Cioaca Înaltă (SW du Banat), *Rev. roum. Géol., Géophys., Géogr., ser. Géol.,* **20**, 1, 147-153.

Constantinescu E. (1977) Filosilicații din zonele de autometamorfism hidrotermal de la Stînăpari, *St. tehn. ec.,* ser. **I**.

Constantinoff D. (1972) Considerații asupra rocilor metamorfice și eruptive din Banatul de vest (zona Fîrliug - Moldova Nouă). *St. cerc. geol., geofiz., geogr., geol.,* **17**, 2, 177-193.

Cotta v. B. (1864) Erzlagerstätten im Banat und im Serbien, 51-55, Wien.

Dewey J., Bird (1971) Plate tectonics and geosynclines. *Tectonophysics,* **10**, 5-6, 625-638.

Didier J. (1973) Granites and their enclaves. Elsevier Co., Amsterdam, London, New York.

Gheorghiță I. (1975) Studiul mineralogic și petrografic al regiunii Moldova nouă (zona Suvorov-Valea Mare). *St. tehn. ec.,* ser. **I**, 11.

Gheorghițescu D. (1975) Considerații privind mineralogia skarnelor cu mineralizații cuprifere de la Vărad. *St. cerc. geol., geofiz., geogr., geol.,* **17**, 1, 49-66.

Giușcă D., Cioflica G., Savu H. (1967) Caracterizarea petrografică a provinciei banatitice. *An. Inst. Geol.,* **XXXV**.

Marka G. (1869) Einige Notizen uber das Banater-Gebirge. *Jahrbuch K. K. Geol. Reich. Wien,* **19**, 299-318.

Mayer C., Hemley J. (1967). Wall-rock alteration. In: Geochemistery of hydrothermal ore deposits, New York.

Muir I.D. (1953). A local potassic modification of the Ballachulish granodiorite. *Geol. Mag.,* **XC**, 3, 182.

Pieptea V., Ciornei A., Weingartner R. (1972). Mineralizația cupriferă de tip diseminat din corpul subvulcanic Suvorov, regiunea Moldova Nouă. *D. S. Inst. Geol.,* **LIX**, 2, 65-80.

Rădulescu D., Săndulescu M. (1973) The plate-tectonics concept and the geological structure of the Carpathians. *Tectonophysics,* **16**, 155-161.

Șeclăman M., Constantinescu E. (1972). Metasomatic origin of some micrographic intergrowth. *Amer. Min.,* **57**, 5-6.

Turekian K.K., Wedepohl K.H. (1961) Distribution of the elements in some major units of the earth's crust. *Geol. Soc. Am. Bull.,* **72**, 175-192.

Vinogradov A.P. (1962) Srednie sederejnaia chimiceskih elementov v glavnîh tipah izverrzenih gornîh parod zemnoi korî. *Geochimia,* **5**, 555-571.

*** Classification and nomenclature of plutonic rocks. Reccomendations by the IUGS, Subcomission on the Systematics of Igneous Rocks. *N. Jb. Miner.,* **4**, 149-164.

Plate I
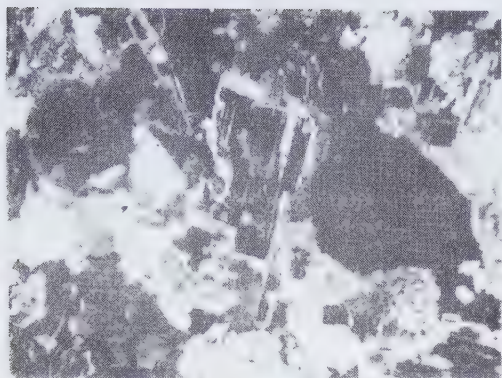
Fig. 1
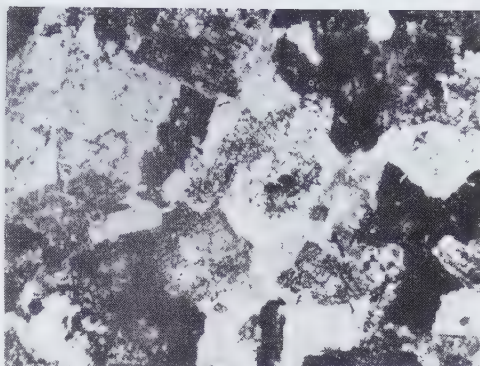
Fig. 2
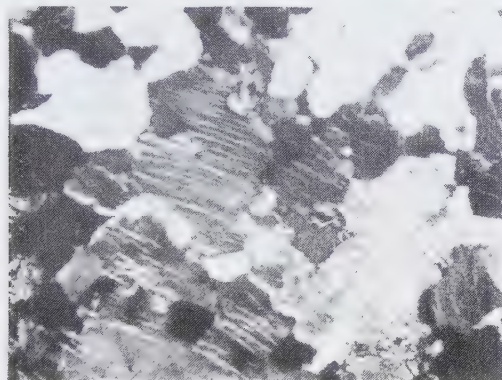
Fig. 3
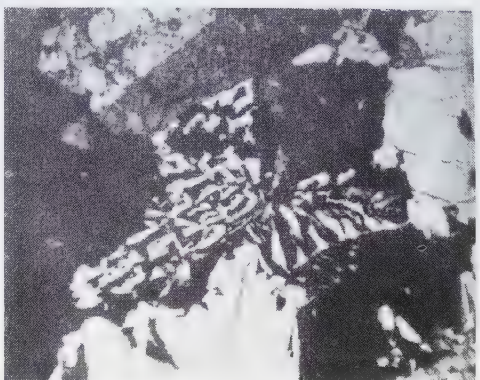
Fig. 4

Fig. 1. Plagioclase crystal in granodiorite, corroded by K-feldspar and bordered by albite; N +, 30x.
Fig. 2. Remnants of plagioclase, biotite and hornblende in orthoclase from feldspathised quartz-diorites; N +, 30 x.
Fig. 3. Microperthites in alkali syenites; N +, 30 x.
Fig. 4. Graphic intergrowth of feldspar and quartz in alkali granite; N +, 30 x.

Mineralogy of Alpine veins from the Romanian Carpathians

EMIL CONSTANTINESCU
GAVRIL SĂBĂU

The Alpine veins, raising interest for their mineralogical and textural peculiarities, are well developed in the Alps (Parker, 1954), the Sudetes (Ansilewski, 1958), the Rhodopes (Kostov, 1965). This paper describes some new occurrences within the Romanian Carpathians. The Alpine veins which were examined consist of some various mineralogical assemblages, being encompassed within different metamorphic rock types.

1. The assemblage: quartz-adularia-chlorite-apatite-actinolite, within migmatites and laminated granites (Parâng Mts.: the Jiu Strait, the Gruniu brook).
2. The assemblage: quartz-chlorite-albite-actinolite-calcite-hematite within amphibolites and amphibolic schists (Făgăraş Mts.: the Cheia Valley, the Gălăşescu Peak, Câineni).
3. The assemblage: quartz-albite-chlorite-actinolite-epidote± rutile.
4. The assemblage: quartz-chlorite-pyrophyllite-paragonite/muscovite, and paragneisses (Leaota Mts.: the Brusture brook).
5. The assemblage quartz-chlorite-pyrophyllite-paragonite/muscovite-chloritoid within chloritoid—bearing pyrophyllitic schists (Parâng Mts.: Izvorul, Jieţ).

The Alpine veins are lenticular in form or appear as irregular nests usually transversally oriented as compared to the schistuosity planes and very seldom along schistuosity (Fig. 1). Cavities are partly or rarely almost completely filled up, sometimes a zoning structure (Fig. 2).
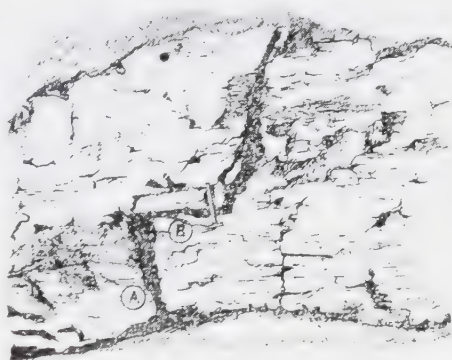
Fig. 1. Alpine veins " en echelon" with partly unconformable setting (A), partly concordant (B) in migmatites (Parâng).
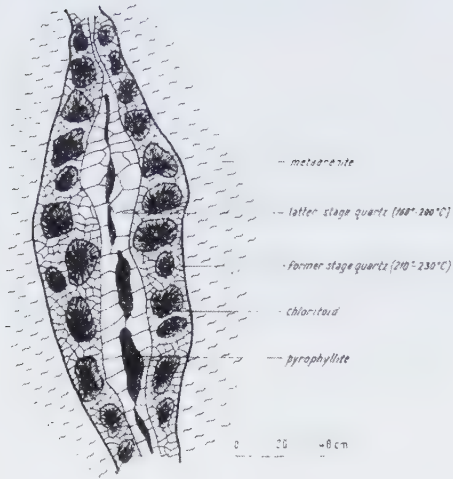
Fig. 2. Quartz, chloritoid and pyrophyllite vein with zoning structure in the Schela Formation (Parâng), after Popescu (1983) (unpublished data).

Description of main minerals

The composing minerals were analysed by a complex mineralogical study in order to find out their morphological aspects, their optical characters and their chemico-structural peculiarities.

Quartz is present in all assemblages, quantitatively dominating the other minerals. Quartz crystals can reach remarkable sizes, up to 20 cm long. Its habit can be columnary - 20/5 cm (Gruniu) or shortly prismatic - 20/15 cm. Face were identified $(10\bar{1}0)$, $(10\bar{1}1)$, $(011\bar{1})$, $(3\bar{1}\bar{2}1)$, $(\bar{2}\bar{1}\bar{1}1)$, as well as some rare forms $(05\bar{5}2)$, $(30\bar{3}1)$, $(033\bar{1})$ (Fig. 3). Face combinations are richer (Gruniu) or simpler (Leaota), Crystals are colourless and glass-like, milky white, smoky or green. Under miscroscope, some chlorite inclusions, marginally disposed and parallel to crystal faces (Figs. 4, 5), or fibrous actinolitewere noticed in the crystal mass notices within green crystals. In some cases they can show fluid inclusions (Jieț); here, the temperature of the fluid phase homogenization was measured on these inclusions (150 deter-

minations); for formation temperatures there were obtained some values between 160-180⁰ C (Popescu, Constantinescu, 1982).
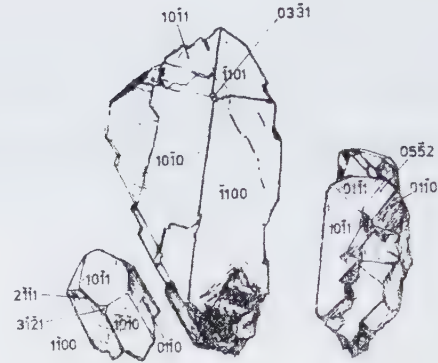
Fig. 3. Morphology of quartz crystals from Alpine veins (Parâng) (coll. R. Strusiewicz).
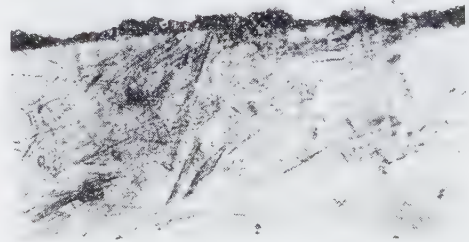
Fig. 4. Setting of chlorite and actinolite inclusions within greenish quartz (thin section, N II, 10X).
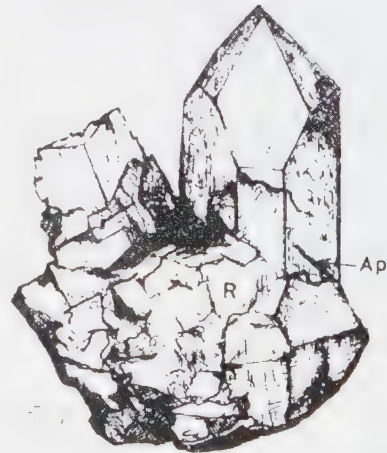
Fig. 5. Assemblage (1) quartz - adularia- ripidolite-apatite (Parâng).

Chlorite is the only mineral found together with quartz in all assemblages. Its crystal dimensions are between 1mm and 1 cm. It shows a lamellar habit and is disposed in radial aggregates (Fig. 6). Its colour varies from yellowish-green to dark green. Taking into account the optical properties and the chemical-structural determinations, ripidolite and clinochlore could be separated.

It is weakly pleochroic from yellowish to green and its birefringence colour is dark grey, often anomalous with bluish shades. Clinochlore which appears within assemblages 2 and 3 is set out in rosettes with undulose extinction (Fig. 8) or in dispersed isolated crystals. Its pleochroism is more intense with chlorites in assemblage 2 and weaker with those in assemblage 3. Its birefrigence colours are usually anomalous (yellow-brown, violaceous), rarely normal, but very low (dark grey).

Fig. 6. Chlorite rosettes associated with quartz and calcite (assemblage 2) (Făgăraş).
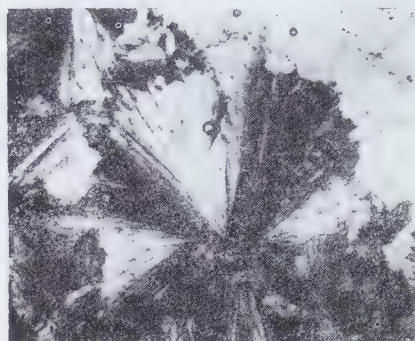
Fig. 8. Radial aggregate of chlorite with undulose exctinction (thin sectionn, N+, 40 X).

Ripidolite is characteristic for assemblage 1 (Parâng Mts., the Jiu Strait and the Gruniu brook) (Fig.5), where it appears within agglomerations of crystals with a helminthic structure (Fig. 7), or as single crystals having a prismatic habit.

The precise identification of mineral species could be carried out by means of X-ray diffraction, IR spectrography and thermodifferential analyses (Fig. 9).

Fig. 7. Helmintic aggregates of ripidolite (thin section, N II, 80 X).
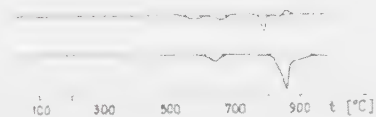
Fig. 9. Thermodiferential curve of ripidolite (Parâng).

Adularia appears only in assemblage 1 (Parâng Mts., Gruniu) associated with quartz, ripidolite, apatite (Fig. 3). Its crystals have a short prismatics habit and dimensions between 1-4 cm. Faces are well represented (110),

(110), (001), (201), with a larger development of face (201), in prejudice of face (001) (Fig. 10). Twins often appear after Manebach, Baveno and pericline+albite laws. Microscopical observations have indicated an optical non-homogeneity marked by a variation of the 2V angle, between 67-83^0 and of the extinction angle $c^\wedge n_m$ between 12-17^0, in different crystal zones. There were noticed some zonal structures, both macroscopically by colour variations, and microscopically by the existence of some lamellae having a different optical behaviour (Fig. 11).

Fig. 10. Morphology of adularia crystals (Parâng).
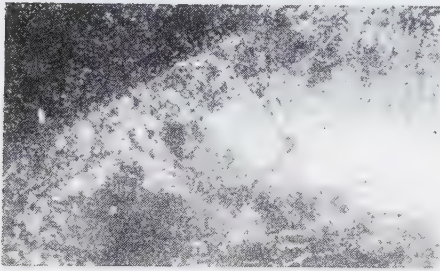
Fig. 11. Lamellar and diffuse optical non-homogeneities in adularia (thin section, N+, 40X).

Chemical analyses (Table 1) allowed calculation of the structural formula $K_{3.092}$ $Na_{0.245}Ba_{0.100}$ $Ca_{0.022}Si_{11.901}Al_{4.427}O_{32}$ and the participation ratio of final terms from the feldspar group: Fk 89%, Ab 7%, Cs 3%, An 1%.

The d/n values and the I/100 corresponding intensities, calculated for the main diffraction lines are included in Table 1. The triclinity calculation yielded a value of 0.8. The sometimes diffuse character of 130 reflections

points out the non-homogeneous chracter of the adularia from the Alpine veins in the Parâng Mts. with monoclinic and triclinic symmetry zones.

Table 1. Chemical analyses of minerals Alpine veins

Minerals/ Oxides	Adularia Gruniu, Parâng Mts.	Pyrophyllite Jiet, Parâng Mts.
SiO_2	64.20	64.19
TiO_2	-	0.01
Al_2O_3	19.26	28.77
Fe_2O_3	0.11	0.40
FeO	0.09	-
MgO	0.05	0.14
CaO	0.12	0.16
BaO	1.42	-
Na_2O	0.70	0.14
K_2O	13.04	0.20
H_2O	0.70	5.73
	99.69	99.74

The main absorption bands in infrared which were obtained on the analysed adularia are characteristic for the stretching frequences Si(Al) -O (1045 cm^{-1}); Si-Al-Si (728 cm^{-1}) and for the deformational frequences Si-O-Si (433 cm^{-1}). The value of transmission minimum from 645cm^{-1} occupies an intermediary position among characteristic values for sanidine 639 cm^{-1} and microcline 650 cm^{-1}, indicating an intermediary state of order, as the order band positions.

Albite appears in assemblage 2 and 3, in association with quartz-chlorite-actinolite-calcite-hematite, and quartz-chlorite-actinolite-epidote, respectively. Its crystals are up to 4-6 mm and form monomineral aggregates where only the mineral faces and the prismatic habit, elongated after the lateral pinacoid (010) can be distinguished. Under microscope it shows a subhedral outline.

The determined optical constants: the refractive index, the extinction angle and the 2V angle show a content of 5-10% An.

Comparing the values of the d/n parameter and those of the I/100 intensitties calculated from the X-ray diffraction analyses made in the domain 2θ: 10-55⁰, with data obtained by Borg and Smith (1969), there comes out that our values correspond to those obtained for the low albite.

This is confirmed by the projection of wavelengths of absorption bands in IR from domains 18.2-18.9 and 15.3-16.2 on Hafner and Lave's diagram (1957) which are included in the characteristic low temperature domain.

Actinolite appears as macroscopically visible crystals (2-3 mm) in assemblage 2 and 3, associated with quartz-chlorite-albite-calcite or epidote, as microscopical inclusions within quartz and adularia in assemblage 1 and as asbestiform aggregates (assemblages 2 and 3).

Pyrophyllite appears in assemblage 4 associated with quartz, chlorite and paragonite/muscovite. Its colour is pearly white. In thin sections it appears as scales and elongated leaflets with an anhedral outline, generally having submillimetric dimensions. It is colourless or with a slightly greenish shade. Its birefringence colours vary from grey to greenish-yellow. The extinction angle c^Np = 8-10⁰. The 2V angle determined in basal sections varies between 54-58⁰.

Its chemical composition is given in Table 1, yielding the following structural formula: $K_{0.031}Na_{0.033}Ca_{0.021}(H_3O)_{0.199}Mg_{0.025}Fe^{3+}_{0.036}$ $Al_{3.803}Si_{7.728}Al_{0.272}O_{20}(OH)_{3.801}/24(O)$.

The values of interplanar distances determined by X-ray diffraction are shown in Table 2 and thermodifferential curve in Fig. 12. The crystallinity index, considered to be a sensible indicator of phyllosilicate genesis (Dunoyer de Segonzac, 1969), was calculated according to the ratio between the height of the peak corresponding to the (002) reflection and its width at half-height. The obtained value, -122, is higher for the crystallinity index of pyrophyllite from pyrophyllitic schists - 47 (representing the average of five analyses) after Popescu and Constantinescu (1982), and very high as compared to the value obtained for hydrothermal pyrophyllites from România - 8 (Ianovici et al., 1981).

Table 2. d/n in Å and I/100 values obtain by X-ray diffraction for minerals of the Alpine veins

1.Adularia			2. Pyrophyllite				3. Ripidolite			
Nr	d/nÅ	I/100	Nr	hkl	d/nÅ	I/100	Nr	hkl	d/nÅ	I/10
1	3.93	10	1	002	9.0544	49.5	1	001	14.10	40
2	3.766	15	2	004	4.5344	7.2	2	002	7.08	100
3	3.45	10	3	006	3.0455	100	3	003	4.71	10
4	3.29	20	4	132	2.4012	3	4	004	3.54	20
5	3.229	100	5	008	2.2905	10	5	005	2.82	10
6	2.985	35	6	0.0.10	1.8391	22	6	131.202	2.59	10
7	2.889	10	7		1.5289	23	7	132.202	2.54	10
8	2.760	10	8		1.3799	6	8	132.203	2.45	15
9	2.55	25	9		1.3644	7	9	132.202	2.38	10
10	2.319	10					10	133.204	2.25	10
11	2.154	10					11	135.204	2.00	15
12	2.119	10								
13	2.049	10								
14	1.887	45								
15	1.795	35								
16	1.615	10								
17	1.449	15								
18	1.406	10								
19	1.382	10								

Together with the above mentioned minerals, the Alpine veins contain as well some locally spread or quantitatively subordinated minerals.

Fig. 12. Thermodifferential curve of pyrophyllite (Parâng).

Calcite appears in assemblage 2 as crystals with rhombohedral habit up to 2 cm with a cleavage perfectly following the colourless rhombohedral faces or in masses having a granular aspect, greyish-white in colour.

Epidote appears as grains or short prismatic crystals, sometims with curved faces (Fig. 13).

Hematite appears in assemblage 2 as lamellar crystals, iron-grey coloured, sometimes disposed in aggregates with a radial aspect.
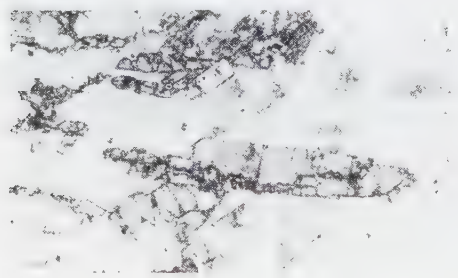
Fig. 13 Epidote and apatite crystals included in adularia (thin section, NII, 10X).

Conclusions

The mineralogical composition of the Alpine veins from the Romanian Carpathians is a simple one and in all the examined assemblages it is closely related to the mineralogical composition of the host rocks. The development of certain minerals is controlled by a specific petrographic environment. Thus, the adularia exclusively appears in gneissic rocks (migmatites, laminated granites) and the pyrophyllite exclusively appears within pyrophyllitic schists. Chlorites, which appear in all assemblages are characterized by the presence of the ferriferous species (ripidolite) within the Alpine veins of gneissic rocks and of the magnesian species (clinochlore) within the Alpine veins from in amphibolites and amphibolic schists. Hematite appears as well only in veins of the amphibolic schists as it formed with iron levigated from amphiboles. These observations, correlated to the partial depletion of the host rocks in chemical elements forming the minerals of the Alpine veins, support the idea of the formation of these minerals by lateral secretion processes.

The reciprocal relationships among minerals of the Alpine veins indicate a depositional succession allowing the separation within certain veins (assemblages 1-3) of an initially alkaline stage, represented by the crystallization of quartz, adularia and albite, followed by a calc-alkaline stage, when actinolite and epidote are formed. Two crystalization stages can be distinguished as well in assemblage 4: a) chloritoid+quartz and b) pyrophyllite ±quartz of lower temperature (Fig. 2).

The crystal morphology for quartz and adularia, the chemical-structural characteristics (order-disorder etc.) for albite and adularia, and the values of homogeneity temperatures for fluid inclusions of quartz indicate medium to low emperatures of formation.

The mobilization and redeposition of these minerals are associated with the action of metatectical fluids which have circulated through open fractures within metamorphic rocks, after their deformation. Therefore, the Alpine type veins represnt the final manifestations of regional metamorphism processes from the Romanian Carpathians.

References

Ansilewski I. (1958) On microcline and triclinic adularia from bialkine gory gneiss (Polish Sudeten). *Bul. Akad. Pol. Sci., Sci Chim. Geol. Geogr.*, **VI**, 10, 275-282, Warsaw.

Borg I.Y., Smith D.K. (1968) Calculated powder patterns. II. Five plagioclases. *Am. Min.*, **53**, Washington.

Brindley G. W., Gillery F.H. (1956) X-ray identification of chlorite species. *Am. Min.*, **41**, 169.

Constantinescu E., Săbău G. (1984) Caracteres cristallographiques, optiques et structuraux de l'adulaire des filons alpins de Roumanie - Contributions au "probleme de l'adulaire" *An. Inst. Geol. Geofiz.*, **LXII** (Trav. du II-ème Congr. Assoc. Geol. Carp.- Balk., 1981).

Hey M.H. (1954) A New Review of the chlorites. *Min. Mag.*, **30**, 277.

Ianovici V., Neacşu Gh. (1981) Pirofilitele din România. *Rev. roum. géol. géophys. géogr., s. Géol.*, **26**.

Ionescu J., Anton L., (1971) Ripidolitul dinmasivul granitic Şuşiţa - Carpaţii Meridionali. *St. cerc. geol., geofiz. geogr., s. Geol.*, **16**, 1, 147-155.

Kostov I. (1965) Alpiiski tip mineralizatia v gnaisitie na tentralnite Rodopi. *Sp. BGD*, **26**, 3 271-278.

Laves F., Hafner S. (1956) Infrared Spectra of Feldspars. *Zeit. Krist.*, **108**.

Parker R.L. (1954) Die Mineralfunde der Schweizer Alpen. Basel.

Popescu Gh. C., Constantinescu E. (1982) Pyrophyllite in the anchimetamorphic schists from the Parâng Mountains (South Carpathians, Romania). Intern. Mineralog. Assoc., 13th General Meeting, Varna.

Tuddenham W.M., Lyon J.P. (1959) relation of infrared spectra and chemical analysis for some chlorites and related minerals. *Analyt. Chem.*, **31**, 377.

*** X-ray Powder data File. ASTM.

III. MINERALOGY OF ORE DEPOSITS

Some observations concerning the skarns and the copper deposits at Sasca Montană (Banat)

EMIL CONSTANTINESCU

The following conclusions may be drawn from the mineralogical-petrographical characterization of magmatic rocks, of metamorphosed rocks from the contact zone and of metalliferous concentrations: Igneous rocks mainly belong to porphyry granodiorites and quartz-diorites. The occurrence of more acid or alkaline types (alkali syenites and granites) has a local character. The present composition of magmatic rocks is complicated by the presence of mineral neoformations resulting from various processes of hydrothermal alternation. Mineralogical associations separated in the contact zone are mainly characteristic of calcic skarns, while associations with magnesium character are less spread. The outstanding development of vesuvianite assigns a characteristic feature to these skarns. Metalliferous concentrations are delimited in three types with different parageneses and structural-textural characters, preferentially localized in skarns, recrystallized limestones and silicified-sericitized magmatic rocks. The presence of chalcopyrite as the main mineral and subordinately, of molybdenite, subordinated in all parageneses, points to the cupro-molybdenic character of the mineralization.

The copper ore-deposit at Sasca Montană occupies a median position in a classical region for the study of contact rocks and ores (Ocna de Fier-Moldova Nouă), included in the Banatitic (Laramian) province. The long-standing interest in this region has been revived over the past decade, by an in-depth investigation of laramic ore-deposits in Banat and in the whole Banatitic metallogenetic province, for their potential economic value. Giuşcă., Cioflică, Savu (1967) have elucidated the petrologic and metallogenic contents of this province and Kissling (1967), Vlad (1969), Constantinof (1967), Superceanu (1956), Gheorghiță (1969), Gheorghițescu.

(1969) et al., contributed to the knowledge of the rocks and mineralization in the above-mentioned region. The following observations are the result of field and laboratory research conducted over the years 1968-1970 in the area of Sasca Montană-Stânăpari. Detailed surface research has been carried out between V. Şuşara-Dealul lui Ciucar and on the material collected from explorations carried out by IPEG Banatul in the Stânăpari sector. The paper aim is to define from a mineralogical and petrographical point of view the Banatitic rocks and the associated metalliferous concentrations.

1. The Banatitic eruptive

It outcrops between the Nera Valley and the Radimna Valley, over 8,5 km, with the main occurrences localized in the territory of the Sasca Română, Sasca Montană, in Valea Gheorghe and in the erosion plateau Stânăpari-Cărbunari, where they reach the maximum width. The magmatic outcrops may be grouped in two alignments oriented from North to South; the main one in the West and another one, less developed, in the East (Fig. 1) both parallel with the Oravița major tectonic line and with the Sasca, Crucea Otmanului and Nera faults (Răileanu et al. 1956, 1963; Bădăluță, Buică 1970).

The development of deep magmatic bodies, is hardly noticeable in the Northern sector where it can be guessed only in the ellipsoidal contour of the surface intercepted by erosion (Valea Morii). Instead it can be clearly traced in the Southern sector, through the East-West profiles made on the basis of bore-holes. Banatites appear here (Fig. 2) in the form of a blade (sphenoid) with a normal width of (G=200 m), oriented North-South and with a 500-550 W inclination, partly concordantly intruded into sedimentary rocks.

The main fissure systems within banatites are: a) N-S /50-60^0 W; b) N 40-50^0 E/E; c) and d) E-W with 80-90^0 slants (c) or N (d). The above-mentioned average values obtained in the surface outcrops of the Dealul Orașului-Dealul lui Ciucar area (Photo 1), are generally

Fig. 1. Geological sketch of the Sasca Română Stânăpari area (Tectonics after Bădăluță, Buică, 1970).

Fig. 2. W-E profile through the Stânăpari Plateau, based on the drill-hole data by I.P.E.G. Banatul: 1. Banatites weakly impregnated with sulfides 2. recrystallized limestones, 3. Garnet vesuvianite-bearing skarns, 4. Mineralization in skarns, 5. Mineralization in silicified banatites.

in agreement with the results of measurements made underground (V. Morii gallery, Gheorghe II gallery; Ciocănelea, Hârlea, 1965).

From the frequency point of view, "c"-type fissures are predominant, while the "a"-type fissures are more clearly expressed. The longitudinal "a"-type fissures are parallel with the direction of the banatite bodies, following the local variations in the direction thereof. The aplitic or quartzitic veins frequently cement such fissures and one may often notice decimetric skarn strips with the same orientation. The "c"-type fissures separate the banatites into regular blocks – with widths varying between 0.50-1 m. They intersect the systems, causing the separation of small quartz veins arranged after the "a" system and, most likely, of exokinetic nature in relation to the "a" and "b" fissures which have an endokinetic character.

The participation of mineral components in various parts of the investigated eruptive rock (Table 1) allowed the separation of various types of rocks, assigned according to the QAP diagram (Streckeisen 1967): diorites, quartz-diorites, granodiorites, monzonites and monzodiorites. Locally, one notices the development of special varieties as the syenites and the alkali granites with aegirine and augite. The structural variation of magmatites is con-

spicuous; one notices a gradual transition from rocks with structures typical of the plutonic facies (diorites, quartz-diorites, granodiorites, monzonites, granites) to rocks of the dacite and andesite type, located in the peripheral zones of the apophysis in Dealul Ciucar. This very clear transition, particularly obvious in the hypabisic rocks, which are dominant in the region, through the alteration of the size of phenocrysts and the components of the fundamental mass, has allowed to separate types pertaining to porphyrytic granodiorites, microgranodiorites and, respectively, porphyrytic diorites and microdiorites. Interesting graphic and myrmekitic textures have been observed in the alkali microgranites in Dealul Oraşului (Photo 3) and in the granophyres and aplites of Valea Gheorghe - Stânăpari.

The mineralogical composition of the magmatites is complicated by the presence of new mineral formations resulting either from the substitution of primary minerals or from direct precipitation. The following typical assemblages have been identified: orthoclase-biotite-quartz; albite-epidote; sericite-chlorite-quartz; sericite-quartz; illite-sericite-chlorite; quartz-carbonates (calcite+siderite); analcime-laumontite-stilbite. A vast array of alterations with hydrothermal character (feldsparization, albitization, biotitization, sericitization, argillization, carbonation, zeolitization) result-

Table 1. The participation of mineral components in the Laramian magmatites from Sasca Montană

Rock type	Minerals %						
	Orthoclase	Plagioclase	Quartz	Hornblende	Biotite	Augite - egirine	Accesso nes
Diorite	4.3-3.1	44.1-47.3	6.9-7.8	43.2-41.2	-	-	1.2-2.3
Quartz-diorite	5.4-6.2	42.3-44.8	9.6-11.2	39.2-37.1	1.4-0.5	0.5-0.1	1.1-0.5
Granodiorite	5.4-6.2	14.6-13.2	52.4-54.3	19.7-20.3	13.2-12.4	-	0.4-
Monzonite	41.8-39.6	41.4-39.4	2.3-3.4	13.2-11.1	3 7-3.2	-	0.3-0.1
Monzodiorite	24.2-26.7	42.4-43.5	17.6-18.1	10.1-15.6	0.7-0.1	-	0.5-2.4
Sienite	41.2	21.7	1.02	16.2	7.0	8.9	3.62
Alkaline Granit	56.9-60.4	0-5.9	6.2-35.2	0-3.4	-	4.9-24.8	0.5-2.5
Graphic micro-granite	72.11-70.88	-	27.89-29.12		-	-	

ed from the circulation of fluids in the fissures formed after the rearrangement of magmatites.

2. The metamorphic rocks in contact aureole

They occur in the Northern sector, along the slopes of Valea Mare and in the Southern one towards Valea Gheorghe, being more developed in the Stânăpari sector, where they are covered by the dump-wastes of older mining works. In the Stânapari sector, the contact area forms an in-depth, almost continuos strip, which follow – with small width variations – the direction of the beds and cover of the banatite blade. In its terminal sectors, the banatite body has direction and inclination fascicles, causing a vaster contact area and the expansion of skarns, which are intercepted in drillings at different levels.

The mineralogical composition shows notable variations. The following associations are typical in the analyzed samples: grandite-vesuvianite; grandite-diopside-vesuvianite; wollastonite-grossularite; grandite-diopside-anthophyllite; scapolite-calcite; diopside-tremolite; grandite-wollastonite-salite-epidote; brucite-calcite; forsterite-flogopite. Of these, the grandites, vesuvianite and tremolite form local monomineralic zones, accompanied only by small amounts of calcite. Alongside the above-mentioned minerals, one notices relic minerals such as apatite, sphene, secondary chrysotile, serpentine, chlorite or some late phases deposited on the fissures: quartz, analcime, laumontite, stilbite.

On the whole, we can distinguish parageneses typical for calcic skarns as well as markedly magnesian assemblages identified in the Carolina gallery and in the drillings on the Stânăpari plateau. Pyroxenes are insignificant compared with the broad dissemination of the grandite-vesuvianite assemblage in all the investigated sectors. The remarkable participation of the vesuvianite in the mineralogy of metasomatites confers a typical aspect to the

Sasca Montană skarns, in comparison to other occurrences in the Banatitic province, where the garnet is followed mainly by wollastonite, diopside (Băița Bihor, Ocna de Fier), hedenbergite, ilvaite (Dognecea) or is clearly dominant (Moldova Nouă). As for the spatial disposition of metasomatites, the microscopic and field research allows to separate the endoskarn zones with a limited development and a simpler mineralogy from the exoskarn ones. The later cover an important area and with notable mineralogical variations. Within them, the distribution of the bi- or monomineral associations mentioned above often has an irregular character.

3. Mineralization

Within the metalliferous concentrations in the Sasca Montană ore deposits, three major types of mineralization have been separated on the basis of mineralogical associations and of structural and textural criteria. They are mainly located in skarns, in recrystallized limestones and in silicified-sericitized banatites:

a) the mineralization associated with skarns is generally defined by the presence of the paragenesis: chalcopyrite-digenite-molybdenite. In the Stânăpari sector, the paragenesis chalcopyrite-pyrite-pyrrhotite-magnetite-hematite is predominant, but appears only sporadically in the other sectors (Sasca Română-Sasca Montană- Valea Gheorghe). The minerals have allotriomorphic contour; there appear various inter-crystalline structures as well as exsolution ones (bornite-chalcopyrite; bornite-chalcocite). The magnetite and hematite are frequently martitized and muskovitized, respectively. The metallic minerals usually replace calcite, garnets or the other skarn minerals. The mineralization appears in the form of local accumulations either in nests or as impregnation in broader areas.

b) The mineralization in the recrystallized limestones. The paragenesis is pyrite ± tetrahedrite-galena, marcasite-molybdenite – usu-

ally located on the outer side of the skarn zone or rather at a distance from the contact. It frequently shows colloidal structures (either concentric or plane-striped). At a larger scale, we can mention the presence in the Stânăpari sector – in some limestone islands with a "roof-pendant" aspect – of pyrite mineralization in parallel strips, following the fissure planes (WE) in recrystallized limestones.

c) The mineralisation in banatitic rocks: chalcopyrite-pyrite-molybdenite. Chalcopyrite appears either disseminated or in veins, in association with pyrite, molybdenite and, seldom, with bornite in quartz gangue. The mineralized zones follow the fissure direction in the mass of intensely hypogenically silicified and sericitized banatites.

A distinct character is that of the mineralization in the tectonic breach in Dealul Gheorghe, followed up to a depth of 300 meters in the Western flank of the syncline affected by Sasca and Crucea Otmanului Faults and made up of irregular elements of recrystallized limestone trapped into black clay. The mineralization: – pyrite, marcasite, tetrahedrite – forms narrow strips (2-7 mm) which follow the contour of the granodiorite and microcrystallized limestone fragments, as well as local replacement zones and diffuse impregnation into the clay mass.

Parageneses typical of the oxidation zone of the copper mineralization were identified at Stânăpari - 8 May mining well sector (cuprite, native copper, malachite, azurite) and in the sectors Sasca Română, Dealul Oraşului, Valea Gheorghe: malachite, azurite, representing, alongside chalcocite, bornite (partly) and covellite, the relics of a broad area of supergeneous alteration (oxidation, cementation) which formed the upper layer of the copper lode. This was almost fully exploited in the past due to its high copper concentration (Cotta, 1864; Marka, 1869).

4. Genetic considerations

The intrusion of Laramian magmatites generated important petrogenetic and metallogenetic processes that affected both the rocks in the adjoining sedimentary complex and the intruded magmatic rock. The thermal effect and the action of post-magmatic fluids caused in the contact aureole a series of transformations resulting in the development of mineralogical phases stable in the new circumstances. The mutual relationships between these minerals and the general character of the newly formed rocks indicate that the formation and evolution processes had three stages, corresponding to a main phase (grandite, pyroxene, vesuvianite, wollastonite), a subsequent one (tremolite, epidote, chrysotile) and a late phase (calcite, quartz, analcime, laumontite, stilbite). The peri-plutonian zoning is generally weak in the investigated area; the regular spatial disposition of the various associations or types of skarns retain, in general, a local character, being limited by the composition variation of the paleosome, the anisotropic character of the rock permeability and the disjunctive tectonics. The magnesian character of some of the mentioned mineralisation, located in the Western part of the deposits, seems to partially reflect the lithologic control exerted through the local presence of Triassic dolomites.

The post-intrusion transformations of the magmatites concern both the endoskarn zones, formed through contact-reaction at the limit of the carbonated rocks and the modification of the mineralogical composition in various internal zones thereof, through varied metamorphisms. The auto-metamorphic processes have developed in a temperature range of 525^0 -600^0 C the lower limit of the stability range for monoclinic K-feldspar (MacKenzie, 1954) and 320^0-450^0 C, the lower limit of stability

for sodium and calcium zeolites in the quartz-rich systems (Coombs et al., 1959).

The observations made on the metallic parageneses and on their correlation with the mineralogical assemblages of the host rocks, as well as on the facies of hydrothermal metamorphism, have a preliminary character.

Thus, the establishment of the succession and discontinuity in the ore genesis must not be treated without reserves. The mentioned paragenesis indicate a high temperature for the formation of skarn mineralisation, the mesothermal character of mineralisation located in banatites and the partially epithermal character of certain deposits located in crystalline limestones.

The tight relationship between the autometamorphic processes and mineralization is well enhanced by the magmatites in the Stânăpari-Cărbunari area which can be assigned - on the basis of the minerals belonging to various alteration facies – to the "quartz-sericite-pyrite" type (Schwartz, 1947). Also noticeable is the dissemination of pyrite into the eruptive bodies, over vast areas – a possible "protore" in the sense defined by Ransome (1919), Park Diarmid (1964) as well as the concentrations of chalcopyrite mainly in the sericitized and silicified zones. The geometric relations between the various minerals of the hydrothermal alteration facies point out especially the association of copper with the sericite-quartz stage, which is the final sequence of the hypogenic alteration process, followed only by late zeolites occurring as fissure fillings. Local enrichment of the primary mineralization is typical for the supergenous alteration zone whose specific features in various sectors of the deposit are determined by the mineral composition, the presence of carbonate rocks and the ground morphology. The oxidation zone is dominated by the presence of iron hydroxides in the Stânapari sector and by the presence of basic copper carbonates in the Sasca Română sector. The hypergenic copper

sulfides (chalcocite, covellite, bornite) are well represented in the Gheorghe-Sasca Montană sector, where chalcocite may form compact concentrations. In certain situations, the action of both oxygen and CO_2 appears to have been sufficient to convert the primary mineralization (chalcopyrite, pyrite magnetite) into limonite and malachite.

In other cases – such as the 8 May sector – the modification in time of the Eh has caused the oxidation of the zone and the appearance of secondary sulfite enrichment, together with the development of a sub-zone rich in cuprite and native copper, with relics of chalcocite in cuprite.

Conclusions

The formation and distribution of the cupriferous mineralization was controlled by the structural elements represented by the deep Laramian dislocations that have governed the emplacement of the magmatites (and probably the character of the fluids). Other elements of structural control were represented by the fissure system which has been reactivated repeatedly, and has facilitated the circulation of these fluids. A lithologic control has been exerted as well. It determined the preferential fixing of metallic components in the contact aureole, where rock permeability and competence were favorable.

The copper-molybdenum character of the mineralization is suggested by the presence of chalcopyrite as the main mineral and by subordinated molybdenum. Such parageneses are confined to skarns, magmatites and recrystallized limestones. The association of the copper mineralization with the grandite-vesuvianite paragenesis in skarns and the quartz-sericite one in magmatites represents a metallogenetic metallotect (Lafitte et al., 1965) and defines the peculiarities of the ore-deposit at Sasca Montană against other occurrences of the Laramian metallogenetic province in Romania.

References

Cotta v. B. (1964) Erzlagerstatten im Banat und im Serbien. 51-55, Wien.

Coombs et al. (1959) the zeolite facies with comments on the interpretation of hydrothermal syntheses. *Geochim et Cosmochim Acta,* **V 17**,. 53.

Giuşcă D., Cioflică G., Savu H. (1967) Caracterizarea petrologică a provinciei banatice. *An. Com. Geol.,* **XXXV.**

Laffitte P., Permingeat F., Routhier P. (1965) - Cartographie metallogenique, metallotecte et Geochimie regionale. *Bull. Soc. Fr. Miner. Crist.,* **88**, 3-6.

Lindgreen W. (1905) The copper deposits of Clifton Morenci, district Arizona. *U.S. Geol. Surv. Pap.,* **43**, 3705, Washington.

MacKenzie W.S. (1954) The orthoclase-microcline inversion. *Mineralogical Mag.,* **30**, 354.

Marka G. (1869) Einige Notizen uber das Banater gebirge. *Jb. K.K.*

Park C., Diarmid R. (1964) Ore deposits. Freeman, San Francisco.

Pandelescu C., Dumitrescu M., Borcea M. (1970) Cercetări privind prepararea minereului de la Sasca Montană. *Stud. Teh. Ec.,* B **45**, 135-151.

Streckeisen A. (1967) Classification and Nomenclature of Igneous Rocks. *N. Jb. Miner. Abh.,* **107**, 14.

Schwartz G. M. (1947) Hydrothermal alteration in the "Porphyry copper" deposits. *Ec. Geol..* **XLII.**, 319-352.

Fissures in granodiorites, Dealul Orașului.

Granodiorite with biotite, N+, 40X
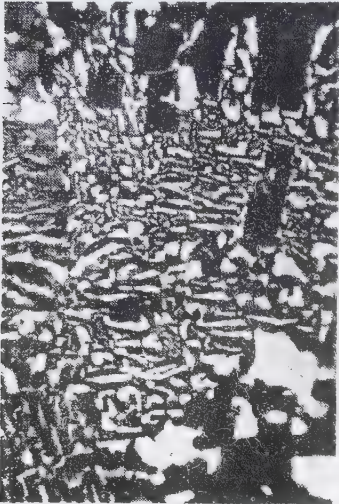
Graphic microgranite, Dealul Orașului, N+, 40X.

Porphyrytic granodiorites with biotite and hornblende, Stânăpari, N+, 40X.
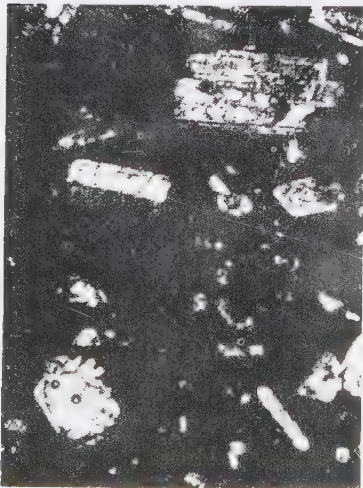
Andesite with biotite, Dealul lui Ciucar, N+, 40X

Quartz-diorite, Cioaca Înaltă, N+, 40X.
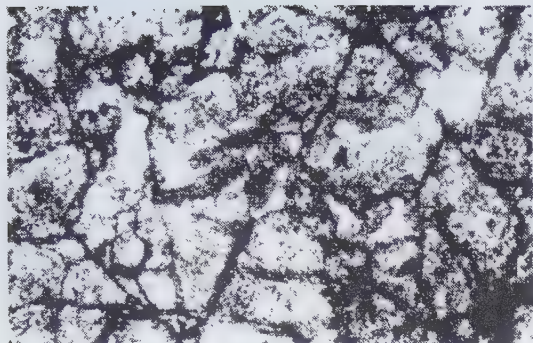
Grandites, N II, 40X.
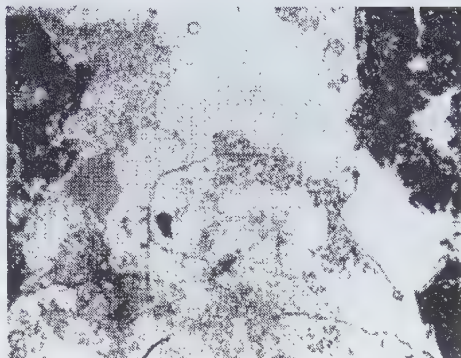
Skarn with garnets (black) and vesuvianite, N+, 40X.
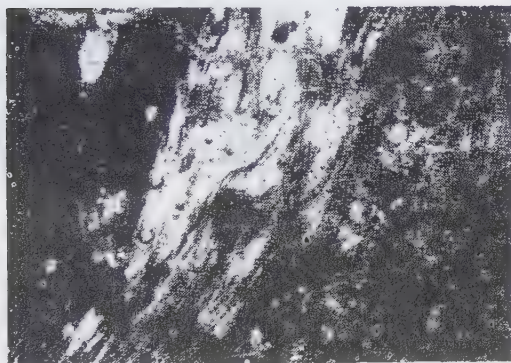
Skarn with garnets and wollastonite, N+, 40X.
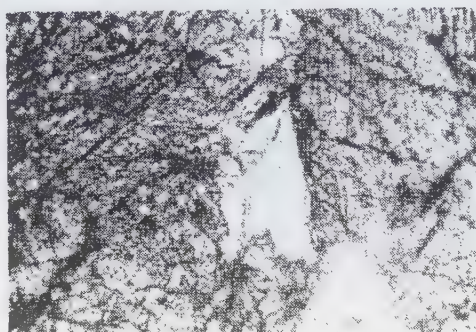
Skarn with garnets and diopside, N+, 40X.
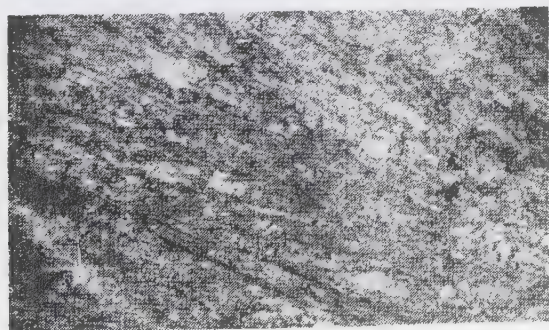
Skarn with tremolite, N II, 40X
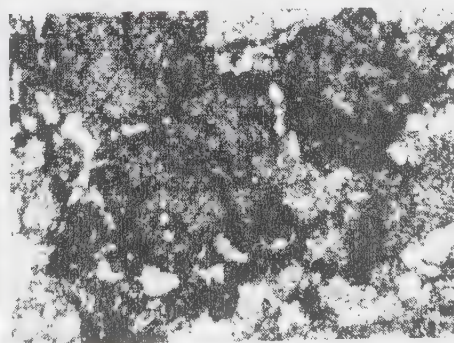
Skarn with garnets and epidote, N+, 40X.
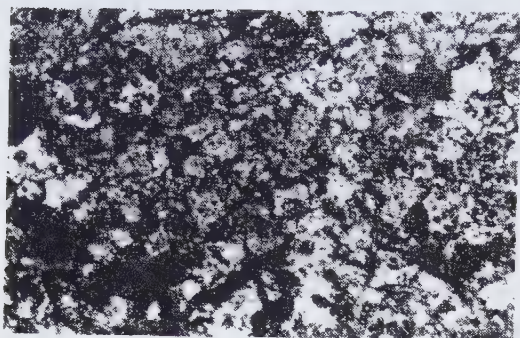
Chalcopyrite and pyrite in skarns, 40X.
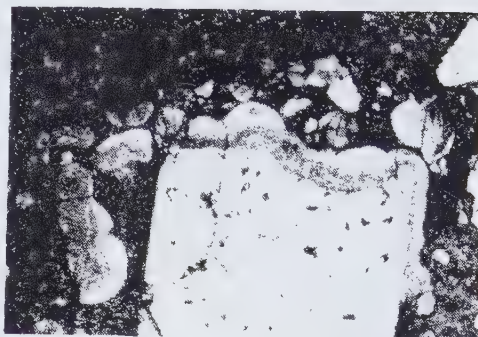
Pyrite replaced by chalcopyrite and covellite, 40X.
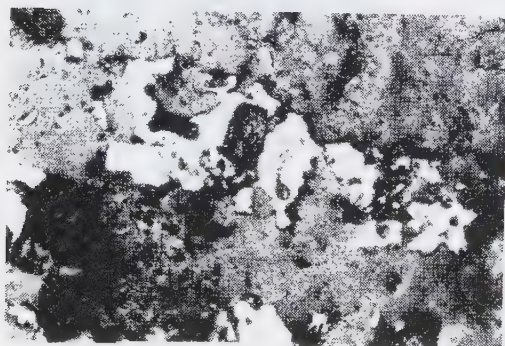
Chalcopyrite and covellite in skarns, 40X.
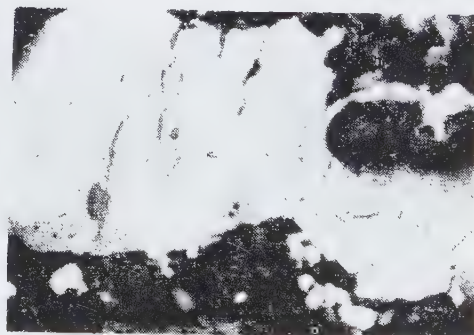
Chalcopyrite relics in bornite, 40X.
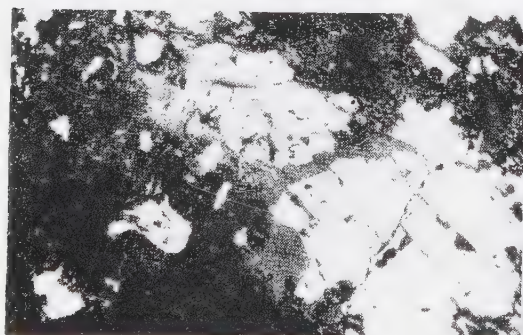
Chalcopyrite and galena in silicified limestones, 40X.
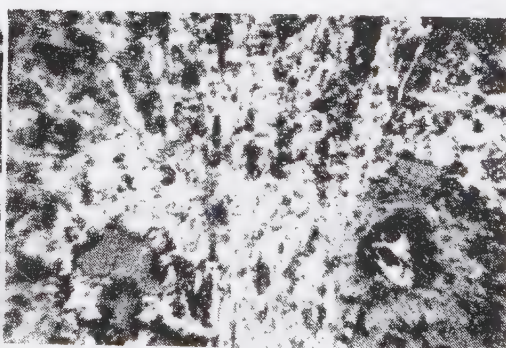
Magnetite pseudomorph after hematite, 40X.

Contributions to the knowledge of the paragenetic aspects of the mineralization associated to the alkaline massif of Ditrău

EMIL CONSTANTINESCU
NICOLAE ANASTASIU
NICOLAE POP
NAZAR GARBAŞEVSCHI

Described for the first time in 1872 by Herbich, the alkaline massif of Ditrău is well known from petrographical, geochemical and structural points of view. We remind the studies concerning its petrogenesis by Ianovici (1933, 1938), Codarcea et al., (1954), Streckeisen (1954, 1960) and completed by the more recent studies of Anastasiu, Constantinescu (1974, 1978, 1980), Jakab (1975) and Zincenco, Vlad (1978).

The observation concerning the associated mineralizations are sporadic among the petrographic studies and limited to the isolated identification of several minerals.

The first informations concerning the mineralizations belong to Ianovici (1933, 1938), who describes occurrences of sphalerite, galena, pyrite, chalcopyrite and goethite localized in the valley of Jolotca, and to Panto (1942), who described pyrite, chalcopyrite, sphalerite.

Other minerals have been identified by Koch (1886) – orthite, Zepharovich (1859) – pyrochlore, Stanciu (1955) – baddeleyte; Codarcea et al. (1958) – rhönite, xenotime, molybdenite, Jakab, Garbaşevschi (1975) – arsenopyrite.

Field studies, detailed microscopic observations and complex laboratory analyses (XRD, TDA, IR, electron microprobe, laser spectrography) enabled the identification of several new mineral occurrences and to precise the chemistry, structure and optical properties of others. There were also studied the mutual relations between these minerals as well as their position during the petrographic and metallogenetic evolution of the massif.

1. Geological background

According to Anastasiu and Constantinescu (1980), the alkaline pluton of Ditrău, with a quasi-circular outline, represents a complex intrusion developed during several stages, in discordant relations with the crystalline schists of the Rebra and Tulgheș Series.

Its geological structure and petrography are complex. Two structural levels are distinguished: a northern, "Jolotca-Putna" compartment, and another, central-southern "Valea Mare-Güdutz-Belcina", consisting of calc-alkaline (matites, diorites, monzonites, syenites, granites) and alkaline rocks (essexites, foidic monzonites, foidic syenites). Both structural levels are cross-cut by a swarm of vein rocks (lamprophyres, aplites, syenitoides).

2. Aspects of the mineralization

Depending on the geological and petrographical background, two distinct chemical and mineralogical types can be separated in the northern and central-southern zones of the massif.

The mineralization of the northern zone located in the complex of mafic and ultramafic rocks which play exclusively the part of host rocks, constitute mostly simple veins or systems of quasi-parallel veins grouped along E-W N trending lineaments. Local impregnation zones, nests or fine networks of veinlets can occur. There is a spatial association between the mineralized zones and the vein rocks (lamprophyres, albitites, carbonatites).

The mineralization from the central-southern zone form impregnations, sometimes largely dispersed, seldom nests or short bands with milimetric widths. They are hosted by leucocratic rocks. The most important concentrations are discontinuously disposed along the contact metamorphic aureoles and are controlled by the complex of alkali-feldspar syen-

ites and by the complexes of quartz-feldspar rocks from the borders of the massif.

3. Description of the main minerals

The mineralization consists of oxides, sulphides, carbonates, phosphates and subordinated silicates and native elements (Table 1). REE minerals dominate quantitatively (phosphates, oxydes), over molybdenum, iron bisulphides and titanium oxides.

Molybdenite. It occurs as veinlets, fine films along microcracks or as very fine impregnations within the rock mass. Crystals of various dimensions are dominant, with thicknesses of 0.04-0.06 mm. They show blade shapes, often curved due to mechanical deformation. XRD analyses (main lines: 6.06, 2.26, 2.038, 1.53) indicate the predominance of the 2H hexagonal polytype and subordinately the presence of the trigonal 3R polytype, marked by increase of the "b" axes value and by decrease in hardness. Values R% (Table 1) are slightly lower than the standard values (Uytenbogaardt, Burke, 1971). Molybdenite is typically associated with carbonates, oxides and sulphides. They frequently occur along the cracks with sphalerite, galena, on ilmenite quartz interfaces, moulding pyrite and sphalerite crystals (Fig. 1), or forming radial carbonate aggregates, obviously deposited subsequently to the forementioned minerals.

Bismuthinite. It appears as patches within galena or forms intergrowths with it; its polishing hardness equals that of galena; it shows a darker yellow color and strong birefringence and anisotropy.

Josëite. Occurs as prismatic-needle shaped crystals, included in galena (Fig. 2) or bismuthinite. It is yellow at the contact with galena, shows medium hardness and higher reflection. reflection and anysotropy are low. It shows a bluish shade at the con-

Table 1. Minerals forming the mineralization associated to the Ditrău alkaline massif

Sulphides	Oxides	Carbonates
arsenopyrite	**anatase**	ankerite
bismuthinite	baddeleyite	azurite
sphalerite	**brookite**	bastnäsite
chalcopyrite	corundum	malachite
chalcopyrrhotite	goethite	parisite
covellite	lepidocrocite	siderite
cubanite	hausmanite	
galena	hematite	
joseite	ilmenite	*Phosphates*
mackinawite	**pyrophanitic ilmenite**	apatite
marcasite	ilmenorutile	monazite
molybdenite	magnetite	xenotime
pyrite	molybdenite	
pyrrhotite	niobite (columbite)	*Silicates*
valleriite	picotite	melanocerite
tetradymite	pyrochlore	melinophane
	pyrolusite	orthite (allanite)
Native elements	**pseudobrookite**	thorite
silver or copper	psilomelane	zircon
	rutile	
Halogenides	thorianite	
fluorite	titanomagnetite	

* the bold lettering indicates minerals mentioned for the first time.

Sphalerite. It occurs as 2-3 cm wide veinlets, nests at the marginal zones of veins, and centimetric patches or tiny allotriomorph grains within the gangue. The value of reticular parameter "a", calculated from the XRD analyses is 5Å, corresponding to a FeS content of 7%. The microhardness VHN is 192 kg/mm². It is associated with chalcopyrite, cubanite and pyrrhotite. It forms myrmekite-like intergrowths with carbonates.

Chalcopyrite. Appears as isolated patches, inclusions in sphalerite or intergranular films associated with pyrite aggregates. When associated with calcite, it forms discontinuous veinlets along the mechanical discontinuities within monazite, rutile, ilmenite and pyrite, or along the cleavage planes of sphalerite.

Pyrrhotite. Appears as xenomorph inclusions in pyrite or as ovoids in magnetite. It can enclose tiny pyrite grains. It show stransformation to marcasite along cracks.

Fig. 2. Spatial relationships between the minerals constituting the mineralization **2a**: cp, chalcopyrite; gn, galena; bl, sphalerite; js, joseite; q, quartz. **2b**: py, pyrite; cp, chalcopyrite; po, pyrrhotite; q, quartz.

Fig. 1. Microphotographs of the Ditrău mineralizations - Jolotca area. **1a**: mo, molybdenite; sphalerite; dark grey, carbonates. **1b**: il, ilmenite; gn, galena.

Monazite. It is the most important mineral concerning the REE contents. It occurs as tabular crystals, forming microgranular or radial aggregates, usually 1-2 mm long and 0.01-0.10 mm wide. It shows a brown-reddish color and waxy luster. Microscopic evidence shows that hydrogoethite and lepidocrocite accumulate on crystal junctions and along cracks, imparting their color. The pleochroism is low. The birefringence is high - $2V\alpha=15\text{-}10^{\circ}$. R% values are low. The main diffraction lines determined are 5.18-4.79-4.18-3.50-3.30-3.09-2.99-2.87-2.60-2.44-2.19-2.14-1.97-1.90-1.87-1.75-1.69 Å. The IR absorption spectra show absorption bands at 1 070, 625, 585, 475 cm^{-1}. They constitute characteristic associations with the carbonates which often occur along cracks, with rutile, pyrite, galena, chalcopyrite, apatite, orthite and zeophyllite

(Figs. 3, 4). The alteration of monazite into orthite is obvious, especially at the zeophyllite contacts.

Xenotime. It appears especially in the SE part of the massif and it is completely subordinated within the northern zone.

Orthite. It occurs as black prysmatic crystals, grouped into radial aggregates. Polysynthetic twining and zoning are common. Pleochroism is intense: colorless - brown reddish - dark red. Biaxial negative. Lines of diffraction: 8.007-5.06-4.68-3.51-3.01-2.89-2.69-2.60-1.62 Å. For some samples both XRD and DTA analyses show the presence of metamictic orthite. It commonly forms associations with calcite, monazite, pyrite, rutile and zeophyllite.

4. Structure and texture of the mineralization

The most usual structure (Fig. 3) is granular, with grain sizes larger than 1-2 mm, except for molybdenite, where the grains attain 0.05 mm.

veins, and cementation with younger and more plastic minerals. Epitaxial intergrowths equally occur too: molybdenite-chlorite, molybdenite-biotite; bismuthinite-joseite.

5. Characteristic associations

Considering the relations between minerals forming the mineralization (Fig. 4), as well as the relationships between these minerals and gangue, a series of characteristic mineral associations have been separated, forming dis-

Fig. 3. Structures and textures of the mineralization from Ditrău - Jolotca sector. **3a**: 1, monazite; 2, pyrite; 3, ilmenite; 4, carbonates. **3b**: 1, quartz; 2, pyrite; 3, monazite; 4, ilmenite and chalcopyrite; 5, molybdenite; 6, carbonates. **3c**: 1, pyrite; 2, monazite and orthite; 3, orthite; 4, pyrite, ilmenite and sphalerite; 5, monazite and orthite nests within carbonates; 6, mylonitic zone with monazite showing brittle deformation.

Replacement structures often occur: ilmenite-rutile; joseite-bismuthinite; monazite-orthite; sphene-ilmenite. Exsolution structures are frequent: ilmenite-hematite; sphalerite-chalcopyrite. The textures are massive and compact in the case of pyrite, and radial or nest type for monazite.

Impregnation textures as well as microbbrecciated, mylonitic textures (Fig. 3c) occur especially in the case of the pyrite, showing brittle deformation mostly in the marginal zones of

Fig. 4. Characteristic mineral associations in the alkaline massif of Ditrău - Jolotca sector. **4a, 4b**: 1, ilmenite; 2, pyrite; 3, monazite; 4, orthite; 5, carbonates; 6, chlorites. **4c**: 1, ilmenite; 2, pyrite; 3, carbonates; 4, chlorites; 5, sphalerite; 6, molybdenite.

tinct parageneses: (1) sphene-apatite-mag-netite-titanomagnetite-ilmenite-rutile-zircon; (2) monazite-rutile-pyrite-carbonates 1 ± (albite); (3) xenotime-rutile-anatase-pyrite-calcite-siderite; (4) monazite-bastnäsite-parisite; (5) rutile-ilmenite (+ilmenorutile - pyrophanitic ilmenite ± hematite ± magnetite)-carbonates 1; (6) monazite-orthite (± metamic-tic orthite) - zeophyllite - carbonates 1; (7) car-bonates 2-quartz-zeophyllite-chlorite (poly-type IIb)-lepidolite-hydromicas (polytype IM); (8) pyrite-sphalerite-pyrrhotite-chalcopy-rite (± chalcopyrrhotite ± mackinawite ± cubanite) - sphalerite (± bismuthinite ± joseite ± tetradymite) ± or - carbonates 3 (dolomite - calcite ± manganocalcite-siderite); (9) molyb-denite (polytype 2H)-carbonates 4-chlorite; (10) goethite-lepidocrocite-covellite-native copper)-malachite-azurite.

6. Mineralogenetic considerations

The mineralization associated to the Ditrău alkaline massif is the result of a series of com-plex processes and of a long evolution in time, during several stages of development:
- the magmatic stage, when the minerals of the parangenesis 1 crystallized: sphene - apatite - magnetite - titanomagnetite - ilmenite - rutile - zircon. These minerals constitute the fraction of the accesory minerals of the syenitic and dioritic-hornblenditic complexes. They are closely associated   (often as inclusions or exsolutions) with the main rock forming min-erals: feldspars, feldspathoids, amphiboles, pyroxenes, micas. They are present in a rather large amount, exceeding 10% of the rock vol-ume, especially in the case of the mafic rocks from the northern area;
- the pneumatolitic stage, during which the parageneses 2-6 have formed, made up of REE minerals (phosphates, carbonates, oxides, sili-cates) and of Ti, Fe, Th, Nb oxides. These minerals are associated especially with car-bonates and albite. During this stage, a meta-logenetic specialization occurred between the northern compartment, characterized by the presence of some light REE - cerium (mon-

azite paragenesis) and the central-southern compartment, with heavy REE - ytrium (xeno-time paragenesis) associated to Th;
- the hydrothermal stage, during which para-geneses 8-9 have formed, represented by sul-phides. The transition from the pneumatolitic stage (carbonate-albite) to the hydrothermal one is marked by the association (7), consis-ting of phyllosilicate-carbonate-quartz,which belongs also to the hydrothermal domain. The presence of Bi and of polyphase inclusions of exsolution type within the sphalerite (chal-copyrite-pyrrhotite-mackinawite-cubanite) indicates the formation at high temperature (meso-hypothermal) and quick cooling, with preservation of the metastable phases (cuban-ite, chalcopyrrhotite). Locally, the paragene-sis (10) is superimposed onto the foremen-tioned supergene associations: goethite-hydro-goethite-lepidocrocite-covellite-native cop-per-azurite-malachite ± molybdite.

The mineralogical features of the mineraliza-tion formed during the main (pneumatolitic and hydrothermal) stages indicate a sequential formation. They are pointed out by the pres-ence of several mineral generations (carbon-ates, orthite, pyrite, magnetite) and by the existence of important discontinuities marked by brecciation intervals. The dominant thioidic or oxidic character of the mineraliza-tion during certain periods reveals the modifi-cation in time of the O_2 and S fugacity ratios.

The REE mineralization: Nb - Ti (±Th) can be considered genetically affiliated to the alkaline rocks, the mineralogical and geochemical obser-vations showing a common geochemical trend of the REE, Ca and Nb with Th. The mineralog-ical complexity and several mineralogical incompatibilities with parageneses described for other known alkaline massifs (Vlasov, 1968; Sörensen, 1974) could be explained by the part-ly agpaitic character of the parageneses showed for several moments by the Ditrău massif. These parageneses were superimposed on a prevailing-ly miaskitic background (Anastasiu, Constantinescu, 1978, 1981).

Although in the southern zone, Nb and Ta appear as major elements within the pyrochlore, bastnäsite, niobite (columbite), associated to the miaskitic alkaline rocks, in the northern zone, they indicate an agpaitic differentiation trend, forming isomorphous substitutions of Ti within ilmenite and ilmenorutile. In what concerns the Mo mineralization, aparently this is not associated genetically with the foidic and ultramafic rocks. Its location in the complex of mafic rocks from the northern zone suggests the "screening" role or of "cathalitic environment" which it used for the precipitation of hydrothermal solutions subsequently to the formation of the REE - Nb - Ti mineralization.

References

Anastasiu N., Constantinescu E. (1974) Observații mineralogice în rocile sienitice din masivul Ditrău, *Com. Șt. Geol., Sesiunea festivă, Decembrie,, 17–18, 1975.*

Anastasiu N., Constantinescu E. (1978) Feldspații alcalini din masivul alcalin de la Ditrău, *D. S. Inst. Geol. Geof.*, **LXIV/1**, București.

Anastasiu N., Constantinescu E. (1980) Structure du massif alcalin de Ditrău, *Analele Univ.*, **XXIX**.

Anastasiu N., Constantinescu E. (1981), Feldspații plagioclazi din masivul alcalin de la Ditrău, *St. cerc. ser. geol. geofiz. geogr., geol.* **26**, 1, 83-95.

Codarcea Al., Codarcea M., Ianovici V. (1954) Structura geologică a masivului de roci alcaline de la Ditrău, *Buletin St. Acad. RPR*, **II**, 3-4, București.

Codarcea A., Ianovici V., Iova I., Lupan S., Papacostea C. (1958) Elemente rare în masivul de la Ditrău. *Com. Acad.* **VIII**, 3 .

Herbich F. (1982) Die geologischen Verhältnisse des nordöslichen Sieben bür-

gens. *Jahrb. ung. geol. Aust.,* 293-350.

Jakab G. (1975) Considerații asupra poziției spațiale a masivului alcalin de la Ditrău. *D. S. Inst. Geol. Geofiz.*, **LXII**, 93-98.

Ianovici V. (1933) Etude sur le massif syenitique de Ditrău, region Jolotca, district Ciuc (Transilvania). *Rev. Muz. Mineral. Univ. Cluj*, **4**, 2, Cluj.

Ianovici V. (1938) Etude mineralogique du gisement metallifere de Pîrîul Baia, Ditrău, district Ciuc (Transylvanie).

Ianovici V., Ionescu J. (1965) Contribution a la connaisance mineralogique du massif des roches alcalines de Ditrău - Roumanie. *Rev. roum. geol., geoph., geograph., ser. geol*, **9**, 1, București.

Koch A. (1886) Mineralogische Mitteilungen aus Siebenbürgen. *Orv. Termes. ert.* Cluj.

Panto (1941-1942). Orotva Ore Prospect near Ditro (Transylvania). *Rel. Ann. Inst. Geol. Publ. Hung.* **II**.

Sörensen H. (1974) The Alkaline Rocks, John Willey, London.

Streckeisen A. (1952/1954) Der Nephelinsyenit - Massif von Ditro (Siebenbürgen), *Schw. Min. Petr. Mitt.*, **32**, II, Sch. Min. Petr. Mitt. 34, Bern.

Streckeisen A. (1960), On the structure and Origin of the Nephelinosyenite Complex of Ditro (Transilvania, Romania), *Rep. 21th Intern. Geol. Congr. Part.* **13**, Copenhagen.

Uytenbogaardt B. (1971) Tables of microscopic identification of ore minerals (Ed. II). Elsevier, Amsterdam.

Vlasov K.A.- Geochemistry and Mineralogy of rare Elements and Genetic Types of their Deposits.

Zepharovich (1859) Mineralogisches Lexicon des Kaiserthuns Österreich, Wien.

Zincenco D., Vlad C. (1978). Raport, Arch. of the Institute of Geology and Geophysics, Bucharest.

Mineralogical observations on the skarns and mineralization from Oravița region

GHEORGHE C. POPESCU
EMIL CONSTANTINESCU

In the Oravița area there are the following types of postmagmatic transformations: pyrometasomatic - characterized by skarns (with grandite, vesuvianite, wollastonite, clintonite, forsterite and scapolite); thermal contact rocks (hornfels with biotite, orthoclase, andalusite and corundum); hydrothermal alteration characterized by four mineral assemblages: K-feldspar-quartz; orthoclase-quartz-biotite; sericite-quartz; chlorite-epidote-actinolite-quartz-calcite. In the same area there are four types of mineralisation: copper in crystalline schists; copper and molybdenum; copper-bismuth-tungsten and titanium in crystalline schists. There are spatial correlations between the copper-bismuth-tungsten mineralisation and the adularia-quartz, sericite-quartz assemblages, as well as between the titanium mineralisation and tourmaline - K-feldspar, and between the copper mineralisation and the propylitic alteration.

The Oravița region has been known for a long time for the richness of its mineral species and for their morphological features. A number of older papers, e.g., Cotta (1865), Koch (1924) or newer ones, e.g., Răileanu et al. (1963), Constantinof (1972), Gheorghitescu (1975), Cioflica et al. (1976, unpublished), have outlined the general petrographic and geologic aspects of the area under study.

The most wide-spread formations are the meso-metamorphic crystalline schists and the Lower Cretaceous calcareous clays. The banatitic rocks outcrop on both sides of the Oravița fault (Fig. 1) and affect both the crystalline schists and the Cretaceous rocks, generating small areas of thermal transformation and extensive areas of metasomatism.

Our observations followed the detailed mineralogical aspects of the skarns and associated mineralisation. Mutual relationship among the skarn and ore minerals and the post-magmatic transformations were analyzed as well, in order to outline some possible prospecting indicators. The studied samples were collected from the dumps of some old mining works in the area. The material was investigated using a wide range of methods: chemical analysis, X-ray diffraction, IR absorption spectroscopy, thermal analysis and UV fluorescence.

On the basis of these observations several types of mineralisation and post-magmatic transformations were identified. Figure 2 shows the location of these types on a simplified geological and structural background.
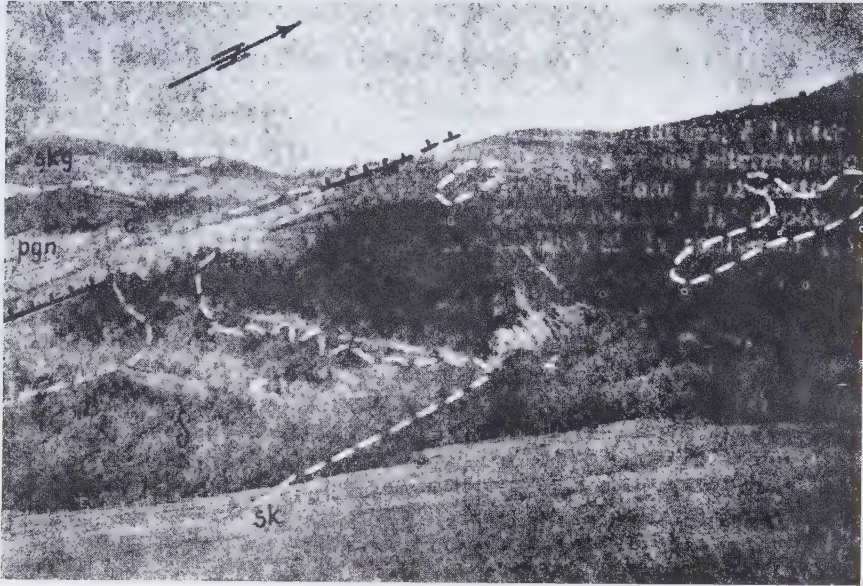
Fig. 1. Geological image of the Oravița Valley, near Lacul Mare: pgn - crystalline schists; c - hornfels; skg,v,cl - skarns with garnets, vesuvianite and clintonite; d - banatites.
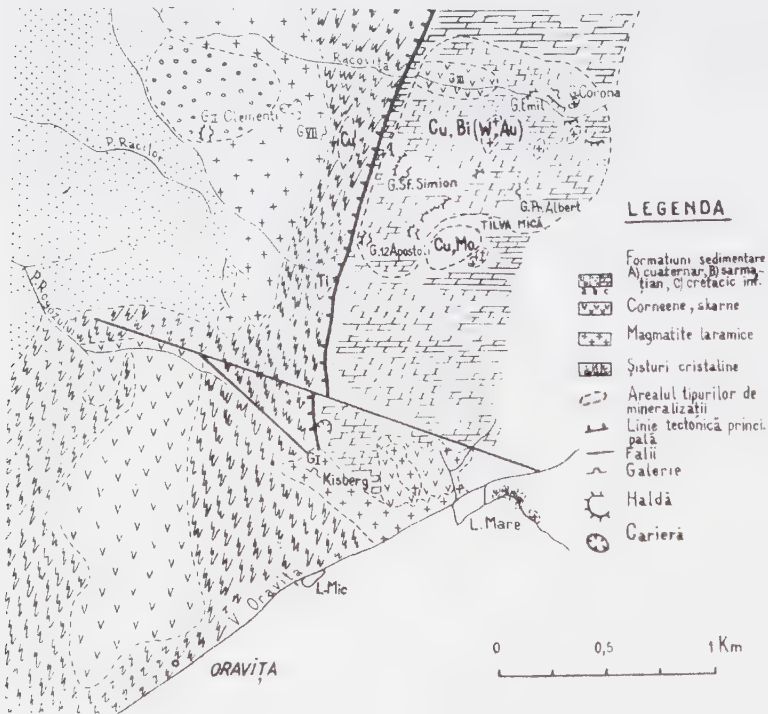
Fig. 2.- The distribution of mineralization types between the Oravița and Racovița Valleys.

1. Post-magmatic transformations

The thermal contact metamorphism is represented by white-gray recrystallized limestones and by fine-grained hornfels with biotite, orthoclase, andalusite and corundum.

The contact metasomatism is represented by layers of skarns with variable width, consisting mainly of grandites (13 - 31 mol % andradite), pyroxenes (diopside, Fe-diopside), vesuvianite, wollastonite, clintonite, forsterite and sporadically, scapolite.

In several favorable outcrops (Lacul Mare, Crişenilor Brook) the following zoning of the contact area between limestones and banatites could be noticed: diorites - periskarns - apobanatitic skarns - apocarbonaceous skarns. The main mineralogical components of the diorites are: 64.55-68.30% plagioclase (22-50% An); 2.8-5.2% K-feldspar (b^γ = 0-5°) and 2V = 65°; 4.19-22.1% quartz; 3.13-6% biotite; 3.12-15.11% hornblende. The color index (M) ranges between 9.12 and 22.4.

The periskarns consist of orthoclase, aegirine-augite, biotite, hornblende, plagioclase relics, sphene and apatite. Besides the skarns formed on banatites and limestones, contact metasomatic rocks formed on paragneisses and hornfels could be identified, too. Such skarns occur in Rîndunicii Brook and are mainly formed by garnets in conformable layers or in cross-cutting veins.

Within the skarns the main difference noticeable concerns the composition of the garnets. The garnets in the apomagmatic skarns are represented by a brown grossularite, in centimetric crystals, and containing up to 5.6 mol % pyralspites.

The brown garnet is included in a matrix of brown-greenish grossularite with 13.7 mol % andradite and 17.5 mol % pyralspites. Both varieties are optically isotropic with only isolated and diffuse optical anomalies.

The garnets in the apocarbonaceous skarns are represented by dark-green grandites with 31 mol % andradite and 7 mol % pyralspites. They display euhedral outlines (rhomboidal dodecahedra and trapezohedra). Under the microscope the garnets show radial and concentrical optical anomalies, the later being given by an alternation of isotropic and anisotropic lamellae disposed parallel to the outlines of the grains. The chemical composition of the three types of garnets is given in Table 1. It may be thus retained that aluminuous garnets prefer the apomagmatic skarns, whereas the ferrous ones, occur mainly in apocarbonaceous skarns.

Table 1. Chemical analyses of garnets from the area between the Oravița and Racovița Valleys

Oxides wt. %	151A	151B	67
SiO_2	38.10	39.26	37.36
TiO_2	0.18	0.04	2.08
Al_2O_3	17.12	20.26	12.38
Fe_2O_3	4.08	2.07	10.99
FeO	2.96	1.17	0.71
MnO	0.03	0.05	0.44
MgO	1.55	2.2	0.89
CaO	35.53	34.12	34.23
H_2O^+	0.15	0.18	0.17
H_2O^-	0.75	0.41	0.30
Total	100.55	99.79	99.55
Number of ions in the basis of 24 (O)			
Si	6.02	6.00	5.877
Al	-	-	0.123
Al	3.001	3.722	2.164
Fe^{3+}	0.464	0.222	1.304
Ti	0.002	-	0.246
Mg	0.323	0.491	0.208
Fe^{2+}	0.570	0.092	0.094
Mn	-	-	0.057
Ca	5.663	5.420	5.764
Participation of end members (mol %)			
and	13.7	5.623	31.6
gross	68.7	84.559	55.319
alm	11.2	1.550	1.813
pyr	6.3	8.226	3.99
spess	-	-	1.092

Pyroxenes are represented by diopside $\gamma \wedge c = 38\text{-}40^o$ and sometimes by salite ($\gamma \wedge c = 40\text{-}42^o$). They occur as small euhedral crystals with short prismatic habit.

Wollastonite shows prismatic crystals, isolated or as radial aggregates in calcite. It may form monomineralic zones of decimetric size (adit III, Racoviţa Valley. Wollastonite is often replaced by calcite.

Clintonite represents a unique occurrence in Romania. The mineral forms lamellar crystals of 0.5-1 cm in size, it has a green color, and occurs as nests associated with brown grossularite. By alteration, clintonite becomes white, transparent, resembling muscovite.

Vesuvianite occurs in short prismatic crystals, sometimes anhedral. The crystals are zoned, with anomalous anisotropy colors: brown and blue. Vesuvianite is often formed along cracks in grossularite.

Hydrothermal alterations. The main mineral assemblages characteristic to the alteration facies are:

1) Tourmaline - K-feldspar - quartz. Macroscopically, tourmaline occurs in black prismatic crystals. Under the microscope it shows euhedral and subhedral outlines with a marked pleochroism (pinkish-yellow to dark olive-green, or light bluish-yellow to blue). The variation in color and birefringence is probably due to different Mg/Fe ratios in the isomorphous series schörl-dravite-elbaite. In all cases, tourmaline is associated with monoclinic K-feldspar. The relationships with surrounding minerals indicate two generations of tourmaline: generation I - with big, green and pink, fractured crystals, corroded by K-feldspar and cut by ilmenorutile and rutile (Pl. I, Fig. 3) and generation II - with small blue crystals, forming together with K-feldspar, small veinlets within the porphyritic banatites.

Usually, the assemblage tourmaline - K-feldspar - quartz is considered typical for greisens, but in this case may be interpreted as a consequence of a high-temperature hydrothermal process, similar to that affecting the sericitized porphyries at Canannea Llalaguoa, Mount Potosi (Schwartz, 1959). At Oraviţa, a particularity is given by the presence of titanium minerals (ilmenorutile, rutile). The association between tourmaline and titanium minerals has been described also at Sasca Montană (Constantinescu, 1976) and seems to be characteristic for the Banat district of the Laramian metallogenic province.

2) K-feldspar (orthoclase, adularia) - quartz - biotite; The K-feldspar occurs as orthoclase in banatites, periskarns and apomagmatic skarns where it replaces plagioclase. The feldsparisation is accompanied by biotitisation and occurs mainly in the alteration zones around mineralized fissures in banatites. Adularia occurs in euhedral, large, limpid and optically inhomogeneous crystals. The 2V angles range between values specific to sanidine and microcline.

3) Illite - quartz; this assemblage occurs in the peripheral, decolored zones of the mineralized veins. The plagioclases are replaced by illite which forms together with quartz (+pyrite) a fine grained, compact aggregate. Sometimes, illite lamellae have remarkable dimensions.

4) Chlorite - epidote - actinolite - quartz - calcite; the assemblage is characteristic for the studied area (Pl. II, Fig. 3). Chlorite, epidote and actinolite confer the altered zones a pale to intense green color. Chlorite is found as pseudomorphs after biotite and hornblende or as sheaflike aggregates in veinlets cross-cutting the host rock. The thermal analyses on veinlet chlorite from banatites indicate an endothermic effect at 621^oC characteristic to magnesian chlorites (Philips, 1963). This was confirmed by the presence of a discriminative IR absorption band at 472 cm^{-1} (Rahden, Rahden, 1972).

Epidote is present in almost all rock types: banatites, skarns, hornfels. Sometimes it forms centimetrical ellipsoidal concentrations (Tîlva Mică) or compact monomineralic masses (Racovița Valley). The optical characters correspond to pistacite and rarely to clinozoisite. Actinolite occurs in veinlets within hornfels and banatites or as fine needles disseminated in quartz. It is often found as relics, almost completely transformed in a matrix of late calcite.

Quartz is also present in the majority of the mineral assemblages. Its relations with primary or late minerals allow the separation of several generations that span from the high temperatures specific to the tourmaline-bearing assemblages to the lower temperature geodes found within the skarns. The presence of opal and chalcedony (lutecite) has also been observed.

Calcite is also characterized by multiple generations illustrated by selective replacements of various associated minerals. Calcite is mostly specific to the final stages of the hydrothermal process, when it cross-cuts all the other minerals or cements larger mineralized veins or quartz- and garnet-bearing geodes.

5) The zeolite assemblage is subsequent to the mineralizing process. Zeolites are largely developed along fissures or in centimetrical nests. They may as well invade the ground mass of the porphyritic banatites generating graphic-like textures.

The assemblages mentioned may be ascribable to the following hydrothermal facies: potassic (orthoclase - biotite), phyllic (illite - quartz) and propylitic (epidote - chlorite - actinolite - calcite - quartz). Even though these assemblages can be very clearly identified both macroscopically and microscopically, they affect a small portion of the bulk banatitic bodies which appear with an overall fresh aspect.

The mineral neoformations are deposited mainly along fissures or as impregnations within a restricted area around these fissures. There is a rather clear relation between the hydrothermal facies and various type types of mineralisation. In this sense, we mention the spatial correlations between the adularia - quartz or illite - quartz assemblages and the Cu - Bi - W (Au), between the tourmaline - K-feldspar assemblage and the Ti mineralisation, as well as between the propylitic facies and the copper mineralisation from the crystalline schists. These correlations may be used as prospecting indicators.

2. Mineralisation

The spatial distribution of the types of mineralisation points out their tight connection with the Oravița main tectonic line and, in the case of the Cu - Bi - W mineralisation, with the banatitic apophyses in Tîlva Mică and Racovița Valley (Fig. 2).

Several types of mineralisation have been separated on the basis of characteristic parageneses and of the host rocks: copper - molybdenum; copper - bismuth - tungsten and subordinately, gold; copper in crystalline schists; copper in hornfels; titanium in tourmaline- and K-feldspar- bearing schists. Only the first two types are more widely spread in the area, whereas the last three ones were outlined only on the basis of samples collected from one mining dump or from isolated outcrops.

The copper mineralisation from the crystalline schists was found in the mining dump of the adit VII. It consist of pyrite, chalcopyrite and magnetite disseminations in hydrothermalized paragneisses. The most conspicuous transformation is the sericitization and the chloritization of biotite.

The copper mineralisation in hornfels was found in the mining dump of the adit I Kiesberg. It occurs as disseminations, rarely as

compact masses, of pyrrhotite, pyrite, chalcopyrite within hornfels altered with biotite and carbonates. Pyrrhotite and pyrite are the main components of the mineralisation. They are associated with chalcopyrite, cobaltite and marcasite. Cobaltite appears as small inclusions in pyrrhotite, whereas marcasite has a tardy veinlet character and replaces the iron monosulfide.

The titanium mineralisation was found in the spring area of the Racilor brook, close to the Oravița tectonic line. It consist of disseminated finely intergrown, ilmenite and rutile, the later being sometimes associated with magnetite. Pyrite is very rare. The titanium minerals often outline altered silicate grains that are partly replaced by neoformation chlorite, sericite, epidote and leucoxene. The host rock is affected by transformations with tourmaline and feldspar. Tourmaline phenocrysts are often broken with a noticeable concentration of titanium minerals in the fractured area (Pl. I, Fig. 3). Taking into account the minerals of the surrounding assemblages, the occurrence of titanium minerals represents the consequence of subsequent transformation that affected the initial rock (mainly transformation with K-feldspar and tourmaline). Thus, the Ti minerals may have formed by the depletion of Ti in the femic minerals (biotite, hornblende), a processes that accompanied the chloritization and the epidotization.

The copper - molybdenum mineralization appears both in breccified garnetiferous skarns and in banatites transformed in skarns or affected by alterations with biotite. Within the later, cross-cutting aplite veins with molybdenite could be identified. The typical paragenesis is: pyrite, chalcopyrite, molybdenite. Chalcopyrite may exhibit sometimes, exsolutions of cubanite. Magnetite is also present, sometimes in skeletal crystals or replacing zoned garnets and ilmenite inclusions in pyrite.

Molybdenite lamellae are rare. Pyrite - the main component of the mineralization - occurs in euhedral cubic or cube-octahedral crystals, of centimetrical sizes. The cubanite exsolutions in chalcopyrite indicate a temperature of approximately 250° C.

The copper - bismuth - tungsten - (gold) mineralization is the most wide-spread in the area. Here, it occupies a large part of the northern slope of Tîlva Mică hill, and a smaller area on the western slope (Fig. 2). The mineralization occurs as centimetrical veinlets in decolored banatites. The metallic minerals are accompanied mainly by calcite, quartz, K-feldspar and sometimes, by relics of garnets and epidote, both partially altered to calcite.

The characteristic mineral assemblage consists of chalcopyrite, bismuth minerals, and subordinately, pyrite, scheelite, cobaltite and glaucodot. The bismuth minerals are represented by: tetradymite, tellurobismutite and native bismuth. Small quantities of gold, tetrahedrite and enargite are present, too.

Mineral description. This section contains a brief description of the metallic minerals forming the copper - bismuth - tungsten - (gold) mineralization.

Chalcopyrite is the main metallic mineral in the veinlets cross-cutting the banatites with superposed skarns and hydrothermal alteration. Spatially, chalcopyrite occurs together with calcite and quartz, including scheelite quartz I and pyrite. In this type of mineralization there are two generations of chalcopyrite. The first generation corresponds to isometric, anhedral grains, newer than quartz I and scheelite. The second generation has a subordinate participation; it is represented by fine borders around tetrahedrite and enargite (Pl. III, Figs. 2 and 3). The two generations of chalcopyrite are separated in time by the deposition of copper sulphosalts.

The copper sulphosalts are represented by tetrahedrite and enargite which are constantly associated with chalcopyrite. They occur as veinlets within chalcopyrite I, as peripheral or as internal patches in the copper-iron sulfide. Compared to the participation of bismuth minerals, the copper sulphosalts are insignificant. The only place where they could be found in some abundance is the mining dump of Emil adit (tetrahedrite and enargite) and 12 Apostles adit (tetrahedrite). Both copper sulphosalts are preceding the bismuth minerals.

The bismuth minerals are, after chalcopyrite, the most wide-spread metallic minerals within the copper - bismuth - tungsten - (gold) mineralization. They are represented by the assemblage: tetradymite - tellurobismutite - native bismuth, sometimes associated with native gold. There are cases when native bismuth is centripetally replaced by tetradymite and tellurobismutite (Pl. II, Fig. 3). The two tellurides are the most frequent bismuth minerals. They are constantly associated with chalcopyrite which they partially replace (Pl. III, Fig. 1). Tetradymite and tellurobismutite are tightly intergrown, the later mineral often forming lamellar, marginal separations within the former. The graphic-myrmekitic intergrowths quoted by Ramdohr (1969) as typical for Oravița zone, are seldom found.

Native bismuth has a subordinate participation in comparison with tetradymite and tellurobismutite, but, judging after their mutual relations, it was the first Bi mineral formed. The most eloquent proof is the centripetal replacement of Native bismuth by tetradymite and tellurobismutite (Pl. II, Fig. 3).

Native gold is constantly found in association with the Bi minerals. In relation to these, native gold has a peripheral position.

The link between native gold and bismuth minerals has been noticed in the case of several tungsten ore deposits from the soviet Far-East (e.g., Vostok - 2), where gold is associat-ed with arsenopyrite, and less with pyrrhotite. The same link has been noticed in the bismuth ore deposits and in the magnetite-bearing skarns in the Kuraminsk Mountains (Chetyrbotskaia et al., 1975). In the Djilău and Tyrniauz ore deposits, gold has a tendency to occur in silicate rocks: silicified granodiorites at Djilau, and amphibolites at Tyrniauz. It thus may be inferred that in the case of tungsten and gold mineralization, the prospects for gold are related to silicate rocks.

Glaucodot and cobaltite are rare. The first mineral occurs as radial aggregates included in chalcopyrite, or as borders around chalcopyrite and tetrahedrite. There are two generations of glaucodot, one included together with cobaltite in chalcopyrite, and another one, younger than chalcopyrite and tetrahedrite (Pl. II, Fig. 2).

Pyrite has a subordinate participation within this mineralization. It occurs as large grains, included by the copper-molybdenum ore. Pyrite precedes glaucodot I and cobaltite.

Scheelite usually occurs with chalcopyrite in the form of veinlets within the banatites. Scheelite was found in samples collected in the mining dumps of adits II and Emil, in Racovița Valley, and of adit 12 Apostles on the western slope of Tîlva Mică hill. The characteristic assemblage include quartz I, K-feldspar, being included or cross-cut by carbonates, quartz II, adularia and chalcopyrite (Pl. II, Fig. 1). Macroscopically, scheelite appears as large grains with a pronounced euhedral character. Observations made with under UV light indicated the concentration of scheelite in the central parts of the veinlets as well as its disperse character within the mineralization.

3. Conclusions

The copper - bismuth - tungsten mineralization is the best represented in the studied perimeter. Its area of spreading has a peripher-

al position in relation with the copper - molybdenum mineralization, both on horizontal and vertical scale. Taking into account the parageneses specific to the two type of mineralization, this behavior is probably the consequence of an evolution in time. Thus, the paragenesis of the copper - molybdenum mineralization is represented by pyrite, molybdenite, chalcopyrite and cubanite, indicating, as mentioned before, a formation temperature of about 250º C.

On the basis of relationship between minerals within the copper - bismuth - tungsten mineralization, one can infer two phases of mineralization. The first phase is represented by the assemblage scheelite, pyrite, cobaltite, glaucodot, tetrahedrite and enargite, whereas the second comprises glaucodot II, chalcopyrite II, Bi minerals and native gold. Quantitatively, the later phase has a subordinate character, only significant through the presence of the Bi-Te minerals (tetradymite and tellurobismutite) and of native gold.

The occurrence of copper sulphosalts in the first phase and of the bismuth minerals in the second one indicates that the copper - bismuth - tungsten mineralization has formed at temperatures inferior to those that characterized the copper - molybdenum mineralization. The post-magmatic transformations accompanying the mineralization, plead for the same idea. In the area occupied by the copper - molybdenum mineralization, skarns are preponderant, whereas in the area of the copper - bismuth - tungsten mineralization, prevail the hydrothermal assemblages. From here, one should not necessarily understand that the former type of mineralization has not a hydrothermal character. In this case, the intensity of the hydrothermal transformations was only weaker, unable to obliterate the effects of initial pyrometasomatic process.

References

Barabanov B.A. (1975) Mineraloghia i geochimia greizenovih obrazovanii mestorozhdenia Vostok II (Primorie), *Min. gheoh. wolf. mest.* Leningrad.

Chetyrbotskaia I., Sahoenok V.V., Smuraeva L. (1975) K zolotnosti wolframy mestorojdenii, *Min. geol. wolf. mest.*, Leningrad.

Cioflica G., Vlad Ş., Iosof V., Panican A. (1976) Scheelite occurences at Băiţa Bihorului, *Rev. Roum. Geol. Geogr. Geoph., Ser. Geol.*, **20/2**.

Constantinescu E. (1976) Tourmaline de la zone de Cioaca Înaltă (SW de Banat), *Rev. Roum. Geol. Geoph. Geogr.,* Ser. Geol., **20-1**, p. 147 - 153.

Constantinof D. (1972) Consideraţii asupra rocilor metamorfice şi eruptive din Banatul de vest (zona Fîrliug - Moldova Nouă), *St. cerc.* **17**, 2.

Cotta V.B. (1865) Erzlagrstatten im Banat und Serbien. W. Braumüller Verl., Wien.

Gheorghiţescu D. (1975) Studiul mineralogic şi geochimic al formaţiunilor de contact termic şi metasomatic de la Oraviţa (Coşoviţa), *D. S. I.G.G.,* **LXI**. (1973-1975).

Koch Al. (1924), Uber der vesuvian und scheelit von Csiklova. *Földt. Kozl.*, **54**.

Phillips W.R. (1963) A differential thermal study of the chlorites. *Min. Mag.*, **33**.

Răileanu Gr., Năstăseanu S., Boldur C. (1963) Date noi asupra limitei tectonice de vest a zonei Reşiţa (Banat), *St. Cerc. Geol.*, **VII**.

Rahden H.V.R., V. Rahden M.J.E. (1972) Some aspects of the identification and characterization of l4 A chlorites. *Minerals Sci. Engng.,* **43**.

Ramdohr P. (1969), The ore minerals and their intergrowths, Pergamon Press.

Plate I
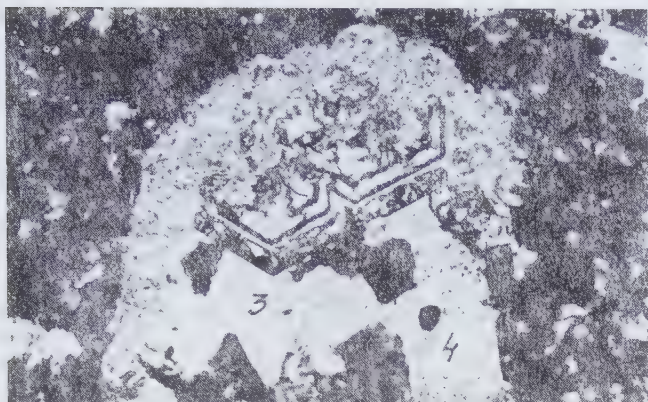
Fig. 1. Garnets replaced by calcite and epidote in adularia-bearing skarns (Racovița Valley, adit III); 1. garnets, 2. epidote, 3. calcite, 4. adularia; N+, 54 X.

Fig. 2. Hydrothermally altered plagioclase feldspar (Racovita Valley, adit III); 1. sericite, 2. chlorite, 3. epidote, 4. quartz; N+, 54 X.
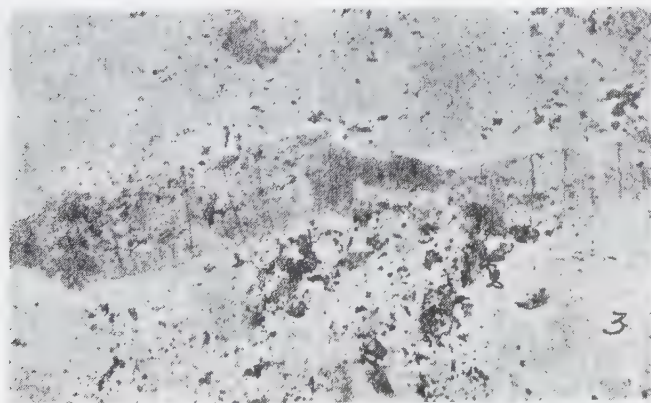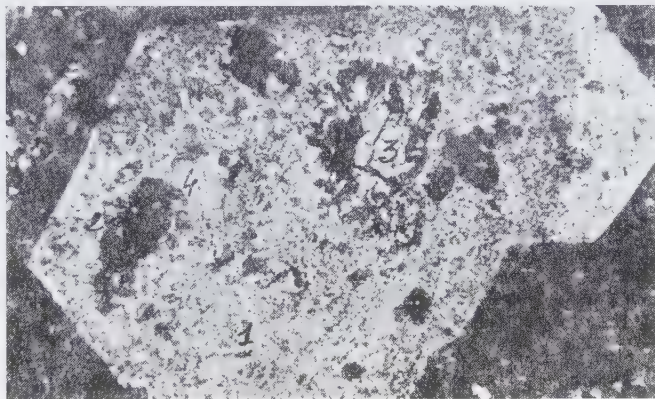
Fig. 3. Fractured tourmaline crystal with Ti-minerals located on the fissures (Tîlva Mică); 1. tourmaline, 2. ilmenorutile and rutile, 3. monoclinic K-feldspar; N II, 54 X.

Plate II
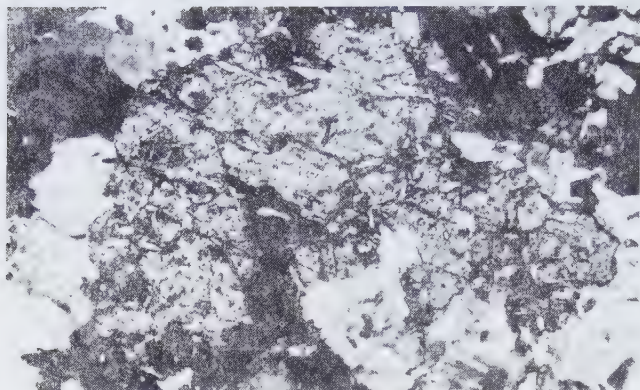
Fig. 1. - Scheelite crystal (1) associated with adularia (2) on fissures in apomagmatic skarns (Racovița Valley, adit II Clementi); N+, 54 X.

Fig. 2. - Cobaltite in chalcopyrite; immersion, NII, 250X.
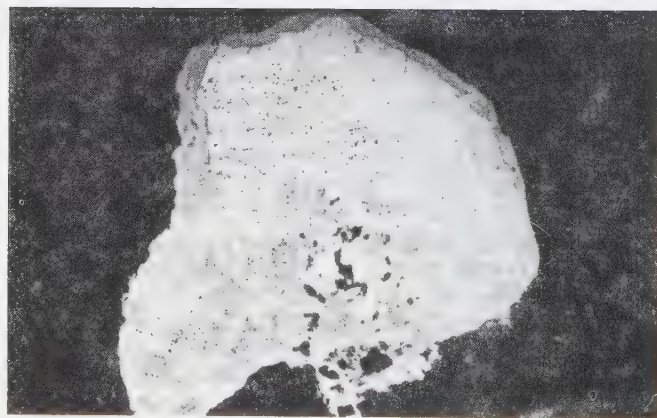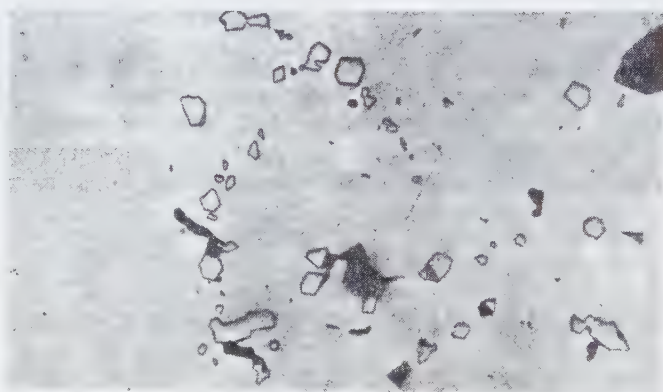
Fig. 3. - Native bismuth replaced by tetradymite (Racovița Valley, adit III); N II, 250 X.

Plate III
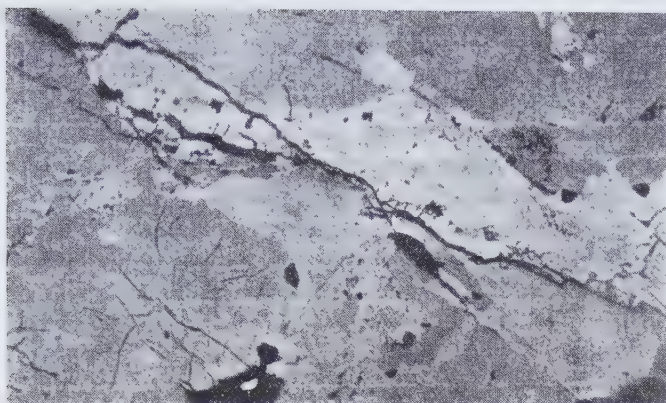
Fig. 1. - Chalcopyrite cross-cut by tetradymite (Racovița Valley, Emil adit); immersion, N II, 160 X.

Fig. 2. - Tetrahedrite bordered by chalcopyrite II (Tîlva Mică, 12 Apostles adit); immersion, NII, 250 X.
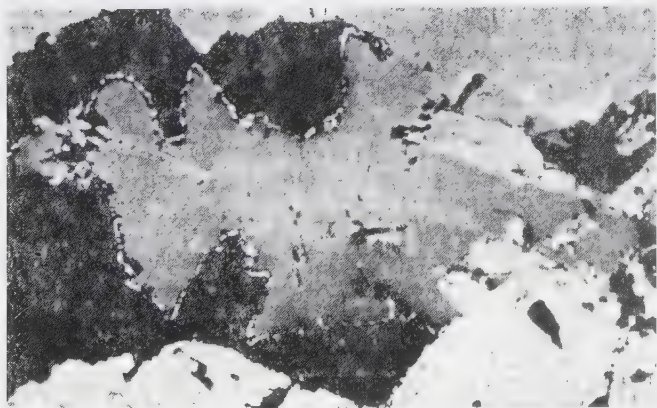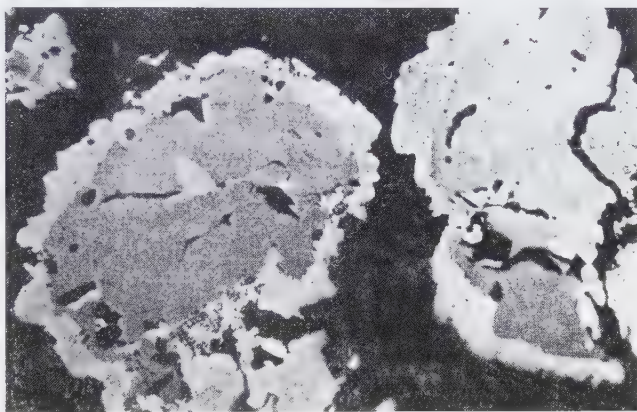
Fig. 3. - Enargite with a seam of chalcopyrite II (Racovița Valley, Emil adit); immersion, N II, 250 X.

Bi - mineral assemblages in copper ore deposits in South-Western Banat (Sasca Montană - Stânăpari- Sasca Română), Romania

EMIL CONSTANTINESCU
GRIGORE ȘIMON

In the Sasca Montană - Stânăpari- Sasca Română area, copper-rich ores located especially in the contact zone between Uper Cretaceous-Eocene magmatites (granodiorites) and carbonate sedimentary formations of Upper Jurasic-Lower Cretaceus age, contain various Bi-minerals. These minerals occur as minute grains frequently included by late chalcopyrite in cupriferous skarns and as individual grains in mineralisation hosted by hornfels and breccia-pipe, in association with base-metal mineralisation.

The following species were identified for the first time in this deposit: bismuthinite, pekoite, krupkaite, aikinite, emplectite, wittichenite, cosalite and kobellite (?).

The deposition of Bi-mineral sequences took place between two important cupriferous stages. Therefore, a strong copper-metaso-matosis affecting the early Bi-minerals may be easily seen especially in mineralisation located in cupriferous skarns and it is represented by replacement products (wittichenite II and emplectite II). The wittichenite I, as primary phase, is related to the main Bi-mineral deposition sequence while the wittichenite II occur as rims around the early emplectite lamellae crystals, when emplectite is included by late chalcopyrite.

Bi-Cu $\pm$ Pb sulphosalts are usually found in cupriferous skarns in association with early and late chalcopyrite, pyrite, tetrahedrite, while Bi-Pb $\pm$ Cu sulphosalts may be seen in mineralisations hosted by hornfels and breccia-pipe in association with pyrite, galena, sphalerite, enargite, bornite, tetrahedrite and lead sulphosalts such as geocronite, boulangerite and jamesonite.

Manganese-bearing minerals association from Răzoare, Preluca massif, Romania.

EMIL CONSTANTINESCU
MONICA PĂLĂȘEANU
SORIN MILUTINOVICI

1. Abstract

The manganese-bearing minerals from Răzoare area (Transylvanian basin) are represented mainly by the oxides and hydroxides group and subordinately by carbonates, phosphates, and silicates. Up to 70 different mineral species were described until now in the manganese-iron ore deposit from Razoare, of which the most recently discovered are sonolite, leucophoenicite and pyrophanite (Hartopanu et al., 1993). In this paper we shall focus our attention at manganese-bearing minerals. A comparison between mineral occurrences from this area and other manganese ore deposits (Iacobeni, the East Carpathians) was carried out, and on these basis, it has been inferred that before Palaeogene the two areas where united in a single and in close relationship with the East Carpathians crystalline schists.

2. Geological setting

The manganese-iron ore deposit at Răzoare is located in Preluca Mountains in the north-western part of the East Carpathians, Romania. The Preluca Massif is one of the seven crystalline islands which separate the Transylvanian Basin from the Pannonic Basin. The crystalline schists in Preluca area are divided in two metamorphic sequences: Răzoare Series (Carelian) and Preluca Series (Baikalian). The first consists of paragneisses and pegmatites followed by crystalline limestones. The Preluca series is transgressive and discordant on the Răzoare Series, which is composed by an alternance of garnet and staurolite bearing micaschists, gneisses with biotite, quartzites, quartzitic schists and black quartzites. The last ones are the host of manganese-iron ores at Răzoare. The upper part of this series is covered by crystalline limestones.

LEGEND:

▨ Quartzitic micaschists

▢ Paragneisses with biotite & staurolite

▧ Black quartzite

▨ Crystalline limestones & dolomites

▨ Pegmatites

▨ Micaschists with garnets

▨ Gneisses with ortoze

⚋ Faults
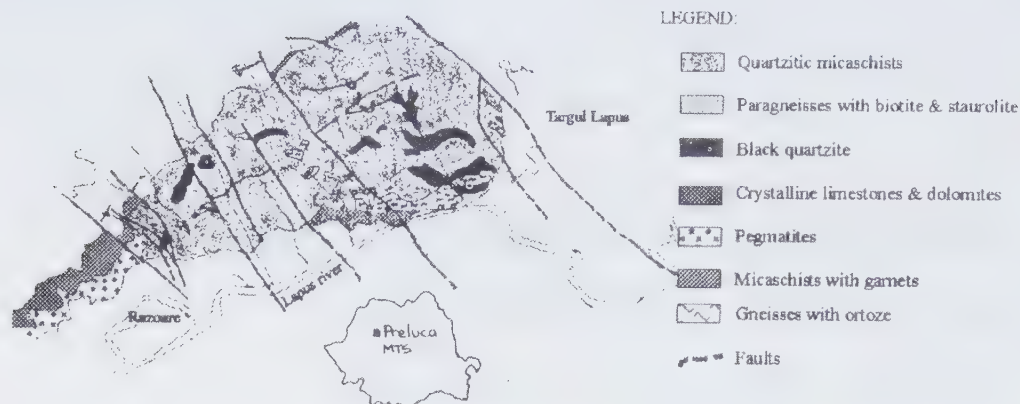
Fig. 1. The simplified geological map of the Răzoare zone.

All these series are covered by a pre-Permian - Cuaternary sedimentary sequences. The synthetic lithostratigraphic column of the Răzoare region is given in Figure 2.

3. Mineralogy

The Mn-bearing minerals from Răzoare belong to oxides and hydroxides, carbonates, phosphates and silicates groups.

3.1. Oxides and hydroxides

Mn-Fe-bearing oxides and hydroxides represent important constituents of the ore deposit. The participation of the primary and the secondary oxides are between 18-24%. Spinels ($Me^{2+}Me2^{3+}O_4$) are the main oxide minerals in the primary mineralization; They are associated with $Me_2^{3+}O_3$ oxides. The secondary Mn-Fe oxides and hydroxides are formed in the upper part of the ore deposit as a consequence of weathering of the primary mineralization.

The primary oxides show either idiomorphic grains dispersed in the carbonatic or silicatic matrix, or xenomorphic grains intimately

1 - paragneisses &micashists; 2 - quartzites, 3- rhodochrosite with jacobsite dissemination, lacking at the footwall (3a), 4 - Mn-fayalite-rich lenses &pods; 5 - tephroite+Mn-humites 6 - dannemorite, 7- magnetite ± pyrrhotite
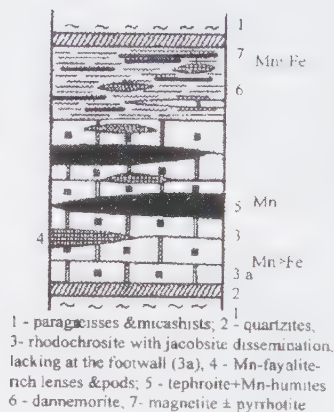
Fig. 2. The lithostratigraphic column of Răzoare (Hârtopanu et al., 1993).

intergrown with carbonatic or silicatic minerals. Jacobsite, Fe-jacobsite, hausmanite, Fe-franklinite from the spinel group, braunite and bixbyite from the $Me_2^{3+}O_3$ group are the main Mn-bearing oxides.

Secondary Mn-oxides and hydroxides occur as pellicules, veinlets or earthy masses, developed on the primary mineralization. By means of microscopic, thermal and X-rays analyses the following Mn-minerals were identified:

Fig. 3. Replacement of rhodochrosite by psilomelane.

psilomelane, pyrolusite, brostenite, wad, nsutite and criptomelane (Figure 3).

Brostenite was defined for the first time by Poni in 1900 in a sample from Broşteni, East Carpathians, Romania. Later on, the name was given for a variety of mixtures dominated either by pyrolusite (Palache et al., 1961) or by chalcophanite (Embrey, Fuller, 1980) or consisting of birnessite, todorokite and γ-MnO_2 (Perseil, 1973).

3.2. Carbonates

Minerals from this group may reach up to 28 % of the mineralization volume. Three generations of carbonates were identified, one primary and the other two secondary.

The primary Mn-carbonates described in Răzoare are rhodochrosite, kutnahorite and manganocalcite with the former as the prevailing mineral. A younger rhodochrosite has also been observed. Rhodochrosite from Răzoare has low contents of Fe, Mg and Ca.

DTA and X-ray analyses pointed out secondary Mn-carbonates formed on the expense of the primary minerals. These are Fe-rich oligonite and ponite, a Fe-bearing rhodochrosite. Ponite has the type locality Broşteni, Romania. It has a rather narrow compositional field, i.e. $CaCo_3$ (0 - 15), $FeCo_3$ (3.3 - 30), (0 - 15) and $MnCO_3$ (70 - 90) (values in mole percents). However, following the IMA recommendation, no names should be given to intermediate members of solid solution series.

3.3. Phosphates

Pop (1976) recognized by X-ray analyses Mn-apatite and carbonate-apatite and volfeite which has not been confirmed by later analyses. Generally, apatite develops isometric grains randomly distributed within the silicatic or carbonatic gangue.

3.4. Silicates

Minerals of this group are represented by olivines, Mn-bearing humites, garnets, innosilicates and phyllosilicates.
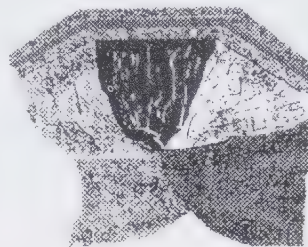
Fig. 4. Optical anomalies in spessartite (drawing after thin section).

3.4.1. Nesosilicates

Olivine series is most frequently represented by intermediary terms of the Mn-Fe solid solutions such as tephroite and knebellite.

Knebellite forms coarse to medium grained aggregates intimately intergrown with dannemorite, apatite or spessartite.

Tephroite occurs in granular aggregates included in pyroxenes and carbonates. Tephroite forms peculiar assemblages with Mn-bearing humites, with which it forms bands or lenses up to 1,5 m thick, especially within the lower, carbonate-rich part of the ore sequence (Hartopanu et al., 1993). The intergrowths between tephroite and Mn-bearing

Table 1. The mineralogical composition of two Mn-bearing ore deposits from the East Carpathians, Romania

GROUP	MINERALS		RĂZOARE	IACOBENI
OXIDES AND HYDROXIDES	PRIMARY	jacobsite	♦	♦
		Fe-jacobsite	♦	♦
		hausmanite	♦	♦
		Fe-franklinite	♦	♦
		braunite	♦	♦
		bixbyite	♦	♦
		banganite		♦
	SECONDARY	psilomelane	♦	♦
		pyrolusite	♦	♦
		brostenite	♦	♦
		wad	♦	♦
		nsutite	♦	♦
		criptomelane	♦	♦
CARBONATES	PRIMARY	rhodochrosite	♦	♦
		kutnohorite	♦	♦
		manganocalcite	♦	♦
	SECONDARY	oligonite	♦	♦
		ponite	♦	♦
PHOSPHATES	Mn - apatite		♦	♦
	Carbonate - apatite		♦	♦
	volfeite		♦	♦
SILICATES	NESOSILICATES	tephroite	♦	♦
		knebellite	♦	♦
		alleghanyite	♦	♦
		leucophoenicite	♦	♦
		sonolite	♦	♦
		spessartite	♦	♦
	INNOSILICATES	rhodonite	♦	♦
		bustamite	♦	♦
		pyroxmangite	♦	♦
		Mn-egirine-augite		♦
		Mn-riebekite		♦
		Mn-antophyllite		♦
		dannemorite	♦	♦
	PHYLLOSILICATES	bementite	♦	♦
		Mn-chlorite	♦	♦
		hissingerite	♦	♦
		melanolite	♦	♦
		pennantite	♦	♦
		neotokite	♦	♦

humite is very tight. Intergrowth of tephroite with carbonate fluorapatite may also occur.

Mn-bearing humites. Until 1991 only the mentioning of alleghanyite indicated the possible occurrence of the Mn-bearing humites at Răzoare. A comprehensive research in this field has been carried out by Hârtopanu et. al. (1993). The following sequence of Mn-bearing humites has been described: alleghanyite-leucophoenicite-sonolite suggesting their formation on the expense of tephroite.

Garnets. The Mn-bearing garnets are represented by spessartite, which is a typical mineral for the mineralization, but also for the host formation, the micaschists. Generally, garnets are isotropic, excepted the coarser grains from Sunătorii Valley. In thin sections, the garnet has a central core with radial structure with numerous quartz inclusions and secondary Mn-chlorite mantled by an alternance of isotrop large garnet ribbons with anisotropic thin garnet ribbons. This phenomenon was firstly pointed out in the pyralspites from Răzoare region. We can distinguish two major type of optic anomalies: 1. ribbon anomalies; 2. sectorial anomalies (Figure 4.)

The optical anomalies of garnets are due to lattice disequillibria linked to cations substitution (primary anisotropy) and to lattice dislocations caused by cooling stress (Constantinescu, 1986).

The garnets show frequent alterations to secondary manganese minerals such as Mn-chlorite or carbonates.

3.4.2. Innosilicates

The Mn-bearing pyroxenoids identified in Răzoare mineralization are rhodonite, bustamite and pyroxmangite. They form compact masses, in association with amphiboles, or irregular aggregates and ribbons in carbonatic rocks.
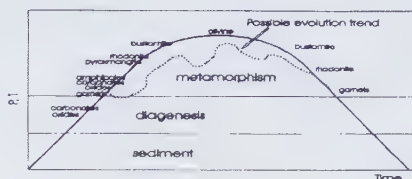
Fig. 5. The possible evolution of the manganese minerals with temperature and pressure

Rhodonite includes or corrodes bustamite and. Sometimes, rhodonite occurs as relics into knebellite grains of newer generation.

Bustamite has a limited development in Răzoare mineralization, where occurs among ribbons of amphiboles, apatite and garnets.

Pyroxmangite is generally prismatic coarser grained crystals usually include xenomorphic grains of knebellite or needle-like crystals of amphiboles and apatite.

The main amphibole in Răzoare mineralization is dannemorite. The mineral has a wide and irregular spreading in mineralization. Sometimes it formes monomineral zones or being in association with knebellite and pyroxmangite. Generally dannemorite is polysynthetically twinned after (100) and shows different stages of alteration to complete replacement by carbonates or chlorites.

3.4.3. Phyllosilicates

Bementite, Mn-bearing chlorite, hissingerite, melanolite, pennantite and neotokite (an amorphous variety of bementite) represent the Mn-bearing phyllosilicates. These minerals are formed on the expense of tephroite, knebellite, spessartite and dannemorite.

4. Genetic considerations

The Răzoare ore deposit is considered of a metamorphic sedimentary origin. The initial
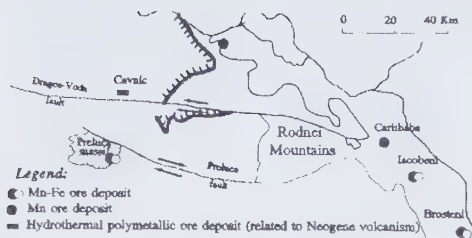
Fig. 6. The movement of Preluca massif along the Preluca Fault during Paleogene (Popescu, 1978).

rocks consisted of silica bearing sediments with high content of manganese hydroxides which have been transformed under a medium grade metamorphism. The present mineralogic composition suggests a polymetamorphic evolution with two or tree generations of each primary mineral (Figure 5).

Together with Răzoare ore deposit other manganese mineralizations in the East Carpathians, form a N-S oriented alignment. These are directly associated with black quartzites similar to those in Preluca area. Their mineralogy is similar to the ore described (see Table 1), and it is necessary to be taken into account in a genetic model. Starting from these considerations and from the geophysical knowledge about the presence

of two crustal faults in the northern part of Transylvanian Basin, Popescu (1976) considered the idea of the two occurences beeing genetically linked. In this hypothesis the Preluca massif moved along the Preluca crustal fault until it reached its actual location during Palaeogene and before this event the massif was a part of the East Carpathians crystalline (Figure 6).

Selected References

Bălan M. (1976) Mineralogia zăcămintelor manganifere de la Iacobeni. Edit. Acad. Române, 123p., Bucureşti.

Constantinescu E. (1986) Mn-bearing minerals from Răzoare, Romania. Communication presented in the Scientific Session of Bucharest University.

Hârtopanu P., Udubaşa G., Udrescu C., Cristea C. (1993) Mineralogy of the Fe-Mn Ore Deposit at Răzoare, Preluca Mts. I. Tephroite and Manganese-bearing Humites. *Romanian Journal of Mineralogy,* **76**, 15–22.

Popescu C. Gh. (1978) Metallogeny of Manganiferous Ore Deposits in the East Carpathians and the Preluca Massif. A Plate Tectonics Attempt. *Rev. Roum. Geol. Geophys. et Geogr.,* **22**, 129-134.

IV. MINERAL TEXTURES

Metasomatic origin of some micrographic intergrowths

MARIN ŞECLĂMAN
EMIL CONSTANTINESCU

Some micrographic intergrowths in a small pegmatite dike from Sebeş Mountains and in alkali granites from Banat Province have formed by replacement of feldspar or other minerals by quartz. The main textural features of these intergrowths are: 1) The graphic quartz is skeletal, and the same skeletal quartz is sometimes included in two or more crystal hosts; 2) Occasionally the feldspar host is obviously deformed, whereas intergrown graphic quartz is nondeformed; 3) Some graphic quartz tends to develop along interfaces between feldspar or other mineral crystals, as well as along clevage planes, fractures, slips and deformation bands of its feldspar host.

Introduction

According to Fersman (1952), Vogt (1928), and many others, graphic texture is a result of simultaneous crystallization of feldspar and quartz. On the contrary, Schaller (1926), Wahlstrom (1939) and Drescher-Kaden (1948), among others, believe that this texture can be formed by replacement of feldspar by quartz or vice-versa. In his recent treatise on migmatites and the origin of granitic rocks, Mehnert (1968, p. 194-199) has critically examined the two points of view on the origin of graphic textures and came to the conclusion that a simultaneous crystallization of quartz and feldspar seems to be the most probable assumption. However, in some cases, the textural features of graphic intergrowth undoubtedly show a metasomatic development of graphic quartz. In order to emphasize these features two examples are presented here.

Sebeş Mountains

In the northern part of the Sebeş Mountains (Southern Carpathians Romania) there are a few small granitic bodies of uncertain age. In one of these bodies, on the Sibişel Valley, there is a small pegmatite dike (about 3m thick) formed of microcline, quartz, acid plagioclase (6-8% An), a little muscovite, and partially or totally chloritized biotite. The microcline and coexistent plagioclase occur either as pure crystals or in mutual perthitic intergrowths. The quartz also occurs either as "free" grains or in micrographic intergrowth with micro-

cline, plagioclase, and even with muscovite or biotite. In the central part of the pegmatitic dike, where granulation is coarser, the graphic quartz is well developed, but near the walls, where there is a fine grained zone, it appears seldom appears. In this external zone a lot of quartz and feldspar crystals have anomalous extinctions, fractures and other deformation features indicating that the fine granulation of the external zone at least partly is due to shearing movements localized near the walls. Between the external and central zones there is a transition, with intermediate granulation, where a large part of the graphic intergrowths are broken and even completely destroyed. It is suggested, therefore, that the graphic intergrowth in the external zone has probably been destroyed by shearing movements.

In the graphic intergrowth, quartz usually occurs as "inclusions" in feldspar, similar in aspect with the so-called "ichtyoglipts", "hieroglyphs", or "rods" described by Fersman (1952), Wahlstrom (1939), and others. The quartz inclusions generally look in thin section as if they were isolated, but many of them have the optical axes directed in the same way as shown by simultaneous extinction. This common optical orientation may be accounted for differently depending on the interpretation of the relations between inclusions. If we consider that they are actually isolated, the common optical orientation might be explained only by admitting that all the quartz inclusions have the same reticular orientation into the host feldspar, as assumed by Fersman. On the contrary, if we consider that quartz inclusions are only apparently isolated, due to the so-called "cut-effect", then all inclusions with the same optical orientation should be interpreted as parts of the same skeletal crystal. Fersman rejects the possibility of connection between quartz inclusion ("icthyoglipts"), noting that when feldspar of macrographic samples is altered, the detached quartz has no skeletal shape. However, Simpson (1962), has demonstrated the skeletal nature of his graphic quartz by series sectioning.

In the above-mentioned pegmatite dike, the reticular connection of graphic quartz inclusions is sometimes obvious even in thin section (Fig. 1A). In many cases, however, the connection between inclusions is not obvious, but it can nevertheless be easily deduced. For instance, the quartz inclusions with the same optical orientation in Fig. 1B and 1C, are included in several hosts differently oriented, indicating that graphic quartz does not display any reticular orientation with respect to its host. In this case, the common optical orientation of quartz inclusions undoubtedly shows their reticular connection.

It is significant that feldspar from graphic texture often shows obvious signs of deformation, e.g., changes of the clevage directions, fractures, or even deformation bands resembling to a certain extent those noticed by Siefert (1965). However, the intergrown graphic quartz has most often almost a perfect uniform extinction, showing that it is not deformed (Fig. 1D). This absence of quartz deformation in contrast with that of intergrown feldspar might be accounted for by three assumptions:

1. The present state of intergrowths is a consequence of a selective deformation. For instance, it might be assumed that under a relatively slight mechanical strain only the feldspar has been deformed while the intergrown graphic quartz has not been deformed. This explanation seems unlikely, because skeletal quartz is much more easily destroyed than its host feldspar, a fact which has been noticed by one of the present authors (Şeclăman, 1971), in the case of macrographic intergrowths from some pegmatite bodies. Şeclăman noticed that skeletal crystals of graphic quartz are broken even in the cases when intergrowths feldspar deforms only plastically. Plastic deformation of feldspar is frequently materialized only as translations along cleavage planes which do not disturb very much its optical and reticular continuity, whereas intergrown gràphic quartz is so much destroyed

that instead of a single quartz rod, optically continuous, there result tens or hundreds of crystal fragments with different optical orientation. This mechanical disturbance of the optical continuity of graphic quartz might explain the fact that sometimes in one and the same quartz rod many quartz crystals are differently oriented (Wahlstrom, 1939; Simpson, 1962).

2. The present state of the intergrowth is the result of two consecutive processes: a) a deformation of both feldspar and intergrown quartz; b) a later recrystallization exclusively of the graphic quartz. As a consequence of this selective recrystallization, the graphic quartz lost its deformation state while feldspar, which was not recrystallized, remained with its previously deformed appearance. However, it is difficult to explain why the quartz recrystallized skeletally and not as ordinary grains. Also exclusive recrystallization requires some spatial redistribution not only of quartz, but even of the intergrown feldspar, and therefore recrystallization of graphic feldspar itself.

3. The graphic quartz developed subsequently by partial replacement of the previous deformed feldspar.

This last hypothesis is the only one to fit with the textural peliculiarites of the graphic intergrowths described above, namely: a) The tendency of graphic quartz to develop along the fractures of the feldspar host (Fig. 1D); b) The development of the same skeletal crystal of graphic quartz in two or several adjacent feldspar or other mineral crystals (Fig. 1B and 1C), as well as the tendency of graphic quartz to develop along some interfaces between different feldspar crystals, a fact that also has been noticed. It is practically impossible to account for these peliculiarites by simultaneous crystallization of graphic quartz and its host. From the metasomatic point of view, however, all these textural features can be explained adequately, because the same quartz crystal could grow by replacement along interfaces or along various fractures and "weakness zones" in one or several neighbouring minerals.

Banat Province

In Banat Province[1] there are many rocks with well-developed micrographic textures. Usually, these rocks are granodioritic but sometimes they can be even alkali granites devoid of plagioclase. These alkali granites occur in the proximity of Sasca Montană (Banat, România), and they are made up mainly of alkali feldspar with perthitic texture and quartz. Quartz occurs usually in micrographic intergrowth with pertithe crystals and only seldom as isolated crustals. In micrographic intergrowth the quartz inclusions with the same optical orientation are often included in hosts with different orientations showing that the graphic quartz is here also skeletal.

At first sight, this micrographic intergrowth (Fig. 2A) shows a resemblance to the products of artificial eutectic crystallization and thus it might lead to the belief that the intergrowth was due to simultaneous crystallization of alkali feldspar and quartz. As Fig. 2A shows, the alkali feldspar is not entirely intergrown with quartz. Some idiomorphic feldspar "phenocrysts" are surrounded by micrographic groundmass. Usually, these "phenocrysts" are interpreted as a previously developed stage of feldspar thet grew alone and free in a homogeneous melt, while intergrown feldspar represents a later generation corresponding to the simultaneous crystallization of feldspar and quartz. A careful examination, however, reveals that these feldspar "phenocrysts" are not genuine phenocrysts like those in igneous rocks of porphyritic texture. For instance, the detail of Fig. 2B reveals that "phenocrysts" I and II are parts of a bigger alkali feldspar crystal that is non-uniformly deformed. In this big

---

[1] Banat Province includes all intrusive and effusive rocks of Senonian-Lower Eocene age of Western Romania, associated with Laramide tectogenesis.

crystal there are some parallel deformation bands, and in many deformation bands there exist numerous inclusions of graphic quartz. The relatively underformed portions between the bands do not contain graphic quartz, and they represent the very "idiomorphic phenocrysts" mentioned above. Further, in some portions all quartz inclusions have a perfect optical continuity, pointing out that graphic deformation bands and curved cleavage planes. The relative absence of deformation of graphic quartz as well as its tendency to develop along deformation bands of feldspar substantiate the subsequent and metasomatic development of graphic quartz. Therefore, those "phenocrysts" should be interpreted as non corroded relics of bigger feldspar crystal, and not as growth during a previous generation of feldspar.

Some of these relics resembling authentic phenocrysts from volcanic rocks are shown in Fig. 2C and 2D. They are sectioned perpendicularly to the "a" axis of feldspar and their plane edges are parallel to the cleavages. Most quartz inclusions appear like "rods" elongated both parallel to cleavages (Fig. 2C) and obliquely (Fig. 2D). At first sight, the impression is of a radial distribution of graphic quartz around the "phenocryst".

Uspenski (1943) and others deduce from such a distribution that graphic quartz develops along directions of feldspar growth. However, these idiomorphic "phenocrysts" are relics and not growth centers of feldspar. In this case the distribution of quartz rods is a consequence of selective replacement of feldspar by quartz along some "weakness zones" which occurred in feldspar crystals during their deformation. These "weakness zones" are sometimes the very cleavage planes (Fig. 2C), but in other cases they correspond to some glides oblique to cleavages (Fig. 2D).

In short, the textural peculiarities of the above described quartz-feldspar intergrowths, may be satisfactorily explained only if we admit

two consecutive stages in their genesis. The first was a non-homogeneous deformation of pre-existent feldspar crystals which were not yet intergrown with quartz. The non-homogeneous character of deformation consists in the fact that some of the portions of feldspar crystals, of regular or irregular shapes, have been less affected by deformation, while others have been the site of development of reticular fractures, slips, and deformation bands, representing "weakness" or reticularly labilized zones. The second stage is a selective replacement of feldspar by quartz along "weakness zones". As a result, the quartz takes a complicated shape, imposed by the shape of "weakness zones". Skeletal quartz is thus generated.

References

Descher-Kaden, F.K. (1948) Die Feldspat-Quartz-Reaktionsgefuge der Granite und Gneisse und ihre genetische Bedeutung. Springer, Berlin;

Fersman, A.E. (1952) The graphic texture of pegmatites and its causes. In *Izbranie Trudi*, **vol. I**, Moskva, 37-50 (in Russian);

Mehnert, K. R. (1968) Migmatites and the Origin of Granitic rocks. Elsevier Publishing Company. Amsterdam - London - New York;

Shaller, W. T. (1926) Mineral replacement in pegmatites. *Amer. Mineral.,* **12**, 59-63;

Seifert, K. E. (1965) Deformation bands in albite. *Amer Mineral.* **50**, 1469-1472;

Simpson, D.R. (1962) Graphic granite from the Ramona pegmatite district, California. *Amer. Mineral.* **47**, 1123-1138;

Şeclăman, M. (1971), On graphic texture. *Studii Cercetări Geol. Acad. R.S.R.,* **16**, 133-146 (in Romanian);

Uspensky, N.M. (1943) On the genesis of granitic pegmatites. *Amer. Mineral.* **29**, 437-447;

Vogt, J. H. L. (1928), On the graphic granite. *Norske Videnskapsels., Forth.* **1**, 67;

Wahlstrom, E.E. (1939), Graphic granite. *Amer Mineral.* **24**, 681-698.
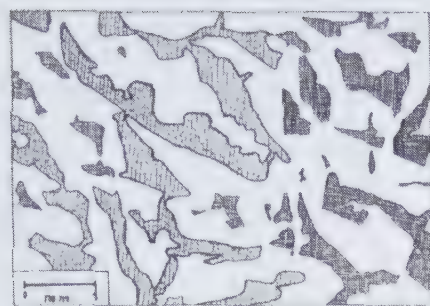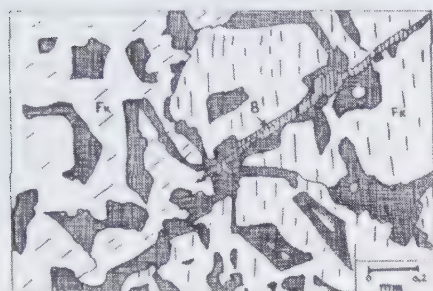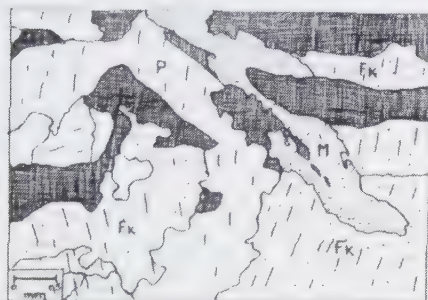
Fig. 1. Micrographic intergrowths from pegmatitic dike (Sibişel Valley), Q = quartz; Fk = K-feldspar; P = plagioclase; B = biotite; M = muscovite. (A) Quartz-microcline intergrowth in a thin section of about 0.05 mm thickness. Note the connection between dotted "hieroglyphs" and skeletal feature of graphic quartz. All quartz inclusions in the figure were connected when the thin section was about 0.1 mm thick. Crossed polars. (B) Alkali feldspar-quartz intergrowth. All quartz inclusions have the same optical orientation, although their hosts are differently oriented. Crossed polars. (C) The graphic quartz rods (black), which have the same optical orientation, are included not only in microcline, but even in plagioclase and muscovite. Crossed polars. (D) Plagioclase-quartz intergrowth . The plagioclase is obviously deformed, while the intergrown quartz is not deformed. Note the tendency of graphic quartz to develop along some fractures in plagioclase host. Crossed polars.

(a)
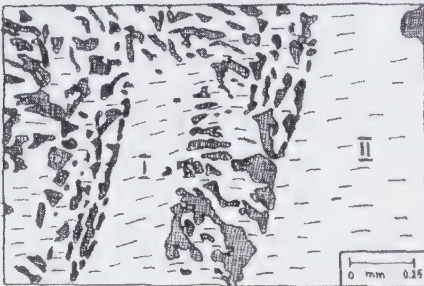
(b)
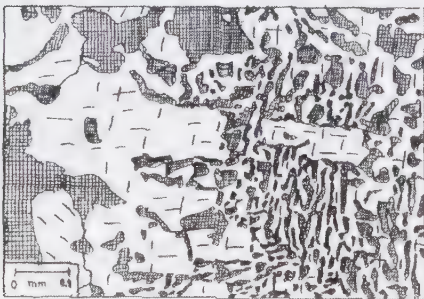
(c)
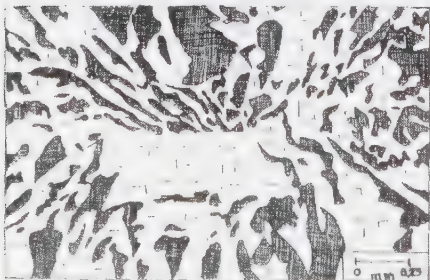
(d)

Fig. 2. Micrographic intergrowths from alkali granite (Sasca Montană). (A) Alkali feldspar-quartz intergrowth. Note the idiomorphic "phenocrysts" af alkali-feldspar surrounded by micrographic intergrowth. The graphic quartz inclusions have the same optical orientation, although their hosts are differently oriented. Crossed polars. (B) Detail within fig. 2A. Note the deformation bands in feldspar crystal. The graphic quartz has developed metasomatically in deformation bands. Some relatively undeformed portions between bands (I and II) have not been replaced by quartz, and they have remainded as relics, representing the very "idiomorphic phenocrysts". Crossed polars. (C) False idiomorphic feldspar phenocrysts surrounded br micrographic intergrowth. The "phenocrysts" and intergrown feldspar belong to the same alkali-feldspar crystal, but nonuniformly deformed. The ""phenocrysts" represents the less deformed parts of feldspar crystals, whereas the intergrown feldspar represents the relatively deformed parts that have been subjected to a selective replacement by quartz along clevage planes. The alkali-feldspar is sectioned nearly parallel to (100). Crosed polars. (D) false idiomorphic feldspar phenocryst surrounded by micrographic intergrowth. The feldspar within graphic texture is not an overgrowth on "phenocryst", but a more deformed part of a bigger and previous feldspar crystal which has been selectively replaced by quartz along fractures and slips oblique to clevages. The alkali feldspar is sectioned nearly parallel to (100). Crossed polars.

Some features of ore fabric, Sasca Montană skarn deposit, Romania

EMIL CONSTANTINESCU
GHEORGHE UDUBAŞA

1. Introduction

The Sasca Montană skarn deposit, Banat, West Romania, belongs to the Laramian metallogeny and exhibits copper-rich ore assemblages. It was already known and mined as von Cotta was writing his book on the ore deposit visited in Banat and Serbia (1864).

The most striking feature of this ore deposit is the lack of any zoning both of the skarn and ore mineral assemblage (Constantinescu 1971, 1981). Some new observational data concerning the ore fabric are here presented. Most of the ore minerals form non-equilibrium assemblages. The occurrence of idaite in Romania is reported for the first with this paper.

2. Ore Mineralogy

About 25 ore- and more than 70 non-metallic minerals have been described to the present from the Sasca Montană ore deposit (Constantinescu, 1981). The copper and iron ore minerals i.e., chalcopyrite, pyrite, chalcocite, bornite, digenite and idaite are the most common. Some sulphosalts such jamesonite and boulangerite appear only in places as well enargite, linnaeite - siegenite, and the near-end members of the fahlore group. Magnetite and molybdenite were observed both within the porphyry-type ore concentrations locally developed in the granodioritic rocks and the skarn bodies. Pyrrhotite and arsenopyrite occur also but only as microscopic constituents of the ore. Fine veinlets and pockets containing sphalerite (iron-poor) and galena appear in places mostly within the recrystallized limestones. The ores hosted by skarns sometimes contain specular hematite. Covellite, cuprite, tenorite, native copper, crhysocolla and aurichalcite occur in the oxidised ores which contain also typically developed anatase grains. A mineral variety of smithsonite, szaszkaite, was also described at Sasca Montană (Cădere, 1925).

3. Ore Fabric

Exsolution textures are widespread, especially of chalcopyrite in bornite, sphalerite in chalcopyrite, and chalcocite in bornite, sphalerite in chalcopyrite, and chalcocite in bornite, well-documented by Superceanu (1969),

Constantinescu (1981), and in the Card Index of Ore Photomicrographs (Maucher and Ramdohr 1962). The high - temperature ore deposition indicated such textures correlates well with the association of these exsolution-rich mineral phases with the skarn assemblages.

Substitution textures are often found and their apparition is mainly related to the polyascendent development of the postmagmatic mineral formation. Zoned garnet crystals show beautiful replacements by magnetite with zoning preservation (Fig. 1). Mention should also be made particularly of the lamellar intergrowths of chalcopyrite (cp) and quartz (Fig. 2). The occasional presence of bornite residuals together with the quartz matrix (Fig. 3) is indicative of a preferential substitution of bornite by quartz under preservation of the cp laths.
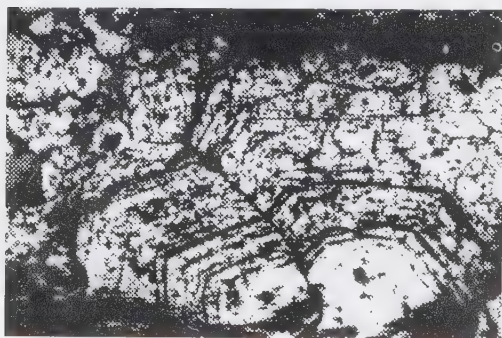
Fig. 1. Zonal replacement of garnet by magnetite. Reflected polarized light (RPL), x10.
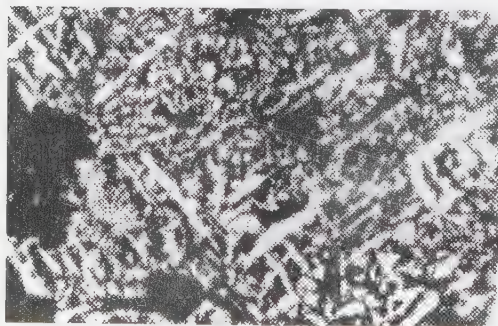
Fig. 2. Lamelar intergrowths of chalcopyrite (white) with quartz (black), RPL, oil immersion, x500.

Intimate intergrowths of enargite-sphalerite, tetrahedrite-cp and cp-chalcocite (cc) develop sometimes myrmekitically; their mode of formation is, however, very different. The rarely observed myrmekites enargite-sphalerite must probably be regarded as products of a simultaneous crystallisation. The very fine intergrowths of cp-fahlore (Fig. 4) probably followed the same way of formation. They are similar in appearance to those mention by Ramdohr (1945, Fig. 17; 1969, Fig. 87). Supergene reworking of bornite may perhaps be invoked in the case of such intergrowths where cp and fahlore irregular aggregates, partly botryoidal in appearance (Fig. 5).

The so-called "disease-cracks" within the monomineralic masses of bornite are related to the development of idaite, locally accompanied by cp and cc during low-temperature decomposition of the primary bornite (Fig. 6). The most frequently observed aspects may perhaps be related to Tufar's (1967) "Vorstufe" (intermediate step) of bornite transformation into idaite.

Incipient alteration of linnaeite-siegenite is a very complex one and commences gradually along the cleavages. Secondary pyrite also forms in places along the cleavages of linnaeite (Fig. 7). The end -product of such a transformation is an aggregate of linnaeite grains cemented by cp and bornite (bn). Ramdohr (1945) suggests that the myrmekitic intergrowths of linn+cp+bravoite could represent the breakdown product of the mineral villamaninite. Sporadically occurring millerite lamellae within these intergrowths at Sasca Montană show that the variant of this interpretation may also be accepted for the Sasca ores.

The globular aggregates or apparent single grains of pyrite form a striking feature of the Sasca Montană copper ores (Fig. 8-11). Rounded aggregates of microgranular pyrite are always enclosed in a matrix of cp and bn. Sometimes atoll-textured or shell-like pyrite

Fig. 3. A,B. Chalcopyrite laths develop both in quartz (q) and in bornite (bn). In **B** bornite is completely replaced by quartz. Scale bars are 0.01 mm.

Fig. 6. "Disease-crack" in bornite (dark grey) with incipient formation of idaite (light grey) and minor chalcopyrite and chalcocite (lighter than idaite). RPL, oil immersion, x200.
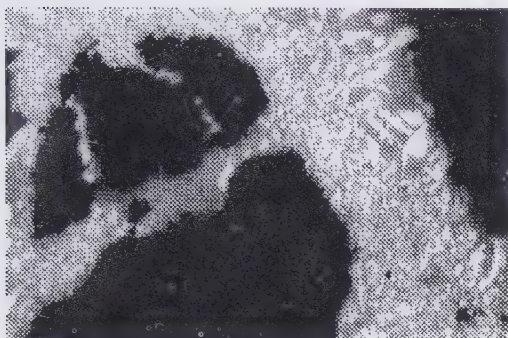
Fig. 4. Myrmekites of chalcopyrite (white) and fahlore (grey). RPL, oil immersion, x400.
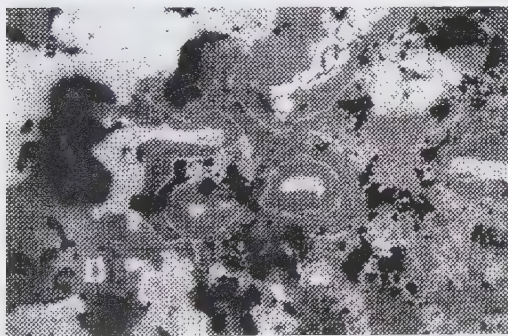
Fig. 5. Intergrowth of chalcopyrite (white) with fahlore (grey). Black — gangue minerals. RPL, oil immersion, x200.
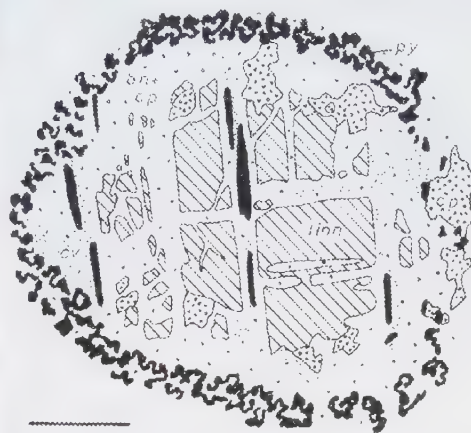
Fig. 7. Transformation of a linnaeite-siegenite grain (linn) into a fine-grained aggregate of cp+bn which bears locally irregular masses of chalcopyrite. Pyrite (py) forms both onto linnaeite cleavage and around the linn grain. Irregular patches of covellite (cv) appear within the bn+cp. Scale bar is 0.15 mm.

grains occur and they have nothing to do with the "mineralised bacteria" as Superceanu (1969) states. Such globular pyrites seem to be descendent in nature but their mode of formation is still not understood. Betechtin et al. (1958) and Vujanovic (1974) described similar forms of the pyrite aggregates occurring in a cp-rich matrix and consider their formation to be of colloidal nature under conditions of volcano-sedimentary ore deposition (Vujanovic, 1974).

Irrespective of whether the pyrite globules are of volcano-sedimentary origin or whether they formed by supergene reworking of some copper-rich pyrite-bearing assemblages the rounded form with varying size (0.1 - 0.5 mm) remains to be explained. As in the case of the

Fig. 8 A-C. Globular pyrite "grains" consisting of very fine pyrite micrograins (py) associated with secondary copper minerals. Inside the pyrite aggregate there is a mixture of bn+cp sometimes developed in flower-like pattern (**A**). Alternating bands of pyrite and bn with a nucleus of secondary copper minerals (sm) (**B**). Simple atoll- or shell-like pyrite grains in cp. Scale bar is 0.5 mm.

"Rogenpyrit" and of the framboidal pyrite the nearly spherical form may be regarded as an equilibrium one. It is, however, worth mentioning that the pyrite of the Sasca Montană ores usually transforms into microgranular aggregates by means of "coating" replacement by cp (Fig. 12). This fact points out that the globular form is here related to destroying mechanism of the early-formed pyrite grains (by an opposite mechanism of the crystal growth) rather than to a coalescent growth of pyrite micrograins. Reliable evidence of mode of formation could not be obtained, despite its abundance in the copper ores in the Sasca deposit. The prevalence the copper in the ores generally seems to indicate instability of the early- or even simultaneously formed pyrite grains in the copper-rich environment. At Jiulesti- Valea Fagului deposit, Apuseni Mountains, Romania, the pyrite occurs subordinately within the copper ores and forms scattered grains either in cp or bn (Udubaşa et al., 1981). In other copper-rich ores, e.g. Vorţa, Metaliferi Mountains, Ilba and Băiuţ, Maramureş, Romania, occasionally occurring globular pyrite is always confined to the presence of the bornite. Therefore bn seems to induce the instabilisation of pyrite. It is likely that such "unstable" pyrites represent in fact

decomposing products of the high-temperature solid solution series FeS_2-CuS_2 (Shimazaki 1969). The low-temperature breakdown of this solid solution results in the formation of a metastable copper-bearing pyrite, perhaps also Ad-baring (tennantite is locally present). Its further alteration leads to the apparition of the "normal" pyrite cemented both by cp, locally associated with bn and more rearely fahlore. Under certain circumstances the globular form of pyrite may indicate also the pre-existence of the mineral fukuchilite which typically forms globular aggregates and transforms easily into pyrite and covellite (Kajiwara, 1969).
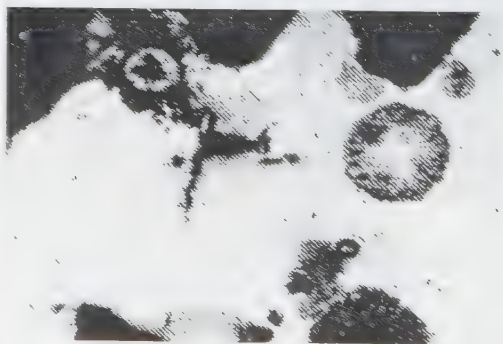
Fig. 9. Globular pyrite in chalcopyrite partly replaced by gangue minerals (black). RPL, x90
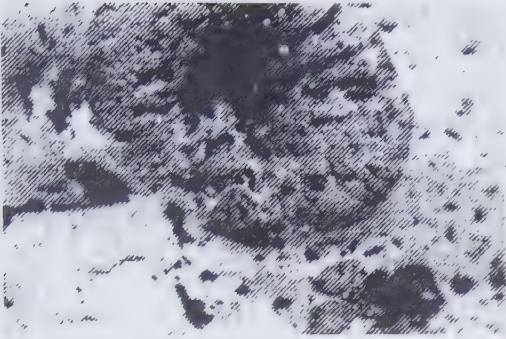
Fig. 10. Globular pyrite (0.5 mm in diameter) in a matrix of chalcopyrite+tetrahedrite. RPL.
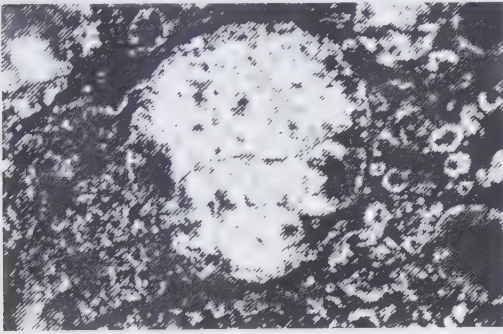
Fig. 11. A globular pyrite grain irregularly replaced by bornite and chalcopyrite, and smaller shell-like pyrite grains in a fine-grained calcite matrix (black) +tetrahedrite. RPL, x90.
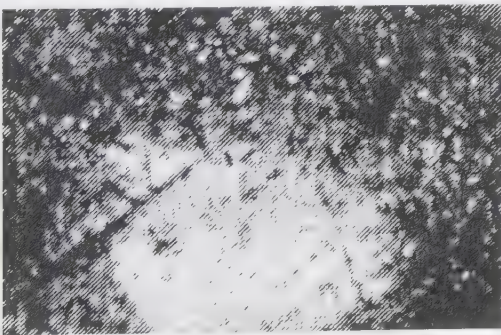
Fig. 12. Pyrite aggregate replaced by chalcopyrite (fine veinlets and patches, indistinguishable on the photograph) which alters further to covellite and secondary copper minerals (black). This matrix contains relict grains of pyrite and chalcopyrite. The sample represents an oxidezed ore, but the similar evolution of pyrite aggregate is presumed to occur at higher temperature. RPL, x90.

4. Discussion

The ore minerals in the Sasca Montană area are assigned to some major deposition environments, i.e., skarns (garnet-vesuvianite-diopside-wollastonite), altered granodioritc rocks (porphyry-type assemblages), recrystallized limestone, and tectonic breccias. The concurrent ore mineral assemblages differ both in composition and in the intergrowth type, depending on their setting (Constantinescu, 1981). The mineralising process took places discontinuously and a non-equilibrium state prevailed during the entire postmagmatic activity. There is no evidence of a regional zoning of the skarn assemblages in the Sasca Montană area, but zoned and brecciated minerals do frequently occur as well as numerous paramorphs and reverse paragenetic sequences. The non-equilibrium state is mainly due to the repeated re-opening of the faults and fissures which favoured a persistent variation in the CO_2 - activity. All this may explain the variety of the ore textures of the Sasca Montană deposit (partly presented in this paper) which characterises ores formed under varying PT conditions and at varying Fe:Cu ratios of the ore solutions.

References

Betechtin, A.G., Genkin, A.D., Flimonova, A.A., Shadlun, T.N. (1958) Structures and textures of the ores. (in Russian). Sci. Tech. Publ. House Geology Environ. Preserv., Moscow.

Cădere, D.M. (1925) Facts with a view to help mineralogical description of Romania. (in Romanian). Mem. Acad. Rom., III/3.

Constantinescu, E. (1981) Skarn genesis at Sasca Montană, Banat (in Romanian). Edit. Academiei, București.

Cotta, B. v. (1864) Erzlagerstätten in Banat und Serbien. Wien

Kajiwara, Y. (1969) Fukuchilite, Cu_3FeS_8, a new mineral from the Hanawa Mine, Akita prefecture, Japan. Mineral J. 5, 399-416.

Maucher, A., Ramdohr, P. (1962) Bildkartei der Erzmikroskopie, Umschau, Frankfurt.

Ramdohr, P. (1945) Myrmekitische Verwachsungen von Erzen. *Neues Jahrb Mineral. Geol. Palaeontol. Abh.* **79A,** 161-191.

Ramdohr, P. (1969) The ore minerals and their intergrowths. Pergamon Press, Oxford Braunschweig.

Shimazaki, H. (1969) Synthesis of a copper-iron disulphide phase (abstr). *Can. Mineral.* **10,** 146.

Superceanu, C.I. (1969) Die Kupfererz-lagerstätte von Sasca Montană im SW-Banat und ihre Stellung in dem alpidisch-ostmittelmeerischen Kupfer-Molybdän-Erzgürtel. *Geol. Rundsch.,* **58,** 798-860.

Tufar, W. (1967) Der Bornit von Trattenbach (Niederösterreich). *Neues Jahrb. Mineral. Abh.* **106,** 334-351.

Udubaşa, G., Istrate, G., Popa, C. (1981) Preliminary data on the Jiuleşti-Valea Fagului mineralizations, Apuseni Mountains. (in Romanian, Engl. Summary). *Dări de Seamă Inst. Geol. Geofiz.,* **LXIV/2,** Bucureşti.

Vujanovic V (1974) The basic mineralogical, paragenetic and genetic characteristics of the sulphide deposits exposed in the Eastern Black-Sea coastal region (Turkey). *Bull. Mineral. Res. Explor. Inst. Turk.* **82,** 21-36.

About fractal features of iron and manganese hydroxides dendrites

EMIL CONSTANTINESCU
MONICA PĂLĂȘANU
SORIN MILUTINOVICI
RĂZVAN CARACAȘ

The iron and manganese hydroxides dendrites (IMHD) are commonly found on the fissures in a variety of host rocks. However, they were not seriously taken into consideration by geologists. Among the interesting characteristics of the IMHD are the geometrical ones. According to the classification of Van Straaten there are two main IMHD types: internal and fissure-confined. From internal dendrites type, the "tree" and "star" dendrites were studied. According to their morphological features the IMHD are fractal objects. In this paper we present a fractal study on this objects, using four methods of measuring the fractal dimension: box counting and mass dimension – for surfaces –, compass method, and the branches length –for outlines –. The branches length method is proposed to become a method for measuring the fractal dimension of the dendritic type of shapes (1). The fractal surface dimensions (box counting and mass dimensions give an average value of 1.64. The outline (compass) dimension, similar to those found with the branches length method, yielded of 1.43.

In an attempt to obtain a characteristic fractal dimension for the IMHD not taking into consideration the branches width susceptible to be influenced by successive incomes of fluid, we carried out errosion tests on dendrites using several algorithms. The most appropriate erossion algorithm for the IMHD is considered to be the one which reduce the objects to lines. The obtained dimensions are similar for all the samples (average1.36).

Dendritic overgrowth is rare event in IMHD. In some of our samples such overgrowths where found and their fractal dimension was measured. The overgrowing dendrites showed a decrease of in fractal dimensions compared with their host objects.

References

(1)Constantinescu E., Pălășeanu M., Milutinovici S.P., Caracaș R., *Romanian Journal of Mineralogy*, in press;

(2)Van Staaten L.M.J.U., 1978,. *Geol. Soc. Lond*, **135**, p.137–151.

Fractal dimension measurements of some manganese dendrites

EMIL CONSTANTINESCU
SORIN MILUTINOVICI
RĂZVAN CARACAŞ
MONICA PĂLĂŞANU

The geometry of the manganese dendrites (MD) was investigated using the fractal dimension method. Four types of MD occurrences were investigated and classified according to their overall geometric features. The obtained fractal dimensions are generally lower than the ones already published in the literature. The difference is probably caused by the selection of samples in the previous studies. The large variance of the fractal dimensions is considered to be caused by: 1. The width of the dendrite branches and 2. The mutual influence of neighboring dendrites during growth. The study confirms partially the conclusion of Garcia-Ruiz et al., (1994) that the MD are amenable by the Viscous Fingering (VF) pattern type. However, some features of the dendrites are not fully consistent with the VF model and thus, more studies are necessary before a more precise genetic model may be constructed.

Introduction

The MD represent branching shapes that appear on various types of rock cracks as well as on the surfaces of many types of rocks. Their mineralogical composition consists mainly in manganese oxides and hydroxides (hollandite, romanechite, cryptomelane, and todorokite) usually with small amounts of quartz, clay minerals and/or carbonates (Potter an Rossman, 1979). Many types of manganese oxide concentration and coatings are known to occur with more or less the same mineralogical composition. Dendrites however are distinct from all other types of manganese concentrations by their geometry. The dendritic shape of some manganese concentration has been a challenging problem ever since their discovery, mainly due to the difficulties related to the kinetic factors (e.g. Tiller, 1991).

The fractal geometry suggests a different approach to the dendritic (and not only dendritic) patterns which may offer a new understanding of their genesis. Fractal geometry however, is detached from the chemical nature of the dendrite, trying to classify shapes according to geometrical features only (Mandelbrot, 1982). Moreover, not all patterns can be analyzed with fractal geometry, this

method being limited to self-similar shapes. A self-similar shape or object is also referred to as a fractal object and the character of that object is also called fractal (Takayasu H., 1990).

The fractal character of MD was demonstrated in several studies (Chopard et al., 1991), (Garcia-Ruiz et al., 1994). With this knowledge, the main purpose of this study is to understand the factors that influence the fractal dimension of a dendrite. Dendrites from several locations were studied, with different host rocks and with different types of supporting surfaces.

Fractal objects were classified according to their shapes and genetic processes. The appurtenance of the MD to any of these classes in still a matter of debate (Garcia-Ruiz J.M., 1994). There could represent either Diffusion Limited Aggregation (DLA) (Witten and Sander, 1983) or Viscous Fingering (VF) (Maloy, 1985) products.

Materials studied

A number of rock and fossil specimens that exhibit manganese dendrites were selected for this study to include a large chemical and physical diversity of supporting surfaces as well as different joint system geometries. The first type was a shell of *Unio sp.*, consisting of fine layers of carbonate material. Due to diagenetic processes, the shell exibit various fissures that are oriented more or less perpendicular to the shell layers. Both fissures and natural pores of the shell were circulated by solutions reach in manganese, which led to the formation of dendrites. The dendrites have less than 3 mm diameter of the bounding circle. The second type of samples was represented by volcanic tuffs from Racoş (East Carpathians). The Racoş tuffs formed an intensely fissured and circulated environment in which multiple types of manganese crusts can be encountered. There are basically two

types of fissures: regular (tectonic) and irregular-discontinuous, the later with a conchoidal shape. The regular fissures are large, with manganese crusts up to 2.5 mm width and with no dendrites. The irregular fissures are discontinuous, extended for 10-20 cm and extremely thin. On these irregular cracks medium to small (less than 1 cm) dendrites can be found. The third type of sample is the well known Solenhofen limestone which exhibit a parallel cleavages, on which large (up to 15 cm diameter of the bounding circle) dendrites can be found. The fourth type of samples are jasps from Poiana Braşov (South Carpathians) The jasps does not show at all regular, paralel fissures but only irregular, conchoidal ones. Medium to small dendrites (less than 1 cm diameter of the bounding circle) can be found on some areas of these fissures

Types of dendrites

The MD currently found on rock cracks were classified according to the following terms:
- single dendrites;
- overgrowing dendrites;
- shared source dendrites.

Single dendrites are shapes characterized by a main stem from which a certain number of branches are developed. In addition, single dendrites are isolated on their support i.e. no other dendrites neighbors can be observed at a distance at least equal with the dendrite bounding box dimension.

Overgrowing dendrites were identified on the *Unio sp.* shell samples, as well as on the Solenhofen limestone. There are small dendrites, usually with a simple pattern, with thin branches growing on the tip of larger dendrites (Fig. 1).

On the same host dendrite several overgrowing dendrites can be identified. The overgrowing phenomenon may be much more common in nature but in many cases it may be obscured

by the similarity between the overgrowing and host dendrites. The overgrowing feature was observed on the basis of the geometrical difference.

In the case of shared source dendrites, one can identify a unique starting area that may be interpreted as a single source of fluid shared by several adjacent dendrites in the same way as parallel crystal growth on a certain substrate. The geometry of these emergence areas

Fig. 2. Double point emergence in the Unio shell. Width of the image in of 3.1 mm.

fractal dimension of the object in cause. Thus, a main part of the fractal analysis consists of measuring the object at various scales, with measuring units changed accordingly. A measurement of a fractal dimension yields two sets of numbers, one consisting of the current measurement units and the other consisting in the actual measure i.e. how many measurement units are needed to cover the whole object. A log-log graph of these two sets should fit well with a straight line if the measured object has a fractal character. In this case, the fractal dimension is represented by the slope of the line.

Fig. 1. Overgrowing dendrites on the shell of a *Unio sp.*a (image width is 2.5 mm).

may vary considerably from point emergence on some *Unio sp.* samples (Fig. 2) through liniar emergence (Fig. 1), to curved or even irregular emergence. However, the most common type is the one-dimensional emergence even if curved.

Methods of investigation

A fractal is defined as a scale-invariant object, i.e., showing similar patterns on different observation scales (Barnsley, 1988). The self-similarity of these patterns is expressed by the

Various methods have been designed for measuring the fractal dimension. The difference lies in the type of measurement units (length units or surface units) and in the way they are applied. Each method has its characteristics and instabilities, especially when used with natural, random fractal objects. Therefore, three different methods were used in the case of MD fractal study. As with almost all type of branching patterns, the fractal dimension is influenced by the branch width, which contribute to the overall dimension of the pattern in a more or less random way. Due to this fact, we performed also a binary erosion on the samples and measured also the fractal dimension of eroded samples.

Box-counting

The box-counting principle is quite simple: the measured object is enclosed in a square bounding box which is covered with squares whose areas are progressively smaller (Barnsley, 1988). According to Barabashi and Stanley (1995), a structure covered with boxes of length Lb has a fractal dimension of:

$$D_{box-counting} = \lim_{L_b \to 0} \frac{\log_{10} Nb(L_b)}{\log_{10} L_b}$$

where L_b is the box side length, $Nb(L_b)$ is the number of such needed to cover the object completely.

Dilation

The dilation dimension is less straightforward than the box-counting. It involves the replacement of every pixel of the digitized object with a progressively larger square. Every replacement operation yelds a new image with multiple nested squares characterized by an area. The log-log graph of square lengths versus obtained areas gives the fractal dimension (e.g. Flock, 1978)

belong to the measured object. The number of pixels (i.e. quantity or "mass") versus the length of the boxes' sides are recorded and the fractal dimension is again obtained from a log-log graph as described above.

Erosion analysis

The branches width of MD may induce significant errors in fractal dimension measurements. In order to estimate the influence of the branches width on the fractal dimensions, we performed a binary erosion analysis (Serra, 1982,) on all the samples used in this study. The algorithm used was "thin erosion", which preserves lines. The evolution of the fractal dimension during progressive binary erosion steps was recorded.

Results

The obtained fractal dimension range from 1.2 to 1.9 with significant dispersions. Within each group of samples large values (e.g. 1.8) as well as small values (e.g. 1.3) may occur. This may be explained by the large geometric variation of the dendrites as well as by the instabilities inherent to the methods of measurement. Average values for the sample groups are given in the Table 1.

Table 1. Means and dispersion of fractal dimensions of analysed manganese dendrites.

Location	Samples	Box - Counting		Dilation		Mass	
		Mean	Disp.	Mean	Disp.	Mean	Disp.
Unio	52	1.603	0.082	1.339	0.330	1.428	0.295
Tuffs	25	1.670	0.068	1.240	0.126	1.593	0.209
Jasps	7	1.576	0.045	*	*	1.594	0.207
Solenhofen	10	1.622	0.061	1.568	0.138	1.568	0.138
Mean	94	1.617	0.064	1.382	0.198	1.545	0.212

* - Not measured

Sandbox

The sandbox dimension is one of the most used method (Vicsek, 1983, Takayasu, 1990). A starting point on the object's surface is chosen and from that point progressively larger circles (or squares) are build. Each circle (or square) contains a number of pixels that

Most of the box-counting graphs showed a straight line fit accounting for the fractal character of the samples. In several cases however, the graphs were curved towards the smaller values of the box side length. This effect was due to the fact that the value of the box side was to small in comparison to the size of the pixel in image. By digitizing the sample at a

higher resolution, this problem was corrected in all cases. The same effect may be seen in some of the dilation graphs. Tests at a higher resolution determined also the correction of the line shape. The sand box graph were rarely perfectly straight. The most general appearance was of a sigmoid-like graph caused by the finite-size effect involved in the measurement of random fractals (Takayasu, 1990). In a number of cases however, the curves were much more complicated, sometimes yielding fractal dimensions larger than 2, that were consequently eliminated from calculations. No significant correlation between abnormal sand-box behavior and fractal dimension values produced by box-counting or dilation were recognized. The reasons behind such anomalies (e.g. multiple fractal dimension) still remain to be investigated.

The fractal dimensions obtained through the dilation method is generally lower than the ones obtained with the box-counting and sand-box method, probably due to the fact that only the outlines were measured with this method.

The cross-comparison of values obtained by dilation box-counting and mass dimension, is indicative for the importance of the branch width. Since in the case of the Solenhofen dendrites (whose branches are extremely thin) the mean value of the dilation dimension is close to that of the box-counting and even equal to that of the sandbox, it may be concluded that the later two methods are strongly influenced by the width of the branches.

Errosion results

Seven successive steps of binary erosion were applied on dendrite images and the fractal dimension using the box-counting algorithm was measured. In all cases the box-counting dimension was reduced after every erosion step. The results are presented in Table 2.

Table 2

Sample	Box-counting (mean)	Box-counting (min.)	Box-counting (max)
Shell	1.35	1.285	1.458
Jasps	1.36	1.216	1.450
Tuffs	1.37	1.312	1.434

It should be noted that the fractal dimension decrease during successive erosion steps was either linear or exponential. No correlation between other variables and the graph shape was observed.

Relationship between dendrites

As mentioned above, vicinal (shared-source) dendrites do not touch each other. This may account for a strong mutual dependence of developing shape on neighboring dendrites. Fractal dimension of neighboring dendrites is usually smaller that fractal dimension of an isolated dendrite in the same conditions (i.e. surface type, emergence type). In the case of dendrites that share a single point of emergence, the fractal dimension is generally slightly larger that in the case of dendrites that share a linear emergence. When the same emergence has an irregular shape, the convex portion (towards dendrite growth sense) gives birth to dendrites with larger fractal dimension that corresponding to the concave portion.

Discussion

The fractal dimension values obtained in this study are not easily comparable with values from previous works probably due to the selective choice of samples within these studies. Our own values are generally lower that the ones published in the literature (e.g. Garcia Ruiz, 1994 values ranging from 1.69 to 1.70 or Chopard et al, 1991, values ranging from 1.51 to 1.78). There are many other factors we may invoke when explaining the smaller fractal dimensions of our MD: rock porosity, irregu-

larity of the surface, vicinity with other dendrites. When selecting samples, one can find singular dendrites with multiple branching orders. Also in our study this type of dendrites approaches the values obtained in previous work.

The difference between the various methods results comes mainly from the influence of the width of the dendrite's branches. It is hard to say however which method gives the best results. When obtaining a high box-counting or sand-box dimension the dilation dimension should be also checked in order to be sure that the effect of the overall surface of the dendrite (i.e. branches width) is not to high. The fact that after performing the binary erosion all the fractal dimensions within every sample group where much close to each other shows that the all the MD investigated are after all in the same class of fractal objects.

Fractal dimensions obtained in this study, together with the general aspect of the dendrites are consistent with both models suggested in previous work for MD: DLA (Chopard et al., 1991) and Viscous Fingering (Garcia-Ruiz, 1994) types, respectively.

The DLA (Diffusion Limited Aggregation, Witten and Sander, 1981) is a process in which a fractal cluster grows from a nucleus or a starting point, and proceeds by addition of matter from the surrounding fluid. Dendrite shapes where experimentally obtained using a clear DLA growth in the case of electrolitic deposition of metals (e.g. Zn,) and the same DLA model is widely used to explain various dendritic growth in thin film epitaxy processes (e.g. Hwang et.al, 1991). VF (Viscous fingering) takes place when a fluid replaces rapidly another, more dense, fluid. In some cases, when the kinetic of the process is extremely fast, patterns resembling DLA may occur. VF may also occur when a fluid is injected into a porous media at high speed. Therefore it is not easy to make the difference between DLA and VF otherwise than from their fractal dimen-

sion. The theoretically calculated fractal dimension of a VF pattern is 1.82 while the fractal dimension of a DLA dendrite is around 1.70. Feder et al (1989) suggest that from a pure geometric point of view, the two models are in the same universality class. Modified computer models of DLA exists (Maloy et al., 1985; Maloy et al., 1987) that can reach the same fractal dimension as the VF products. Moreover, experiments showed that the fractal dimension of VF patterns may drop dramatically depending mainly of the injection speed.

For the MD growth model however, as well as for geological background of this phenomenon the distinction between DLA and VF is very important. In the case of DLA, the crack on which dendrites are found should be filled with fluid containing dissolved dendrite material while in the case of VF, the fluid containing the dissolved dendrite material should arrive in situ and form a fluid dendrite that dries up afterwards without changing shape.

Fractal dimensions obtained in this study are well below both VF and DLA models but several well developed samples showed dimensions between 1.78 - 1.85 which fall in the VF domain. Moreover, the complicated shape of some sandbox graphs may account for the multifractal properties of the dendrites, i.e., another factor that can affect fractal dimension.

VF experiments (Ben-Jacob, 1994) showed that the fractal dimension of VF patterns as well as their branching is influenced also by the growth space. This is consistent with the fact that in shared source dendrites the fractal dimension is smaller than in the case of isolated dendrites.

Previous works by Garcia-Ruiz et al., (1994) showed that the dendritic growth is more likely to be associated with VF than with DLA. The authors explained the VF growth by placing dendritic growth in the early diagenesis, when rock cracks may have been filled with

colloidal suspensions that provided the highly viscous fluid to be replaced via the VF mechanism by the manganese oxide solution. Although the present study support most of the conclusions of Garcia-Ruiz, the presence of colloidal suspension in the interlaminar space of the *Unio sp.* shell can hardly be explained.

Conclusions

Fractal dimension of MD, as an image of the complexity of natural patterns, depends of a high number of genetic factors. More research is needed however, before the genetic factors may be inferred from fractal dimension. However, the fractal dimension of our samples can indicate that the VF model is the most appropriate formation process for describing the MD formation. The geological application of the VF model in the MD case yields the following observations:

1. The MD shapes are not "solid state" shapes; they are produced by the rapid intrusion of the manganese solution on the cracks surfaces. More studies are necessary in order to establish what could be the cause of such an event.
2. The VF mechanism consists in fluid replacement. The presence of a more dense fluid (i.e. gel) in all the environments where dendrites can be found is not easy to be explained, especially in the case of *Unio sp.* shells.

References

Barabashi A.L., Stanley H.E. (1995) Fractal concepts in surface growth. *Cambridge University Press*, New York.

Barnsley M. (1988) Fractals everywhere. Academic Press Inc., Boston.

Ben-Jacob E., Shochet O., Tenenbaum A., Cohen I., Czirók A., Vicsek T. (1994) Communication, regulation and control during complex patterning of bacterial colonies. *Fractals*, **2(1)**, 15–44.

Chopard B., Herrmann H.J., Vicsek T. (1991) Structure and growth mechanism of mineral dendrites. *Nature,* **353**, 409–412.

Flock A. G. (1978) The Use of Dilation Logic on the Quantimet to Achieve Fractal Dimension Characterization of Textured and Structured Profiles. *Powder Technology*, **21**.

Garcia-Ruiz J.M., Otalora F., Sanchez - Navas A. (1994) The formation of mineral dendrites as the mineral record of flow structures. In J.H. Kruhl, Ed. Fractals and dynamic systems in Geoscience,307–318. Springer Verlag.

Maloy K.J., Feder J., Jossang T. (1985) Viscous fingering fractals in porous media. *Physical Reviews Letters*, 2681–2691.

Mandelbrot B.B. (1967) How long is the coast of Britain: Statistical self-similarity and fractal dimension. *Science*, **155**, 636–638.

Mandelbrot B.B. (1982) The Fractal Geometry of Nature. WH Freeman, New York.

Matsushita M., Sano M., Hayakawa Y., Honjo H., Sawada Y. (1984) Fractal structures of zinc metal leaves grown by electrodepozition. *Physical Review Letters*, **53(3)**, 286–289.

Potter R.M., Rossman G.R. (1979) Mineralogy of Manganese Dendrites and coatings. *American Mineralogist*, **64**, 1219–1226.

Rosenfeld A., Kak A.C. (1982) Digital picture processing. Academic Press, New York.

Smith T.G., Lange G.D, Marks W.B. (1996) Fractal Methods and results in cellular morphology - dimensions, lacunarity and multifractals. *Journal of Neuroscience Methods,* **69**, 123–136.

Tiller A.W. (1987) The science of crystallisation: macroscopic phenomena and defect generation, *Cambridge University Press,* Tokyo, **1987**, 231–253.

Takayasu H. (1990) Fractals in physical sciences. Manchester University Press, Manchester.

Vicsek T. (1983) Fractal growth phenomena. World Scientific, Singapore.

Witten T.A. Sander L.M. (1983) Diffusion Limited Aggregation. *Physical Review B*, **27**, 5686–5697.

V. MINERALOGY AND PETROGENESIS

Contributions to the study of the Oravița-Ciclova skarn occurrence, South-Western Banat

EMIL CONSTANTINESCU
GHEORGHE ILINCA
AURORA ILINCA

The Oravița-Ciclova skarns are developed at the contact between the Laramian magmatites and the Upper Kimmeridgian-Valanginian limestones, marls and calcareous clays. The main types of skarns are defined by the following assemblages grandite (grossularite $_{30-50 and}$); wollastonite-grandite-tremolite; wollastonite-grandite; grandite-scapolite (meionite); wollastonite-diopside-grandite I-grandite II-vesuvianite-clintonite; grandite I-grandite II-vesuvianite: diopside-melilite (gehlenite); wollastonite-diopside-chondrodite-grandite-vesuvianite. Skarns were formed in a medium rich in mineralizers (F, Cl, B), suggested by the appearance of vesuvianite, chondrodite, scapolite and, probably, szajbelyite. According to the more basic character of the Laramian magmatites occurring here, the temperature reached in the contact aureole was, in all probability, higher (750°C) than in the case of other skarn occurrences in Banat. The sequence of skarn minerals at the contact of the Oravița Valley diorites indicates the existence of two main phases in the evolution of the temperature: a heating phase (diopside-gehlenite)' and a cooling phase (wollastonite-diopside II-grandite-vesuvianite-clintonite).

1. Introduction

Remarkable for their mineralogical complexity, the pyrometasomatic formations related to the Oravița - Ciclova Laramian magmatites were the subject matter of numerous researches. Beside the pioneering works of earlier authors: Born (1774, 1780), Cotta (1865), Castel (1869), Marka (1869), Halaváts (1884), Koch (1885), it is worth mentioning the important contributions of Koch (1924), Superceanu (1958), Pieptea (1964), Mînzatu (1964), Gheorghițescu (1974), Cioflică et al. (1976, 1977, 1980), Popescu, Constantinescu (1977), Constantinof (1980), Cioflică, Vlad (1981), by which a marked advance in the geological knowledge of this region was attained.

The rich mineralogical list of the Oravița-Ciclova thermal and metasomatic contact zone is broadly represented in the earlier or later literature, e.g. Marka (1869), Zepharovich (1859, 1870, 1888), Koch (1885), Cădere (1927), Koch (1948), Rădulescu, Dimitrescu (1966).

This paper is intended to offer the main typological and mineralogical aspects of the skarns in the Oravița - Ciclova area. By means of these observations, an outlining of the essential petrogenetic features is attempted.

2. General data on the geology and petrology of the region

2.1. Crystalline schists

The regional metamorphic rocks in the Oravița - Ciclova area belong to the southern part of the Bocșa Montană - Oravița - Ilidia Crystalline Massif (Codarcea, 1931; Constantinof, 1980), namely, to the complex of retromorphosed micaceous gneisses of the Bocșița - Drimoxa Series (Constantinof, 1980). Muscovite-biotite paragneisses with gradual transitions to muscovite schists with albite porphyroblasts form the background of the crystalline schists suite.

The frequency of the muscovite schists increases towards the Oravița overthrust line. Quartz-feldspathic gneisses, amphibolites and amphibolic gneisses, muscovite-bearing quartzites and granite gneisses occur subordinately as intercalations.

Eastwards, along the Oravița tectonic line, the crystalline schists overlap Paleozoic and Mesozoic deposits of the Reșița - Moldova Nouă sedimentary zone.

2.2. Sedimentary deposits

The Paleozoic formations are represented by grey lithic sandstones with surrounded lithoclasts of quartzites and micas, alternating with brown-violaceous or black-violaceous shales of Permian age. They form a band of variable thickness, extending north-southwards near the Oravița overthrust line (Fig. 1).

The Mesozoic sedimentary is widely spread in the area of study; it is included in the Natra anticline structure and in the Cornetul Mare and Jitin synclines, covering the Upper Oxfordian - Lower Aptian interval. It is represented by limestones with stratiform or lens-shaped siliceous intercalations (Valea Aninei limestones, Upper Oxfordian - Lower Kimmeridgian), micrites with rare bioclasts and centimetric separations of shally marls (Brădet limestones, Upper Kimmeridgian - Lower Tithonian), yellowish - grey sublithographic limestones with marl intercalations in the upper part (Marila limestones, Upper Tithonian - Berriasian), marls and calcareous clays (Crivina Beds, Valanginian), blackish-grey calcareous clays with ellipsoidal silicolite concretions and marly-calcareous intercalations which grade upwards into massive limestones with numerous bioclasts of requiens and corals (Plopa limestones, Barremian - Lower Aptian).

The Mesozoic deposits are mainly carbonatic, with some compositional peculiarities given both by silicolite intercalations and by the wide development of calcareous clays and marls within the Crivina Beds and the Hauterivian formations.

2.3. Laramian magmatites

Together with the similar occurrences at Tincova - Nădrag, Bocșa Montană, Ocna de Fier, Dognecea, Sasca Montană and Moldova Nouă, the Oravița - Ciclova igneous rocks belong to the western principal alignment of the Laramian magmatites in Banat (Cioflică et al., 1977), which trends parallel to the Oravița line.

In the Oravița - Ciclova area, the outcrop pattern display several main intrusive bodies both within the crystalline schists and the sedimentary rocks.

In the north-easternmost part of the area, between the Cuptorului brook and Chinisea Valley, there is a large-sized body, chiefly consisting of biotite- and green hornblende-bearing porphyritic granodiorites, within which numerous transitions to microgranodiorite-porphyritic and dacitic apophysis facies may be observed. Quite locally, small separations of porphyritic diorites occur (e.g., Popii brook area).
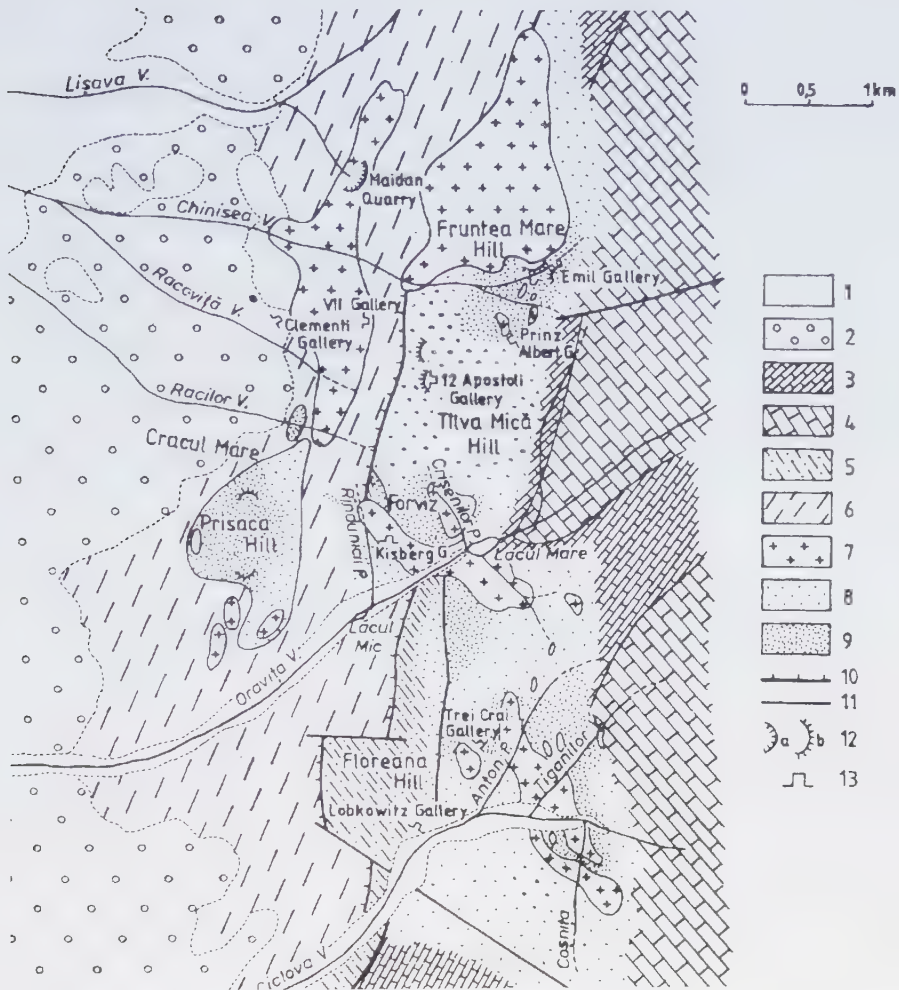
Fig. 1. Geological sketch of Oraviṭa-Ciclova zone. 1, Pleistocene (gravel, sand, clays); 2, Miocene (conglomerates, sandstones); 3, Cretaceous (marls, calcareous clays, chert-bearing limestones, reef limestones); 4, Jurassic (chert-bearing limestones, sublithographic limestones); 5, Permian (lithic sandstones, shales); 6, Precambrian (muscovite-biotite paragneisses, muscovite schists with albite porphyroblasts, amphibolites, muscovite-bearing quartzites; 7, Laramian magmatites (granodiorites, diorites, monzodiorites); 8, hornfels; 9, skarns; 10, Oravita tectonic line; 11, faults; 12 a, quarry; b, mining dump; 13, gallery.

Between the Popii brook and Racilor brook, west of the Oravita fault, there is a N - S elongated body, located entirely in crystalline schists. Here, granodiorites with biotite and green hornblende are transitional from equigranular or megaporphyritic and phaneritic structures, in the north, to porphyritic textures in the south. South of Poiana Crucii Hill, in the Forviz area, there occur a body with a relatively complicated morphology, trending approximately WSW - ESE; it crosses Oravița Valley and follows up to the springs of Coliliilor brook. The body is characterized by a wide petrographic variety, with a stronger basic character as compared with the above-mentioned intrusive types: diorites with green and/or

brown hornblende, porphyritic diorites, quartz-microdiorites, monzodiorites and syenites.

Around the springs of Anton brook, crossing Ciclova Valley and reaching the area of Coşniţa brook, develops a body, also with a complicated morphology, consisiting mainly of monzodiorites, within which there are local gradings into hornblende + biotite diorites. A similar composition is observed for small-sized bodies occurring in Floreana area and Poienilor brook.

The intrusions in Oraviţa Valley and Ciclova Valley are considered to represent a unique body (Cioflică et al., 1980), with the existent discontinuities depending on the actual level of erosion.

The main intrusive bodies occur in association with small-sized satellite bodies as well as with numerous dykes of porphyritic diorites (Oraviţa Valley), biotite granodiorites (Anton brook and Coliliilor brook), hornblende latiandesites (Racilor Valley, Ţiganilor Valley), quartz-syenites (Oraviţa Valley), augite+aegirine-bearing alkali-feldspar syenites (Ţiganilor Valley), augite+aegirine-bearing albitized oligoclase akerites (Coşniţa brook, Anton brook) and micrographic alkali-feldspar granites (Ţiganilor Valley).

2.4. Hornfels
The thermal contact metamorphic rocks, develop around all intrusive bodies, irrespective of the country rocks they are ascribable to the albite-epidote hornfels and hornblende hornfels facies.

Within the crystalline schists, the hornfels contain orthoclase, quartz, biotite and andalusite, sporadically accompanied by corundum and cordierite.

The contact metamorphism underwent by the Permian sedimentary is materialized by the appearance of quartz, acid plagioclase, biotite and clinozoisite hornfels or of mostly biotitic

hornfels. Also produced by the isochemical contact metamorphism, are widely spread micro- or mesoblastic recrystallized limestones, formed on the Mesozoic carbonatic deposits. Separations of clay minerals, epidote, quartz and pyrite are found locally in association with calcite, which is the main mineralogical component.

3. Skarns'

3.1. Petrographic types, spreading
The skarns outcrop on large areas in the Oraviţa - Ciclova zone. The main types of skarns, according to mineralogical criteria are defined by the following assemblages:

- *grandite* (*grossularite $_{3-50and}$*): widespread in Chinisea Valley and in the NW slope of Tîlva Hill and Anton and Ciclova valleys;
- *wollastonite-grandite-tremolite*: visible in the upper course of Chinisea Valley and in the southern side of Fruntea Mare Hill;
- *wollastonite-grandite*: in Lacul Mare-Crişenilor brook area;
- *grandite-scapolite*: first outlined as such in the skarn vein body in the, spring zone of Rîndunicii brook;
- *wollastonite-diopside-grandite I-grandite II-vesuvianite-clintonite*: in Lacul Mare-Crişenilor brook zone;
- *grandite I-grandite II-vesuvianite*: in the middle and lower course of Anton brook, in Ţiganilor Valley and in the Coşniţa brook zone;
- *diopside-melilite* (*gehlenite*): identified in the right bank of Crişenilor brook;
- *wollastonite-diopside-chondrodite-grandite-vesuvianite*: in the right Bank of Ţiganilor Valley.

Skarns form columns and irregular bodies and are locally found as veins within the crystalline schists. The occurrence of the vein body in Rîndunicii brook seems to have been conditioned by the existence of a limestone lamina planed in front of the Oraviţa overthrust and brought in an unconformable posi-

Table 1. Chemical analyses of the garnets from the skarns in the Maidan - Tîlva Mare - Oraviţa zone

Oxides	151A*	151 B*	67*	C_2	68	O_2	O_1
SiO_2	38.10	39.26	37.36	34.90	32.30	35.38	34.36
TiO_2	0.18	0.04	2.08	0.13	0.10	0.35	0.45
Al_2O_3	17.12	20 26	12.38	16.00	13.80	16.58	18.24
F_2O_3	4.08	2.07	10.99	11.00	18.00	3.66	4.69
FeO	2.96	1.17	0.71	0.70	0.34	0.29	0.42
MnO	0.03	0.05	0.44	0.38	0.40	0.10	0.10
MgO	1.35	2.20	0.89	2.00	1.22	5.20	4.50
CaO	35.53	34.12	34.23	31.36	32.76	35.01	34.03
H_2O^+	0.15	0.18	0.17	-	-	-	-
H_2O^-	0.75	0.41	0.30	0.34	0.26	1.12	0.16
Total	100.55	99.79	99.55	100.04	99.98	99.77	99.73

* from Popescu, Constantinescu (1977).

Table 2. Atomic proportions of garnets, in the basis of 24 (oxygen)

	151A	151B	67	C_2	68	O_2	O_1
Si	6.02	6.00	5.877	5.459	5.177	5.453	5.403
Al	-	-	0.123	0.541	0.822	0.5473	0.597
Al	3.001	3.722	2.164	2.407	1.799	2.464	2.762
Fe^{3-}	0.464	0.222	1.304	0.292	2.178	0.423	0.0532
Ti	0.002	-	0.246	0.015	0.0125	0.041	0.551
Mg	0.323	0.491	0.208	0.467	0.293	1.195	1.049
Fe^{2+}	0.570	0.092	0.094	0.091	0.046	0.038	0.055
Mn	-	-	0.057	0.050	0.055	0.013	0.013
Ca	5.663	5.420	5.764	5.263	5.667	5.789	5.708
Participation of end members (mole %)							
and	13.7	5.623	31.6	34.79	54.6	14.46	16.36
gross	68.7	84.559	55.319	54.87	38.9	67.84	67.27
alm	11.2	1.550	1.813	1.55	0.76	0.54	0.81
pyr	6.3	8.226	3.99	7.95	4.83	16.98	15.37
spess	-	-	1.092	0.85	0.91	0.18	0.19

tion against the crystalline schists. The field observations indicate a certain tendency of zoning given by the peripheral disposition of the garnetiferous skarns as compared with the garnetiferous-vesuvianite ones.

3.2. Mineralogy of skarns

Garnets predominate over the other skarn minerals. Macroscopically, they exhibit a great morphological and colour variety. Garnets can form monomineralic accumulations within which the crystal sizes vary from 2 - 3 mm to 8 - 10 cm; other times they form nests, small voids and veinlets or they can occur as dodecahedral crystals within a groundmass of calcite or quartz.
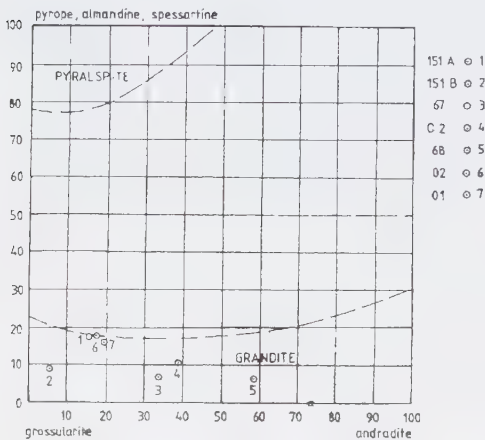
Fig. 2 - Boecke diagram (1914); plots of the values representing the percentage participation of end members (mol %) obtained for garnets in Oravița zone: 151 A - green-yellowish garnet, Oravița Valley, 151 B - brown garnet - Oravița Valley; 67 - dark green garnet-Chinisea Valley (Popescu, Constantinescu - 1977), C₂ - dark green garnet - Rîndunicii brook, 68 - dark green garnet - Chinisea Valley, O₂ brown-yellowish garnet - Crișenilor brook, O1 - light green garnet - Crișenilor brook.

The colour varies from brown and reddish-brown to honey yellow, yellowish-green and China green. It is difficult to establish a correlation between the variation of the colour and that of the chemical composition; however, the appearance of the green colour in andradite-rich terms can be retained as a general tendency.

The chemistry of garnets was investigated by means of several chemical analyses on the basis of which the percentage compositions were established in end members (Table 1 and 2).

The resulting values, plotted on Boecke diagram (1914, from Winchell, 1958), point out their appurtenance to the grandite fields (Fig. 2). The significant participation of the pyralspitic terms is obvious, three of the analysed samples following the limit of the miscibility gap between grandites and pyralspites. High contents in pyralspitic moles were observed in other occurrences, too: Ocna de Fier (Kissling, 1967), Dognecea (Vlad, 1974), Sasca Montană (Constantinescu, 1980). This fact can be retained as a remarkable mineralogical particularity of the garnetiferous skarns in Banat, the more so as the grandite-pyralspite miscibility is considered, on the basis of numerous experimental data (Schreyer, 1976), to be hardly achievable under the thermo-baric conditions of the pyrometasomatic reaction zones.

Microscopically, garnets occur as xenoblastic or idioblastic crystals, colourless or with a brown-yellowish colour, with a high relief. Generally, two garnet generations can be emphasized:
- generation I - colourless garnet in plane polarized light, usually, displaying idioblastic forms;
- generation II - brown-yellowish garnet with a higher refringence than the first one, commonly showing xenoblastic forms. Rather as a rule than as an exception, the garnets from Oravița-Ciclova display anomalous optical anisotropy, locally very obvious.

Certain morphological particularities of the anomalies allowed the separation of the following types:
- sectorial anomaly (Pl. I, Fig. 1): crystalloblasts sectioned in a median plane reveal a structure divided into six triangular-shaped birefringent sectors, with the peak in the centre of the crystal;
- concentric anomaly (Pl. I, Fig. 2): lamellae of variable sizes, alternatively isotropic and

anisotropic, parallel to the crystal faces; the crystalloblasts with concentric anomaly reveal the evolution of the crystallographic form from rhomboidal dodecahedron to trapezohedron (Pl. II, Fig. 1), a fact also observed in case of Ocna de Fier garnets (Kissling, 1967); - mixed anomaly: a complex joining of the two mentioned types: the anisotropic sectors are divided by lamellae parallel to the margins of the grain.

The birefringence of the sectorial areas and of the anisotropic lamellae is generally low; a positive or negative biax character, with a variable angle of the optical axes (2 V = 23-30°) can be observed. The main plane of optical symmetry of the lamellae of the concentric anomaly is approximately parallel to the crystal faces however without a perfect coincidence. In accounting for the appearance of the double refraction in these grandites, several causes may be invoked: internal tensions due either to forced isomorphic mixtures between the pyralspitic and the granditic terms or to particular processes connected with the skele-

metasomatic substitution of monzodiorite plagioclases by garnet, comparable, in morphological respect, with the quartz-feldspar micrographic intergrowths (Pl. III, Fig. 1). In the hydrometasomatic phase, garnets are replaced by calcite, epidote, scapolite and quartz. Locally, pseudomorph epidote after garnet idioblasts, preserving a mixed-type divided structure, was identified.

Table 3. Chemical analysis of the vesuvianite from Țiganilor Valley

Oxides	Content %	Number of ions in the basis of 76 (O, OH, F)		
SiO_2	37.64	Si	18.01	
Al_2O_3	20.38	Al	—	Sum = 18.00
		Al	11.50	
TiO_2	0.121	Ti	0.04	
Fe_2O_3	5.15	Fe^{3+}	1.85	
FeO		Fe^{2+}	—	
MnO	0.08	Mn	~	
MgO	2.72	Mg	1.94	Sum = 15.53
CaO	33.19	Ca	17.03	
Na_2O	0.33	Na		
K_2O	—	K		
H_2O^+	0.303			
H_2O^-	0.192	OH	0.97	
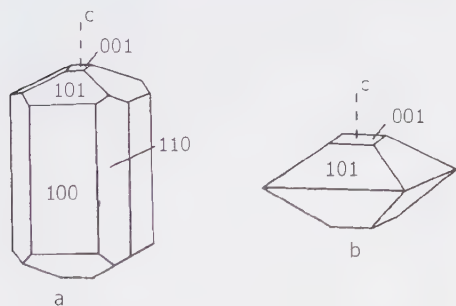
Fig. 3 - The habit of vesuvianite crystals: a) forms specific to Sasca Montană- vesuvianite (Orașului Hill), b) forms specific to Oravița and Ciclova vesuvianite.

tal growth. In some cases, certain morphological features of the garnets, difficult to infer from a selective substitution suggest an incomplete skeletal development (Pl. II, Fig. 2). Garnets replace wollastonite, diopside and chondrodite and are substituted by vesuvianite. There were also observed structures of

Vesuvianite is, after grandites, the most frequent mineral in the Oravița-Ciclova skarns. It forms compact masses, locally with a vein character within granditic accumulations or crystal agglomerations with sizes up to 10 cm (Țiganilor Valley). It is brown or yellowish-brown, and hence its macroscopic separation from grandite, particularly when its crystallographic shape is not obvious becomes, to a great extent, difficult.

Vesuvianite crystals show a typical bipyramidal habit (Pl. III, Fig. 2) characterized by the disappearance of the prism faces (100) and (110), the development of the tetragonal bipyramid faces (101), as well as of the basal pinacoid (001) (Fig. 3).

The chemistry of the Țiganilor Valley vesuvianite points out, in comparison with other chemical analyses on samples from known

occurrences, average values of the main cations. The relatively high amount of Fe_2O_3, is not connected with a decrease of the content in Al_2O_3 as in the case of other types of high-iron vesuvianites. The Al_2O_3/Fe_2O_3, ratio in the Ciclova vesuvianite is 20.38 - 5.15% in comparison with 17.29 - 4.87 % (FeO 0.36%) in the Sasca Montană vesuvianite (Constantinescu, 1980), 12.66 - 4.36 % (FeO 1.55%) in Akhmat-Ural (Miashnikov, 1940, in Deer et al. 1965), 13.36 - 4.15% (FeO 2.15%) in the Iron Mountains vesuvianite (New Mexico, Deer et al., 1965) and 15.62 - 2.81% (FeO 2.96%) in the Turnback Lake vesuvianite (Canada; Meen, 1968 in Deer et al., 1965).

In comparison with the mentioned occurrences, the Ciclova vesuvianite is characterized either by the absence or by extremely small amounts of FeO: 0.58 or 0.25% (Cioflică et al., 1980).

Under the microscope vesuvianite displays a xenoblastic or idioblastic contour and a high refringence. Its colour, in plane polarised light, is almost brown-yellow; in crossed polars vesuvianite shows a low birefringence in anomalous colours: Prussian blue, purple, light-yellow and brown. The disposition of the birefringence colours frequently yields a marked zoning in the plane perpendicular to (001). Both negative uniaxial crystals and anomalous negative biaxial crystals were identified; in the later cases the optic plane is parallel to (110). Vesuvianite replaces all the other associated skarn minerals, suggesting its appurtenance to the late phases of the pyrometasomatic process. The replacement of the high-andradite garnets by vesuvianite determines a significant increase of vesuvianite birefringence in the reaction zone between the two minerals and, implicitly, a change of colour towards light hues, corresponding to an enrichment in Fe (Pl. IV, Fig. 1). Similar situations were described in the vesuvianite occurrence at Sasca Montană (Constantinescu, 1980).

During the hydrometasomatic phase vesuvianite is highly substituted by clintonite, epidote, calcite and quartz. Very interesting mineralogical aspects were observed in the contact zone of the Țiganilor Valley skarns with the alkali-feldspar syenites, where a pseudomorph vesu-
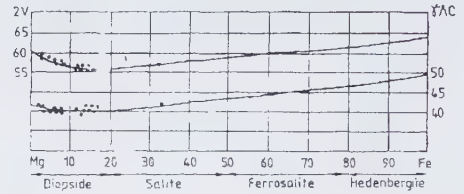
Fig. 4. Plotting of 2V and $\gamma \wedge c$ angles measured for the calcic pyroxenes from the Oravița-Ciclova skarns on the Hess diagram (1949).

vianite after a fibrous-radial mineral was identified (Pl. IV, Pig. 2). The X-ray diffraction, carried out on such samples, pointed out traces of serpentinite and szajbelyite.

Wollastonite occurs frequently in the Oravița-Ciclova skarns. Macroscopically, wollastonite can be easily distinguished due to the long prismatic habit, locally needle-shaped, as well as to its bright white or white-grey colour. Commonly it forms monomineralic with crystals often exceeding 5 - 6 cm (Chinisea Valley, Crișenilor brook, Țiganilor Valley).

Microscopically, wollastonite occurs as hipidioblastic or xenomorphic, corroded crystals. The optic angle is 2V = 89 - 40°, the extinction angle $\alpha \wedge c = 30°$ and the optic sign is negative. Wollastonite is replaced by all the other associated skarn minerals, thus suggesting an early stage of the pyrometasomatic process. In the hydrometasomatic phase, wollastonite is very sensitive to the substitution with calcite, quartz and epidote.

Pyroxenes belong to the diopside-hedenbergite series and are found in the skarns from Crișenilor brook and Țiganilor Valley. In thin sections, the pyroxenes form hipidioblastic crystals with short-prismatic habit and good

cleavage. The extinction and optic angles measured for 17 crystals from different thin sections and plotted on the Hess diagram (1949-in Troger, 1952), indicate a significant concentration of the values in the diopside field (Fig. 4).

In the Crişenilor brook - Lacul Mare skarns, diopside is replaced by gehlenite or forms after wollastonite, being eroded by garnet and vesuvianite, which may indicate the presence of two generations. In Ciclova area, diopside contemporaneous with chondrodite replaces wollastonite, being substituted by garnet and vesuvianite. In the hydrometasomatic phase, diopside is corroded by calcite and quartz.

Gehlenite was identified in association with diopside or forming small monomineralic accumulations in the skarns from Crişenilor brook. Macroscopically, it occurs as crystals (up to 0.5 cm) of a dark green colour with brownish spots, trapped in a groundmass of diopside and clay minerals. Microscopically (Pl. V, Fig. 1), it displays xeno- or hipidioblastic outlines, with a visibly lower relief as compared with garnets and vesuvianite. In comparison with vesuvianite, gehlenite differs clearly due to the quality of the cleavage - medium to good - along two orthogonal directions. Gehlenite occurs frequently in normal birefringence colours of the first order; some thin sections may reveal however, anomalous hues of lavender-blue. The uniaxial character has been checked; the optic sign is negative indicating the presence of gehlenite. Locally, crystals are covered by a brown-greenish pigment, resembling a clay mineral which is, however, undeterminably.

Chondrodite was identified in the Ţiganilor Valley skarns. Microscopically, they occur as idioblastic crystals, locally isometric or short prismatic, with a weak pleochroism in yellow and light brown hues. The cleavage parallel to (001) is poor, often unseen. The relief is medium to high, giving a chagrin-like aspect similar to that of olivine. Chondrodite is positive

biaxial; the values of the optic angle range between 68° and 75° and the extinction angles β ^ c are large (26 - 27°), differentiating chondrodite from the other minerals in the humite group. Radial intergrowths of chondrodite with diopside are characteristic, indicating their simultaneous appearance in the pyrometasomatic process (Pl. V, Fig. 2). Chondrodite is corroded by garnet, vesuvianite, epidote, calcite and quartz.

Clintonite was first described at Oraviţa by Popescu, Constantinescu (1977); it was identified in association with brown-yellowish, xenoblastic vesuvianite and with grandite in the skarns from Crişenilor brook. This mineral was also found in the mining dump of the adit II Clementi, but in this case, its source could not be established.

Macroscopically, it occurs as green, leafy, pseudohexagonal crystals. The crystals usually underwent a supergene decolouring, locally with a wider extension, yielding a muscovite-like aspect. In thin sections it shows a light green colour, with a strong positive relief and a perfect cleavage parallel to (001). The birefringence colours are vivid, randomly spread. The optic angle is small, and the optic sign is negative; the optic plane is perpendicular to (010), which differentiate clintonite from xantophyllite where the optic plane is parallel to (010). Clintonite is preferentially developed along some fissures in garnets or vesuvianite (Pl. VI, Fig. 1) suggesting its late position versus the other two minerals.

Scapolites are associated with grandite (35 and), epidote, calcite and zeolites in the skarn vein body at Rîndunicii brook. Scapolites form colourless, limpid hipidioblastic or idioblastic crystals, with a marked pseudoabsorption; the relief is weakly positive after w, decreasing sensibly after ε. The cleavage parallel to the prism faces is good and in basal sections one can observe two orthogonal cleavage directions, typical for minerals in the tetragonal system. The stages of growth and

evolution of the crystals from a tetragonal prism to a ditetragonal one, through the development of the face. (110) (Pl. VI, Fig. 2) can be distinguished in basal Sections. Birefringence is very high, according to the appearance of the pseudoabsorption. The relief variation and the high birefringence indicate a term closer to meionite.

Meionite represents a subsequent phase in relation to garnet, being, in its turn, replaced by calcite and zeolites.

Tremolite occurs as crystals with a long prismatic up to acicular habit, of a greyish-white colour, spotted by iron oxides. Microscopically, it forms needle-shaped or radial fibrous aggregates, colourless or of a light green colour, which cement or corrode garnet crystalloblasts. Extinction $\gamma \wedge c$ is 16 - 18° with lower values in the coloured terms. Tremolite is corroded by quartz and opacized by iron oxides.

3.3. Petrogenetic considerations
The intrusion of the Laramian magmatic bodies was accompanied by the release; of significant amounts of post-magmatic fluids with a pneumatolytic and hydrothermal character.

The Mesozoic sedimentary, with a mostly carbonatic nature, was sensitive to the action of the pneumatolytic fluids, and thus the pyrometasomatic products are preferentially linked. to it. The Permian deposits and the crystalline schists underwent only thermal metamorphism therefore displaying an isochemical character.

The main petrogenetic factors whose influence is proved by observation data refer to: petrographic and chemical features of the paleosome, circulation possibilities of the post-magmatic fluids, chemical composition of these solutions, pressure and temperature of the metasomatic reactions.

The influence of the paleosome is well illustrated by the fact that the skarns with complex mineralogical associations are developed only on the background of Crivina Beds, mostly with a marly and clay-calcareous character, whereas the zones presumed to exist in the extension of the Brădet and Marila limestones include skarns with a relatively simple composition. In this latter case, a diversification of the mineralògical associations may be the result of the marly intercalations at the upper part of the Marila limestones. The absence of periplutonic zoning, the skarn development as columns, veins or irregular bodies as well as the petrographic characters of the Mesozoic paleosome, plead for processes of metasomatosis by infiltration and quite locally by diffusion at the contact between the marly and calcareous levels.

The access ways opened to the metasomatosis by infiltration were represented by fissures, fractures, bedding planes, as well as by separation planes between the calcareous levels and the marly or siliceous ones.

The tendency of zoning, locally manifested within pyrometasomatic deposits, indicates the local preponderance of a bimetasomatosis-type mechanism related, in this case, to the development of Brădet and Marila limestones. The zoning displayed by the disposition of the garnetiferous skarns versus the garnetiferous-vesuvianitic ones is a result of the different relative mobility of the chemical components within the exchange of substance yielded between the eruptive mass and the calcareous paleosome.

The chemical components of the system within which the pyrometasomatic processes took place are very numerous as one can see from the described mineralogical associations: SiO_2-Al_2O_3-CaO-MgO-Fe_2O_3-FeO-CO_2-H_2O, etc., and they cannot be accounted entirely by the Mesozoic paleosome. In this respect, there

is the fluid composition whose supply of substance is always significant, justifying more than the paleosome composition, the diversity of the skarn minerals and the particularities of their succession, that must be taken into account.

Pressure and temperature played an important role in establishing the succession of the skarn minerals. As regards pressure, one shall distinguish the lithostatic pressure corresponding to the pyrometasomatic reaction zone level and given by the Laramian overlying rocks and, on the other hand, the fluid pressure. It may be reasonably inferred that the lithostatic pressure corresponding to pyrometasomatic reaction zones - at depths of 1 - 1.5 km and with an average specific weight for the overlying rocks of 2.5 - 2.6 - was approximately of 250 - 400 bar. This approximation is due to the impossibility of an exact estimation of the erosion rate affecting the overlying deposits and of the load induced during the Laramian by the eastward extension of the crystalline schists in the Bocşa Montană - Oraviţa - Ilidia massif.

A notable permeability of the reaction system for the volatile components is suggested by certain particularities of the succession of skarn minerals, i.e. by the preferential replacement of mineralogical phases along geometric discontinuities. Thus, it may be accepted that the total pressure of the fluids was subordinated to the lithostatic one, and it ranged between a maximum value close to the lithostatic pressure and a minimum value corresponding to the atmospheric pressure.

Like the fluid pressure, temperature constituted a variable factor in time and space as it ranged between a minimum value corresponding to the geothermal gradient of the reaction zone (cca 50°C) and a maximum value corresponding to the intruded magma. Some indications on the maximum temperature reached in the Oraviţa Valley contact aureole, is given by the frequent transitions from ferrotschermakite to brown hornblende which are considered to occur at temperatures of 750°. In agreement with the strong basic character of the Laramian magmatites in this area, the reaching of so high values conditioned the appearance
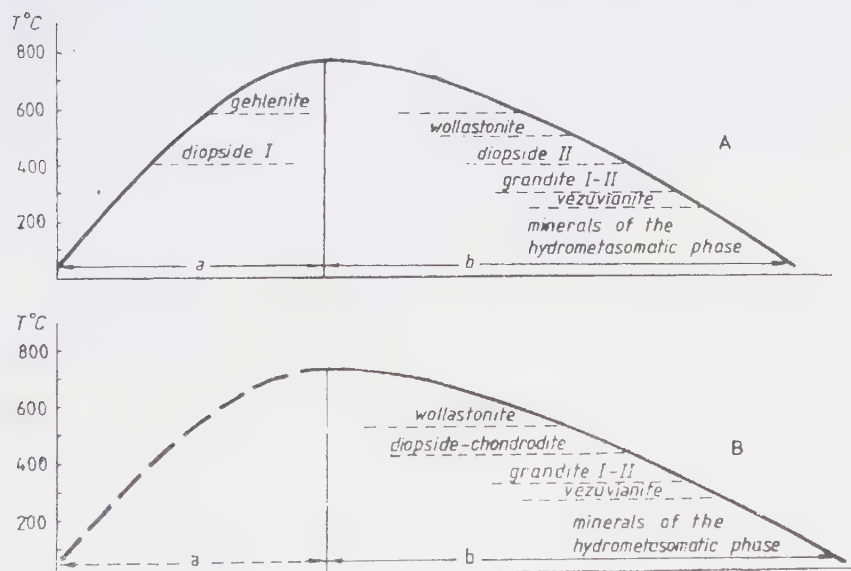
Fig. 5. The evolution of the temperature described by the sequence of skarn minerals for the contact aureoles in Oraviţa Valley (A) and Ţiganilor Valley - Ciclova (B).

of gehlenite which differentiates the Oravița skarns from other occurrences in Banat.

The crystallisation sequence of the skarn minerals illustrates the variability in time of the temperature factor. Thus, the associations identified in the aureole of the Oravița body indicate the existence of two main stages in the evolution of temperature:

- a progressive (heating) phase represented by the diopside I-gehlenite association;
- a regressive (cooling) phase during which wollastonite-diopside II + calcite - garnet I - garnet II - vesuvianite - clintonite - quartz - calcite - epidote were formed (Fig. 5A).

In the case of the Țiganilor Valley skarns there are no elements to suggest the manifestation of the two main phases in the evolution of temperature and therefore the existence of the progressive phase can be only presumed (Fig. 5B).

4. Conclusions

The ample pyrometasomatic processes generated by the intrusion of the Oravița - Ciclova magmatites differently affected the pre-existent formations. Skarns are confined to the contact zones between the intrusions and the Mesozoic sedimentary represented by the Crivina Beds, Marila and Brădet limestones.

Within the crystalline schists, the Permian sedimentary and partly, the Mesozoic one, isochemical metamorphites were generated which can be ascribed to the facies of hornblende hornfels or of albite and epidote hornfels. The particularities of the Oravița - Ciclova skarn occurrence refer to:

- the presence of mineralizers of F, Cl, B type in the reaction zones, materialized by the appearance of minerals such as: vesuvianite, chondrodite, scapolite and probably szajbelyite;
- the occurrence of gehlenite as a result of the high temperature (ca 750° C) reached in the contact aureole of Oravița Valley, in agreement with the more basic character of the Laramian magmatites occurring here;
- the confining of the substitution zones of the early skarn minerals by more recent mineralogical phases along microfissures and cleavages, indicating a good permeability of the reaction medium for the volatile components;
- the frequent absence of a clear periplutonic zoning beside the development of skarns as irregular bodies or columns, indicating the metasomatosis by infiltration and, subordinately, the bimetasomatosis as mechanisms of emplacement;
- the development of skarns with a complex composition on a background of a marly of clay-calcareous paleosome and of those with a simple composition against a calcareous paleosome;
- the microfissures occurring in skarn crystals which host the late depositions of vesuvianite and minerals of the hydro- metasomatic phase, indicating a general tendency of contraction manifested towards the end of the pyrometasomatic process;
- the existence of two main phases in the temperature evolution, at least in case of the contact zone of the Oravița Valley diorites: a heating phase, represented by the diopside I - gehlenite association, and a cooling phase, represented by the wollastonite - diopside II + calcite - garnet - vesuvianite - clintonite succession.

References

Born I. v. (1774), Briefe über mineralogische Gegenstände auf einer Reise durch das Temeswarer Banat, Siebenbürgen, Ober- und Nieder Hungarn - 9,47 Frankf. U.L.

Born I. v. (1780), Voyage minéralogique fait en Hongrie et en Transylvanie. M. Monet. Paris.

Castel M. (1869), Mémoire sur les mines et usines métalliques du Banat. *Annales des mines, 6-éme serie*, **XVI**, 440 - 449, Paris.

Cădere D. M. (1927), Fapte pentru a servi la descrierea mineralogică a României. *Mem. Acad. Rom.,* **2**, **8**, **4**, **5**, București.

Cioflică G., Popescu Gh., Constantinescu E. (1976) Raport, Arh. Cat. Min. Univ. București.

Cioflică G., Istrate Gh., Ştefan A., Vlad S. (1977) Contact metamorphism related to Laramian magmatism in Romania. Congr. Carpato-Balcanic Kiew.

Cioflică G., Vlad Ş., Vlad C. (1980) Magmatismul laramic şi metasomatoza asociată de la Ciclova (Banatul de sud). *An. Univ. Bucuresti*, **XXIX**, 56 - 69.

Cioflică G., Vlad S. (1981) Mineralizaţia cupriferă de la Ciclova. *An. Univ. Bucuresti*, **XXX**, 3 - 17.

Codarcea Al. (1930) Studiul geologic şi petrografic al regiunii Ocna de Fier - Bocşa Montană (jud. Caraş - Banat). *An. Inst. Geol.*, **XV**, Bucuresti.

Koch S. (1948) Bismuth Minerals in the Carpathian Basin. *Acta Szeged.*, **2**, Szeged.

Marka G. (1869) Einige Notizen über das Banater Gebirge. *Jahrb. d. k. k. geol. R. A.*, **XIX**, 318 - 349, Wien.

Mînzatu S. (1964) Şisturile cristaline din aureola de contact termic a banatitelor de la Oraviţa (Banat). *D. S. Com. Geol. Rom.*, **L/1**, Bucureşti.

Năstăseanu S., Constantinof D., Orăşanu Th., Stancu J., Rogge-Taranu E. (1967) Harta geologică a R.S.R. Scara 1: 50000 Foaia Oraviţa, Inst. Geol. Geofiz. Bucureşti.

Pieptea V. (1964) Contribuţii la cunoaşterea skarnelor din regiunea Oraviţa. *D. S. Inst. Geol. Geofiz.*, **XLIX/2**, 69 - 79, Bucureşti.

Popescu Gh., Constantinescu E. (1977) Observaţii mineralogice asupra skarnelor si mineralizaţiilor din regiunea Oraviţa. *An. Univ. Bucureşti*, **XXVI**, 45 - 58.

Rădulescu D., Dimitrescu R. (1966) Mineralogia topografică a României. Ed. Acad. RSR., p. 376, Bucureşti.

Schreyer A.V. (1976) Experimental metamorphic petrology of low pressures and high temperatures. In: Evolution of Crystalline Rocks. Academic Press London.

Scolari G., Lille H. (1973) Nomenclature et classification des roches sédimentaires. *Bull. B.R.G.M.*, **2/IV.2**.

Superceanu C. (1958) Skarne vezuvianice şi granatice cu conţinut de beriliu şi bor în zăcământul de contact de la Ciclova-Banatul de SV. *Rev. minelor*, **9**, **12**, 552 - 562.

Plate I

Fig. 1. Sectorial-type optical anomaly of garnets (Anton brook-Ciclova) N +, 250 x.
Fig. 2. Concentric-type optical anomaly of garnets (Chinisea Valley) N +, 250 x.

Plate II

1
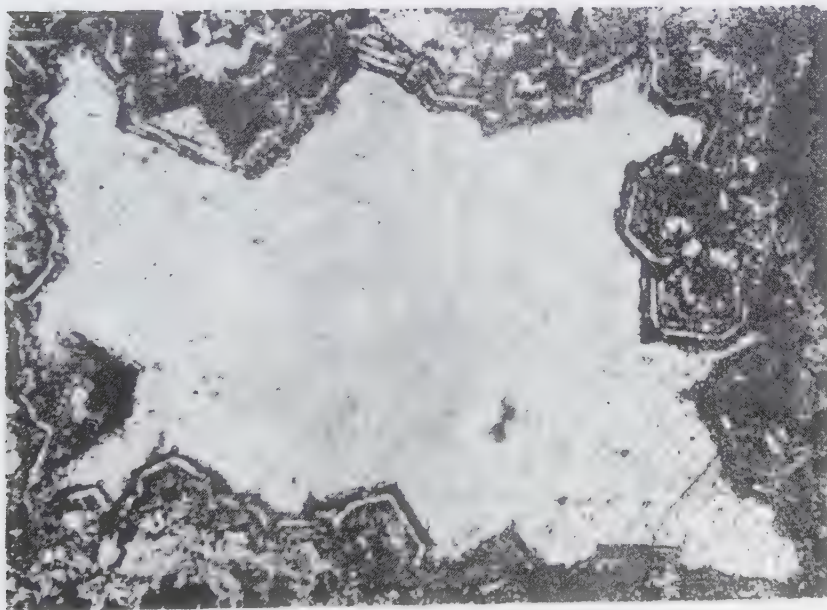
Fig. 1. Evolution of a garnet crystalloblast from rhomboidal dodecahedron to trapezohedron (Prisaca Hill) N +, ~ 300 x.
Fig. 2. Skeletal garnet crystalloblasts (Chinisea Valley) NII, 60 x.

Plate III
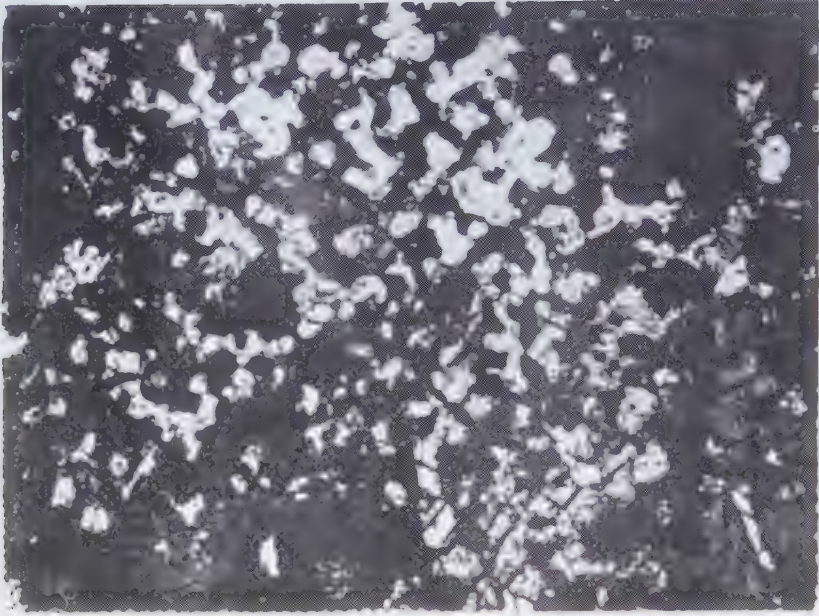
1

2

Fig. 1. Substitution structures of monzodiorite plagioclase feldspar by garnet (black) (Țiganilor Valley) N+, 150 x .
Fig. 2. Bipyramidal crystals of vesuvianite (Țiganilor Valley).

Plate IV
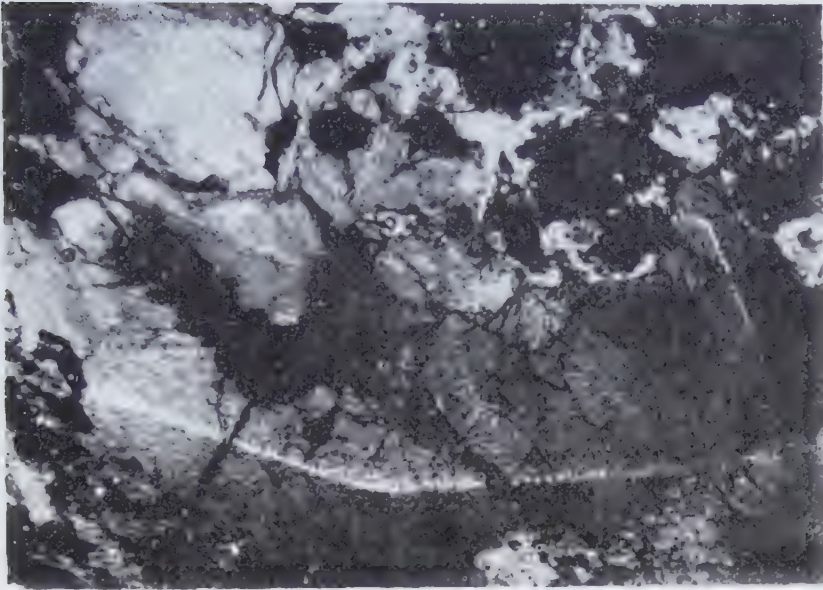
1
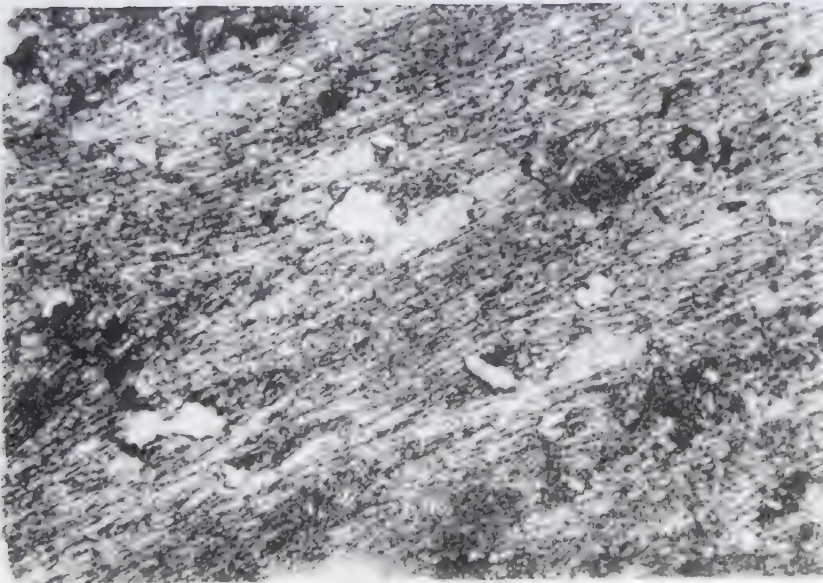
2

Fig. 1. Remnants of andraditic garnet in vesuvianite; an increase of the vesuvianite birefringence in the reaction zone is visible (Țiganilor Valley) N+, 250x.
Fig. 2. Vesuvianite pseudomorph after a fibrous-radial mineral (Țiganilor Valley) N II, 160 x.

Plate V
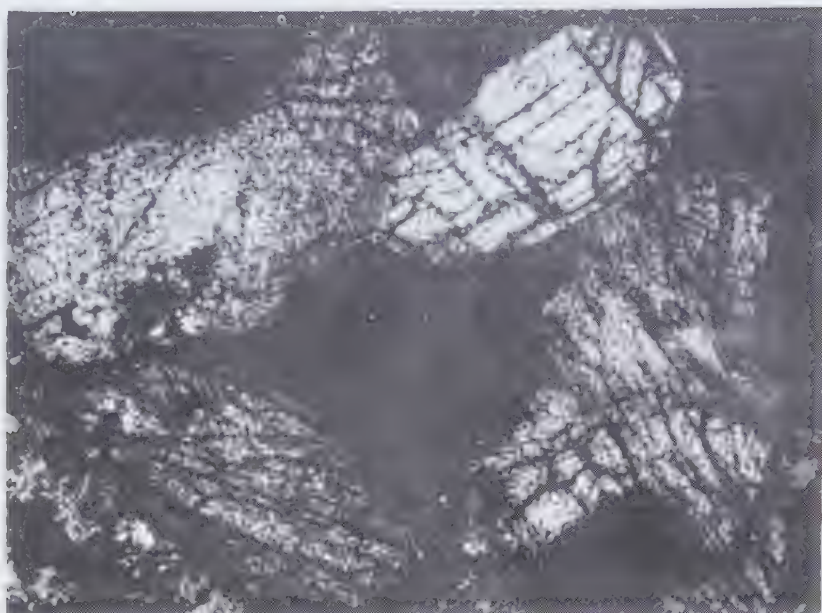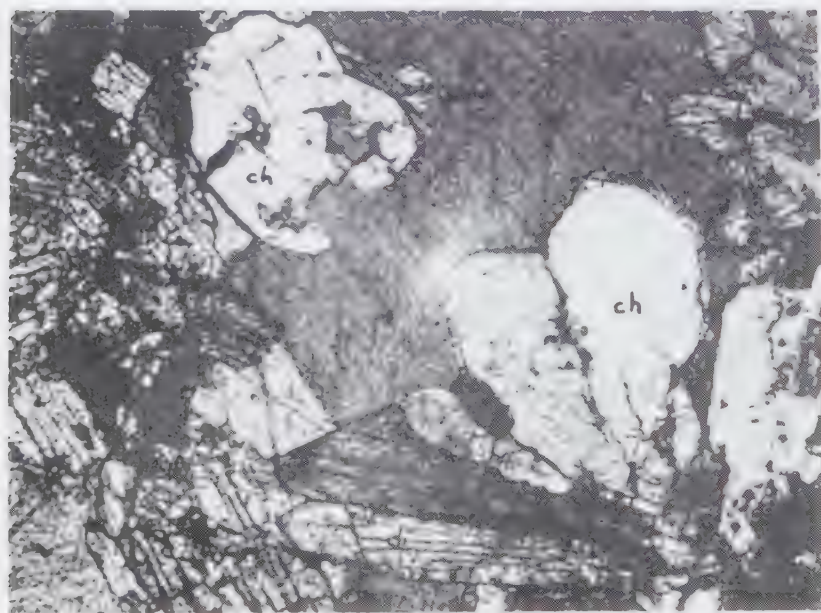
Fig. 1. Gehlenite (Crişenilor brook) N+, 60 x.
Fig. 2. Radial intergrowths of chondrodite (ch) and diopside (di). (Ţiganilor Valley), N+, 160 x.

Plate VI
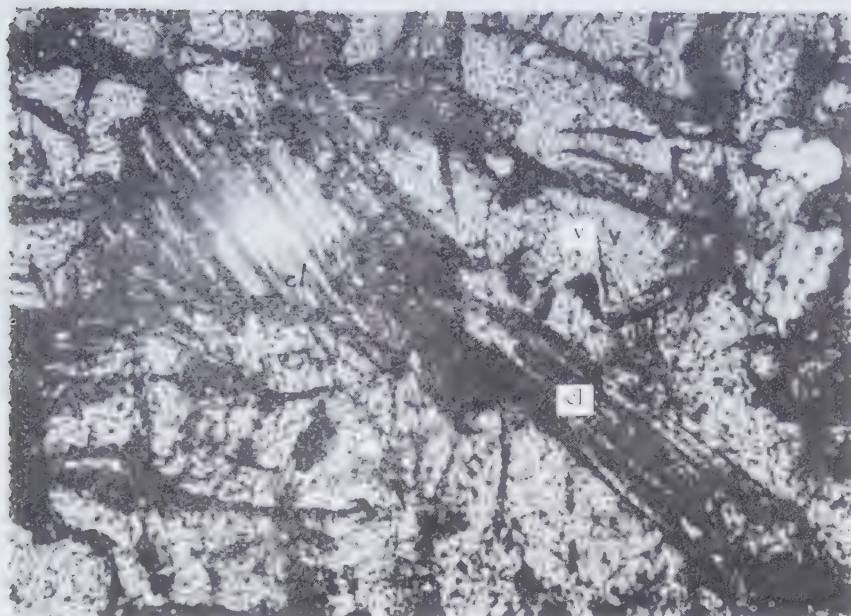
1
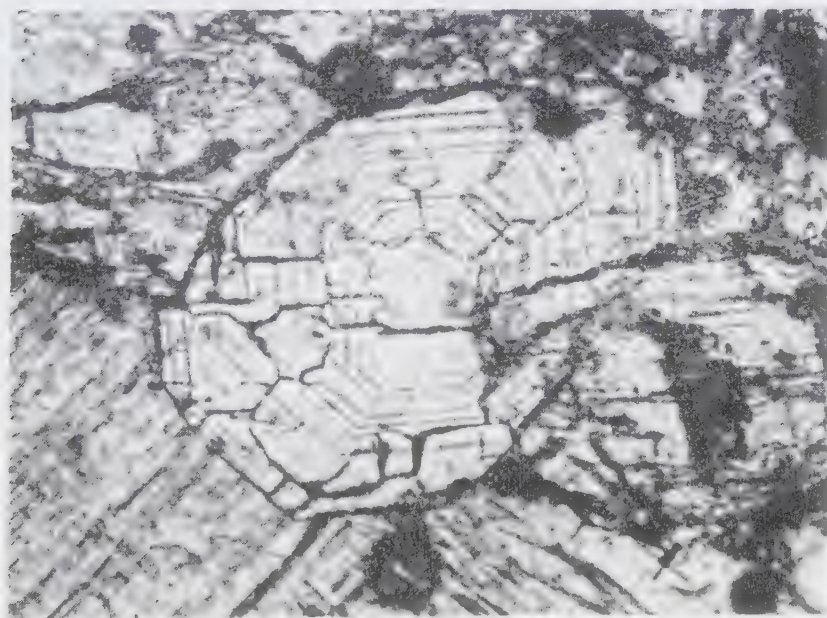
2

Fig. 1. Clintonite (cl) in vesuvianite (v) (Crişenilor brook) N II, 300 x.
Fig. 2. Basal section of a scapolite crystal; the stages of growth from tetragonal prism to ditetragonal prism by the development of the (110) face are visible. N II, 300 x.

The petrography and petrogenesis of the vein rocks from the alkaline massif of Ditrău

NICOLAE ANASTASIU
EMIL CONSTANTINESCU
NAZAR GARBAŞEVSKI
GYULA JAKAB

In the Ditrău alkaline massif vein rocks are represented both by salic types – leucosyenites, porphyry microsyenites, bostonites, albitites, foidic syenites, tinguaites, alkali granites, aplites, pegmatites and mafic types   vogesites, kersantites, spessartites, camptonites, odinites. The vein rocks were intruded in two stages – late-magmatic and post-magmatic – characterized by hypersolvus (liquidus-solidus) and recrystallization processes. Old faults and "needle" joints controlled the emplacement of the veins; a connection between mechanical strain and recrystallization was observed.

One of the petrographical and structural features of Ditrău alkaline massif is the frequency and the great variety of the vein rocks. Their presence within the massif has been previously noticed (Ianovici, 1933, 1938; Streckeisen, 1952, 1954), but without detailed petrographic description or correlation between petrogenesis and metallogenesis.

The recent interest on vein rocks was due to their spatial location and their apparent relationship with the mineralization from Jolotca and from Aurora-Hereb zone. The petrographic observations allow a better systematic of the vein ores (Anastasiu, Constantinescu, 1980) and implicitly yield a more complete petrogenetic image.

Petrographic types

The frequency of vein rocks in Ditrău massif is an obvious proof of successive insets of magmatic differentiation products related to the alkaline melt, rich in salic or femic minerals. The intrusion was structurally controlled by an irregular system of faults and diaclases (Anastasiu, Constantinescu, 1980). The cooling conditions of magma explain their structural diversity: micro-, mesocrystalline and pegmatoid facies. The connection with the main types of massif rocks is revealed by the mineralogical composition.

The vein rocks are represented by leuco-syenites, porphyry microsyenites, bostonitic

microsyenites, albitites, foidic syenites and microsyenites, tinguaites, alkali granites, aplites and pegmatites as prototypes with leucocrate trend – and by lamprophyres – vogesites, kersantites, spessartites, camptonites and odinites - as prototypes with melanocratic trend. Less spread are the veins with carbonates, epidote, sodalite and biotite.

Leucosyenites. Leucosyenite veins occur in the ultramafites and diorites from the northern compartment, cropping out along the basin of Jolotca Valley and all the mining adits of the perimeter; they frequently display zoning structures (Fig.1). In the central compartment, they occur within essexites along Ditrău -

varieties constitute the most frequent vein rocks. They cut the ultramafites, diorites, essexites and even massive syenites or monzonites. These veins crop out in the basin of Jolotca valley, in Valea Mare of Ditrău, in the road Ditrău- Tulgheş, in the basin of Belcina Valley (Aurora - Hereb - Cianod zone) and in the Chiurutz Creek. In outcrops the rocks appear white or pink in color. They have a microcrystalline structure and are poor in femic minerals; therefore they are described as aplites (despite the fact that rocks do not contain quartz !). Their porphyry structure, which is due to the inequigranular character of feldspars, or the bostonitic structure, suggested by the slight orientation of albite and of K-
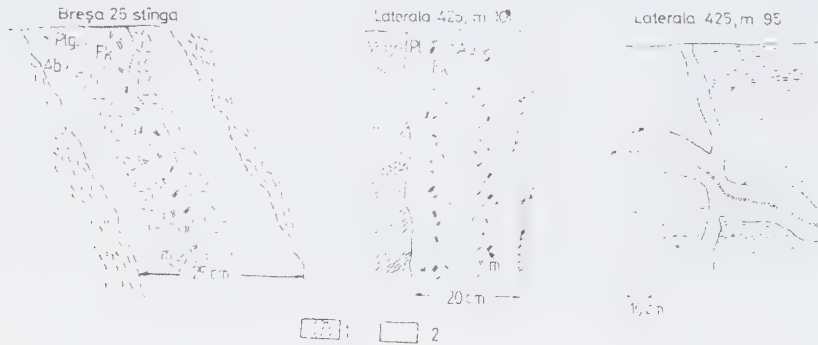
Fig. 1. Zonal structure of syenitoid veins (2) piercing hornblendite and diorite (1) Jolotca Valley; Fk - perthite potassium feldspar; Plg. plagioclase; Ab, albite.

Tulgheş road and in the upper basin of Putna Creek. The veins appear either isolated, or as vein networks, with successive injections. The mineralogical composition is given by: alkalifeldspar (microcline and albite) 60%; plagioclase (An_{10-15}) 30%; biotite ($\pm$) and/or hornblende 8%; accessory minerals (zircon, corundum, calcite, epidote) 2%.

Porphyry microsyenites and bostonitic microsyenites. In the marginal zone of the alkaline massif of Ditrău, the microsyenite

feldspar in the ground mass, could be observed only microscopically.

The veins have centimetrical and decimetrical thickness and cut the host rocks on lengths of tens or hundreds of meters. Most of them have a discordant character related to the structural elements of the host rocks; some of them are concordant separations (especially, in meladiorites). They crop out as parallel systems, with apparently normal strike on the contour of the massif. Their mineralogical composition comprise: alkali-feldspar

(microcline and albite) 60-75%; plagioclase (An_{10-18}) 10-25%; muscovite 2-4%; biotite 5-7%; amphibole 2-3%; accessory minerals (zircon, apatite, corundum, calcite) 2% (Pl. I, Fig. 1).

Albitites. The rocks are formed mainly by albite and have been intercepted by XX and XXV adits (Jolotca basin). They crop out in Valea Mare - Ditrău, Cianod Creek-Hereb and in the Belcina-Aurora zone, where they intersect meladiorites and diorites, and essexites and syenites respectively.

The mineralogical composition is simple: albite 70-80%, microcline and/or plagioclase 10-15%, muscovite 5%, accessory minerals (zircon, corundum, apatite) 3% (Pl. I, Fig. 3).

At the periphery of the central body of foidic syenite from Valea Mare-Güdütz-Priczke and in the vicinity of the apophyses from Teascul hill, veins of nepheline syenite with meso- and microcrystalline structures are developed (Pl. I, Fig.2).

The mineralogical composition is represented by: alkali-feldspar 50-70%; nepheline 20-40%; plagioclase 5-10%; biotite and/or hornblende 5-10%; accessory minerals (zircon, apatite, cancrinite) 3-5%.

In the central zone of the alkaline massif of Ditrău (Valea Mare-Prizcke Peak and subordinately in the peripheral parts) tinguaite veins are associated with foidic rocks or intersect monzonites and syenitoides; the mineralogical composition comprises: alkali-feldspar (microcline and albite) 40-55%; nepheline 30-35%; augite-aegirine 4-8%; biotite 4-8%; amphibole 3-5%; accessory and secondary minerals (zircon, apatite, cancrinite, analcime, calcite, sodalite) 3%.

In the massif of Ditrău, the veins of quartz-feldspar rocks occur accidentally and belong to various petrographic categories, as alkali granites, aplites and pegmatites.

Lamprophyres. The veins of lamprophyres constitute a distinct feature for the alkaline massif of Ditrău. They are well spread both in the northern and southern compartment and exhibit sharp limits in the mass of ultramafites, mafites, diorites, syenitoides, granitoides, foidic syenitoides and essexites, as well as in the peripheral zone of the massif. Their position and the relationship with the leucocrate veins suggest multistage occurrences. Thus, it could explain the presence of, both, fresh and highly altered rocks in the same area.

The veins expose variable thickness – from centimetrical to metrical – and spans over hundreds of meters Their systems usually comprise parallel, subparallel, branching or anastomosing branch veins. Inward, the rocks are black, black-grayish or dark green, with microcrystalline structure, wherein appear phenocrystals of femic minerals (amphibole or pyroxene). The porphyric structure can also be noticed microscopically.

The mineralogical varieties of lamprofires can be separated only at microscopic scale: biotite calc-alkaline lamprophyres (minettes and kersantites), amphibolic (vogesites and spessartites) and alkaline lamprophyres (camptonites) (pl. I, fig. 4).

Beside the leucocrate vein rocks and lamprophyres, in the alkaline massif of Ditrău appear veins or vein networks, with monomineral - or almost monomineral compositions, corresponding to late hydrothermal deposition along dislocations and various systems of fractures that affected the body. This is the case of carbonate, epidote, sodalite and biotite accumulations.

Petrogenetic considerations

The petrographic diversity and the complex structure of the alkaline massif of Ditrău are the result of a polystadial petrogenetic processes accomplished over a long period of

time. In its evolution, the occurrences of vein rocks marked a final moment of geological structure (Anastasiu, Constantinescu, 1980; Anastasiu and colab., 1983). The presence of veins in the massif pleads for a magmatic stage, whereas their petrographic nature confirms the comagmatic character.

The examination of the petrographic types revealed the existence of a great number of rock, which support "vein" facies but, excepting the lamprophyres, they have identical mineralogical constitutions with those of the main "body" facies or of "marginal" one. These affinities characterize the calc-alkaline and alkaline rocks, feldspar and quartz-feldspar foidic rocks; the rocks which do not expose a "vein" facies are mafites, ultramafites and essexites, while the vein ones without an equivalent in lareg "body" facies are albitites, lamprophyres and the concentrations rich in epidote, carbonate, sodalite and biotite. The presence of magmatic differentiates with obvious consanguinity within the massif and in the peripheral zone, illustrates the great extent in time of magmatic porcess. The relationship between the veins and their the host rocks reveal the polystadial character of the massif and allow to establish the stages of its evolution.

Thus, one could separate two main stages in which vein rocks occurred: late-magmatic and post-magmatic stages, characterized by: (A) crystallization processes hipersolvus (liquidus-solidus) and (B) recrystallization processes, preceded and/or followed by deformations in subsolvus conditions (Fig. 2).

During late-magmatic stage, when the huge magmatic mass was generating the main "body" facies, residual products successively occurred. In a first stage (late-magmatic I) calc-alkaline vein rocks occurred; leucosyenites, alkali granites, aplites, pegmatites and, during the second (late-magmatic II), the alkaline ones: foidic syenites and tinguaites. Now appeared the first generation of lamprophyres
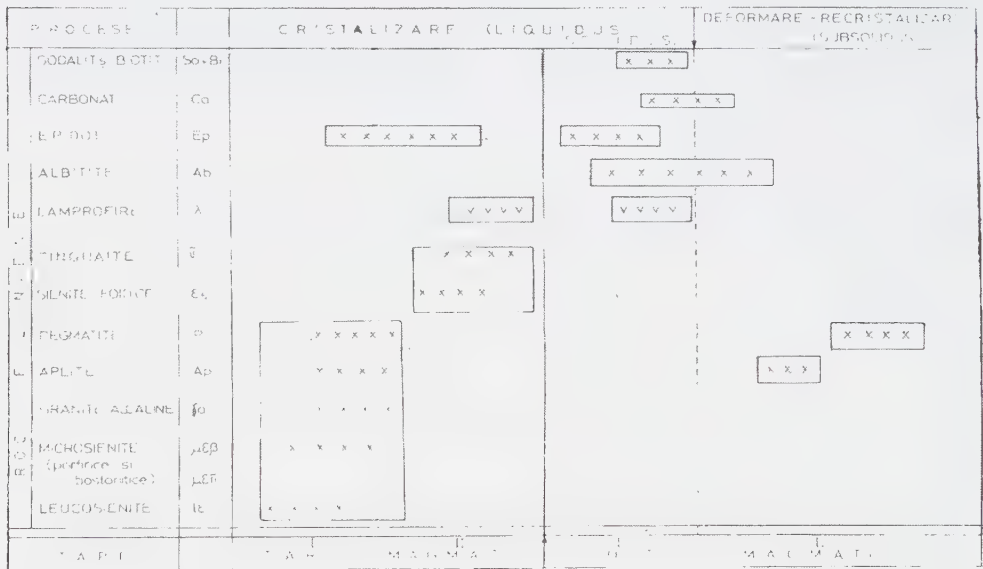
Fig. 2. The succession of vein rocks from alkaline massif of Ditrău – stages and processes.

(highly altered, with primary paragenesis obliterated almost entirely) and a part of the epidote veins.

The differentiation of the vein rocks is of Atlantic type, framed by the sodic character, very peculiar for the whole assemblage of rocks. There is an advanced differentiation between the vein rocks and the massif rocks. The tinguaites evolved towards the nonsaturation in SiO_2 (the Kenedy trend), and the lamprophyres towards the increasing of the alkaline character. The vein products cluster around the final crystallization points of alkali-feldspar-nepheline eutectic and under the curve of alkali-feldspar-quartz eutectic.

The access ways of the magma coincided partly with some rupture deformations massif; such a coincidence appears between the system of diaclases from Jolotca perimeter (NW-SE and NE-SW) and some veins of lamprophyres.

In the post-magmatic stage, after the consolidation of the massif and, probably, simultaneously with the cooling stages, the appearance of vein rocks was due to successive crystallization processes from volatile-rich solutions (A) and to recrystallization processes triggered by plastic and rupture deformations, which changed the previous thermodynamic equilibrium (B).

During the post-magmatic stage I, the second generation of lamprophyres developed and differentiated rich in albite (albitites) and concentrations of, epidote, carbonates, fluorite, sodalite and biotite.

The ways of access had a fissural character. In all the alkaline massifs where they have been identified, these minerals represented late depositions from solutions rich in volatile (F, CO_2, O_2 etc.) and having an excess of alkaline elements (Na, K).

A second stage (post-magmatic II) occurred during the slow cooling of the massif and was characterized by subsolvus processes (exsolution, remobilization and substitution at small scale, recrystallization etc.), with a local character or extended along rupture dislocations. In such conditions, associations of feldspar minerals became stable (perthites, albite recrystallizations, quartz-feldspar intergrowth). Some veins of albitite and pegmatite are the result of such processes. For the albite neoformations, the nonequilibrum could mean a dissolution process, with the release of sodic phase and its remobilization by diffusion at microscopic scale.

The microscopic study revealed a strong connection between the mechanical deformation (marked by relics of bent micas, clastic feldspar) and recrystallization (albite euhedral crystals, decalcification, loss of alteration etc.).

The fragmentation of old crystals increase their reaction surface and the appearance of new crystalline germs; their growth during mechanical deformations involves the multiplication of crystalline grains and thus a general increasing of transformation speed, every "granoclast" becoming a new growth core. A solid state process (favored by an intergranular fluid) can also be accepted to interpret the substitution relationships between the maximum microcline and plagioclase feldspar from the syenitoides and foidic syenite veins.

The occurrence of leucocrate veins was controlled by old dislocations or fissures which affected the massif during its cooling or immediately afterwards (usually, "needle"-like diaclases). The same path was followed by lamprophyres, individualized as veins, subparallel with syenitoids, orientated NW-SE, E-W and, subordinately NW-SE in the perimeter Valea Mare-Güdutz.

References

Anastasiu N., Constantinescu E. (1980) Structure du massif alcalin de Ditrău, *Anal. Univ. Bucuresti*, **XXIX**.

Anastasiu N., Constantinescu E., Garbasevschi N., Jakab G. (1983) Controlul structural al amplasării filoanelor în masivul alcalin de la Ditrău, *Anal. Univ. Bucureşti* (sub tipar).

Jakab G. (1982) Studiul mineralogic şi geochimic al mineralizaţiilor metalifere dintre Voslobeni si Corbu, Teză de doctorat. Biblioteca Univ. "Al. I. Cuza", Iaşi.

Ianovici V (1933) Etude sur la massif syenitique de Ditrău region Jolotca, district Ciuc (Transilvania), *Rev. Muz. Mineral. Univ. Cluj*, **4**, 2.

Ianovici V (1938) Consideration sur la consolidation du massif syenitique de Ditrău en relation avec la tectonique de la region. *C.R. Ac. Şci. Roum.*, **II**, **6**, 689 - 694.

Streckeisen A. (1952, 1954) Das Nephelinsyenit - Massif von Ditro, Schw. *Min. Petr. Mitt.*, **32** (I) - **34** (II), Bern.

Plate I.
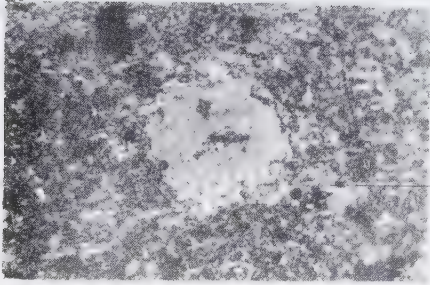
Fig. 1. Porphyry microsyenite; vein in the Cianod quarry, N+; x 20
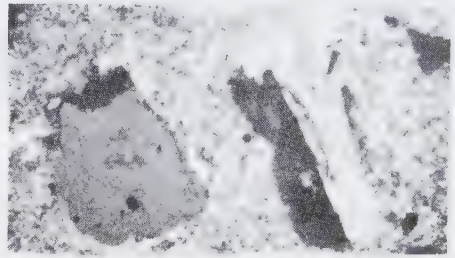
Fig. 2. Foidic microsyenite with porphyry structure; vein in the Cianod quarry; N+, x 20.
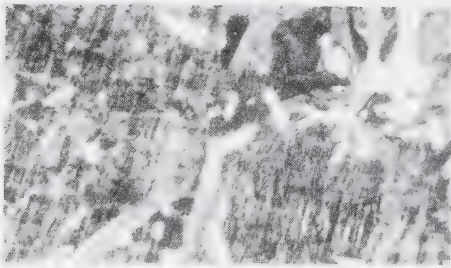
Fig. 3. Recrystallization albite in an albitite vein; Hereb gallery; N+; x 20.
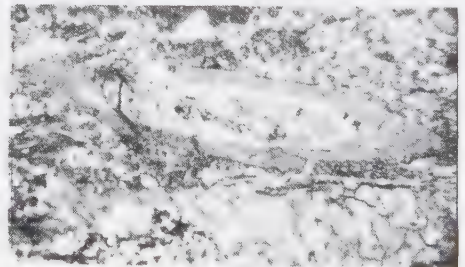
Fig. 4. Zonned barkevikite in camptonite; lamprophyre vein in Cianod Creek; N+; x 20.

Petrographical and structural criteria for the outlining of vein fields in the alkaline massif of Ditrău

NICOLAE ANASTASIU
EMIL CONSTANTINESCU

In the area of the alkaline massif of Ditrău, the vein rock occurrences are frequent, with distinct petrographical and structural features. Their presence within the massif signify a distinct moment in the evolution of the magmatic processes. The vein rocks may also represent metallogenic indicators.

The spatial distribution of the vein rocks in uneven. They concentrate in the marginal zones of the massif and denote structural "access ways", usually in the form of dislocations or areas of low free energy, compatible with subsolvus transformations. In the central part of the massif, the veins are hardly distinguishable. Here, the presence of the vein rocks may be deduced from specific relations between microcrystalline and normal-grained facies.

The delimitation of vein fields in the marginal areas of the massif is determined by: (1) mineralogical and petrographical affinities of the veins, (2) their structural and textural features, (3) the connection or the lack of connection with the mineralized zones. The control exerted by the major structural frame work is also obvious; it is noticeable through the frequency and the position of the veins, their shape and their concordant or discordant character. From this perspective, the veins are an expression of (1) the disjunctive tectonics manifested prior to their emplacement and (2) the existence within the massif of "S"-type planes, with a visible directional continuity (Anastasiu, Constantinescu, 1980).

From a petrographical point of view, the vein rocks may be classified in felsic facies - leucosyenites, porphyritic and bostonitic microsyenites, foidic syenites and microsyenites, tinguaites, alkali granites, aplites and mafic facies - various lamprophyres (vogesites, kersantites, spessartites, camptonites, odinites). A part of the vein rocks are represented by monomineralic agglomerations such

as albitites, epidotites, carbonate veins, or correspond to simple assemblages, e.g., sodalite and biotite. The bulk mineralogical composition of the vein rocks reflect a tight connection with the rocks of the main massif. Their structural diversity (e.g., microcrystalline, medium-grained and seldom pegmatoid facies, reflect the cooling conditions of the parental magma and sketch the temporal extension of the magmatic processes.

In the two structural compartments of the massif-expressed in the relief by their uneven vertical extensions (Anastasiu, Constantinescu, 1980) - the following vein rock fields can be outlined on the basis of the above-mentioned criteria:

In the northern compartment - "Jolotca", the veins concentrate in two sectors:

I. "Pietrari - Teascului" vein field;
II. "Jolotca - middle course" vein field.

In the central-southern compartment - "Valea Mare - Güdutz - Belcina", there are seven vein fields:

III. "Valea Mare" vein field;
IV. "Güdutz" vein field;
V. "Chiuruţ" vein field;
VI. "Cianod" vein field;
VII. "Hereb - Balas - Lorincz" vein field;
VIII. "Aurora" vein field;
IX. "Putna - Călugăr" vein field.

In the northern compartment, the vein rocks cross-cut ultramafites (pyroxene- and biotite-bearing hornblendites), mafites (meladiorites), diorites and monzodiorites. They are represented by medium- or microcrystalline, biotite-bearing syenites and by lamprophyres (vogesites and spessartites). The separation of the two fields has been made possible by applying petrographic and metallogenic criteria. Thus, in "Pietrari - Teascului" field (I) we distinguished in addition to the already mentioned types, albitites and kersantites. Here,

the lamprophyres and epidotites are emplaced parallel with veins of sulfides (pyrite, chalcopyrite, sphalerite, pyrrhotite, molybdenite), oxides (Ti, Fe, Th, Nb) and phosphates (monazite-Ce) in a gangue with calcite, orthite, rutile, anatase, siderite, parisite, albite. "Jolotca - middle course" field (II) lacks kersantites and mineralized veins. In both fields the veins appear either discordant or concordant with the planar elements of the mafites (S2 planes defined by the orientation of micas and amphiboles).

In the "Valea Mare - Güdutz - Belcina" compartment the vein rocks show a larger mineralogical and petrographical diversity, often suggesting a petrogenetical link with the "main body" facies. The individuality of the vein rocks is given by the nature of the rocks forming the association in question as well as by the nature of the host rocks. The structural control of the emplacement of the vein rocks is given here by the S1, S2 planes (with which the veins are both concordant and discordant) and by the disjunctive dislocations - fractures and diaclases. Thus, in the fields III and IV, the position of the syenitoides coincides partially with the direction of the S2 planes. In the field V, veins are concordant with the fractures in the area, oscillating slightly around NS, but discordant with the structural elements of the host rocks. In the field VI, the felsic veins and the lamprophyres are grouped in two systems emplaced one after another. The syenitoides and microsyenites are older than the tinguaites. The sub-horizontal lamprophyres are sheared by the vertical lamprophyres. In the fields VII and VIII the vein rocks are concordant with the NS fissure system in the area, whereas the sulfide mineralisation are concordant with the porphyritic microsyenites. In the field IX the vein network is anastomosed. Here, the lamprophyres shear the tinguaites.

In "Valea Mare - Güdütz - Belcina" compartment, the most frequent veins are those of porphyritic microsyenites. The syenites and tinguaites are confined to this area only.

Table 1. Rock assemblages in the vein fields of the alkaline massif of Ditrău

Vein field	Petrographic assemblages	Host rocks	Associated mineralisation
I Pietrari Teascului	biotite-bearing syenites, porphyritic microsyenites, albitites, lamprophyres (K+S+V)	hornblendites meladiorites diorites	molybdenite, pyrite, sphalerite, chalcopyrite, monazite (Ce), Ti, Th, Nb-oxides
II Jolotca	leucosyenites, porphyritic microsyenites, lamprophyres (V+S)	diorites, monzodiorites	
III Valea Mare IV Güdütz	leucosyenites, porphyritic microsyenites, albitites, tinguaites, lamprophyres (K+S+C)	essexites, foidic monzodiorites	
V Chiuruţ	albitites, porphyritic microsyenites, alkaline granites, pegmatites, lamprophyres	syenitoides, granites, crystalline schists	
VI Cianod	leucosyenites, porphyritic microsyenites, bostonitic microsyenites, tinguaites, lamprophyres (S+C)	foidic syenites foidic monzonites, syenites, alkaline granites, crystalline schists	
VII Hereb Balaş Lorincz	porphyritic microsyenites, albitites, sodalite + biotite, lamprophyres	syenitoides, alkaline granites, crystalline schists	
VIII Aurora	leucosyenites, porphyritic microsyenites, bostonites, aplites, tinguaites, lamprophyres	white syenites, pink syenites nepheline	molybdenite, pyrite, sphalerite, galena, xenotime (Y), Nb,Ti ± Th oxides
IX Putna – Călugăr	tinguaites, foidic syenites		

K – kersantite; S – spessartite; V – vogesite; C – camptonite

Pegmatites are rare, occurring only in field V. Their overall properties and the shape are not constant along the direction of the veins. The dimension of the component crystals is also variable. The occurrence of pegmatites is accompanied the development of muscovite, albite and zircon.

Albitite veins are characteristic for the southern compartment. They are often located along highly mobile fractures and contain minerals with various degree of deformation, suggesting the continuity of the (re-)crystallization processes after the cessation of the movements.

On the entire border of the massif, the vein rocks overrun the limit between the magmatic body and the crystalline schists, thus getting a clear discordant character. In the southern

compartment, the lamprophyre veins form two clearly distinct generations: spessartites and camptonites, with the former type prevailing.

In all the studied fields the density of the veins is higher where the host rock has a mafic character (ultramafites and mafites).

The mineralisation is genetically related to the alkaline rocks and occurs as disseminations and subordinately, as veins (e.g., Hereb vein field and Aurora - inside the massif, and Belcina - outside it). At Hereb and Aurora the sulfide mineralisation (molybdenite, pyrite, sphalerite and galena) together with REE and a gangue containing fluorite, calcite, Nb- and Ta-bearing pyrrochlore, bastnäsite, niobite, occurs concordantly with syenitoide and partly lamprophyre veins. At Belcina the mineralisation takes a clear vein form and consists of sulfides (sphalerite, galena, arsenopyrite, pyrite, molybdenite), xenotime (with Th and REE), siderite, fluorapatite, chlorite, calcite, quartz, rutile, anatase (Jakab, 1982).

The vein mineralisation is located in the crystalline schists in the aureole of the Ditrău massif. The petrogenetical and structural study of the mineralisation (Constantinescu et al., 1981) pointed out two characteristics which are in a sense similar to the situations described for the vein rocks:

1) the existence of multiple generations of minerals (e.g., pyrite-1, pyrite-2; orthite-1, orthite-2);
2) the existence of breccification structures signifying the tight relationship between breccias and mineralisation; similarly, for the vein rocks a relationship between deformation and recrystallisation could be described, suggesting the role played by the recrystallisation processes in the attainment of the present mineralogical relations. Such a conclusion may direct the prospecting works toward areas with known post-magmatic deformations, a plausible host for the reconcentration of the mineralisation.

Conclusions

The emplacement of the vein rocks has marked a moment of completion of the geological structure of the alkaline massif of Ditrău, pleading for the existence of a magmatic stage of evolution. The petrographical nature of the veins confirms their co-magmatic character. The number of rock types found in vein facies is large. With the exception of the lamprophyres, their mineralogical composition is identical with that found in the "main body" or marginal facies.

The relation between the veins and the host rocks suggests the multistage character of the massif and the generation of the vein rocks in two stages: late-magmatic and post-magmatic (Anastasiu, Constantinescu, 1983).

The frequency of the vein rocks increases in the neighborhood of the areas affected by fractures. However, no permanent correlation could be established between these two elements: the rupturing deformation followed by recrystallisation in subsolvus conditions, probably had a role in the formation of the albitites, aplites and carbonate-bearing veins. The separation of the vein fields is possible in areas with high frequency of vein rocks and imposes itself as a premise for a better understanding of the potentially economic zones. The criteria for their outlining are viable and regard the mineralogical and petrographical nature of the rocks, elements of major structural nature (rupturing dislocations), the host rocks and their position within the massif.

Taking into account the nature of the metallic concentrations within the massif and their position in the vein fields, the following metallogenic indicators - useful in directing prospecting and exploration work - can be considered:
- the identification of the access ways in areas with old and regenerated disjunctive dislocations, which allowed remobilizations of the mineralisation in zones other than the known ones (Jolotca, Aurora);
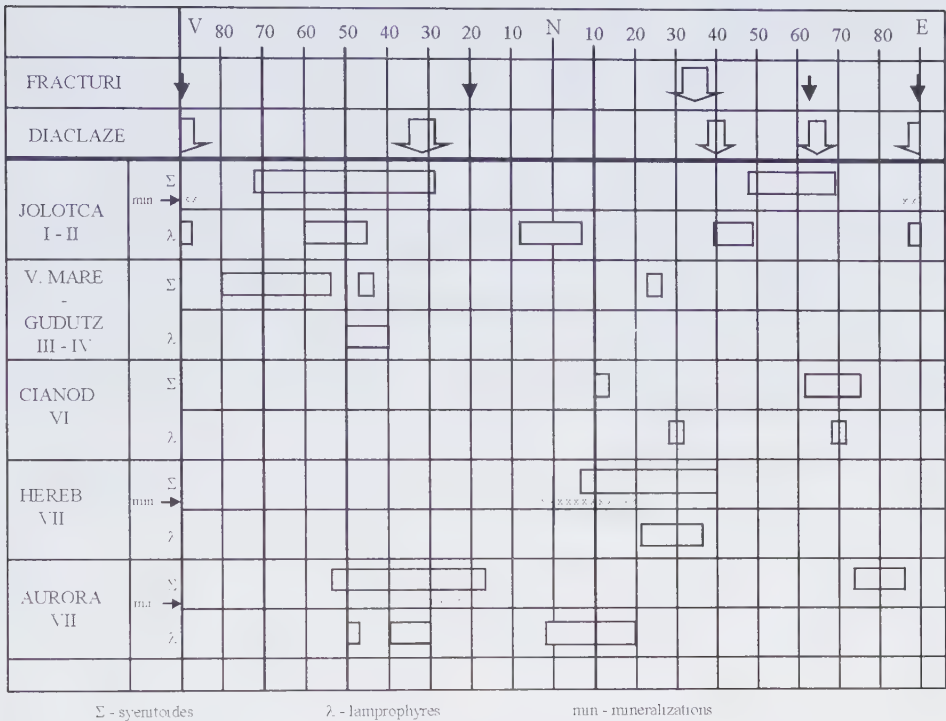
Fig. 1. The repartitión of the directions corresponding to syenitoides, lamprophyres and mineralization veins in the alkaline massif of Ditrău (I VIII: field veins).

- the following-up of areas with deformations and recrystallisations;
- the identification of the areas petrographically similar to those hosting metallic concentrations; from this point of view, Chiurutz and Cianod fields are potentially interesting;
- secondary phenomena such as argillizations, epidotizations, in the areas of hydrothermal circulation represent in their turns, important criteria for following-up and extending mineralized zones.

References

Anastasiu N., Constantinescu E. (1980) Structure du massif alcalin de Ditrău. *Analele Univ. Bucureşti*, **XXIX**.

Anastasiu N., Constantinescu E., Garbasevschi N., Jakab G. (1982) Controlul structural al amplasării filoanelor în masivul alcalin de la Ditrău. *Analele Univ. Bucureşti*, **XXXIV**, 43-55.

Anastasiu N., Constantinescu E., Garbaşevschi N., Jakab G. (1983) Petrografia şi petrogeneza rocilor filoniene din masivul alcalin de la Ditrău. *St. cerc. geol., geofiz., geogr., s. geol.*, **28**, 17-23.

Jakab G. (1982) Studiul mineralogic şi geochimic al mineralizaţiilor metalifere dintre Voşlobeni şi Corbu. Teza de doctorat, Univ. Al. I. Cuza, Iaşi.

Ianovici V., Constantinescu E., Anastasiu N. (1982) Petrochimia lamprofirelor din masivul alcalin de la Ditrău. *Rev. roum. géol., géoph., géogr., s. géol.*, **29**, 5-17.

Ianovici V. (1933) Etude sur le massif syenitique de Ditrău, region Jolotca, district Ciuc (Transylvanie). *Rev. Muz. Mineral., Univ.* Cluj, **4**, 2.

Ianovici V. (1938) Considerations sur la consolidation du massif alcalin de Ditrău en relation avec la tectonique de la region. *Compt. R. Acad. Sci. Roum.*, **II-6**, 689-694.

Streckeisen A. (1952-1954) Das Nephelinsyenit - Massif von Ditro. *Schw. Min. Petr. Mitt.*, **32(I)-34(II)**, Bern.

Contributions to the petrological and structural knowledge of the Ditrău alkaline massif – metallogenic implications

NICOLAE ANASTASIU
EMIL CONSTANTINESCU

Petrographic and structural studies show that the Ditrău alkaline massif is a quasi-circular body, discordantly emplaced in the crystalline schists of the East Carpathians. The massif is made up of several petrographic types: hornblendites, diorites, essexites, monzodiorites, monzonites, foidic monzonites, alkali feldspar syenites, foidic syenites, granites; vein rocks include: tinguaites, aplites, mariupolites, minettes, spessartites, kersantites, vogesites, camptonites. A zonality is suggested by the distribution of the main rock types in the central part and of the dykes in the marginal zone of the massif. The metallogenetic specialization of the massif is a consequence of magma fractioning, of the primary processes controlling its crystallization and of secondary – postmagmatic processes. The main metallic elements concentrated in the massif – Zr, Ti, Nb, V, Th, Mo, REE, Fe, Pb, Zn, P are constituents of two metallogenetic formations: 1) the primary formed by segregation or magmatic dissemination; 2) postmagmatic pneumatolitic-hydrothermal formation.

In order to determine its metallogenetic potential, the Ditrău alkaline massif, well known in the entire world for its mineralogical and petrographical features, was the object of numerous geological and geophysical prospecting during the late decades. Following a series of important studies (Ianovici, 1933, 1938; Codarcea, Ianovici, 1954; Streckeisen, 1954, 1960, 1974) which yielded various petrogenetic models of the massif, recent studies (1974-1982) emphasized a series of distinct mineralogical, petrographical and structural features; they concentrated on defining the phases of evolution, defining the metallogenetic indicators and the diversification of possibilities to emphasize all the mineral resources within the massif.

The mineralogical studies – carried out by modern physical methods – have enriched the mineralogical inventory with 17 mineral species of which four are rare minerals described for the first time in Romania: kalsilite, magnesium, riebeckite (Constanti-

nescu, Anastasiu, 1979); zeophyllite, pyro-phanitic ilmenite (Constantinescu et al., 1981).

Quantitative determinations of the mineral participation in the main petrographic assemblages enabled the precise separation of rock types: hornblendites, diorites, essexites, monzodiorites, monzonites, foidic monzonites, alkali-feldspar syenites, foidic syenites, tinguaites, microsyenites, aplites, mariupolites, minettes, spessartites, kersantites, vogesites, camptonites, as well as their spatial distribution.

The optic analyses, the X-ray diffraction, the IR absorption carried out on the main minerals – feldspars, amphiboles, feldspathoids, micas – pointed out a series of structural features such as order/disorder, polytypes, structural defects. The main petrogenetic information obtained are the crystallization temperature for plagioclase, K-feldspar and nepheline (550-660° C). The observations on the spatial distribution of feldspar crystallization temperatures have classified the assymetry of the massif in respect with the present level of erosion, as well as its development towards SE, beneath the metamorphic rocks.

Other interesting aspects are the cryptic intergrowths identified in arfvedsonites, the exsolution and replacement microperthites and the magmatic epitaxial intergrowths as well as the important role of the processes developed during subsolidus phase.

The petrographic and structural studies show that the Ditrău is a quasi-circular alkaline massif, discordantly emplaced into an upper structural level with a partly retrograde evolution. Lithostratigraphic units of cycles 1 and 2 occur within this structural level – the Carpian and Marisian supergroups (Bretila-Rarău, Late precambrian A, older than 850±50 ma, with amphibolite facies metamorphic rocks; Rebra series, Late Precambrian B - 850-600 ma, with greenschist facies metamorphic rocks) (Kräutner et al., 1980; Mureşan, 1982; Balintoni, 1983).

The contacts with the green schists are usually sharp; the northern and eastern contacts are almost vertical, while the southern slope is smooth. The contacts are marked by a discontinuous and limited thermal aureole, showing specific mineralogical transformation – neoformations of andalusite, corundum, spinel, sillimanite – and by structural and fabric changes of the host metamorphic rocks. The massif is affected by postkynematic faults and shows a complex, sometimes assymetric structure, marked by the development and orientation of the petrographic complexes (usually in the northern, "Jolotca" compartment). Sometimes a ring distribution is suggested by the facies succession from the center (in the central-southern compartment " Valea Mare - Güdütz - Belcina) (Anastasiu, Constantinescu, 1980). The zonality is marked by the concentrical distribution of the various rock bodies in the central part and by the vein structures in the marginal part of the massif.

The mafic rocks occur in the western part of the northern compartment, successively grading eastward to diorites, which in turn grade to monzonites and syenites; hybrid rocks develop at the border zones of these petrographic complexes. The foidic rocks, represented by nepheline syenites and tinguaites, are accidental and lack zonalityl; they cross-cut other rock types and make up discordant circular apophyses.

The massif shows a strong zonality within its central-southern compartment. Its middle part corresponds to the center of the area occupied by foidic syenites with phaneritic structure and by tinguaitic separations where two "dome" type structures with massive fabric develop. The oriented fabric prevails toward the periphery of the central body, where it shows a foidic monzonite composition. The essexite complex shows an assymetric development, occurring in the western part of the massif, between the foidic syenites and monzosyenites. The zonality is most pregnant at the border of the central body, which grades to

monzonites and syenites and sometimes to granites and alkali granites in the vicinity of the crystalline schists.

The Ditrău massif shows an autochthonous, intrusive character, and its rooting tendency was often demonstrated, based on various evidence: petrological (Ianovici, 1934; Codarcea et al., 1954; Streckeisen, 1974), mineralogical and structural (Anastasiu, Constantinescu, 1977, 1980) or geophysical (Iakab, 1975; Botezatu, Calotă, 1979; Cristescu, 1981).

Complex recent geophysical investigations (gravity, aero-magnetism and aero-radiometry) have shown its development in depth and also outlined the magnetic anomalies produced by the basic bodies (Cristescu, Strugaru, 1982).

The polystadial emplacement and consolidation of the Ditrău massif within the tecto-structural space of the East Carpathians was controlled by crustal faults and by the mobility of the structural compartments they delimited. Based on gravimetric anomalies (Socolescu et al., 1975) and of deep geophysical surveys (Rădulescu et al., 1976), a line of maximum – Miercurea Ciuc-Gheorgheni-Topliţa-(G_8) – was identified, marking a continental crustal fault at the border between the cystalline-Mesozoic zone and the Neogene volcanic chain. Its trace is confined to a fault complex which started to be active before the Neogene (maybe during the Paleozoic). In the Gheorghieni-Topliţa area, where the G_8 crustal fault is crossed by other fault systems – G_9 and G_4 – the emplacement of the Ditrău massif is related to the presence of several tectonic blocks with various degrees of mobility.

The tectonic movements subsequent to the emplacement indicate a rejuvenation that enable relative displacements of the structural blocks, with the following effects: 1) the submersion of the area between Jolotca Valley and Valea Mare and 2) a strong uplift of the central zone relative to the northern part, even if the present erosion level exposes two dis-

tinct structural levels of the Ditrău massif: a) a superficial, but petrographically older zone where the foidic syenites remain at depths or appear as apophyses and b) a deeper level, where erosion has reached the central part of the youngest intrusions of foidic rocks which partly include the essexites.

The petrochemical analyses indicate the dominant sodic geochemistry of the massif and the presence of both alkaline and calc-alkaline rocks. The geochemical specialization of the part where rocks showing miaskitic features coexist with others displaying agpaitic features justifies the mineralogical and chemical complexity of the petrograhic associations, as well as the presence of mineralogical incompatibilities with the assemblages described in other alkaline massifs. The petrogenesis of the vein rocks and the metallogenetic process were controlled, at different times and with various intensity, by the tarde- and post-kynematic tectonization of the alkaline massif, as well as by the development of faults.

The spatial distribution of vein rocks is irregular; they concentrate within the marginal zones and commonly represent disjunctive displacements, in areas with low values of free energy, capable of triggering subsolvus changes. In the peripheral zones of the massif, the vein fields is based on mineralogical and petrographical features of the veins, on structural and fabric features of their constituent rocks, on their relationship (or its absence) with the mineralized zones. The control of the main tectonic background is always obvious. Based on these criteria, nine vein fields have been separated within the two compartments of the massif (Fig. 3).

Metallogenetic consequences

The petrographic heterogeneity of the massif, as well as the geochemical incompatibilities, the presence of suprasaturated rocks – the granitoids – together with unsaturated rocks – the foidic syenites – suggest the existence of

Geological sketch of the Ditrău alkaline massif (scale 1:1.000.000). 1, cover deposits; 2, granitoide complex; 3, syenitoide complex: syenites, monzonites; 4, foidic rock complex: foidic syenites, essexites; 5, diorite complex; 6, ultramafic and mafic complex; 7, Rebra series, Tulgheş series; 8, mineralized zones; 9, fault; 10, vein fields (I-IX).

two deep magmatic sources, whose emplacement was controlled by deep fractures within the host rocks, divergent in the beginning and convergent in the end.

The metallogenetic specialization of the Ditrău alkaline massif is a consequence of the parent magma fractionation, of the primary processes controlling their crystallization and of secondary – postmagmatic – processes which ended the petrogenetic evolution.

The main metallic elements concentrated within the massif – Zr, Ti, Nb, V, Th, Mo, REE, Fe, Pb, Zn, P – belong to both structural levels:

1) the "primary" formation – segregation or magmatic dissemination – includes two distinct parageneses:

a) Zr-P-Nb-Ti-REE minerals: zircon, apatite, ilmenite, orthite, xenotime, pyrochlore, niobite, garnet and Pb, Zn, Mo, Fe, Cu, Sb sul-

fides, related to syenitoides and foidic syenites, located in Aurora, Hereb, Várbükk, Balas Lorincz areas (Iakab, 1982).

2) postmagmatic formation with pneuma-tolitic-hydrothermal features and with veins with distinct mineralogy in the two distinct compartments:

a) in the Jolotca-Tarnița area, the Mo-REE-Ti-Nb-Fe-(Pb, Zn) minerals (molybden-ite, xenotime, loparite, monazite, ilmenite, titanomagnetite, pyrite, galena, sphalerite) are concentrated in veins (Constantinescu et al., 1981);

$\vdash\!\!\!-\!\!\!\dashv$ 1 km

Fig. 3 Simplified structural section in the Ditrău alkaline massif.

b) in the southern area – the Belcina valley basin – Th-V-REE-Zr-F-Mo minerals are con-centrated: pyrochlore, bastnäsite, thorite, xenotime, niobotantalite, zircon, fluorite and Pb, Zn, Cu, Mo, Fe sulfides.

The mineralogical, petrographical, petrochem-ical and structural investigations rise the met-allogenetic potential of the massif and enhance the possibilities for exploiting the rocks. The quality of hornblendites was emphasized for their Fe, P, Ti contents and that of the foidic syenites for their Al contents and for their usage in the ceramic industry. We also estab-lished the metallogenetic indicators used to orient the geological explorations.

References

Anastasiu N., Constantinescu E. (1974) Observații mineralogice în rocile sienitice din masivul Ditrău, *Com. Șt., Geol.* Facultatea de Geologie și Geografie.

Tipografia Univ. București.

Anastasiu N., Constantinescu E. (1978) Feldspații alcalini din masivul alcalin de la Ditrău, *D.S. Inst. Geol. Geof.*, **LXIV/1**, București.

Anastasiu N., Constantinescu E. (1980) Structure du massif alcalin de Ditrău, *Analele Univ. București,* **XXIX**.

Anastasiu N., Constantinescu E. (1981) Feldspații plagioclazi din masivul alcalin de la Ditrău, *St. cerc. geol. geofiz. geogr., s. geol.* **26**, 1, 83-95.

Anastasiu N., Constantinescu E. (1982) Tectostructural position of the foidic rocks in the Romanian Carpathians. *Rev. Roum. Geol., Geophyz., Geogr., s. Geol.,* **26**.

Anastasiu N., Constantinescu E. (1983) Criterii petrografice pentru cercetarea cim-purilor filoniene in masivul alcalin de la Ditrău, vol. Carpații, Gheorgheni.

Anastasiu N., Constantinescu E., Iakab G., Garbasevschi N. (1983) Petrografia si petrogeneza rocilor filoniene în masivul alcalin de la Ditrău. *St. cerc. geol. geofiz.,geogr., s. geol., Acad. RSR,* **28**.

Botezatu R., Calotă C. (1979) Ipoteză aupra anomaliei magnetice produsă de masivul de roci alcaline de la Ditrău rezultată din aplicarea unui procedeu de analiză spec-trală. *St. cerc. geol. geof., geogr., s geofiz-ică,* **17**, 1, București.

Codarcea Al., Codarcea D.M., Ianovici V. (1957) Structura geologică a masivului de roci alcaline de la Ditrău, Buletin *St. Acad. RPR,* **II,** 3-4, București.

Constantinescu E., Anastasiu N. (1979) Nepheline du masif alcalin de Ditrău. *Analele Univ. Buc., Geologie,* **XXVIII**.

Constantinescu E., Anastasiu N., Pop N., Garbașevschi N. (1982) Contributions a la connaisance des aspects paragénétiques du massif alcalin de Ditrău. *Travaux 12-eme Congres de Asoc. Géol. Carpatho-Balc.,* Bucharest.

Ianovici V. (1938) Considérations sur la con-solidation du massif siénitique de Ditrău en relation avec la tectonique de la region, *Comp. R. Acad. Sci, Roum.,* **II,** 6.

Ianovici V. (1973) Etude sur le massif syenitique de Ditrău, region Jolotca, district Ciuc (Transilavania). *Rev. Muz. Mineral. Univ. Cluj*, **4/2**.

Ianovici V., Ionescu I. (1972) Contribuţii la mineralogia masivului alcalin de la Ditrău. I. Amfibolii. *St. cerc. Acad.* **XIV**, 2.

Ianovici V., Constantinescu E., Anastasiu N. (1984) Petrochimia lamprofirelor din masivul alcalin de la Ditrău. *St. cerc. Acad.* **29**.

Iakab G. (1975) Consideraţii asupra poziţiei spaţiale a masivului alcalin de la Ditrău, *D. S. Inst. Geol. Geof.*, **LXII**, Bucureşti.

Iakab G. (1982) Studiul mineralogic şi geochimic al mineralizaţiilor metalifere dintre Voşlobeni şi Corbu. *Rez. teza doctorat.*, Univ. Al. I. Cuza, Iaşi.

Rădulescu D., Cornea I., Săndulescu M., Constantinescu I., Rădulescu F., Pompilian R. (1976), Structure de la croute terrestre en Roumanie - essai d'interprétation des études seimiques profondes. *An. Inst. Geol. Geof.*, **L**, Bucureşti.

Streckeisen A. (1952/1954) Der Nephelinsyenit Massif von Ditro (Siebenburgen), *Schw. Min. Petr. Mitt.*, **32**, II.

Streckeisen A. (1960), On the structure and origin of the nephelinosyenite complex of Ditro (Transilvania, Romania), *Rep. 21th Intenr. Geol. Congr. Part.* **13**, Copenhagen.

Streckeisen A., Giuşcă D. (1932) Der Nepheline-Cancrinite Syenit von Orşova, *Bul. Soc. Rom. Geol.*, **I**, Bucureşti.

Streckeisen A., Hunziker J. C. (1974) On the origin and age of the nephelin syenite massif of Ditro (Romania), *Schw. Min. Petr. Mitt.*, **54**, 1, 59-77, Bern.

VI. MINERALOGY OF SECONDARY PROCESSES

The mineralogical study of the hydrothermal alterations of the Sasca Montană banatites

EMIL CONSTANTINESCU

The mineralogical assemblage of the hydrothermal alteration of banatitic rocks is represented by illites, kandites, smectites, chlorites, zeolites, Ti-oxides (rutile, brookite, anatase), tourmaline, fluorite. The illite polytypes (1M and 2M) and several randomly interlayered structures (chlorite-montmorillonite, illite-montmorillonite and nontronite-saponite) were identified by X-ray and IR analyses. The formation of illite polymorphs and of randomly interlayered structures is the result of a continuous flux of K-rich hydrothermal solutions, as well as of differential leaching of some elements of the primary minerals. The development of montmorillonite in the argillic zone is related to the existence of a Mg-rich medium (dolomites and Mg skarns) in the proximity of the magmatic rocks. The thermal range of the hydrothermal metamorphism is extended from 400° C (tourmaline-brookite association) to 50-100° C (zeolite facies).

The emplacement of the Laramic igneous intrusions' in the Sasca Montană region was accompanied by important petrogenetic and metallogenetic phenomena which affected both the host rocks and the intruded igneous rocks. The mineralogical composition of the igneous rocks is complicated by the presence of post-magmatic minerals resulted either through the substitution of the primary minerals either by direct crystallization from solutions. The microscopic and chemical studies as well as X-ray diffraction, infrared absorption spectrography and thermal analysis lead to the identification of several mineralogical phases, to the determination of chemical and structural peculiarities as well as to the deciphering of

the relations between the minerals of the alteration zone. The interpretation of the data obtained allowed the interpretation of the thermodynamically and geochemical characteristics of the hydrothermal autometamorphism in the studied area.

I. The description of minerals

1. Tourmaline

Appears macroscopically as black prismatic crystals with ditrigonal habit, isolated as radial aggregates or compact masses. Microscopically, it displays a strong pleochroism, colorless, green, yellowish, olive dark green and

birefringence in various colors. (Δ: 0.024-0.034) refraction indexes: ω=1.670; ϵ=1.641.

The variation of the birefringence colors has a zonal character, the zones with euhedral contour being parallel to the faces of the prism. The chemical analysis, the unit-cell parameters, the IR absorption bands and the thermal effects are characteristic to the schörl variety.

2. Fluorite

Macroscopically, it appears as euhedral crystals or compact aggregates associated with quartz and pyrite. When exposed to light it tends to alter its violet colors to lighter shades. Microscopically, it displays a good cleavage along (111). The refractive index is n = 1.43. The unit-cell parameter calculated on the basis of X-ray diffraction analysis a = 5.46±0.02Å.

3. Titanium oxides

Three polymorph of TiO_2 have been recognized: rutile, brookite and anatase.

3.1. Rutile, frequently found as a primary accessory mineral, is represented by the sagenite variety developed as needles along two directions in biotite. It also appears as neoformation mineral through the transformation of the accessory Ti-magnetite in the banatites at Stânăpari. It appears as isolated crystals with needle to prismatic habitus, always associated with pyrite.

3.2. Brookite appears exclusively in association with tourmaline in the autometamorphosed banatites at the Cioaca Înaltă. Microscopically, it appears as well developed short-prisms, colored in red and with obvious pleochroism. Its participation is significant in tourmaline-affected areas. In diffractograms made on the material collected in these alteration areas, brookite is pointed by the intensity of its first five characteristic diffraction lines (see Constantinescu, 1976).

3.3 Anatase was identified in the hydrothermally transformed and mineralized banatites in the Stânăpari plateau. (the area of the 8 May mining pit). Microscopically, it was identified, both in thin and polished sections, as subhedral grains of sub-millimetric dimensions, associated with pyrite, chalcocite and covellite (Photo 3). In reflected light, it appears gray-brown, with a reflection capacity higher than that of covellite; it is isotropic and shows typical green-blue internal reflexes.

4. Clay minerals

Are represented by minerals from the illite, kandite and smectite groups.

4.1. Illite (sericite). Macroscopically, the sericitized zones show a light, almost white color and are characterized by decomposition of hornblende, biotite, plagioclase. In other cases, the sericite appears as veinlets which cross-cut the banatitic rock. Microscopically, it forms aggregates with high birefringence, sometimes as prismatic crystals with perfect cleavage. In an initial phase, the sericite replaces both the plagioclase from phenocrysts and the groundmass, the K-feldspars remaining untouched; the femic minerals (biotite, hornblende) are chloritised. In the final stage, both the phenocrysts and the matrix of the porphyry rock are totally substituted by very fine sericite and granular quartz (± pyrite) resulting in a compact or micro-granular aggregate, in which the outline of the original feldspar is sometimes still distinguishable. Pyrite appears as euhedral crystals, with granular aspect, or as small veins associated with chalcopyrite.

The chemical analysis of a completely sericitised banatite is presented in Table 1. In comparison with an unaltered porphyry granodiorite from the same area (Constantinescu, 1977) we can note the relatively constant (slight increase) quantities of SiO_2 and Al_2O_3 the decrease contents of MgO, Na_2O, CaO and enrichment in K_2O, FeS_2, and $CuFeS_2$.

Table 1. Chemical analysis of a fresh por-
phyrytic (1) and sericitized (2) granodiorite,
Stânăpari.

Oxides %	1	2
SiO_2	66.56	70.50
Al_2O_3	17.74	15.29
Fe_2O_3	3.05	0.38
FeO	2.31	0.09
MnO	0.08	-
MgO	2.03	0.79
CaO	2.53	0.13
Na_2O	5.26	0.21
K_2O	2.87	4.98
TiO_2	0.16	0.17
P_2O_5	0.09	0.13
H_2O^+	0.13	0.96
H_2O^-	0.24	2.83
FeS_2	-	3.69
$CuFeS_2$	-	0.27
Total	100.05	99.97

Fig. 1. Diffractograms of the minerals from the
hydrothermal alteration zone of the banatites.

In the strongly altered, fine-granular areas, in
which the sericite appears intimately associat-
ed with other neo-formation minerals, the
sericite has been detected on the basis of its
characteristic X-ray (Fig. 1, 2), on the IR
absorption band (Fig. 3) and on the basis of
thermal effects on the TDA curves (Fig. 4).

4.2 Kandites. The kandites are mainly repre-
sented by kaolinite. Macroscopically it
appears as white-gray colored, soft areas. The
areas that are intensely kaolinised can not be
analyzed microscopically but, in the rocks in
which the process is in its incipient stage we
can notice the preferred pseudomorphose of
the K-feldspar.

Kaolinite has been identified through the
X-ray diffraction, IR absorption spectrography
and thermal analysis.
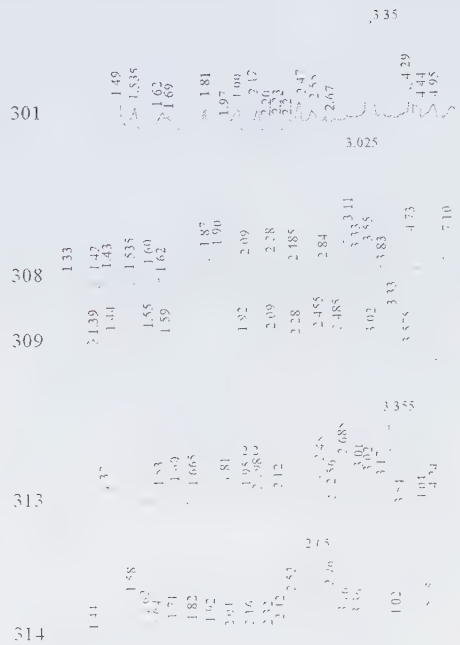
The XR diffractograms (Fig. 1) show a kaoli-
nite with a generally fully crystallized struc-
ture. On the IR absorption spectra, its pres-
ence, even in small quantities, is marked by
the occurrence of the characteristic 3.700
cm^{-1} absorption band and on the thermo-dif-
ferential curves by the 980° C exothermal
effect.

4.3 Smectites. The smectites are represented
by montmorillonite, nontronite and nontron-
ite-saponite. Macroscopically, the smectites
are colored in greenish white, sometimes pink-
ish white and, as a consequence of their pres-
ence, the transformed rocks underwent a sig-
nificant increase in volume.

X-ray analysis on oriented samples saturated
in etilene-glycol were performed for the sepa-
ration of the minerals from the smectite group
from the ones in the kandite group. The smec-
tites are showing an obvious 17.27 Å maxi-
mum, characteristic to the expandable miner-
als. The different varieties of smectites were
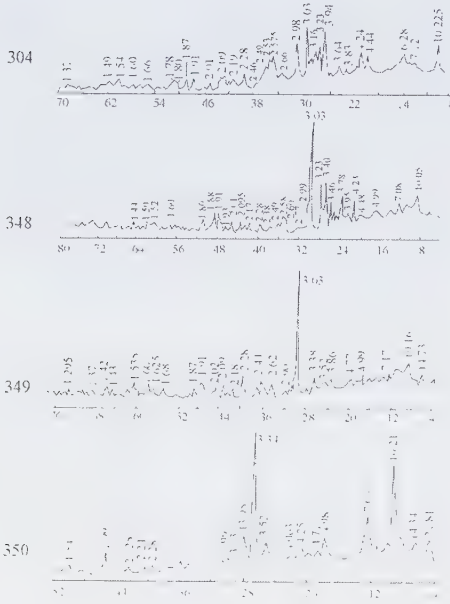
Fig. 2. Diffractograms of the minerals from the hydrothermal alteration zone of the banatites.

Fig. 3. IR absorption spectra of the minerals from the hydrothermal alteration zone of the banatites.

identified based on the comparison of the diffraction line value, absorption band and thermal effects (Figs. 1, 2, 3, 4) with the standard values (Van der Marel, 1976; MacKenzie, 1952; Smykatz, Kloss, 1974).

5. Chlorite

Macroscopically, the chloritized rocks display a greenish color, sometimes dark green to black. One may notice the preferential alteration of the mafic minerals.

Microscopically, they have weak pleochroism, low or anomalous birefringence in shades of brown or purple. Different phases of substitution of the hornblende and biotite can be noticed, sometimes all the way to their total replacement.

The X-ray analysis revealed the presence of the peaks of 14.7 Å, 7.17 Å, and 4.77 Å (on oriented samples: 14.5 Å, 7.08 Å, 4.73 Å) and 4.70 Å, 3.52 Å, 2.28 Å characteristic to orthochlorite and to the association of sericite (illite), calcite, hidrogoethite.

The thermodifferential curves (Fig. 5) display the 621° C endothermic effect, characteristic to the magnesian chlorites (Phillips, 1964; Smycatz, Kloss, 1972). The 850° C exothermal peak is sometimes masked by the strong exothermal effect of the calcite.

On the IR absorption spectra (Fig. 3 and 4) the values of the 472 cm^{-1} band whose position varies with the Mg-Fe substitution (Rahden et Rahden, 1972) also indicates the presence of the magnesian chlorites. The position of the Si-O vibrations at 1034 cm^{-1}, correlated with the X-ray diagram, indicates, both for chlorite and for the sericite, a complex structure in the octahedral layer.

6. Silica

6.1. Quartz, as a neo-formation mineral, appears both in cracks and as a substitute of the primary minerals that make the matrix of

Fig. 4. IR absorption spectra of the minerals from the hydrothermal alteration zone of the banatites.

Fig. 5. Thermo-differential curves of the minerals from the banatite alteration zone.

lar to that of the noble opal. Vitreous luster; the refractive index: n= 1.42, indicates a high water content.

7. Iron hydroxides

Microscopically, it appears as red-brown powdery aggregates. The optical, thermal and X-ray studies indicate the presence of goethite and lepidocrocite.

8. Carbonates

Microscopical observations, as well as X-ray, thermal and IR analysis (Figs. 1, 2, 3, 4) show that the carbonates (calcite, ankerite, siderite) are present in the altered rocks, sometimes in remarkable amounts.

8.1 Calcite appears as isolated crystals in veins or geodes, as well as through the calcitization of some phenocrysts and of the ground-mass. The crystals may have up to 4-5 cm and display different combinations of faces of scalenohedron ditrigonal, rhombohedral and hexagonal bi-pyramid. The observed shapes: $(11\bar{2}1)$, $(\bar{1}2\bar{1}1)$, $(\bar{2}111)$, $(\bar{1}\bar{1}21)$, $(2\bar{1}\bar{1}1)$, $(01\bar{1}2)$,

the phenocrysts of the banatite. In some rare cases, the high degree of silicification of the rock creates a situation resembling the secondary quartzites that include relics of the altered banatite. The silicified areas typically have a mosaic structure. The quartz grains of microgranular dimensions sometimes display a dentured structure, specific to the vein deposits. The neo-formation quartz appears in association with the majority of the alteration minerals, the most common parageneses being quartz-sericite-pyrite; quartz-carbonates-pyrite-chalcopyrite; quartz-molybdenite.

6.2 Chalcedony appears in nests and it is formed either cracks from solutions or via the transformation of opal. Optical characteristics (extinction, elongation); indicate the variety lutecite.

6.3 Opal is well developed in some areas, as veins and sub-parallel bands in the sericitized banatites. The yellowish brown color is simi-

Table 2. Chemical analysis of the zeolite from Dealul lui Ciucar – Sasca Montană

Oxides %	
SiO_2	58.27
Al_2O_3	13.50
Fe_2O_3	0.89
FeO	1.16
MgO	4.22
CaO	1.05
Na_2O	0.47
K_2O	1.00
H_2O^+	19.40
H_2O^-	--
Total	99.96
SiO_2 Al_2O_3 4.	

Table 3. Values of 2q, d, i/100 for the zeolite from Dealul lui Ciucar   Sasca Montană

Nr.	2è	d/n Å	I/100
1	9.76	9.06	100
2	19.14	4.65	45
3	32.24	2.70	52
4	36.13	2.48	12
5	38.34	2.36	16
6	43.84	2.06	9
7	47.96	1.89	-
8	51.19	1.78	8
9	56.04	1.64	7
10	57.89	1.59	10
11	59.49	1.55	11
12	64.72	1.44	18
13	69.12	1.36	24
14	72.64	1.30	15

$(\bar{1}012)$, $(\bar{1}\bar{1}02)$, $(31\bar{4}2)$, $(14\bar{3}2)$, $(\bar{4}312)$, $(\bar{1}\bar{3}\bar{4}2)$. (1432), (4132) are very similar to those described by Mareş et al. (1970) for the calcite from Vărad mine. Microscopically, one can observe zonal structures, probably due to cyclic inflows from solutions and common extinctions for all the crystals deposited in certain micro-cracks systems.

8.2. Siderite and ankerite, identified by thermal analysis are associated with sulfides which they corrode as they come in contact with.

9. Sulfates

The drillings in the Stânăpari plateau have identified isolated occurrences of gypsum and anhydrite. In the large framework of the entire Sasca Montană site, these minerals are rarely found, in contrast with their large distribution in the Moldova Nouă-Suvorov ore site (Gheorghiţă, 1975).

10. Zeolites

They appear veinlets, in association with calcite and quartz or substituting plagioclase in banatites. Stilbite (α = 1.49³; c^γ = 4-6°; 2V = 35), laumontite (γ = 1.51; c^γ = 26-27°; 2V = 24-26°) and thompsonite (c^γ = 0; 2V = 60°) varieties have been identified microscopically.

The chemical analysis and the main diffraction lines of a zeolite (stilbite) sample are presented in Tables 2 and 3.

II. Chemical and structural features of the minerals in the alteration zone

The X-ray diffraction studies, IR spectrography and thermal analysis revealed the detailed chemical and structural properties of the minerals in the alteration area at the Sasca Montană: polytypes, randomized interstratification, hydration level, exchange capacity of the phiyllosilicates; the degree of crystalinity (order-disorder) of the iron hydroxides.

1. The polytypes of mica minerals

An important problem in the mineralogy of contact areas is the delimitation of clay micas, (globally referred to as sericite) from the minerals of the illite and the mica groups, including the position of the hydro-muscovite. The problem can be solved in a satisfactory manner through the study of polytypes; according to Burnham (1962), the sericite minerals can

display a variation in composition and structure ranging from disordered illites (polytype 1 Md) to hydromica (3 mol % K). Yoder and Eugster (1955) have shown that the polytypes 1 Md and 1 M are characteristic to the low-temperature, di-octahedral micas. At higher temperatures these polytypes are transformed to the polytype 2 M1 which created the support for establishing the thermal history of these minerals.

According to the results of the X-ray analyses, the 2M1 and 1M polytypes are differentiated through the presence and respectively absence of the complete series of hkl reflexes. In standard conditions, the width of the diffraction lines can be correlated with the disordered stratified structures. When quartz is absent form the sample, the separation of polytypes can be made on the basis of the presence (2 M1) and respectively absence (1M) of the IR absorption band at 803 cm^{-1}. The percentage ratio between the 1Md and 2 M polytypes can be deduced from the ratio of the intensities of the reflexes 3.74Å/2.58Å (Velde, Hower, 1963). The determinations carried out on the Sasca Montană micas have indicated the predominant presence of the 1M polytype and totally subordinated, (10-15%) of the 2M polytype. The later appears in the sericite + quartz facies. The obtained results are consistent with Burham's observations (1962) according to whom the 1Md and 1M polymorphs appear in proportion of 90% when montmorillonite is present and 90% when the association montmorillonite + kaolinite is present.

2. Randomized inter-stratification in clay minerals

Part of the studied clay minerals display mixed irregular structures of the chlorite-montmorillonite, illite-montmorillonite and nontronite-saponite type. This last type is characteristic to the sample no. 348 from the Stânăpari plateau.

The Si-O absorption bands at 465 – 523 cm^{-1} and 1000 cm^{-1} on the IR absorption spectrum (Fig. 3) indicate the presence of clay minerals with octahedral Mg and Fe. The lack of the bands attributed to the Al-OH vibrations, from 920 cm^{-1} and 3630 cm^{-1} shows that we are in the presence of a mixture of tri-octahedral minerals. This is confirmed by the 970 cm^{-1} inflexion, indicating the presence of octahedral Fe and Mg in a tri-octahedral framework. The water band from 1640 cm^{-1}, underlines a relatively high hydration state, also confirmed by the intense maximum at 3440 cm^{-1}.

The thermo-differential curve (Fig. 5) displays a large maximum given by a mixture of clay minerals. The two stages de-hydrolisation, at 470° C and at 600° C indicate the predominance of Fe in the octahedral layers. The flattened effects, which are accompanied by gradual loss of weight on the TG curve during the de-hydrolisation suggests the occurrence of a complex mixture of clay minerals of the hydrobiotite-nontronite-saponite group.

The diffractogram (Fig. 1) shows the presence of tri-octahedral micaceous mineral with diffraction lines at 10.05 - 4.48 - 4.23 - 3.78 - 3.40 - 2.90 - 2.71 - 2.57 -2.52 - 2.17 - 2.01 Å. The existence of intense diffraction lines at 3.78 - 2.40 - 3.23 Å, in association with the predominant trioctahedral structure and the state of hydration of the ions in the interlayer space, suggest that a smectite-type mineral with a randomized, nontronite-saponite type stratification may be present.

3. The degree of crystalinity of the iron hydroxides

The separation of different mineralogical phases within the iron hydroxides in the alteration area has been facilitated by the crystalinity studies (degree of disorder: Kulp, Trites, 1952) with the help of differential thermal analysis. The temperature of the endothermic peak, representing the dehydration and decomposition Smykatz, Kloss, 1974) displays higher values: 410° C for goethite

(FeOOH) then for lepidocrocite (FeOOH): 345° C. The high value of the endothermic peak (411° C) for the analyzed goethite indicates a high degree of disorder by comparison with the standard values (Kelly, 1956).

Lepidocrocite also displays an exothermal peak at 4700° C which indicates a high degree of disorder, the thermal effect marking the recrystalisation of the strongly disordered phases (MacKenzie, 1952) with increasing temperatures.

III. Metallogenetic considerations

The structural and chemical characteristics of the neo-formation minerals, their associations and spatial distribution offer interesting information regarding the thermal and geochemical characteristics of the hydrothermal autometamorphism. The minerals identified in the alteration area can be attributed to the clay facies and phyllic facies (Burnham, 1962) or to the intermediate clay association and to the sericite association (Meyer, Hemley, 1967).

The chemistry of the neo-formation minerals in the area under consideration suggests and important inflow of B, F (mineralizers) and K as well as a remobilization of the Mg, Fe, Ca, Si. Starting with a granodiorite to diorite composition, and with a high potential of H_2O in the argillitic zone, the banatitic rocks have evolved towards an enrichment in Al_2O_3 and a depletion of CaO, NaO and K_2O.

The phyllic zone is characterized nevertheless by a considerable inflow of K. The fact that the K-feldspars in the sericitised banatites remain unaltered is a proof in this respect. Observing the variation of K content in the illite lattice, on the basis of I_{001}/I_{002} ratio (the White index, 1969) values between 1.5-1.7 have been obtained for the illites in the phyllitic zone (high K content) and between 1.8-2.1 for the illites in the argillitic zone lower K contents exists.

Thus, the kaolinisation appears subsequent to sericitisation and correlates with the moment of the partial K consumption in the illite zone. A similar relationship, followed spatially along the main access cracks of the hydrothermal solutions, was noticed in the case of the andesite volcanics at Bocşa-Săcărîmb (Udubaşa et al. 1976).

The occurrence of randomized inter-stratifications and of many polytypes of the illite is induced by the action of chemically stable hydrothermal solutions upon the clay minerals formed previously (Frank-Komenetsky et al. 1972).

Within the alkaline elements, the ratio K/Na was always favorable to K throughout the entire duration of the post-magmatic processes, as the low proportion of albite illustrates it.

Magnesium has an important role in the determination of the parageneses in the alteration zone. The existence, in the neighborhood of the banatites, of a Mg-rich environment (magnesian skarns, dolomitic paleosome) determined not only the appearance of parageneses specific to these areas (chrysotile, antigorite, amiant, sepiolite, saponite), but acted as a control factor for the kandite/smectite ratio, favoring the appearance of the montmorillonite in the hydrothermal autometamorphism area. If it is possible that part of the kaolinite in the argillitic zone could be of supergene origin. As suggested by the development of an intense alteration process in the galleries in the Stânăpari sector. However the occurrence of the montmorillonite is indicative of conditions that characterize hydrothermal alteration. The existence in some minerals (tourmaline) of zones richer in Fe, and respectively Mg, and that of phases with a more or less significant Mg content (smectites, chlorites) indicates a high variability of the Mg/Fe ratio in the composition of the hydrothermal solutions. The modification of this ratio can be attributed to the levigation of Fe ions from the primary minerals of the banatites.

The titanium is constantly present in the alteration area contained in rutile, brookite and anatase. These phases result either from the transformation of accessory minerals (titanomagnetite, sphene) or from the chloritisation of Ti-rich biotite.

The weak mobility of Al_2O_3 explains the abundant formation of zeolites in the final phases of the hydrothermal alteration of the banatites. Their preference for a more basic environment determines a preferential development in plagioclase-rich rocks that have been incompletely transformed. Zeolites are seldom found in the sericite-quartz facies.

The thermal stability domain of the minerals identified in the alteration zone of the banatites is wide.

The quartz-tourmaline association, as well as the presence of some particular forms of tourmaline (tourmaline suns) could be correlated with the tourmaline-quartz facies the greisenisation process (Nacovnic fide Kurek, 1954), but the presence of the tourmaline would rather characterize the high temperature hydrothermal alteration similar to that which affected the Canannea, Lalagua and Mount Potosi deposits (Schwartz, 1947, 1959).

The temperatures of tourmaline crystallization can be deduced from the fact that the brookite is present in the paragenesis. From the phase diagram of the TiO_2-Na_2O-H_2O system made by Kessman 1966 (fide Lerz, 1968) we notice that, in the presence of Na^- brookite is not stable at temperatures higher than 486° C. The microscopic observations which indicate a high degree of sericitisation of the tourmaline in the Cioaca Înaltă area, correlated with the experimental data (Kessman ibid.) allow us to estimate that the forming temperature of the tourmaline-brookite paragenesis that we examined is around 360° C-420° C.

The existence in the alteration area of the other two forms of TiO_2: rutile (associated with pyrite)

and anatase (associated with covelite and chalcosine) show the important role played by the pH and the chemical composition of the hydrothermal solutions in determining the thermal stability domain of these minerals.

The predominance of the the 1M polytype, the illites, associated with montmorillonite ± kaolinite, indicate, for the argillitic facies, temperatures bellow 350° C (the 1M polytype is stable, according to Yoder, Eugster, 1955, at temperatures ranging from 250° C – 350° C) and the existence of the 2M polytype at the illite in the filic facies indicates temperatures higher than 350° C.

The abundance of zeolites in the study area, marks the extension of the hydrothermal alteration process to temperatures, as low as under 100° C (Coombs, 1960).

Acknowledgments

References

Burnham C.W. (1962) Facies and types of hydrothermal alteration, *Ec. Geol.* **57**, 768.

Constantinescu E. (1976), Tourmaline de la zone Cioaca Înaltă (SW de Banat), *Rev. Roum. Geol. Geoph., Geogr., ser. Geol.* **20**, 1, 147-153.

Constantinescu E. (1977) Mineralogia și petrologia magmatitelor laramice dintre valea Nerei si valea Radimniuței, *St. cerc. Geol., Geoph., Geogr., ser. Geol.* **22**, 1, 87-102.

Coombs D. S. (1960) Lower grade mineral facies in New Zealand. *Internat. Geol. Congr. Reports XXI*, **13**, Copenhagen.

Frank-Kamenetskj V., Kotov N., Golio E., Klotchkova G. (1973) Some aspects of structural transformations of clay minerals under hydrothermal conditions, *Proc. Internat. Clay Conf.*, Madrid.

Gheorghiță I. (1975) Studiul mineralogic și petrografic al regiunii Moldova Nouă (zona Suvorov - Valea Mare), *St. tehn. ec.* ser. I, **11**.

Keesmann I. (1966) Zur hydrothermalen Synthese von Brookit. *Z. anorg. allg. Chem.*, **346**, 30-43.

Kurek H.H. (1954) Izmenennîe okolorudnîe porodî i ih poiskovoe znacenie, Gos. Izd. Moskva.

Lerz H. (1968) Über eine hydrothermale Paragenese von Anatas, Brookit, und Rutil von Dorfer Keesfleck, Pragaten Osttirol, *N. Jb. Min. Mh.*, **11**, 411-414.

Mareș I., Popescu I. C., Mareș I. (1970) Contribuții la studiul calcitelor de la Vărad (Moldova Nouă), *St. cerc. Geol., Geogr., Biol., Muzeul.* - Muzeul de științe nat. Piatra Neamț.

Mayer C., Hemley J. J. (1967) Wall rock alteration in geochemistry of hydrothermal ore deposits, New York.

Măldărescu I., Măldărescu M. (1965) Asupra unor probleme privind alterările hidroter-male din regiunea Baia Mare, *Analele Univ. Buc., Geol.*, **1**, 27-39.

Phillips W. R. (1964) A differentiation thermal study of the chlorites, *Min. Mag.* **33**.

Rahden H. V. R., Rahden M. J. E. (1972) Some aspects of the identification and characterization of 14A chlorites, *Min. Sci. Eng.*, **43**.

Schwartz (1959) Hydrothermal alteration. *Ec. geol.* **54**,'161-183.

Smykatz Kloss (1975) Differential thermal analysis, New York.

Udubașa G., Istrate G., Dafin E., Braun A. (1976) Mineralizațiile polimetalice de la Bocșa (N de Săcărîmb, Munții Metaliferi), *D. S.* **LXII**, 97-124.

Velde Hoover (1963) Petrological significance of illites polztipes, *Am. Min.* **48**, 11-12, 1239.

White J. l. (1969) Influence of potassium content on intensities of basal reflections and b-dimensions of dioctahedral micas. *Trav. Intern. Etude des bauxites, des Oxydes et des Hydroxides d'Aluminium*, Zagreb.

Plate I
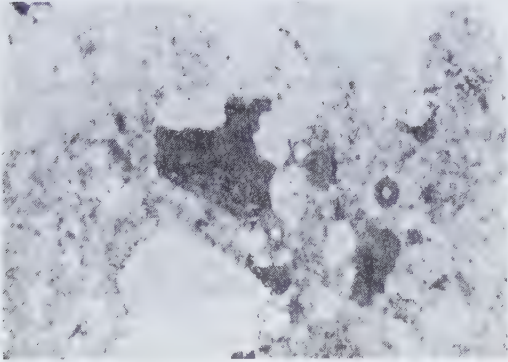
Photo 1. Zoned tourmaline crystals, corroded by quartz and partly altered to illite.
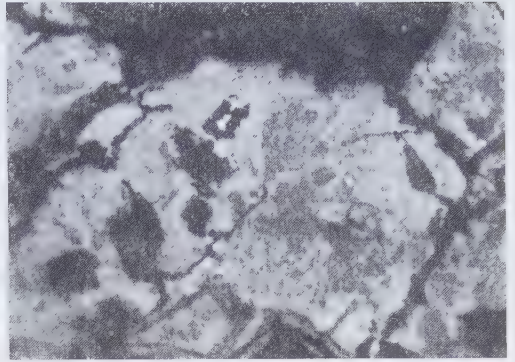
Photo 3.. Anatase (an) in hydrothermally altered banatite; cp = chalcopyrite.
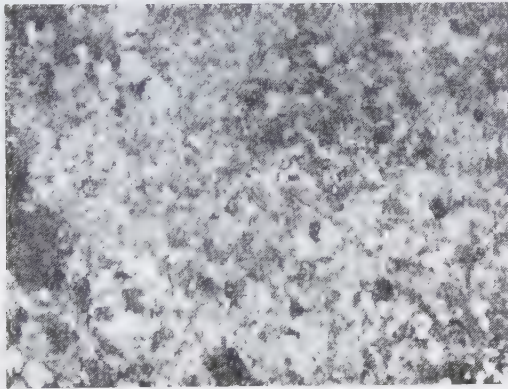
Photo 2.. Sericitized granodiorite; il = illite; Q = quartz; Py = pyrite; mafic minerals are altered to chlorite (cl).
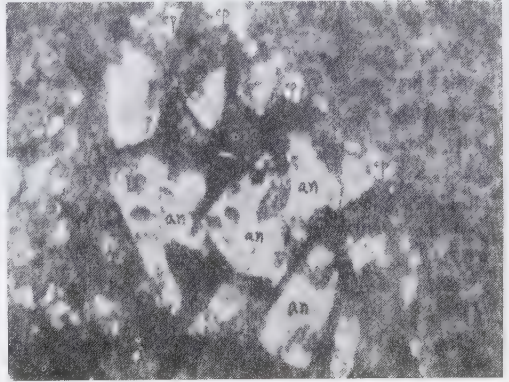
Photo 4. Goethite (Gt) and lepidocrocite (lp) in the hydrothermal alteration zone.

Laramian hydrothermal alteration and ore deposition in the Oravița-Ciclova area. South-Western Banat

EMIL CONSTANTINESCU
GHEORGHE ILINCA
AURORA ILINCA

In the Oravița-Ciclova area, the following mineralisation types were identified: Cu + Mo (in granodiorites), Cu + Bi + W (in garnetiferous skarns, granodiorites, and hornfels), Cu + pyrite (in recrystallized limestones), Cu + Mo + W (in garnetiferous-vesuvianitic skarns and monzodiorites), Cu + Co + As (in propylitized skarns and monzodiorites), Cu + Pb + Zn (in monzodiorites). Within the mineralisation, a mineral was identified for the first time in our country: kobellite $5PbS - 4(Bi, Sb)_2S_3$. Although the ore deposits, in their large majority, are hosted by skarns, they are genetically related to the hydrothermal evolution stage. The identified hydrothermal assemblages (i.e. tourmaline-orthoclase-quartz; K-feldspar (orthoclase-adularia)-biotite; quartz-epidote-actinolite-chlorite-calcite; quartz-sericite; zeolites-calcite) reflect a relatively continuous evolution of hydrothermal solutions from an acid-oxidizing to a basic-reducing character. Spatial-genetic correlations between the tourmaline-orthoclase-quartz assemblage and the scheelite mineralisation from Chinisea Valley as well as between the propylitic association with its gradings to phyllic facies and the Cu + Bi + W, Cu + Mo + W and Cu + Co + As mineralisation can be established.

Although known and mined in a rudimentary manner as far back as in antiquity, the Oravița-Ciclova mineralisation became the subject of some early geological mentions not before the second half of the 18th century.

Within the mineralisation, several rare minerals were described, namely scheelite, wolframite, argentite, cubanite, bismuthinite, native bismuth, bismite, cobaltite, smaltite, glaucodot, erythrite, löllingite, hoernesite, native tellurium, tetradymite (Marka, 1869; Zepharovich, 1859, 1875, 1893; Cădere, 1925, 1926, 1927, 1928).

In 1948, Köch described for the first time in samples from Ciclova, a bismuth telluride, which he called csiklovaite. In the case of two minerals which have remained unidentified, i.e. a Ni and Co sulpharsenide and a bismuth telluride, only the chemical analyses carried out by Sipocz and Grasselly (1886 and 1948, respectively, fide Rădulescu, Dimitrescu, 1968) are available.

A complex view of the Oravița-Ciclova ore deposits and their relations with the intrusive bodies and contact aureole has been given by means of the last decades studies (e.g.

Gheorghițescu, 1974; Cioflica et al., 1976; Constantinof, 1980).

In 1977, Popescu and Constantinescu carried out detailed studies on the mineralisation, emphasizing the physiographic relationships between the ore minerals as well as the main hydrothermal replacement features. Five types of mineralisation have been outlined.: (1) copper in crystalline schists, (2) copper-molybdenum, (3) copper-bismuth-tungsten and subordinately gold, (4) copper in hornfels and (5) titanium in crystalline schists.

A complex study of the metallogenesis related to Ciclova Laramian magmatism and its contact aureole, by Cioflica and Vlad (1981), has pointed out the main types of mineralisation (Cu ± Mo, Cu - Co ± As, Cu ± W, Cu ± Pb - Zn), the ores deposition sequence and their essential geochemical and genetic characters.

1. General data

The Oravița-Ciclova ore deposits are mainly hosted by the pyrometasomatic contact zone, in association with skarns. The main types of skarns are given by the following assemblages: *1) grandite (grossularite 30   50 and), (2) wollastonite-grandite-tremolite, (3) wollastonite-grandite, (4) grandite-scapolite (meionite) (5) wollastonite-diopside-granditevesuvianite-clintonite, (6) grandite-vesuvianite, (7) diopside-gehlenite, (8) wollastonitediopside-chondrodite-grandite-vesuvianite.*

Subordinately, the ore deposits are associated with thermal contact, metamorphites represented by hornfels with: orthoclase-quartz-biotite-andalusite (± corundum, cordicrite); quartz-acid plagioclase-biotite-clinozoisite and recrystallized micro- or mesoblastic limestones with separations of epidote, quartz and pyrite. To the same effect, ores are to be found in association with Laramian magmatites (hornblende-biotite granodiorites and porphyritic microgranodiorites, monzodiorites, porphyritic monzodiorites).

2. Hydrothermal alterations

The Laramian igneous rocks, the skarns and hornfels are marked by intense hydrothermal alterations. A brief description of the identified hydrothermal assemblages will given further on.

The *tourmaline-orthoclase-quartz I* assemblage is developed in the upper course of Chinisea Valley against the background of garnetiferous skarns and porphyritic granodiorites. A correlation may be assumed between the Chinisea Valley tourmaline and the scapolite occurrences in the Rîndunicii Brook, as they could signify a first wave of high temperature, acidic and rich in mineralizers solutions, to all appearances transitional from pneumatolytic   to   hydrothermal   conditions. Tourmaline occurs as tiny radiated crystal aggregates with a marked pleochroism: pink, greenish-yellow and greenish-blue, indicating a member of schorlite   elbaite series. Tourmaline constantly appears associated with sericitized orthoclase and quartz, but their mutual relations are wavering.

The *K-feldspar (orthoclase II-adularia)-biotite* assemblage (K-silicate facies) is confined to a small part of the intrusive bodies, partially affecting the porphyritic granodiorites from Chinisea Valley and Racilor Brook. The alteration consists in hornblende biotitization processes as well as in replacements and corrosions of plagioclase by orthoclase. Locally, along the fissures, K-feldspar is represented by adularia, which occurs as limpid euhedral crystals. In the Chinisea Valley granodiorites, adularia replaces orthoclase.

The *quartz II-epidote-actinolite-chlorite-calcite I (± albite)* assemblage defines the propylitic facies for the Oravița-Ciclova area. Propylitization affects a wide range of rocks: porphyritic granodiorites, diorites, monzodiorites, skarns and hornfels, often being superposed on other assemblages which were already mentioned.

Epidote occurs mainly at the expense, of skarn minerals: garnets, wollastonite, vesuvianite, which are replaced peripherally or along fissures. Such processes may result locally in pseudomorphs after garnets. Epidote also appears against the background of Laramian magmatites, especially syenites, where it substitutes K-feldspar along fissures and cleavages. Within propylitized recrystallized limestones from the northern and northeastern slopes of Tîlva Mică, epidote frequently forms monomineralic concretions ranging from 1 to 10 cm in diameter. Chlorite is abundant in skarns and Laramian magmatites. Its occurrence at the expense of tourmaline-orthoclase-quartz and K-feldspar-biotite assemblages, is always typical. Within the magmatites, chlorite replaces hornblende and biotite, often resulting in pseudomorphs.

The chloritization of magmatic primary biotite (to distinguish it from the biotite in the K-silicate assemblage), is accompanied by a detitanization process which is marked by the appearance of sphene or rutile. Actinolite occurs frequently as inclusions in quartz and calcite or as small monomineralic vein-like accumulations within porphyritic granodiorites.

The *quartz III-sericite* assemblage (phyllic facies) develops in the porphyry-microgranodiorite and dacitic apophyses of the Chinisea Valley intrusive body and, more frequently in the Ciclova monzodiorites and dykes. Members of quartz-sericite facies overlap the tourmaline-orthoclase-quartz assemblage and often obscure the effects generated. by propylitization.

The *zeolite-calcite II* assemblage is ascribable to the lowermost temperature phase of the hydrothermal alteration. Zeolites are represented by stilbite, thomsonite, scolecite – which occur mainly in skarns – and by laumontite which is found mostly in Laramian magmatites.

3. Description of ore minerals

Scheelite forms millimetric accumulations in a body of tourmalinized and feldsparized granodiorites in Chinisea Valley as well as in monzodiorites and garnet-vesuvianite skarns at Ciclova. Quite seldom, scheelite nodules over 1 cm in diameter can be observed. Under the microscope, scheelite appears as anhedral, high relief crystals, associated with tourmaline, K-feldspar and quartz or with anisotropic garnets and vesuvianite. Sometimes, crystals are rounded or peripherally corroded by calcite or adularia. In the Ciclova zone, two generations of scheelite can be emphasized.

Molybdenite appears in the following characteristic assemblages:
    in granodiorites: + chalcopyrite, pyrite, zeolites, calcite;
    in skarns and monzodiorites: + chalcopyrite, quartz.

Molybdenite occurs as veinlets, fine films or discrete flakes. Mutual relationship with chalcopyrite provides evidence for the tardy character of molybdenite (Plate I, Fig. 1).

Chalcopyrite is the most wide-spread ore mineral. Its characteristic associations are:
- in granodiorites: + molybdenite, pyrite, zeolites, calcite;
- in garnetiferous skarns, granodiorites and hornfels (north of Oravița Valley): + glaucodot, cobaltite, enargite, tetrahedrite, tetradymite, tellurobismutite, kobellite, sphalerite, chalcocite, covellite, cuprite, malachite, azurite, erythrite, goethite, lepidocrocite, epidote, quartz, calcite, actinolite, chlorite;
    in garnetiferous skarns and monzodiorites (Ciclova): (a) + cubanite, molybdenite, pyrite, azurite, malachite; (b) + glaucodot, pyrite, arsenopyrite, tetrahedrite, tennantite, bornite, covellite, chalcocite, native copper, erythrite, scorodite;
    in recrystallized limestones: + pyrite, pyrrhotite, cobaltite, marcasite;

– in phyllitized monzodiorites: + galena, sphalerite, pyrite.

Chalcopyrite has numerous mineralogical particularities, mainly in connection to the Vickers hardness variation, optical anisotropy and relations. with other ore minerals. The early chalcopyrite generations associated with garnetiferous skarns and monzodiorites, are represented by crystals with relatively strong birefringence, in dark brown hues, revealing a multiple twinned structure. After Uytenbogaard and Burke (1971), an increase in the birefringence of chalcopyrite is dictated by a higher iron content. The Vickers hardness measurements in these particular cases, show very high values: VHN_{20} – 195 – 221 kg/mm^2, i.e. at the uppermost limits of the chalcopyrite microhardness range.

The appearance of strong anisotropic chalcopyrite pleads for its formation at high temperatures characteristic to the first stages of hydrothermal process. At the same time, a direct correlation between the iron content and microhardness number may be reasonably inferred.

The high temperature chalcopyrite replaces or cements glaucodot and cobaltite. Sometimes it shows exsolutions of cubanite which are considered to occur at temperatures ranging between 235 and 400º C (Borchert, 1934; Ross, 1934 fide Schwartz, 1955). High temperature chalcopyrite is frequently substituted by copper sulphosalts, native bismuth, bismuth tellurides and sulphosalts. The late chalcopyrite generations, optical anisotropy is invisible and the Vickers hardness values are appreciably lower: VHN_{20} = 169 – 182 kg mm^2.

Low temperature chalcopyrite forms borders around enargite and tetrahedrite being in its turn replaced by native bismuth and bismuth tellurides and sulphosalts. Within the mineralisation associated with the monzodiorites from south of Oravita Valley and with propylitized

skarns from the Floreana, Țiganilor and Ciclova Valley, chalcopyrite is replaced by tetrahedrite, tennantite, and quite locally by galena and sphalerite. Within the ores associated with the Ciclova Valley monzodiorites, there are frequent exsolutions of chalcopyrite in sphalerite. In recrystallized. limestones, mutual relationships between chalcopyrite and other ore minerals are hesitating. Within the supergene enrichment zone, chalcopyrite is replaced by bornite, chalcocite, covellite and, in the oxidized zone by goethite and lepidocrocite.

Glaucodot seems to he the most abundant ore mineral in the Ciclova Valley monzodiorites, its participation being somehow reduced in the mineralisation associated with the Chinisea Valley garnetiferous skarns and magmatites and with the Tîlva Mică hornfels. Characteristic assemblages:
– in garnetiferous skarns, granodiorites and hornfels: + cobaltite, chalcopyrite, copper and bismuth sulphosalts, pyrite;
– in propylitized skarns and phyllitized monzodiorites (Ciclova): + pyrite. chalcopyrite, arsenopyrite, gersdorffite, copper sulphosalts, sphalerite, galena.

Glaucodot, forms euhedral crystals with seemingly prismatic or rhombic outline (Fig. 1A) and more frequently anhedral ones. They are brilliant-white colored and. their anisotropy is invisible even under strongest lighting. The Vickers hardness values are high: VHN_{70-100} = 900 – 1000 kg/mm^2, but it is difficult to establish a true hardness range due to the intense fractured indentation. Glaucodot is penetrated and cemented by chalcopyrite (Fig. 1B) as well as by copper or bismuth sulphosalts (Fig. 1C). In the oxidized zone. glaucodot passes into erythrite and iron oxides and hydroxides.

Cobaltite (Pl. I, Fig. 2) seldom occurs as euhedral crystals, with high relief and visible anisotropy in gray and brownish-gray hues. It is associated with chalcopyrite, pyrrhotite and
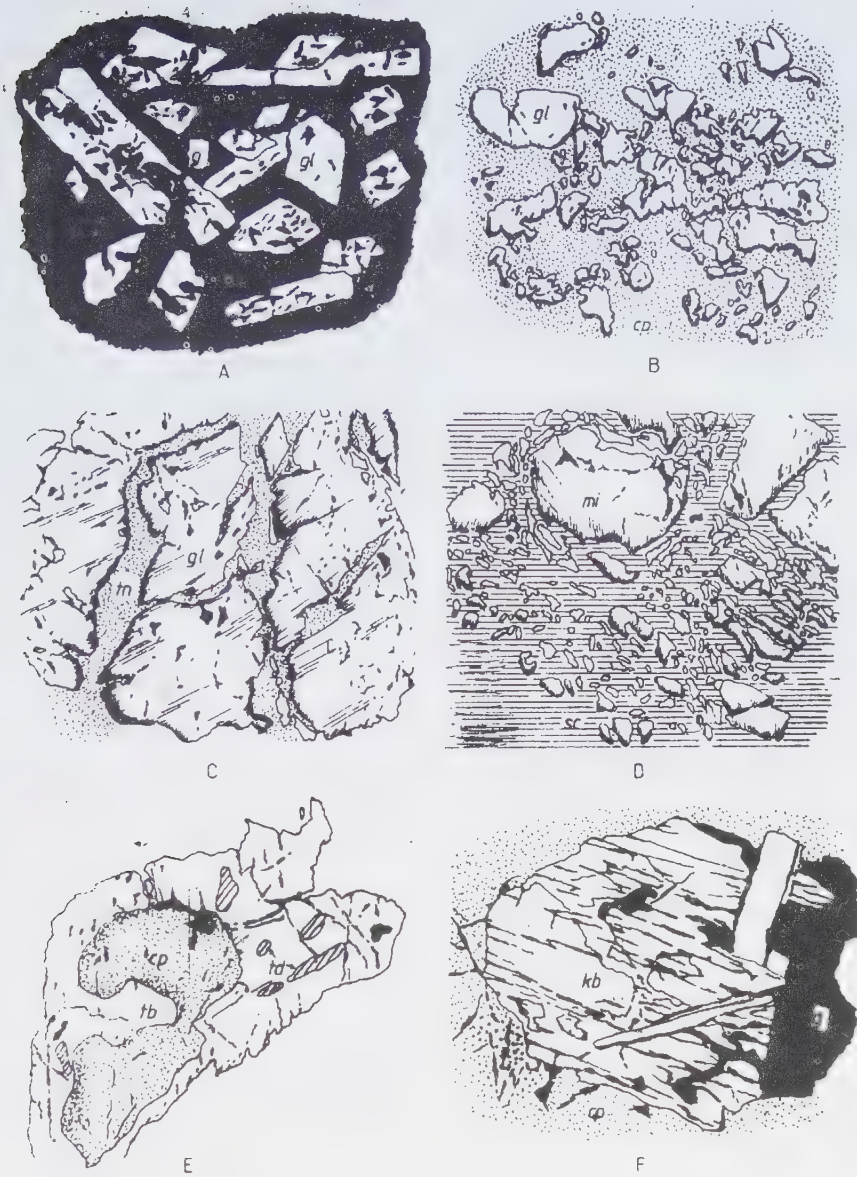
Fig. 1. A, Glaucodot crystals (gl) in a quartz gangue (g) (Trei Crai gallery, Ciclova); B, glaucodot (gl) cemented by chalcopyrite (cp), (Emil gallery, Chinisea Valley); C, glaucodot (gl) replaced by tennantite (tn), (Lobkowitz gallery, Ciclova); D, arsenopyrite (mi) replaced by scorodite, (sc) (Trei Crai gallery, Ciclova); E, tellurobismutite (tb) with tetradymite (td) inclusions forming a border around chalcopyrite (cp) (Emil gallery, Chinisea Valley); F, kobellite (kb) associated with chalcopyrite (cp) and quartz gangue (g), (Emil gallery, Chinisea Valley).

R%
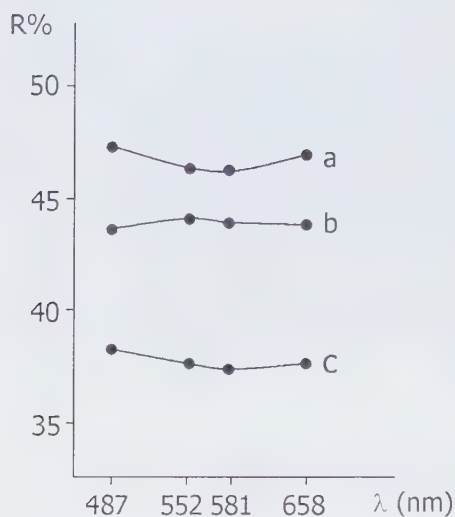
Fig. 2. Reflectance spectra of gersdorffite (a) and kobellite (b-c).

Table 1. Calculated d/n and I values for a scorodite and arsenopyrite mixture (Trei Crai gallery)

d/n	I	d/n m [1]	d/n s [2]	
5.5672	56		5.56	s
4.9509	19		4.95	s
4.4541	100		4.44	s
4.0720	22		4.06	s
3.7891	22		3.78	s
3.6584	30	3. 669		m
3.3623	19		3.36	s
3.1662	90		3.16	s
3.0516	63		3.05	s
2.9867	34		2.98	s
2.8455	22	2.843	2.84	m.s
2.7863	20	2.783		m
2.7191	16			
2. 6503	100	2.662		m
2.5785	47		2.58	s
2.4951	31		2.50	s
2.4471	80	2.443		m
2.4047	73	2.412		m
2.2132	33	2.206		m
2.1126	19		2.11	s
2.0480	25		2.04	s
1.9998	22		2.00	s
1.9467	32	1.943		m
1.8135	70	1.817		m
1.7945	16		1.79	s
1.7659	28			
1.7502	28		1.75	s
1.6606	28		1.66	s
1.6321	29	1.629		m
1.6255	29	1.629		m

1) d/n m – d/n values for arsenopyrite (from Miheev, 1957)
2) d/n s – d/n values for scorodite from Durango   Mexico (Miheev, 1957).

pyrite in the mineralisation hosted by recrystallized limestones.

Gersdorffite appears quite locally as low relief inclusions in a body of glaucodot and arsenopyrite. Its color is white with a weak yellowish tint as compared to that of glaucodot or arsenopyrite and in crossed polars is isotropic. The Vickers hardness at 100 g loading ranges between 730 and 910 kg/mm^2. Measured. reflectance for 487, 552, 591 and 658 nm are: 47.48; 46.52; 46.35; 40.87%. The reflectance spectrum is given in Fig. 2.

Arsenopyrite occurs in association with glaucodot, cobaltite, gersdorffite, tetrahedrite, tennantite and scorodite. It forms anhedral crystals with marked anisotropy. In the oxidized zones, replacements of arsenopyrite by scorodite are common (Fig. 1D).

Scorodite $Fe(AsO_4)*2H_2O$ is a typical mineral of the arsenopyrite-bearing oxidized zones in the Ciclova area. This occurrence, previously not mentioned, is significant as it provides evidence for supergene alteration processes, carried. on in. a warm and moist climate. X-ray diffraction study of scorodite was carried out

and the obtained d/n values are given in Table 1.

Copper sulphosalts are represented by tetrahedrite, tennantite and enargite. Characteristic associations:
– in garnetiferous skarns and hornfels: + chalcopyrite I, II, bismuth sulphosalts;
– in propylitized skarns and monzodiorites: + glaucodot, chalcopyrite, sphalerite, galena, arsenopyrite.

Vickers hardness values are as follows: tetrahedrite VHN_{40-50} = 380 – 403 kg/mm^2; tennantite VHN_{40} = 270 – 335 kg /mm^2; enargite VHN_{40} = 290 – 360 kg /mm^2.

Tetrahedrite and enargite replace high temperature chalcopyrite within the mineralisation associated with the Chinisea Valley skarns and magmatites and with Tîlva Mică hornfels (Plate II, Fig. 1, Fig. 2). These are in turn substituted by low-chalcopyrite or by bismuth sulphosalts and tellurides. In the mineralişation hosted by the Ciclova Valley monzodiorites and skarns, tetrahedrite and tennantite in association with sphalerite, replace glaucodot and arsenopyrite.

Native bismuth occurs in the Chinisea Valley mineralized skarns, opening the deposition sequence of the bismuth minerals. It has a brilliant creamy-pink color and strong optical anisotropy. The grains are frequently anhedral, but tiny euhedral, short prismatic crystals, often localized along fissures in tetrahedrite can be identified, too. The VHN_{10} values range between 21 and 24 kg/mm². Native bismuth is corroded by tetradymite.

Bismuth tellurides and *sulphosalts* are represented by *tetradymite, tellurobismutite* and *kobellite.* Tetradymite and tellurobismutite are associated with chalcopyrite and copper sulphosalts, the later being replaced along fissures and bordered by the former. Sometimes, tetradymite forms inclusions in tellurobismutite (fig. 1E). The Vickers hardness values are as follows: tetradymite – $VHN_{10} = 35 – 69$ kg/mm²; tellurobismutite – $VHN_{10} = 52 – 87$ kg/mm². Kobellite – in fact, an intermediary member of kobellite – tintinaite series ($5PbS–4Bi_2S_3–6PbS–4Sb_2S_3$) characterized by a Bi/Sb ratio greater than unity – was identified only in the Emil gallery dump in Chinisea Valley. As the available amounts of kobellite proved insufficient for a chemical analysis, information about the chemical composition was obtained by means of electron-microprobe investigations (Plate III and IV). Kobellite (Fig. 1F) shows a weak bireflectance in white and grayish-white with pale violaceous tints. It occurs as tabular or columnar crystals with good cleavage, aligned to elongation (Plate V, Fig. 1). Optical anisotropy is strong (Plate V fig. 2) in grayish-brown hues and has straight extinction in all sections parallel to the cleavage. The Vickers microhardness values are $VHN_{10} = 65–164kg/mm²$. Measured reflectances Rg:Rp: for 487, 552, 591 and 658 nm wavelengths are 43.70–38.23; 44.19–37.79; 44.00–37.49; 43.81–37.64 %. The reflectance spectrum is rendered in Fig. 2. Kobellite is associated with chalcopyrite, tetradymite, tellurobismutite and native bismuth.

Native gold appears sporadically as minute grains associated with tetradymite and tellurobismutite.

4. Discussion

The identified ore minerals in correlation with their country rock and spreading area, outline the following types of mineralisation:

– Cu + Mo: associated with hornblende-biotite granodiorites from Maidan zone (chalcopyrite, molybdenite, pyrite);
– Cu + Bi + W (± Te, Pb, Co, Ni, As, Zn, Au): associated with garnetiferous skarns and granodiorites from Chinisea Valley as well as with the Tîlva Mică hornfels (scheelite, glaucodot, cobaltite, chalcopyrite I, enargite, tetrahedrite, chalcopyrite II, native bismuth, tetradymite, tellurobismutite, kobellite, native gold and in the supergene enrichment and oxidized zones, chalcocite, covellite, cuprite, malachite, azurite, erythrite, goethite, lepidocrocite);
– Cu + pyrite (± Co): represented by small lens-shaped bodies associated with recrystalized limestones in the Forviz-Kiesberg gallery zone .(pyrite, pyrrhotite, chalcopyrite and subordinately cobaltite and marcasite);
– Cu + Mo + W: associated with the garnetiferous-vesuvianitic skarns and with the monzodiorites in the Floreana-Ciclova Valley zone (scheelite I, scheelite II, chalcopyrite, cubanite, molybdenite, pyrite and in the oxidized zone: azurite, malachite, goethite, lepidocrocite);
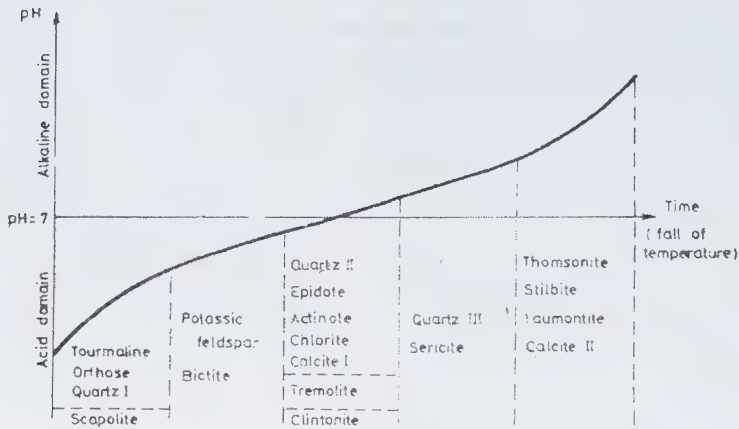
Fig. 3. Evolution of the pH of the hydrothermal solutions.

– Cu + Co + Ai (± Ni, Sb, Pb, Zn): associated with propylitized skarns in the Floreana, Ţiganilor Valley and Ciclova Valley zones, as well as with the monzodiorites from south of

Fig. 4. Variation limits of pH and Eh at high temperatures (interrupted line) and in exogene conditions (uninterrupted line).

Oraviţa Valley (glaucodot, pyrite, chalcopyrite, arsenopyrite, gersdorffite, tetrahedrite, tennantite and quite subordinately sphalerite and galena; in the enrichment and oxidized zones occur: bornite, covellite, chalcocite, native copper, azurite, malachite, erythrite and scorodite);

– Cu + Pb + Zn: less developed, is associated

with the Ciclova zone monzodiorites (galena, sphalerite, chalcopyrite I, chalcopyrite II, pyrite).

It may be noticed that the Cu + Bi + W mineralisation is preponderant at north of Oraviţa Valley, whereas the Cu + Mo + W and Cu + Co + As ones are prevailing in the Ciclova, zone.

Although the Oraviţa-Ciclova ore deposits, in their large majority, are hosted by skarns, they are genetically related to the hydrothermal stage of postmagmatic evolution. The described hydrometasomatic assemblages, as seen from the angle of deposition temperatures, of acidity degree which they reflect (Schwartz, 1955) and of specific superposition relationships, suggests for the whole area a relatively continuous evolution of the hydrothermal solutions pH from acid to basic (fig. 3).

The recurrence described sometimes by the repeated occurrences of quartz and K-feldspar within the hydrothermal assemblages suite, could be explained by taking in account both pH and Eh variation ranges (fig. 4). Commonly, these ranges are given for exogene conditions (Ianovici et al., 1982), but we have considered that at high temperatures which involve a higher dissociation degree of water, the state of the variation limits of Eh and pH

may be described in a similar manner, considering the exogene conditions field as being shifted to the diagram's upper left area. Thus, the whole variation field moves to the bottom-right area as the hydrothermal solutions evolved from acid-oxidizing to basic-reducing conditions.

Several spatial-genetic correlations may be established between the tourmaline-orthoclase-quartz assemblage and the scheelite occurrences from Chinisea Valley, as well as between the propylitic assemblage with its frequent passings to phyllic facies and the Cu + Bi + W mineralisation from north of Oravița or the Cu + Mo + W and Cu + Co + As mineralisation in the Ciclova zone. Mutual replacing relations occurring between the ore minerals or between these and the gangue ones, are relevant for the polyascending character of the mineralizing fluids materialized by successive crystallizing moments separated by intense fracturing stages.

Based on about 2200 measurements, a computer based microtectonic study was carried out. Thus, it became obvious that the ore distribution was subordinated to a strict structural control. The main tension fracture system which controls the disposition of both igneous dykes and mineralisation, trends SW – SE. This fact is pointed out by the disposition of molybdenite and chalcopyrite-bearing fissures in the Maidan granodiorites, of pyrrhotite and chalcopyrite bodies in the Kiesberg zone, of the glaucodot lens-shaped bodies from Țiganilor Valley as well as of chalcopyrite and glaucodot veinlets from Floreana Hill. This tension fracture system can be emphasized all over the study area and its development within the Laramian magmatites, aureole formations, sedimentary deposits and crystalline schists pleads for an exokinetic character. The system intensely affects the skarns and hornfels thus providing evidence for being active even after the emplacement of the main intrusive bodies.

Acknowledgements

References

Cădere D. M. (1925, 1926, 1927, 1928) Fapte pentru a servi la descrierea mineralogică a României. *Mem. Acad. Rom.,* **2**, **3**, **4**, **5**, București.

Cioflică G., Popescu Gh., Constantinescu E. (1976) Raport – Arhiva Cat. de Min. Univ. București.

Cioflică G., Vlad Ș. (1981) Mineralizația cupriferă de la Ciclova. *An. Univ. București*, **XXX**.

Constantinof D. (1980) Complexul banatitic de la Oravița-Ciclova (Banat.). Teză de doctorat. Univ. București.

Gheorghițescu D. (1974) Studiul mineralogic și geochimic al formațiunilor de contact termic și metasomatic de la Oravița (Coșovița). *D. S. Inst. Geol.,* **LXI**.

Ianovici V., Stiopol V., Măldărescu I. (1982) Geochimie (partea I), Tip. Univ. București.

Koch S. (1948) Bismuth minerals in the Carpathian Basin. *Acta Szeged.,* **2**. Szeged.

Marka G. (1869) Einige Notizen über das Banater-Gebirge, *Jahrb. d.k.k. geol. R.A.* **XIX**, 318   349.

Miheev V. I. (1957) Rentghenometriceskii opredelitel mineralov. Gosgheoltehizdat, Moskva.

Popescu Gh., Constantinescu E. (1977) Observații mineralogice asupra skarnelor și mineralizațiilor din regiunea Oravița. *An. Univ. București*, **XXVI**.

Rădulescu D., Dimitrescu R. (1966) Mineralogia topografica a României. Edit. Acad. RSR, 376 p. Bucuresti.

Schwartz G. M. (1955) Hydrothermal alteration as a guide to ore. *Econ. Geol.,* **50**.

Uytenbogaard W., Burke I. (1971) Tables for microscopic identification of ore minerals – Elsevier, Amsterdam.

Zepharovich V. v. (1859, 1875, 1883) Mineralogisches Lexikon für das Kaiserthums Österreich, I, II, III Wien.

Plate I
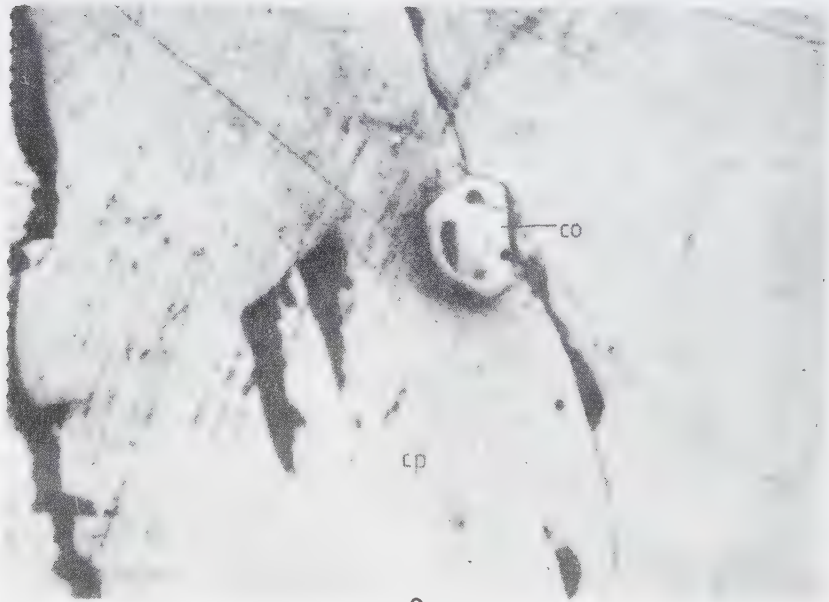
Fig. 1. Molybdenite (mo) associated with chalcopyrite (cp) in porphyritic granodiorite. Maidan quarry: N II, 160 X.
Fig. 2. Cobaltite (co) in chalcopyrite. Emil gallery, Chinisea Valley: N II, 250 X.
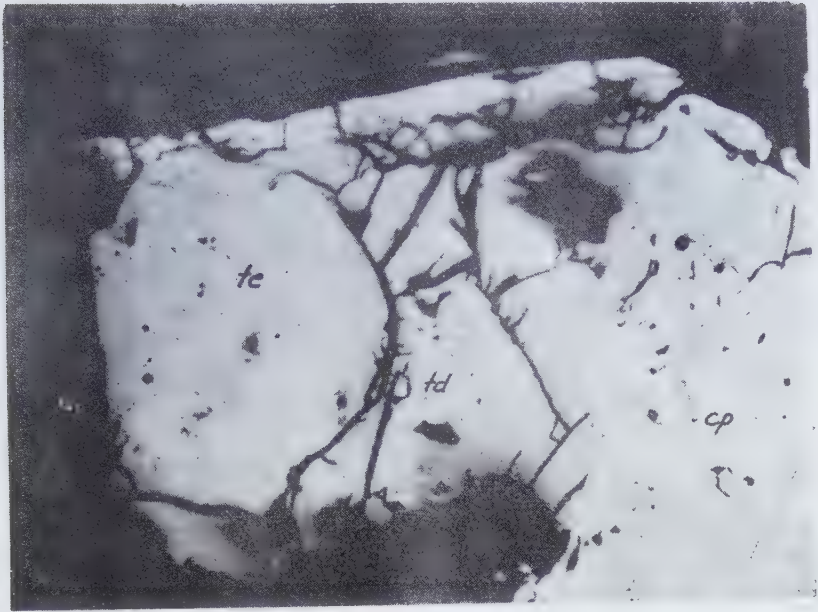
Plate II

1
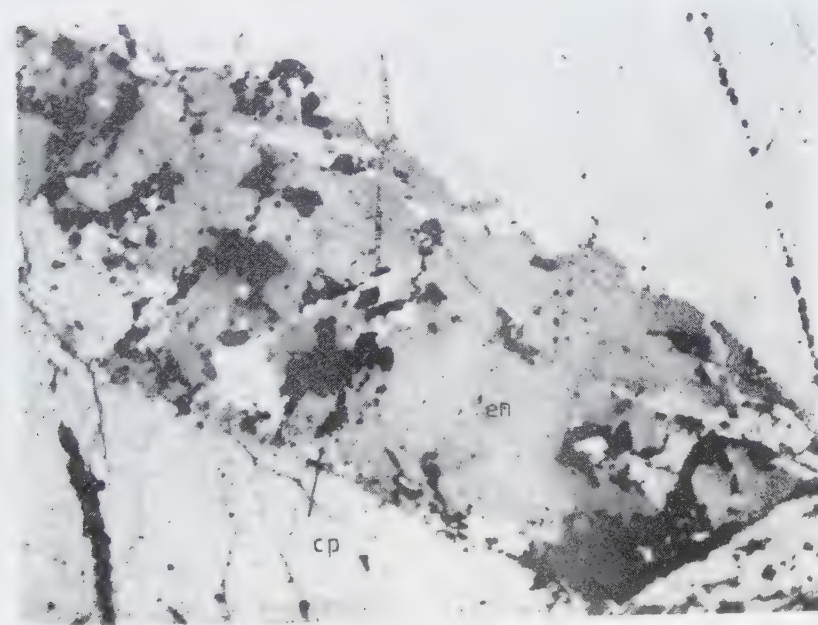
2

Fig. 1. Tetrahedrite (te) associated with chalcopyrite (cp) and tetradymite (td). Emil gallery Chinisea Valley: N II, 160 X.
Fig. 2. Vein-shaped enargite (en) in chalcopyrite (cp). Prinz Albert gallery, Tîlva Mică; N II, 160 X.

Plate III
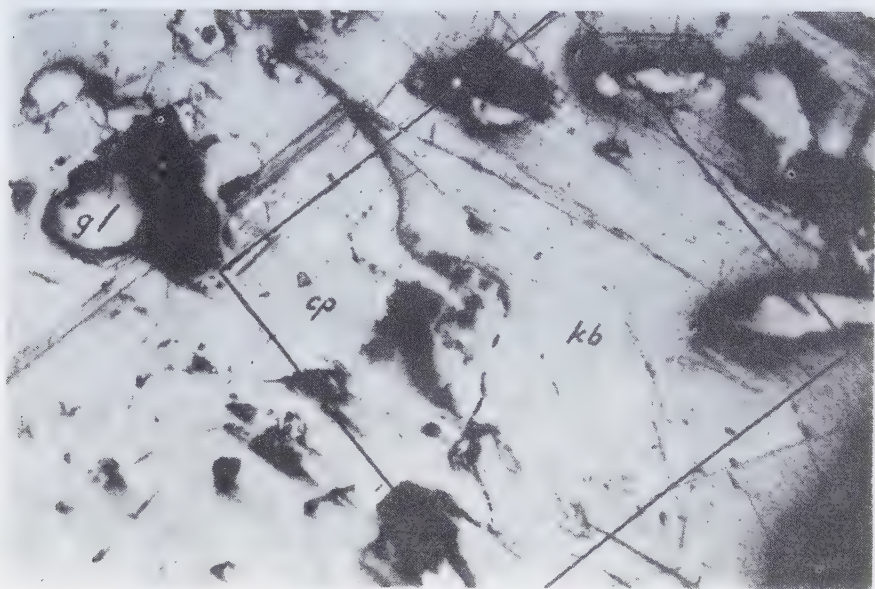
1
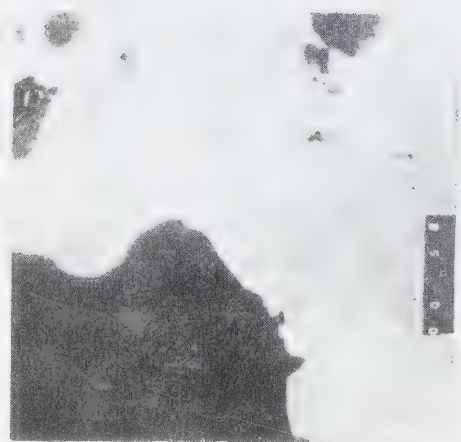
2
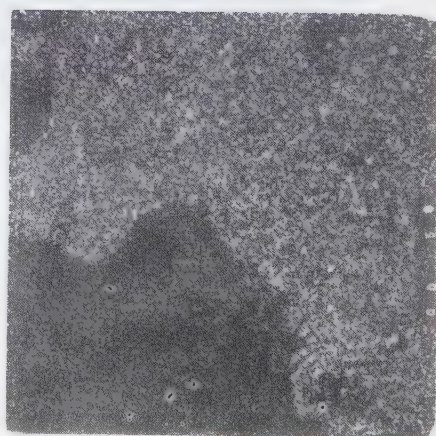
3

Fig. 1. Kobellite (kb) associated with chalcopyrite (cp) and glaucodot (gl); the field investigated with the electron microprobe; N II, 300 X.

Fig. 2. BSE image of the investigated field; 300 X.

Fig. 3. X-ray image showing the distribution of Bi; 300 X.

Plate IV
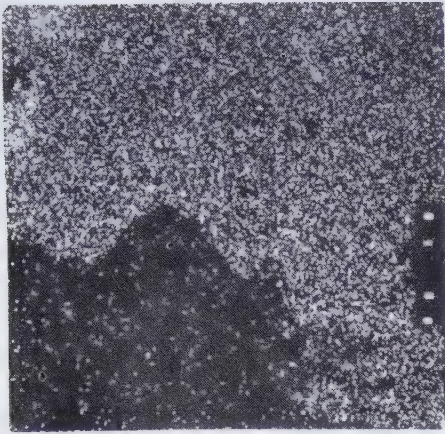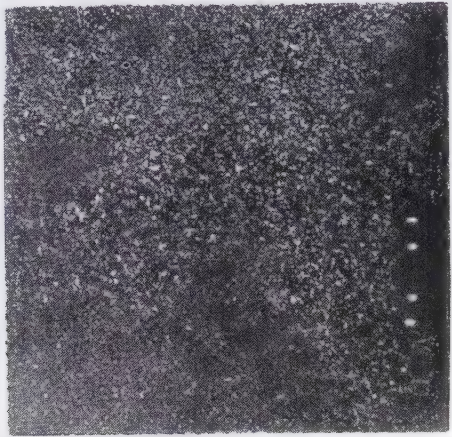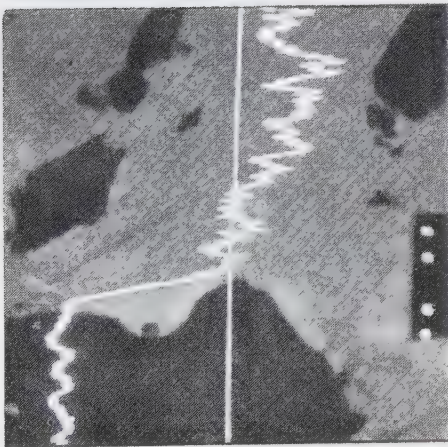
Fig. 1. X-ray image showing the distribution of Pb; 300 X.
Fig. 2. X-ray image showing the distribution of Sb; 300 X.
Fig. 3. Variation of Sb content; 300 X.

Plate V
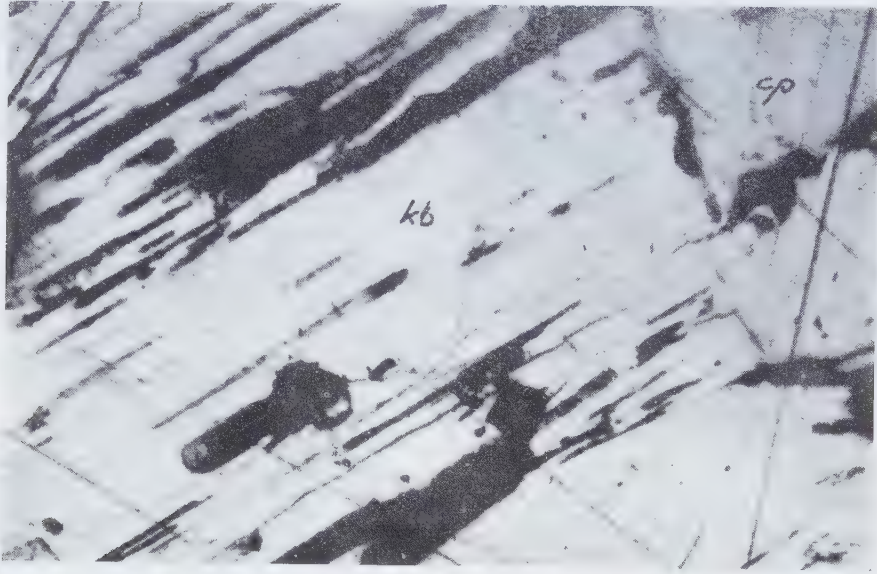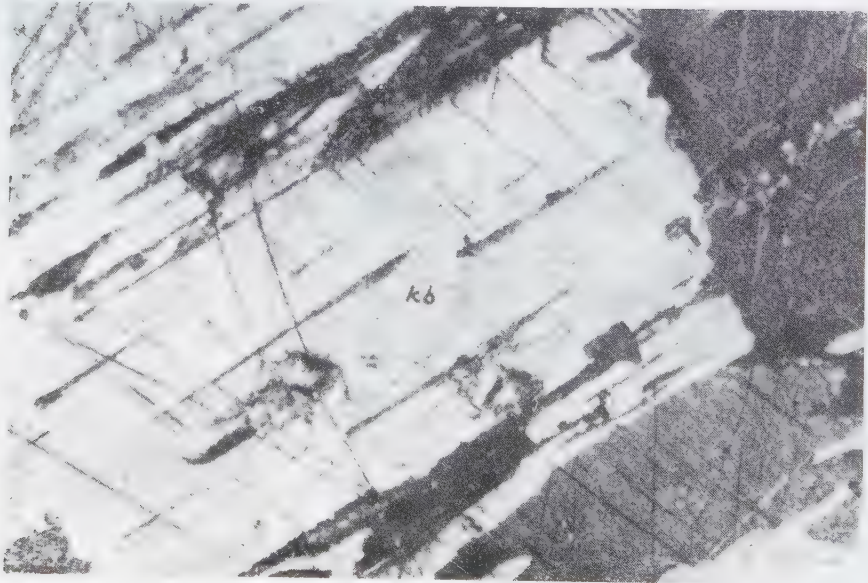
Fig. 1. Kobellite (kb) associated with chalcopyrite (cp) (Emil gallery , Chinisea Valley);. N II, 250 X.
Fig. 2. Same image in N + .

VII. MINERALOGY AND PETROCHEMISTRY

Chemical-mineralogical investigation on the Triassic-Lower Cretaceous sedimentary rocks between Nera and Radimna Valleys

EMIL CONSTANTINESCU
NICOLAE ANASTASIU

The mineralogical composition of the studied rocks, comprises the following main minerals: microcline, quartz, clay minerals, micas, carbonates, iron oxides and hydroxides. The X-ray analyses and infrared absorption spectroscopy pointed out the presence of calcite, dolomite, aragonite, kaolinite, nacrite, dickite and illite-muscovite. Chemical composition of rocks indicates a tendency of grouping in three domains, coresspondind to limestones, dolomites and dolomite limestones. The succession of the Triassic-Cretaceous sedimentary deposits, highly differentiated between the Nera and the Radimna Valleys, has three importants moments: Rhaetian, Liassic and Albian- which are correlated with a significant terrigene supply, accumulated in the marginal zones of the sedimentary basin of these epochs. In each stratigraphic interval, the detrital terrigene sequence are followed by carbonatic sequences; the simutaneous presence of kandite and illite in the clay formation of the Mesozoic deposits confirms the accumulation of the primary sediments in the marginal zones of the basin.

The sedimentary rocks belonging to the Triassic-Cretaceous cycle are well-known from the stratigraphic point of view. they belong to the Reşiţa-Moldova Nouă synclinorium of the Getic domain in the SW part of the South Carpathians (Răileanu et al., 1964; Mutihac, Bădăluţă, 1964, 1973).

By their presence in the Laramian magmatism area, they exerted a lithological control in the formation of the mineralized skarns in the Ocna de Fier-Moldova Nouă zone and determined, by their particular aspects the development of some specific mineralogical occurrences in the studied area (Constantinescu, 1971, 1977).

The specification of the mineralogical and chemical-structural nature of constituents of these deposits, as well as their reconsideration

from the petrographical point of view provide new elements for the petrogenetic interpretation and definition of the paleomedium conditions under which these formations accumulated.

Petrographical data

Definition of the petrographical types requires mineralogical and structural-textural criteria. The mineralogical associations of the studied stratigraphical series (Table 1) indicate the evolution of the sedimentation process during the Triassic, Jurassic, Lower Cretaceous as well as the post-depositional transformations of the sediments during lithification and after. The mineralogical parageneses within the Triassic deposits are defined by their alloge-

neous constituents: (1:4) - *quartz + feldspar + micas*, and authigene ones : (6:7) - *calcite - dolomite*. In the upper part of the series, calcite and dolomite occur in distinct levels, having different crystallization degrees.

The Jurassic deposits, except the Liassic (8) - *quartz-muscovite*, include simple mineral associations in which calcite is the common term:
(9, 10, 13) calcite + aragonite + allogeneous micas;
(11, 14) calcite + clay *minerals (kaolinite, dickite, nacrite);*
(12) calcite + chalcedony;
(15) calcite + opaque minerals (iron hydroxides);

Table 1. Lithostratigraphical mineralogical and petrographical features of Mesozoic from Nera Valley - Radimna Valley (stratigraphy by A. Bădăluță 1974, 1973). q, quartz; F, feldspars; L, lithical fragments; Ar, aragonite; Mu, muscovite; A, clay minerals; Bi, biotite; c, calcite.

In the Cretaceous deposits, mineral associations (17-20) are also simple and similar to those in the Jurassic deposits. A mineralogical peculiarity is represented by the quartz+lithic fragments (allogeneous) associations (21) found in a transgressive series at the Albian level.

According to the structural-textural criterion, the clastic rocks have been defined on the basis of the allogeneous constituent, the binding matter (liant) and the granulometric parameters (Pettijohn, Potter Siever, 1973). The carbonatic rocks have been separated on the basis of the crystallinity degree of the carbonates and the ratio among the allochemes ("figurative elements"), extraclasts and orthochemes (binding matters) (Folk, 1959).

In the stratigraphic succession (Table 1), the Triassic series includes, in the base, *quartz conglomerates, subarkoses, arkoses with calcitic cement* which, by the increase of the carbonatic grains, pass gradually to *bioclastic calcarenites*. In the upper part of the Werfenian, levels of *dolosparites* and *microdolosparites* occur concordantly with calcarenites. In the Lower Anisiam they form compact blocks of meter range. The bioclastic material, abundant in the Upper Anisian, characterizes the *biosparites* and the *biomicrites*. The diagenesis of the mentioned rocks consist mainly in ana-and epidiagenetic recrystallizations that determined the sparitic facies.

The Jurassic series begins with transgresive, subarkose sandstones, (Liassic), and continues with *allochemic limestones, bioclastic micrites, marls*, and intercalations of *calcilutites, silicolites* and *siltites*, up to the base of Cretaceous. In late Jurassic, micrites are partly recrystallized (recrystallatelization sparites); it is a diagenetic phenomenon.

The Cretaceous series: Valanginian-Upper Aptian is represented, from the petrographic point of view, by two types of association: *calcilutites* and *calcisiltites* with intercalations of marls, silicolites and biolithites of the reef type, in Urgonian facies. The late orogenesis affected especially the rock texture and the bioclastic structure.

Mineralogical data

The mineralogical composition of the studied rocks, (see Table 1), comprises the following main minerals: microcline quartz, clay minerals, micas, carbonates, iron oxides and hydroxides, sulphides.

Carbonates: X-ray analyses pointed out the presence of calcite (3.025 (1014) - 1.921 - 1.863 - 1.039Å), dolomite (2.862 (1.014) - 2.661 - 2.179 - 1.783Å) and aragonite (1.97 - 3.31Å).

The IR absorption spectra of the rombohedral carbonates show absorption bands in the area specific to the anionic group CO_3 713 cm^{-1} calcite - 729 cm^{-1} dolomite and to the M-O connections at 1418 cm^{-1} (Ca-O), 1435 cm^{-1} (Mg-O), respectively. The values of the absorption bands obtained on the analysed samples are close to the standard ones (Zussman, 1967).

Aragonite is individualized by the presence of an additional absorption band of low-intensity at 1065 cm^{-1}.

The DTA curves, show endothermic peaks at 890^0 C(calcite) and at 650^0 C and 800^0 C (dolomite). Strong thermic effects at the same temperatures appear on the TG and DTG curves, corresponding to the loss of the CO_2.

Qualitative determinations have been completed with qualitative analyses in view of specifying the participation rate of the calcitic phase (dolomitic, repectively) in the carbonatic rocks composition. The determinations have been carried out on 35 samples collected from the marked horizons. The ratio of the intensity of the reflexes 3.03 Å (calcite) 2.88 A (dolomite) projected on the Tennan-Berge curve (1975) wasused in the X-ray diffraction study.

The IR absorption spectroscopy used the absorption band from 713 to 729 cm^{-1}, whose position varied with the proportion of Mg-Ca substitution (Adler, Kerr, 1969).

The measurement on the thermogravimetric curves and of the weight losses corresponding to the CO_2 release connected with Mg and Ca, respectively, (MacKenzie, 1971; Todor, 1976; Constantinescu, 1977) was carried out by thermal analysis. The results obtained are given in Table 2.

For the clay minerals, the determinations (X-ray, IR and DTA) analyses pointed to the presence of minerals belonging to the kandite, illite and mica group. Kandites are mostly represented by kaolinite (the main reflexes 7.151-3.568-1.485 Å; absorption bands at 472, 539, 1009, 1033 cm^{-1}; endothermal peak at 620^0 C

and exothermal peak at 1080^0 C) and subordinately by nacrite and dickite.

The minerals of the illite-muscovite type are widespread. Illite corresponds to two polytypes—2M$_1$ and 1M—differentiated, on the diffractograms of unoriented samples, by the presence of the complete and incomplete series of *hkl* lines, respectively. When is absent, the separation of the two polytypes is possible by the (2M$_1$) presence or (1M) absence of an infrared absorption band at 803 cm^{-1}. It is possible that some of the large-crystallized muscovites migh represent the result of an illite recrystallization in zones close to the contact of the banatitic massifs (Cioflica, 1974; Vlad, 1974). However, some other times muscovite seems to have an obvious allogeneous character.

Table 2. Chemical composition of the carbonatic fraction from sedimentary mesozoic deposits (Nera - Radimna Valley)

Sample	Location	CaO %	MgO %	FeO %	SiO$_2$ mg/g	Cations in the basis of 2	Mineralogy of carbonatic fraction
601	Dl. Redut	19.85	12.73	0.35	1.03	Ca1.046 Mg0.933 Fe0.011	1 phase: dolomite
602	Dl. Redut	14.30	7.60	0.41	0.85	Ca1.130 Mg0.837 Fe0.022	1 phase: dolomite
603	Dl. Redut	47.25	5.10	0.36	0.93	Ca1.729 Mg0.258 Fe0.010	2 phases: calcite, dolomite
604	Dl. Redut	43.15	6.27	0.91	1.17	Ca1.640 Mg0.330 Fe0.025	2 phases: calcite, dolomite
605	Dl. Redut	49.02	3.80	0.16	0.36	Ca1.799 Mg0.183 Fe0.004	2 phases: calcite, dolomite
606	Dl. Redut	29.70	19.56	0.43	0.98	Ca0.040 Mg0.953 Fe0.003	1 phase: dolomite
607	Dl. Redut	45.18	8.66	0.35	0.63	Ca1.580 Mg0.398 Fe0.007	2 phases: calcite, dolomite
608	Dl. Redut	38.42	13.20	0.57	1.13	Ca1.340 Mg0.640 Fe0.013	2 phases: calcite, dolomite
609	Dl. Redut	42.15	8.15	0.38	1.15	Ca1.566 Mg0.421 Fe0.010	2 phases: calcite, dolomite
610	Dl. Redut	38.82	7.90	0.60	1.30	Ca1.541 Mg0.427 Fe0.017	2 phases: calcite, dolomite
611	Dl. Redut	37.20	3.15	0.22	3.15	Ca1.781 Mg0.209 Fe0.008	2 phases: calcite, dolomite
612	Dl. Redut	32.12	2.10	0.10	0.90	Ca1.827 Mg0.166 Fe0.003	2 phases: calcite, dolomite
613	Dl. Redut	13.16	0.73	0.19	0.35	Ca1.946 Mg0.045 Fe0.005	1 phase: calcite
614	Dl Calvaria	49.20	0.65	0.23	0.88	Ca1.956 Mg0.035 Fe0.006	1 phase: calcite
615	Dl Calvaria	51.32	0.56	0.43	1.30	Ca1.955 Mg0.029 Fe0.010	1 phase: calcite
616	Dl Calvaria	53.60	0.70	0.15	1.90	Ca1.959 Mg0.034 Fe0.004	1 phase: calcite
617	Dl Calvaria	48.56	1.17	0.75	0.73	Ca1.911 Mg0.064 Fe0.022	1 phase: calcite
618	Dl Calvaria	41.38	5.25	1.17	0.56	Ca1.667 Mg0.294 Fe0.036	2 phases: calcite, dolomite
619	Dl Calvaria	35.56	9.10	1.08	0.73	Ca1.479 Mg0.484 Fe0.032	2 phases: calcite, dolomite
620	Dl Calvaria	36.45	7.13	1.13	0.43	Ca1.540 Mg0.417 Fe0.035	2 phases: calcite, dolomite
621	Dl Redut	21.13	5.80	0.31	0.83	Ca1.135 Mg0.845 Fe0.015	1 phase: dolomite
622	Dl. Redut	17.90	10.86	0.93	1.15	Ca1.060 Mg0.894 Fe0.039	2 phases: dolomite, calcite
623	Dl. Redut	20.15	12.30	0.63	0.95	Ca1.066 Mg0.906 Fe0.023	1 phase: dolomite
624	Dl. Redut	21.70	0.86	0.00	2.13	Ca1.891 Mg0.102 Fe0.000	1 phase: calcite
625	Dl. Redut	21.80	0.72	0.10	1.80	Ca1.902 Mg0.083 Fe0.004	1 phase: calcite
626	Dl. Redut	34.30	0.15	0.10	0.70	Ca1.982 Mg0.009 Fe0.003	2 phases: calcite, aragonite
627	Dl. Redut	21.05	6.15	0.25	0.35	Ca1.411 Mg0.572 Fe0.011	2 phases: dolomite, calcite
628	V. Susara	21.18	6.40	0.42	0.72	Ca1.390 Mg0.582 Fe0.018	2 phases: dolomite, calcite
629	V. Susara	50.15	0.36	0.45	0.17	Ca1.964 Mg0.017 Fe0.013	1 phase: calcite
630	V. Susara	41.13	0.82	0.05	0.40	Ca1.943 Mg0.053 Fe0.000	1 phase: calcite
631	V. Susara	35.42	0.22	0.15	0.45	Ca1.975 Mg0.015 Fe0.006	2 phases: calcite, dolomite
632	V. Susara	41.10	0.95	0.20	0.85	Ca1.928 Mg0.060 Fe0.005	1 phase: calcite
633	V. Susara	51.15	1.15	0.00	0.10	Ca1.937 Mg0.059 Fe0.000	1 phase: calcite
634	V. Susara	24.35	3.80	0.35	0.90	Ca1.627 Mg0.352 Fe0.015	2 phases: calcite, dolomite
635	V. Susara	42.50	1.17	0.48	1.15	Ca1.908 Mg0.073 Fe0.015	1 phase: calcite

Chemical of the mesozoic carbonatic rocks

35 samples collected from three main outcrops – Redut Hill, Calvaria Hill and Şuşara Valley – have been analysed in order to point out the chemical composition of the Mesozoic carbonatic deposits. The results are presented in Table 2. The main cations Ca, Mg, Fe are given as oxides, in weight percents. The siliceous residuum is expressed in milligrams of SiO_2 per gram of rock (column 6). The total amount of the cations, supposed to belong to the carbonatic fraction, is given in column 2 and the proportions obtained for these cations are shown in column 7. In case of a unique constituent, this may be considered an attempt to establish the structural formula; in case of a mixture of two phases, the figures do not have a crystal-chemical significance; they can be, however, significant for the location of the average chemical composition of the two main phasis calcite and dolomite. For an easier correlation with mineralogical determinations, the mineralogical nature of the carbonatic fraction established by thermic analyses and X-ray diffraction is mentioned in column 8.

A synthetic image has been obtained by the projection of these results on a Ca, Mg and Fe ternary diagram. The ternary diagram rendered in Fig. 1, points to a composition averaging between calcite and pure dolomite. At the same time a tendency of grouping in three

Fig. 1. Chemical composition of the carbonatic fraction of the studied samples.

domains, corresponding to limestones, dolomites and dolomite limestones, in obvious.

The domain of limestones, especially of dolomites, shows greater homogeneity; in case of dolomite limestones, the dispersion is higher and a tendency of division into two subgroups limited by a compositional gap is outlined (Fig. 1, detailed sketches).

The some carbonatic rocks between the Nera and the Radimna Valleys, as compared to the chemistry of the Mesozoic formations in the Ezeriş-Cârnecea syncline (Kissling, 1967) and in the southern zone of the Reşiţa-Moldova Nouă synclinorium (Suvorov - Vărad - Gheorghiţă, 1975; Gheorghiţescu, 1972) point out higher amounts of Mg^{+2}, Al^{+3}, K^+.

Petrogenetical data

The succession of the Triassic-Cretaceous sedimentary deposits, highly defferentiated between the Nera and the Radimna valleys, has three important moments: Rhaetian, Liasic and Albian which are correlated with a significant terrigene supply accumulated in the marginal zones of the sedimentary basin of these epochs and correspond to some transgression moments of the sea.

Within each chronostratigraphical interval, the detrital terrigenme sequence continue with carbonatic sequences. The carbonatic sedimentation was dominated by the precipitation of the weak magnesian calcite, isolated the Anisian level on dolomite precipitation. Its presence at this level suggests changes in the water composition, mainly concerning the increase of the activity coefficient $K = aMg^{2+}/aCa^{2+}$ above the value specific to marine waters with normal salinity (k = 8.37, Usdowski, 1967).

The dolomite primary precipitation in distinct levels was probably achieved in tidal zones with shallow water and high alkalinity. These conditions did not last during the Triassic - Cretaceous sedimentary cycle. The outline, on the Ca, Mg, Fe ternary diagram, of the fields indicating the presence of limestones and dolomites and the X-ray results plead for the primary origin of dolomites levels. The diagenetic changes, subsequent to the lithification of the carbonatic deposits led to partial dolomitizations as suggested by the compositional diagrams.

Aragonite, identified by X-ray analyses, is a subordinated phase found in the Jurassic deposits. Within the evolution of carbonatic deposits, it may be exclusively regarded as an epidiagenetic product.

The simultaneous presence of kandites and illites in the clay formation of the Mesozoic deposits between the Nera and the Radimna valleys also confirms the accumulation of the primary sediments in the marginal zones of the basin.

Kaolinite – identified by thermal and X-ray analyses occurs in the transition terms from the epiclastic to the carbonatic rocks and remains in their clay residuum. Its presence in the respective levels has to be connected with the reworking processes in the adjacent continental area where the emerged formations were affected by a kaolinitic alteration.

The arkosian levels in the base of the carbonatic series plead for the presence in the source area of some feldspathic rocks (Millot, 1967; Keller, 1970).

Dickite, which was found in some diffractograms, occurs sporadically and insufficiently for getting a clear genetic significances. Its presence could be connected with local diagenetic changes took place in an acid environment (Muller, 1967).

Illite – the main term of the clay formation – is typical of the marine formations with normal alkalinity and saturated in potassium. Its for-

mation in zones close to the continental areas, against the background of an active carbonatic sedimentation may correspond to aggradation processes (transformation by iron addition) of allogeneous filosilicates rather than to a neo-formation by direct precipitation (Keller, 1970; Hans, 1971; Spears, 1973).

The Triassic-Lower Cretaceous cycle offered in all periods conditions favourable for the development of organisms with carbonatic test and subordinately of those with siliceous test (in the Oxfordian and Hauterivian levels).

The reef sedimentation, in Urgonian facies, was achieved only in the Barremian - Lower Aptian level.

References

Adler H. H., Keer P. P. (1962) Infrared study of aragonite and calcite. *Am. Miner.*, **47**, 700.

Adler H. H., Keer P. P. (1963) Infrared absorption frequency trands for anhydrous normal carbonates. *Am. Miner.*, **48**, 124.

Constantinescu E. (1971) Observații asupra skarnelor și mineralizației cuprifere laramice de la Sasca Montană. *Anal. Univ. Buc.*, **XX**, 65-74.

Constantinescu E. (1977) Mineralogia și petrologia magmatitelor laramice dintre valea Nerei si valea Radimniuței. *St. Cerc. Geol. Geogr., s Geol.*, **22**, 87-102.

Chilingar G.V., Bissel H. J., Fairbridge R. W. (1967) Carbonate Rocks. Elsevier, Amsterdam.

Gheorghiță I. (1975), Studiul mineralogic și petrografic al regiunii Moldova Nouă (zona Suvorov-Valea Mare). *St. tehn. econ.*, I, 11.

Gheorghițescu D. (1972) Considerații privind

mineralogia skarnelor cu mineralizații cuprifere de la Vărad. *St. Cercet. Geol. Geof. Geogr., s. Geologie*, **17**, 49-66, Buc.

Jeans C. V.(1971) The neoformation of clay minerals in brackish and marine waters. *Clay Minerals*, **9**, 209-217.

Keller C. V. (1970) Environmental aspects of clay minerals, *L. Sedim. Petrol*, **40**, 3, 788-813.

Kissling A., (1967) Studii mineralogice și petrografice în zona de exoskarn de la Ocna de Fier, Banat, Ed. Academiei, București.

Miller G. (1967) Diagenesis of argillaceous sediments. Diagenesis in sediments, *Develop. Sedimentology*, **8**, Elsevier, Amsterdam.

Millot G. (1967) Signification des études recents sur les roches argilleuses. *Sedimentology*, **8**, 259-280.

Pettijohn F. J., Potter P. E., Siever R. (1973) Sand and Sandstone, Springer Verlag, Berlin.

Răileanu GR., Năstăseanu S., Boldur C. (1964), Sedimentarul paleozoic și meso-zoic al domeniului getic din partea de sud-vest a Carpaților Meridionali. *An. Com. Geol.* **XXXIV**.

Spears D. A. (1973) Relationship between exchangeable cations and paleosalinity. *Geoch. Cosmoch. Acta*, **37**, 1, 77-85.

Todor N. (1972) Analiza termică a min-eralelor, Editura tehnică, București.

Usdowski H. E. (1967) Die genese von dolomit in Sedimenten, Springer Verlag, Berlin.

Vlad Ș. (1974) Mineralogeneza skarnelor de la Dognecea, Ed. Academiei, București.

Zussman J. (1969) Physical Methods in Determinative Mineralogy, Academic Press, London.

Petrochemistry of lamprophyres in the alkaline massif of Ditrău

VIRGIL IANOVICI
EMIL CONSTANTINESCU
NICOLAE ANASTASIU

The wide development of lamprophyres is one of the distinctive features of the alkaline massif of Ditrău. Chemical analyses of lamprophyres have been carried out since early in 1867, by Felner, followed by Mauritz (1912) and Vendel and Harwood (1923). Petrographical and petrochemical research on lamprophyres has been done by Ianovici (1934) and Streckeisen (1954). The research resumed with a more comprehensive petrographical and structural study of the vein rocks (Anastasiu et al., 1983) that pointed out the necessity of a petrochemical approach in the complex petrological characterisation of the lamprophyres.

The petrochemical study carried out within this study concerned the assemble of vein rocks at Ditrău. The study aimed at establishing the position of the lamprophyres in the context of other vein counterparts, as well as the relations between the chemical composition of lamprophyres and that of rocks belonging to the main massif. At the same time, the chemistry of lamprophyres inside the massif was compared to that of the lamprophyres inside the surrounding crystalline schists.

The chemical composition was followed by means of 42 analyses carried out on dominant types of vein rocks, within the limits of natural outcropping. Also, a systematic sampling has been done following the spatial distribution of the lamprophyres. Thus, the selected samples could be considered as representative from both petrographical and spatial points of view.

Beside the 42 new analyses, some data in the literature (Ianovici, 1934; Streckeisen, 1954; Garbaşevschi, Naumescu, 1976 - 1980, unpublished; Jakab, 1976 - 1980, unpublished) were included in the calculations. Interpretation of data was carried out both by direct comparison of the oxide contents and by calculation of petrographical parameters and norms.

By comparing the values of Niggli and Zavaritsky parameters and the plotting of points and vectors in appropriate diagrams, with the standard values determined on average samples (Daly, 1933; Johansen, 1962) it has been possible to check satisfactorily the degree of precision of the chemical analyses in
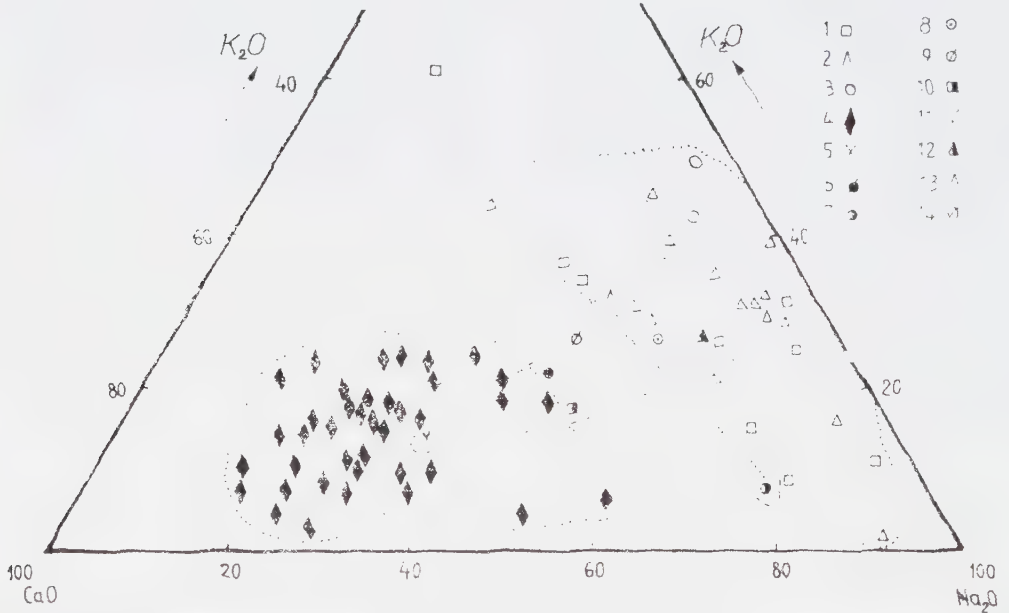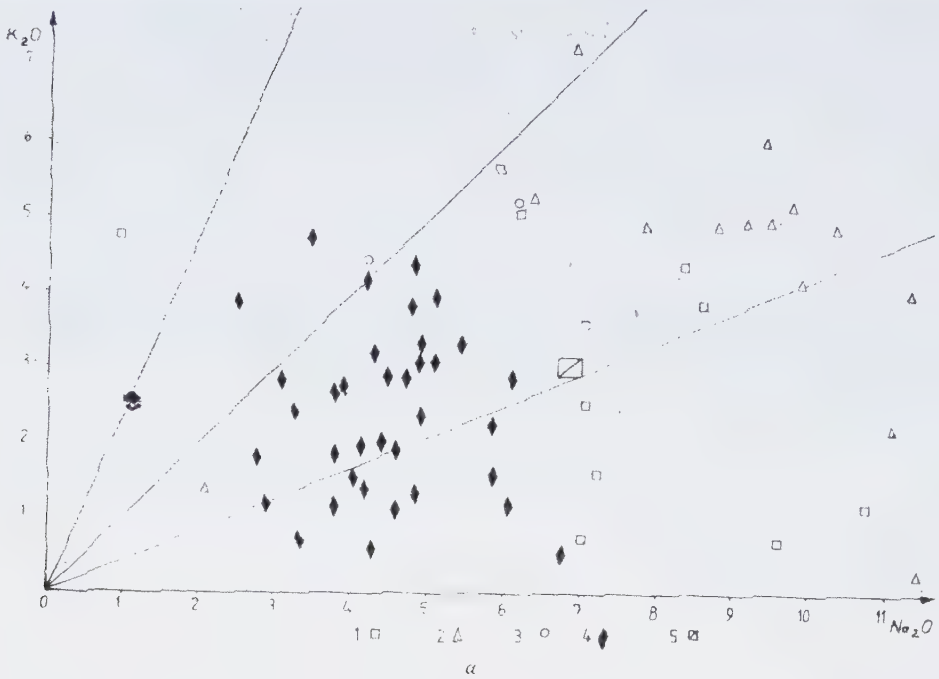
Fig. 1. Plots of analyses of the vein rock from the alkaline massif of Ditrău (oxide weight percentages) in the diagrams K_2O/Na_2O (a) and K_2O - CaO - Na_2O (b): 1, syenitoide vein rocks; 2, tinguaites; 3, aplites; 4. lamprophyres; 5, average composition of the rocks of the main massif. Several other average values corresponding to the main types of rocks in the massif are given: 5, granitoides; 6, alkali-feldspar syenites; 8, monzonites; 9, monzodiorites; 10, diorites and meladiorites; 11, hornblendites; 12, foidic syenites; 13, foidic monzonites; 14, global composition of the rocks of the massif (after Anastasiu, Constantinescu, 1980).

comparison with the microscopical analyses carried out on the same samples.

From the point of view of average oxide content, the main types of vein rocks are well individualised by the comparison between their main components.

The lamprophyres were tested chemically by means of 38 analyses. The quantity of SiO_2 varies between 34% and approximately 49% (with some isolated values exceeding 57% or lower than 32%), placing the lamprophyres in the fields of alkaline rocks and of intermediary (diorite - gabbroic) rocks. The Al_2O_3 percentage maintains between 17 - 19 % and 13 - 15%. The limits for other oxides are: $CaO = 3.5 - 12.96\%$; $Na_2O = 2.52 - 7.06\%$; $K_2O = 0.55 - 9.10\%$; $MgO = 2 - 9.64\%$ (with accidental contents either exceeding 10% or below 1%).

In tinguaites, which were tested by means of 9 analyses, the contents of the main oxides vary as follows: $SiO_2 = 43.50 - 57.66\%$; $Al_2O_3 = 20.69 - 24.49\%$; $CaO = 0.92 - 3.24\%$; $Na_2O - 2.12 - 11.92\%$; $K_2O = 1.36 - 5.24\%$; $MgO - 0.05 - 3.22\%$ (with two samples under the detection limit); $Fe_2O_3 = 0.2 - 5.2\%$; $FeO = 0.18 - 4.8\%$. In foidic microsyenites (6 analyses) the extreme values are largely the same: $SiO_2 = 54.71 - 66.3\%$; $Al_2O_3 = 16.2 - 23.55\%$; $CaO = 0.26 - 1.82\%$; $Na_2O = 6.84 - 12.7\%$; $K_2O = 0.21 - 7.25\%$; the Fe and Mg contents are relatively low and constant.

Two analyses of aplites show peculiar contents of SiO_2 (59.8 and 76%), Al_2O_3 (12.91 and 20.94%), $Fe_2O_3 + FeO$ (1.02 and 5.52%) and quite similar values for the other oxides. These contents correspond to a granitic aplite and to a syenitic aplite, respectively.

In what concerns the syenitoide veins (9 analyses), several distinguishing features can be pointed out in comparison with the tinguaites and foidic syenites: $SiO_2 = 52.54 - 63.7\%$; $Al_2O_3 = 16.7 - 25.17\%$; $Na_2O = 5.9 - $

10.78%; $K_2O = 0.75 - 5.66\%$; $CaO = 0.46 - 4.34\%$.

For the whole vein assemblage, the acidity varies between 31 and 76%, the alkalies between 0.93 and 12.74% (0.21% for sodium and 7.25% for potassium), and calcium between 0.26 - 12.96%, suggesting significant petrochemical variations.

The $Na_2O - K_2O$ (wt. %) diagram (Fig. 1a) shows the general sodic character of the vein rocks. Only five analyses (a foidic microsyenite, a tinguaite, a granitic aplite and two lamprophyres) lie above the bisectrix of the diagram. This behaviour resembles that of the main massif, whose sodic character is well documented. The values corresponding to the vein rocks lie around the areas occupied by the rocks of the main massif. One can note the grouped character of the lamprophyres, located in sectors with low Na and K contents, as well as the high dispersion of foidic vein rocks, suggesting a somewhat inverse correlation.

The plotting of the weight percents for K_2O, Na_2O and CaO in a ternary diagram (Fig. 1b) suggests two compositionally distinct domains: one for the mafic vein rocks (lamprophyres) - richer in Ca, and another one for the felsic vein rocks (syenitoides, foidic syenites and aplites) - richer in alkalies. Following in parallel the positions corresponding to the vein rocks with those corresponding to the rocks of the massif (granitoides, alkali-feldspar syenites, syenites, foidic syenites, monzonites, foidic monzonites, monzodiorites, diorites, hornblendites), we can observe that the hornblendites lie in the domain of the lamprophyres, whereas granitoides, foidic monzonites, and foidic syenites, in the domain of the felsic vein rocks. Between the two domains there are points representative for alkali-feldspar syenites, monzodiorites, diorites and meladiorites. Compared to all diorites and meladiorites or partly, to hornblendites, the lamprophyres are located in a sector with
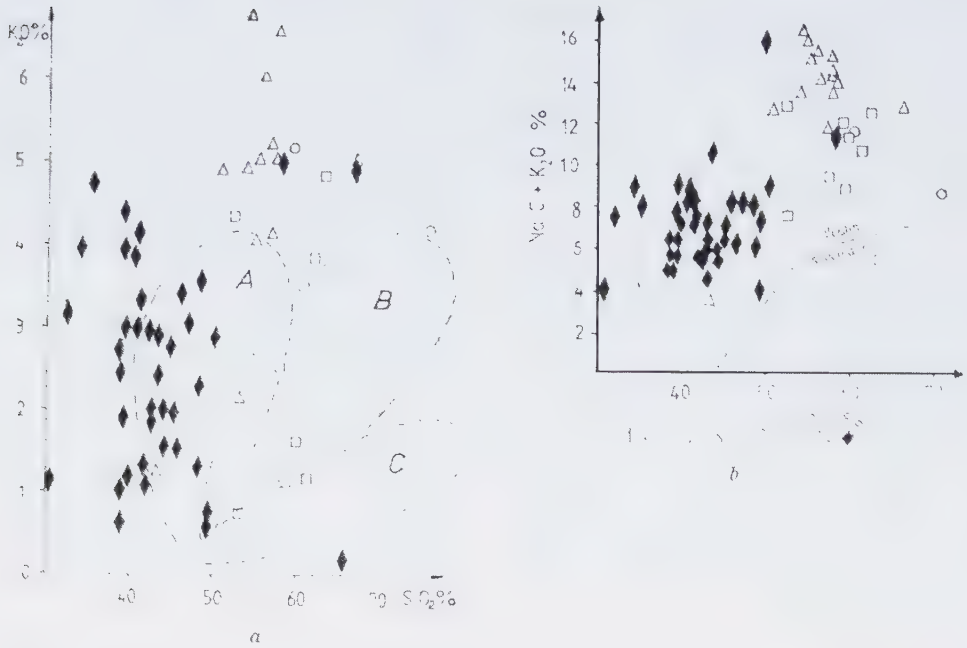
Fig. 2. Plot of analyses of the vein rocks from the alkaline massif of Ditrău (oxide weight percentages) in the diagrams K_2O/SiO_2 (a) and K_2O+Na_2O/SiO_2 (b): 1, syenitoide vein rocks; 2, tinguaites; 3, aplites; 4, lamprophyres. Outlined zones in (a) represent shoshonitic (A), calc-alkaline (B) and tholeiitic (C) domains.

higher contents of calcium. Similarly, the syenitoides, tinguaites and aplites are located in an area with higher contents of alkalies in comparison with massive syenites and foidic syenites. This fact suggests a higher differentiation of the vein products in comparison to the rocks of the massif.

The projection of weight percentages for K_2O and Na_2O in the binary diagram in Figure 2a, shows a shoshonitic composition for a part of the lamprophyres (minettes, kersantites, spessartites, vogesites) - the zone marked with A, or an alkaline composition - for another part (camptonites, monchiquites) - the zone situated in the left side of A. On the same diagram, the syenitoide veins are located in the subalkaline and partly in the alkaline domains, whereas the tinguaites and the aplites show a clear alkaline character. The binary diagram in Figure 2b (sum of alkalies vs. SiO_2) expresses well both the alkaline character of the majority of the vein rocks and their evolution

towards a higher desaturation in SiO_2, i.e., the Kennedy tendency.

On the basis of diagrams built with Niggli parameters, the following observations cab be made:

- The diagram al-alk (Fig. 3a) shows a marked grouping of all vein types between the lines alk = al and alk = 2/3al, characteristic to the alkaline rocks; it also shows the concentration of some lamprophyres and syenitoides in the domain of intermediary and subalkaline rocks as well as the location of tinguaites and foidic microsyenites in the domain of the peralkaline (alk>al) rocks.
- The diagram al-fm (Fig. 3b) points out an inverse correlation between these parameters. The lamprophyres tend to concentrate in the femic field, whereas the other vein rocks tend to gather in the salic field. The isofalic area concentrates all the other types of vein rocks.
- In the diagram c/fm (Fig. 3c) a large disper-
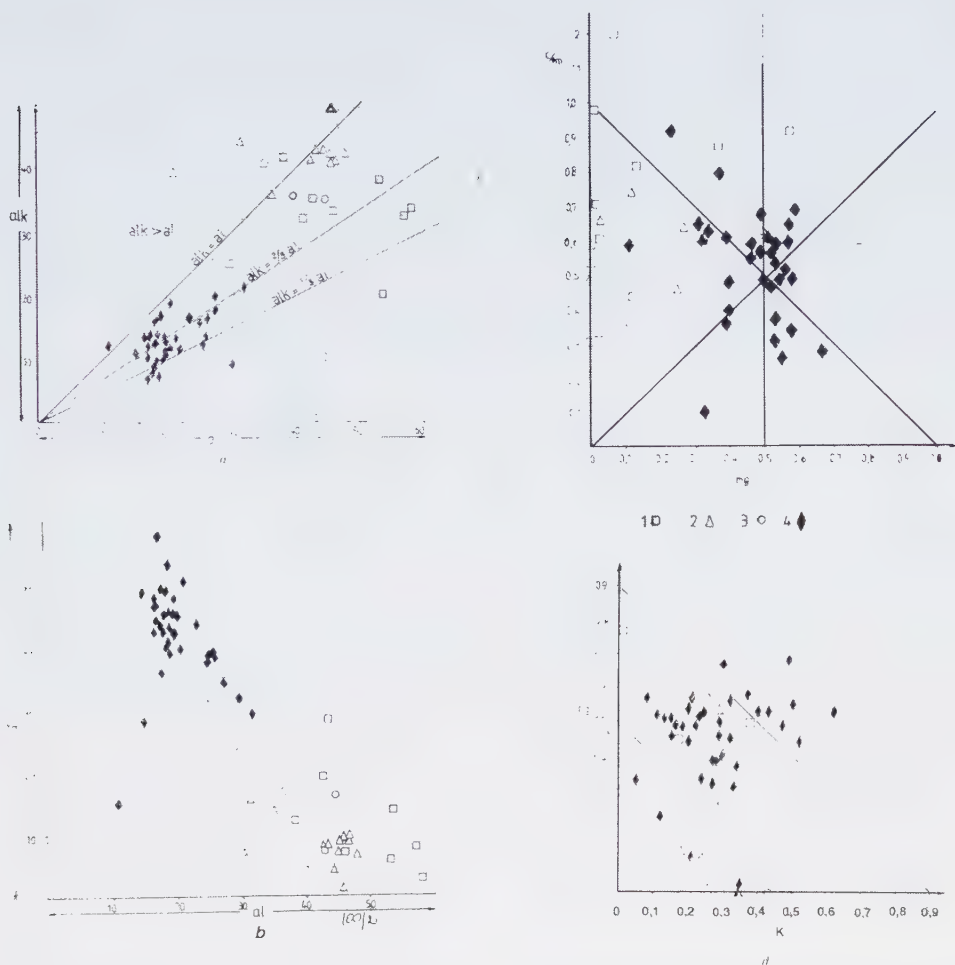
Fig. 3. The ďiagrams al-alk (a), al-fm (b) and mg-c/fm (c) built on the basis of Niggli parameters calculated for the vein rocks of the alkaline massif of Ditrău: 1, syenitoide vein rocks; 2, tinguaites; 3, aplites; 4, lamprophyres.

sion of the values can be noticed. However, the lamprophyres tend to concentrate around the intersection of the Fe, Ca, Mg, Ca-Fe-Mg and Ca-Mg-Fe fields, whereas the other vein rocks gather around the c/fm line.
- In the diagram k-mg (Fig. 3d), the area delimited by 0.5mg - 0.5k and 0.9mg - 0.9k corresponds to the maximum frequency of lamprophyres. In turn, the tinguaites and aplites concentrate under the line 0.5mg-0.5k or even on the abscissa. A detail of this dia-

gram (Fig. 4) renders the points corresponding to the lamprophyres from Ditrău in comparison with data from the literature. One can thus notice the intermediary character of the lamprophyres from Ditrau as well as the presence of several types ascribable to calc-alkaline (minettes, kersantites, vogesites, spessartites) and alkaline lamprophyres (camptonites). A series of features shared by the vein rocks from Ditrău and from the East Carpathians, can also be noticed.
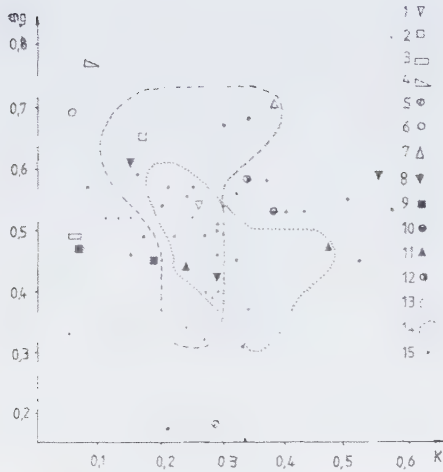
Fig. 4. Detail of the area occupied by lamprophyres in the diagram k-mg. 1-7 average values for various types of lamprophyres published in the literature: 1, camptonites; 2, monchiquites; 3, beerbachites; 4, odinites; 5, tinguaites; 6, spessartites; 7, kersantites. 8-12 Niggli values of lamprophyres from East Carpathians: 8, camptonites; 9, monchiquites; 10, spessartites; 11, kersantites; 12, lamprophyre. Domains of maximal frequency of recent volcanic rocks (after Burri, 1959): 13, Atlantic province (508 analyses, Bohemia); 14, Pacific province (878 analyses, North American Cordillera); 15, our own analyses.

Fig. 5. The Zavaritsky variation diagram (the ac SB surface) for the vein rocks in the alkaline massif of Ditrău. Explanation of symbols as in Figure 4.

In the Zavaritsky diagram, the large majority of the lamprophyres concentrate in the lower zone of the SoB and SA(c)B areas, characteristic for higher Fe and Mg contents. A larger dispersion of the points is characteristic for vein syenitoides, tinguaites and aplites. Within the ac SB area, the vectors reflect for the majority of the samples, higher Na/K ratios, but also, in some isolated cases, very high contents of K (vectors are almost horizontal). The diagram in Figure 5 contains, beside the symbols corresponding to various vein types in Ditrău area, a series of other values published in the literature. One can notice the tendency of lamprophyres to separate into two distinct

Fig. 6. The Zavaritsky variation curves for the vein rocks in the alkaline massif of Ditrău (A). On the diagram, there are also: the Etna line of variation (1), the Synir line of variation (2) (after Tihonenkova et al, 1973) and the line of Variation of the rocks in the alkaline massif of Ditrău (3) (after Constantinescu, Anastasiu, 1980).
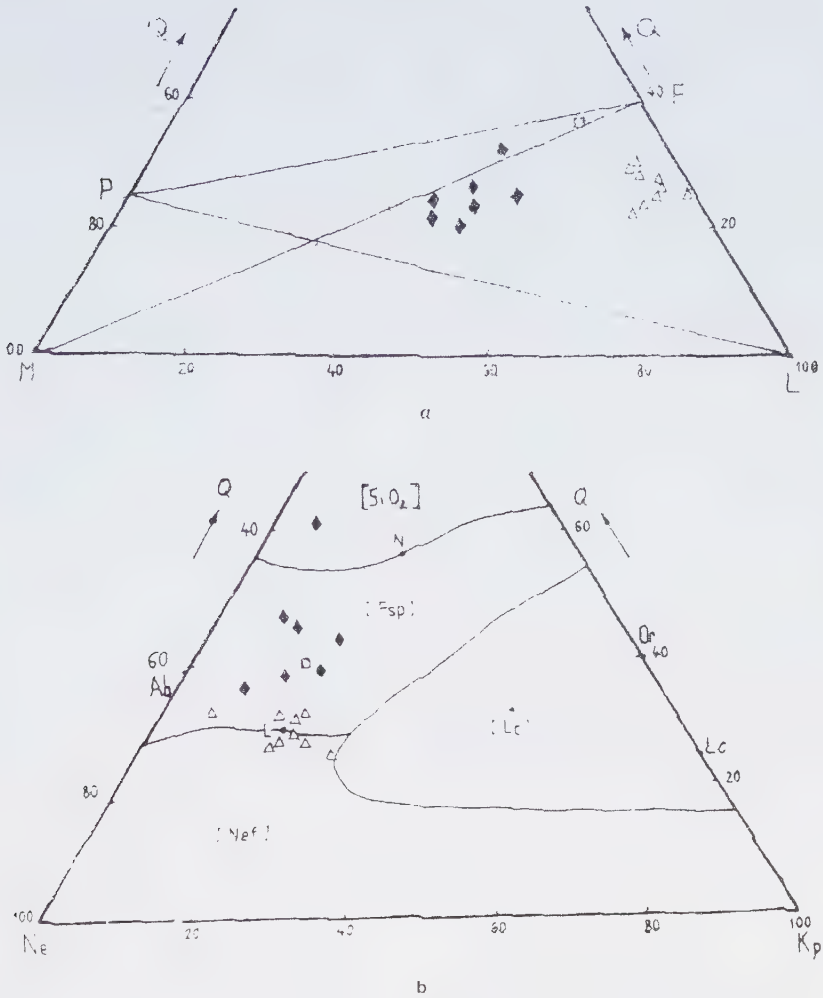
Fig. 7. The QLM (a) and Q.Ne.Kp (b) diagrams for the vein rocks of the alkaline massif of Ditrău. Explanation of symbols as in Figure 1.

fields corresponding to calc-alkaline (minettes, kersantites, vogesites, spessartites) and alkaline types (camptonites, monchiquites).

The variation curve built for the vein rocks (Fig. 6) superpose on the line corresponding to the Edna type (line 2) which separates the calc-alkaline and alkaline fields, and lies in the left side of the Synir massif line (line 3) characteristic to the alkali-potassic type (Tihonenkova et al., 1971). In relation with the line of variation of the vein rocks, the distribu-

tion of the values in the terminal part of the curve towards the field of the alkaline-rich rocks denotes a more pronounced alkaline tendency. A calc-alkaline tendency is also illustrated by the B branch which is oriented in the SB direction.

The QLM diagram (Fig. 7) shows a general image of the probable evolution of the differentiation process which developed mainly under the PF line. It may be observed that the tinguaites are located under the MF line, in an approximately central area. The syenitoide

veins lie on the conjunction of the PF and MP lines, whereas the aplites occupy different positions: the alkali-granitic aplite, over the PF line, half way between F and D (the granitic eutectic), and the syenitic aplite, under the MF line. In the ternary system silica - nepheline - kaliophilite, the tinguaites and foidic microsyenites occupy the area near the alkali-feldspar - nepheline eutectic. The lamprophyres, the vein rocks, the syenitoides and the aplites, are located between the eutectic curves alkali-feldspar - nepheline and alkali-feldspar - quartz.

Both diagrams indicate an evolution from an ultrabasic composition given by the formation of Ca-pyroxenes and amphiboles, to an alkaline differentiation, where the vein products are grouped around the final points of crystallization of the eutectic alkali-feldspar - nepheline and under the eutectic curve alkali-feldspar - quartz.

From a petrochemical point of view (as it has also been observed from mineralogical and petrographical points of view - Anastasiu et al., 1983) one can notice the presence of several types of lamprophyres, between which a series of gradual transitions exist: lamprophyres with alkaline composition - camptonites and subordinately monchiquites, lamprophyres with shoshonitic composition - minettes, kersantites, spessartites, vogesites. The camptonites predominate clearly from a quantitative point of view. They represent the differentiates of an alkaline-basic magma under the influence of the volatiles in the alkaline massif. The shoshonitic lamprophyres are hybrids of basic magma and of crust material. The monchiquites have probably resulted from the crystallization of the camptonitic magma in certain isolated areas characterized by a high activity of CO_2.

References

Anastasiu N., Constantinescu E. (1980) Structure du massif alcalin de Ditrău. *Analele Univ. Bucureşti. s. Geol.*, **XXIX**.

Anastasiu N., Constantinescu E., Garbaşevschi N., Jakab G. (1983) Petrografia şi petrogeneza rocilor filoniene din masivul alcalin de la Ditrău. *St. cerc. geol., geofiz., geogr., s. Geol.*, **28**, 17-23.

Burri C. (1959) Petrochemische Berechnungsmethoden auf äquivalenter Grundlage. Kirekhäuser Verl., Basel - Stuttgart.

Ianovici V. (1938) Considérations sur la consolidation du massif syénitique de Ditrău en relation avec la tectonique de la region. *C.R. Ac. Sci. Roum.*, **II**, 6, 689-694.

Johansen A. (1963) A descriptive petrography of the igneous rocks. Chicago Univ. Press.

Streckeisen A. (1954) Das Nephelinsyenit - Massif von Ditro (Siebenbürgen). *Schw. Min. Petr. Mitt.*, **34**, 336-409.

Tihonenkova R.P., Neciaeva I.A., Osochin E.D. (1971) Petrologhia kalievykh shelocynikh parod. Akad. Nauk USSR, Moskow.

VIII. SYNTHESES

A thermodynamic model
of the calcic skarn formation

EMIL CONSTANTINESCU

Introduction

As a basis for conceiving and applying the proposed thermodynamic model, several calcic-skarn occurrences in South Banat (Romania) have been chosen: Moldova Nouă (Gheorghiță, 1975), Vărad (Gheorghițescu, 1972), Sasca Montană, Stânăpari (Constantinescu, 1980), Oravița, Ciclova (Constantinescu et al., 1988) and partly, Dognecea (Vlad, 1974) and Ocna de Fier (Kissling, 1966).

The particularities of the skarns in South Banat are given by:

- the lack of an obvious peri-plutonic zonality;
- the presence of Al in the system (grossularite, vesuvianite, epidote - in the metasome; kandites, illites - in the paleosome);
- the presence of mineralizers: B, F, Cl (scapolite, B-bearing vesuvianite, tourmaline, fluorite);
- the existence of fractures and deformations of various orders: faults, fissures, diaclases;
- geometrical discontinuities visible at crystal level, suggesting interruptions of the forming process;
- wavering relations among minerals: in the case of the main skarn assemblage: grossularite - vesuvianite there have been noticed: coexisting euhedral grains, grossularite inclusions with compromising interfaces in zoned vesuvianite, pseudomorph vesuvianite after grossularite;
- multiple generations of the same mineral: isotropic garnets, anisotropic grossularite with younger, andraditic zones, late garnets on fissures inside other minerals, vesuvianite I, vesuvianite II.

The mentioned characteristics reflect the predominance of a disequillibrium state (successions of monomineral zones corresponding to "local equilibria" - Thompson, 1959 - are practically absent) and a weak correlation between the distance to the intrusive body (or the hot center) and the isograde surfaces.

1.Theoretical considerations

A prerequisite of all theoretical analyses of thermodynamic models is the setting of certain constraints. The definition of the system and of its relation with the exterior, is of particular importance, bringing out the inevitable alternative: closed system - open system. If the hypothesis of an open system is accepted, then a next problem to be considered is the selection of the components for which the system is defined.

In fact, the essential element of the theoretical approach is establishing the status of the components.

In the suite of models advanced by Korjinsky (1948, 1950, 1965, 1968) to explain the metasomatosis phenomenon, two main types of components are considered: inert components (IC) and mobile components (MC), the later allowing to be transferred freely by infiltration and/or diffusion from the system to the exterior or vice versa. A convenient way two distinguish among these two categories of components is given by the use of the chemical potential.

In the case of IC, the chemical potential depends on their initial concentration, pressure and temperature, whereas in the case of MC, the same potential becomes an independent variable imposed by the external environment and playing the same role as pressure, temperature and the initial concentration of the IC.

Korjinsky showed that for open systems, at given P pressures and T temperatures, the phase law takes the form:

$$\Phi = c - MC = IC$$

where c represents the number of components and Φ, the number of phases. The relation suggests that for constant P and T, the maximum number of the existing phases is equals the number of IC. Thompson (1959) demonstrated that in fact, this is not a modification of the

phase law by Gibbs, but a consequence of putting the system in particularly extreme conditions.

Another category is represented by the "buffer components" which, by their properties related to the chemical potential, are in some ways analogous with the MC.

A series of examples may suggest the nature and the role of these components. If we consider an assemblage with hematite and magnetite in equilibrium, at determined T and P, their equilibrium may be expressed by the relation:

$$2Fe_3O_4 + 1/2O_2 = 3Fe_2O_3$$
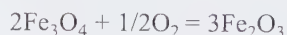
If a determined quantity of O_2 is introduced in the system and if the reaction speed is sufficiently high, a certain amount of magnetite will be transformed in hematite until the equilibrium is re-established. If O_2 is extracted from the system, then a corresponding amount of hematite will transform in magnetite.

Which is then the status of oxygen in the system? By adding or subtracting a certain component, the system becomes open for that component, that is a MC, in Korjinsky's view. ON the other hand, the component is an IC because its chemical potential is not controlled by the environment. Its chemical potential is fixed (buffered) by the simultaneous presence of hematite and magnetite.

2. Possible reactions of formation of the main minerals

The main minerals formed by metasomatic reactions in the skarns of South Banat are: wollastonite, diopside, grandites (grossularite - andradite), vesuvianite. Essentially, the paleosome is formed by limestones, dolomites, carbonatic and detrital rocks with aluminous minerals (kaolinite, micas). The theoretically possible reactions that could generate skarn minerals are:

A. The wollastonite reaction

$$3CaCO_3 + 3SiO_2 \rightarrow Ca_3[Si_3O_9] + 3CO_2\uparrow$$

calcite   quartz   wollastonite
            (silica)

B. The diopside reaction

I. $$CaMg(CO_3)_2 + 2SiO_2 \rightarrow CaMg[Si_2O_6] + 2CO_2\uparrow$$

   dolomite   quartz   diopside
               (silica)

II. $$CaCO_3 + MgO + 2SiO_2 \rightarrow CaMg[Si_2O_6] + CO_2\uparrow$$

   calcite   Mg   quartz   diopside
           oxide   (silica)

C. The grossularite reaction

I. $$3CaCO_3 + Al_2[Si_2O_5](OH)_4 + SiO_2 \rightarrow Ca_3Al_2[SiO_4]_3 + 3CO_2\uparrow$$

   calcite   caolinite   quartz   grossularite
                            (silica)

II. $$3CaCO_3 + Al_2O_3 + 3SiO_2 \rightarrow Ca_3Al_2[SiO_4]_3 + CO_2\uparrow$$

   calcite   corundum   quartz   grossularite
                      (silica)
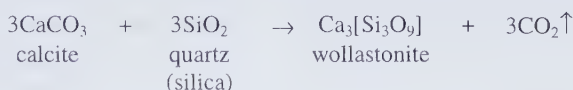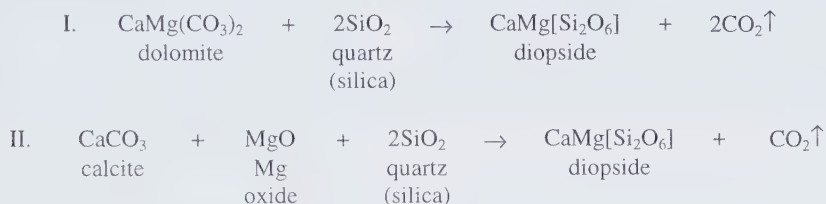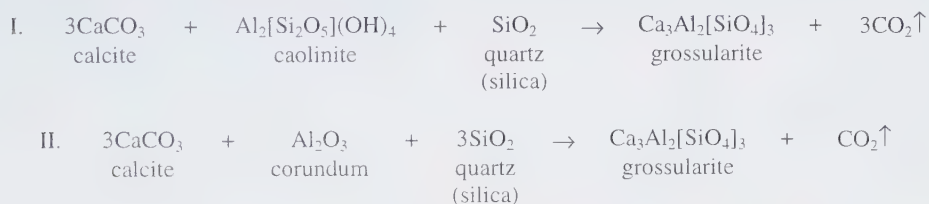
D. The andradite reaction

$$CaCO_3 + Fe_2O_3 + 3SiO_2 \rightarrow Ca_3Fe_2[SiO_4]_3 + 3CO_2\uparrow$$

calcite   Fe   quartz   andradite
            oxide   (silica)
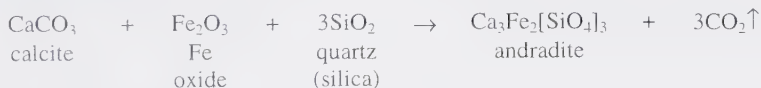
E. The vesuvianite reaction

The chemical composition of vesuvianite is given by the formula:

$$Ca_{20}Mg_4Al_8Si_{18}O_{68}(OH)_{8-n}H_2O$$

Due to the complexity of the chemical composition, the formation of vesuvianite cannot be deduced from simple reactions. In principle, we may accept either its direct formation during the skarn forming process - like in the case of grossularite, with a rather similar chemical composition:

$$calcite + clay\ minerals + SiO_2 + MgO? + H_2O \rightarrow vesuvianite + CO_2\uparrow$$

$$dolomite + clay\ minerals + SiO_2 + H_2O \rightarrow vesuvianite + CO_2\uparrow$$

or by reaction between existing skarn minerals (Ito, Arem, 1970):

$$\text{diopside+hydrogarnet+} Ca_2SiO_4nH2O \rightarrow \text{vesuvianite}$$
$$\text{wollastonite+monticellite+mellilite+} H_2O \rightarrow \text{vesuvianite}$$
$$\text{grossularite+diopside+wollastonite+calcite+ } H_2O \rightarrow \text{ vesuvianite+quartz+} CO_2 \uparrow$$

F. The tremolite reaction

$$5CaMg(CO_3)_2 \quad + \quad 8SiO_2 \quad + \quad H_2O \quad \rightarrow \quad Ca_2Mg_5[Si_4 O_{11}](OH)_2 \quad + \quad 3CaCO_3 \quad + \quad 7CO_2 \uparrow$$

| dolomite | quartz (silica) | | tremolite | calcite |
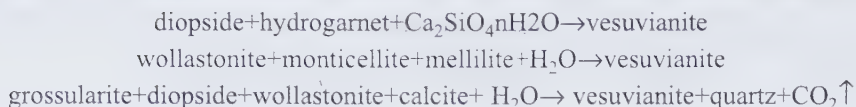
3. The definition of the system and of its limits

A system includes a undetermined number of chemical components which are chosen according to the mineral assemblages identified in the studied skarns. The limits of the system are defined by the status of the existent components.

Choosing the components is relatively simple. All minerals present in the skarns of South Banat can be discussed in the system: CaO - FeO - MgO - SiO_2 - Al_2O_3 - CO_2 - H_2O.

The lack of any important concentrations of magnetite pleads for omitting O_2 from the system. The role of oxygen being limited to that of a buffer component. The existence of distinct parageneses within the skarns requires the taking into account of two subsystems:

A) the aluminous subsystem CaO - MgO - SiO_2 - Al_2O_3 - CO_2 - H_2O represented by the assemblage: grossularite - vesuvianite ± epidote, wollastonite;
B) the non-aluminous subsystem CaO - FeO - MgO - SiO_2 - CO_2 corresponding to the assemblage wollastonite - Fe-diopside - andradite.

The small number of minerals formed by reaction of a large number of components and the specific structural conditions at Sasca Montană, indicate clearly the existence of a system that maintained open during the whole duration of the skarn forming process.

Establishing the status of the existing components is more delicate. Firstly, we shall discuss the components whose position is clear in all the investigated geological conditions.

-CaO: all skarn minerals contain important amounts of Ca. As the contents in the paleosome are very high, it is natural to consider this as the main source of Ca. We shall therefore consider CaO as a inert component.
-CO_2: skarn minerals are almost completely devoid of Carbon dioxide. It is therefore normal to consider it as a mobile component, transferred from the system to the exterior.
-H_2O: even though it subsists in certain skarn minerals, its behavior during the metasomatic process is somewhat analogous with that of CO_2. Thus, H_2O will also be considered a mobile component.

Establishing the status of other components (Fe, Mg, Si, Al) is more complicated and requires the cross comparison of the mineral assemblages specific to skarns and to paleosome. Several characteristic examples will be treated further on.

A) The aluminous system

The grandite - epidote assemblage. If CaO and Al_2O_3 are taken as IC and the system is considered open for all the other components, this assemblage is bivariant. Starting from the assemblage calcite + kaolinite, the reaction may be written as follows:

$$[5CaCO_3] + [(2 - 0.5x)Al_2Si_2O_5(OH)_4] +$$
$$((2 + x)SiO_2) + ((1 + x)FeO) + (0.75O2) \rightarrow$$
$$[Ca_2(Al_2Fe)Si_3O_{12}(OH)]+Ca_3(FeAl_2- x)Si_3O_{12}$$
$$+ ((3.5 - x)H_2O) + (5CO_2),$$
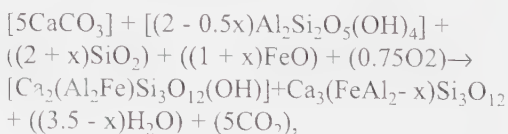
with $0 \leq x \leq 2$ and

$$\frac{a_{H_2O}^{3.5-x} \cdot a_{CO_2}^{5}}{a_{SiO_2}^{2+x} \cdot a_{FeO}^{1+x} \cdot a_{O_2}^{0.75x}} K_{15}$$

at a given P and T.

The ratio Al/Fe in grandite will depend on: the ratio calcite/kaolinite, the oxidizing conditions, the temperature and the activity of silica and iron. The temperature and the oxidizing conditions of SiO_2 and FeO are controlled by the external environment and may be considered constant. Therefore, the ratio calcite - kaolinite remains essential for the fixation of the Al/Fe ratio in grandites.

B) The non-aluminous system

B_1 - A single mineral - andradite. The system is necessarily open for silica and iron and has two degrees of liberty (bivariant). The paleosome was a pure limestone transformed by a ferrous and siliceous metasomatosis, into a monomineral garnetiferous skarn.

B_2 - Two minerals - andradite + wollastonite. There are two possibilities:

- The system is open for silica and iron; the mineral assemblage is monovariant. The paleosome was a pure limestone transformed by a ferrous and siliceous metasomatosis, into a bimineral, andradite- and wollastonite-bearing skarn.
- The system is open either for silica or iron; the mineral assemblage is bivariant. The paleosome was a ferrous or siliceous limestone transformed into a bimineral, andradite- and wollastonite-bearing skarn.

B_3 - Three minerals - andradite + Fe-diopside + wollastonite. There are three possibilities:

- The system is open for silica and iron (mag-

nesium); the mineral assemblage is invariant. The paleosome was a pure limestone transformed by a ferrous (magnesian) and siliceous metasomatosis, into an andradite-, Fe-diopside- and wollastonite-bearing skarn.
- The system is open either for silica or iron (magnesium); the mineral assemblage is monovariant. The paleosome was a ferrous (slightly magnesian) or siliceous limestone transformed by a ferrous and siliceous metasomatosis, into an andradite-, Fe-diopside- and wollastonite-bearing skarn.
- The system is closed for silica and iron (magnesium); the mineral assemblage is bivariant. The paleosome was a ferrous (slightly magnesian) limestone with a siliceous detrital fraction, transformed into an andradite- and wollastonite-bearing skarn.

In order to select among these various possibilities a good knowledge of the mineral peculiarities of the paleosome is essential. In South Banat the paleosome consisted of pure limestones, limestones with aluminous and siliceous impurities and dolomites, practically with no participation of ferrous limestones. On this basis we may consider FeO as a MC in all cases; SiO_2 - mostly MC, and in isolated cases, IC; MgO - MC, and in isolated cases, IC; Al_2O_3 - always IC.

4. Physical parameters controlling the skarn formation. Stability diagrams

In order to identify the physical parameters controlling the skarn formation, several methods of investigation have been suggested, most of them regarding the temperature. We consider that a more efficient solution is to take into account the genetic conditions of the main skarn forming minerals. The method suggested has the advantage of enhancing the subtle variations of temperature and pressure in various particular conditions, as well as the exact role played by the partial pressures of CO_2 and H_2O.

4.1. Physical conditions of the main mineral reactions

4.1.1. The stability of wollastonite

The formation of wollastonite has been studied experimentally, in the absence of water, by Harker, Tuttle (1956, fide Turner, 1968) (Fig. 1), and, in the presence of a fluid phase with variable proportions of H_2O and CO_2, by Greenwood (1963) (Fig. 2) and Winkler (Fig. 3).
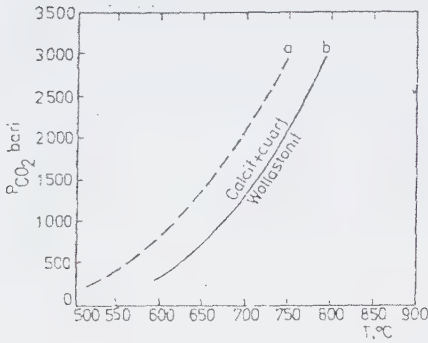
Fig. 1. The stability curve of wollastonite: (a) after Danielson (1950); (b) after Harker, Tuttle (1956).
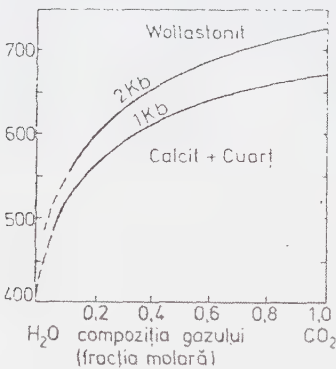
Fig. 2. The stability curve of wollastonite in the presence of a fluid phase ($H_2O + CO_2$) (after Greenwood, 1967).

As may be seen in these diagrams, the temperature of wollastonite reaction is strongly influenced by the partial pressure of CO_2. When the pressure of CO_2 equals the total fluid pressure ($PCO_2 = P_F$), the formation temperature of wollastonite is minimal ($\sim 300°$ C) at atmospheric pressure and increases rapidly with pressure, reaching the value of $750°$ C at 2 kbar. From the experimental works by Greenwood (1967), it results that in the presence of water, the partial pressure of CO_2 decreases proportionally with the concentration of CO_2 in the fluid phase. Thus, for a given xCO_2 concentration, the partial pressure of CO_2 is given by the relation:

$$PCO_2 = P_F \cdot xCO_2$$

The decrease of the partial pressure of CO_2 as a consequence of water being present in the system, determines a significant decrease of the reaction temperature (Fig. 3).
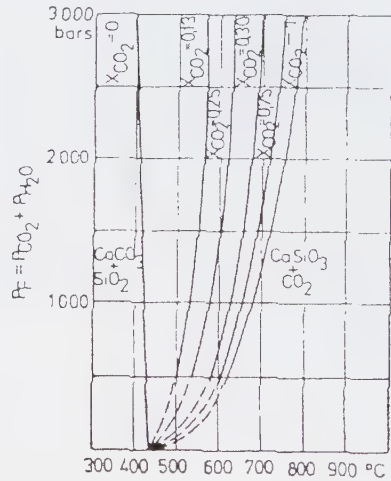
Fig. 3. Univariant curves of stability for wollastonite (ISO - XCO_2) as functions of P and T (after Winkler, 1965).

It must be stressed that the available experimental data do not refer to low-pressures of CO_2. Thus, the diagrams presented in Figures 1-3 do not cover the domains under 300 atm.

Starting however from the thermodynamic constants involved in reactions and taking into account that the equilibrium temperature

varies with pressure according to the equation:

$$\left(\frac{dT}{dP}\right)_{\Delta G=0} = \frac{\Delta V_s + \Delta V_F \dfrac{dP_F}{dP_S}}{\Delta S}$$

where $\Delta G=$ the free energy of reaction, $\Delta S =$ the reaction entropy, $\Delta V_F =$ the volume of the gases resulted from reaction, $\Delta V_s =$ the volume variation of the solid phases - we may extrapolate the experimental data to a minimum pressure of 1 atm.

From the stability diagram of the wollastonite reaction (Fig. 4) it results that at a maximum pressure of CO_2 of 250 atm, the minimal temperature of wollastonite formation is 500° C. At lower pressures, the temperature decreases; at a CO_2 pressure of 50 atm. wollastonite may form even at temperatures of 400° C.
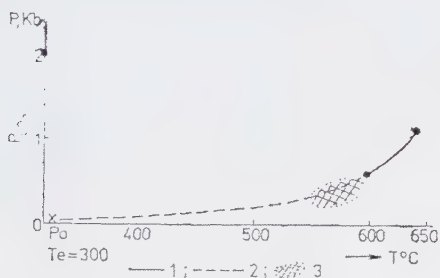
Fig. 4. The stability curve of wollastonite calculated for low pressure conditions presumed for the skarns in South Banat (h = 1 km, P = 270 bar ≈ 0.3 kbar); 1. experimentally determined curve; 2. calculated curve; 3. probable condition.

4.1.2. The stability of diopside

The stability of diopside was analyzed on the basis of the chemical reaction given above. The calculations started from the free energies at different temperatures. The equilibrium pressures of the reaction were calculated on the basis of the following equation:

$$\log P_{e_t} = \frac{\Delta G_T}{2.3R}$$

where $P_{e_t} =$ the equilibrium pressure of CO_2 at temperature T, $\Delta G_T =$ the free energy of the reaction at temperature T, R = the universal constant of gases (1.98 cal/mole).

The corresponding free energies, equilibrium pressures and temperatures (Te) are given in Table 1.

The partial pressures of CO_2 and of the equilibrium temperatures were transposed in the diagram in Figure 5.
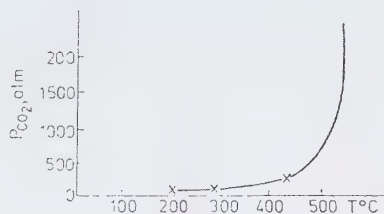
Fig. 5. The stability curve of diopside calculated on the basis of reaction free energies at different temperatures.

4.1.3. The stability of tremolite

For the tremolite forming reaction, the free energies are given in Table 2. The reaction entropy is of about 200 cal/mole and the reaction volume of the solid phase (ΔVs) is of 112 cm³. The temperatures corresponding to various equilibrium pressures of the tremolite reaction are given in Table 2 and transposed graphically in Figure 6.
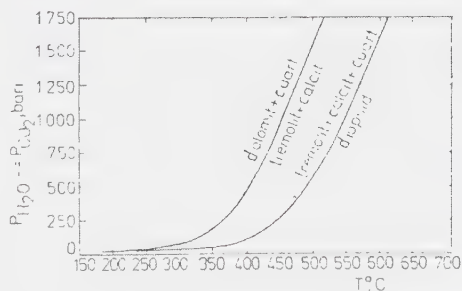
Fig. 6. The stability curve of tremolite: (a) calculated according to the data in Table 2; (b) reproduced after Turner, Verhoogen (1963).

Table 1. The thermodynamic constants of the diopside reaction.

Te, °K	300	400	500	600	700	800	900
Te, °C	25	125	225	325	425	525	625
ΔG_T, kcal	16	6	-3	-10	-17	-25	-33
P_e, atm	$10^{-5.7}$	$10^{-1.7}$	$10^{0.35}$	$10^{2.8}$	$10^{2.8}$	$10^{2.1}$	10^4

Table 2. The free energy of formation for tremolite, at different temperatures.

Temperature (° C)	ΔG_T (kcal)	Temperature (° C)	ΔG_T (kcal)
25	+36	325	-37
125	+14	425	-62
225	-16	525	-88

Equilibrium temperatures and pressures for the tremolite reaction

Te, °C	25	125	225	325	425	525
Pe, atm	$10^{-4.3}$	$10^{-1.3}$	$10^{1.3}$	$10^{2.1}$	$10^{3.1}$	10^4

Table 3. Thermodynamic constants of the grossularite reaction.

	Calcite	Caolinite	Quartz	Grossularite	CO_2	H_2O
S	22.15	8.53	9.88	57.7	51	45
V, cm³	37	100	22.7	125.3	–	–
Hf	288	979	217	1588	94	57
Gf	267	902	204	1500	94	54

4.1.4. The stability of grossularite

We considered that one of the most probable ways of forming grossularite in the skarns from Sasca Montana is the CI reaction given in the previous paragraphs. Starting from the values in Table 3, it results that in standard conditions, this reaction is characterized by $\Delta G = -17$ kcal; $\Delta S = 175$ cal; $\Delta Vs = -108$ cm³.

On the basis of the relation:

$$Te = To + \frac{\Delta G}{\Delta S}$$

we may deduce that for the extreme case of a minimal pressure (1 atm), grossularite can form at very low temperatures, of about 100° C. The formation temperatures increase with the pressure of volatiles, as indicated in Fig. 7.

4.1.5. The stability of vesuvianite

The stability conditions of vesuvianite are less known in comparison with other skarn minerals. One cause concerns the chemical complexity of this mineral, yielding a large variation of the stability domain, not only as a function of the physical proprieties of the compo-

nents involved in the forming reactions, but also in relation with the physical conditions of the environment.
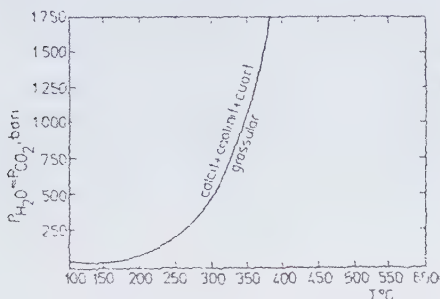
Fig. 7. The stability curve of grossularite calculated with the data in Table 3.

Experimental research concerning the synthesis of vesuvianite have been carried out by Levy (1967), Ito and Arem (1970). According to Ito and Arem (1970) (Fig. 8), at constant chemical-composition:$Ca_{20}Mg_4Al_8Si_{18}O_{68}$ $(OH)_{8-nH_2O}$, the stability of vesuvianite is dependent on pressure and temperature. Thus, at pressures exceeding 0.5 kbar, vesuvianite is stable only between 350 and 700° C (Fig. 8a). This domain reduces with approximately 50° C for alkaline environments (Fig. 8b). At pressures below 0.5 kbar, vesuvianite with the composition given by Ito and Arem, breaks-down into grossularite and wollastonite - melilite. It is noteworthy that hydro-grossularite forms at lower temperatures than vesuvianite.

Unfortunately, the experimental data do not give indications on the behavior of vesuvianite at temperatures below 350° C.

Starting from the physical proprieties of vesuvianite and hydro-grossularite (molar volumes and entropies), we considered that in the presence of water, at low pressures of the water vapors (P_{H_2O} = 500 bar), the stability domains of the two minerals can be traced like in Fig. 9.
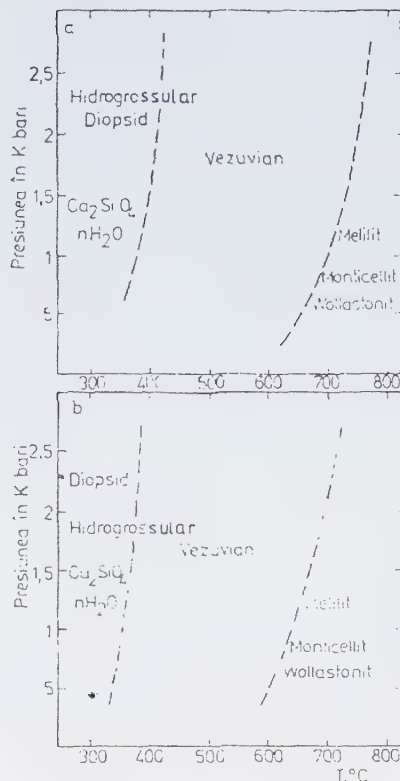
Fig. 8. Stability diagrams of vesuvianite according to the experimental data by Ito and Arem (1970, simplified).
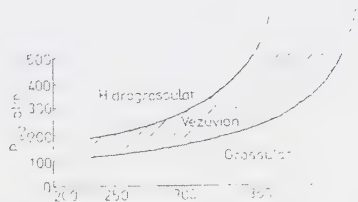
Fig. 9. Hypothetical diagram of the vesuvianite stability at low P_{H_2O} values.

4.2. The definition of the factors controlling the skarn formation.

Essentially, the factors influencing the formation reactions of skarns are: temperature and fluid pressure. Bringing together the particular

images of the calculated or experimental curves for the skarn forming minerals (Figs. 1 - 9), we notice that the curve separating the stability domains of the carbonate paleosome and of the skarns may represented schematically like in Figure 10.
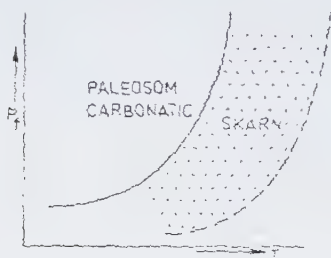
Fig. 10. The stability curve paleosome - skarn.

It becomes obvious that no discussion on the forming temperate of the skarns is possible without knowing the fluid pressure and vice versa. Consequently, for outlining an even general image of the formation conditions of skarns, it is necessary to state the maximal values of the pressure and of the temperature.

4.2.1. The pressure factor.

The total maximal fluid pressure. In the idea that the system is closed to volatile components, the maximal pressure of the fluids is approximately equal with the lithostatic pressure:

$$P_F = P_t - \rho \cdot g \cdot h$$

where P_t = the total pressure; h = the depth at which the reaction occurs; ρ = the average height of the rock column from surface to depth h; g = the acceleration of gravity ($\doteq$ 981 cm/s^2).

In order to estimate the total pressure of skarn formation at Sasca Montana, we have considered h = 1 km and ρ = 2.5 g/cm^3. By replacing these values in the above equation we obtain: P_{tmax} = 250 bar.

Partial pressure of CO_2 (H_2O). All skarn forming reactions assume the release of CO_2 conferring the partial pressure of CO_2 an important role in the evolution of the metasomatic processes. Unfortunately, only the maximal possible pressure of CO_2 can be estimated. If we admit that the system has been impermeable for CO_2 and CO_2 has been the only volatile substance in the system, then the maximal pressure of CO_2 must have been equal with the total pressure:

$$P_{CO_2} \max = P_t = 250 \text{ bar.}$$

It is however impossible not to accept the existence of any permeability for CO_2, as this volatile has had a mobile character and has migrated freely on any access ways inside the system. Had a permanent way of communication between the reaction zones and surface existed, then the partial pressure of CO_2 may have been as low as the atmospheric pressure.

One must not neglect that the skarn forming reactions assume the existence of fluid transport medium, characterized by the presence of water vapors. A series of reactions affecting a clayey paleosome, imply also the circulation of H_2O molecules. The existence of water in the system diminishes the pressure of CO_2. In the presence of H_2O:

$$P'_{CO_2} \doteq P_{F\,max} \cdot x \cdot CO_2$$

where P_{CO_2} = the partial pressure of CO_2; P_F = the total fluid pressure; x = the molar fraction of CO_2. As a consequence, the estimated range of variation for CO_2 pressure is

$$P_{CO_2} \max \leftrightarrow P_{CO_2} \doteq 250 \text{ bar} \leftrightarrow 1 \text{ bar}$$

4.2.2. The temperature factor

It is almost certain that in the contact aureole, the temperature has been a time- and space-dependent variable, which has oscillated between a minimal value corresponding to the geothermal level of the affected paleosome,

and a maximal value, corresponding to the intruded magma. In the case of skarn forming reactions at Sasca Montana, we assume the following limits of temperature variation:

$$T_{max} \approx 750^\circ \text{ C} \leftrightarrow T_{min} \approx 50^\circ \text{ C}$$

The existence of several mineral assemblages which are thermally incompatible, plead for the idea that, in time, each point of the contact aureole underwent an initial heating phase, followed by a cooling one, corresponding to a prograde and retrograde stage, respectively. It is probable that the later phase had a longer duration.

As concerns space, it is logical to assume that the temperature decreased more or less constantly from the contact to the exterior, yielding isothermal surface parallel to the contact surface. This idea has been used by Jaeger (1959) for calculating the thickness of various zones corresponding to different contact metamorphic facies around igneous dykes.

In his studies concerning the zonality of the metamorphic factors in the contact area of Salmo (Canada), Greenwood (1967) noted that when the contact surfaces are not flat, the isothermal curves tend to be closer to each other in the convex areas and farther from each other in the concave ones. This fact was due to the longer maintaining of higher temperatures in the concave areas.

It is noteworthy that the morphology of the contact areas in South Banat may be described from both points of view. Both quasi-linear contacts between magmatic bodies and sedimentary formations (e.g., Stănăpari, Sasca Montană) and concave contacts (e.g., Sasca Montană, Oravița) are present. In the later cases, the preferential development of the assemblage wollastonite - diopside, pleads for the existence of a higher temperature in comparison with the bulk of other skarn occurrences in the corresponding areas.

A more delicate situation may occur when the relation between isothermal surfaces and mineral assemblages is analyzed. the problem concerns the existence or non-existence of a concordance between the two terms of this relation.

In the event that the only factor controlling the skarn forming reactions is the temperature, the isothermal surfaces should coincide with the isograde ones. the thermodynamic calculations show however, that such a coincidence is likely to occur only in the case of a very high pressure of CO_2, i.e., higher than 2 kbar. At lower pressures of CO_2, we must admit that the reactions are influenced both by temperature and the pressure of CO_2. As the pressure of CO_2 has been estimated at 250 bar, it is likely that the importance of this factor should not be neglected.

5. The proposed thermodynamic model.

The modeling of the skarn forming process represents an attempt to reconstruct the spatial-temporal relation between two petrographic entities: the metasome (known by direct information) and paleosome (able to be reconstructed by extrapolation of unaffected sedimentary formations). In order to obtain a valid solution for the suggested scheme, the knowledge of the tectonic elements likely to act as physical supports for the variation of physical conditions, is also of importance.

Starting from the basic theoretical elements, already mentioned, a multitude of thermodynamic models have suggested to explain the evolution of metasomatic processes in several particular occurrences: Turinsk (Korjinsky, 1948), Kamioka (Fonteilles, 1962) San Leone (Verkaeren, 1974), Ocna de Fier (Kissling, 1967), Dognecea (Vlad, 1974) etc.

The application of these models to the South Banat deposits is important because of the differences concerning: the characteristics of the

skarns (reaction skarns at Kamioka and partially, at San Leone), the metasomatic zonality (clearly defined monomineral zones at Turinsk, San Leone, Ocna de Fier, Dognecea), the components involved in skarn forming reactions (at Dognecea, the system Ca - Fe - Si was applied in the majority of cases: the diagram CaO, FeO, SiO_2, CO_2, O_2 by Korjinsky, 1965; at San Leone, the diagram Si - Ca - Fe - μO_2 - $2\mu CO_2$, by Burt, 1970, was applied).

In the discussion about the physical conditions governing the main reactions involving skarn forming minerals, we noticed that in their majority, the equilibrium curves based on experimental data and published in the literature do not cover the low-pressure domains of CO_2 (under 300 atm).

Starting from the generalized equilibrium curve of the skarn forming process (Fig. 11), it is clear that a skarn assemblage may be obtained not only through the raise of temperature, but also through the decrease of pressure CO_2.
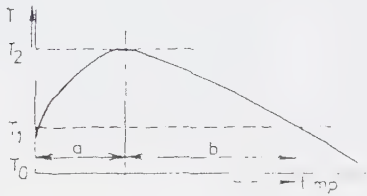
Fig. 11. The curve of temperature variation with time, within the contact aureole. T_0 = the temperature of the geothermal level; T_1, T_2 = the minimal and maximal temperatures of the skarn forming reactions; a = the prograde phase; b = the retrograde phase.

The possible ways to attain the transition from the carbonate paleosome to the skarn parageneses are given schematically below (Fig. 12):

A) on the path 1 - 2, through the isobaric increase of temperature;

B) on the path 1 - 3, through the isothermal decrease of CO_2;

C) on the path 1 - 4, through the simultaneous decrease of temperature and pressure.
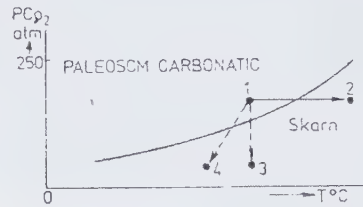
Fig. 12. Hypothetical diagram suggesting the possible paths of attaining the skarn parageneses at low-pressure of CO_2, characteristic to the calcic skarn occurrences in South Banat: 1. paleosome mineral assemblages; 2,3,4, skarn mineral assemblages.

In South Banat, the isograde surfaces cannot be paralleled with the isothermal ones, otherwise than in some rare and isolated cases.

Thus, we may conclude that the essential factor determining the non-concordance of isograde and isothermal surfaces, is the fluctuation of the CO_2 pressure, which can vary idependently of the variation of temperature. The main factors controlling this fluctuation are:

- the tectonic factor which opens or blocks the access of CO_2 to the surface;

- the presence of variable quantities of water vapors and of other volatiles (B, F), able to be correlated with the polyascending character of the skarn forming fluids or with some coupled reactions releasing H_2O.

Following this idea, in the retrograde phase corresponding to the cooling stage, a series of minerals may form, not necessarily typical for cooling processes (e.g., the tremolitisation of diopside). Taking into account that during cooling, the pressure of CO_2 may have decreased unevenly, it is possible that for short moments both senses of the transition between
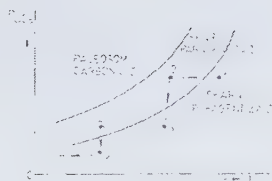
Fig. 13. Hypothetical diagram illustrating the change of stability conditions of skarn minerals in the retrograde phase.

carbonatic paleosome and skarns, may have been gone around (Fig. 13).

In consequence, in a given point, multiple generations of skarn minerals may have formed (see the examples given above), not necessarily through thermal recurrences, but through a pulsating decrease of the CO_2 pressure.

We believe that the model proposed for the dynamic of the skarn forming process at Sasca Montană, may be applied to other skarn occurrences where the pulsating activity of the disjunctive tectonics has facilitated the periodical variation of the CO_2 pressure and the polyascending evolution of the mineralizing fluids.

References

Burt D.M. (1970) Some phase equilibria in the system Ca-Fe-Si-C-O, *Carn. Inst. year-book*, **70**;

Constantinescu E. (1980) Mineralogeneza skarnelor de la Sasca Montană. 158 p., Edit. Academiei, Bucureşti.

Constantinescu E., Ilinca Gh., Ilinca A. (1988) Contributions to the study of the Oravita - Ciclova skarn occurrence, southwestern Banat. D.S. Inst. Geol. Geof., 72-73/2 (1985;1986), 27-45.

Fointeilles M. (1962) Contribution á l'étude des skarnes de Kamioka, Japon, Journ. *Fac. Sci Univ. Tokio*, **XIV**, 1, Tokio;

Gheorghiţă I. (1975) Studiul mineralogic şi petrografic al regiunii Moldova Nouă (zona Suvorov - Valea Mare. Studii

Tehnice şi Economice, I/11, 188 p.

Gheorghiţescu D. (1972) Consideratii privind mineralogia skarnelor cu mineralizatii cuprifere de la Varad. St. cerc. geol. geof. geogr., s. geol., 17/1, 49-66.

Greenwood H.I. (1967) Wollastonite: stability in H_2O-CO_2, mixtures and ocurrence in a contact metamorphic aureole near Salmo, British Columbia, Canada, *Amer. Miner.*, **52**, 1669-1680;

Holser W.T. (1950) Metamorphism and associated mineralisation in the Philipsburg region, Montana, *Bull. Geol. Soc. Amer.*, **61**;

Ito I., Arem E. (1970) Idocrase: synthesis, phase relations and crystal chemistry, *Amer. Miner.*, **55**, 880-912;

Jaeger J.C. (1959) Temperature outside a cooling intrusive sheel, *Amer. Journ. Sci.*, **257**;

Kissling Al. (1967) Studii mineralogice şi petrografice în zona de exoskarn de la Ocna de Fier (Banat), Edit. Acad. R.S.R., Bucureşti;

Korjinsky D.S. (1948) Pétrographie des gisements de cuivre ŕ skarns de Turinask, *Trudy Inst. geol. Nauk SSSR*, **68**, Trad. M. Szyszn B.R.G.M. Paris;

Korjinsky D.S. (1950) Differential mobility of components and metasomatic zoning in metamorphism, Intern., Congr. G.B., 1948, London;

Korjinsky D.S. (1965) Abriss der metasomatischen Prozesse, Akad. Verlag, Berlin;

Korjinsky D.S. (1968) The theory of metasomatic zoning, Min. Dep. Berlin;

Lévy C. (1967) Contribution à la minéralogie des sulfures de cuivre de type CU_3XS_4, *Mem. Bur. Rech. Ggeol. Min.*, **54**,178;

Lindgren W. (1933), Mineral deposits, New York;

Loomis A.A. (1966) Contact metamorphic reactions and processes in the Mt. Tallac Roof Remnant, California, *Journ. Petr.*, 7;

Măldărescu I.C. (1976) Asupra limitelor de aplicabilitate ale metodei omogenizarii incluziunilor fluide, *Mine, petrol şi gaze*, **27**, 3, 140-143;

Pomîrleanu V. (1971) Termometria şi apli-

carea ei la unele minerale din România, Edit Academiei, Bucureşti;

Thompson J.B. jr. (1959) Local equilibrum in metasomatic processes, in Researches in Geochemistry, ed. *P.H. Abelson Wiley*, London;

Turner F.I. (1968) Metamorphic petrology, New York - san Francisco;

Turner F.I., Verhoogen I. (1963) Igneous and metamorphic petrology, New York;

Verkaeren J. (1974) Les skarns a magnétite de san Leone, sardaigne Sud-occidentale, *Mém. Inst. géol.*, Univ. Louvain, **XXVII**, 2, 1-163;

Vlad S. (1974) Mineralogeneza skarnelor de la Dognecea, Edit. Acad;

Winkler H.G.F. (19650 Die genese der metamorphen Gestein, Berlin.

Tectostructural position of the foidic rocks in the Romanian Carpathians

NICOLAE ANASTASIU
EMIL CONSTANTINESCU

In the Romanian Carpathians there are only few petrographic associations that include foidic syenites: the Ditrău pluton (Giurgeu Mts., East Carpathians), the Strineac and Cărbunăria Bodies (Almăj Mts. in the South Carpathians) and the Mălaia occurrences (Lotru Mts., Central South Carpathians). They are located in orogenic areas with sialic basement and form complex alkaline provinces (those in the Ditrău Massif contain ultramafites, sienytoides and foidic syenitoides) and simple provinces (with syenitoides and foidic syenitoides at Strineac, Cărbunăria and Mălaia) in which tinguaitic veins, lamprophyres and, sometimes, pegmatoidic differentiates with rare earths can be separated. The structural control of the emplacement of such alkaline bodies is, often, evident. Their intrusion, due to the stopping mechanism along convergent crustal fractures or in areas with conjugated fractures at the intersection of major faults, represents a Mesozoic magmatic reactivation of Proterozoic consolidated structures. The intrusions have a polyphasic character, are polystadial and crystallized slowly, in a long time. The generation of the parental melt took place at great depth in the crust, at high pressures and temperatures, and their emplacement followed moments of relative tectonic calm, in overseated structural stages.

The petrographic associations including foidic rocks, are usually rare and mark a special moment in the evolution of the magmatism in a tectostuctural unit. The origin of the magmas nonsaturated in silica is still uncertain. The differentiation lines are complicated and hard to be explained, and their manifestation in the crust – as bodies, apophyses or alkaline veins – constitutes isolated events.

The foidic syenites and monzonites or essexites take part in the evolution of massifs associated to the stable crustal zones – the old shields – or to the orogene areas with eusialic basement. The spatial distribution of the large bodies of foidic rocks in the continental areas points to the stuctural control of their distribution:

– along certain old crustal fractures: the massifs in Gardar – South Greenland (Upton, 1974), in the Monteregian province—Canada (Philpotts, 1974), in the French Central Massif (Wimmenauer, 1974), in the Midland Valley Zone – Scotland (Sorensen, 1974), and in the south-west of Africa (Mathias, 1974);

– in the zones of conjugate fractures, in the intersection points of major faults in cratonic areas: Hibin and Lovozero massifs in Kola

Peninsula (Gherasimov et al., 1974), alkaline massifs in Bohemia (Kopecky, 1966) and Alden zone – northeast of Baikal (Butacova, 1974) and those in the Udzin province – Siberia, east of the Lena River (Butacova, 1974);

– in the neighborhood or inside orogenic belts: massifs in the Tuva province – Mongolia (Pavlenko, 1974), in Arkansas – USA (Barker, 1974) and in the Altai-Sayan and Taimîr-Siberia regions (Butacova, 1974);

– along young rift zones: in East Africa (Bailey, 1974) and the Rhine-Oslo Graben (Wimmenauer, 1974).

Nowadays, the elaborated petrogenetic models seek for a support in the subduction mechanisms along convergent crustal contacts or in the processes accompanying the crustal changes in the vicinity or above hot "spots". The formation of certain foidic magmas occurred, however, several times in the earth's geological history. In the mentioned zones the age of the massifs ranges between 1700-1800 m.y. and 20-30 m.y.; it excludes the discussion on a temporal control on certain time periods during wich the generation of such magmas might have taken place.

General geological setting

Within the Carpathians area, the Ditrău alkaline massif   East Carpathians (Ianovici, 1932, 1933, 1938; Streckeisen, 1935, 1952, 1974; Codarcea et al., 1957; Anastasiu and Constantinescu, 1978, 1980) - well known by its mineralogical associations, petrographic variety and structural-textural variety; small bodies with foidic rocks occur at Strineac and Cărbunăria – Autochtonous Realm, South Carpathians (Streckeisen and Giuşcă, 1932; Codarcea, 1936; Anastasiu, 1973, 1976) and Mălaia – Getic Realm, South Carpathians (Savu, 1965) (Fig.1).

Within the tectostructural units the bodies with the foidic rocks are spread in the orogenic belts, in crystalline formations of different ages and different degrees of metamorphism (Table 1).

Fig.1. The spreading of foidic rocks in Carpathian orogen: 1) crystalline formations; 2) crustal fractures (G8, G9); 3) the boundary of the Carpathian orogene; 4) foidic rocks bodies:D-Ditrău, M-Mălaia, S-Strineac, C-Cărbunăria.

The Ditrău alkaline massif

The Ditrău alkaline massif is outlined as a quasicircular pluton occuring unconformably in an upper structural stage with a partly retromorphous evolution; within it several litostratigraphic units of the cycles 1 and 2 - Carpian and Marisian supergroups (Kräutner, 1980) assigned to the Bucovinian Nappe (Săndulescu, 1975), (Table 1), have been distinguished: The Bretila-Rarău Series, Upper Precambrian A (older than 850±50 m.y. Kräutner, 1980; Bercia et al., 1976), including metamorphosed cristalline schysts in the amphybolite facies; the Rebra-Barnar Series, Upper Precambrian B (850-600 m.y., Kräutner, 1975, Popescu, 1976, Zincenco, 1978), constituted of quartz-muscovite schists, quartz-biotite schists, crystalline limestones with tremolite, metamorphosed in the greenschists facies; the Negrişoara Series of the "Pietrosul – Bistriţa" Formation (Balintoni and Gheuca, 1978; Balintoni, 1981), metamorphosed in the greenschist facies; the Tulgheş Series, Vendian-Lower Cambrian (550-505 m.y., Popa, 1974; Mureşan, 1976; Popescu, 1974; Kräutner, 1980), includes crystalline schists, metamorphosed in the greenschists

Table 1

Tectostructural unit	DITRĂU	CĂRBUNĂRIA STRINEAC		MĂLAIA
	East Carpathians	South Carpathians		
		Autochtonous realm	Getic realm	
1. Carpian 2. Marisian	a) Bretila-Rarău series b) Rebra-Barnar series (Negrişoara s.) c) Tulgheş series (Mîndra formation)	a) Neamţu series b) Ogradena granitoides	a) Sebeş-Lotru series	
Petrography	a) gneisses b) quartz-muscovite schist, quartz-muscovite schist, quartz-biotite sc., crystalline limestones+tremolite; c) phyllites, biotite quartzite, black quartzites, graphite schist	a) gneisses, amphibolites, retromorphites, cataclasites b) gneisses and massive granitoides	a) gneisses (cordierite + sillimanite); amphybolites, micaschists, migmatic rocks	
Age Facies	a) Pcb. (850-1600 m.y.) amphibolite facies b) U. Pcb. (850-600 m.y.) greenschist facies c) Vendian-Cambr. L. (505-550 m.y.) greenschist facies	a) Pcb. (older 850 m.y.) amphibolite and greenschist facies b) Baicalian	a) Pcb. (older 850 m.y.) amphibolite facies	

facies (phyllites, biotite quartzites, black quartzites, graphite schists).

The Mîndra Formation, with a medium-grade metamorphism and partly retromorphous (Balintoni, 1980), has been separated in the easternmost part of the Tulgheş Series; no obvious contacts with the Ditrău Massif have been observed.

The contacts with the crystalline schists are usually smooth, almost vertical in the north and east or with a gentle slope in the south and are marked by a thermal aureole, spatially limited and discontinuous, within wich specific mineralogical modifications – neoformations of andalusite, cordierite, corundum, spinel, sillimanite – and less changes of the texture and structure of the crystalline schists can be observed.

On the whole, the pluton is divided postkinematically (Fig. 2) and has a complex structure, in places asymmetrical, due to the spreading and orientation of the petrographic series (especially in the northern compartment – "Jolotca") and sometimes circular, due to the succession of the petrographic facies as against the centre of the massif (in the central-southern compartment – "Valea Mare-Gûdutz-Belcina"; Anastasiu and Constantinescu, 1980). The zonality of the massif is marked by the development of the "body" structures, in the central part, and of the "dyke" structures in the marginal areas.

In the northern compartment, the mafites occupy an outermost position and pass successively, to the east, to diorites, the latter to monzonites and syenites; granodiorites occur in the easternmost part of the compartment. At the limit between these petrographic complexes hybrid rocks develop in places. The foidic rocks, represented by nephelinic syenites and tinguaites, are azonal and occur accidentally. They cut other types of rocks and are individualised as unconformable apophyses with circular outline.

In the central-southern compartment, the zonality of the massif is conspicuous. Its median part corresponds to the centre of the pluton formed of foidic syenites with phaneritic structure and tinguaitic separations, within wich two "dome"

Table 2

	DITRĂU	CĂRBUNĂRIA STRINEAC	MĂLAIA
Morphology	-quasicircular pluton -dykes, veins	-quasicircular bodies -veins	-tabular bodies
Size	19 km/14 km	400 m/300 m	300m/140 m
Petrography	N:-ultramafites, mafites, diorites, syenitoides, granitoides; C, S:1) foidal syenites, 2) monzonites, 3)essexites; Veins: tinguaites, pegmatites, aplites, alcalisienites	-1) foidal sienites 2) sodalites sienites 3) alc.-feldspar syenites -tinguaites, trachytes	-1) foidal sienites 2) syenites
Mineralogy (crystallisation order)	1)F_k+Ne±Bi±Plg$_{5-15}$±Ho±Px; +can+se+parag 2) F_k ±Plg$_{10-20}$+Ne+Bi+Ho± Px; +can+zr+il+ap; 3)Plg$_{15-30}$+F_k+Ne+Bi+Ho±Px (acc. min., pirox., nepheline, Na-amph., biotite I, plg., microcline, bi. II, albite...)	1)F_k +Ne+Mi+Ab+Aug-eg; +can+se; 2) F_k +Ab+Se+Aug-eg 3) F_k +Ab+Parg. (acc. min., Ti-aug., aug.-eg., nephelin, K-feldspar, albite cancrinite, sodalite)	1Plg+ F_k+Ne+Eg 2)Plg+F_k+Bi (acc. min., egirine, plag., microcline, nepheline, liebn.)
Chemistry $Na_2O + K_2O/Al_2O_3$	miaskitic, partly agpaitic 0,73-0,93; 1,09-1,89	miaskitic 0,31-0,67	miaskitic 0,51-0,65

structures with massive textures are outlined; the oriented textures are commonly found toward the margins of the central body, where its composition becomes foidic monzonite. The essexite complex has an asymmetrical development and, in the western part of the massif, it interposes between the foidic syenites and monzosyenites. At the margin of the central body the zonality of the massif is more obvious, passing from monzonites to syenites and, in places, to granites and alkali granites can be observed in close vicinity of the cristalline schists.

The Ditrău Pluton has an autochtonous, intrusive character and its tendency of enrootment has been proved several times; the arguments have been either petrological (Ianovici, 1934; Codarcea et al., 1957; Streckeisen, 1974), or mineralogical (Anastasiu and Constantinescu, 1977) or geophysical (Gohn, 1973; Gyula, 1975; Botezatu and Calotă, 1979; Cristescu, 1981). Without specifying its autochtonous character, Balintoni (1981) has concluded, on

the basis of some interpretative profiles, that Ditrău alkaline massif intersects the mentioned crystalline series (according to the author the Pietrosu, Putna, Borsec and Rarău nappes).

The polystage distribution and the consolidation of the Ditrău Massif within the tectostructural space of the East Carpathians have been controlled by crustal fractures and by the mobility of the stuctural compartments limited by them. Thus, the geophysical data pointed out, on the basis of the gravimetric anomalies (Socolescu et al., 1975) and of the geophysical deep sounding (Rădulescu et al., 1976), the existence of a maximum line – Miercurea Ciuc-Gheorgheni-Toplița – which marks, at the limit between the Mesozoic-Crystalline zone and the Neogene volcanic chain, a crustal fracture of continental type, occurring, as a "fault field". Its line comprises a complex of fractures, which began to work (probably during the Paleozoic) and continued to be active,

by regeneration, during Mesozoic. The same geophysical data (Socolescu et al., 1975; Cernea et al., 1979) outline in the Gheorgheni-Topliţa sector an area in which the old G_8 crustal fracture intersects with other systems of fracture - G_9 and G_4 - the junction of some compartments with distinct mobility degrees and the emplacement of the Ditrău alkaline massif being thus achieved. The interdependence between the adjacent major fractures and the disjunctive dislocations, which divide the massif, with those which control structurally the displacement of the vein rocks, is shown in the diagram in Figure 2, in which the tendencies of the directions for these structural elements have been projected (Anastasiu, Constantinescu, 1980).

The disjunctive tectonics, subsequent to the emplacement of the massif, shows a regeneration character which has facilitated the movement of compartments thus delimited and allowed their relative shifting; the main effects were: 1) the sinking of the sector between the Jolotca Valley and Valea Mare and 2) the strong uplift of the central sector as compared to the northern one. Thus the present level of erosion opened, in the Ditrău Massif, two distinct structural levels: a) a shallow zone, older from the petrographical point of view, within which the foidic syenites remain at depth or individualize as apophyses and b) a deeper level, in which the erosion reached the central part of the young intrusions of foidic rocks which partly include the essexites.

The Ditrău Massif constitutes a multistage magmatic intrusion in superior levels of the earth's crust. Its petrographic heterogenity and the petrochemical incompatibilities – the presence of supersaturated rocks, granitoides, beside the nonsaturated ones, foidic syenites – points to the existence of two deep magmatic sources, whose emplacement has been controlled by deep-seated fractures in contact zones, at the beginning divergentin the beginning and convergent later on.
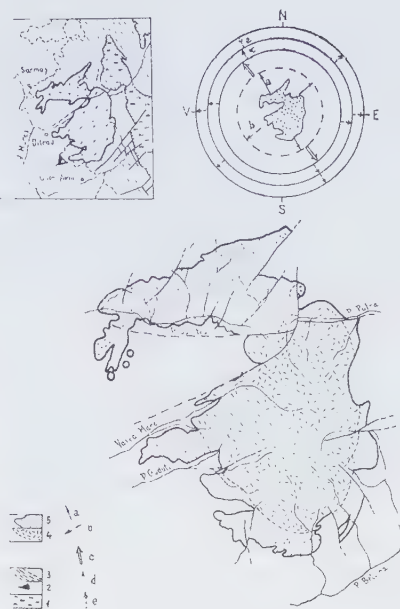
Fig. 2. The tectostructural position and the structure of the Ditrău alkaline massif: Rebra-Barnar Series, 2) Rarău-Bretila Series, 3) Tulgheş Series, 4) central zone with foidic rocks, 5) marginal zone; a) G8 crustal fracture strike, b) the fault strikes in Tulgheş Series, c) the joint strikes in contact zone, d) the joint strikes in the northern compartment, e) the joint strikes in the central-southern compartment.

The Strineac and Cărbunăria alkaline bodies

The foidic rocks also appear in the Strineac and Cărbunăria hills, the Almăj Mts., South Carpathians. They are quasicircular bodies, well delimited as concerns the morphology and as a vein sequence with a marginal disposition (Fig. 3).

The "Strineac" body has an eliptical shape, with a diameter of 200-300 m, and is located in the crystalline schists of the Carpian Supergroup, the Neamţu Series, represented by amphibolites, retromorphites and cataclasites. This series is considered to be of Upper Precambrian age (Prebaikalian; Anastasiu, 1976; older than 850 m.y.; Kräutner, 1980) and
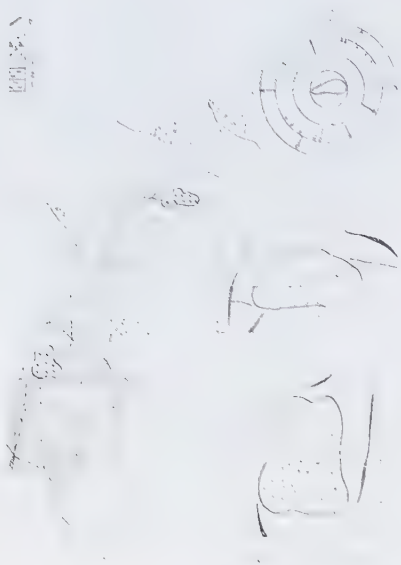
Fig. 3. The tectostructural position and the structure of Cărbunăria and Strineac bodies: 1) quartz-feldspar-biotite rocks, 2) amphibolite rocks, 3) cata-clasites and retromorphites, 4) Ogradena granitoides, 5) foidic rocks, 6) tinguaites and syenite por-phyries, 7) normal-granular facies, 8) aplitic-micro-crystalline facies, 10) alkali syenites; a) the vein strike from Strineac, b) the vein strike from Cărbunăria, c) major fault strike.

underwent a metamorphism process in he amphibolite facies. The body outcrops in the close vicinity of an E-W transversal disloca-tion and in the southernmost part of a tectonic element which accompanies the limit between retromorphites and amphibolites. The central part of the body consists of foidic syenites with a visible granulation variation: the inter-nal zones show phenocrystalline tendencies and the marginal zones microcrystalline ten-dencies. In the peripheral part of the foides decrease quantitatively and are visibly altered.

The Cărbunăria body, also with an elliptical shape, has an E-W tendency of development and does not exceed 400 m in diameter. It intersects both the biotite-bearing paragneisses of the Neamțu Series and the Ogradena grani-toids, considered of Baikalian age (Anastasiu,

1976). The central part of the body is also con-stituted of foidic syenites with structural vari-ations from the interior to the exterior and rare hydrothermal alterations; alkali syenites and syenites with sodalite appear at the periphery of the body.

The veins have thicknesses varying from 0,50 to 5m and occur both in crystalline schists and in granitoides; they appear isolatedly and may form parallel systems. In the vicinity of the bodies they seem to have a circular disposition which is likely to be the result of a tectonic control: emplacement on systems of fractures surrounding the central outcrops.

The presence of the foidic rocks on the same alignment trending NE-SW, within the Neamțu Series, and nearby disjunctive dislocations with an E-W strike is not accidental. The geo-physical data also confirm the existence, in this sector, of crustal fractures (Airinei, Ștefănescu, 1976). However, the simultaneous projection on diagrams of tendency for tectonic elements of the bodies, veins and main systems of frac-tures, indicates the structural control in the rock genesis (Fig. 2).

The lack of the chemical, mineralogical and structural affinities between the bodies of foidic rocks and Ogradena granitoides obscure the genetic affinities between them. The emplacement of the foidic rocks was the result of processes of partial melting in the basement of the Ogradena granitoides and of the Neamțu crystalline produced at the limit between two structural compartments with convergent con-tacts at a cronostratigraphic moment earlier than the Mesozoic (probably Laramian: Anastasiu, 1976).

The Mălaia alkaline body

The Mălaia alkaline body - in the Sebeș Mts. – has been pointed out and described by Savu (1965). Like the bodies in the Almăj Mts., it has an elliptical shape and small dimensions (300/140 m). This body occurs unconformably

in the crystalline schists in the Getic Realm, the South Carpathians, the Sebeş-Lotru Series of the Carpian Supergroup and represents a late orogene intrusion, without thermal aureole (Fig. 4). It comes into contact with gneisses, micaschists, amphibolites, and migmaţic rocks of Upper Precambrian-A Age (Pre-Riphean, Savu, 1965, older than 850 m. y.).

The foidic syenites in pegmatoid facies occupy its central part; they pass laterally to normal facies and are bordered marginally by alkaly-feldspathic syenites. The structure of the body is of "primary flow" and the structural and petrographical zonality is obvious; the oriented structures are generated by the disposition of the femic minerals.
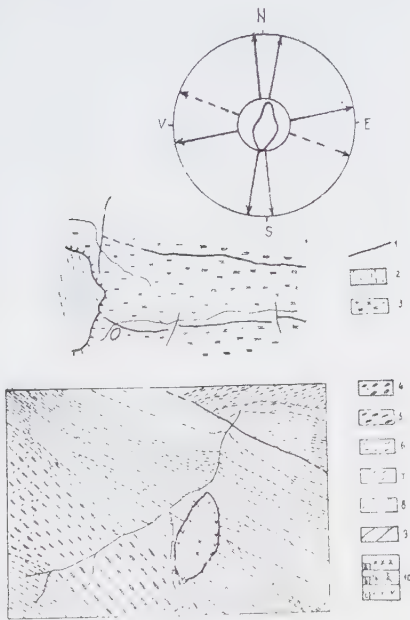
Fig. 4. The tectostructural position and the structure of Mălaia bodies: 1) crustal fractures, 2) Autochtonous Realm, 3) Getic Realm, 4) cordierite+sillimanite gneisses, 5) migmatic rocks, 6) paragneisses, 7) amphibolites, 8) quartz-feldspar gneisses, 9) quartzites, 10) pegmatoide foidic syenites, 10) b) aegirine foidic syenites, 10) c) alkali syenites

Without clear connections with disjunctive dislocations its presence is observed immediately south of the Lotrului fault and relatively close to the contact between the Getic Realm and the Autochtonous Realm. Savu (1965) considered that the primary melting constituted a subcrustal differentiate of a basic and ultrabasic magma, mobilized under stress during Paleozoic and subjected to progressive thermobaric variations.

In the Romanian Carpathians the foidic rocks constitute three occurrences and are individualized as bodies of very different sizes. Their petrographic diversity and structural complexity increase in direct correlation with their sizes. The Ditrău alkaline massif constitutes an exception within the Carpathian area; obvious similarities occur between the small bodies Strineac, Cărbunăria and Mălaia .

In spite of the very different context of their spreading as well as of the absence of relations with formations able to be dated stratigraphically, the foidic rocks are to be found in the central zones of the bodies. The bodies occur in the direction or in the vicinity of crustal fractures pointed out by geophysical data and frequently with important geological effects.

Considering all this and accepting the regeneration of the dislocations during Paleozoic or Mesozoic, it may be ascertained that the petrogenesis of the foidic rocks is linked to an old disjunctive tectonics. Its implications at the limit between the structural compartments and their temporal reopening for the creation of the access way for the nepheline-rich meltings.

The omnipresence of the veins of foidic rocks in the neighbourhood (Cărbunăria, Strineac) or inside the respective bodies (Ditrău) is a further proof for the continuity of the differentiation mechanisms as against the moment of the generation of the primary melting and its emplacement. The erosion levels where plutonic structures or terminal parts of some

intrusions exist are clearly equivalent; under them is possible – especially in the case of small bodies1 – the development in the depth, the complication of the structures and their petrographic diversification.

Regardless of the size and complexity of the alkaline bodies, the foidic fraction gives them a certain petrographic particularity. In the case of the Romanian Carpathians and within the tectostructural context, the origin of the foidic magmas has to be connected to the crustal events. The generation of such meltings took place at (20-40 km below the Conrad disconti-nuity), at highpressures and temperatures (700-800°C and pressures of 8-10 kilobars - Yoder, Tilley, 1962; O'Hara, 1968; Bailey, 1968). Their emplacement was subsequent to moments of relative tectonic calm at upper structural levels. In the Carpathians, the foidic rocks occur in alkaline provinces, which include either an almost complete succession of products or the terminal parts of this suc-cession formed exclusively of foidic syenites.

The complex bodies (Ditrău) consist of multi-ple phase intrusions, are multistadial and crys-tallized during a very long time interval (1-10 m.y.). The structural control of the disposition of the alkaline massifs is very often conspicu-ous. Their emplacement by "stopping" mecha-nisms in sectors with repeated "subsidence" represent, in the cases presented, a Mesozoic (or Paleozoic?) magmatic "activation" in con-solidated Proterozoic structures.

References

Anastasiu N. (1973) Corpurile de roci sienitice din cristalinul seriei de Neamțu (Carpații Meridionali), *Analele Univ. București*, **XXII**.

Anastasiu N. (1976) Masivul granitoid Ogradena – studiu petrografic și geochim-ic, *An. Inst. Geol. Geof.*, **XLIX**, .

Anastasiu N., Constantinescu E. (1978) Feldspații alcalini din masivul alcalin de la Ditrău, *D. S. Inst. Geol. Geof.*, **LXIV**, 1,.

Anastasiu N., Constantinescu E. (1980) Structure du massif alcalin de Ditrău, *Analele Univ. București*, **XXIX**.

Balintoni I. (1981) The importance of the Ditrău alkaline massif emplacement moment for the dating of the basement overthrusts in the eastern Carpathians, *Rev. Roum. Géol., Géophys., Géogr., Géologie*, **25**, 1.

Botezatu R., Calotă C. (1979) Ipoteză asupra anomaliei magnetice produsă de masivul de roci alcaline de la Ditrău rezultată din aplicarea unui procedeu de analiză spec-trală. *St. cerc. Geol. Geof., Geogr., Geofizică*, **17**, 1.

Codarcea Al. (1936) Note préliminaire sur cer-taines roches éruptives alcalines et sur quelques lamprophyres de la region d'Ogradena. *Bul. St. Geol.*, **XVII**. București.

Codarcea Al., Codarcea D. M., Ianovici V. (1957) Structura geologică a masivului de roci alcaline de la Ditrău, *Buletin St. Acad. RPR*, **II**, 3-4.

Cornea I., Drăgoescu I., Popescu M., Visarion M. (1979) Harta mișcărilor crustale verti-cale pe teritoriul României, *St. Cerc. Geol. Geof. Geogr., Geofizică*, **17**, 1.

Ianovici V.(1933-1934) Etude sur le massif siénitique de Ditrău, region Jolotca. *Rev. Muz. Mineral., Univ. Cluj*, **4**, 2.

Ianovici V. (1938) Considérations sur la con-solidation du massif siénitique de Ditrău en relation avec la tectonique de la region, *Comp. R. Acad. Sci, Roum.*, **II**, 6.

Iakab G. (1974-1975) Considerații asupra poziției spațiale a masivului alcalin de la Ditrău, *D. S. Inst. Geol. Geof.*, **LXII**.

Mureșan M. (1976) O nouă ipoteză privind pânzele bucovinice din partea sudică a zonei cristalino-mezozoice a Carpaților Orientali, *D. S. Inst. Geol. Geof.*, **LXII**, 5.

Rădulescu D., Cornea I., Săndulescu M., Constantinescu I., Rădulescu F., Pompilian R. (1976) Structure de la croute terrestre en Roumanie – essai d'interprétation des

études sismiques. *An. Inst. Geol. Geof.*, **L**.

Săndulescu M. (1975) Essai de synthése structurale des Carpathes , *B.S.G.F.* (7), **XVII**, 3, Paris.

Socolescu M., Airinei St., Ciocîrdel R., Popescu M. (1975) Fizica şi structura scoarţei terestre din România, Ed. tehnică, Bucureşti.

Sorensen H. (1974) The Alkaline Rocks, John Wiley, London.

Streckeisen A. (1952-1954) das Nephelinsfen Massif von Ditro Siebenburgen, Schw.

Min. Petr. Mitt., 32, 34, Bern.

Streckeisen A. (1960) Of the structure and origin of the nephelinsyenite complex of Ditro (Romania), *Rep. 21th Inter. Geol. Con. Part.* **13**, Copenhagen.

Streckeisen A., Giuşcă D. (1932) Der Nepheline-Cancrinite Syenit von Orşova, *Bul. Soc. Rom. Geol.*, **I**, Bucureşti.

Streckeisen A., Hunziker J. (1974) On the origin and age of the nephelin syenite massif of Ditro (Romania), *Schw. Min. Petr. Mitt.*, **54**, 1, Bern.

Structural control of vein setting in the alkaline massif of Ditrău

NICOLAE ANASTASIU
EMIL CONSTANTINESCU
GYULA JAKAB
NAZAR GARBASEVSKI

The vein rocks from the alkaline massif of Ditrău are represented by leucosyenites, porphyrytic microsyenites, bostonitic mycrosyenites, albitites, syenites and foidic microsyenites, tinguaites, alkali granites, aplites and pegmatites as petrotypes with leucocratic tendency and by various lamprophyres (vogesites, spessartites, kersantites, camptonites) as petrotypes with melanocratic tendency. The emplacement of the vein rocks has marked a moment of completion of the geological structure of the alkaline massif of Ditrău. It was controlled by old displacements or by fissures which affected the massif during its cooling or immediately after that. As compared to the disjunctive displacements and to fissures systems, the directions of leucocratic veins and of lamprophyres are not always conformable.

The vein rocks from the alkaline massif of Ditrău belong both to the leucocratic and melanocratic types. They have a high frequency and a preferential distribution within this massif; they are concentrated in its marginal sectors and are rare towards its central part.

The presence of vein rocks in the massif was noticed in many studies (Ianovici, 1933, 1938; Streckeisen, 1952, 1954; Codarcea et al., 1954), but without trying to correlate with the structural elements of the massif. The vein rocks associated with mineralized zones, in the northern part of the massif (Jolotca valley) and in its southern part (Aurora and Hereb zones) may with the orientation of microstructural elements (planes S2 given by the orientation of micas and amphiboles) and tectonic elements (fissures, faults, etc.).

The vein rocks (Anastasiu et al., 1983) are represented by leucosyentes, porphyrytic microsyenites, bostonitic microsyenites, albitites, syenitic and foidic microsyenites, tinguaites, alkali granites, aplites and pegmatites, them–as petrotypes with leucocratic tendency and by various lamprophyres - vogesites, spessartites, kersantites, camptonites–as petrotypes with melanocratic tendency; carbonate, sodalite and biotite-bearing veins are much less frequent (Anastasiu, Constantinescu, 1974). The vein frequency in the massif and their

relationship with with the main pluton are an evident proof of the successive emplacement of some magmatically differentiated products. The cooling subsolvus processes explain on the one hand their structural diversity, namely, the microcrystalline, medium-grained and pegmatoid facies. On the other hand, they explain their petrogenetic conection with the main rocks of the massif.

Veins are widely spread on tens and hundreds of meters in length and appear both conformably and unconformably as compared to microtectonic and structural elements of the massif. Their limits with host rocks are clear for unconformable veins and rather diffuse for the ones conformable to host the "foliation" of host rocks. Veins are usually associated in parallel systems or form networks with successive generations; the anastomosing aspect is also common.

The petrographic similarities, their frequency and dimensions of the veins their space relationships with host rocks, provide the criteria to delimit nine vein fields (Anastasiu, Constantinescu, 1983): Pietrari-Teascului, Jolotca, Valea Mare, Güdutz, Chiuruţ, Hereb-Balas, Lorincz, Aurora and Putna-Călugăr.

Setting of structural elements

The late- and postkinematic division of the alkaline massif from Ditrău and the development of disjunctive displacements have controlled the vein rocks petrogenesis during distinct periods and with different intensities.

The orientation of foliation planes S2 - within oriented textured rocks - meladiorites, diorites, essexites, foidic syenites - is clear in the two compartments of the massif (Anastasiu, Constantinescu, 1980). In the northern compartiment their setting leads to an "axial" group–N40°E/30°NW–. In the southern compartment a tendency of "garland" emplacement can be noticed–settings between NS and

N40°E/60-70°NW.

The disjunctive displacements between the two compartments are pointed out by the existence of some breccias and milonites and by shiftings of some petrographic sectors. These are confirmed by geological mapping and by mining works.

Within the northern compartment, the main fractures form a quasiparallel system having a NE-SW general orientation, extending over the massif limit. Fractures do not affect too much the continuity of petrographic complexes, and do not reflect strong correlations with the vein systems.

Within the southern compartment, fractures develop marginally and have a radial distribution as compared to the limit with the crystalline schits.

Fissure systems (diaclasses-D), having a transversal ("ac") and longitudinal ("bc") character, were delimited in the massif, clase to the disjunctive displacements or far outside them.

Within the "Jolotca" sector, the poles of "D" planes form several maxima corresponding to the following directions: E-W/70-90° towards N and S; N45°E/60-80° towards NW and SE and N30°E/30 - 50°NE and SW.

Within the "Valea Mare - Güdütz - Belcina" sector, the maxima of "D" planes tend to form a belt with a symmetry plane parallel to the direction of the dominant diaclase system: N0-40° W/60-70°NE is weakly outlined.

All diaclase systems of the massif have a postkinematic character; their age is not the same: the oldest seem to be the longitudinal system ("bc"- as to the elongation of the adjacent crystalline). The most recent ones, are the transversal diaclases - "ac" type, which appear as support - fissures.

Setting of the vein rocks

The setting of the vein rocks as compared to the setting of structural elements (planes S2) and of tectonical elements (displacements fissures) in each vein field, shows several partially correlable cases.

In the "Pietrari-Teascului" field, the syenitoidseveins cross hornblendites, meladiorites and diorites and are usually unconformable as to their planar elements (S2). Their direction is between N30-72°W/30-70°NE and N48-68°E/45-90° towards NW and SE (Fig. 1).

Fig. 1. Projection of poles of syenites veins direction. (1) porphyrytic microsyenites; (2) lamprophyric microsyenites; (3) from Pietrari-Teascului and Jolotca vein fields as compared to the main fissure planes (D) and of foliation planes (S2 poles).

The lamprophyre veins located in hornblendites and meladiorites are hardly distingnishable from their background. Therefore, their frequency is probably higher than that observed from mapping. They sometimes cross syenitoide veins. They are grouped in four maxima corresponding to the following directions: N-E, E-W, N45-60°W and N40-50°E with variable dips towards NE and SE.

In the "Jolotca-middle course" field, syenitoides cross diorites and monzodiorites and

appear as single veins or, more frequently, with two or three branches, of which, one can be conformable to planar elements of the host rock. Leucocratic veins lose their individuality and quickly fade within monzodiorites and hornblende-bearing syenites. Their directions are grouped into two maxima: N50-75°E/70-90°S and N30-60°W/40-65°NE, which are sometimes subhorizontal.

In the "Valea Mare" and "Güdutz" fields the vein rocks (without foidic leucosyenites, porphyry microsyenites, albitites) are more abundant towards the margins of the perimeter. They cross essexites, foidic monzodiorites and diorites. As compared to their S2 plane, they are both comformable and uncomformable. Their directions are grouped in three maxima (Fig. 2): N25°E/60°W; N45°W/70°SW and N55-80°W/70°SW Lamprophyres are of two generations, which are spatially recognized by mutual intersections vein. Their directions are more constant: N40-50°W/10-40°NE or /60-70°SW.

Fig. 2. Projection of poles of syenites veins directions (1), and lamprophyres (2), from Valea Mare and Güdütz fields as compared to the projection of the main fissure planes (D) and of foliation planes (S2 poles).

In the "Chiuruț" field, the albitites, porphyrytic microsyenites and pegmatites veins cross syenitoides, granitoides and crystalline schits

of the Tulgheş Series and are mostly unconformable as to the structural elements of the host rocks. Their direction is conformable to the fractures of the perimeter and varies around N-S. Dips are almost vertical. Lamprophyres veins have subhorizontal tendencies.

In the "Cianod" field the leucosyenite, bostonitic microsyenite and tinguaite veins intersect foidic syenites, foidic monzonites, syenites, alkali granites and phyllites. They are unconformable as to the structural elements of the host rocks. Syenitoides are previous to porphyrytic microsyenites and are crossed by tinguaites.

The directions of leucocratic veins are grouped into two systems: N10°E/80°NW and N65-75°E/20°SE and /70°E.

In the "Hereb-Balas Lorincz" field, leucocratic veins cross syenitoides, granitoides and crystalline schits, following the direction of main fissure systems (Fig. 3.).

The mineralization identified in mining works is conformable to porphyrytic microsyenite veins. The direction of syenitoid veins varies between N5-40°E/70°NW or SE.

In the "Aurora" field, the leucocratic veins and lamprophyres cross pegmatoid syenites and lieberitized foidic syenites. The emplacement succession, 'suggested by these relationships would be: syenitoides, porphyrytic, microsyenites, lamprophyres I, tinguaites, aplites, lamprophyres II, carbonate- and fluorinebearing veins. In the VII - Aurora gallery zone, molybdenum mineralizations are parallel with porphyrytic microsyenites and with NW-SE oriented fissures. Leucocratic rocks are individualized in two vein systems: N45°W/45°NE and N75-85°E/30-60°NW. and lamprophyres have directions between N 0-20°E/20-60şNW and N30-40°W (Fig. 4).

Fig. 4. Projection of poles of syenitoide veins (1) and of mineralized zones; (2) from the mining works at gallery VII - Aurora, as compared to the projection of the main fissures planes (D).

Fig. 3. projection of poles of leucosyenite veins directions (1), porphyrytic microsyenites (2), lamprophyres (3) and mineralized zones (4) from the hereb mining works, compared with the projection of the main fissure planes (D).

In the "Putna-Călugăr" field, tinguaites and foidic syenites form an anastomosing veinlet network trap a microsyenitic differentiate; lamprophyres are rectangular and displace tinguaites. The carbonate veins, well individualized in this field, have a N80°W/80°S direction.

appear in a relative conformity with the "ac" dia-clase system and are subparallel with to the "Jolotca" fracture. The lamprophyre veins, very differently oriented, are partly conformable to the main disjunctive displacements of the zone.

Fig. 5. Projection of poles of foidic syenite veins directions: (1) tinguaites; (2) lamprophyres; (3) from he mining at gallery XI - Aurora, as com-pared to the projection of the main fissures planes (D) of the zone.

Final remarks

The vein rock emplacement has marked a moment of completion of the geological struc-ture of the alkaline massif from Ditrău. The vein formation was controlled by old displace-ments or by fissures which affected the massif during its cooling time or immediately after that.

By simultaneous projection of the S2 plane poles, of diaclase ("D") poles and of poles cor-responding to the direction of leucocratic and melanocratic veins, one can observe the sys-tematic relationship between these elements.

As compared to disjunctive displacements and to fissure systems, directions of leucocratic veins and of lamprophyres are not always per-fectly conformable (Figs. 6, 7).

In the northern compartment of the massif (Jolotca - Putna), the syenitoid veins are grouped into two systems with preferential orientations: N25-70°W and N50-70°E/60-80°SW. They

Fig. 6. Projection of the main fracture direction (F), of diaclase systems (D), of mineralized veins (M), of lamprophyres (L), and of syenitoides (S), from the northern compartment (Jolotca) of the alkaline massif Ditrău.
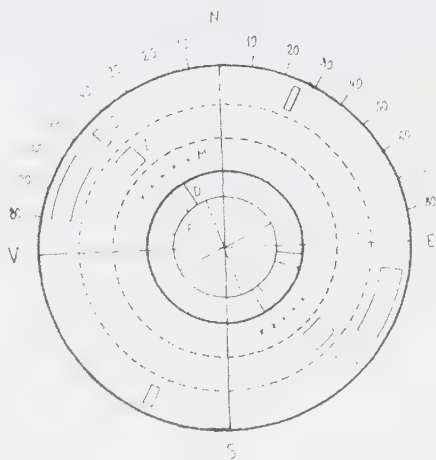
Fig. 7. Projection of the main fracture direction (F), of diaclase system (D), of mineralized zones (M), of lamprophyres (L), and of syenitoides (S) from the central-southern compartment (Valea Mare - Güdütz-Belcina) of the alkaline massif from Ditrău.

The mineralized veins (with molybdenite-xenotime-loparite-monazite-ilmenite-titano-magnetite-pyrite-galena-sphalerite; Constantinescu et al., 1981) are E-W oriented and are grouped in discontinuous alignments but often conformable to one of the lamprophyres systems (the E-W one) (Fig. 6).

In the central-southern compartment, namely "Valea Mare-Güdütz-Belcina", the syenitoide veins have two preferential directions: N45 (55-80°) W and N25°E of which the first is conformable with the disjunctive displacements setting. The lamprophyres veins direction (N40-50°W) can be correlated with the direction of "bc" longitudinal diaclase system and to that of some marginal fractures (Fig. 7). The mineralizations from the Hereb and Aurora field (molybdenite-pyrite-sphalerite-galena-REE) is located on alignments conformable to syenitoide and lamprophyre veins.

References

Anastasiu N., Constantinescu E. (1980) Structure du massif alcalin de Ditrău. *An. Univ. Buc., s. geol.*, **XXIX**.

Anastasiu N., Constantinescu E., Iakab G., Garabaşevschi N. (1983) Petrografia şi petrogeneza rocilor filoniene în masivul alcalin de la Ditrău. *St. cerc.geol. geofiz. geogr., s. geol.*, **28**.

Anastasiu N., Constantinescu E. (1983) Criterii petrografice pentru cercetarea câmpurilor filoniene în masivul alcalin de la Ditrău. vol. "Carpaţii – Gheorgheni".

Codarcea Al., Codarcea D. M., Ianovici V. (1954) Structura geologică a masivului alcalin de la Ditrău. *Bul. St. Acad. R.S.R.*, **II, 3-4**.

Constantinescu E., Anastasiu N., Iakab G., Garabasevschi N. (1982) Contribution à la connaissance des aspects paragénetiques du massif alcalin de Ditrău. Travaux 12-eme Congres de l'Asoc. Gèol. Carpatho. Balc.

Streckeisen A. (1960) On the structure and origin of the nephelinosyenite complex of Ditro (Transilvania, Roumania). Rep. 21, th IGG. Part. 13.

Streckeisen A., Hunsiker J.C. (1974) On the origin and age of the nephelin syenite Massif of Ditro (Transilvania, Roumania). *Schw. Min. Petr. Mitt.*, **54/1**, 59-77.

Structure of the alkaline massif of Ditrău

NICOLAE ANASTASIU
EMIL CONSTANTINESCU

The alkaline massif of Ditrău, well-known for its mineralogical and petrografical characteristics represented, over the past two decades, the object of geological and geophysical explorations whose target was to establish its metallogenic potential.

As a continuation of a wide series of studies (Ianovici, 1933, 1939; Codarcea, Ianovici, Codarcea, 1954; Streckeisen, 1954, 1960, 1974) that offered a general overview on the petrogenesis of the massif, the research undertaken over the past three decades revealed some peculiarities that emphasize the mineralogical and petrographical diversity of this massif. At the same time, the research work enabled us to deal with new aspects regarding its microtectonic and petrostructural characteristics. These characteristics, as well as the spatial relations among the petrographical complexes made it possible to identify some elements of disjunctive tectonics, generated by the location of the massif in the area of the East Carpathians. All the pre-requisites are thus created for the structural classification of the compartments of the Ditrău massif, decoding its structure and evolution, its location in space and time, as well as the moment of ore deposition.

Microtectonic analysis

The microtectonic elements (S planes and lineations) represent a primary argument for the general evaluation of the structure of the magmatic body found in the upper structural levels and, therefore, of their stages of evolution. The petrographical complexity of the Ditrău massif and its spatial relations with the neighbouring formations required microtectonic analyses whose role was to define the relations between "the massif" and "the crystalline area", to decode the structural compartments and to reveal the major structural elements. For this purpose we looked in the main outcrops (Jolotca Valley river and its tributaries, Valea Mare, the Güdütz river, the medium and upper basin of the Belcina valley) The study attempts to identify te "S" planes occurring in the massiv and in the surrounding crystalline area, as well as their accompanying linear (L) elements.

Planar elements

The microtectonic study of the petrographical complexes forming the massif emphasized, along with the massive aspects, the presence of the orientated textures in all the types of

rocks: hornblendites, diorites, monzodiorites, essexites and nepheline syenites. The first researchers described them as fluid textures (Ianovici, 1934; Streckeisen, 1974) or as gneiss textures (Codarcea, 1954), thus assigning them with an evident genetic significance.

The femic minerals (amphiboles and/or biotite) of the mentioned petrographical types have a tendency to concentrate in parallel or sub-parallel planes. Most often have "schlieren" or lens-like aspect with clear orientation. On the planes concentrating of the amphiboles (S_2 planes), hornblende crystals are arranged in clusters and never have a lineation tendency.

The foliation planes of the crystalline schists where the intrusion of the massif occurred, that is S_2 planes, represent schist-like planes where the "mica" minerals prevail: chlorite, sericite, biotite etc. These minerals lead to the formation of oriented textures and, sometimes, in case they is an alternate with quartz, to "agglomerations", to primary ribbon textures or to metamorphic differentiated textures.

The third category of planar elements which can be easily recognized show the diaclase systems – "D" planes – that can be found everywhere in the massif, as well as in the adjacent formations.

The S_2 planes – measured up inside the rocks of the massive - emphasize the NS/N – 70° E general orientation with constant inclinations to the SE between 30 - 70°. The maxima on the microtectonic stereograms (Fig.1) point out a clear tendency of grouping shared by the diorites and monzodiorites of the Jolotca river basin as compared with the essexites and syenite-foidic rocks from the center area of the massif (the basin of the Valea Mare and Güdütz rivers).

The S_2 poles of the orientated textures of the Jolotca sector rocks have no evident symmetries, but display an "axial grouping" (N 40° E
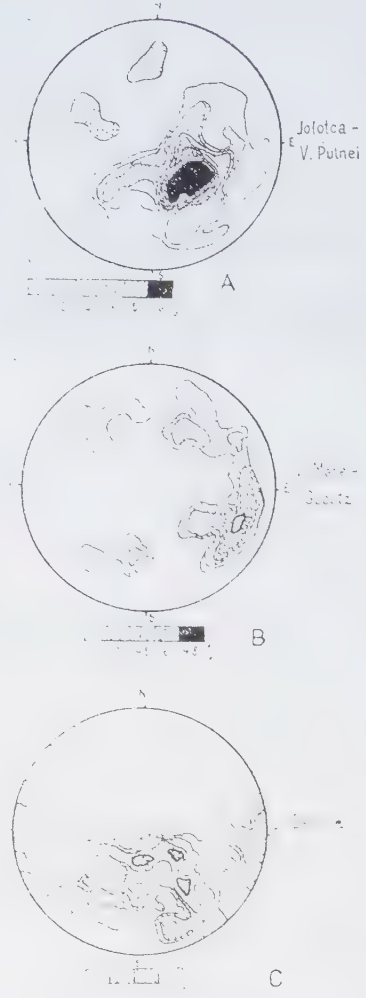
Fig. 1. The microtectonic diagrams for the S planes: A and B- rocks of the massif; C-crystalline schist.

30° NW). The S_2 poles the rocks in the center area of the massif are spread in "clusters" (between NS and NW 40° E/ 60-70° NW). The angle formed between the poles varies from 15° to 20°.

The foliation of the crystalline schists given in the general diagram of the S_1 planesfalls in three maxima close to each other, showing the directions NE-SW (N30° E - N80° E) and inclinations that seldom exceed 50° NW. The

diagram lacks symmetry due to the change of direction of the "micro-wrinkles" the crystalline complex. The three maxima are inscribed in a belt which is approximately oriented towards the EW.

The planar elements of the massif rocks (S_2) and those of the surrounding area (S_1) do not correspond to each other. The overlapping of the few sectors in the two types of diagrams is accidental and hardly reflects an element of continuity between the "crystalline" and "the massif". Thus the origins of the S plans appear to be different.

The S_2 planes emphasize the recurrent gravitational accumulation of the femic minerals, along with a slow cooling and successive emplacement of melted magma that generated the main petrographical complexes. The differences between the two sectors of the massif (Jolotca and Valea Mare - Güdütz) suggest the existence of two structural compartments disturbed by tectonic movements. To a lower extent, differences created by the separation of the rock bodies or by the basic changes of the emplacement direction.

The S planes point out the orientation of the crystalline schists within the Tulgheş series and reflect the distortions that occurred during the last phase of metamorphism.

Diaclases

The Ditrău massif and the surrounding crystalline area are affected by a large number of fissures which, together with other microtectonic elements may bring information about the behavior of the rocks during the post-cinematic periods.

The "D" planes (diaclases) measured up in the massif and in its contact aureole (in the area of the crystalline schist) are very numerous and have different orientations. The poles of these diagrams were plotted on stereograms (Fig. 2). Several pole maxima in the plane of the massif

are to be seen, due to the concentration of the poles of the diaclases into several sectors corresponding to the following systems: E-W / 50 - 60° S; E / 60 - 70° SE; N 30-35° W / 40-70° NE; N85° W / 60 - 70° N, NE.
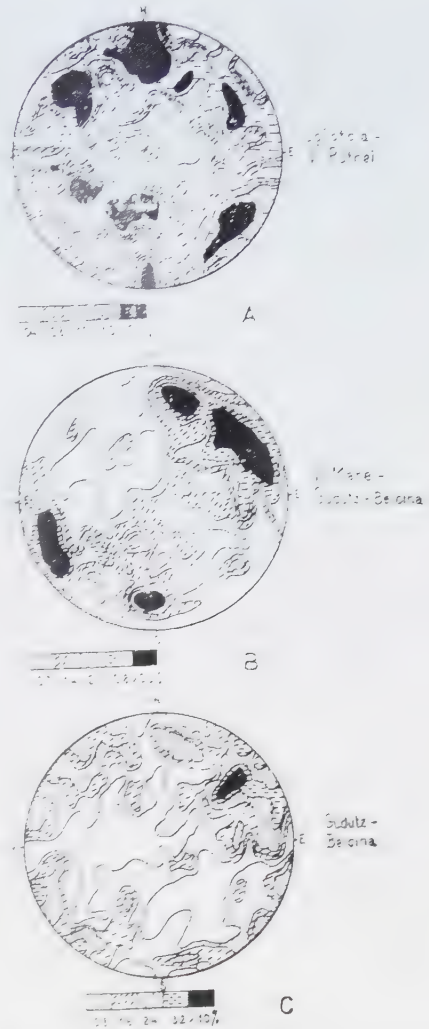
Fig. 2. The microtectonic diagrams for the diaclases. A and B - rocks of the massif; C - crystalline

The distribution of the maxima in the diagram differs from one sector to another. For example:

- in Jolotca - Valea Putnei area, the diagram lacks symmetry; the maximua are distributed

at the periphery (showing inclinations above 45º) and correspond to diaclase systems; a'c' - transversal; bc - longitudinal, concordant, with the general structure of the crystalline area, but discordant as to the S_2 planes measured in Jolotca sector.

- in Valea Mare - Güdütz - Belcina area, the maxima described by the poles of D planes tend to inscribe themselves in a belt whose symmetry plan coincided with the direction of the prevailing system of diaclases - N 30-40ºW with inclination either to the NE (60-70º), or to the SW (70-80º); a second system (N 85º W/60-70ºN, NE) is only very vaguely defined. This systems has longitudinal "bc" diaclases, but, in this area too, it crosses the S_2 planes.

In the contact halo of the massif, the D plans mainly represent the "bc" type systems, that fit into the general orientation of the crystalline area: N 40º/60-70º SW. This system also crosses the S_1 foliation planes. The microtectonic diagram lacks symmetry (Fig. 2).

Both in the massif and in its contact aureole, all the diaclase systems have a postcinematic character. Some of them represent cooling fissures (bc), others are tension (ac, a'c') or decompositions fissures. The diaclase systems are not synchronous. The oldest system seem to be the "bc" that complies with the general orientation of the crystalline. Their formation is followed up by the formation of the "a'c'" cracks, with an approximate orientation E-W. The most recent are the tension.

The analysis of the microtectonic data provide additional arguments for the separation of the two structural components: "Jolotca" and "Valea Mare - Güdütz".

Lineations

The only linear elements that can be mapped are the mechanical ones. Despite the frequent occurrence of the prismatic minerals, no mineral lineations could be separated.

The mechanical lineations are represented by gliding strikings that were identified both in the Jolotca basin and in the central area of the massif. They develop along major planes of the diaclases or along the foliation planes.

Most of the lineations of the massive have orientations that vary between N 45º and E-W. They are to be found in the diorite bodies from Jolotca valley, in the essexites from Valea Mare and Valea Putnei. Their orientation coincides with the direction of the disjunctive dislocations of the massif and result from the stike-slip movements.

In the area of the crystalline schists, the contact aureole of the massif has frequent mechanical lineation - the Belcina basin, the eastern and southern sectors of the massif. The lineation represent associations oriented N 80º E and N 70º E, indication on the time they were formed. These lineation are also concentrated along the surfaces of the diaclase planes and along the schist foliation, suggesting that they also formed as a result of the stike-slip movements.

The axes of the micro- and macro-"wrinkles" characteristic for the contact aureole could not be followed up in the crystalline schists.

Petrostructural analysis

The petrostructural characterization of a magmatic boy as well as of the surrounding formations is based upon measuring of the orientation of the optical axes of the felsic minerals (quartz and feldspar) as well as the orientation of the biotite, amphiboles and feldspars. The present analysis aims to clarify the relations among different petrographical complexes representative for the Ditrău massif and to identifying its position as to the adjacent crystalline. The main petrotypes sampled in the massif and in its contact aureole following: diorites (sample 1969), monzodiorites (sample 915, 975) and quartzites (sample 822).

By means of a universal stage, we examined the orientation of the optical axes of the quartz from granites and quartzites, as well as the orientation of the cleavage planes - (001) in biotite and (001) in the K-feldspar from diorites and monzodiorites. The study alowed the identification of petrostructural types. The data were projected on Schmidt networks (in the lower hemisphere).

Orientation of quartz

The orientation of the optical axes in quartz crystals of the granitoides from Jolotca valley (petrotypes 955 and 975) leads to diagrams that have no symmetry. The diagram of the 955 petrotype (microcrystalline granite) emphasizes a very weak orientation of the quartz crystals and the tendency of the pole maxima to group in a oriented garland, which corresponds to a tectonite placed between the B and S types (Fig. 3). The diagram of the 975 petrotype (massive fan-structured granites show the concentration of the maximum value poles of the optical axes of the quartz in three different sectors, with no possibility toconnect in a belt. This suggests the role played by the blastesis (mainly by recrystallization) in stress conditions. Such maxima suggests the elimination of the unstable granules and the formation of new crystals, with preferential orientations (Fig. 3).

The orientation of the optical axes in quartz crystals of the adjacent crystalline schists (Sărmaş - Jolotca area) are completely different from that of the massive quartz crystals.

The petrostructural diagrams of the two examined petrotypes (sample 822 from Sărmaş and sample 842 from Cibi-Iacob-Tarniţa) are characteristic by the symmetric distribution of the pole maxima.

The crystalline schists from Sărmaş area form an S tectonite whose symmetry plane is oriented NW-SE. The concentration of the poles

in relation to this plane suggests the role played by the primary blastesis in the orientation of the optical axes of quartz crystals and enable us to differentiate, from a petrostructur-
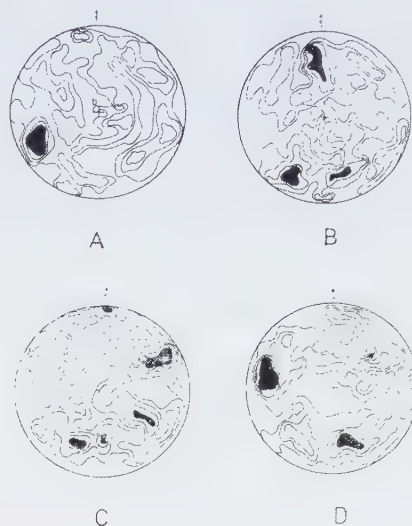
Fig. 3. The petrostructural diagrams for the orientation of the optical axes of the quartz: A and B - crystalline schists; C and D - granitoides.

al point of view the Sărmaş sector from the Cibi-Iacob-Tarniţa sector.

The petro-structural diagram of the homogenous quartzite sampled in the contact aureole of the massif is more complex. The characteristic of the S tectonite rock is maintained, due to the distribution of the two pole maxima on both sides of an E-W orientated plane. However, the general symmetry of the diagram is disturbed by the individualization tendency of a WE-SW orientated belt.

This kind of image reveals the overlapping of the two periods of formation, a primary one – caused by the blastesis of the pre-metamorphic material – and a secondary one, caused by the emplacement of the massif and the recrystallization of the rock under thermal impact.
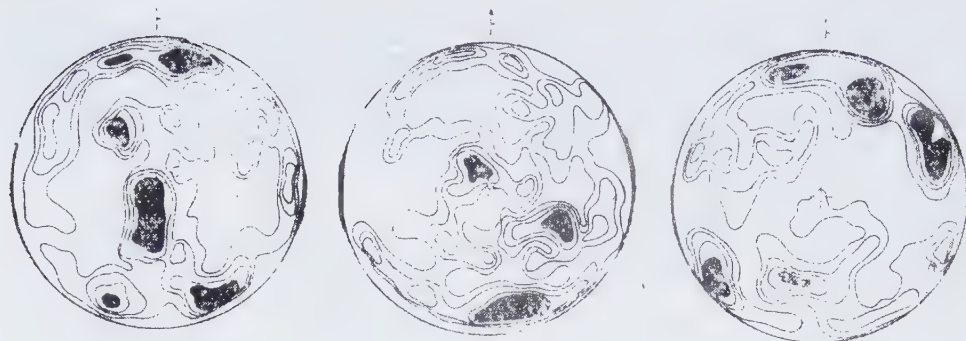
Fig. 4. The petrostructural diagrams for the orientation of the cleavage planes (001) in biotite: A - diorites; B - granitoides; C - monzonites.

Orientation of the cleavage plans (001) of biotite

The orientation of the cleavage plans of the biotite was followed by means of the universal plate bar along thin, orientated sections, made on diorite samples (Jolotca valley, petrotype 969), on monzodiorite samples (Jolotca valley, petro-type 405) and on granite samples (Turcu river, petrotype 975). The symmetry of the petrostructural diagrams was deduced from the projection of the poles of the cleavage plans - (001) in the lower hemisphere of the projection sphere (Fig. 4).

The perpendicular pole (001) of the diorites is concentrated in distinct pole maxima, of which some fall within a circular belt specific for the B tectonites, while others represent a maximum central value corresponding to the "S" pole of the orientated textures of the diorites This perpendicular distribution of the poles (001) in two petrostructural models of diorite suggest the existence of at least two petrogenetic moments: 1) formation of diorites and split of the mica layers along the "foliation" plane – a process that explains the formation of the maximum central value and 2) the formation of the neo-biotite with a disorderly distribution which gives the rock a B tectonite.

In monzosyenites, the symmetry of the petrostructural diagram with its marginal belt around the "B" axis is characteristic to the "B" tectonites. In granitoides we can see the dispersion of the pole maxima; the diagram has no symmetry at all and does not correspond to a clearly expressed tectonite.

Major structural elements

The geological evolution of the East Carpathians has been controlled, by deep fractures and by the mobility of the structural compartments delimited by these fractures.

The geophysical data provided by the gravimetric anomalies (Socolescu et. al., 1975) and by the deep seismic probing (Rădulescu et. al., 1976) emphasize the existence of a maximum line : Miercurea-Ciuc-Gheorgheni-Toplița. This line marks out, within the limits between the crystalline-mesozoic area and the Neogene volcanic chain, a deep continental fracture, under the form of a "field of faults" whose trajectory is perfectly correlated with the development area of the recent volcanites. However, this "field of faults", very instable in the tectonic sense, includes a complex of fractures that started to be activated long before the Neogene (perhaps in the Paleozoic).

The geophysical data provided by Socolescu et. al. (1975) emphasize, in the Gheorghieni-Toplița sector, an area where the old deep G 8 fault intersects with the G 9 and G 4 fault sys-

tems and joins here several compartments with variable mobility.

The quasi-circular shape of the Ditrău massif, within the erosion limits, corresponds to the upper part of a pluton with a complex structure. Its presence, on the trajectory of these faults suggests a genetic interdependence (Fig. 5).

The rooting tendency of this body and, consequently, its autochtonous-intrusive-character were repeatedly demonstrated with petrologic arguments (Ivanovici, 1934; Codarcea and others, 1953; Streckeisen, 1974), mineralogical data (Anastasiu, Constantinescu, 1977) and geophysical arguments (Gohn et. al., 1973; Gyula, 1975; Botezatu and Calotă, 1979). The radiometric anomalies from Remetea-Ditrău, Jolotca-Dealul Înalt, as well as the general geophysical anomaly are arguments in support of the deep rooting of the massiv. The magnetic anomalies represent, according to Botezatu and Calotă (1979) "the total amount of three dissimulated individual sources". The theoretic model calculated on the basis of these anomalies is formed of six vertical prisms, with different underground positions and uniformly magnetized, of which three, coaxial. These prisms have increasing vertical dimensions and are situated at ever greater depths.

The Ditrău pluton has a complex constitution due to the spatial, temporal, and genetic relations that appear among the petrographical associations uncovered by erosion. Several major disjunctive dislocations could be identified in the massif. They allowed the separation of the structural compartments and provided new opportunities for the understanding of the evolution and the metallogenic specialisation of the massif.

The disjunctive dislocations and the structural compartments

On regional scale, several petrographical types display spatial discontinuities. The main gaps in the massif are: Jolotca - Putna Intunecoasa

fault, with an E - W orientation, and Valea Mare - Comarnic Hill - Fagul Înalt Hill fault, with a WSW-ENE orientation (Fig. 6).

The Jolotca -Putna Întunecoasă fault is an old fracture regenerated after the formation of the

Fig. 5. Position of the Ditrău massif within the East Carpathians, related to the main structural elements of the Mesozoic-Crystalline Zone and the deep G 8 fracture.

massif; it worked as a primary strike-slip plane along which the northern compartment moved westwards of the southern compartment. The "field of faults" related to these fractures was intercepted south of Jolotca, in the XXVIII adit. The relief and orientation of the hydrographic network follows the tectonic accident.

The Valea Mare - Comarnic Hill - Fagul Înalt Hill fault is more recent. It meets the Jolotca - Putna fault in the Czengeler sector, thus limit-

ing, to the south, a submerged compartment of the massif, covered with magmatites. Neogene pyroclastic products and Quaternary formations. This fault also represents the N - NW limit of the southern structural compartment of the massif outcropping in the Valea Mare - Güdütz - Belcina sector.

The two major faults limit on the surface two structural compartments well distinct from petrographical and tectonic points of view: A) the Jolotca - Putna compartment and B) the Valea Mare - Güdütz - Belcina compartment.

In the Jolotca - Putna compartment, the disjunctive dislocations are particularly noticeable in the contact area of the massif. They are almost parallel one to each other and trend NE-SW: the Pietrari fault, the Teascul-Holoşag fault, the Rez fault, the Nagyag-Lukone fault. In the Southern part of the compartment there are two faults transversal on Jolotca valley, situated to the E from its conflu-

ence with the Turcu river. The fractures have no significant impact on the continuity of the petrographical complexes and do not correlate with the dyke system in the area. The fractures of the Teascu and Pietrari areas were revealed by the mining excavations. In the Valea Mare - Güdutz - Belcina compartment, the fractures always appear in the marginal area, but with a radial distribution. All the dislocations visible on the map intersect the limit between the massif and the crystalline schists and cut the circular development of the petrographical complexes on the periphery of the massif (Fig.7).

The distribution of the diaclases between the two sectors appears to be a late effect of compression and of tension movements that affected the massif after its consolidation.

Conclusions

The correlation of the mineralogical, petrographical (Anastasiu, Constantinescu, 1977, 1978, 1979) and geophysical data (Botezatu, Calotă, 1979) with the microtectonic and petrostructural elements emphasized in this paper, allowes to us conclude that the Ditrău massif is a quasi-circular pluton with an unconformable placement in an upper structural level. It had a retromorphic evolution and its separation into compartments has a post-cinematic character.

The clear contacts with the crystalline schists wherein the pluton generated a thermal aureole are almost vertical in the northern and eastern parts of the massif and inclined to the S, SW and W.

The pluton, taken as a whole, has asymmetrical structure because of the extension and orientation of the petrographical complexes (mainly in the Jolotca compartment). A circular structure may be described, too, due to the characteristics of its central part and to the dyke structures in the marginal sectors.
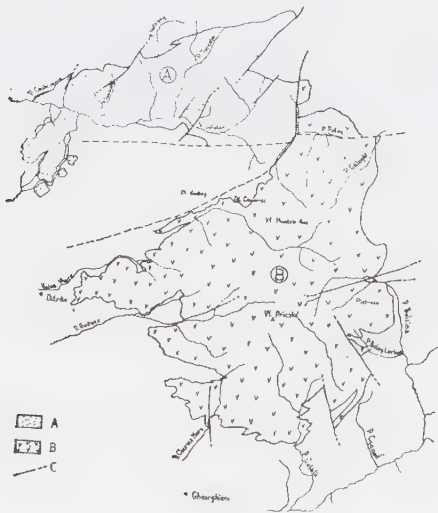
Fig. 6. Structural compartments of the Ditrău alkaline massif : A - Jolotca - Putna compartment; B - Valea Mare - Güdütz - Belcina compartment; C - faults.
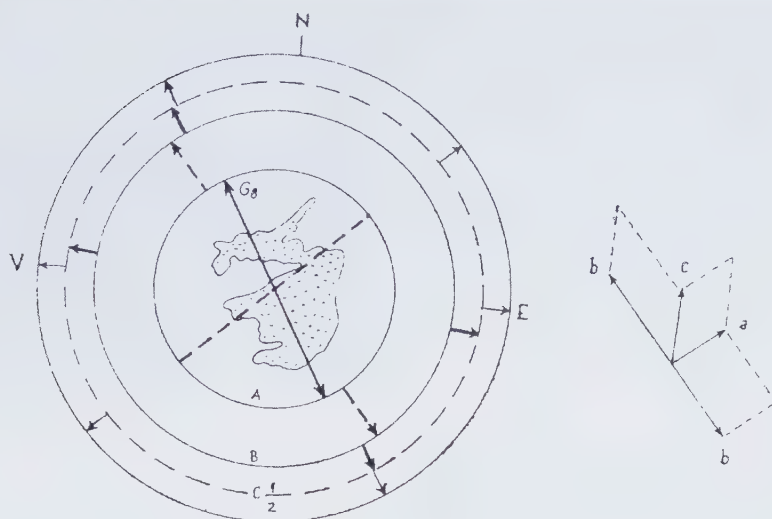
Fig. 7. A) Position of the massif in relation with the direction of the deep G 8 fault. The general orientation of the crystalline area and the prevailing direction of the Tulgheş faults. B) Orientation of the longitudinal "bc" diaclases in the contact halo of the massif. C) Orientation of the crystalline diaclases in the massif: C1) Jolotca - Putna compartment; C2) Valea Mare - Güdütz - Belcina compartment.

The spatial distribution of the petrographical types in the two structural compartments has a distinctive zonality .

Except for the northern marginal area, the mafic minerals occupy an external, western position in the Jolotca - Putna compartment. There are transitions between hornblendites, generally developed as lenticular bodies elongated to the NE and SW and diorites. The transition are made trough meladiorites. There are sectors where the frequency of the salic minerals increases. Thus, to the east, the diorite complex pases to monzosyenites and to syenites that assume a "body" structure.

In the eastern extremity of the compartment we can notice only granitoides. There are no clear limits between the syenites and the granitoides. The transition from one complex to the other occurs through the development and the increased concentration of quartz (as revealed by the cross-section in Turcu valley).

The foidic rocks appear accidentally and they are not distributed into large areas. They cross other types of rocks and take the form of unconformable apophyses with a circular outline (Teascu river and Bordea Simo river).

In the Valea Mare - Güdütz - Belcina compartment, zonality of the massiv is more obvious. Its middle-center part – Muntele Înalt (the High Mountain), the Prizcke peak – corresponds to the central part of the pluton formed by foidic syenites with a faneritic structure and tinguaitic segments where one can distinguish two types of "dome" structures, on either sides of the Valea Mare, both having a massive texture. The oriented textures become dominant towards the periphery of the main body where the composition passes to monzonite-foidic.

The essexite complex develops asymmetrically and interposes in the western part of the massif, between the foidic syenites and the monzosyenites. In the Putna basin, on the NW extremity of the compartment, the essexites represent lenticular insertions within the massif.

The zonality of the massif is noticeable at the periphery of the main body. Here, the transition from monzonites to syenites is general, even in the case of granites and alkali granites,

in the proximity of the crystalline schists. The regional distribution of the petrographical complexes suggests a discontinuous circular distribution.

In the two sectors, the ultramafites and the mafites (hornblendites, diorites and essexites) never appear as dykes or bodies that cross the other petrographical complexes. On the contrary, they appear as enclaves in leucodiorites, syenites and foidic syenites.

The contact aureole of the alkaline massif Ditrău preserves the metamorphic structures of the crystalline schists. The microtectonic and petrostructural analysis could not identify elements of discontinuity between the massif and the surrounding area. The few coincidences are accidental.

References

Anastasiu N., Constantinescu E. (1974) Observații mineralogice în rocile sienitice din Masivul Ditrău. *Comunicări Geologice*, Tipografia Universității București.

Botezatu R., Calotă C. (1979) Ipoteză asupra anomaliei magnetice produsă pe masivul de roci alcaline de la Ditrău rezultată din aplicarea unui procedeu de analiză spectrală, *St. Cerc. Geol. Geof.*, **17.1**, p. 47 - 66.

Codarcea I., Codarcea D. M., Ianovici V (1057) Structura geologică a masivului de roci alcaline de la Ditrău. *Buletin Șt. Acad. R.S.R.*, **II/3 - 4**, Bucharest.

Cornea I., Drăgoescu I., Popescu M., Visarion M. (1979) Harta mișcărilor crustale verticale recente pe teritoriul României. *St. Cerc. Geol. Geof. Geogr.*, **11/1** p. 3 - 11.

Gohn E., Isvoreanu I., Scurtu S , Heredea N. (1973) Cercetarea aero-radiometrică a

masivului Ditrău și formațiunilor adiacente. *St. Cerc. Geol. Geof.*, **11/1**, p. 3 - 11.

Ivanovici V. (1933 - 34) Etude sur le massif syenitique de Ditrău, region Jolotca, district Ciuc (Transilvania). *Rev. Muz. Mineral., Univ. Cluj*, **4/2**.

Ivanovici V. (1938) Considerations sur la cionsolidation du massif sienitique de Ditrău en relation avec la tectonique de la region. *Comp. R. Ac. Sci. Roum.*, **II/6**, 689-694.

Iakob G. (1974 - 1975) Considerații asupra poziției spațiale a masivului alcalin de la Ditrău. *D. S. Inst. Geol. Geof.*, **LXII**, p. 93-98.

Mureșan M. (1976) O nouă ipoteză privind pînzele bucovinice din partea sudică a zonei cristalino-mezozoice a Carpaților Orientali. *D. S. Inst. Geol. Geof.*, **LXII**, 5.

Rădulescu D., Cornea I., Săndulescu M.. Constantinescu I., Rădulescu F., Pompilian R. (1976) Structure de la Croite terrestre en Roumanie – essai d'interpretation des etudes seimiques profonds. *An. Inst. Geol. Geof.*, **L**, București.

Socolescu M., Airinei Șt., Ciocîrdel R., Popescu M. (1975) Fizica și structura scoarței terestre din România. Ed. Tehnică, București.

Streckeisen A. (1952 - 54) Das Nephelinsfen – Massiff von Ditro Siebenbürgen. *Schw. Min. Petr. Mitt.* **32**, 249-310; *Schw. Min. Petr. Mitt.* **II 34**, 336-409.

Streckeisen A. (1960) On the Structure and Origin of the Nephelinsyenite Complex of Ditro (Transylvania, Rumania). *Rep. 21 th. I.G.G.*, **13**, 228-238.

Streckeisen A., Hunnsiker J.C. (1974) On the Origin and Age of the Nepheline Syenite Massif of Ditro/Transylvania, Rumania. *Schw. Min. Petr. Mitt.*, **54/1**, 59-77.

Plate I
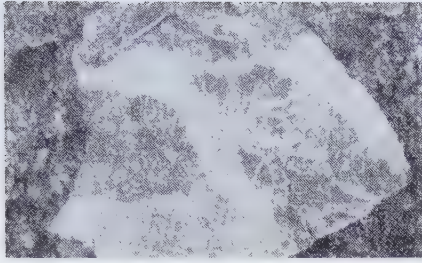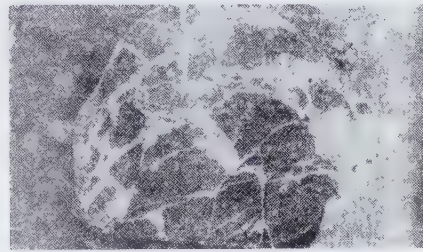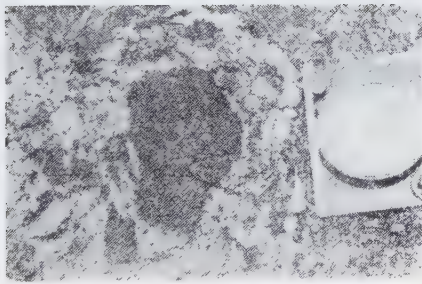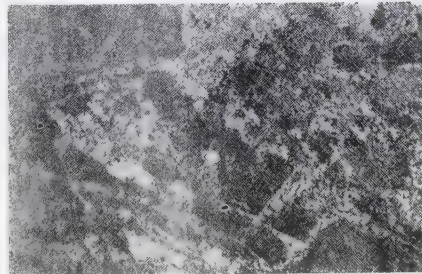
Fig. 1. Hornblendite enclaves in syenites, Pietrari brook.
Fig. 2. Hornblendite enclaves in syenites, Teascu brook.
Fig. 3. A separation of meladiorites into diorites at Valea Mare.
Fig. 4. Relations among diorites, essexites (black) and syenites (white), Güdütz brook.

Plate II
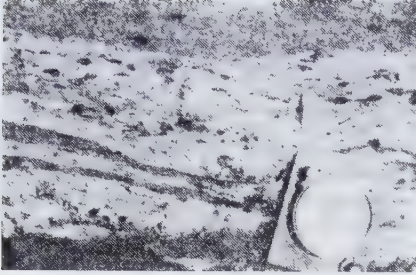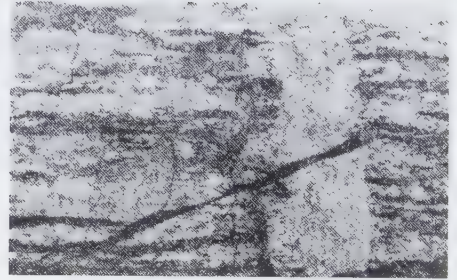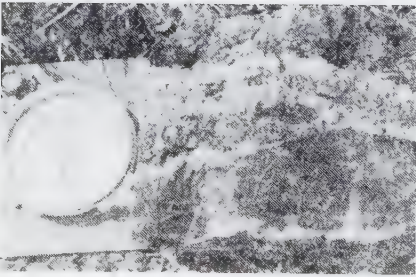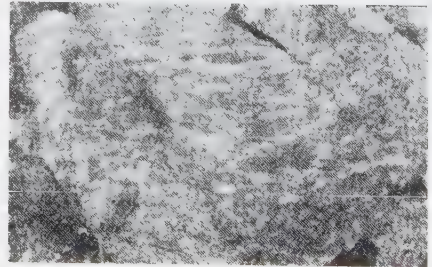
Fig. 1. Concordance of the fabric of foidic syenites and the foidic monzo-diorites in Valea Mare.
Fig. 2. A discordant dyke of foidic microsyenites in the essexites with a ribbon-like fabric, Valea Mare.
Fig. 3. Concordant dykes of tinguaites (black) and foidic pegmatites (white), Cetate brook.
Fig. 4. Diorites with lens-shaped cuttings of meladiorites, Pietrari brook.

Plate III
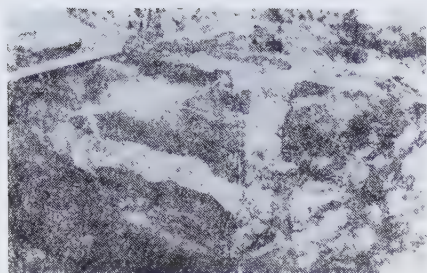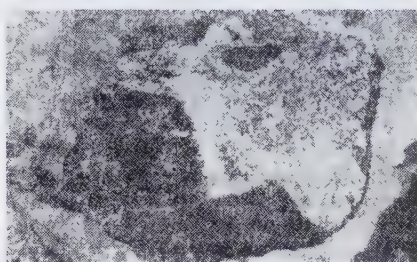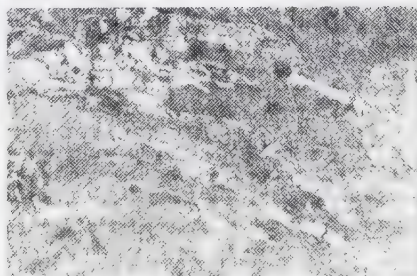
Fig. 1. "Breccia" type fabric, Balas-Lorincz brook.
Fig. 2. Contact between the hornblendites and the pegmatite diorites, Pietrari brook.
Fig. 3. Enclaves of biotitic quartzites in nephelinic syenites, Cianod brook.
Fig. 4. Dykes of foidic syenites in meladiorites, Valea Mare.

Plate IV

1

2

3

4

Fig. 1. Dykes of alkali-feldspar syenites concordant with monzonites that have an orientated fabric, Güdutz brook.
Fig. 2. Dyke of feldspar alkali syenites in foidic monzonites, Valea Mare (Ditrău-Tulgheş road).
Fig. 3. Dyke of amphibolic pegmatites, Cetate brook.
Fig. 4. Consistant dyke of syenites in meladiorites, Jolotca valley.

The alkaline massif of Ditrău: a petrogenetical retrospective view

NICOLAE ANASTASIU
EMIL CONSTANTINESCU

The massif was discovered in 1859 by Herbich and soon visited by many eminent geologists. Many geologists were concerned with its investigation: Koch (1877-1880), Berwerth (1905), Mauritz (1910-1925), Ianovici (1929, 1932-1968), Streckeisen (1931-1938, 1952-1954, 1960, 1974), Codarcea, Codarcea M. D. Ianovici (1958), Rădulescu (1956), Anastasiu, Constantinescu (1974-1984), Zincenco (1975), Iakab (1982).

According to Ianovici (1929-1932) the Ditrău alkaline rocks are the result of phenomena of magmatic differentiation and assimilation of quartzites and adjacent limestones, respectively. The massif is described as a laccolith with a concentrical structure, its margins consisting of granites and alkalisyenites and its central parts of nepheline syenites.

Codarcea, Codarcea M.D., Ianovici (1958) explained the fluidal texture of the massif as a replica, in the apical part, of batholit which altered by metamorphosis the crystalline schists of the Tulgheş Series (amphibolites, micaschists, phyllites). At various stage of the investigation, Strckeisen explain the formation of the massif by Daly's theory of limestone synthesis but finally abbandoned this idea and accepted a magmatic origin, accompanied by widespread hybridization phenomena and metasomatic changes (for many reasons: sharp contact, thermal contact aureole, dike rocks, structure of the massif); according to determinations, the intusion occurred in the Jurassic time.

According to Anastasiu and Constantinescu the polystage distribution and the consolidation of the Ditrău massif within the tectostructural space of the East Carpathians were controlled by crustal fractures and the mobility of the structural compartments limited by them. The geophysical data point out, on the basis of the gravimetric anomalies (Sococlescu et al., 1975) and of the geophysical deep sounding (Rădulescu et al., 1976), the existence of a maximum line which marks, at the limit between the crystalline-Mesozoic zone and the Neogene volcanic chain, a continental crustal fracture type. The Ditrău massif has an autochthonous, intrusive character and its tendency of enrootment has been proved by petrological, mineralogical or geophysical arguments. It constitutes a multistage magmatic intrusion in a superior level of the earth's crust. Its petrographic heterogeneity and the petrochemical incompatibilities - the presence of the supersaturated rocks, granitoides, beside the nonsaturated ones (foidic syenites)- point to the existence of two deep magmatic sources.

Contribution to gold mineralogy in Romania

EMIL CONSTANTINESCU
GHEORGHE C. POPESCU

In Romania there are numerous native gold occurrences known since ancient times. Most occurrences, especially those in the Metaliferi Mountains (Apuseni Mountains) and in the Gutâi Mountains (East Carpathians) consist of "free" gold of macroscopic size, either individualized, as geodes or as inclusions in other minerals or as alluvial gold grains. The complex mineralogic study of Romanian gold occurrences is based on the great amount of gold samples from mineral collection in our country and numerous museums abroad.

Mode of occurrence: Various Romanian occurrences of native gold, in free and large crystals or marvelous aggregates, allowed the examination and the elaboration of complete morpho-crystallographical studies.

Main genetical occurrence types are related to Precambrian terrains (A.); banatitic igneous activity (B.); Neogene hydrothermal vein deposits (C.); recent or old alluvia (D.)

1. Main occurrences

- Abrud (Fig. 2. a) (C.): Crystals with tabular development with predominant faces (001), (100), (111) ;
- Băiţa (Fig. 2. a, b) (C.): Simple cube-octahedron crystals, crzstals twinned cyclically or after (111);
- Boteş (C.): Crystals dominated by octahedrons and hexahedrons;
- Măgura Topliţa (Ilia) (C.): Cubic crystals;
- Musariu (C.): Dodecahedron faces present;
- Roşia Montană (Fig. 3 c - f, h-j, m) (C.): crystal forms: (111), (100), (112); frequent combinations of cubes and icosi-tetrahedrons; rarely (012), (113); anisotropically developed crystals , prismatic or lamellar were also described; twinning after (100) or (111); negatively striated faces; octahedral faces with positive pyramidal-shaped individuals; dendrites, as intergrowths of lamellar-developed skeletal crystals in which (111) faces have dominant sizes; small crystals disposed in

Legend:

- Crystalline schists
- Gabbros, peridotites
- Mesosoic ophiolites
- Laramian (K_3-Pg_1)
- Neogene Igneous Province
- Sedimentary rock basins

0   50   100 km

BULGARIA

Fig. 1. Map of gold occurences quoted in text: 1. Abrud; 2. Băița; 3. Botes; 4. Musariu; 5. Roșia Montană; 6. Ruda Barza; 7. Valea Morii; 8. Băița Bihor; 9. Baia Sprie; 10. Băiuț; 11. Bucium; 12. Cavnic; 13. Dognecea; 14. Fața Băii; 15. Musariu; 16. Pianu; 17. Săcărâmb; 18. Stănija; 19. Trestia, Contu (Brad); 20. Valea lui Stan.

cluster aggregates or as leaf-like forms; lamellar, granular; old alluvia from this region display gold nuggets with cylindrical, spherical or lamellar forms; sometimes as immature grains slightly rounded.

- Ruda Barza (Fig. 3 b) (C.): Anisotropically developed skeletal crystals intergrowths with (100) and (012) forms;

- Valea Morii (C.): (110) rhomboidal dodecahedrons faces described.

2. Morphology of the intergrowths

- Băița Bihor (B.): Thin, flattened pellets;
- Baia Sprie (C.): Thin wires or lamellar aggregates;
- Băiuț, Văratec (C.): Wire-shaped;
- Bucium (C.): Moss-shaped agregates;
- Cavnic (C.): As plane or curved coatings, rarely whire-shaped

- Dognecea (B.): Agreggates composed at thin crystals, whires or lamellae;

- Fața Băii (C.): Whire-shaped, skeletal intergrowths in which (012) form seems to predominate;

- Musariu (C.): Zoomorphic peculiar aspects (the "gold lizard")

- Pianu, Pătroaia (D.): Alluvial gold is described as thin sheets and coatings, up to a few mm in size, presenting irregular limits; sometimes interesting zoomorphic aspects;

- Săcărâmb (C.): Skeletal films;

- Stănija (C.): Lamellar, whire-shaped;

- Trestia, Conțu (Brad area) (C.): Moss-like, lamellar; cubic crystals associated with sphalerite or calcite;

- Valea lui Stan (A.): Skeletal thin films

- Transylvania: Imprecisely localized crystals presenting simple forms: (100) or (111).
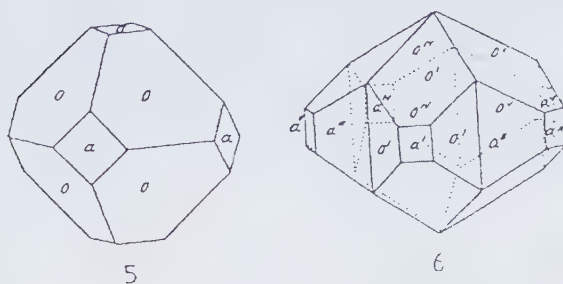
Fig. 2. Morphology of gold crystals from Abrud and Băiţa (see text for details).

3. Chemical-physical properties

The Ag content ranges within large limits (4.92 - 34%), being characterized by a zoned arrangement with increasing contents towards the grain periphery in the case of hydrothermal gold (Metaliferi Mts, Gutâi Mts.) and decreasing contents towards the grains boundaries in the case of alluvial gold samples (Semenic, Sebeş Mts.). The Cu content is usualy low to 1% and only ocassionally 23% (Baia de Arieş). The reflactivity and microhardnes measurements performed on several samples have proved the increase of reflectivity related to high Ag contents and its decrease with respect to high Cu contents, as well as the linear growth of microhardnes concomitantly with the increase of Ag content.

4. Mineral assemblages and genesis

The gold of pyrometasomatic-hydrothermal (banatitic) deposits is related to Bi (tetradymite, tellurobismutite, native bismuth), Cu (digenite, chalcocite, chalcopirite) and Ag (pyrargyrite) minerals. The main assemblages of the Neogene hydrothermal deposits are: quartz-bearing gold-silver assemblages; Au and Ag sulphides and tellurides (sylvanite, nagyagite, krennerite, hessite, petzite etc.) ± adularia, alabandine, rhodocrosite, fluorite, ankerite. The free gold

of the hydrothermal deposits (Apuseni Mts., Gutâi Mts.) is a late mineral deposited subsequently to pyrite and arsenopyrite, but synchronous with or after sphalerite, chalcopyrite, galena, prior to or simultaneously with tellurides (hessite, petzite). The gold dissemination within quartz suggest the role of gold transport through colloidal solutions and finally as deposition environment. The gold in crystalline schists is associated with quartz, arsenopyrite, chalcopyrite, sphalerite. The alluvial deposits contain gold related to heavy minerals (garnet, ilmenite, rutile, zircon, magnetite).

In the South Carpathians area, especially in the Sebeş and Semenic Mountains several gold occurences have been pointed out, mainly Au-Ag associated with some shear zones. The mineralization hosted by medium metamorphic rocks, sometimes showing a retrograde metamorphism of various intensities, and Mesozoic sedimentary deposits. Based on their general geological features, three types of mineralization can be distinguished: synshear-zone mineralization, pre-shear-zone mineralization and mixed-shear-zone mineralization. The main occurrence are reported to synshear-zone mineralization. This category contains the shear-zone related mineralization formed by leaching of mineral components
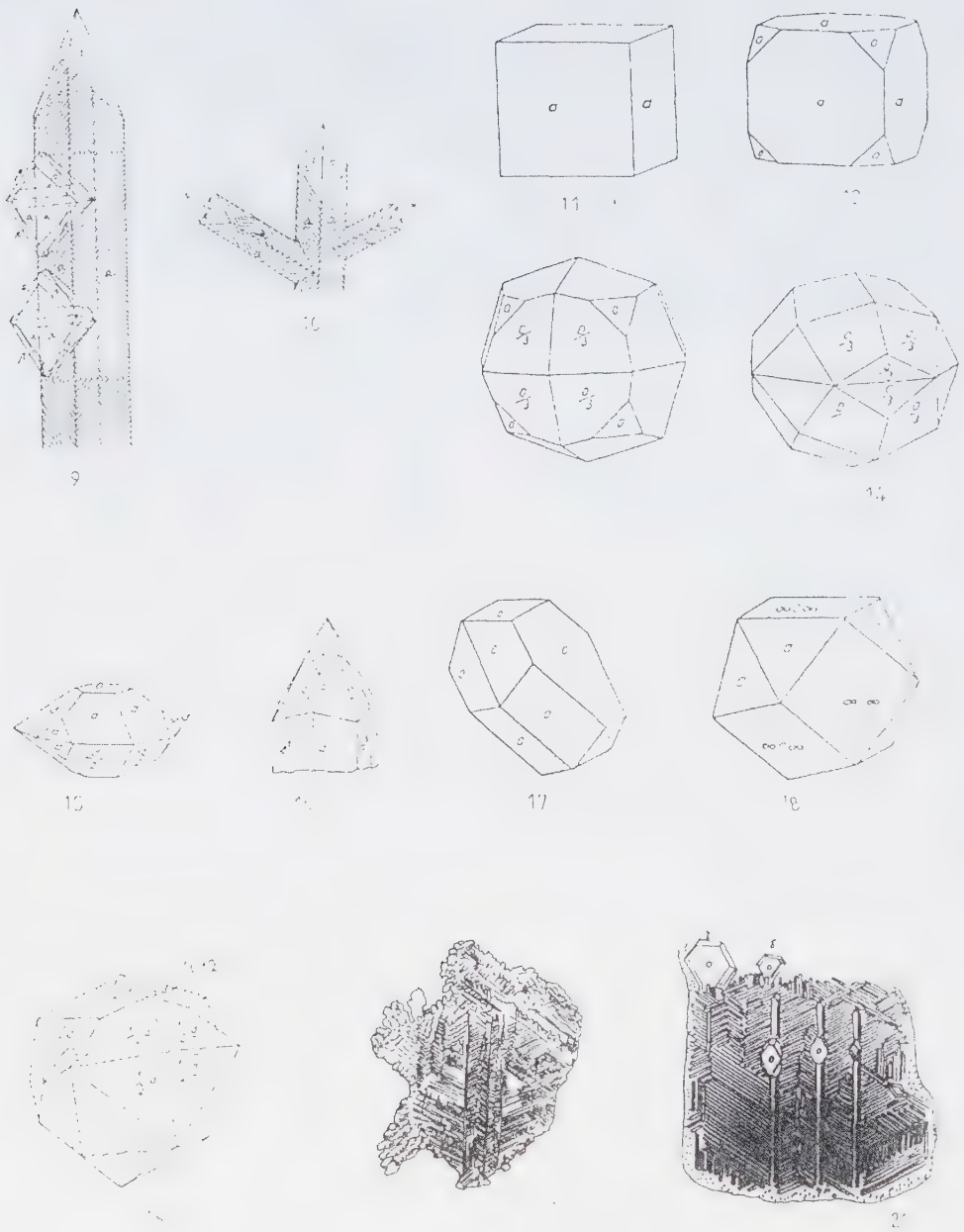
Fig. 3. Morphology of gold crystals and intergrowths (see text for details)

from the country rocks/minerals and their deposition in the dilation zones. The Valea lui Stan and Văliug occurrences can also be included here.

References

Ackner M. (1855) - Mineralogie Siebenbürgens mit geognostischer Andentung, Hermannstadt.

Baumauer (1889) - *Reich d. Kryst.*, **314**, fig. 264.

Cochet Y.R. (1957) - Contributii geologice asupra zacamintelor aurifere de la Baia de Aries, *Rev. Min.*, **8/10.**

Constantinescu E. (1999) - Crystallographic Atlas of Romania, Bucharest University Press (in press).

Constantinescu E., Matei L. (1996) - Mineralogie Determinativă, Bucharest University Press.

Dufrénoy A. (1856) - Traité de mineralogie, pl. 7, fig. 42; pl. 34, fig. 507, Paris.

Haüy C. (1823) - *Mineralogical Magasine*, London, pl. 6, fig. 20;pl. 86, fig. 1.

Helke A. (1938) - Die jungvulkanischen Gold- und-Silber-Erzlagerstätten des Karpathenbogens Archiv. Lagerstättenforsch., 66.

Hessenberg F. (1866) - Abhsnlungen der Senckenbergschen Gesellschaft, Frankfurt am Main, 6, pl. 3, fig. 35, 36.

Hârtopanu I. et al. (1986) - Raport geologic, Arh. IGG.

Ianovici V. et al. (1961) - Privire generală asupra regiunii Baia Mare, Ghid Congr. Carp. Balcan.

Koch Ant. (1885) - Übersicht der Mitteilungen über das Gestern und die Mineralien des Aranyaer Berges und neuere Beobachtungen darüber, *Math.t.-t Ért.*, **3**, Ref. Z.K., 1886, 11.

Mohs F., Haidinger M.V. (1825) - *Mineralogical Magasine*, London, **2**, pl. 7, fig. 113; pl. 9, fig. 48; pl. 28, fig. 151; pl. 33, fig. 184.

Mügge (1899) - *Jahrb. Min.*, **2**, p. 57, fig. 1.

Popescu Gh.C. (1986) - Metalogenie aplicată şi prognoză geologică. Partea II-a, Ed. Universitatii Bucuresti.

Popescu Gh.C., Lupulescu M. (1996) - Shear-zone related gold sulfide mineralization in the South Carpathians (Romania), Terranes of Serbia, Ed. Knezevic V. & Kristic B., pp. 299-304, Belgrade.

Rădulescu D., Dimitrescu R. (1966) - Mineralogia topografică a României, Ed. Acad. Rom., Bucureşti.

Rath G.v. (1877) - *Zeitschrift für Kristallographie*, Leipzig, **1**, pl. 1, fig. 1, 3, 4, 8, 9; pl. 25, fig. I, Ia.

Rose (1831) - *Poggendorf's Annalen der Physik und Chemie*, Leipzig, **23**, pl. 1, fig. 2, 3, 4, 7, 12, 14, 15, 16.

Udubaşa G. et al. (1986) - Studii in vederea elaborarii atlaselor paleontologic si mineralogic al Romaniei. I. Elemente native si sulfuri, Arh. IGG.

Udubaşa G., Ilinca Gh., Marincea Şt., Săbău G., Rădan S. (1992) - Minerals in Romania: The Sate of the art 1991, Rom. J. Mineralogy, 75, p. 1-51, Bucureşti.

Werner (1881) - *Jahrb. Min.*, **1**, pl. 1, fig. 2, 3, 21, 22, 23.

Zepharovich V.v. (1859, 1873, 1893) - Mineralogisshes Lexicon des Kaiserthums Österreich, Wien.

Upper Cretaceous magmatic series and associated mineralisation in the Carpathian - Balkan fold belt

TUDOR BERZA
EMIL CONSTANTINESCU
ŞERBAN-NICOLAE VLAD

The Alpine Orogen contains in South East Europe, from the Carpathians to the Balkans-Srednogorie, an Upper Cretaceous, ore bearing, igneous belt: a narrow, elongated, body which runs discontinuously from the Apuseni Mountains, in the North, to the western part of the South Carpathians (Banat), in Romania, and further South to the Carpathians of East Serbia and still further East to Srednogorie (Bulgaria). This results in a belt of 750 Km/30-70 Km, bending from N-S in Romania and Serbia, to E-W in Bulgaria. Using the well established, century-old, terminology of this region, we describe it in this paper as the Banatitic Magmatic and Metallogenetic Belt (BMMB). Plate tectonics models of the Alpine evolution of South-East Europe involve Mesozoic rifting, spreading and thinning of the continental crust or formation of oceanic crust in the Tethyan trench system, followed by Cretaceous-Tertiary convergence of Africa with Europe and opening of Eastern Mediterranean and Black Sea troughs. The result of successive stages in the collision process is not only the continental growth of Europe from N to S by the docking of several microplates formerly separated from it by Mesozoic palaeo-oceans, but also the rise of mountain belts by overthickening of the crust, followed by orogenic collapse, lateral extrusion, exhumation of metamorphic core complexes and post-collisional magmatism connected to strike-slip or normal faulting. The BMMB from the Carpathian-Balkan fold belt is rich in ore deposits related to plutons and/or volcano-plutonic complexes. Serbian authors have proposed an Upper Cretaceous Paleorift in Eastern Serbia for the Timok zone and some Bulgarian geologists have furnished geologic, petrological and metallogenetic support for this extensional model along the entire BMMB. The existence and importance of previous westwards directed subductions of Transylvanides (=South Apuseni = Mures Zone) and Severin-Krajina palaeo-oceans, popular in Romanian literature, seems to have little relevance to BMMB generation, but the well documented northwards directed subduction of the Vardar-Axios palaeo-ocean during Jurassic and Lower Cretaceous is a good pre-conditionfor the generation, during the Upper Cretaceous, of banatitic magmas in extensional regime, by mantle delamination due to slab break-off. Four magmatic trends are found: a tholeiitic trend, a calc-alkaline trend, a calc-alkaline high-K to shoshonitic trend and, restricted to East Srednogorie, a peralkaline trend. For acid intrusives, the typology is clearly I-type and magnetite-series, pointing to sources in the deep crust or the mantle; however, some high $^{87}Sr/^{86}Sr$ ratios recorded in banatites prove important contamination from the upper crust.

The calc-alkaline hydrated magmas, most common for banatitic plutons, can be considered as recording three stages of evolution: more primitive - the monzodioriric, dioritic to granodioritic trend (S Apuseni, S Banat, Timok, C and W Srednogorie); more evolved - the granodioritic-granitic trend (N Apuseni, N Banat, Ridanj-Krepoljin); the alkaline trend (E and W Srednogorie, western part of N

Banat). Correlating the composition of the host plutons with the types of mineralisation, several envinronments can be found in the BMMB, function of timing of fluid separation (porphyry versus non-porphyry envinronments), depth of emplacement, size of intrusion and geology of intruded rock pile, biotite versus hornblende crystallisation, involving the evolution of K/Na ratio in fluids, i.e. development of potassic and phyllic alteration zones: a) non-porphyry envinronment with granodi-oritic to granitic magmas, plutonic level, skarn mineralisation prevails; b) porphyry envinronment with monzodioritic or dioritic to granodioritic magmas, subvolcanic-hypabyssal-plutonic level; porphyry Cu with skarn halo at hypabissal-subvolcanic level; c) porphyry envinronment with monzodi-oritic or dioritic to granodioritic magmas, volcano-plutonic complexes with porphyry copper plus massive sulfide mineralisation at subvolcanic-volcanic level; d) non-porphyry envinronment with magmas of alkaline tendency, volcanic level, vein ("mesothermal" and "epithermal") mineral-isation.

1. Introduction

In South-East Europe, the Alpine Orogen is looping like a horse-shoe around a small but strange continental block: the Moesian Platform, docked from Late Jurassic to the East European Platform. Rising at 2000-2500 m, the South Carpathians to North and West and the Balkans (including also the Srednogorie Mountains) to South are now mountain ridges dominating the lowlands of the Moesian Platform and morphologically express the tectonic imprint of this spur (Wallachishe sporn - Stille, 1953), or foreland promontory with corner effect (Ratschbacher et al., 1993). Despite important Tertiary basins frequently hiding the contacts with surround-ing mountain belts (the Apuseni Mountains to North, the Serbo-Macedonian Mountains to West and the Rhodope Mountains to South), the South Carpathians - Balkan and Srednogorie (SC-BS) belt interfere with the adjacent orogenic belts and have to be dis-cussed in a larger framework, together with the rest of the Carpathians and the Alpides-Dinarides-Hellenides. This complicates the approach, as to Romania, Serbia and Bulgaria, where the SC-BS belt outcrops, regions of Hungary, FYROM and Greece also have to be considered. Based on papers printed in the last decade in the six mentioned countries, but also in international journals, we shall try to present facts and discuss models of evolu-tion for the alpine granitoid series and associ-ated mineralisations from the Carpathian - Balkan orogen.

In his famous book published in 1864, the aus-trian geologist Bernhardt von Cotta described Cretaceous igneous rocks from Banat (now SW Romania) and Serbia as "banatites", meant as a family of cognate intrusive and effusive rocks; the predominance of the gran-odiorites between these lead to an equivalent sense for the term "banatite" (see discussion of Johannsen, 1958, p 348-349). The term is still extensively used by Romanian and Serbian geologists for acid to intermediate suites of Upper Cretaceous to Paleocene age, even if the alternative "Laramian Magmatites" was also proposed (Cioflică and Vlad, 1973). For Bulgarian geologists the more common term is "Late Cretaceous" magmatism (Boccaletti et al., 1978; Popov, 1981, 1995, 1996; Vassilieff and Stanisheva-Vassilieva, 1981; Bayraktarov et al., 1996), also used by some Romanian authors (Cioflică, 1989; Cioflică et al., 1992, 1996, 1997).

In the last ten years the understanding of the tectonic evolution of the eastern part of the Alpine Europe registered a huge advance due to the aplication of new structural, paleomag-netic, isotopic and metamorphic petrology techniques on an area well mapped by local geologists in the previous decades. Several Ph D theses and dozens of papers propose models for the Mesozoic-Cenozoic history of the South Eastern Europe and already there is consensus around basic steps of the evolution from the rift stage to the present shape of the Carpathian-Balkan mountain belt and its west-ern and southern hinterland.

On the other hand, igneous petrology and associated metallogenetic studies of the Alpine magmatic belts from the eastern part of Alpine Europe also registered important progress due to the new techniques and concepts, leading to various models for the genesis of Triasic to Pleistocene magmatic rocks and associated ore deposits. Cu, Mo, W, U, Pb, Zn deposits of small size to world class associated with Upper Cretaceous magmatism were discussed and modelled in many papers, especially published within the framework of IGCP Project No 356 "Plate Tectonic Aspects of the Alpine Metallogeny in the Carpathian-Balkan Region". The advance of tectonic, petrologic and metallogenetic studies made possible the evaluation of controversial models of the Upper Cretaceous, ore bearing, igneous belt from the Carpathians and the Balkans-Srednogorie. This is a narrow and elongated belt, 280 km long in Romania, that runs discontinuously from the Apuseni Mountains, in the North, to the western part of the South Carpathians (Banat). It extends further south to the Carpathians of East Serbia (Yugoslavia) and still further east to Srednogorie (Bulgaria), over other 470 km, never exceding 70 km in width. This results in a belt of 750 Km/30-70 km, bending from N-S in Romania and Serbia, to E-W in Bulgaria (Fig. 1). Using the well established, century-old, terminology of this region, we shall refer in this paper to the Banatitic Magmatic and Mellogenetic Belt (BMMB).

2. Discussion of tectonic models of South-East Europe

Since the pioneering work of Roman (1970, 1971, 1973), Rădulescu and Săndulescu (1973, 1980), Bocaletti et al. (1973, 1974), Dewey et al., (1973), Bleahu (1974), Hertz and Savu (1974), Grubic (1974), Dewey and Shengor (1979) and Burchfiel (1980), plate tectonics models of the Alpine evolution of South-East Europe involved Mesozoic rifting, spreading and thinning of the continental crust or formation of oceanic crust in the Tethian
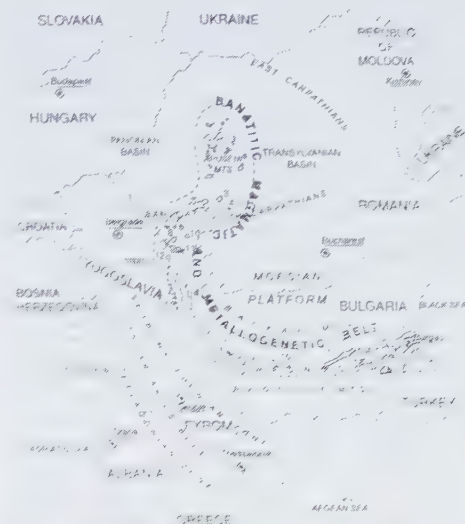
Fig. 1 Banatitic Magmatic and Metallogenetic Belt in South East Europe. 1 Vlădeasa volcano-plutonic complex, 2 Rusca Montană volcano-sedimentary basin, 3 Demsus volcano-sedimentary basin, 4 Baru Mare intrusions, 5 Bocşa composite pluton, 6 Ocna de Fier apophysis, 7 Surduc pluton, 8 Oraviţa intrusions. 9 Sasca-Moldova Nouă intrusions, 10 Lăpuşnicel-Teregova area of dykes, 11 Lilieci-Purcariu area of dykes, 12 Ridanj intrusions, 13 Krepoljin intrusions, 14 Timok volcano-plutonic complex, 15 West Srednogorie sector (Vitosha), 16 Central Srednogorie Sector (Panagyurishte), 17 Jambol volcanics, 18 Manastir intrusions, 19 Bakadjik volcanics, 20 Burgas volcano-plutonic complex, 21 Zeljaskovo intrusive.

trench system, followed by Cretaceous-Tertiary convergence of Africa with Europe and opening of Eastern Mediterranean and Black Sea troughs. The last twenty years of research improved these models due to constraints from palaeogeographic, palaeomagnetic, shear sense indicators and palaeostress data. Further new concepts, especially concerning late stage orogenic extension and gravitational collapse of overthickened orogenic wedges and exhumation of metamorphic core complexes, had evolved recently.

The **Hallstadt-Meliata Palaeo-ocean** from East Alps and West Carpathian domain (Neubauer et al., 1996; Dallmeyer et al., 1996) and the **North Dobrogea Palaeo-aulacogen**

(Vlad, 1978; Seghedi, 1998) with Triassic spreading and Jurassic closure, as not being relevant to the topic of this paper, will not be discussed here, just as other ophiolitic remnants from the Rhodope, Serbo-Macedonian and Circum-Rhodope belts (Papanikolaou, 1989). The Penninic, Pindos, Vardar, Severin, Pieniny and Silesian-Moldavidic oceans opened and closed at various epochs between Middle Jurassic and Tertiary, while East Mediterranean Sea and Black Sea opened in Late Cretaceous and still preserve oceanic crust. Products of the **Penninic Palaeo-ocean** are now exposed, in various metamorphic grades, in the Engadine, Tauern and Rechnitz windows from the East Alps. They reveal Early to Middle Jurassic rifting of the Variscan continental crust and opening of a basin with basaltic magmas injected in sediments, followed by development of a basin floored by oceanic crust from Late Jurassic to Early Cretaceous, subducted below the Austro-Alpine domain (Koller and Hock, 1992). **Ophiolites and turbidites from the Pindos Palaeo-ocean** are preserved in the Hellenides and are considered to have evolved in the same time-span (Papanikolaou, 1989). **Severin-Krajina ophiolites and flysch** from the South Carpathians (= **Ceahlău-Czywczyn flysch** from the East Carpathians = **Nis-Trojan flysch** from the Balkans) also cover the Late Jurassic - Early Cretaceous interval and are considered to have been subducted below the Getic-Supragetic (= Bucovinian in East Carpathians = Srednogorie in the Balkans) domain (Săndulescu, 1984). **Pieniny turbidites and basalts** run as a belt from the East Alps to the West Carpathians and the north of the East Carpathians, where according to Schmid et al. (1998) they end, while for Săndulescu (1984) they are just offset by a fault from a similar belt (**Transylvanides**) in the basement of the Neogene Transylvanian basin. **Silesian-Moldavidic flysch** was deposited from Late Cretaceous to Miocene on an oceanic crust now consumed below West and East Carpathians (Roman 1970, 1971, 1973; Rădulescu and Săndulescu, 1973

Schmid et al., 1998). Given its considerable extent and complexity, the **Vardar-Axios Palaeo-ocean** is the most important from South East Europe. It runs southwards from Belgrade to the Aegean Sea, then across it eastwards to Izmir-Ankara belt of Turkey; the river Vardar (=Axios in Greek) gives its double name. North of Belgrade the belt bifurcates below the Neogene deposits of the Pannonian basin, a western limb going into Croatia and an eastern one into Romania, to outcrop in the **South Apuseni Belt** (= Metaliferi Mountains = Mures Zone) and, after an other gap appearing again below the Neogene Transylvanian basin, in the uppermost (**Transylvanides**) nappes of the East Carpathians (Săndulescu, 1984).

With the exception of the East Mediterranean and the Black Sea oceanic crust floor, just as in most orogenic belts, the oceanic crust and its turbidic cover from the above mentioned palaeo-oceans from South-East Europe were rapidly consumed in subduction zones, resulting in major magmatic activity in the upper slab. The time-span of this period is variable, just as the moment of collision of the continental crust from the various microplates involved. However, several intervals are significant for the closure of the palaeo-oceans in most models proposed for this region of the Alpine Orogen:
  - Lower-Middle Jurassic for Hallstadt-Meliata, North Dobrogea, Rhodope, Circum-Rhodope and Serbo-Macedonian ophiolites;
  - Lower Cretaceous for Penninic, Axios-Vardar-South Apuseni and Trojan-Nis-Krajina-Severin-Ceahlău-Czywczyn palaeo-oceans;
  - Lower Tertiary for Pindos and Pieniny palaeo-oceans;
  - Miocene to Lower Pliocene for Silesian-Moldavidic and East Mediterranean palaeo-

The result of these succesive collisions is, for some of the proposed models, not only the continental growth of Europe from N to S by

the docking of several microplates formerly separated from it by the mentioned palaeo-oceans, but also the rise of mountain belts by overthickening of the crust, followed by orogenic collapse, lateral extrusion, exhumation of metamorphic core complexes and post-collisional magmatism connected to strike-slip or normal faulting. Evidently, these morphologic, structural and igneous effects have occured after the above metioned time for the closure of the respective palaeo-oceans.

Considering the Upper Cretaceous age of the Banatitic Magmatic and Metallogenetic Belt and the palaeo-oceans postulated in the Carpathian-Balkan area, the Axios-Vardar-South Apuseni and Trojan-Krajina-Severin-Ceahlău-Czywczyn troughs are relevant and will be further discussed in this paper.

In northern Greece (Macedonia), Former Yugoslav Republic of Makedonia (FYROM), and Serbia the Axios-Vardar belt separates the Pelagonian-Dinaric microcontinent to the West from the Serbo-Macedonian - Rhodopian one to the East (Papanikolaou, 1989; Serafimovski et al., 1995; Jankovic, 1997). It is not a homogeneous ophiolitic-turbiditic belt, as slabs of pre-Alpine crystalline basement (the Paikon and Stip-Axios massifs - Kockel (1986) and granitoid plutons (intruded at 150 My - Christofides et al., 1990) also occur. Vardar ophiolites and turbidites were subject of many papers in the last decades and the tectonics of this belt were recently discussed by Arsovski and Dumurdzanov (1995) and Arsovski et al. (1997). References about associated mineral deposits can be found in the reviews of Serafimovski et al. (1995), Jankovic (1996), Jankovic (1997). The eastward and northward subduction of the Vardar-Axios ocean below the Serbo-Macedonian-Rhodopian microcontinent was proposed from the beggining of plate-tectonic interpretation of the geology of Balkan Peninsula (Dewey et al., 1973; Bocaletti et al., 1974; Karamata, 1974, 1982; Chanell and Horvath, 1976; various papers by Karamata and Jankovic in:

Jankovic ed., 1977) and are central to the theory of Mesozoic-Cenozoic tectonics of this segment of the Eurasian Alpine Orogen. Some of these papers, Sillitoe (1980), Vassiliev and Stanisheva-Vassilieva (1981) and more recent ones by Jankovic (1996, 1997), Skenderov (1996), Kuikin (1996), Bayraktarov et al. (1996) ascribed to this subduction the generation of the Upper Cretaceous magmas in the Banat and Srednogorie area.

The eastern part of the Vardar-Axios belt was described in northern Greece as Circum-Rhodope belt, with Lower to Middle Jurassic flysch and ophiolites and Upper Jurassic discordant molasse cover (Mountrakis, 1994), cut by granitoid plutons of 50 My, while the adjacent Serbo-Macedonian belt is crossed by granites of 130, 43 and 29 My isotopic ages respectively (Magganas, 1998).

The South Apuseni belt is thrusted northwards upon the pre-Senonian pile of basement nappes of the North Apuseni Mountains and cut southwards by the dextral South Transylvanian fault; below Neogene deposits it continues westwards to Belgrade in the Vardar belt, while eastwards it forms the basement of the Transylvanian basin and repears, as outliers of the Transylvanian nappes, at the top of the Mid-Cretaceous nappe pile of the East Carpathians (Săndulescu, 1984). It contains slabs of pre-Alpine basement, thick piles of Lower-Middle Jurassic tholeiitic volcanics with small gabbroic intrusions followed calc-akaline volcanics, covered by Upper Jurassic limestones, Lower Cretaceous flysch and Upper Cretaceous chaotic formations (Nicolae et al., 1992, Nicolae, 1995), all involved in several tectonic units, of Mid-Cretaceous and Laramian age (Lupu, 1976; Bleahu et al., 1981; Balintoni, 1998). The tholeiitic series was interpreted by Savu (1980) as ocean floor MORB type crust and well documented by Cioflică et al. (1980) as island arc volcanics resulted by subduction of the Transylvanian ocean below the Austro-Bihor microcontinent. For the calc-alkaline series, all authors agree

upon island arc origin (see Nicolae, 1995, and references therein), resulting from a Jurassic-Lower Cretaceous subduction. The volcanic and sedimentary formations from the South Apuseni belt are crossed by younger plutons of Lower Cretaceous and Upper Cretaceous (banatites) ages and Neogene volcano-plutonic complexes. The Săvârşin, Cerbia and Căzăneşti granitoid plutons, formerly considered as Upper Cretaceous (banatites), have K-Ar ages of ~120 My (Lemne et al., 1983; Savu et al., 1986) and are now considered Lower Cretaceous mature arc-acid differentiates, connected with the previous immature arc-ofiolitic (sensu lato) series (Stefan, 1986). Banatitic dykes and small plutons cross Senonian or older deposits and cross as well the South Apuseni belt (Transylvanides), as the North Apuseni nappe pile (Apusenides) (Balintoni, 1998); their origin was also connected with the subduction of the Transylvanian ocean (Roman 1970, 1971; Rădulescu and Săndulescu, 1973; Rădulescu, 1974). Neogene volcano-plutonic complexes with world-class gold deposits and Cu porphyries are associated with small graben-like sedimentary basins in the central zone of the South Apuseni. These 14 to 7 My old (Pecskay et al., 1995) calc-alkaline rocks were considered as subduction related by Roman (1971), Rădulescu and Săndulescu (1973) and Mitchell (1996) but, based on an early interpretation by Vlad (1980), Balintoni and Vlad (1998) reconsidered them as connected with NW-SE oriented extensional structures and controlled by centers of rising asthenospheric isotherms.

The Czywczyn-Ceahlău-Severin-Krajina-Nis-Trojan belt is in fact outcropping in three separate sub-belts disposed en relais along the Carpathian - Balkan mountain chain: Czywczyn-Ceahlău in the East-Carpathians of Ucraina and Romania; Severin-Krajina in the western part of the South Carpathians of Romania and Serbia and Nis-Trojan in the Balkans of Bulgaria. All these have in common the large developpment of carbonatic turbitites in the Upper Jurassic - Lower Cretaceous interval and more or less abundent ophiolitic suites. In the East Carpathians, Czywczyn-Ceahlău is a a tectonic unit composed of Upper Jurassic - Lower Cretaceous flysch, underlying Mid-Cretaceous basement nappes of the Bucovinic system and overlying the Miocene pile of the Moldavidic nappes (Săndulescu, 1984) and no magmatic-metallogenetic products were described as connected with this sub-belt. In the South Carpathians the Severin nappe (Krajina nappes in Eastern Serbia - Grubic, 1997) contains similar Upper Jurassic - Lower Cretaceous flysch sequences, but also important volumes of peridotites and pillow basalts (Mărunţiu, 1983; Djordjevic et al., 1997). This unit is located between two piles of basement nappes: the Getic-Supragetic ones on top and the Danubian nappes below (see references about regional tectonics in Berza, 1997 and Grubic, 1997). Since the papers of Roman (1971), Rădulescu and Săndulescu (1973) and Rădulescu (1974), to that of Vlad (1997), the origin of the banatites and associated mineral deposits from the South Carpathians was ascribed by most Romanian authors to the partial melting of subducted oceanic crust and sediments from the Severin palaeo-ocean. The Nis-Trojan flysch (Nachev, 1989) is also Upper Jurassic - Lower Cretaceous and is located between Balkans and Srednogorie, in a position equivalent to the Getic/Danubian location of the Severin nappe from the South Carpathians. No magmatic-metallogenetic products of this sub-belt were described.

From many of the above mentioned papers concering the Axios-Vardar-Southern Apuseni and Severin-Krajina belts, it results a postulated Cretaceous eastward directed subduction of the Axios-Vardar ophiolitic belt and a coeval westward directed subduction of the South Apuseni belt and of the Severin-Krajina belt, with the same result: the generation of the banatitic magmas and associated ore deposits. For Romanian authors these magmas are derived from the consumption of the Transylvanian trough in the Apuseni

Mountains and from the Severin trough in the South Carpathians, while for many of the Yougoslav and Bulgarian geologists they were born from the consumption of the Vardar trough. This duality reflects a more general conception of the Africa versus Europe collision, respectively the change at the level of the South Trasylvanian Fault of the direction of subduction for Late Cretaceous: soutwards directed North of this fault and northwards directed South of it (Burchfiel, 1980). But the BMMB has an L shape crossing this boundary in western Romania and therefore it is difficult to relate it so simply with the (Jurassic-)Early Cretaceous subductions of the Transylvanides, Severin-Krajina or Vardar palaeo-oceans.

During Tertiary the Late Alpine tectonics were also active in South East Europe, complicating considerably the reconstruction of the Early Alpine structures. Burchfiel (1980), Robertson and Dixon (1984), Balla (1984), Săndulescu (1984, 1988), Royden and Baldi (1988), Papanikolau (1989), Csontos et al. (1992), Jones et al. (1992), Ratschbacher et al. (1993), Pătrașsu et al. (1994), Csontos (1995), Linzer (1996), Morley (1996), Marton (1997), Matenco (1997), Matenco et al. (1997), Balintoni (1997, 1998), Girbacea (1997), Panaiotu (1998), Girbacea and Frysch (1998), Sanders (1998), Lips (1998), Schmid et al. (1998), Neubauer et al. (1998) and many others have contributed to model the Tertiary evolution of the Carpathian-Balkan-Dinaric-Hellenic Early Alpine orogens.

The general picture involves: Paleogene to Miocene flysch deposition and compression in the Outer Carpathians; lateral extrusion of East Alps towards East; 50° to 90° clockwise rotation of the preNeogene formations from the Apuseni Mountains and South Carpathians; dextral orogen-parallel stretching in the South Carpathians and dextral wrenching along the boundary between them and the Moesian Platform; dextral strike-slip along the Mid-Hungarian line of ALCAPA (=Alpine-North Pannonian=Pelso) terrane north of it and Tisza (=Tisia) - Dacia (=Getia) terrane south of it; Neogene extension and crustal thinning in the Pannonian basin, syncronous subsidence in the Transylvanian and many smaler intramontane basins in the Carpathians and the Balkan Peninsula; Oligocene magmatism in North Hungary and Rhodopes, Neogene magmatism at the interior of the East Carpathians, in the Serbo-Macedonian belt and in western Turkey; Neogene uprise of the Carpathians, Balkans, Rhodope and Pindos mountains up to 4000-5000 m and erosion to the present altitudes; Neogene southwards jumping of the trench in the Hellenic arc, up to its actual position south of Crete; active volcanoes north of Crete.

3. Petrology of the Upper Cretaceous magmatites from the Carpathian-Balkan orogen

Since the study of von Cotta (1864), hundreds of papers, doctorate theses and books have discussed mineralogical, petrographical and chemical data of the Late Cretaceous effusive, subvolcanic and intrusive rocks from the Banatitic Magmatic and Metallogenetic Belt (reviews in: Divljan and Karamata, 1967; Drovenik et al., 1967; Cioflică and Vlad 1973; Rădulescu, 1974; Bocaletti et al., 1978; Russo-Săndulescu and Berza, 1979; Stanisheva-Vassilieva, 1980; Vassilieff and Stanisheva-Vassileva, 1981; Popov, 1981; Cioflică et al., 1995, Djordjevic et al., 1997). But if the traditional (wet) chemical analyses performed in Romania, Bulgaria and Yougoslavia in the sixties, seventies and even eighties were reliable, little geochemical information is offered by the optical spectrometric data for the few trace elements recorded. Recently some accurate geochemical and isotopic data were published (Cioflică et al., 1991, 1996; Ștefan et al., 1992; Karamata et al., 1997, Nicolescu, 1998), but much work with modern anlytical techniques is still needed before bringing the knowledge of the petrology of banatites to international level. For this reason our survey will be restricted to comparision of the distribution of rock types and major element chemistry along the BMMB, from Apuseni Mountains to Black Sea.

In the Apuseni Mountains Upper Cretaceous magmatism is well illustrated in the vulcano-plutonic Vlădeasa Massif of North-West Apuseni Mts. (Giuşcă, 1950; Istrate, 1978; Ştefan, 1980, Ştefan et al., 1992), but in North-East and South Apuseni only minor intrusions and dyke swarms are now considered as banatites. Described by Giusca (1950) as "taphrolite" bordered by normal faults, the Vlădeasa vulcano-plutonic complex is located in a Gosau-type Senonian basin, with a lower sedimentary formation and an upper volcano-sedimentary formation, overlain by pyroxene andesites, hornblende andesites, biotite-hornblende dacites, ignimbritic rhyolites and banded biotite rhyolites, all crossed by quartz dioritic, monzogranitic and dioritic intrusions; late rhyolitic and basaltic dykes pierce earlier metamorphic, sedimentary, volcanic and intrusive formations (Istrate, 1978). In the Vlădeasa taphrolite, andesites are relatively scarce, while rhyolites prevail in the West and dacites in the East and (Ştefan et al., 1992). At the scale of all North Apuseni Mountains, intrusions are widespread on a much wider area, piercing preAlpine basement and Mesozoic formations building the Mid-Cretaceous nappe stack, granodioritic-granitic intrusions (e.g. Băiţa Bihor - Dedes batholith) being more important as frequency and volume as quartz monzodioritic and quartz dioritic ones (Ştefan et al., 1992); frequent resset of K-Ar ages from crystalline schists all around the North Apuseni to 60-70 My indicate a regional heating due to major banatitic intrusions undelying them (Bleahu et al., 1984).

Based mainly on 31 analyses from Istrate (1978), Ştefan (1980) and Ştefan et al. (1992), we present the fields for plots of banatites from North Apuseni in the SiO_2-K_2O (Fig. 2), SiO_2-Na_2O+K_2O (Fig. 3) and Alk-FeO*-MgO (Fig. 4) diagrams. The calc-alkaline character and the prevalence of acid rocks are obvious.

Ştefan et al. (1992) present also REE anlyses pointing to similar trends in volcanic and plutonic rocks, important LREE differentiation and enrichment, in contrast with HREE and a negative Eu anomaly, stronger with the decrease of plagioclase content. They also report ^{86}Sr/^{87}Sr ratios of 0.7058 to 0.7084 for andesites, of 0.7053 to 0.7086 for dacites, of 0.7054 to 0.7090 for rhyolites and 0.708 for Bihor granitic batholith.

In the Romanian South Carpathians, Late Cretaceous magmatism was mainly intrusive, but important volcanism is recorded in Gosau-type Senonian basins from Poiana Ruscă Mts., overlying both Getic and Supragetic nappes (Năstăseanu et al., 1981). Unpublished work of Krautner and Krautner and the geological maps published by Krautner et al. (1972) and Maier and Lupu (1979) show the absence of volcanic products in the Cenomanian, Turonian and Coniacian to Lower Maastrichtian, but the development of an Upper Maastrichtian volcano-sedimentary formation with andesitic aglomerates and tuffs. Upper Cretaceous deposits and undelying metamorphic basement are crossed by dioritic and granodioritic plutons and dyke swarms of andesite, dacites and rhyolites, followed by lamprophyric dykes, all considered as banatites. Eastwards, in the Senonian deposits from Demsus area, andesitic and rhyolitic flows or tuffs are found in the Maastrichtian pile (Maier and Lupu, 1979) and south of Barul Mare porphyry granodiorite intrusions cross Upper Campanian-Lower Maastrichtian deposits (Berza et al., 1986). 120 km southwards, near Danube, the Gosau-type basin of Sopot preserves Cenomanian to Middle Campanian deposits lacking volcanic products, but are crossed by monzodioritic to granodioritic intrusions (Cioflică et al., 1992).

Intrusive banatites have been ascribed to three lineaments by Giuşcă et al. (1966), to three magmatic trends that cross at low angle this lineation by Vlad (1979), respectively to a plutonic zone in the west and to a hypabyssal one in the east, by Russo-Săndulescu and Berza (1979). The plutonic zone is represented by the alkali-calcic Surduc (Russo-Săndulescu et al., 1986 a), Bocşa West (Russo-Săndulescu et al., 1978) and Hăuzeşti (Cioflică et al., 1994) intrusions and by the calc-alkaline plutons Ascuţita, Tincova, Gavojdia, Eastern Bocşa-
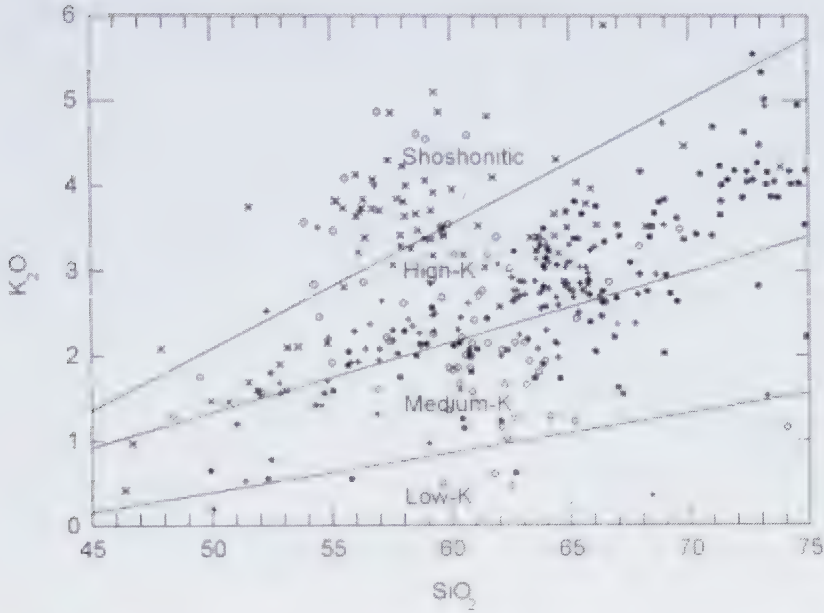
Fig. 2 SiO_2-K_2O diagram for banatites from Romania

* North Apuseni;
x Bocşa W, Surduc;
+ Ascuţita, Bocşa E, Ocna de Fier, Oraviţa, Sasca, Moldova Nouă;
o Lilieci-Purcariu, Lăpuşnicel-Teregova.
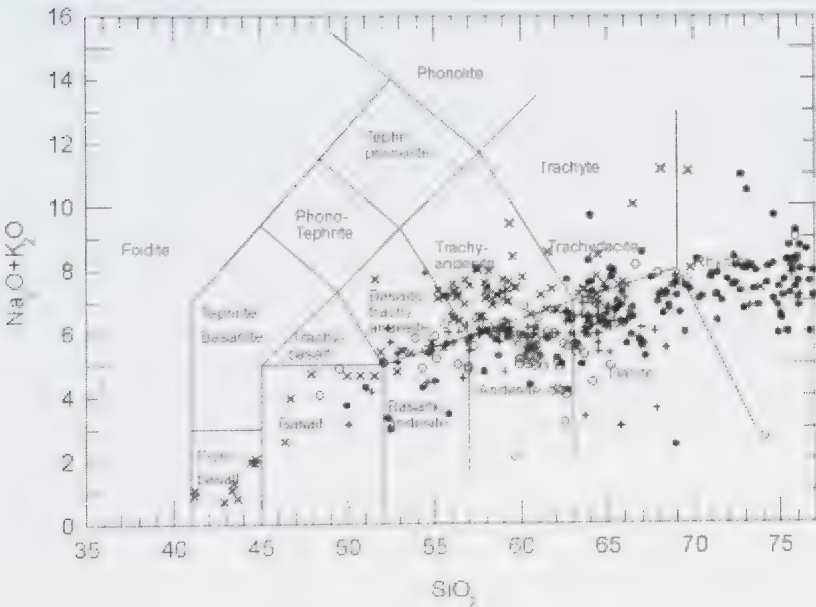
Fig. 3 SiO_2-K_2O+Na_2O diagram for the banatites from Romania

*North Apuseni;
x Bocşa W, Surduc;
+ Ascuţita, Bocşa E, Ocna de Fier, Oraviţa, Sasca, Moldova Nouă;
o Lilieci-Purcariu, Lăpuşnicel-Teregova.

Ocna de Fier-Dognecea (Russo-Săndulescu et al., 1978, 1986 b; Krautner et al., 1986; Nicolescu, 1998) and Oraviţa - Ciclova - Sasca -Moldova Nouă (Gheorghiţă, 1975; Gheorghiţescu, 1975; Constantinescu, 1977); south of Danube, this zone is known as Ridanj-Krepoljin, but with hypabyssic facies (Karamata et al., 1997; Djordjevic et al., 1997). The envinronment of the plutons is represented by crystalline schists from the Supragetic nappe, or Carboniferous to Lower Cretaceous cover formations of the Reşiţa, Sasca-Gornjac and Getic nappes (Năstăseanu et al., 1981). The hypabissal zone follows estwards after 20 km of interruption and is represented by dyke swarms and small plutons of
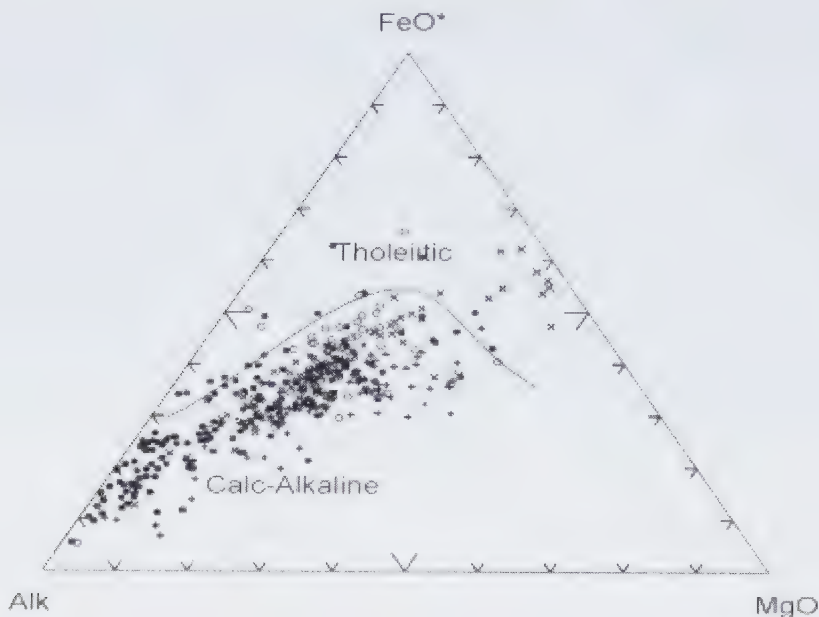
Fig. 4. Alk*-FeO-MgO diagram for banatites from Romania; * North Apuseni; x Bocşa W, Surduc; + Ascuţita, Bocşa E, Ocna de Fier, Oraviţa, Sasca, Moldova Nouă; o Lilieci-Purcariu, Lăpuşnicel-Teregova.

porphyry quartz diorite, monzodiorite or granodiorite; lamprophyres and andesites are also reported (Gunnesch et al., 1975, 1978; Întorsureanu, 1986; Cioflică et al., 1991, 1993). These intrusions cross crystalline schists from the basement of the Getic nappe or Cenomanian to Middle Campanian formations of the Gosau-type basin of Sopot (Năstăseanu et al., 1981). South of the Danube, this zone is represented by the volcanics and intrusions of Timok area (Djordjevic et al., 1997; Karamata et al., 1997).

Isotopic dating of effusive and intrusive banatites from the Romanian South Carpathians (Russo-Săndulescu et al., 1986; Krautner et al., 1986, Strutinski et al., 1987; Cioflică et al., 1994, Nicolescu, 1998) points to K-Ar ages between 91 and 65 My, but andesitic and lamprophyric dykes can reach 54-43 My; U-Pb zircon ages of 75 My for the Eastern Bocşa-Ocna de Fier-Dognecea pluton indicates an Upper Campanian intrusion. Based on 229 analyses from Gheorghiţescu (1975), Constantinescu (1977), Russo-

Săndulescu et al. (1978, 1979, 1986a, 1986 b), and Cioflică et al. (1991, 1993), we present the fields for plots of banatites from Romanian South Carpathians in the SiO_2-K_2O (Fig. 2), SiO_2-Na_2O+K_2O (Fig. 3) and Alk-FeO*-MgO (Fig. 4) diagrams. Western Bocsa and Surduc intrusions show the largest chemical variation, constantly at higher level of alkalies compared with the other rocks. ORG normalised spidergrams shaw Rb, K, Ba and Th enrichment and Ta, Nb, Ce, Hf, Zr, Sm, Y and Yb depletion, while [86]Sr/[87]Sr ratios varies between 0.703-0.706 and 143Nd/144Nd ranges between 0.51255-0.51275 (Cioflică et al., 1996, 1997).

An interesting feature of the banatites from Romania, both from Apuseni Mountains and South Carpatians, is the average 81º Declination, 47º Inclination and 27º N Palaeolatitude, computed from 56 sites confirming, along with data from sedimentary formations, a 20º clockwise rotation and norward drift of 25º in the Eocene - Middle Miocene

time span, followed by 60° more rotation in Late Badenian to Early Sarmatian (Panaiotu, 1998).

South of Danube, in the Serbian South Carpathians, banatites are found in two N-S oriented parallel zone: Ridanj-Krepoljin to the west and Timok to the east (Djordjevic et al., 1997), representing prolongations of the plutonic, respectively hypabissal zones from Banat.

In the Ridanj-Krepoljin zone dykes, shallow intrusions, volcanic breccias or tuffs, mainly dacitic but also andesitic or rhyolitic, intrude or overlie Permian to Lower Cretaceous formations from the Sasca-Gornjac or Getic nappes; in boreholes porphyritic quartz diorites and granodiorites were also found (Karamata et al., 1997). Compared to the intrusions north of the Danube, the banatites exposed in the Ridanj-Krepoljin zone represent a shallower level, hypabissal or even volcanic. No Upper Cretaceous deposits are preserved, but K-Ar ages in the 70-74 My range (Peczkay et al., 1992) are in good agreement with the U-Pb ages found north of Danube (Nicolescu, 1988) and suggest Upper Campanian to Lower Maastrichtian igneous activity. The SiO_2 content of 21 analyses varies from 59% to 75% and the mean is 65%; the general trend is calc-alkaline (Djorjevic et al., 1997).

The Timok zone is situated 20 km eastwards from the Ridanj-Krepoljin zone and is a 60/20 km belt of volcanics with rare intrusions, located 30 to 90 km south of Danube, in the continuation of the hypabissal zone from Banat. Timok is a volcano-plutonic complex where volcaniclastics, lavas and feeder dykes of andesites and basaltic andesites prevail, but dacites and latites also occur; dykes and rare plutons of monzonites, diorites and granodiorites cross the volcanics and northwards, to the Danube, only andesitic dykes are known (Karamata et al., 1997). According to the rela-

tions with the Upper Cretaceous formations and the K-Ar data, the volcanic activity started in the eastern part in Turonian to Campanian (90-80 My) with andesites and continued up to the Upper Maastrichtian (70-63 My) with dacites, while in the western part Campanian to Lower Maastrichtian (80-72 My) andesites and basaltic andesites with rare latites were erupted; intrusions of monzonites, diorites, granodiorites and syenites occurred simultaneously with the youngest lavas at 75-62 My (Karamata et al., 1997). The substratum of the Timok zone is represented by pre-Alpine crystalline schists and granitoids from the basement of the Getic nappe (Krautner, 1996), but the several kilometers thick pile of Upper Cretaceous sedimentary and volcanic formations has enabled Antonijevic et al. (1974) to consider here a palaeorift structure. 100 chemical analyses recorded by Djordjevic et al. (1997) have a SiO_2 content from 49% to 65%, with a mean at 56% and express both calc-alkaline and tholeiitic differentiation trends. $^{86}Sr/^{87}Sr$ ratios between O.706 and 0.710 (Jankovic, 1996) are contrasting with the relatively basic character of the Timok vulcano-plutonic complex and express clear crustal components of some of the magmas.

East from the Timok river, in Srednogorie Mountains from Bulgaria, the BMMB first continues in West Srednogorie on the NW-SE strike, then takes an E-W trend in the Central and East Srednogorie, up to the Black Sea. Reviews concerning Late Cretaceous igneous rocks from Srednogorie were presented by Stanisheva-Vasilieva (1980), Vassilieff and Stanisheva-Vassilieva (1981), Popov (1981, 1996) and Bayraktarov et al. (1996), all pointing to important along-arc differences.In West Srednogorie the volcanic activity is confined to the Coniacian-Campanian time span, lati-andesites with lati-basalts and andesites with basalts being crossed by several gabbro-monzonite-syenite plutons, from which Vitosha is is the most important (Popov, 1981). In Central Srednogorie, a large volcano-plutonic complex is located in the area of

Panagyurishte, composed of volcanic structures crossed by the Elsica, Medet, Vlaikov vrah, Tsar Asen intrusions, but other intrusions are also found some tens of kilometers East and South from the Panagyurishte complex; rhyolites, dacites and andesites are the main volcanics and gabbros, diorites and granodiorites the most common intrusives (Popov, 1981). Eastern Srednogorie has a great variety of Late Cretaceous magmatites, preserving huge volcano-plutonic structures, with radial and concentric dyke complexes; plutons of gabbro-diorite-granite composition are common in the South (Bayraktarov et al., 1996). Stanisheva-Vassilieva (1980) and Stanisheva-Vassilieva and Daieva (1990) have stressed the across-arc variation of the geochemistry of Upper Cretaceous igneous rocks in East Srednogorie, with increase in K_2O content from South to North, but Kuikin (1996) has revealed the importance of the Zlatograd-Yambol trans-crust fault, separating a normal crustal block to the West from one with reduced granite layer (10 km, against 25 km) and total crust (28-39 km, against 50-55 km) to the East. Campanian tephryte-trachyte, latiandesite-latibasalt and andesite-basalt associations are crossed by gabbro-monzonite-syenite intrusions at Rosen, Burgas and Sozopol (Popov, 1981; Boccaletti et al., 1978). The basement of the Upper Cretaceous sedimentary and volcanic formations is the same type of crystalline schists and granitoides as for the Timok zone, a prolongation in the Balkan Mountains of the Getic nappe from the Carpathians (Tari et al., 1997).

Synthesis of the chemical data on banatites from Srednogorie were presented by Stanisheva-Vassilieva (1980) -- 1200 analyses, Popov (1981) – 1236 analyses and Bayraktarov et al. (1996) ~ 1000 analyses, from which it results that: in the Bulgarian segment of BMMB all the main petrographic types are present, from ultrabasic to acid ones and from silica-oversaturated to silica-undersaturated, but dominant are the basic and intermediate groups, mainly in the alkali-calcic trend; andesites are dominating in the Central Srednogorie, and basalts in West and East Srednogorie; acid rocks, also with alkali-calcic trend, are restricted to the Panagyurishte area; alkaline and ultrabasic rocks are characteristic for E Srednogorie, where in a shoshonitic envinronment leucitic basanites, limburgites and picrites are found (Boccaletti et al., 1978).

Scarce $^{86}Sr/^{87}Sr$ ratio data quoted by Bayraktarov et al. (1996) indicate for monzonites and syenites from the Vitosha pluton 0.7042 to 0.7044 and for andesites from West and Central Srednogorie 0.7040 to 0.7060.

4. Ore deposits associated with the Upper Cretaceous magmatites in the Carpathian-Balkan orogen

Economic mineralisation in the Banatite Magmatic and Metallogenetic Belt of the Carpathian-Balkan orogen is represented especially by porphyry copper, massive sulfide, skarn and vein (epithermal and mesothermal) deposits. The mining activity throughout this area has been unbalanced. The northern part of the belt (i.e. the Apuseni Mts., Banat Mts.) have been exhaustively mined for metallic ores since pre-Roman times, including under the Austrian rule in XVIII - XIX century period and lately activities of national companies. These ore deposits were described in the last century by such well known geologists (from the Freiberg school) as von Cotta and Posepny. Accordingly, the skarn deposits at Dognecea, Ocna de Fier and Băiţa Bihorului became famous the world over. They have a rich and complex paragenesis, with up to 200 ore and gangue minerals. Several minerals were described from these deposits for the first time: ludwigite, szajbelyite, rezbanyite, csiclovaite, veszelyite and dognacskaite. The southern portions of the belt, namely the Eastern Serbia and Srednogorie underwent a long Ottoman occupation resulting in very restricted mining exploitation. Accordingly, exploration developed in the last decades promoted impor-

tant discoveries, especially in terms of large porphyry Cu-Au deposit (e.g. the world-class deposit at Majdanpek, Timok with 1000 Mt, grading 0.6% Cu and 0.3 ′g/t Au) and high sulfidation volcanogenic Cu-Au-As deposits (e.g. Chelopech in the Central Srednogorie, the largest gold deposit in Europe with 60 Mt, grading 1.24 % Cu and 3.38 g/t Au).

The Banatitic Magmatic and Metallogenetic Belt is subdivided into several segments, i.e. metallogenetic sub-belts with associated zones and districts. In Romania, the Banatitic Belt is comprised of the Apuseni Mountains and South Carpathian segments. These subdivisions are presently distributed along major N-S lineation, but have different tectonic settings.

The North Apuseni Mts. sub-belt is characterized by acid volcanism plus granodiorite-granite plutonism and widespread base-metal metallogenesis. Two metallogenetic zones have been recognized in non-porphyry envinronment (Cioflică and Vlad, 1984):

1. The southern zone exhibits a complex metallogenesis in the Bihor-Gilău Mts. It contains Fe, Mo, Bi, W, Cu, Co, Ni, Pb, Zn, B, Au and Ag in skarns, stratiform-impregnation bodies, and veins in the Băişoara, Băiţa Bihor and Luncşoara-Brusturi-Poiana districts. Băiţa Bihor is the most important deposit. The ore zoning around the Băiţa Bihor-Dedes batholith at Băiţa Bihor is Mo-Bi-W-Cu-U-Pb-Zn-B and is expressed in a vertical column extending up to 1.5 km away from the granite pluton. Calcic and magnesian skarns of proximal and distal setting contain molybdenite, bismuthinite, Bi sulfosalts and tellurides, scheelite (three generations), Cu minerals, common sulfides and borates as szajbelyite, ludwigite, fluoborite and kotoite. Metasomatised siliciclastic hornfelses contain U and Cu ores in stratabound lenses and molybdenite in impregnations and veinlets, whereas Palaeozoic siliciclastic rocks and crystalline schists situated far from the pluton enclose bands and veins of common sulfides. The same granitic major intrusion

yielded "pentametallic" (U, Ni, Co, Ag, Bi) in veins and Cu-U ores as stratiform impregnations at Avram Iancu and replacement base-metal ores at Brusturi and Luncşoara.

2. The northern zone is noted for base metals and is located in the Vlădeasa Massif, i.e. hydrothermal Pb-Zn ores in the Scrind-Răchiţele and Bucea-Corniţel districts.

The South Apuseni Mts. sub-belt is represented by monzodiorite to diorite-granodiorite magmatism with calcic Fe-skarn deposits at Magureaua Vatei.

The South Carpathian (Poiana Ruscă Mts. - Banat Mts) sub-belt consists of two zones (Vlad, 1979):

1. The southern zone exhibits in the South Banat Mts. a monzodiorite to diorite>granodiorite magmatism and related Cu-Mo porphyries. The porphyry deposits and prospects have in common the occurrence of porphyritic tongue-like apophyses of deeply buried plutons of monzonite or diorite to granodiorite composition. Such apical setting represents centres of zoned hydrothermally developed sulfide mineralization and rock alteration controlled by intensivelly fractured host rocks. These porphyries are of classic calc-alkaline type or (Arizona type), two subtypes being outlined, i.e. Suvorov-Moldova Nouă and Sasca with skarn halo and Bozovici with pyrite halo. The large scale zonality is: Cu-Mo stockwork in potassic/phyllic altered igneous host-calcic/magnesian skarn Cu ± Mo, W-replacement Pb-Zn telethermal As-Sb-presumable Carlin gold.

2. The northern zone exposes in the North Banat-Poiana Ruscă Mts. granodiorite-granite magmatism with Fe, Cu, Pb-Zn skarn deposits at Dognecea and Ocna de Fier, Mo-W-Cu skarn deposits at Ciclova-Oraviţa and Pb-Zn skarn deposits and prospects at Tincova, Ascuţita and Ruşchiţa. Such non-porphyry environment is characterised by proximal grandite skarns with Fe (Cu) ores (Ocna de Fier) and distal Mn-hedenbergite skarns with Pb-Zn ores (Dognecea) in calcareous environ-

ment. When wall-rocks are various meta-sedimentary rocks and coeval or older igneous rocks refered to granitic intrusion, Pb-Zn mineralization is found away from the pluton and suggests remobilization during the banatitic event (Ruşchiţa). These contrasts are the result of proceses that proceeded to different extent in response to similar felsic magmatism and wall-rock / protores of various origin.

A recent review of the regional occurrences, tectonic characteristics, alteration and zoning, ore mineralogy and other elements form the outline of metallogenetic models of the Romanian part of the BMMB (Vlad and Borcoş, 1997). Metallogenetic models in porphyry envinronment are represented by the Suvorov model with skarn halo and the Bozovici model with pyrite halo in Banat. Metallogenetic models in non-porphyry envinronment are defined as Ocna de Fier model and Dognecea model in Banat of carbonate host with proximal and distal Fe-Cu/Pb-Zn skarn formation and Băiţa Bihor model in the Apuseni Mountains with extended skarn formation and Mo-Bi-W-Cu-Pb-Zn-B mineralisation throughout the whole contact aureole of the pluton.

In Yugoslavia, the Eastern Serbian sector of the South Carpathian subbelt contains two parallel metalogenetic alignments that strike N-S, i.e. the Ridanj-Krepoljin zone in the west and the Timok volcano-plutonic complex in the east. These units represent the extension south of the Danube of the above mentioned zone of North Banat - Poiana Ruscă Mts. and respectively the zone of South Banat Mts. (e.g. Jankovic, 1997; Karamata et al., 1997):

1. The Timok volcano-plutonic complex contains andesites, subordinately basaltic andesites and dacites at high level and deep-seated corespondant monzodiorites, diorites and quartz diorite intrusions. The mineralization is of Cu ± Mo, Au and marginal Zn character. Worth mentioning is the recovery of Pt and Pd recorded at Bor. Ore types are located at volcanic and subvolcanic levels and consists

of porphyry Cu ± Au, Mo, high sulfidation massive sulfide Cu-As-Au or Pb-Zn ± Au and subordinately skarn Pb-Zn. Significant porphyry copper deposits as Majdanpek and Veliki Krivelj or Borska Reka (Bor) and prospects as Cerova, Valja Strz and Dumitru Potok show a wide variation in mineralization style and metal contents which points to fundamental difference in the metal budgets of adjacent hydrothermal systems (e.g. Majdanpek deposits grades 0.3 g/t Au whereas Veliki Krively only 0.07 g/t Au). These porphyry deposits are commonly closely associated with massive sulfide high-sulfidation deposits, e.g. the famous Bor deposits (porphyry at Borska Reka with 400 Mt grading 0.9% Cu, 0.35 g/t Au and massive sulfide at Coka Dulkan, Tâlva Roşie, Tâlva Mică with 40 Mt grading 3% Cu and 3 g/t Au).

At Majdanpek the porphyry is tectonically controlled by a 300 m wide linear "graben" within crystalline basement that served to inhibit interaction between the porphyry system and the possible wall-rock fluid sources. The development of high-sulfidation mineralization in restricted to the very apex of the porphyry. These high sulfidation ore bodies are also base metal rich, similar to the distal epigenetic Zn-Cu ± Pb, Au, Ag Coka Marin recently discovered deposit. By way of contrast, at Bor, the Borska Reka porphyry intrudes a thick sequence of subvolcanic and extrusive andesites and this led to intensive advanced argillic alteration. Large high-sulfidation ore bodies with pyrite, bornite, chalcopyrite, enargite, covellite, chalcocite and gold developed with gold-bearing silica cap.

2. The Ridanj-Krepoljin zone exhibits a more differentiated and crustal contaminated granodiorite-granite magmatism with associated Pb-Zn-Ag, locally Sb-W mineralization. Base metal replacement and skarn ores are related to andesite-dacite subvolcanic bodies, e.g. Kucajna, whereas Permian sandstones contain epigenetic Sb-W-Cu ores, e.g. Krepoljin.

In Bulgaria, the Banatitic Magmatic and

Metallogenetic Belt is well expressed in Srednogorie and represents the eastward extension of the N-S striking South Carpathian (Banat - Eastern Serbia) sub-belt. The characteristic BMMB transversal zonality of the South Carpathian sub-belt in both Romanian and Serbian sectors is replaced in the Srednogorie subbelt by significant along-arc differentiation. This peculiarity is represented spatially by three clusters, i.e. Western Srednogorie sub-belt, Central Srednogorie sub-belt and Eastern Srednogorie subbelt (e.g. Vassiliev and Stanisheva-Vassilieva, 1981; Popov, 1996):

1. The Sofia ore district in Western Srednogorie contains the products of intermediate to basic calc-alkaline magmatism with subalkaline trend that lacks economic importance. So far, deposits of industrial importance are only the Kremikovtsi metasomatic Fe deposits in dolostone and the Pozharevo volcano-sedimentary Mn deposits. Anyway, recent investigations sugests that low-sulfidation epithermal systems virtually carrying gold are to be taken into consideration (e.g. Vakarelets).

2. The Panagyurishte ore district in Central Srednogorie is characterized by intermediate to felsic calc-alkaline magmatism with subalkaline trend. The related metallogeny is represented by spatial association of volcanogenic high-sulfidation massive sulfide deposits and porphyry Cu ± Au, Mo deposits. The porphyry copper occur at different levels of the volcano-plutonic complex intruding thick continental crust, i.e. hypabysal at Medet, subvolcanic at Petelevo, Vlaykov Vrh and Tsar Assen, and volcanic at Assarel. This feature correlates with progressive involvement of meteoric water in the porphyry system, increase of gold content and development of advanced argillic alteration.

Major massive sulfide bodies in andesite piles are Elshitsa (mainly pyrite), Krassen and Chelopech (Cu-pyrite ± Au,As) and Radka (Cu-Pb-Zn-pyrite). Mineralization comprises sulfide-rich zones of pervasive silicification within halos of silica-sericite-propylitic alteration. The ore bodies are tectonically controlled and contain gold, common sulfides, enargite, luzonite, tennantite, bornite, complex sulfides and arsenides, especially at Chelopech. In all deposits sulfide and sulfosalts show a significant ability to concentrate gold. Highest gold concentration is in bornite, tennantite and enargite and early generation of pyrite.

3. The Eastern Srednogorie districts contain commonly tholeiite (basalts to andesites and corespondent gabbros and diorites), subalkaline (latibasalts to latiandesites and corespondent gabbro-monzonite-syenite rocks) and alkaline (tephrytes and trachytes) magmatic suites emplaced in rift-like environment. The associated mineralization is Fe, base metal and precious metal veins and skarn deposits. The Yambol district is located near the central part of the Eastern Srednogorie and contains Fe-skarns (Krumovo) and Au-base metal veins of "mesothermal" type (Bakadzik). The Burgas ore district is situated in the easternmost part of Srednogorie. The magmatism is of subalkaline to alkaline character, represented by volcano-plutonic complexes with thick volcanic piles emplaced above thin basified crust. The metallogeny is of "mesothermal" vein type and comprises Cu ± Au; Au ± Pb, Zn, Cu; Mo, U, Fe and Co-pyrite deposits at Rosen, Varly Bryag and Zhidarevo ore fields. Gold contents are higher at Zhidarevo. The Malko Tarnovo /Stranja district exhibits calc-alkaline to tholeiitic magmatism that penetrated a basement of intermediate thickness compared with thin crust at Burgas and thick crust at Panagyurishte. This district is located in the south-eastern corner of Bulgaria and extends into Turkey. Skarn metallogeny prevails and "skarn hosted ore deposits" are characteristic of this setting. Major deposits are Malko Tarnovo (Cu-Mo skarn-porphyry), Velikovets (Fe-Ti magmatic skarn) and Gramatikovo (Cu-Fe stratiform remobilised).

5. Proposed genetic model for the formation of the Banatitic Magmatic and Metallogenetic Belt from the Carpathian-Balkan orogen

To the dozens of models already proposed for parts from, or for the entire, BMMB in the literature published in the last 25 years, and implying plate-tectonics for the generation of magmas and related ore deposits, it is difficult to add a really new one. But we will try to present our choice from the existing ones in tectonics and to propose some ideas about the correlation between the petrografic composition of the host/cause igneous formations and the associated types of minerallisation.

From the North Apuseni Mountains, through the Poiana Ruscă Mts. of North Banat , the Timok complex of East Serbia, the West, Central and East Srednogorie of Bulgaria, up to the Black Sea, a series of Upper Cretaceous sedimentary, volcanic and plutonic formations are preserved in elongated grabens, up to 100 km long/30 km large (Fig. 1); plutons or dykes are also found in the intervals between these grabens, or parallel to them, and help to delineate the BMMB. As early as 1974, Antonijevic et al. have proposed an Upper Cretaceous Paleorift in Eastern Serbia for the Timok zone and Popov (1981, 1996) has found geologic, petrological and metallogenetic support for this extensional model along the entire BMMB, making it relatively popular in the Bulgarian literature. We also accept it, with the mention that the extensional regime, following the Middle Cretaceous compression responsible for the overthrusts recorded by the nappes from Apuseni Mountains, the Bucovinic system from the East Carpathians and the Getic-Supragetic system from the South Carpathians, was restricted to the Austro-Bihor (= PreApulian) and Getic (= Bucovinian = Rhodopian) blocks, as in the Danubian (=Stara Planina) block flysch deposition and nappe empilement were ongoing. The tectonic model of the South Carpathians presented by Neubauer et al. (1998) can thus

be extended for the Upper Cretaceous along the entire Carpathian-Balkan orogen, with Gosau-type (± banatitic magmatism) basins in the back and accretionary wedges in the front. As palaeomagnetic data prove an 80o clockwise rotation of the Apuseni Mts. and Banat sectors of BMMB, it results that, despite the present-day L shape, BMMB was originally a linear, E-W striking, extensional structure. The existence and importance of previous westwards directed subductions of Transylvanides (=South Apuseni = Mureş Zone) and Severin-Krajina palaeo-oceans, popular in Romanian literature, seems to have little relevance to BMMB generation, but the well documented northwards directed subduction of the Vardar-Axios palaeo-ocean during Jurassic and Lower Cretaceous is a good precondition for the generation during the Upper Cretaceous of banatitic magmas, in extensional regime, by mantle delamination due to slab break-off. Evidently, the later Laramian compression, the transpressional to transtensional Tertiary tectonics, the northern drift and clockwise rotation of the western part of BMMB, and Oligocene to Neogene volcanism, all due to the Africa/Europe collision, contributed essentially to the present-day geology of the Carpathian-Balkan orogen.

Considering the whole BMMB, the chemical diagrams presented here for the Romanian sector and those of Karamata et al. (1997) and Djordjevic et al. (1997) for the East Serbian sector and Stanisheva-Vassilieva (1980) and Popov (1981) for the Bulgarian sector show the wide chemical variation of composition for banatitic effusive and intrusive rocks. According to the above quoted authors, four magmatic trends are found: a tholeiitic trend, a calc-alkaline trend, a calc-alkaline high K to shoshonitic trend and, restricted to East Srednogorie, a peralkaline trend. Plotted on the Pierce geochemical diagrams, considered relevant for the tectonic setting, Upper Cretaceous rocks from BMMB spread from volcanic arc to intraplate fields, confirming the criticism of these diagrams for post-collisional magmatism (e.g. Liegeois, 1998). For acid

A **B** **C** **D** 13

| SKARN DEPOSITS RELATED TO PLUTONS | PORPHYRY-SKARN DEPOSITS RELATED TO SUBVOLCANIC-PLUTONIC STRUCTURES | PORPHYRY-MASSIVE SULFIDE DEPOSITS RELATED TO VOLCANIC-SUBVOLCANC STRUCTURES | MESOTHERMAL-EPITHERMAL VEIN DEPOSITS RELATED TO VOLCANIC STRUCTURES |

I-type/Magnetite series granitoid suite of BMMB

1 Pluton
2 Apophyses of pluton
3 Volcanic structure
4 Dyke
5 Fault

6 Skarn deposits (Apuseni Mts)
7 Proximal skarn deposits (N Banat)
8 Distal skarn deposits (N Banat)
9 Skarn porphyry deposits (S Banat)

10 Porphyry-pyrite halo deposits (S Banat)
11 Porphyry deposits (C Srednogorie)
12 Porphyry-masive sulfide deposits (C Srednogorie, Timok)
13 Mesothermal-Epithermal vein deposits (W and E Srednogorie)

Fig. 5 Cartoon presentation of the banatitic magmatic-metallogenetic model.

intrusives, the typology is clearly I-type (Chappel and White, 1974) and magnetite-series (Ishihara, 1977), pointing to sources in the deep crust or the mantle; however, some high $^{86}Sr/^{87}Sr$ ratios recorded in banatites prove important contamination from the upper crust. The calc-alkaline hydrated magmas, most common for banatitic plutons, can be considered as recording three stages of evolution: more primitive - the monzodioriric, dioritic to granodioritic trend (S Apuseni, S Banat, Timok, C and W Srednogorie); more evolved - the granodioritic-granitic trend (N Apuseni, N Banat, Ridanj-Krepoljin); the alkaline trend (western part of N Banat, E and W Srednogorie). Correlating the composition of the host plutons with the ore types, several environments can be found in the BMMB, function of: timing of fluid separation (porphyry versus non-porphyry environments);

depth of emplacement; size of intrusion and geology of intruded rock pile; biotite versus hornblende crystallisation, involving the evolution of K/Na ratio in fluids, i.e. development of potassic and phyllic alteration zones:

a) non-porphyry environment with granodioritic to granitic magmas (Fig.5 A), plutonic level, skarn mineralisation prevails (North Banat, North Apuseni);

b) porphyry environment with monzodioritic or dioritic to granodioritic magmas (Fig. 5 B), subvolcanic-hypabyssal-plutonic level; porphyry Cu with skarn halo at hypabissal-subvolcanic level (South Banat);

c) porphyry environment with monzodioritic or dioritic to granodioritic magmas (Fig. 5 C), volcano-plutonic complexes with porphyry copper plus massive sulfide mineralisation at subvolcanic-volcanic level (Timok, Panagyurishte in Central Srednogorie);

d) non-porphyry environment with magmas of alkaline tendency (Fig. 5 D), volcanic level, vein "mesothermal" and "epithermal" mineralisation (East and West Srednogorie).

Acknowledgements

References

Antonijevic, I., Grubic, A., Djordjevic, M. (1974) The Upper Cretaceous Paleorift in Eastern Serbia. In: S. Karamata, editor "Metallogeny and Concepts of the Geotectonic Development of Yugoslavia", **315-339**.

Arsovski, M., Dumurdzanov, N. (1995) Alpine tectonic evolution of the Vardar Zone and its place in the Balkan region. *Geologica Macedonica*, **9**, 15-22.

Arsovski, M., Dumurdzanov, N., Petrov, G. (1997) Manifestations of the Alpine Orogene Phases in the Vardar Zone. In: B. Boev and T. Serafimovski, editors "Proceedings Magmatism, Metamorphism and Metallogeny of the Vardar Zone and Serbo-Macedonian Massif", Symposium Annual Meeting IGCP Project No 356, Stip-Djoran - 1997, 77-82.

Balintoni, I. (1995) Alpine plate boundaries on the Territory of Romania. *Studia Univ.*

Babes-Bolyai, Geologia, **XL**, 1, 55-72.

Balintoni, I. (1997) Geotectonica terenurilor metamorfice din România. Ed. Carpatica, Cluj-Napoca, 176 p.

Balintoni, I. (1998) The Apuseni Mountains. In: J. Sledzinski, editor "Monograph of Southern Carpathians", *Warsaw Univ. of Techn., Reports on Geodesy,* **7** (37), 93-110.

Balintoni, I. and Vlad, Ş. (1998) Tertiary magmatism in the Apuseni Mountains and related tectonic setting. Studia Univ. Babes-Bolyai, *Geologia*, in press.

Balla, Z. (1984) The Carpathian loop and the Pannonian basin: a kinematic analysis. *Geophys. Trans.,* **30**, 4, 313-353.

Bayraktarov, I., Antova, N., Nikolov, G., Rankova, T. and Chemberski, H. (1996) Geodynamic enviroments during the Late Cretaceous in Bulgaria and their metallogeny. In: "Plate tectonic aspects of the Alpine metallogeny in the Carpatho-Balkan region", IGCP Project No 356 Annual Meeting, Sofia 1996, 1, 45-56.

Berza, T. (1997) A hundred years of tectonic studies in South Carpathians: The state of the art. In: A. Grubic and T. Berza, editors "Geology of Djerdap Area", Belgrade, 271-276.

Berza, T., Seghedi, A., Pop, Gr., Szasz, L., Hârtopanu, I., Săbău, G., Moisescu, V., Popescu G. (1986) Geological map of Romania scale 1:50.000, Lupeni sheet. Inst. Geol. Geof., Bucuresti.

Bleahu, M. (1974) Zone de subducţie in Carpaţii românesti. *D.S. Inst. Geol.,* **LX/5**, 5-25.

Bleahu, M., Lupu, M., Patrulius, D., Bordea, S., Ştefan, A., Panin, S. (1981) The Structure of the Apuseni Mountains. Guide to excursion B 3, Carp.-Balk. Geol. Assoc. XII Congr. Bucharest-Romania, 106 p.

Bleahu., M., Soroiu, M., Catilina R. (1984) On the Cretaceous tectono-magmatic evolution of the Apuseni Mountains as revealed by the K-Ar dating. *Rev. Roum. Phys.,* **29**, 367-377.

Bocaletti, M., Manetti, P., Peltz, S. (1973) Evolution of the Upper Cretaceous and

Cenozoic Magmatism in the Carpathians arc. Geodynamic significance. *Mem. Soc. Geol. Ital.*, **XII**, 367-377.

Boccaletti, M., Manetti, P., Peccerillo, A. (1974) The Balkanids as an Instance of Back-Arc Thrust Belt: Possible Relation with the Hellenids. *Geol. Soc. Amer. Bull.*, **85**, 1077-1084.

Boccaletti, M., Manetti, P., Peccerillo, A.,Stanisheva-Vassilieva G. (1978) Late Cretaceous high-potassium volcanism in eastern Srednogorie, Bulgaria. *Geol. Soc. Amer. Bull.*, **89**, 439-447.

Burchfiel, B.C. (1980) Eastern European alpine system and the Carpathian orocline as an example of collision tectonics. *Tectonophysics*, **63**, 31-61.

Channell, J.E.T., Horvath, F. (1976) Adria - the African/Adriatic promontory as a paleogeographical premise for Alpine orogeny and plate movements in the Carpatho-Balkan region. *Tectonophysics*, **35**, 71-101.

Chappel, B.W., White, A.J.R. (1974) Two contrasting granite types. *Pacif. Geol.*, **8**, 173-174.

Christofides, G., Soldatos, T., Koroneos, A. Geochemistry and evolution of the Fanos granite, N. Greece. *Mineralogy and Petrology*, **43**, 49-63.

Cioflică, G. (1989) Copper mineralisation related to Upper Cretaceous-Paleogene magmatites in Romania. *Rev. Roum. Geol. Geophyš. Geogr., Geologie*, **33**, 13-24.

Cioflică, G., Vlad, Ş. (1973) The correlation of Laramian metallogenic events belonging to the Carpatho-Balkan area. *Rev. Roum. Geol. Geophys. Geogr., Geologie*, **17**, 2, 217-224

Cioflică, G., Lupu, M., Nicolae, I., Vlad, Ş. (1980) Alpine Ophiolites of Romania: Tectonic Setting, Magmatism and Metallogenesis. *An. Inst. Geol. Geog.*, **LVI**, 79-95.

Cioflică, G., Vlad, Ş. (1984) Alpine metallogeny in Romania. *An. Inst. Geol. Geof.*, **LXIV**, 175-184.

Cioflică, G., Jude, R., Lupulescu, M.,Udrescu, C. (1991) The banatitic magmatites of the Lilieci-Liubcova area (Banat). *Rev. Roum. Geologie*, **35**, 3-22.

Cioflică, G., Jude, R., Lupulescu, M. (1992) Evidence of porphyry copper mineralizations and additional remobilisation phenomena in the Lilieci-Purcariu area (Banat, Romania). *Rev. Roum. Geologie,* **36**, 3-14.

Cioflică G., Jude, R., Lupulescu, M. (1993) Magmatitele banatitice din arealul Lapuşnicul Mare (Banat). *St. Cerc. Geologie*, 3-22.

Cioflică, G., Pecskay, Z., Jude, R., Lupulescu, M. (1994) K-Ar ages of Alpine granitoids in the Hăuzeşti-Drinova area (Poiana Ruscă Mountains, Romania). *Rev. Roum. Geologie*, **38**, 3-8.

Cioflică, G., Jude, R., Lupulescu, M. (1995) Petrometallogenetic models in the areas the End Maastrichtian- Paleocene granitoid intrusions of Romania. *Studia Univ. Babes-Bolyay, Geologia*, **XL**, 1, 41-54.

Cioflică, G., Jude, R., Lupulescu, M., Ducea, M. (1996) Lower crustal origin of the Late Cretaceous-Eocene arc magmatism in the western part of the South Carpathians, Romania. In: Knezevic, V. and Krstic, B., editors "Terranes of Serbia", Belgrade, 103-107.

Cioflică, G., Jude, R., Lupulescu, M. (1997) Late Cretaceous-Eocene arc magmatism related porphyry-type deposits in Romania. *Rev. Roum. Geologie*, **41**, 3-18.

Constantinescu, E. (1977) Mineralogia şi petrologia magmatitelor laramice dintre valea Nerei şi valea Radimniuţei. *St. Cerc. Geol. Geof. Geogr., Geologie*, **22**, 87-102.

Constantinescu E. (1980) Mineralogeneza skarnelor de la Sasca Montană. Edit. Acad. R.S. România, 158 p, Bucureşti.

Cotta, B. v. (1864) Uber Eruptivgesteine und Erzlagerstatten in Banat und Serbien. Edit. V. Braunmuller, Wien, 105 p.

Csontos, L. (1995) Teriary tectonic evolution of of the Intra-Carpathian area: a review. *Acta Vulc.*, **7**, 1-13.

Csontos, L., Nagymarosy, A., Horvath, F., Kovac, M. (1992) Tertiary evolution of the

Intra-Carpathian area: a model. *Tectonophysics*, **208**, 221-241.

Dallmeyer, D.R., Neubauer, F., Handler, R., Fritz, H., Muller, W., Pana, D., Putis, M. (1996) Tectonothermal evolution of internal Alps and Carpathians: Evidence from 40Ar/39Ar mineral and whole-rock data. *Ecl. Geol. Helv.*, **89**, 1, 203-227.

Dewey, J.F., Pitman, W.C., Ryan, W.B.F., Bonnin, J. (1973) Plate tectonics and the evolution of the Alpine system. *Geol. Soc. Amer. Bull.*, **84**, 3137-3180.

Dewey, J.F., Sengor, A.M.C. (1979) Aegean and surrounding regions: complex multiplate and continuum tectonics in convergent zone. *Geol. Soc. Amer. Bull.*, **90**, 84-92.

Divljan, M., Karamata, S. (1967) Les roches eruptives de la zone de Ridan-Krepoljin. In: "Les roches magmatiques cretacees-tertiaires des Carpatho-Balkanides yougoslaves". *Acta Geol. Acad. Sci. Hung.*, **11**, 1-2, 131-135.

Djordjevic, M., Banjesevic, M., Ralevic, B , Milicic, M. (1997) Mesozoic magmatism of Djerdap Area. In: A. Grubic and T. Berza, editors "Geology of Djerdap area", 121-128.

Drovenik, M., Djordjevic, M., Antonijevic, I., Micic, I. (1967) Les roches magmatiques de la region eruptive de Timok. In: "Les roches magmatiques cretacees-tertiares des Carpatho-Balkanides yougoslaves". *Acta Geol. Acad. Sci. Hung.* **11**, 1-3, 115-129.

Gîrbacea, R.A. (1997) The Pliocene to Recent tectonic evolution of the Eastern Carpathians (Romania). Ph D Thesis, Univ. of Tubingen, TGA A 37, Tubingen, 136 p.

Girbacea, R.A., Frysch, W. (1998) Slab in the wrong place: Lower lithospheric mantle delamination in the last stage of the Eastern Carpathian subduction retreat. *Geology*, **26**, 7, 611-614.

Gheorghiță, I. (1975) Studiul mineralogic și petrografic al regiunii Moldova Nouă (zona Suvorov-Valea Mare). *St. tehn. Econ. Inst. Geol. Geof.* , **I/11**, 188 p.,

Bucureşti.

Gheorghițescu, D. (1975) Studiul mineralogic si geochimic al formatiunilor de contact termic si metasomatic de la Oravița (Coşovița). *D.S. Inst. Geol. Geof.*, **LXI/1**, 59-103.

Giuşcă, D. (1950) Le massif eruptif de la Vlădeasa. *An. Com. Geol.* **XXVIII**, 1-53.

Giuşcă, D., Cioflică, G., Savu, H. (1966) Caracterizarea petrologică a provinciei banatitice. *An. Com. Stat. Geol.*, **XXXV**, 13-45.

Grubic, A. (1974) Eastern Serbia in the Light of the New Global Tectonics: Consequences of This Model for the Interpretation of the Tectonics of the Northen Branch of the Alpides. In: S. Karamata, editor "Metallogeny and Concepts of the Geotectonic Development of Yugoslavia", 179-212.

Grubic, A., Dokovic, I., Marovic, M. (1997) Tectonic of the Yugoslav South Carpathians in Danube Gorges. In: A. Grubic and T. Berza, editors "Geology of Djerdap Area", Belgrade, 105-109.

Gunnesch, K., Gunnesch M., Seghedi I., Popescu C. (1975) Contribuții la studiul rocilor banatitice din zona Liubcova-Lăpuşnicul Mare (partea vestică a munților Almăj şi sud-vestică a munților Semenic). *D.S. Inst. Geol. Geof.*, **LXI/1**, 169-189.

Gunnesch, K., Gunnesch, M., Vlad, C. (1978) Consideratii petrografice si petrochimice asupra banatitelor din zona Teregova-Lapùsnicel (Muntii Semenic). *St. cerc. Geol. Geol. Geogr., Geologie*, **23**, 2, 239-248.

Herz, N., Savu, H. (1974) Plate Tectonics History of Romania. *Geol. Soc. America Bull.*, **85**, 1429-1434.

Ishihara, S. (1977) The magnetite-series and ilmenite-series granitic rocks. *Mining Geol.*, **27**, 293-305.

Istrate, Gh. (1978) Petrologic Study of the Vlădeasa Massif (Western Part). *An. Inst. Geol. Geof.* **LIII**, 177-298.

Intorsureanu, I. (1986) Banatitic eruptive rocks in the Bozovici-Liubcova zone

(Banat). *D.S. Inst. Geol. Geof.*, **70**, 53-67.

Jankovic, S. (1996) Comparision between metallogeny af Serbo-Macedonian metallogenic province and the Bor-Srednogorie zone. In: "Plate tectonic aspects of the Alpine metallogeny in the Carpatho-Balkan region", IGCP Project No 356 Annual Meeting, Sofia 1996, 1, 47-53.

Jankovic, S. (1997) The Carpatho-Balkanides and adjacent area: a sector of the Tethyan Eurasian metallogenetic belt. *Mineralium Deposita,* **32**, 426-433.

Johannsen, A. (1958) A descriptive petrography of the igneous rocks. Volume II, The quartz bearing rocks. Univ. of Chicago Press, Chicago, 428 p.

Jones, C.E., Tarney, J., Baker, G.H., Gerouki, F. (1992) Tertiary granitoids of Rhodope, northern Greece: magmatism related to extensional collapse of the Hellenic Orogen? *Tectonophysics,* **210**, 295-314.

Karamata, S. (1974) Evolution of the magmatism in Yugoslavia. In: M. Mahel, editor "Tectonics of the Carpathian-Balkan regions", Bratislava, 354-357.

Karamata, S., Knezevic, V., Pecskay, Z., Djordjevic, M. (1997) Magmatism and metallogeny of the Ridanj-Krepoljin belt (eastern Serbia) and their correlation with northern and eastern analogues. *Mineralium Deposita,* **32**, 452-458.

Kockel, F. (1986) Die Vardar-(Axios) Zone. In: V. Jacobshagen, editor "Geologie von Griechenland". Gebrueder Barntraeger, Berlin, 150-168.

Koller, K., Hoeck, V. (1992) the Mesozoic ophiolites in the Eastern Alps: A review. In: F. Neubauer, editor "The Eastern Central Alps of Autria - ALCAPA Field Guide", Graz, 115-126.

Kräutner, H.G., Kräutner, F., Orăşanu, T., Potoceanu, E., Dincă Al. (1972) Geological map of Romania scale 1:50.000, Nădrag sheet, Inst. Geol. Geof., Bucureşti.

Kräutner, H.G., Vâjdea, E., Romanescu O. (1986) K-Ar dating of the banatitic magmatites from the Southern Poiana Rusca Mts. (Rusca Montana sedimentary basin).

D.S. Inst. Geol. Geof., **70-71/1**, 373-388.

Kräutner, H.G. (1996) Alpine Rifting, Subduction and Collision in the Romanian Carpathians. In: G. Amann et al., editors "6. SymposiumTektonik-Strukturgeologie-Kristallingeologie, Salzburg, 10-15 April 1996", Wien, 230-234.

Kuikin, S (1996) The joining of the Balkanide and the Pontide island arc systems and the Late Cretaceous-Tertiary metallogeny in Bulgaria. In: "Plate tectonic aspects of the Alpine metallogeny in the Carpatho-Balkan region", IGCP Project No 356 Annual Meeting, Sofia 1996, 2, 181-187.

Lemne, M., Vâjdea, E., Borcoş, M., Tănăsescu, A., Romanescu, O. (1983) Des datation K - Ar concernant surtout les magmatites subsequentes alpines des Monts Apuseni. Assoc. Geol. Carp. Balk. Congress XII, 1981, Bucharest, *An. Inst. Geol. Geophys.*, **LXI** : 375-386.

Liegeois, J.P. (1998) Some words on the post-collisional magmatism. Lithos Special Issue on " Post-collisional magmatism", *Lithos*, **45**.

Linzer, H.G. (1996) Kinematics of retreating subduction along the Carpathian arc, Romania. *Geology,* **24**, 2, 167-170.

Lips, A.L.W. (1998) Temporal constrains on the kinematics of the destabilisation of an orogen; syn- to post-orogenic collapse of the North Aegean region. Geol. Ultraiectina, 166, Ph D Thesis, Univ. of Utrecht, 223 p.

Lupu, M. (1976) The main tectonic features of the South Apuseni Mts. *Rev. Roum. Geol. Geophys. Geogr., Geologie,* **20/1**, 21-25.

Magganas, A. (1998) Serbomacedonian Zone: Geological Framework. In: Sideris K., editor "Eurogranites '98 Macedonia and Thrace, Northern Greece", Univ. of Athens.

Maier, O., Lupu, M. (1979) Geological map of Romania scale 1:50.000, Băuţar sheet. Inst. Geol. Geof., Bucuresti.

Marton. E. (1997) Paleomagnetic aspects of plate tectonics in the Carpatho-Pannonian

region. *Mineralium Deposita*, **32**, 441-445.

Mărunțiu, M. (1983) Contributions to the petrology of ophiolitic peridotites and related rocks of the Mehedinți Mts. (South carpathians). *An. Inst. Geol. Geof.*, **LXI**, 215-22.

Matenco, L.C. (1997) Tectonic evolution of the Outer Romanian Carpathians: Constraints from kinematic analysis and flexural modelling. Ph D Thesis, Free University Amsterdam, 160 p.

Matenco, L.C., Bertotti, G., Dinu, C., Cloething, S. (1997) Tertiary tectonic evolution of the external South Carpathians and the adjacent Moesian platform (Romania). *Tectonics*, **16**, 896-911.

Mitchell, A.H.G. (1996) Distribution and genesis of some epizonal Zn-Pb and Au provinces in the Carpathian-Balkan region. *Trans. Inst. Min. metall.*, B, **105**, 127-137.

Morley, C.K. (1996) Models for relative motion of crustal blocks within the Carpathian region, based on restorations of the outer Carpathians thrust sheets. *Tectonics*, **15**, 885-904.

Mountrakis, D. (1994) Introduction to the geology of Macedonia and Thrace. Aspects of the geotectonic evolution of the Hellenides Hinterland and Internal Hellenides. *Bull. Soc. Geol. Greece Spec. Publ.*, **1**, 63-90.

Nachev, I. (1989) Paleogeodynamics of Alpine flysch on the Balkans. *Geologica Balcanica*, **19**, 3, 23-40.

Năstăseanu, S., Bercia, I., Iancu, V., Vlad, S. , Hartopanu, I. (1981) The Structure of the South Carpathians (Mehedinți-Banat Area). Guide to excursion B 2, Carp.-Balk. Geol. Assoc. XII Congr. Bucharest-Romania, 100 p.

Neubauer, F., Dallmeyer, R.D., Fritz, H., Reichwalder, P. (1976). Zur Geodynamik und Kinematik der Meliata-Decke in Westkarpaten und Ostalpen. In: G. Amann et al., editors "6. Symposium Tektonik-Strukturgeologie-Kristallingeologie, Salzburg, 10-15 April 1996", Wien, 300-303.

Neubauer, F., Berza, T., Bojar, A.V., Dallmeyer, D.R., Fritz, H., Willingshofer, E. (1998) Cretaceous terrane boundary and oblique continent-continent collision in Romanian Southern Carpathians. *Tectonophysics*, in press.

Nicolae, I., Soroiu, M., Bonhomme, M.G. (1992) Ages K - Ar de quelques ophiolites des Monts Apuseni du Sud et leur signification geologique (Roumanie). *Geologie Alpine*, 1992, **68**: 77-83.

Nicolae, I. (1995) Tectonic setting of the ophiolites from the South Apuseni Mountains: Magmatic Arc and Marginal Basin. *Rom. J. Tect. & Reg. Geol.*, **76**, 27-39.

Nicolescu, S. (1998) Skarn Genesis at Ocna de Fier - Dognecea, South-West Romania. Ph D Thesis, Univ. of Goteborg, A 36, 116 p.

Panaiotu, C. (1998) Paleomagnetic constraints on the geodynamic history of Romania. In: J. Sledzinski, editor "Monograph of Southern Carpathians", Warsaw Univ. of Techn., *Reports on Geodesy*, **7** (37), 205-216.

Papanikolau, D. (1989) Are the Medial Crystalline massifs of the Eastern Mediterranean drifted Gondwanian fragments? *Geol. Soc. Greece Spec. Publ.*, **1**, 63-90.

Pătrașcu, S., Bleahu, M., Panaiotu C.E. (1990) tectonic implication of paleomagnetic research into Upper Cretaceous magmatic rocks in the Apuseni Mountains, Romania. *Tectonophysics*, **180**, 309-322.

Pătrașcu, S., Bleahu, M., Panaiotu, C., Panaiotu, C.E. (1992) the paleomagnetism of the Upper Cretaceous magmatic rocks in the banat area of the South Crapathians: tectonic implications. *Tectonophysics*, **213**, 341-352.

Pătrașcu, S., Panaiotu, C., Șeclăman, M., Panaiotu, C.E. (1994) Timing of rotational motion of Apuseni Mountains (Romania): paleomagnetic data from Tertiary magmatic rocks. *Tectonophysics*, **233**, 163-176.

Pecskay, Z., Edelstein, O., Seghedi, I., Szakacs, A., Kovacs, M., Crihon, M., Bernad, A. (1995) K-Ar datings of Neogene-Quaternary calc-alkaline volcanic rocks in Romania. *Acta Volcan.*, **7**, 2, 53-61.

Popov, P. (1981) Magmatectonic features of the Banat-Srednogorie Belt. *Geologica*

Balcanica, **11**, 2, 43-72.

Popov, P. (1995) Postsubduction Alpine metallogenic zones in the Balkan Peninsula. *Geologica Macedonica*, **9**, 97-101.

Popov, P. (1996) Characteristic features of the Banat-Srednogorie metallogenic zone. In: "Plate tectonic aspects of the Alpine metallogeny in the Carpatho-Balkan region", IGCP Project No 356 Annual Meeting, Sofia 1996, 1, 137-154.

Rădulescu, D.P. (1974) Unele observatii asupra magmatismului alpin din teritoriul carpatic. *D.S. Inst. Geol.*, **LX/5**, 105-117.

Rădulescu, D.P., Săndulescu, M. (1973) The plate tectonics concept and the geological structure of the Carpathians. *Tectonophysics*, **16**, 155-161.

Rădulescu, D.P., Săndulescu, M. (1980) Correlation des phases de deformation, de metamorphisme et de magmatisme dans les Carpathes. *Memoire du B.R.G.M.*, **115**, 301-302, Orleans.

Ratschbacher, L., Linzer, G.H., Moser, F., Strusievicz, R.O., Bedelean, H., Har, N. , Mogos, P.A. (1993) Cretaceous to Miocene thrusting and wrenching along the central South Carpathians due to a corner effect during collision and orocline formation. *Tectonics*, **12**, 855-873.

Robertson, A.H.F., Dixon J.E. (1984) Introduction: Aspects of the geological evolution of the Eastern Mediterranean. In: "The geological evolution of the Eastern Mediterranean". Geol. Soc. Spec. Publ., 17, Blackwell Sci., Publ. Oxford.

Roman, C. (1970) Seismicity in Romania - Evidence for the Sinking Lithosphere, *Nature*, **228**, 5277, 1176-1178.

Roman, C. (1971) Plate Tectonics in the Carpathians: a case in development. Proc. XII European Seismol. Comm., Luxembourg, 21-29 Sep. 1970, 101,37, 30, 179-185.

Roman, C. (1973), Rigid Plates, Buffer Plates and Sub-Plates - Comment on paper "Active Plates in the Eastern Mediterranean" by D.P. Mc Kenzie. *Geophys. J. Roy. Astr. Soc*, **33**, 369-373.

Royden, L.H., Baldi, T. (1988) Early Cenozoic tectonics and paleogeography of the Pannonian and surrounding regions. In: L.H. Royden and F. Horvath, editors "The Pannonian Basin - A study in basin evolution". *Amer. Ass. Petrol. Geol. Mem.*, **45**, 1-16.

Russo-Săndulescu, D., Berza, T., Bratosin, I. and Ianc, R. (1978) Petrological study of the Bocsa banatitic massif (Banat). *D.S. Inst. Geol. Geof.*, **LXIV/1**, 105-172.

Russo-Săndulescu, D., Berza, T. (1979) Banatites from the western part of the Southern Carpathians (Banat). *Rev. Roum. Geol., Geophys. et Geogr., Geologie*, **23**, 2, 149-158.

Russo-Săndulescu, D., Bratosin, I., Vlad, C. , Ianc, R. (1986 a) Petrochemical study of the Surduc banatitic magmatites (Banat). *D.S. Inst. Geol. Geof.*, **70-71/1**, 97-121.

Russo-Săndulescu, D., Berza, T., Bratosin, I., Vlad, C., Ianc, R. (1986 b) Petrological study of banatites in the Ocna de Fier-Dognecea zone. *D.S. Inst. Geol. Geof.*, **70-71/1**, 123-142.

Russo-Săndulescu, D., Vâjdea E., Tănăsescu A. (1986 c) Significance of K-Ar radiometric ages obtained in the banatitic plutonic area of Banat. *D.S. Inst. Geol. Geof.*, **70-71/1**, 405-417.

Sanders, C. (1998) Tectonics and erosion - competitive forces in a compressive orogen: A fission track study of the Romanian Carpathians. Ph D Thesis, Free University of Amsterdam, 204 p.

Săndulescu, M. (1984) Geotectonica Romaniei. Editura Tehnica, Bucuresti, 336 p.

Ceahlău, M. (1988) Cenozoic tectonic history of the Carpathians. In: L.H. Royden and F. Horvath, editors "The Pannonian Basin - A study in basin evolution". *Amer. Ass. Petrol. Geol. Mem.*, **45**, 17-25.

Savu, H. (1980) Genesis of the Alpine Cycle Ophyolites from Romania and Their Associated Calc-Alkaline Volcanics. *An. Inst. Geol. Geof.*, **LVI**, 55-77.

Savu, H., Vajdea, E., Romanescu, O., (1986) The Radiometric age (K - Ar) and the ori-

gin of the Săvârşin Granitoid Masiff and of other Late Kimmerian Intrusions from the Mureş Zone. *D. S. Inst. Geol. Geophys., Bucharest*, **70-71/1**: 419-429.

Schmid, S.M., Berza, T., Diaconescu, V., Froitzheim, N., Fugenschuh, B. (1998) Orogen-parallel extension in the Southern Carpathians. *Tectonophysics*, in press.

Seghedi, A. (1998) The Romanian Carpathian Foreland. In: J. Sledzinski, editor "Monograph of Southern Carpathians", *Warsaw Univ. of Techn., Reports on Geodesy*, **7** (37), 21-48.

Serafimovski, T., Jankovic, S., Cifliganec, V. (1995) Alpine metallogeny and plate tectonics in the SW flank of the Carpatho-Balkanides. *Geologica Macedonica*, **9**, 3-14.

Sillitoe, R.H. (1980) The Carpathian-Balkan Porphyry Copper Belt - A Cordilleran perspective. In: "European Copper Deposits" Belgrade, 28-35.

Skenderov, G. (1996) Alpine tectono-magmatic development and metallogenesis of the Strandzha zone in Bulgaria. In: "Plate tectonic aspects of the Alpine metallogeny in the Carpatho-Balkan region", IGCP Project No 356 Annual Meeting, Sofia 1996, 1, 201-209.

Stanisheva-Vassilieva, G. (1980) The Upper Cretaceous magmatism in Srednogorie Zone, Bulgaria: A classification attempt and some implications. *Geologica Balcanica*, **10**, 2, 15-36.

Stanisheva-Vassilieva, G., Daieva, L. (1990) Across-arc geochemical variations of the Late Cretaceous magmatism in Eastern Srednogorie, Bulgaria. *Geologica Balcanica*, **20**, 4, 78.

Ştefan, A. (1980) Petrographic Study of the Eastern Part of the Vlădeasa Eruptive Massif. *An. Inst. Geol. Geof.*, **LV**, 207-325.

Ştefan, A. (1986) Eocretaceous granitoids from the South Apuseni. *D.S. Inst. Geol. Geof.*, **LXII/1**, 145-179.

Ştefan, A., Rosu, E., Robu, L., Robu, N., Bratosin, I., Grabari, G., Stoian, M., Vajdea, E. (1992) Petrological and geo-

chemical features of banatitic magmatites in northern Apuseni Mountains. *Rom. J. Petrology*, **75**, 97-11.

Stille, H. (1953) Der Geotektonische Werdegang der Karpaten. *Geol. Jhb. Beih.*, **8**, 1-239.

Strutinski, C., Soroiu, M., Paica, M., Todros, C., Catilina R. (1986) Preliminary data on the K-Ar ages of the Alpine magmatites between, Tincova and Ruschiţa (soth-western Poiana Rusca). *D.S. Inst. Geol. Geof.*, **70-71/1**, 492-503.

Tari, G., Dicea O., Faulkerson, J., Georgiev, G., Popov, S., Ştefănescu M., Weir G. (1997) Cimmerian and Alpine Stratigraphy and Structural Evolution of the Moesian Platform (Romania/Bulgaria). In: A.G. Robinson, editor " Regional and petroleum geology of the Black Sea and surrounding region", *Amer. Assoc. Petrol. Geol. Mem.*, **68**, 63-90.

Vassilieff L., Stanisheva-Vassilieva, G. (1981) Metallogeny of the Eurasian Copper Belt: Sector Bulgaria. *Geologica Balcanica*, **11**, 2, 73-87.

Vlad, S. (1978) Metalogeneza triasica din zona Tulcea (Dobrogea de nord). *Stud. Cerc. Geol. Geof. Geogr., Geologie*, **23**, 2, 249-258.

Vlad, S. (1979) A survey of banatitic (Laramian) metallogeny in the Banat region. *Rev. Roum. Geol., Geophys. et Geogr., Geologie*, **23**, 1, 39-44.

Vlad, S. (1980) Alpine Plume-generated Triple Junction in the Apuseni Mountains and the Metallogenetic Implications. *Rev. Roum. Geol., Geophys., Geogr., Geologie*, **24**, 71-81.

Vlad, S.N. (1997) Calcic skarns and transversal zoning in the Banat mountains, Romania: indicators of an Andean-type setting. *Mineralium Deposita*, **32**, 446-471.

Vlad, Ş., Borcoş, M. (1998) Alpine Metallogenesis of the Romanian Carpathians. *Rom. J. Mineral Deposits*, **78**, 5- 20.

Afterword

EMIL CONSTANTINESCU

- A Profile -

Anniversaries bring back memories and memories bring to the fore the personality of those we celebrate.

On 19th November 1999, Emil Constantinescu will be sixty. As a close friend and long-standing associate, it is a pleasure and a privilege to attempt to draw an outline of his distinguished academic career, which spanned over the past forty years.

His first degree in Law was followed by a brief spell as a Junior County Court Judge, at Piteşti. At this stage, we shall hardly be surprised if the young Emil reverted to his "first love" for Earth Sciences, which was in fact his true vocation. This is how it occurred that, in 1966, when he took his degree in Geology, Prof. Virgil Ianovici, then at the Chair of Mineralogy, encouraged him to join the staff of the Department of Mineralogy of Bucharest University. It was a beginning of a career, when Emil's interests focused on Mineralogy and Crystallography, an activity which he doubled with teaching, filed work and laboratory research alike.

His Ph.D. supervisor was Professor Dan Giuşcă and the subject of his dissertation was "The Mineral Genesis of the Sasca Montană Skarns", a topic of great interest in the 70's. In the mean time, Emil Constantinescu's activities of combined research and field-work gave him an early opportunity of spotting the talent of his students, with the view of creating an elite School of Mineralogy. This was indeed a "hot house", where the potential of each individual was stretched to the limit. The rewards of this selective process was not long to materialise, as Emil encouraged each member of his team to express his creativity and forge, at the same time, his academic individuality. This highly inspiring environment created, through excellence, a new Romanian School of Mineralogy, which made its mark both in Romania and abroad. Here I should emphasise that the credit undoubtedly goes to Prof. Emil Constantinescu, for his persistent enthusiasm and passion of his profession, qualities which, in turn, he managed to instil in his pupils.

His work on the "The Mineral Genesis of Skarns" was awarded the "Cobălcescu Prize", the highest scientific accolade of the Romanian Academy. This was a tribute to a new concept, as well as to a new method of investigation, which were meant to become a classic benchmark for the young generation of academics. But all these achievements may not have been possible in the Romanian environment, if they were not complemented by some truly outstanding personal qualities. I venture to say this, because first and foremost Emil Constantinescu was a leader of opinion, a man of character, the spokesman of a coherent and clear message, determined in the courage of his opinions, always inspired and inspiring, This trait of character made its mark at the Chair of Mineralogy, then in the Faculty of Geology and in the University at large, where he was elected Chancellor. Those of us, who had the privilege of working with him, were direct beneficiaries of his charisma.

In retrospect, it is obvious that Emil Constantinescu's evolution was not fortuitous, but an intelligent structure, based on the strong belief in the twin tenets of Culture and Education, which were happily complemented by Pragmatism and Efficiency. It is indeed, on these strong principles that we find the secret of his ongoing success in an amazing variety of fields, a success which is based on the sine-qua-non attributes of competence and responsibility. The responsibilities he was given in Academia, as Rector of the Bucharest University, President of the Council of Rectors of Romania and President of the National Council for Educational Reform, where the reflection of his deep-seated faith in the Romanian Education, which he proceeded to improve gradually, through restructuring.

Emil Constantinescu's distinct personality left a remarkable impression on the Romanian School of Geology through his scientific work. His gift for academic teaching is demonstrated by his long career on the staff of the University of Bucharest, where he started first as demonstrator, then as lecturer and finally, professor. I say "finally" because, as we know too well, all academic positions were frozen under the previous Communist administrations and we had to wait until 1990, before these restrictions were lifted and our Academic life reached some sense of normality. Although December 1989 marked a crucial watershed in our lives, as a result of which Emil Constantinescu took on new challenges, it is a tribute to the Scientist that he carried on, in parallel, with his Academic activities to the present day. He did so, in spite of added duties in public life, in a context that brought so many changes to Romania as a whole.

Despite the singular evolution of his career, during the past decade, Emil Constantinescu's relationship with his colleagues and friends remained unaltered. During this latter period, although he inevitably relinquished his position at the Chair of Mineralogy, he kept in constant touch with the Department by giving lectures, contribution with new ideas and projects, enhancing our mineralogical collection with samples brought from his foreign trips, or endowing our library with gifts of books and journals. More significantly, Emil encouraged the young Romanian graduates to apply for scholarships at the best universities around the world, whilst the Ph.D. students had

their theses approved by external examiners from foreign universities. This statement may sound superfluous if we did not consider in retrospect the restrictive practices and vexations perpetrated by the Communist dictatorship. After four long decades of isolation from the main stream of European thinking, which seemed like an unending spell of the Dark Ages, now the Romania Academia had woken up to find its natural vocation within the family of world scientists. Here I could say, without fear of contradiction, that this constant dialogue, this seminal meeting of minds is largely, if not mainly due to the impact made by Emil Constantinescu, both as a Scientist and as a Public Figure.

His international recognition passed its acid test, whether in the award of the degrees of Doctor Honoris Causa of Many Academic establishments around the world, the honorary membership of learned societies, or the lectures which he delivered as our roving ambassador around the globe.

If it is true to say that Professor Constantinescu's extramural activities enhanced the image of Romania, then it stands to good reason to add that the Romanian Academia at large was the direct beneficiary of his mission. Indeed, we consider this renewed dialogue with the rest of the world, which now we take for granted, as an implicit recognition of the Romania cultural and scientific values, Moreover, as a Geologist I am bound to state that this regained ethos is the natural extension of the old tradition of the Romania School of Geology and in particular of the long array of preceding Scholars, such as Ludovic Mrazec, Matei Drăghiceanu, Gheorghe Murgoci, Al. Codarcea, Virgil Ianovici, Dan Giuşcă, Ion Simionescu, Saba Ştefănescu, to mention just a few.....

At the turn of a new Millennium, this historic legacy gives us strength in our faith for the future and it is a particular privilege to pay this tribute to the Scientist, whilst we celebrate, on his 60th Birthday, the man who is a very special friend.
La Mulţi Ani Emil!

Prof. Nicolae Anastasiu
Chair of Mineralogy, University of Bucharest

September 1999

CURRICULUM VITAE
Prof. dr. Emil Constantinescu

Born November 19, 1939
Married. Two children

EDUCATION

· DIPLOMA IN LEGAL SCIENCES FACULTY OF LAW BUCHAREST UNIVERSITY1960
· DIPLOMA IN GEOLOGYFACULTY OF GEOLOGY-GEOGRAPHY BUCHAREST UNIVERSITY 1966
· DOCTOR IN GEOLOGY BUCHAREST UNIVERSITY
· DOCTOR AS SCIENCE DUKE UNIVERSITY (U.S.A.)

CAREER

· HONORARY PRESIDENT OF BUCHAREST UNIVERSITY SENATE 1996-to present
· RECTOR (PRESIDENT) OF BUCHAREST UNIVERSITY 1992 - 1996
· PRESIDENT OF NATIONAL UNIVERSITIES RECTORS COUNCIL - ROMANIA 1992 - 1996
· VICE RECTOR (VICE PRESIDENT) OF BUCHAREST UNIVERSITY 1990 - 1992
· VISITING PROFESSOR - NATURAL SCIENCE DEPARTMENT - DUKE UNIVERSITY, NORTH CAROLINA, U.S.A. 1991 - 1992
· FULL PROFESSOR MINERALOGY - BUCHAREST UNIVERSITY 1991 - to present
· ASSOCIATE PROFESSOR, ASSISTANT PROFESSOR - CRYSTALLOGRAPHY, MINERALOGY, PETROGRAPHY AND PHYSICAL METHODS OF MINERALS ANALYSIS FAC. OF GEOLOGY, GEOGRAPHY & GEOPHYSICS - BUCHAREST UNIVERSITY 1966 - 1991
· JUNIOR JUDGE - DISTRICT COURT - PITESTI, ROMANIA 1960 - 1961

RESEARCH ACTIVITIES

· PH. D., THESIS COORDINATOR IN MINERALOGY, BUCHAREST UNIVERSITY PETROGRAPHY & METALOGENY - ECOLE DE MINE, LYON, FRANCE UNIVERSITY OF SEVILLA, SPAIN 1990 - to present
· HEAD OF TERMAL ANALYSIS LABORATORY FAC. OF GEOLOGY, GEOGRAPHY &

GEOPHYSICS BUCHAREST UNIVERSITY 1970 - 1982
· HEAD OF THE X-RAY DIFFRACTION LABORATORY FAC. OF GEOLOGY, GEOGRA-
PHY & GEOPHYSICS BUCHAREST UNIVERSITY 1980 - 1987
· SCIENTIFIC COUNSELLOR ENTERPRISE FOR GEOLOGICAL EXPLORATION
1987 - 1990

LECTURES - UNIVERSITIES AND RESEARCH INSTITUTES

· Tubingen University, Department of Petrography, 1980 - Germany
· Mining and Geology Institute, Sofia, 1982 - Bulgaria
· Institute of Mineralogy and Geochemistry, Guyang, 1989; Geological Institute, Sinica
Academy, Beijing, 1989 - China

· Berkeley University, CA, 1992; Indiana University, Bloomington, IN, 1992; University of
South California, Los Angeles, CA, 1992;
Standfort University, CA, 1993; Georgetown University, Washington D.C., 1993; Columbia
University, New York, 1998 - U.S.A., National Geographical Society - Washington 1998 - USA
· Oxford University, 1994; British Geological Survey, Nottingham, 1991 - United Kingdom
· Turku University, 1993; Geological Survey of Finland, Helsinki, 1993 - Finland
· East European Institute, Lublin, 1993 - Poland
· National University, Cairo, 1994 - Egypt
· Rio de Janeiro University, 1995 - Brazil
· Sydney University, 1995 - Australia
· Patras University, 1996 - Greece
· Ecole Normale Superieure, Paris, 1997-France
· Caroline University, Prague 1997, Czechia
· The Norwegian Nobel Committee, 1997- Norway

SCIENTIFIC PUBLICATIONS

BOOKS (10); SCIENTIFIC STUDIES IN PERIODICALS (54); FIELD TRIP GUIDEBOOKS
(2); GEOLOGICAL REPORTS (36); GEOLOGICAL EXPERTISE (5); GEOLOGICAL MAPS
(3)

BOOKS

· MINERAL GENESIS OF SKARNS AT SASCA MONTANA, in Romanian, 170 p., Romanian
Academy Press, Bucharest, 1980.
· MINERALOGY. TREATISE., in Romanian, 927 p., Didactica Press, Bucharest, 1979.
Coauthors: Ianovici V. and Stiopol V.
· PRINCIPLES OF CLASSIFICATION AND SYSTEMATIZATION OF MINERALS, in
Romanian, 120 p., Bucharest University Press, 1979. Coauthor: Stiopol V.
· DETERMINATION OF OPAQUE AND TRANSPARENT MINERALS, in Romanian, 183 p.,
Bucharest University Press, 1979.
· PHYSICAL PROPERTIES AND CHEMISTRY OF MINERALS, in Romanian, 223 p.,
Bucharest University Press, 1983. Coauthors: Ianovici V. and Stiopol V.

· MINING ENGINEER'S TEXTBOOK, Chapter on CRYSTALLOGRAPHY AND MINER-ALOGY, in Romanian, Technical Press, Bucharest, 1984.
· METHODS OF PHYSICAL ANALYSIS OF MINERALS AND ROCKS, in Romanian, Bucharest University Press, 1986. Coauthors: Matei L., Cioran A., Crăciun C.
· CRYSTALLOGRAPHY - MINERALOGY, in Romanian, Bucharest University Press, 1990. Coauthors: Fabian C., Ştefan L.
· RISK AND THE ECOLOGICAL POLICY IN ROMANIA, Nefrit Press, Bucharest, 1994. Coauthor: Matei L.
· DETERMINATIVE MINERALOGY, in Romanian, 550 p., Bucharest University Press, 1966. Coauthor: Matei L.

MAIN PAPERS

· Metasomatic Origin of Some Intergrowth, in American Mineralogist, 1972, Vol. 57, No. 5-6, p. 932-940, 1972. Coauthor: Şeclăman M.
· Tectonostructural Position of the Foidic Rocks in the Romanian Carpathians, 13 p., Revue Roumaine, Serie des Geologie, Tome 27, Academia Română, 1982. Coauthor: Anastasiu N.
· Some Features of Ore Fabric, in Ore Genesis. The State of the Art, p. 784-793, G. Amstutz, editor, Springlere Verlag, Heidelberg, London, New York, 1982. Coauthor: Udubaşa Gh.
· Caractér cristallographiques, optiques et chimico-structuraux de l'adulaire cantonnée dans les filons alpins de Roumanie; contributions au "probleme de l'adulaire", in Travaux du 12-eme Congres de l'Assoc. Geol. Carpatho-Balc. An. Inst. Geol. Geofiz. LXII, p 9-18, 1983, Coauthor: Săbău G.
· Mineralogy of Alpine Veins from the Romanian Carpathians, An Inst. Geol. Geofiz. LXIV, Special Issue, The 27th International Congres on Geology, p. 33-43, 1984. Coauthor: Săbău G.
· Isomorphism and Chemical Peculiarities of Some Ludwigites and Szaibelytes from Romania, in Proceedings of International Geological Congress, 29th Congress, Kyoto, 1992. Coauthor: Marincea Şt.
· About fractal features of iron and manganese hydroxides dendrites. Abs. of 30th International Geol. Congress, Beijing, China, v. 2, p.490, Beijing, 1996. Coauthor: Pălăşeanu E., Milutinovici, Caracaş R.
· Pyrophylite in the Anchimetamorphic Schists of the Parâng Mountains. Southern Carpathians, Romania. Petrogenetic Significance., in Crystal Chemistry of Minerals. Schweizerb. Verlagbuchhandlung Stuttgart New York, 1987. Coauthor: Popescu Gh.
· Gold Mineralogy in Romania. Proceedings of the International Symposium on Gold Geology, Publishing House of North University Schenyang, China, 1989.
· First Occurrence of the Coloradoite in Romania, in Revue Roumaine, Serie des Geologie, Tome 36, p. 33/34, 1992, Bucharest. Coauthor: Popescu Gh.
· Bi-Mineral Assemblages in Copper Ore Deposits in South-Western Banat, Romania, Abstract suppl no.1 to Terra Nova 5, 443-444, Strasbourg, 1993. Coauthor: Şimon Gr.
· The alkaline massif of Ditrau; a petrogenetical retrospective view. Anal. Univ. Bucuresti, Geologie, XLIII, Bucharest, 1994. Coauthor: Anastasiu N.
· Plagioclase feldspars in the banatites from Maidan-Oravita, Romania. Anal. Univ. Bucuresti, Geologie, XLIII, Bucharest, 1994. Coauthor: Bindea G.
· Measuring fractal dimension - iron and manganese hydroxides dendrites. Rom. J. of Mineralogy,
77, Bucharest, p. 13-14, 1995. Coauthor: Pălăşeanu E., Milutinovici S., Caracaş R.
· Relatively unoxidized vivianite in limnic coal from Căpeni, Baraolt Basin, Romania. Canadian

Mineralogist 35, 3, p. 713-722, Ontario, Canada, 1997. Coauthor: Marincea Şt., Ladriere I.
· Alpine Granitoid Series and Associated Mineralisation in the Carpathian - Balkan Fold Belt in
Journal of Resource Geology, Tokio, Japan, 1998. Coauthors: Berza T., Vlad Ş. N.

INTERNATIONAL SCIENTIFIC EVENTS. SECTION CHAIRMAN. INVITED SPEAKER, KEYSPEAKER.

· Conference of the International Association of University Presidents : The University of the
21st Century Towards a New Ethics of Responsibility, Brussels,1999.
· Cultural Values and Human Progress Symposium, The Borders of civilizations: Clash or
Dialogue, Harvard University, 1999.
· European Universities Association Conference, A University Politics for Europe, Budapest,
Hungary, 1994.
  European Conference, Perspectives of Higher Education Reform in Central and Eastern
Europe, Menaggio, Italy, 1993.
  European Community Conference, The European Community and the Balkans, Corfu Island,
Greece, 1993.
  European Conference, The Universities in the Service of Students Development, Barcelona,
Spain, 1993.
  Transatlantic Conference of American and European Rectors (ACE CRE) New Demands,
Enduring Values: The Challenge of Human Resources, Williamsburg, VA., USA, 1993.
  Conference AUPELF-UREF, Jours des reflections sur les filieres francophones, Paris, France,
1992.
  International Symposium on International Policy and Strategy, München, Germany, 1992.
  International Conference on Geological Research in Eastern European Countries, London,
United Kingdom, 1991
  European Conference on Technology - Integration of Technology Assessment and Humanities
in Engineering Education, Karlsruhe, Germany, 1991
  UNESCO Conference, The Blue Danube Ecological Programme, Vienna, Austria, 1990.
  Balkan Rectors' Conference on University Education and Research Interaction, Istanbul,
Turkey, 1990.
  International Symposium Gold Geology, Shenyang, China, 1989.
  International Symposium on Genesis of Minerals, Heidelberg, Germany, 1983.
  XIII Congress of the International Association of Mineralogy, Varna, Bulgaria, 1982.
  Conference of the International Association of Mineralogy, Orléans, France, 1980.
  International Congress of Geology, Paris, France, 1980.

PERSONAL CONTRIBUTIONS IN THE FIELD OF GEOLOGY. HIGHLIGHTS.

  Identified and fully described nine rare minerals, so far unknown in Romania: clintonite, idaite,
stegenite, kalsilite, crandalite, kobellite, scorodite, coloradoite.
  Described over 90 new minerals for various classical occurences in Romania.
  Author of a new hypothesis on the metasomatic origin of micrographic intergrowths.
  Model of skarn mineralogenesis under recurrent variations of CO_2 pressure.
  Several genetic models of manganese minerals association and of RE and uranium minerals
association in metamorphic formations.

· Identified and described Alpine veins on the territory of Romania.
· Fractal features of dendrites.
· Author of the first CRYSTALLOGRAPHIC ATLAS OF ROMANIA.
· Scientific collection MINERALS OF ROMANIA, at the University of Bucharest: samples, crystals, thin sections, polished sections.
· Coauthor, Project of the Faculty of Geology and Geography, University of Algiers, Algeria.

CONTRIBUTIONS IN OTHER FIELDS

· Strategy of Education and Scientific Research. Environmental Protection. Political and socio-economic analyses. Over 100 papers and interviews published in volumes and periodicals: USA, Australia, Austria, United Kingdom, The Netherlands, France, Belgium, Germany, Poland, Spain, Finland, Italy, Canada.

ELECTED MEMBER OF ACADEMIC FORA

· European Universities Association, (C.R.E.) Permanent Committee, 1993; re-elected 1994-1998.
· International Association of University Presidents (I.A.U.P.), 1994-1996.

· Member of the Royal British Geological Society, since 1991
· Member of the Mineralogical Society of America, since 1992.
· Honorary Member of the German Mineralogists Society, since 1993.
· Member of the Geological Society of South Africa, since 1993.
· Honorary Member of the Geological Society of Greece, since 1995.
· Honorary Member of the Mineralogical Society of Great Britain and Ireland, since 1996.
· Honorary Member of the Society of Resource Geology, Japan, since 1996.
· Honorary Member of the Geographical Society of Paris, France, 1996
· Honorary Member of the National Geographical Society of Washington, USA, 1998
· Romanian Geological Society, General Secretary, 1987-1990, 1990-1993.

· National Committee of Romanian Geologists, member since 1991.
· High Commission for Academic Degrees Accreditation, Romania, 1990-1996.
· Editorial Board, Geological Review, of the Romanian Academy, member since 1988.

· Civic Academy, President, 1990-1992.

HONOURS AND AWARDS

· DOCTOR HONORIS CAUSA Conferred by the ECOLE NORMALE SUPERIEURE, PARIS, FRANCE
· DOCTOR HONORIS CAUSA Conferred by the THE UNIVERSITY OF LIEGE BELGIUM
· DOCTOR HONORIS CAUSA Conferred by the POLYTECHNION UNIVERSITY, ATHENS, GREECE
· DOCTOR HONORIS CAUSA Conferred by the UNIVERSITY OF MONTREAL, CANADA

· DOCTOR HONORIS CAUSA Conferred by the NEW DELHI UNIVERSITY, INDIA
· DOCTOR HONORIS CAUSA Conferred by the THE UNIVERSITY OF BEIJING
THE PEOPLE S REPUBLIC OF CHINA
· DOCTOR HONORIS CAUSA Conferred by the"BILKENT UNIVERSITY", ANKARA,
TURKEY
· DOCTOR HONORIS CAUSA Conferred by the UNIVERSITY OF CHISINAU, REPUBLIC
OF MOLDOVA
· DOCTOR HONORIS CAUSA Conferred by the UNIVERSITY OF MARIBOR, SLOVENIA

· MEDAL conferred by the UNIVERSITE de PARIS - SORBONNE
· MEDAL conferred by the CAROLINE UNIVERSITY, PRAGUE, THE CZECH REPUBLIC
· MEDAL conferred by ACADEMIE DES SCIENCES, INSTITUT DE FRANCE, PARIS,
FRANCE
· MEDAL conferred by UNIVERSITY OF AMSTERDAM, THE NETHERLANDS
· MEDAL conferred by UNIVERSITY OF SZEGED, HUNGARY

· "GR. COBĂLCESCU" AWARD (1980) FOR OUTSTANDING SCIENTIFIC CONTRIBU-
TIONS IN THE FIELD OF GEOLOGY conferred by the ROMANIAN ACADEMY,
BUCHAREST, ROMANIA (the highest Romanian scientific distinction).

· ARISTIDE CALVANI AWARD for peace, democracy and human development, Paris, 1997
· THE AWARD FOR DEMOCRACY Democratic Center Washington D.C., 1998
· EUROPEAN STATESMAN OF THE YEAR AWARD, conferred by the Institute for East-West
Studies, New York, USA, 1998
· EUROPEAN COUDENHOVE-KALERGI AWARD for the contribution to development of
Europe and free movement of ideas, Bern, 1998

· THE GREAT CROSS OF THE LEGION OF HONOUR OF THE FRENCH REPUBLIC, 1996
· THE ORDER OF THE SUN OF PERU - THE GREAT CROSS WITH BRILLIANTS, 1998
· THE ORDER OF THE WHITE ROSE OF FINLAND - THE GREAT CROSS WITH NECK-
LESS, 1998

· HONORARY CITIZEN of Athens, Prague, Budapest, San Francisco, Helsinki

INDEX